



First report of the genus *Woonpaikia* Park, 2010 (Lepidoptera, Lecithoceridae) from China, with the description of two new species

Shuai Yu^{1,2}, Shuxia Wang²

¹ College of Life Sciences, Liaocheng University, Liaocheng 252000, China

² College of Life Sciences, Nankai University, Tianjin 300071, China

Corresponding author: Shuxia Wang (shxwang@nankai.edu.cn)

Abstract

The lecithocerid genus *Woonpaikia* Park, 2010 and *Woonpaikia angoonae* Park, 2010 are newly recorded from China. *Woonpaikia similangoonae* Yu & Wang, **sp. nov.** and *W. imperspicua* Yu & Wang, **sp. nov.** are described as new to science. Images of adults of the Chinese *Woonpaikia* species are provided, along with a key to the males of all the known species of *Woonpaikia*.

Key words: Gelechioidea, Lecithocerinae, new record

Introduction

Woonpaikia Park, 2010 is a small genus of lepidopteran classified in the family Lecithoceridae, subfamily Lecithocerinae. Park (2010) erected the genus to accommodate *W. villosa* and *W. angoonae* from Thailand, with *W. villosa* as the type species. Since then, no more species have been described. *Woonpaikia* is morphologically similar to the type genus of Lecithoceridae, *Lecithocera* Herrich-Schäffer, 1853, in sharing a similar wing pattern and venation, but it can be distinguished by presence of a ventrodistal pectin-like scale tuft on the scape of the antennae, labial palpi dorsally with dense, long, hair-like scales, male genitalia with the juxta decrescent and the sacculus produced apically to form a process.

Here we describe two new species of *Woonpaikia*. We also provide new distribution records for other known species in China, as well as a key to identify males of all the known species of this genus.

Materials and methods

The specimens examined were collected in China using 450 W high-pressure mercury lamps. Morphological terminology in the descriptions follows Gozmány (1978). Wingspan was measured from the tips of the left to right forewings. Slides of genitalia were prepared following the methods introduced by Li (2002). Photographs of the adults were taken with a Leica M205A stereomicroscope, and



Academic editor: Mark Metz

Received: 1 November 2023

Accepted: 26 January 2024

Published: 19 February 2024

ZooBank: <https://zoobank.org/60D64310-7AF2-4451-8C43-DFCB31D9CF94>

Citation: Yu S, Wang S (2024) First report of the genus *Woonpaikia* Park, 2010 (Lepidoptera, Lecithoceridae) from China, with the description of two new species. ZooKeys 1192: 1–7. <https://doi.org/10.3897/zookeys.1192.115033>

Copyright: © Shuai Yu & Shuxia Wang.

This is an open access article distributed under terms of the Creative Commons Attribution License ([Attribution 4.0 International – CC BY 4.0](https://creativecommons.org/licenses/by/4.0/)).

photographs of genitalia were taken with a Leica DM750 microscope plus the Leica Application Suite v. 4.6. All photographs were refined with Photoshop CC.

Materials examined, including the type series of the new species, are deposited in Liaocheng University, Liaocheng, China (**LCU**), except for several specimens of *W. angoonae*, which are deposited in the Insect Collection of Nankai University, Tianjin, China (**NKU**).

Taxonomic accounts

Woonpaikia Park, 2010

Woonpaikia Park, 2010: 239. Type species: *Woonpaikia villosa* Park, 2010.

Key to the males of *Woonpaikia*

- 1 Apical process of sacculus extending posteriorly at least as far as apex of cucullus (Fig. 3A, C) **2**
- Apical process of sacculus extending much less than length of cucullus (as in Fig. 3B)..... **3**
- 2 Cucullus capitate; aedeagus with a needle-like apical extension (Fig. 3C)...
..... ***W. similangoonae* sp. nov.**
- Cucullus acuminate; aedeagus without apical extension (Fig. 3A)
..... ***W. angoonae***
- 3 Apical process of sacculus triangular; width of cucullus at middle about twice width at base (Fig. 3B) ***W. imperspicua* sp. nov.**
- Apical process of sacculus horn-shaped; width of cucullus at only middle slightly greater than at base (Park 2010: 241, fig. 10) ***W. villosa***

Woonpaikia angoonae Park, 2010

Figs 1A–C, 3A

Woonpaikia angoonae Park, 2010: 241. Holotype male collected in Thailand (Chiang Mai) deposited in Osaka Prefecture University, Osaka, Japan (OPU).

Materials examined. CHINA • 1♂; Yunnan, Mengla County, Bubeng; 21.60°N, 101.60°E; 652 m elev.; 14 July 2013; SR Li et al. leg.; slide no. YS19297, NKU • 1♂; Yunnan, Xishuangbanna, Yexianggu; 22.17°N, 100.87°E; 762 m elev.; 9 July 2015; KJ Teng & X Bai leg.; slide no. YS19298, NKU • 1♂; Yunnan, Jinghong; 21.90°N, 100.77°E; 640 m elev.; 2 Aug. 2016; KJ Teng et al.; slide no. YS19293, NKU • 1♂; Yunnan, Menghai County, Nabanhe; 22.25°N, 100.61°E; 1210 m elev.; 4–5 Aug. 2022; S Yu & KJ Teng leg.; slide no. YUS061, LCU • 3♂; Yunnan, Jinghong, Mt Jinuo; 21.98°N, 100.89°E; 1425 m elev.; 6–7 Aug. 2022; S Yu & KJ Teng leg.; slide no. YUS063, LCU.

Description. Adult wingspan 10.5–12.5 mm (Fig. 1A).

Diagnosis. This species can be recognized by the smoothly arcuate apical process of the sacculus which extends posteriorly beyond the apex of the cu-



Figure 1. External features of *Woonpaikia* spp. **A–C** *W. angoonae* Park, 2010, male, YUS063 **B** lateral view of head **C** close-up of scape **D–F** *W. imperspicua* sp. nov., holotype, male, YUS064 **E** lateral view of head **F** close-up of scape **G–I** *W. similangoonae* sp. nov., male, YUS062 **H** lateral view of head **I** close-up of scape. Scale bars: 2.0 mm.

cullus (Fig. 3A). It is most similar to the new species, *W. similangoonae*. The differences between these species are detailed below.

Distribution. China (Yunnan, new record), Thailand.

Remarks. This species was originally described from Thailand based on a single male. It is recorded here from China for the first time.

***Woonpaikia imperspicua* Yu & Wang, sp. nov.**

<https://zoobank.org/90F5CE81-246C-4C58-9D51-A37832D89FF0>

Figs 1D–F, 2A, 3B

Type materials. Holotype: CHINA • ♂; Yunnan, Jinghong, Mt Jinuo; 21.98°N, 100.89°E; 1425 m elev.; 6 Aug. 2022; S Yu & KJ Teng leg.; slide no. YUS064, LCU. **Paratype:** 1♂; same data as holotype; slide no. YUS060, LCU.

Diagnosis. The new species can be distinguished by the triangular apical process of the sacculus which extends for less than 1/2 the length of the cucullus, and by the aedeagus which has dorsal and ventral extensions at the apex; in *W. similangoonae* and *W. angoonae*, the apical process of the sacculus is long, extending posteriorly at least as far as the apex of the cucullus (sometimes further). *Woonpaikia villosa* has a transverse fascia in the hindwing (Park 2010: 240, fig. 1), whereas *W. imperspicua* lacks this fascia.

Description. Wingspan 13.5–14.0 mm (Figs 1D, 2A). Head brown. Antenna orange white; scape with a small imperceptible pectin-like scale tuft ventrodistally. Labial palpus dorsally with dense, long, hair-like scales; third palpomere shorter than second palpomere. Forewing slightly widened distally, costal margin almost straight, apex produced, termen gently concave; ground color dark brown; orange-yellow along costal margin from before middle to apex; discal stigma black, small, rounded; plical stigma black; discocellular stigma black, larger than plical stigma; fringe greyish brown, with an orange-white basal line; R₃, R₄ and R₅ stalked, R₅ to termen, CuA₁ and CuA₂ with short stalk. Hindwing and fringe pale greyish brown; M₃ and CuA₁ stalked.

Male genitalia (Fig. 3B). Uncus with caudal lobes thumb-shaped. Gnathos with basal plate distally semi-ovate, with rounded apex; median process almost uniformly wide in basal 2/3, thereafter sharply narrowed to a pointed apex, curved ventrad at basal 2/3 by a right angle. Costal bar narrow, taeniod. Valva with basal part subquadrate; cucullus arising from upper corner of basal part of valva, narrowed at base, widened to middle, width at middle about twice width of base, thereafter narrowed to blunt apex, nearly straight on costal margin, bearing a row of needle-like setae along ventral margin; sacculus wide, straight on its ventral margin, with a triangular apical process extending less than 1/2 length of cucullus and bearing a row of needle-like setae. Juxta elliptical, wider than long, with a subquadrate process at middle on anterior margin. Vinculum rounded on anterior margin. Aedeagus slightly shorter than valva, almost uniformly wide, with a horn-like dorsal extension and a spiniform ventral extension; cornuti consisting of a flake-like plate placed beyond middle and three spinules near apex.

Female. Unknown.

Distribution. China (Yunnan).

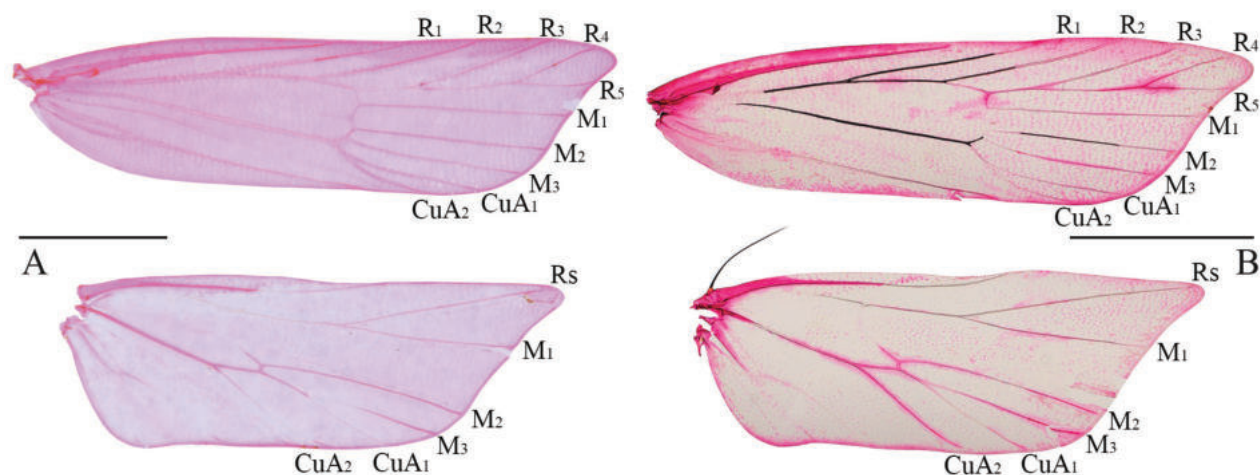


Figure 2. Wing venation of *Woonpaikia* spp. **A** *W. imperspicua* sp. nov., paratype, slide no. YUS060 **B** *W. similangoonae* sp. nov. paratype, slide no. YUS075. Scale bars: 2.0 mm.

Etymology. The specific name is derived from the Latin *imperspicuus*, referring to the small imperceptible pectin-like scale tuft on the scape of the antenna.

***Woonpaikia similangoonae* Yu & Wang, sp. nov.**

<https://zoobank.org/039D1A18-1348-4893-A6F8-4B5D5A086F33>

Figs 1G–I, 2B, 3C

Type materials. Holotype: CHINA • ♂; Yunnan, Mang City, Mt Banggunjian; 24.39°N, 97.84°E; 1758 m elev.; 14 Aug. 2022; S Yu & KJ Teng leg.; slide no. YUS062, LCU. **Paratype:** 1♂; same data as holotype; slide no. YUS075, LCU.

Diagnosis. The new species is similar to *W. angoonae*, but it can be distinguished by the capitate cucullus and the aedeagus with a needle-like apical extension. In *W. angoonae*, the cucullus is acuminate and the aedeagus lacks an extension on the apex.

Description. Wingspan 14.0–15.0 mm (Figs 1G, 2B). Head yellowish brown. Antenna yellow; scape ventrodistally with a small imperceptible pectin-like scale tuft. Labial palpus with dense, long, hair-like scales dorsally; third palpomere shorter than second palpomere. Forewing slightly widened distally, with costal margin almost straight, apex produced, termen gently concave; ground color yellowish brown; orange-yellow along costal margin from about basal 2/5 to apex; discal stigma black, rounded; plical stigma black, nearly same size as discal stigma; discocellular stigma black, elliptical; fringe greyish brown, with an orange-white basal line; R_3 , R_4 , and R_5 stalked, R_5 to termen, CuA_1 and CuA_2 with short stalk. Hindwing and fringe yellow, dark brown scales along vein M_2 ; M_3 and CuA_1 shortly stalked.

Male genitalia (Fig. 3C). Uncus nearly inverted trapezoidal; caudal lobes semi-ovate. Gnathos with basal plate roundly produced on posterior margin; median process narrowed slightly from base to basal 2/3, thereafter sharply narrowed to a pointed apex, curved ventrad at basal 2/3 by a right angle. Costal bar narrow, arched taenioid. Valva with basal part trapezoidal; cucullus capitate, arising from upper corner of basal part of valva, sinuate, narrow basally, widened to about basal

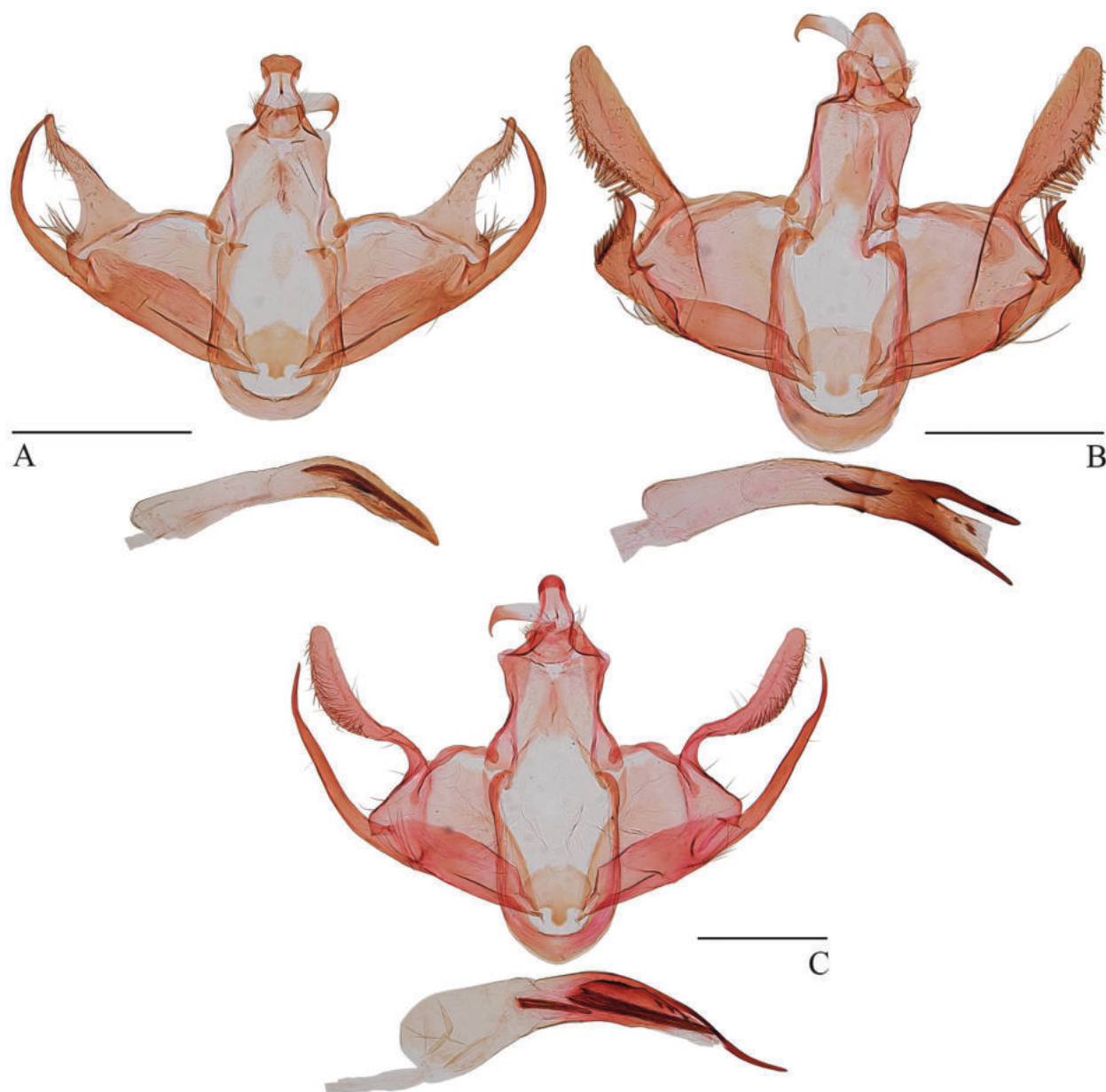


Figure 3. Male genitalia of *Woonpaikia* spp. **A** *W. angoonae* Park, 2010, slide no. YUS063 **B** *W. imperspicua* sp. nov., holotype, slide no. YUS064 **C** *W. similangoonae* sp. nov., slide no. YUS062. Scale bars: 0.5 mm.

2/3, thereafter narrowed slightly to rounded apex, costal margin arched in basal 1/2 and straight in distal 1/2; sacculus wide, straight on its ventral margin, with a long, apical process extending posteriorly as far as apex of cucullus. Juxta elliptical, wider than long, with a thumb-like process at middle on anterior margin. Vinculum subrounded on anterior margin. Aedeagus slightly shorter than valva, wide at base, narrowed to apex, with a needle-like apical extension; cornuti consisting of two needle-like spines of different sizes and a flake-like plate bearing three spinules.

Female. Unknown.

Distribution. China (Yunnan).

Etymology. The specific epithet is derived from the Latin *simile* (likeness) and *angoonae*, referring to the similarity between this new species and *W. angoonae*.

Acknowledgements

We express our cordial thanks to the reviewers, Kyu-Tek Park (Incheon National University, South Korea) and Yang-Seop Bae (Incheon National University, South Korea) for their valuable suggestions. We also thank all the team members for their participating in the field collection.

Additional information

Conflict of interest

The authors have declared that no competing interests exist.

Ethical statement

No ethical statement was reported.

Funding

This study is supported by the National Natural Science Foundation of China (no. ZR2022QD130).

Author contributions

All authors have contributed equally.

Author ORCIDs

Shuai Yu  <https://orcid.org/0000-0003-3670-2701>

Shuxia Wang  <https://orcid.org/0000-0002-9316-6661>








Data availability

All of the data that support the findings of this study are available in the main text.

References

- Gozmány L (1978) Lecithoceridae. In: Amsel HG, Reisser H, & Gregor F (Eds) *Microlepidoptera Palaearctica*, Vol. 5 Georg Fromme & Co., Vienna, 306 pp.
- Herrich-Schäffer GAW (1847–1855) *Systematische Bearbeitung der Schmetterlinge Von Europa, zugleich als Text, Revision und Supplement zu Jakob Hübner's Sammlung europäischer Schmetterlinge, Fünfter Band. Die Schaben und Federmotten*. Regensburg, 394 pp.
- Li HH (2002) *The Gelechiidae of China (I) (Lepidoptera: Gelechioidea)*. Nankai University Press, Tianjin, 504 pp.
- Park KT (2010) A new genus *Woonpaikia* Park, gen. nov. (Lepidoptera: Lecithoceridae) with descriptions of two new species. *Journal of Asia-Pacific Entomology* 13(3): 239–242. <https://doi.org/10.1016/j.aspen.2010.04.004>

First amphibious Crinocheta (Isopoda, Oniscidea) from the Neotropics with a troglobitic status: a relictual distribution

Carlos Mario López-Orozco¹, Ivanklin Soares Campos-Filho², Livia Medeiros Cordeiro^{3,4},
Jonas Eduardo Gallão^{1,3}, Yesenia M. Carpio-Díaz^{1,5}, Ricardo Borja-Arrieta^{1,5}, Maria Elina Bichuette^{1,3}

1 *Laboratório de Estudos Subterrâneos, Universidade Federal de São Carlos, São Carlos, São Paulo, Brazil*

2 *Department of Biological Sciences, University of Cyprus, Lefkosia (Nicosia), Cyprus*

3 *Instituto Brasileiro de Estudos Subterrâneos, São Paulo, Brazil*

4 *Grupo de Espeleologia Serra da Bodoquena, São Paulo, Brazil*

5 *Grupo de Investigación en Biología Descriptiva y Aplicada, Universidad de Cartagena, Programa de Biología, Campus San Pablo, Cartagena de Indias, Colombia*

Corresponding author: Carlos Mario López-Orozco (clopezo1610@gmail.com)

Abstract

The first freshwater amphibian representative of Crinocheta (Oniscidea) from the Neotropics is described from caves within the Brazilian Cerrado biome, state of Mato Grosso do Sul. *Kadiweuoniscus rebellis* **gen. et sp. nov.** is placed in the family Philosciidae. The present work represents a significant contribution to future studies seeking to understand the ecological and evolutionary processes of Crinocheta within the Neotropical region. Moreover, it highlights the importance of biodiversity surveys in subterranean environments toward effective conservation efforts of these unique habitats and their surroundings.

Key words: Cave fauna, new genus, new species, Serra da Bodoquena, southwestern Brazil, terrestrial isopods, troglobitic species



Academic editor: Stefano Taiti

Received: 15 October 2023

Accepted: 4 December 2023

Published: 19 February 2024

ZooBank: <https://zoobank.org/66B3F257-E9D4-48A5-830D-0D3FC7426CB5>

Citation: López-Orozco CM, Campos-Filho IS, Cordeiro LM, Gallão JE, Carpio-Díaz YM, Borja-Arrieta R, Bichuette ME (2024) First amphibious Crinocheta (Isopoda, Oniscidea) from the Neotropics with a troglobitic status: a relictual distribution. ZooKeys 1192: 9–27. <https://doi.org/10.3897/zookeys.1192.114230>

Copyright: © Carlos Mario López-Orozco et al. This is an open access article distributed under terms of the Creative Commons Attribution License ([Attribution 4.0 International – CC BY 4.0](https://creativecommons.org/licenses/by/4.0/)).

Introduction

Terrestrial isopods (Oniscidea) are considered the most diverse group of isopods, with more than 4000 species in more than 500 genera in 38 or 39 families (Schmalfuss 2003; Taiti 2004; Javidkar et al. 2015; Sfenthourakis and Taiti 2015; Dimitriou et al. 2019; Campos-Filho and Taiti 2021). These organisms are distributed in almost all terrestrial environments on the planet, ranging from the supralittoral zone to high mountains, and from tropical zones to deserts (Schmalfuss 2003; López-Orozco et al. 2022). Additionally, a considerable number of species inhabit subterranean environments (Vandel 1973; Schmalfuss 2003; Taiti and Gruber 2008; Bedek et al. 2011; Taiti and Xue 2012; Tabacaru and Giurginca 2013; Reboleira et al. 2015).

Regarding the phylogeny of the group, morphological studies show Oniscidea as monophyletic, including the Sections Ligiidae, Tylidae, Mesoniscidae, Synocheta, and Crinocheta (Schmalfuss 1989; Wägele 1989; Erhard 1998; Schmidt 2008). All these authors recognized Synocheta as the sister group of Crinocheta. The last section is the most diverse, representing more than 80% of the entire suborder inhabiting various types of habitats (Schmidt 2002, 2003,

2008; Schmalzfuss 2003). Recent molecular evidence has revealed that the genus *Ligia* Fabricius, 1798, is closer to marine groups of isopods, which raises doubts about the monophyly of Oniscidea (Lins et al. 2017; Dimitriou et al. 2019). However, future studies with integrative approaches will be necessary to clarify the phylogenetic relationships of the group.

In the last two decades, studies of terrestrial isopods have increased globally (Vittori and Dominko 2022). To date, Brazil holds the highest diversity of species in the Neotropical region, comprising more than 250 species (see Campos-Filho et al. 2018, 2019, 2020; Cardoso et al. 2020a, 2020b, 2021). Among them, more than 40 are considered obligatory cave-dwellers (trogllobites), grouped in the families Armadillidae, Philosciidae, Pudeoniscidae, Scleropactidae and Styloniscidae (Campos-Filho et al. 2018, 2019, 2020, 2022a, 2022b, 2022c, 2023; Cardoso et al. 2020a, 2020b, 2021; Cardoso and Ferreira 2023; López-Orozco et al. in press). Moreover, Styloniscidae comprise the highest number of trogllobitic species, some of which have amphibious habits (e.g., *Xangoniscus* spp. and *Spelunconiscus* spp.) (Campos-Filho et al. 2014, 2022a; Bastos-Pereira et al. 2017, 2022; Cardoso et al. 2020a).

Most of the amphibian species of Oniscidea found in caves belong to the Section Synocheta, primarily from the families Styloniscidae and Trichoniscidae (Vandel 1973; Taiti and Gruber 2008; Bedek et al. 2011; Taiti and Xue 2012; Tabacaru and Giurginca 2013; Campos-Filho et al. 2014, 2019, 2022a, 2022b, 2022c; Souza et al. 2015; Cardoso et al. 2020a, 2021; Bastos-Pereira et al. 2022; Reboleira et al. 2015). In Crinocheta, this type of habit has been described in the family Olibrinidae, which includes species found in caves and marine littoral environments in the genera *Castellanethes* Brian, 1952, *Olibrinus* Budde-Lund, 1912 and *Paradoniscus* Taiti & Ferrara, 2004 (Taiti and Ferrara 2004; Taiti and Gardini 2022; Moutaouakil et al. 2023). Regarding the American continent, there is only the record of *Olibrinus antennatus* (Budde-Lund, 1902) in the marine coast of the state of Rio Grande do Norte, Brazil, inhabiting mangrove swamps and under coral rock in the coastal environment (Araujo and Taiti 2007; Campos-Filho et al. 2018). In the family Philosciidae, this habit is present in some representatives of *Haloniscus* Chilton, 1920 from Australia (Taiti and Humphreys 2001; Guzik et al. 2019; Stringer et al. 2019), and epigeal species *Androdeloscia tarumae* (Lemos de Castro, 1984) in the Central Amazon (Warburg et al. 1997). This amphibious habit has been considered as a secondary condition that appeared several times within Oniscidea (Schmidt 2008; Taiti and Xue 2012; Taiti et al. 2018; Sfenthourakis et al. 2020).

In the present study, a freshwater amphibian representative of Crinocheta (Philosciidae) with trogllobitic status is described for the first time in the Neotropical region. *Kadiweuoniscus rebellis* gen. et sp. nov. is described from caves in the Brazilian Cerrado biome, state of Mato Grosso do Sul, Serra da Bodoquena karst area.

Materials and methods

Study area

The material was collected from three limestone caves of Serra da Bodoquena karst area, located in the Bodoquena municipality, state of Mato Grosso do Sul,

southwestern Brazil (Figs 1, 2). The caves occupy an area about 220 km N to S and may reach 40 km E to W, encompassing many flooded caves beside a few sparse limestone hills, located about 100 km N to W along the Paraguay Belt. The area belongs to the Corumbá (geomorphological) Group, Bocaina Formation, and it is classified as having an Aw (tropical) climate, characterized by a dry winter and humid summer (Bedek et al. 2018, 2020). It is known for its high diversity of troglobites (Camargo and Lourenção 2007; Cordeiro et al. 2014), surpassing 34 species, many of them aquatic (Trajano et al. 2016). The native vegetation in the area consists of savanna in contact with semi-deciduous seasonal forest, within the Cerrado Biome (Galati et al. 2003; Boggiani et al. 2011). Two of the caves are located within the Serra da Bodoquena National Park (PNSB, Parque Nacional Serra da Bodoquena), a National Conservation Unit created in 2000 that covers an area of 76,481 hectares and contains numerous caves (Camargo and Lourenção 2007; Lobo 2007; Cordeiro et al. 2014). Currently, livestock is the main economic activity in the region, followed by tourism, including speleotourism. The latter has grown in economic importance for the municipalities of Bonito, Bodoquena and Jardim (Lobo 2007; Cordeiro et al. 2014).

Collections and taxonomy

Specimens were collected by active search with the aid of tweezers and brushes, and stored in 75% ethanol; microhabitat data was also recorded. The identifications were based on morphological characters with the use of micropreparations in Hoyer's medium (Anderson 1954). The illustrations were made with the aid of a camera lucida mounted on a Zeiss Stemi SV6 stereomicroscope and Leica DMLS microscope. The final illustrations were prepared using the software GIMP v.2.8 with the method proposed by Montesanto (2015, 2016). For scanning electron microscopy (SEM), two individuals were used, one male and one female, without performing dissections. The specimens were dried using Critical Point Drying and mounted on a plastic sheet. Uncoated SEM preparations were examined using an FEI Quanta 250 (at the UFSCar). The figures were edited using GIMP v.2.8.

The material examined is deposited in the zoological collection of the Laboratório de Estudos Subterrâneos (LES), Universidade Federal de São Carlos, São Carlos, Brazil (curator: Maria E. Bichuette).

Systematic account

Suborder Oniscidea Latreille, 1802

Family Philosciidae Kinahan, 1857

Genus *Kadiweuoniscus* López-Orozco, Campos-Filho & Bichuette, gen. nov.

<https://zoobank.org/C1386E76-7F74-45AA-9097-C7A757FD39C3>

Type species. *Kadiweuoniscus rebellis* López-Orozco, Campos-Filho & Bichuette sp. nov., by present designation and monotypy.

Diagnosis. Troglotic species with amphibious habit; animals about 5 mm long; dorsal surface weakly granulated; *noduli laterales* absent; cephalon with lateral lobes weakly developed, frontal and suprantennal lines absent; pleonites 3–5 with epimera elongated, forming acute tips; telson triangular; antennula of

three articles, distal article separated from medial article by fine suture; antenna with flagellum of three articles, apical organ long; molar penicil of mandibles dichotomized; maxillule outer branch with eight teeth; maxilla bilobate; maxilliped endite without penicil; male pereopods 1–7 gradually elongated; dactylar seta short and simple; uropod endopod inserted slightly proximally; pleopods 3–5 exopods with fringe of thin setae on all margins.

Etymology. The new genus is named after the Kadiwéu indigenous people. The Kadiwéu are known as “Indian riders”, due to their horse-riding prowess, keeping in their mythology, art and rituals the way of being of a hierarchical society between masters and captives.

Remarks. The family Philosciidae comprises more than 600 species in 113 genera widely distributed in Australia, southern Asia, Africa, Europe and the Americas (Leistikow 2001; Schmalzfuss 2003; Boyko et al. 2023). To date, the family is considered paraphyletic due to characteristics shared with the Halophilosciidae and Scleropactidae (Leistikow 2001; Schmidt 2003, 2008).

The family has great morphological plasticity and the representatives are mainly recognized by the ‘runner-type’ habitus (sensu Schmalzfuss 1984), body with a dorsal surface smooth or slightly tuberculated, pereonites 1–7 with one or two lines of *noduli laterales* per side (sometimes present on cephalon and pleonites), antennula and antennal flagellum of three articles, mandibles with molar penicil simple or dichotomized, maxillula outer endite with outer set of teeth simple or cleft or pectinated, maxilla bilobated, maxilliped endite bearing ventral penicil or triangular seta (sometimes absent), uropod branches unequal or similar in length and inserted at same or on distinct levels, and pleopod exopods with out respiratory areas or with covered monospiracular lungs (Taiti and Ferrara 1980, 1982; Ferrara et al. 1994; Araujo and Leistikow 1999; Leistikow and Araujo 2001; Leistikow 2001).

Kadiweuoniscus gen. nov. is included in Philosciidae by having most of these mentioned characters. The new genus is easily distinguishable from the other genera of Philosciidae due to its amphibian habit, and the pleonites 3–5 epimera elongated. As mentioned, the amphibious behavior is also present in species of *Haloniscus*; however, the new genus differs in the cephalon lacking frontal and suprantennal lines (vs. present in *Haloniscus*, except *H. anophthalmus* Taiti, Ferrara & Iliffe, 1995), pleonites 3–5 epimera elongated (vs. pleonites 3–5 epimera reduced in *Haloniscus*), antennula distal and medial articles separated by fine suture (vs. antennula with three distinct articles in *Haloniscus*), antennal flagellum with long apical organ (vs. short in *Haloniscus*), maxillula outer branch with 4 + 4 teeth, long and curved (vs. maxilla with 4 or 5 + 6 in *Haloniscus*), and maxilliped endite without penicil (vs. present in *Haloniscus*).

***Kadiweuoniscus rebellis* López-Orozco, Campos-Filho & Bichuette, sp. nov.**

<https://zoobank.org/F5A2614F-20F7-44CC-865F-C2A16F2329D1>

Figs 1–7, Suppl. material 1

Type material. BRAZIL • 1♂, **holotype**, Flor da Bodoquena Cave, Bodoquena, state of Mato Grosso do Sul, 20°45'19"S, 56°48'8"W, 14.VIII.2011, leg. LM Cordeiro, LES 0029048 • 1♂, 1♀ (part in micropreparations), **paratypes**, Dente de Cão Cave, 20°44'48"S, 56°47'4.2"W, 13.VI.2022, leg. LM Cordeiro, A Chagas-Jr, ME Bichuette, LES 0029049 • 2♀♀, **paratypes**, same data as previous, LES 0029050

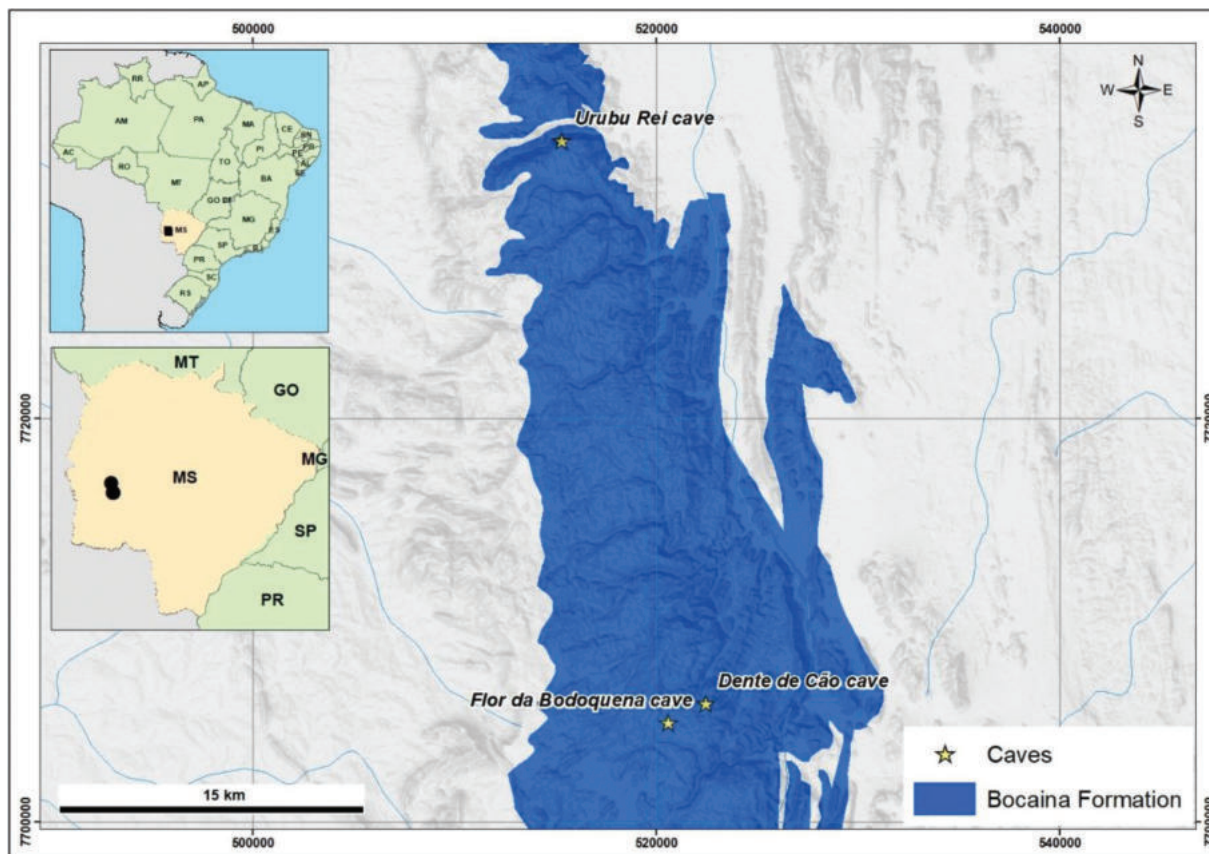


Figure 1. Map of the study area and distribution of *Kadiweuoniscus rebellis* López-Orozco, Campos-Filho & Bichuette gen. et sp. nov. in the Serra da Bodoquena, Mato Grosso do Sul.

- 1 ♀, **paratypes**, same data as holotype, LES 0029051
- 1 ♀, **paratypes**, Urubu Rei Cave, 20°29'40"S, 56°51'11"W, 16.VI.2022, leg. LM Cordeiro, A Chagas-Jr, ME Bichuette, LES 0029052
- 1 ♀, **paratypes**, same data as previous, LES 0029053
- 1 ♂, same data as previous, LES 0029054.

Description. Maximum body length: male 4.5 mm, female 5 mm. Body outline as in Fig. 3A, B. Colourless (Fig. 3B). Dorsal surface granulated bearing pointed scale-setae (Fig. 3A, C, D). Cephalon (Fig. 3E–G) with small semicircular antennary lobes; eyes absent. Pereonites 1–2 with epimera semicircular, 3–7 with posterior corners gradually more acute (Fig. 3A, B, D, F, G). Pleon (Fig. 3H) narrower than pereon, pleonite 3–5 epimera elongated and acute. Telson (Fig. 3H) broader than long, lateral sides almost straight, rounded apex. Antenna (Fig. 3I) distal article longest with four apical aesthetascs. Antenna (Fig. 4A) long, not surpassing pereonite 3 when extended backwards; flagellum of articles subequal in length; apical organ shorter than basal article of flagellum, bearing small free sensilla. Mandibles with molar penicil of six to seven branches; right mandible (Fig. 4B) with 1+1 free penicils; left mandible (Fig. 4C) with 2+1 free penicils. Maxillula (Fig. 4D) inner endite bearing two setose penicils, distal margin rounded; outer endite with 4 + 4 teeth simple, elongated and curved. Maxilla (Fig. 4E) with setose lobes; outer lobe slightly smaller than inner lobe, quadrangular and covered with thin and long setae; inner lobe rounded and covered with thin and thick setae. Maxilliped (Fig. 4F) basis rectangular; first article of palp bearing two setae; endite rectangular, medial seta overpassing distal margin, ventrally with setose sulcus. Uropod (Fig. 4G) protopod and

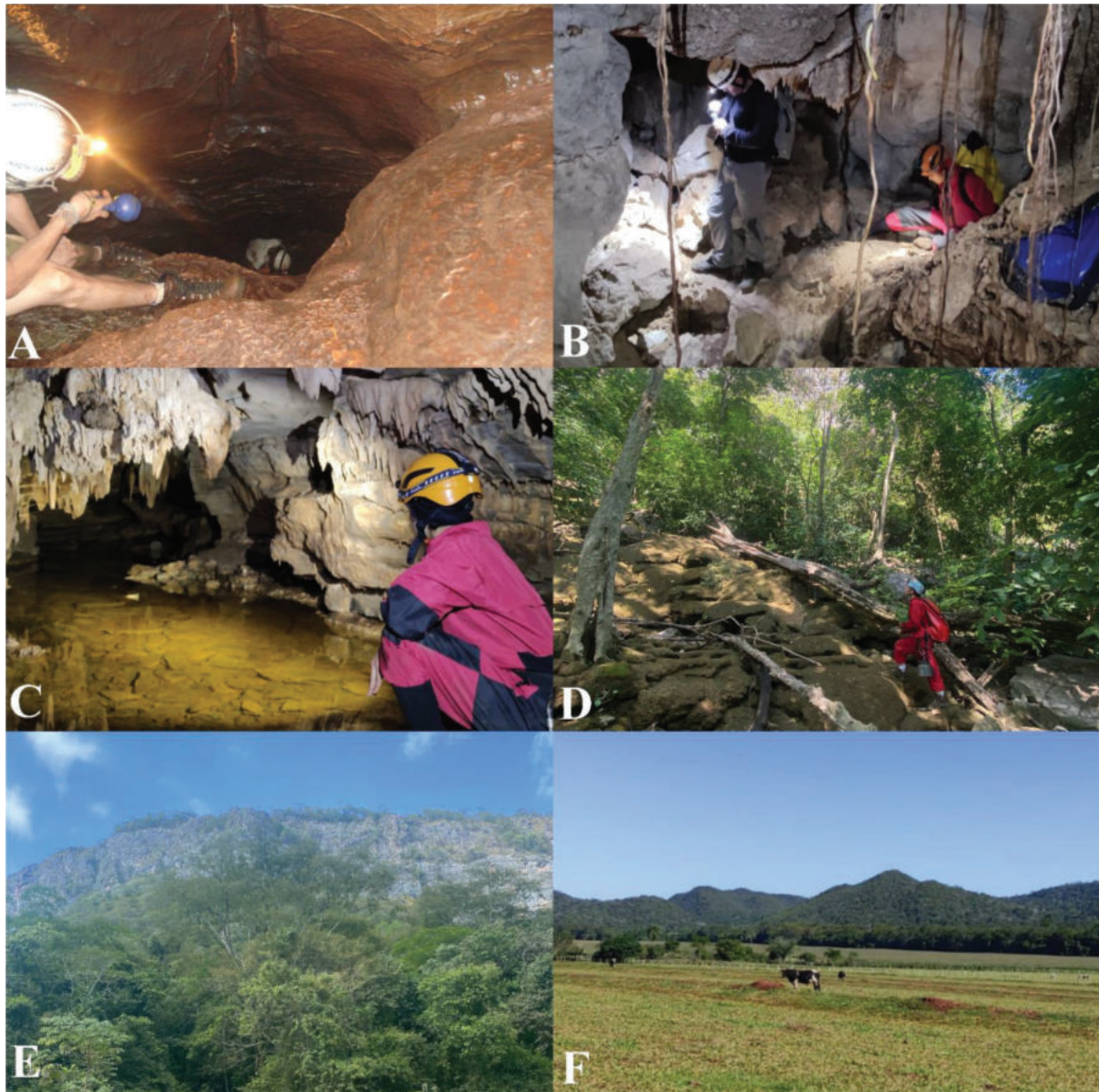


Figure 2. Study area: **A** Flor da Bodoquena Cave **B** Urubu Rei Cave **C** Dente de Cão Cave **D** epigeal environment in Flor da Bodoquena Cave **E** limestones in the Serra da Bodoquena karst area **F** livestock and agriculture in the Serra da Bodoquena.

exopod grooved on outer margin. Pereopods 1–7 bearing sparse setae on sternal margin. Pereopod 1 (Fig. 5A) carpus with antennal grooming brush reduced, composed by short scale-setae; dactylus with unguis and dactylar setae simple (Fig. 5B). Pleopod exopods without respiratory areas.

Male. Pereopod 1–7 (Fig. 5A–H) gradually more elongated, without particular modifications. Genital papilla (Fig. 6A) with lanceolate ventral shield; papilla longer than ventral shield bearing two subapical orifices. Pleopod 1 (Fig. 6A) exopod ovoidal, inner margin with one small seta; endopod stout, three times longer than exopod, slightly bent outwards, apex bearing setae on inner margin. Pleopod 2 (Fig. 6E) exopod triangular, outer margin concave bearing four setae; endopod flagelliform, slightly longer than exopod. Pleopod 3 and 4 (Fig. 6C, D) exopods rhomboid, outer margin with four setae, inner margin slightly convex. Pleopod 5 (Fig. 6E) exopod rhomboid, longer than wide, distal and outer margins rounded bearing four small setae.

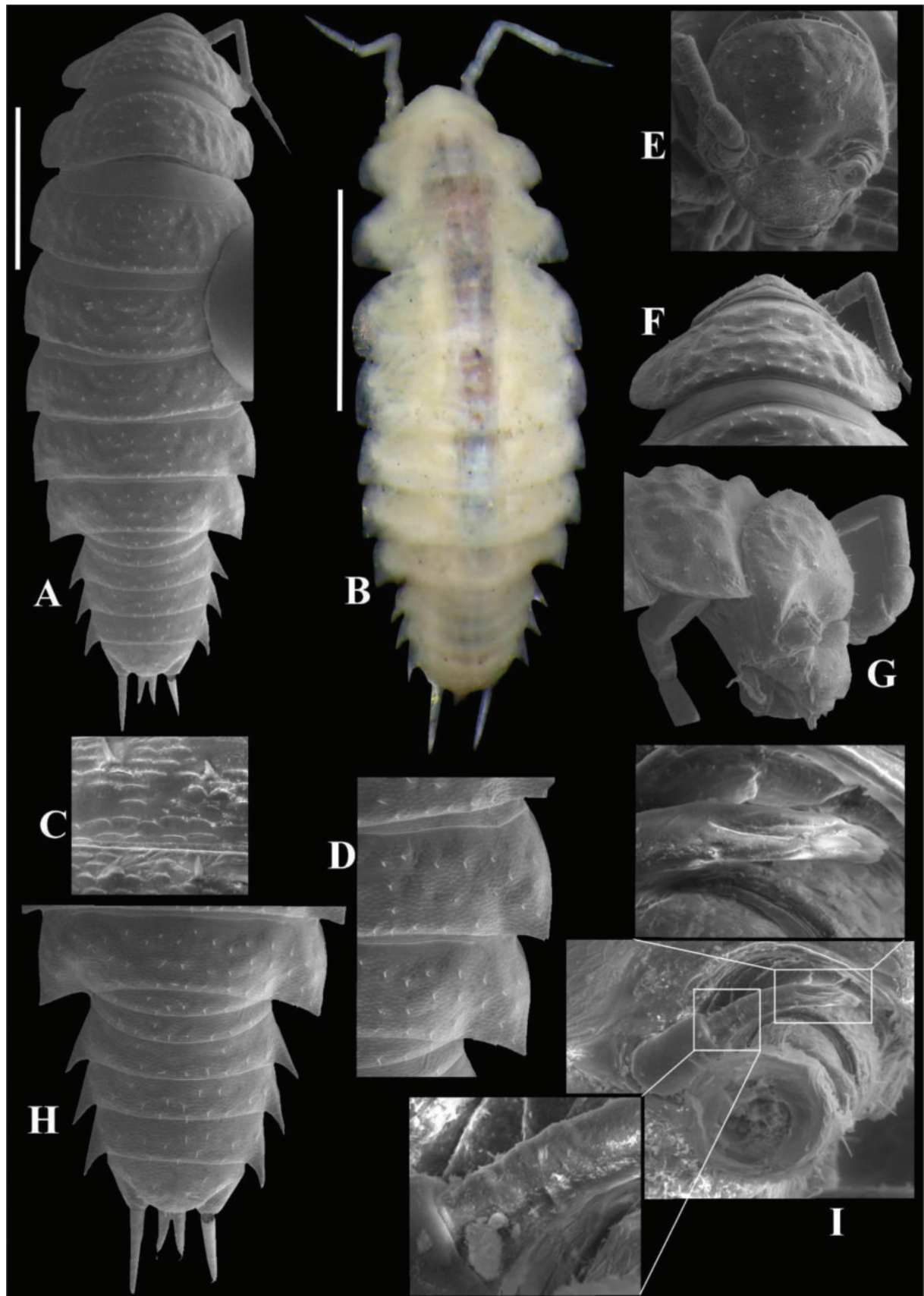


Figure 3. *Kadiweuoniscus rebellis* López-Orozco, Campos-Filho & Bichuette gen. et sp. nov. (♀ paratype, LES 0029050) **A, B** habitus, dorsal view **C** dorsal scale-seta **D** epimera 6–7 **E** cephalon, frontal view **F** cephalon and pereonite 1, posterior view **G** cephalon and pereonite 1, lateral view **H** pleon, telson and uropods **I** antennula. Scale bars: 1 mm.

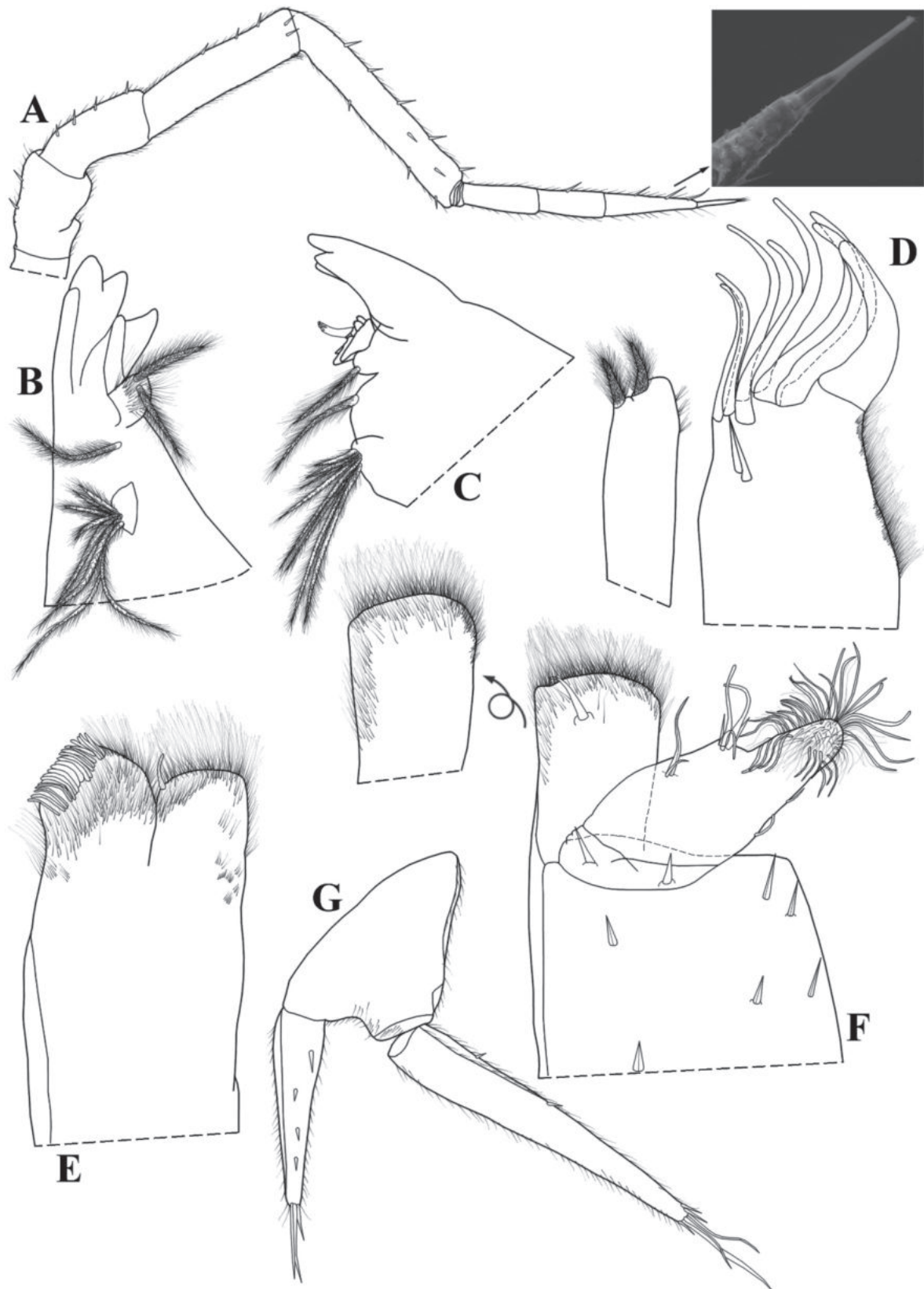


Figure 4. *Kadiweuoniscus rebellis* López-Orozco, Campos-Filho & Bichuette gen. et sp. nov. (♀ paratype, LES 0029049) **A** antenna, with flagellum detail **B** left mandible **C** right mandible **D** maxillula **E** maxilla **F** maxilliped, arrow illustrating the endite in caudal view **G** uropod.

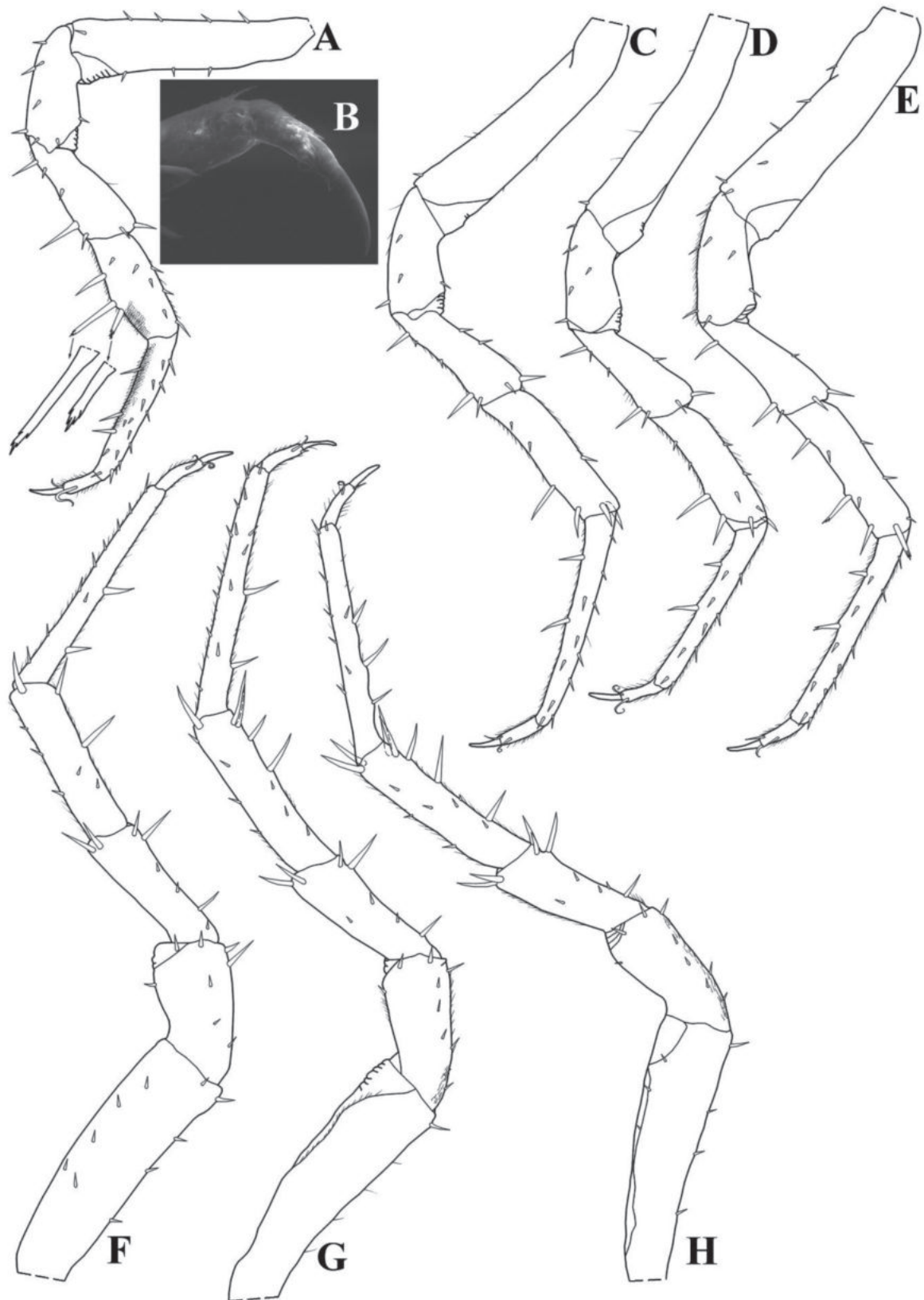


Figure 5. *Kadiweuoniscus rebellis* López-Orozco, Campos-Filho & Bichuette gen. et sp. nov. (♂ holotype, LES 0029048) **A** pereopod 1 **B** dactylus in rostral view; (♂ paratype, LES 0029049) **C** pereopod 2 **D** pereopod 3 **E** pereopod 4 **F** pereopod 5 **G** pereopod 6 **H** pereopod 7.

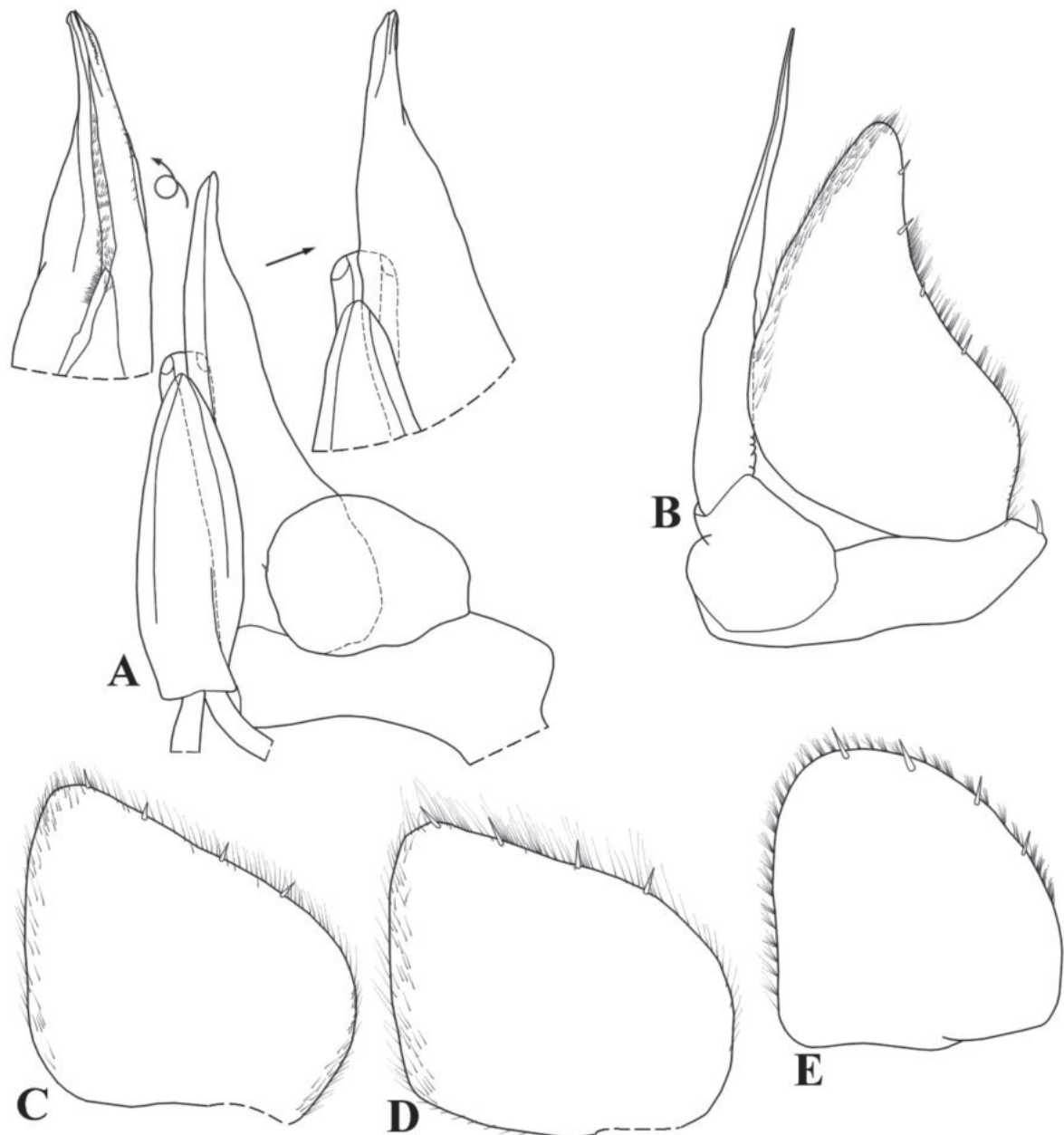


Figure 6. *Kadiweuoniscus rebellis* López-Orozco, Campos-Filho & Bichuette gen. et sp. nov. (♂ paratype, LES 0029049) **A** genital papilla and pleopod 1 **B** pleopod 2 **C** pleopod 3 exopod **D** pleopod 4 exopod **E** pleopod 5 exopod.

Etymology. The new species name alludes to the resistance group from the Star Wars fiction series, the Rebel Alliance, that fights against the Empire. The Kadiwéu indigenous people were known as warriors, and they fought for Brazil in the Paraguayan War to reclaim and secure their lands in the Serra da Bodoquena region. Today, they are confined to the outskirts of the Bodoquena plateau and the Pantanal plain. The designation 'rebellis' is used as an adjective for the genus name.

Ecological remarks. The physicochemical data of microhabitats of *Kadiweuoniscus rebellis* gen. et sp. nov. are: pH = 7.5, high conductivity (c. $0.450 \mu\text{S}\cdot\text{cm}^{-1}$), moderate temperature (22°C) and moderate dissolved oxygen (ca. $6.0 \text{ mg}\cdot\text{l}^{-1}$). pH values (neutral to basic) are typical of karst waters. The abundance is particularly low in each cave, and they have a preference for rocky substrates with a silty and pebble bottom (Fig. 7A, B). Amphibious habit (see Suppl. material 1).

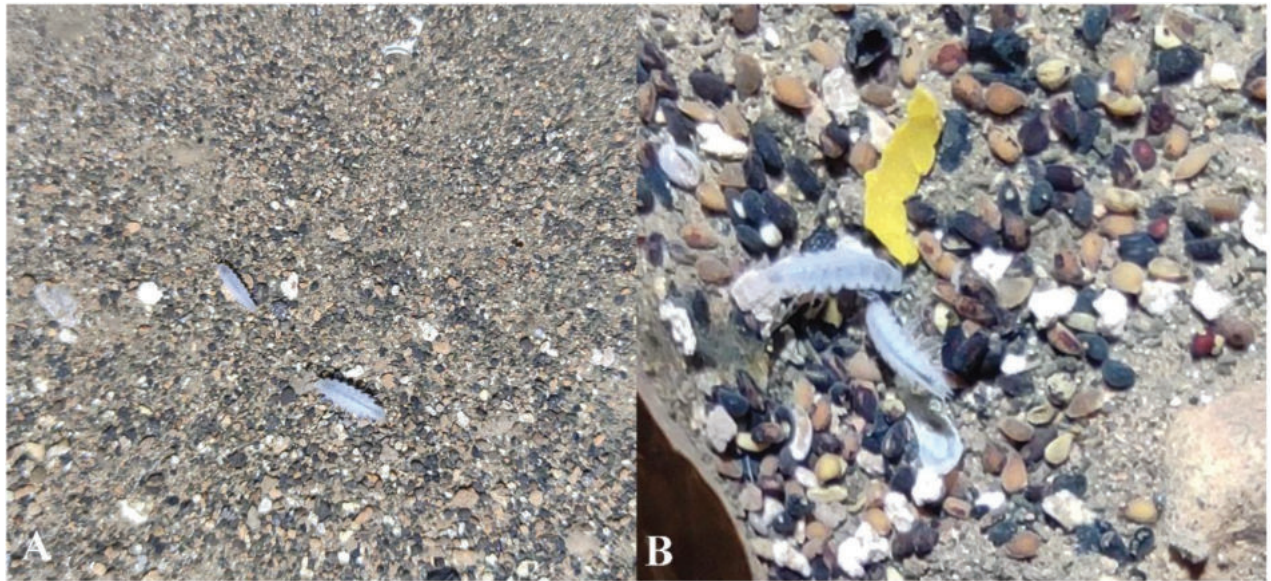


Figure 7. A and B *Kadiweuoniscus rebellis* López-Orozco, Campos-Filho & Bichuette gen. et sp. nov. submerged on rocky substrate with silt and pebbles.

Discussion

The Serra da Bodoquena karst area exhibits taxonomic singularities among invertebrates, housing some remarkable phylogenetic relicts among peracarid crustaceans, such as *Potiicoara brasiliensis* Pires, 1987 (Spelaeogriphacea) and *Megagidiella azul* Koenemann & Holsinger, 1999 (Amphipoda) (Pires 1987; Koenemann and Holsinger 1999). To date, no records of such singularities within Isopoda, particularly Oniscidea, have been documented. Cordeiro et al. (2014) reported a low diversity of terrestrial isopods in this region. At present, the records include *Circoniscus intermedius* Souza & Lemos de Castro, 1991 and *Diploexochus carrapicho* Campos-Filho, López-Orozco & Taiti (Campos-Filho et al. 2014, 2023). The discovery of a new freshwater amphibian genus highlights the taxonomic significance to both Serra da Bodoquena karst areas and the Neotropical region. Moreover, *K. rebellis* gen. et sp. nov. represents a significant addition to our ecological knowledge of Neotropical Philosciidae, considering its amphibious habit. It is worth noting that the majority of species within this family commonly inhabit the edaphofauna in the epigeal environment (Leistikow 2001).

Kadiweuoniscus rebellis gen. et sp. nov. exhibits several distinctive features, including troglomorphisms, such as the absence of eyes and body pigments, as well as the elongation of the pereopods. These characteristics are typical traits found in amphibious troglobitic Oniscidea (Campos-Filho et al. 2014, 2019, 2022a, 2022b; Souza et al. 2015; Cardoso et al. 2020a, 2020b, 2021; Bastos-Pereira et al. 2022). One key trait common among representatives with this type of habit is the absence of *noduli laterales*, which represents an important character in the classification of some groups of terrestrial isopods (Schmidt 2008). This characteristic is observed in several genera with epigeal species within Philosciidae (e.g., *Oxalaniscus* Leistikow, 2000, *Ischioscia* Verhoeff, 1928, *Parischioscia* Lemos de Castro, 1967, *Mirtana* Leistikow, 1997, *Pentoniscus* Richardson, 1913, *Yaerikima* Leistikow, 2001, *Formicascia* Leistikow, 2001, *Roraimoscia* Leistikow, 2001, *Oreades* Vandel, 1968 and *Ecuadoroniscus* Vandel, 1968 (Leistikow 2001). However, the signifi-

cance of this character remains unknown in many fields of biology, and further research is needed to elucidate its usefulness (Leistikow 2001; Schmidt 2008).

Based on the phylogeny of South American Philosciidae, the genera *Quintanoscia* Leistikow, 2000 and *Oxalaniscus* were recovered as basal groups (Leistikow 2001). These two genera show typical characters of the ground-pattern Oniscidea, such as a subrectangular maxilla, the maxilliped palp with prominent setal tufts and the endite with a prominent penicil (Leistikow 2000, 2001). *Kadiweuoniscus* gen. et sp. nov. shares the first two characteristics, however, it lacks the penicil in the endite of the maxilliped, which may suggest it is basal within Philosciidae. Further investigations including molecular data are necessary to clarify the position of the new genus within the family. Our discovery marks the initial documentation of the troglobitic amphibian Crinocheta in the Neotropics, serving as a pivotal link for comprehending aspects related to the biology, ecology, morphology, distribution and evolution of Philosciidae.

The Flor da Bodoquena Cave is a vertical fracture (Fig. 2A), with the water reaching 20 m deep and extending only 150 meters. Specimens of *K. rebellis* gen. et sp. nov. were found in the walls of the cave. The fracture ends at the level of the sheet, where the stygobitic catfish *Trichomycterus dali* Rizzato, Costa, Trajano & Bichuette, 2011 is also recorded, possibly a predator of the isopods. During the rainy season, the current increases and the water level rises, oscillating between 10 and 12 m. Dispersion of the species possibly follows this oscillation. This cave is at a higher altitude compared to the other two where the species occurs (Urubu Rei and Dente de Cão, Fig. 2B–D), and may represent the source population. Urubu Rei and Dente de Cão caves have conduits with lentic waters and bottoms formed by silt, pebbles and rocky substrate (Fig. 2B, Urubu Rei Cave). In the case of Urubu Rei, the water rises drastically in the rainy season, becoming extremely lotic, which also could disperse/spread the isopods; the same is not observed for Dente Cão Cave.

Considering the species distribution, although the limestones are continuous at the surface (Fig. 2E), hydrological barriers have been formed due to fluvial incisions that, in the north plateau, have cut down to non-carbonate rocks, forming compartments corresponding to micro-basins (Cordeiro et al. 2014). The species occurs in the upper part of these compartments, and its distribution in the three caves could be explained by one colonization event and, after the regional uplifting prior to the Pliocene/Pleistocene transition, raising the area to altitudes of 1000 m, followed by the current subsidence responsible for the formation of the adjacent Pantanal Basin. The three populations may be isolated by geological processes, as suggested by Moracchioli and Trajano (2002) for *P. brasiliensis*. These facts, allied with the marked troglomorphisms and unique characteristics, could indicate a relictual occupation of the Serra da Bodoquena subterranean habitats.

Conservation remarks

The species occurs in caves within the boundaries of the Serra da Bodoquena National Park, and is, a priori, legally protected. However, the caves are not controlled or even inspected by governmental bodies dealing with tourism and visitors. Furthermore, their surroundings have deforested areas with livestock farming and agriculture activities (Fig. 2F), which drastically reduces the quality of the habitat. These facts make the species vulnerable in relation to its effective protection. Ecological monitoring projects can help in the understanding of the distribution

and singularities of the species, which would assist in conservation efforts. The restricted distribution makes the species vulnerable and potentially endangered.

Finally, considering that specimens of the taxon described here have been collected since 2011, it is essential to emphasize the significance of scientific collections in the study of biodiversity. These collections serve as repositories of historical information about natural environments. Therefore, it becomes crucial to review the materials collected over extended periods and stored in such institutions. By doing so, we can enhance our understanding of the vast taxonomic diversity present in our ecosystems. Scientific collections play a crucial role in research, allowing the examination of specimens over time and across different locations, and safeguarding our biodiversity. Without these collections, our knowledge of the natural world and the species it harbors would be severely limited.

Acknowledgements

We thank to A. Chagas-Jr, D. M. Borges, S. G. Jimenez and D.F. Torres for help in the fieldtrip and collections; to B. D. Lenhare for preparation of map of Fig. 1; to LES team (UFSCar) for help in the organization of scientific collection, especially to M. F. C. Zancheta and E. L. da Silva; to L. B. R. Fernandes for help in taking SEM images; to Odete Rocha for the loan of her laboratory facilities for the development of illustrations; to Sistema de Autorização e Informação em Biodiversidade/ICMBio for collection permits to MEB (SISBIO # 28992); to CAPES (Coordenação de Aperfeiçoamento de Pessoal de Nível Superior – Brasil) for a scholarship to CML-O and RB-A and CNPq (Conselho Nacional de Desenvolvimento Científico e Tecnológico), for the scholarship to YMC-D; to Research Project titled “Biodiversity of terrestrial isopods (Crustacea, Isopoda, Oniscidea) from Cyprus in the light of integrative taxonomy”, “ONISILOS Research Program – 2018”, funded by the University of Cyprus, for the postdoctoral fellowship granted to ISC-F; to Vicerrectoría de Investigaciones of the University of Cartagena for the financial support to the Grupo de Investigación en Biología Descriptiva y Aplicada (Project Semilleros, Acta de Compromiso N° 053–2022).

Additional information

Conflict of interest

The authors have declared that no competing interests exist.

Ethical statement

No ethical statement was reported.

Funding

The research was partially granted by ICMBio (Instituto Chico Mendes de Conservação da Biodiversidade)/Vale S.A. (TCCE 02/2020), under the project “Teste de metodologias propostas em Legislação Ambiental relacionadas à fauna subterrânea e proposição de novas áreas prioritárias para conservação de cavernas”, coordinated by MEB with operational management carried out by the IABS (Instituto Brasileiro de Desenvolvimento e Sustentabilidade). This study was financed in part by the Brazilian funding agencies CAPES (Coordenação de Aperfeiçoamento de Pessoal de Nível Superior – Brasil) – Finance Code 001 (PROAP/CAPES PPGERN).

Author contributions

Conceptualization: MEB, CMLO, JEG. Data curation: CMLO, YMCD, JEG, MEB. Formal analysis: ISCF, CMLO, MEB. Funding acquisition: LMC, MEB, JEG. Investigation: YMCD, MEB, RBA, LMC, CMLO, ISCF. Methodology: CMLO, RBA, ISCF, YMCD, MEB. Project administration: MEB, LMC, JEG. Supervision: MEB. Visualization: RBA, YMCD. Writing – original draft: CMLO, RBA, YMCD, ISCF. Writing – review and editing: JEG, LMC, CMLO, ISCF, RBA, YMCD, MEB.

Author ORCIDs

Carlos Mario López-Orozco  <https://orcid.org/0000-0002-3251-7739>

Ivanklin Soares Campos-Filho  <https://orcid.org/0000-0001-6139-8241>

Livia Medeiros Cordeiro  <https://orcid.org/0000-0002-0742-897X>

Jonas Eduardo Gallão  <https://orcid.org/0000-0002-5268-7946>

Yesenia M. Carpio-Díaz  <https://orcid.org/0000-0001-5116-9736>

Ricardo Borja-Arrieta  <https://orcid.org/0000-0002-5064-5080>

Maria Elina Bichuette  <https://orcid.org/0000-0002-9515-4832>

Data availability

All of the data that support the findings of this study are available in the main text or Supplementary Information.

References

- Anderson LE (1954) Hoyer's solution as a rapid permanent mounting medium for bryophytes. *The Bryologist* 57(3):e242. [https://doi.org/10.1639/0007-2745\(1954\)57\[242:HSARP\]2.0.CO;2](https://doi.org/10.1639/0007-2745(1954)57[242:HSARP]2.0.CO;2)
- Araujo PB, Leistikow A (1999) Philosciids with pleopodal lungs from Brazil, with description of a new species (Crustacea, Isopoda). *Contributions to Zoology (Amsterdam, Netherlands)* 68(2): 109–141. <https://doi.org/10.1163/18759866-06802004>
- Araujo PB, Taiti S (2007) Terrestrial isopods (Crustacea, Oniscidea) from Rocas Atoll, northeastern, Brazil. *Arquivos do Museu Nacional. Museu Nacional (Brazil)* 65: 347–355.
- Bastos-Pereira R, Souza LA, Ferreira RL (2017) A new amphibious troglobitic styloniscid from Brazil (Isopoda, Oniscidea, Synocheta). *Zootaxa* 4294(2): 292–300. <https://doi.org/10.11646/zootaxa.4294.2.11>
- Bastos-Pereira R, Souza LA, Sandi BDS, Ferreira RL (2022) A new species of *Spelunconiscus* (Isopoda: Oniscidea: Styloniscidae) for Brazilian caves: new record for the type species and an emended diagnosis for the genus. *Nauplius* 30: e2022018. <https://doi.org/10.1590/2358-2936e2022018>
- Bedeck J, Taiti S, Gottstein S (2011) Catalogue and atlas of cave-dwelling terrestrial isopods (Crustacea: Oniscidea) from Croatia. *Natura Croatica* 20(2): 237–354. <https://hrcak.srce.hr/75047>
- Bedeck HE, Zimmermann NE, McVicar TR, Vergopolan N, Berg A, Wood EF (2018) Present and future Köppen-Geiger climate classification maps at 1-km resolution. *Scientific Data* 5(1): e180214. <https://doi.org/10.1038/sdata.2018.214>
- Bedeck HE, Zimmermann NE, McVicar TR, Vergopolan N, Berg A, Wood EF (2020) Publisher Correction: Present and future Köppen-Geiger climate classification maps at 1-km resolution. *Scientific Data* 7(1): e274. <https://doi.org/10.1038/s41597-020-00616-w>

- Boggiani PC, Trevelin AC, Sallun-Filho W, Oliveira EC, Almeida LHS (2011) Turismo e conservação de tufas ativas da Serra da Bodoquena, Mato Grosso do Sul. *Pesquisas em Turismo e Paisagens Cársticas* 4: 55–63.
- Boyko CB, Bruce NL, Hadfield KA, Merrin KL, Ota Y, Poore GCB, Taiti S (2023) [Onwards] *Philosciidae* Kinahan, 1857. Accessed by World Marine, Freshwater and Terrestrial Isopod Crustaceans database. <https://www.marinespecies.org/aphia.php?p=taxdetails&id=246825> [Accessed on 10th April, 2023]
- Camargo RR, Lourenção MLF (2007) Levantamento espeleológico da Serra da Bodoquena. In: Brazilian Society of Speleology (Ed.) *Proceedings of the 29th Congresso Brasileiro de Espeleologia*, July 2007, Ouro Preto. SEE/SBE, Ouro Preto, 1–7.
- Campos-Filho IS, Taiti S (2021) Oniscidea taxonomy: present and future. Abstract book of the 11th International Symposium on Terrestrial Isopod Biology. Spinicornis, Ghent, 9. <https://spinicornis.be/istib2021/presentations/>
- Campos-Filho IS, Araujo PB, Bichuette ME, Trajano E, Taiti S (2014) Terrestrial isopods (Crustacea: Isopoda: Oniscidea) from Brazilian caves. *Zoological Journal of the Linnean Society* 172(2): 360–425. <https://doi.org/10.1111/zoj.12172>
- Campos-Filho IS, Cardoso GM, Aguiar JO (2018) Catalogue of terrestrial isopods (Crustacea, Isopoda, Oniscidea) from Brazil: An update with some considerations. *Nauplius* 26(0): e2018038. <https://doi.org/10.1590/2358-2936e2018038>
- Campos-Filho IS, Fernandes CS, Cardoso GM, Bichuette ME, Aguiar JO, Taiti S (2019) Two new species and new records of terrestrial isopods (Crustacea, Isopoda, Oniscidea) from Brazilian caves. *Zootaxa* 4564(2): 422–448. <https://doi.org/10.11646/zootaxa.4564.2.6>
- Campos-Filho IS, Fernandes CS, Cardoso GM, Bichuette ME, Aguiar JO, Taiti S (2020) New species and new records of terrestrial isopods (Crustacea, Isopoda, Oniscidea) of the families *Philosciidae* and *Scleropactidae* from Brazilian caves. *European Journal of Taxonomy* 606(606): 1–38. <https://doi.org/10.5852/ejt.2020.606>
- Campos-Filho IS, Gallo JS, Gallão JE, Torres DF, Carpio-Díaz YM, López-Orozco CM, Borja-Arrieta R, Taiti S, Bichuette ME (2022a) Expanding the knowledge on the diversity of the cavernicolous *Styloniscidae* Vandell, 1952 (Oniscidea, Synocheta) from Brazil, with descriptions of two new species from the semiarid karst regions. *ZooKeys* 1101: 35–55. <https://doi.org/10.3897/zookeys.1101.79043>
- Campos-Filho IS, Gallo JS, Gallão JE, Torres DF, Horta L, Carpio-Díaz YM, López-Orozco CM, Borja-Arrieta R, Aguiar JO, Bichuette ME (2022b) Unique and fragile diversity emerges from Brazilian caves – two new amphibious species of *Xangoniscus* Campos-Filho, Araujo & Taiti, 2014 (Oniscidea, *Styloniscidae*) from Serra do Ramalho karst area, state of Bahia, Brazil. *Subterranean Biology* 42: 1–22. <https://doi.org/10.3897/subtbiol.42.75725>
- Campos-Filho IS, Cardoso GM, Bichuette ME (2022c) Isopoda, Oniscidea. In: Zampaulo RA, Prous X (Eds) *Fauna cavernícola do Brasil*. Editora Rupestre, Belo Horizonte, Brazil, 363–387.
- Campos-Filho IS, Sfenthourakis S, Gallo JS, Gallão JE, Torres DF, Chagas-Jr A, Horta L, Carpio-Díaz YM, López-Orozco CM, Borja-Arrieta R, Araujo PB, Taiti S, Bichuette ME (2023) Shedding light into Brazilian subterranean isopods (Isopoda, Oniscidea): Expanding distribution data and describing new taxa. *Zoosystema* 45(19): 531–599. <https://doi.org/10.5252/zoosystema2023v45a19>
- Cardoso GM, Ferreira RL (2023) New troglobitic species of *Benthana* Budde-Lund, 1908 and *Benthanoidea* Lemos de Castro, 1958 from iron-ore caves and their important

- record in the Amazon biome (Crustacea: Isopoda: Philosciidae). *Zootaxa* 4(27): 548–562. <https://doi.org/10.11646/zootaxa.5319.4.5>
- Cardoso GM, Bastos-Pereira R, Souza LA, Ferreira RL (2020a) New troglobitic species of *Xangoniscus* (Isopoda: Styloniscidae) from Brazil, with notes on their habitats and threats. *Zootaxa* 4819(1): 084–108. <https://doi.org/10.11646/zootaxa.4819.1.4>
- Cardoso GM, Bastos-Pereira R, Souza LA, Ferreira RL (2020b) New cave species of *Pectenoniscus* Andersson, 1960 (Isopoda: Oniscidea: Styloniscidae) and an identification key for the genus. *Nauplius* 28: e2020039. <https://doi.org/10.1590/2358-2936e2020039>
- Cardoso GM, Bastos-Pereira R, Souza LA, Ferreira RL (2021) *Chaimowiczia*: A new luliniscinae genus from Brazil (Oniscidea, Synocheta, Styloniscidae) with the description of two new troglobitic species. *Subterranean Biology* 39: 45–62. <https://doi.org/10.3897/subtbiol.39.65305>
- Cordeiro LM, Borghezán R, Trajano E (2014) Subterranean biodiversity in the Serra da Bodoquena karst area, Paraguay river basin, Mato Grosso do Sul, Southwestern Brazil. *Biota Neotropica* 14(3): e20140114. <https://doi.org/10.1590/1676-06032014011414>
- Dimitriou AC, Taiti S, Sfenthourakis S (2019) Genetic evidence against monophyly of Oniscidea implies a need to revise scenarios for the origin of terrestrial isopods. *Scientific Reports* 9(1): e18508. <https://doi.org/10.1038/s41598-019-55071-4>
- Erhard F (1998) Phylogenetic relationships within the Oniscidea (Crustacea, Isopoda). *Israel Journal of Zoology* 44: 303–309.
- Ferrara F, Paoli P, Taiti S (1994) Philosciids with pleopodal lungs? The case of the genus *Aphiloscia* Budde-Lund, 1908 (Crustacea: Isopoda: Oniscidea), with a description of six new species. *Journal of Natural History* 28(6): 1231–1264. <https://doi.org/10.1080/00222939400770631>
- Galati EAB, Nunes VLB, Boggiani PC, Dorval MEC, Cristaldo G, Rocha HC, Oshiro ET, Gonçalves-de-Andrade RM, Naufel G (2003) *Phlebotomines* (Diptera, Psychodidae) in caves of the Serra da Bodoquena, Mato Grosso do Sul state, Brazil. *Revista Brasileira de Entomologia* 47(2): 283–296. <https://doi.org/10.1590/S0085-56262003000200017>
- Guzik MT, Stringer DN, Murphy NP, Cooper SJB, Taiti S, King RA, Humphreys WF, Austin AD (2019) Molecular phylogenetic analysis of Australian arid-zone oniscidean isopods (Crustacea: Haloniscus) reveals strong regional endemism and new putative species. *Invertebrate Systematics* 33: 556–574.
- Javidkar M, Cooper SJB, King RA, Humphreys WF, Austin A (2015) Molecular phylogenetic analyses reveal a new southern hemisphere oniscidean family (Crustacea: Isopoda) with a unique water transport system. *Invertebrate Systematics* 29(6): 554–577. <https://doi.org/10.1071/IS15010>
- Koenemann S, Holsinger JR (1999) *Megagidiella azul*, a new genus and species of cavernicolous amphipod crustacean (Bogidiellidae) from Brazil, with remarks on its biogeographic and phylogenetic relationships. *Proceedings of the Biological Society of Washington* 112(3): 572–580. <https://biostor.org/reference/74272>
- Leistikow A (2000) Terrestrial Isopoda from Guatemala and Mexico (Crustacea: Oniscidea: Crinocheta). *Revue Suisse de Zoologie* 107(2): 283–323. <https://doi.org/10.5962/bhl.part.80131>
- Leistikow A (2001) Phylogeny and biogeography of South American Crinocheta, traditionally placed in the family “Philosciidae” (Crustacea: Isopoda: Oniscidea). *Organisms, Diversity & Evolution, Electronic Supplement* 4: 1–85. <https://doi.org/10.1078/1439-6092-00020> [Accessed 6 Feb. 2020]
- Leistikow A, Araujo PB (2001) Morphology of respiratory organs in South American Oniscidea (“Philosciidae”). *Crustacean Issues* 13: 329–336.

- Lins LSF, Ho SYW, Lo N (2017) An evolutionary timescale for terrestrial isopods and a lack of molecular support for the monophyly of Oniscidea (Crustacea: Isopoda). *Organisms, Diversity & Evolution* 17(4): 813–820. <https://doi.org/10.1007/s13127-017-0346-2>
- Lobo HAS (2007) Método para avaliação do potencial espeleoturístico do Parque Nacional da Serra da Bodoquena, MS. *Caderno Virtual de Turismo* 7(3): 99–110.
- López-Orozco CM, Carpio-Díaz YM, Borja-Arrieta R, Navas GR, Campos-Filho IS, Taiti S, Mateos M, Olazaran A, Caballero IC, Jotty K, Gómez-Estrada H, Hurtado L (2022) A glimpse into remarkable unknown diversity of oniscideans along the Caribbean coasts revealed on a tiny island. *European Journal of Taxonomy* 793: 1–50. <https://doi.org/10.5852/ejt.2022.793.1643>
- López-Orozco CM, Campos-Filho IS, Gallo JS, Gallão JE, Carpio-Díaz YM, Borja-Arrieta R, Bichuette ME (2024) Iron-Isopods: New records and new species of terrestrial isopods (Isopoda, Oniscidea) from Brazilian Amazon iron ore caves. *European Journal of Taxonomy* 921: 116–135. <https://doi.org/10.5852/ejt.2024.921.2421>
- Montesanto G (2015) A fast GNU method to draw accurate scientific illustrations for taxonomy. *ZooKeys* 515: 191–206. <https://doi.org/10.3897/zookeys.515.9459>
- Montesanto G (2016) Drawing setae: A GNU way for digital scientific illustrations. *Nauplius* 24(0): e2016017. <https://doi.org/10.1590/2358-2936e2016017>
- Moracchioli N, Trajano E (2002) Bodoquena karst area, southwest Brazil: a hotspot of biodiversity for aquatic troglobites. In: XVIth International Symposium of Biospeleology, Verona, 84–84.
- Moutaouakil S, Boulanouar M, Ghamizi M, Lips J, Ferreira RL (2023) Two new sympatric cave species of *Castellanethes* (Isopoda, Oniscidea, Olibrinidae) from Western High Atlas of Morocco. *Subterranean Biology* 45: 17–37. <https://doi.org/10.3897/subtbiol.45.95845>
- Pires AMS (1987) *Potiicoara brasiliensis*: a new genus and species of Spelaeogriffithacea (Crustacea: Peracarida) from Brazil with a phylogenetic analysis of the Peracarida. *Journal of Natural History* 21(1): 225–238. <https://doi.org/10.1080/00222938700770101>
- Reboleira ASPS, Goncalves F, Oromí P, Taiti S (2015) The cavernicolous Oniscidea (Crustacea: Isopoda) of Portugal. *European Journal of Taxonomy* 161(161): 1–61. <https://doi.org/10.5852/ejt.2015.161>
- Schmalfuss H (1984) Eco-morphological strategies in terrestrial isopods. *The Symposium Held at the Zoological Society of London* 53: 49–63.
- Schmalfuss H (1989) Phylogenetics in Oniscidea. *Monitore Zoologico Italiano* 4: 3–27.
- Schmalfuss H (2003) World catalog of terrestrial isopods (Isopoda: Oniscidea). *Stuttgarter Beiträge zur Naturkunde, Serie A* 654: 1–341.
- Schmidt C (2002) Contribution to the phylogenetic system of the Crinocheta (Crustacea, Isopoda). Part 1 (Olibrinidae to Scyphacidae s. str.). *Zoosystematics and Evolution* 78(2): 275–352. <https://doi.org/10.1002/mmzn.20020780207>
- Schmidt C (2003) Contribution to the phylogenetic system of the Crinocheta (Crustacea, Isopoda). Part 2 (Oniscoidea to Armadillidiidae). *Mitteilungen aus dem Zoologischen Museum in Berlin, Zoologische Reihe* 79: 3–179. <https://doi.org/10.1002/mmzn.20030790102>
- Schmidt C (2008) Phylogeny of the terrestrial Isopoda (Oniscidea): A review. *Arthropod Systematics & Phylogeny* 66(2): 191–226. <https://doi.org/10.3897/asp.66.e31684>
- Sfenthourakis S, Taiti S (2015) Patterns of taxonomic diversity among terrestrial isopods. *ZooKeys* 515: 13–25. <https://doi.org/10.3897/zookeys.515.9332>

- Sfenthourakis S, Myers AA, Taiti S, Lowry JK (2020) Terrestrial environments. In: Thiel M, Poore G (Eds) Evolution and Biogeography of the Crustacea, the Natural History of the Crustacea. Oxford University Press, Oxford, 375–404. <https://doi.org/10.1093/oso/9780190637842.003.0014>
- Souza LA, Ferreira RL, Senna AR (2015) Amphibious shelter-builder Oniscidea species from the New World with description of a new subfamily, a new genus and a new species from Brazilian Cave (Isopoda, Synocheta, Styloniscidae). PLOS ONE 10(5): e0115021. <https://doi.org/10.1371/journal.pone.0115021>
- Stringer DN, King RA, Taiti S, Guzik MT, Cooper SJ, Austin AD (2019) Systematics of *Haloniscus* Chilton, 1920 (Isopoda: Oniscidea: Philosciidae), with description of four new species from threatened Great Artesian Basin springs in South Australia. Journal of Crustacean Biology 39(5): 651–668. <https://doi.org/10.1093/jcobiol/ruz044>
- Tabacaru I, Giurginca A (2013) Cavernicolous Oniscidea of Romania. Travaux de l'Institut de Speologie. Emile Racovitza 42: 3–26.
- Taiti S (2004) Crustacea: Isopoda: Oniscidea (woodlice). In: Gunn J (Ed.) Encyclopedia of caves and karst science. Fitzroy Dearborn, Taylor and Francis Group, New York, United States, 547–551.
- Taiti S, Ferrara F (1980) The family Philosciidae (Crustacea Oniscoidea) in Africa, south of the Sahara. Monitore Zoologico Italiano Supplemento 13(1): 53–98. <https://doi.org/10.1080/00269786.1980.11758549>
- Taiti S, Ferrara F (1982) Revision of the family Philosciidae (Crustacea, Isopoda, Oniscoidea) from South Africa. Annals of the South African Museum 90(1): 1–48.
- Taiti S, Ferrara F (2004) The terrestrial Isopoda (Crustacea: Oniscidea) of the Socotra Archipelago. Fauna of Arabia 20: 211–325.
- Taiti S, Gardini P (2022) The family Olibrinidae in Italy (Malacostraca Isopoda Oniscidea). Redia (Firenze) 105: 97–105. <https://doi.org/10.19263/REDIA-105.22.13>
- Taiti S, Gruber GA (2008) Cave-dwelling terrestrial isopods from Southern China (Crustacea, Isopoda, Oniscidea), with descriptions of four new species. In: Latella L, Zorzin R (Eds) Research in South China karsts. Memorie del Museo Civico di Storia Naturale di Verona, Monografie Naturalistiche, 101–123.
- Taiti S, Humphreys WF (2001) New aquatic Oniscidea (Crustacea: Isopoda) from groundwater calcretes of Western Australia. Records of the Western Australian Museum 64(1): 133–151. <https://doi.org/10.18195/issn.0313-122x.64.2001.133-151>
- Taiti S, Xue Z (2012) The cavernicolous genus *Trogloniscus* nomem novum, with descriptions of four new species from southern China (Crustacea, Oniscidea, Styloniscidae). Tropical Zoology 25(4): 183–209. <https://doi.org/10.1080/03946975.2012.751240>
- Taiti S, Argano R, Marcia P, Scarpa F, Sanna D, Casu M (2018) The genus *Alpioniscus* Racovitza, 1908 in Sardinia: Taxonomy and natural history (Isopoda, Oniscidea, Trichoniscidae). ZooKeys 801: 229–263. <https://doi.org/10.3897/zookeys.801.24102>
- Trajano E, Gallão JE, Bichuette ME (2016) Spots of high diversity of troglobites in Brazil: The challenge of measuring subterranean diversity. Biodiversity and Conservation 25(10): 1805–1828. <https://doi.org/10.1007/s10531-016-1151-5>
- Vandel A (1973) Les isopodes terrestres et cavernicoles de l'île de Cuba. In: Orghidan T, Núñez A, Botosaneanu L, Decou V, Negrea Ș, Viña N (Eds) Résultats des Expéditions biospéologiques cubanoroumaines à Cuba, Vol. 1. Editura Academiei Republicii Socialiste România, Bucharest, 153–188.
- Vittori M, Dominko M (2022) A bibliometric analysis of research on terrestrial isopods. ZooKeys 1101: 13–34. <https://doi.org/10.3897/zookeys.1101.81016>

Wägele JW (1989) Evolution und phylogenetisches System der Isopoda. *Zoologica* 140: 1–262.

Warburg MR, Adis J, Rosenberg M, Schaller F (1997) Ecology and the structure of respiratory organs in a unique amphibious/terrestrial isopod from the Neotropics (Oniscidea: Philosciidae). *Studies on Neotropical Fauna and Environment* 32: 52–63.

Supplementary material 1

Supplementary video

Authors: Carlos Mario López-Orozco, Ivanklin Soares Campos-Filho, Livia Medeiros Cordeiro, Jonas Eduardo Gallão, Yesenia M. Carpio-Díaz, Ricardo Borja-Arrieta, Maria Elina Bichuette

Data type: mp4

Explanation note: *Kadiweuoniscus rebellis* López-Orozco, Campos-Filho & Bichuette gen. et sp. nov. locomotor behavior in the Flor da Bodoquena Cave, in rocky substrate with silt and pebbles. Video on YouTube: <https://youtube.com/shorts/bNqp97PdP-cY?feature=share>.

Copyright notice: This dataset is made available under the Open Database License (<http://opendatacommons.org/licenses/odbl/1.0/>). The Open Database License (ODbL) is a license agreement intended to allow users to freely share, modify, and use this Dataset while maintaining this same freedom for others, provided that the original source and author(s) are credited.

Link: <https://doi.org/10.3897/zookeys.1192.114230.suppl1>

Pseudoscorpions (Arachnida, Pseudoscorpiones) from French Polynesia with first species records and description of new species

Katarína Krajčovičová¹, Thibault Ramage², Frédéric A. Jacq³, Jana Christophoryová⁴

1 Bratislavské regionálne ochrannárske združenie – BROZ, Na Riviére 7/a, 841 04, Bratislava, Slovakia

2 14 impasse Jeanne Dieulafoy, 29900, Concarneau, France

3 BP 41 405 Faretony, 98713 Papeete, Tahiti, French Polynesia

4 Department of Zoology, Faculty of Natural Sciences, Comenius University, Mlynská dolina, Ilkovičova 6, 842 15, Bratislava, Slovakia

Corresponding author: Jana Christophoryová (christophoryova@gmail.com)

Abstract

A new species *Olpium caputi* **sp. nov.** from Tahiti is described here based on external characters. This is the first record of the family Olpiidae Banks, 1895 from French Polynesia. Additionally, the genus *Paratemnoides* Harvey, 1991 is recorded from French Polynesia for the first time with the full description of new-found specimens of *Paratemnoides assimilis* (Beier, 1932). New localities of *Geogarypus longidigitatus* (Rainbow, 1897) are added. An identification key to pseudoscorpions of French Polynesia is provided.

Key words: Endemism, insular fauna, Oceania, Society Islands, taxonomy



Academic editor: Fedor Konstantinov

Received: 17 August 2023

Accepted: 14 January 2024

Published: 19 February 2024

ZooBank: <https://zoobank.org/1CBEA82C-9071-4943-A022-529CCC06B947>

Citation: Krajčovičová K, Ramage T, Jacq FA, Christophoryová J (2024) Pseudoscorpions (Arachnida, Pseudoscorpiones) from French Polynesia with first species records and description of new species. ZooKeys 1192: 29–43. <https://doi.org/10.3897/zookeys.1192.111308>

Copyright: © Katarína Krajčovičová et al. This is an open access article distributed under terms of the Creative Commons Attribution License ([Attribution 4.0 International – CC BY 4.0](https://creativecommons.org/licenses/by/4.0/)).

Introduction

The Pacific Ocean contains about 25,000 islands, which have various geological origins such as continental fragments or volcanic hot-spots. Most of these islands are very distant from continents, and the most remote islands are northern and eastern Polynesia, in the Hawaiian Islands and French Polynesia (Dupon et al. 1993; Gillespie 2002; Gillespie et al. 2008). French Polynesia consists of 118 islands and atolls spread over 5 million km² with a total land area of approximately 3660 km². The islands form five archipelagos: Austral Islands, Gambier Islands, Marquesas Islands, Society Islands, and Tuamotu Islands (Gillespie et al. 2008). Biologists have been attracted to these regions since the 18th century, but French Polynesia, by comparison to the Hawaiian Islands, has received much less attention, especially since the 1930s (Gillespie et al. 2008; Ramage 2017).

A phenomenon called taxonomic disharmony (Roderick and Gillespie 2016) can be observed in the arachnids of French Polynesia. No Amblypygi, Opiliones, Palpigradi, Ricinulei, Solifugae, or Thelyphonida are reported from the islands until now (Ramage 2017; WPC 2022). On the other hand, some of the arachnids of French Polynesia are represented by a high degree of endemism. Araneae of French Polynesia includes 113 species, of which 49 are endemic. The highest

number of endemic forms occur in the families Salticidae and Tetragnathidae (Ramage 2017). A total of 248 species of Acari are known in French Polynesia. Most of the species belong to Sarcoptiformes of which 59 are endemic (Ramage 2017; WSC 2023). Two species of Scorpiones are reported from French Polynesia, the pantropical *Isometrus maculatus* (De Geer, 1778) and *Liocheles australasiae* (Fabricius, 1775), which is widely distributed in Asia and the Pacific (Vaucel et al. 2022; Rein 2023). Recently one species of Schizomida has been discovered in French Polynesia. *Zomus bagnallii* (Jackson, 1908) has been collected in the Society Islands (Bora Bora, Huahine, Raiatea, Tahiti, and Tetiaroa) and Tuamotu archipelago (Anaa) (J. Cokendolpher pers. comm.; unpublished data).

Pseudoscorpions on these remote islands have received only a little interest. Contributions to the knowledge of pseudoscorpions of French Polynesia date back to the 1930s and are associated with the Pacific Entomological Survey (Chamberlin 1938, 1939a, 1939b). Since then, the French Polynesian pseudoscorpion fauna has been thought to be comprised of four species in four genera divided into three families (WPC 2022). The first record from French Polynesia was of *Americhernes kanaka* (Chamberlin, 1938), which was described from Ua Pou in the Marquesas Islands and collected on Mount Tekohepu in dead stipes of *Cyathea* sp. (Chamberlin 1938). The record of *A. kanaka* in Chamberlin (1938) lacks a description of the species, which was given later by Chamberlin (1939b). The species' description is based on a single male specimen that was originally classified in the genus *Lamprochernes* Tömösváry, 1883 (Chamberlin 1938, 1939b). Harvey (1990) transferred the species to the genus *Americhernes* Muchmore, 1976 based on the following characters: leg IV with four tactile setae, trichobothrium *it* farther from fingertip than the distance between *isb* and *ist*. Several specimens of *Haplochernes funafutensis* (With, 1907) were collected on pandanus and *Talipariti tiliaceum* (L.) Fryxell, 2001 trunks on Tahiti, Society Island (Chamberlin 1939a). Chamberlin (1939b) recorded the presence of *Oratemnus samoanus* Beier, 1932 on two neighbouring Marquesas islands, Eiao and Hatuta'a. The specimens of *O. samoanus* were found in dead wood, under bark, and under stones (Chamberlin 1939a). *Geogarypus longidigitatus* (Rainbow, 1897) was reported and described as *Geogarypus marquesianus* Chamberlin, 1939 from French Polynesia in the first place (Chamberlin 1939b). It was later synonymised and reported from several islands in the Marquesas, Society, and Tuamotu archipelagos (Harvey 2000; WPC 2022).

During surveys led by two of the authors (TR and FJ) in French Polynesia between 2017 and 2020, a few pseudoscorpion specimens were collected on Huahine and Tahiti in the Society Islands. These few specimens include a new species described as *Olpium caputi* sp. nov. and another species, *Paratemnoides assimilis* (Beier, 1932), which is a new record and redescribed here based on well-conserved material.

Materials and methods

The samples from Motuhionoa on Huahine were collected as part of an environmental diagnostic for the French Polynesian Agricultural Service, and those from Mount Marau on Tahiti as part of a large-scale survey of the arthropods of Society Islands led by two of the authors (TR and FJ).

All specimens were immersed in lactic acid for clearing and studied on temporary slide mounts. After the study, they were rinsed in water and returned to 75% ethanol.

Morphological and morphometric analyses were performed using a Leica DM1000 compound microscope with an ICC50 camera module (LAS EZ application v. 1.8.0). Measurements were taken from digital images using the Axio-Vision 40LE application. Digital photographs (Fig. 2) were taken using a Canon EOS 5D Mark II camera attached to a Zeiss Axio Zoom V16 stereomicroscope. Image stacks were produced manually, combined using Zerene Stacker software, and subsequently edited in Adobe Photoshop CC. Terminology follows Chamberlin (1931), Harvey (1992), and Judson (2007).

All specimens presented in this paper are deposited in the zoological collections of the Naturhistorisches Museum Wien, Austria (NHMW). For proper identification, specimens of *Paratemnoides assimilis* (Beier, 1932) were compared with *Paratemnoides* specimens deposited in NHMW.

Abbreviations

Setae on chelicera: **bs**–basal, **es**–exterior, **gls**–galeal, **is**–interior, **ls**–laminal, **sbs**–subbasal.

Trichobothria of moveable chelal finger: **b**–basal, **sb**–subbasal, **st**–subterminal, **t**–terminal; trichobothria of fixed chelal finger: **eb**–exterior basal, **esb**–exterior subbasal, **est**–exterior subterminal, **et**–exterior terminal, **ib**–interior basal, **isb**–interior subbasal, **ist**–interior subterminal, **it**–interior terminal; **pc**–coupled sensillum.

Results

Taxonomy

Family Atemnidae Kishida, 1929

Genus *Paratemnoides* Harvey, 1991

Paratemnoides assimilis (Beier, 1932)

Figs 2A, 3

Materials examined (Fig. 1). FRENCH POLYNESIA • 2 ♂♂, 5 ♀♀, 1 tritonymph, 1 deutonymph; Huahine, Motuhionoa [16°46'16"N, 151°00'14"W]; 82 m a.s.l.; 06 Nov. 2020; F. Jacq leg.; decaying *Falcataria moluccana* trunk; NHMW 29976. • 1 ♀; Huahine, Motuhionoa [16°46'11"N, 151°00'10"W]; 32 m a.s.l.; 06 Nov. 2020; F. Jacq leg.; Malaise trap; NHMW 29977.

Description. ♂ (♀) (Figs 2A, 3).

Carapace (Fig. 3A). Carapace 0.96 (0.95) × longer than broad, conically narrowed; epistome absent; with 2 distinct eye spots; smooth, without transverse furrows; anterior half brown distinct darker than posterior half; with 49 (44) acuminate setae apically with a dentition, 8 (9) setae on posterior margin; for lyrifissures see Fig. 3A. **Chelicera** (Fig. 3B, C). Chelicera 2.33 (2.47) × longer than broad; 4 setae on hand, **sbs** absent, **bs** and **es** denticulate; moveable finger with 1 short seta; 2 slit-like lyrifissures on hand; galea long with 5 rami (Fig. 3B); serula exterior with 22 blades; rallum consisting of 4 blades, distal one long and

serrated (Fig. 3C). **Pedipalps** (Fig. 3D, G). Pedipalps smooth, only anterior face of femur with minute denticles (Fig. 3G), trochanter and femur lighter than chela (Fig. 2A). Trochanter 1.59×, femur 2.16 (2.19) ×, patella 1.91 (1.94) ×, chela 2.59 (2.63) ×, hand with pedicel 1.67 (1.69) × longer than broad. Venom apparatus present only in fixed finger terminating in nodus ramosus slightly proximal to trichobothria et (Fig. 3D). Fixed chelal finger with 8 trichobothria, moveable chelal finger with 4 trichobothria. Fixed chelal finger with 39 small marginal teeth; moveable chelal finger with 42 (43) small marginal teeth (Fig. 3D). Trichobothria *eb* and *esb* adjacent and located basally; *est* midway between *esb* and *et*; *st* closer to *sb* than to *t*. For a complete trichobothrial pattern see Fig. 3D. **Coxae** (Fig. 3E). Coxae smooth, all setae acuminate or with fine dentition apically; manducatory processes with 6 (5) setae; palpal coxae with 13–14 (16–17) setae; pedal coxae I–IV chaetotaxy: 9–11 (8–10): 6–8 (9): 6–7 (7): 17–19 (15–17); for lyrifissures see Fig. 3E. **Abdomen** (Fig. 2A). Tergites I–III undivided, IV–V partly divided, VI–XI with fine division; sternites IV–XI divided. All setae acuminate or with fine dentition apically. **Tergal chaetotaxy I–XI**: 8: 8: 8: 4–5: 6–7 (6–7): 6 (6–7): 6 (6–7): 6 (7): 7: 9: 5. **Sternal chaetotaxy IV–XI**: 4: 5–7 (7): 6 (7–8): 7 (8): 8 (7–8): 9 (7): 7: 5. **Genital area II–III**. Short acuminate setae [slit-like lyrifissures]: 15 [2] (8 [4]): 6 [4] (4 [2]). **Genital area** (Fig. 3F). Male rod Y shaped, female with several cribriform plates externally (Fig. 3F). **Leg I** (Fig. 3H). Trochanter 1.21×, femur I 1.25 (1.26) ×, femur II 2.86 (2.63) ×, tibia 2.77×, tarsus 3.22 (3.33) × deeper than broad. **Leg IV** (Fig. 3I). Trochanter 1.44×, femoropatella 3.15 (3.23) ×, tibia 3.18 (3.29) ×, tarsus 2.77 (2.69) × deeper than broad. Leg IV with 1 tactile seta basally on tarsus (Fig. 3I). Claws simple, arolium slightly shorter than claws (Fig. 3H, I).

Measurements (in mm, length/width or, for legs, length/depth). ♂ (♀). Body length 2.98 (3.38). Pedipalps: trochanter 0.43/0.27, femur 0.69 (0.70)/0.32, patella 0.67 (0.68)/0.35, chela 1.27 (1.29)/0.49, hand with pedicel 0.82 (0.83)/0.49, hand without pedicel 0.72 (0.73), fixed finger 0.62 (0.63). Chelicera 0.35 (0.37)/0.15, moveable finger 0.28. Carapace 0.85 (0.88)/0.89 (0.93). Leg I: trochanter 0.17/0.14, femur I 0.25 (0.24)/0.20 (0.19), femur II 0.40 (0.42)/0.14 (0.16), tibia 0.36/0.13, tarsus 0.29 (0.30)/0.09. Leg IV: trochanter 0.23/0.16, femoropatella 0.82 (0.84)/0.26, tibia 0.54/0.17, tarsus 0.36 (0.35)/0.13.

Identification. *Paratemnoides assimilis* is most similar to *P. pallidus* (Balzan, 1892) as both possess similar proportions of the palpal segments (femur 0.62–0.83 mm long/2.10–2.30× longer than broad, patella 0.59–0.78 mm long/1.80–1.90× longer than broad, chela 1.27–1.44 mm long/2.40–2.70× longer than broad, finger 0.47–0.63 mm long), minute denticles on the palpal segments while other body segments are smooth, and a carapace without transverse furrows. They differ by the presence of minute denticles on different segments of the pedipalps; in *P. assimilis* denticles are present on the anterior margin of the palpal femur, but with other palpal segments smooth, but in *P. pallidus* denticles are present on femur as well as on patella (Beier 1932a, 1932b; Mahnert 1978a; Harvey 1988). Measurements of the palpal hand with pedicel also differ (*P. assimilis* 0.62–0.83 mm long vs *P. pallidus* 0.80–1.06 mm long) (Mahnert 1978a; Harvey 1988).

Remarks. New-found specimens of *P. assimilis* were compared with selected *Paratemnoides* species deposited in NHMW: *P. assimilis* [NHMW-Zoo-AR 25115, NHMW-Zoo-AR 25124]; *P. ceylonicus* Beier, 1932 [NHMW-Zoo-AR 25064, NHMW-Zoo-AR 25065]; *P. curtulus* (Redikorzev, 1938) [NHMW-Zoo-AR

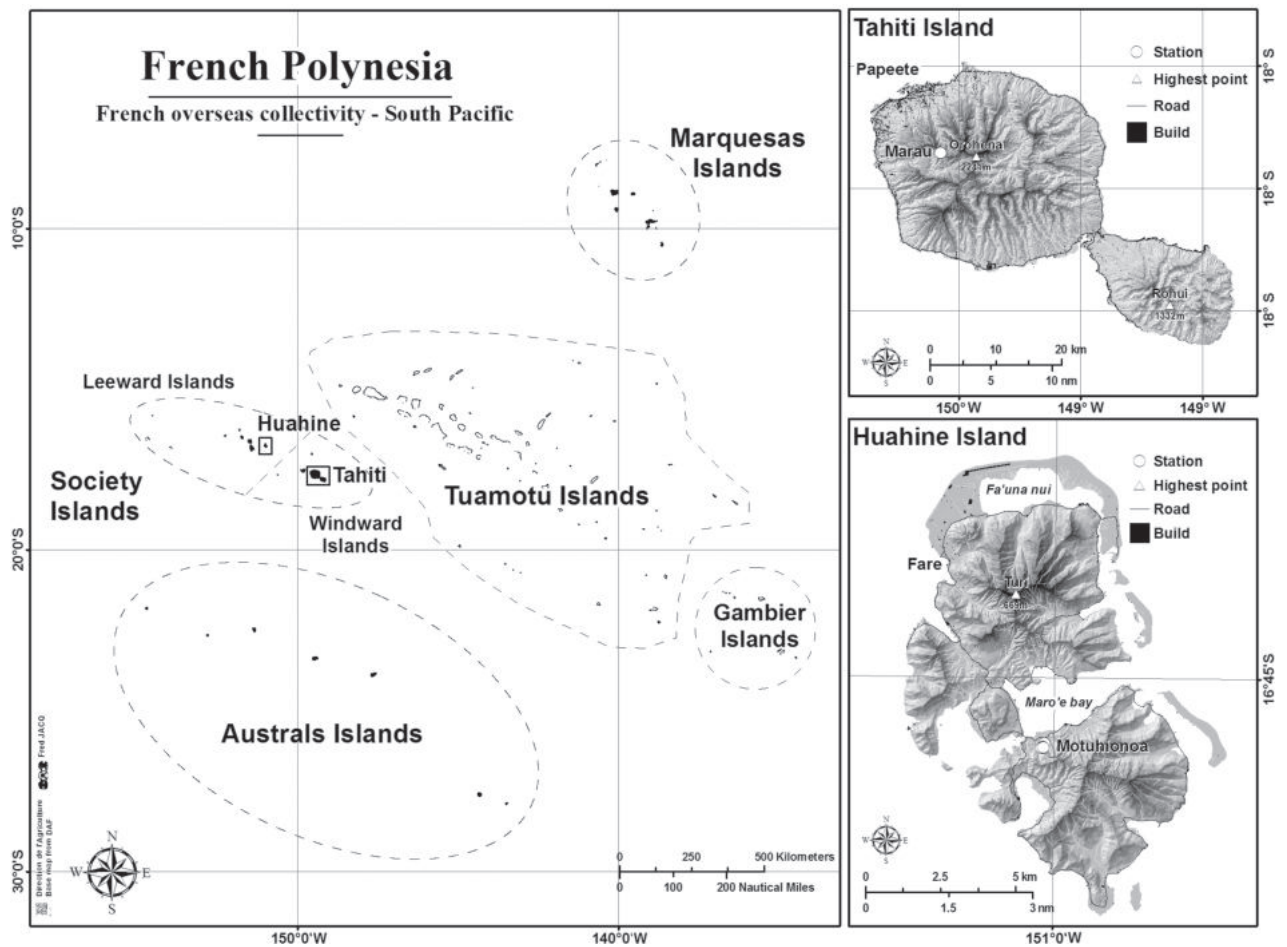


Figure 1. Map of archipelagos of French Polynesia with details of Tahiti and Huahine islands with marked studied localities.

25117]; *P. laosanus* (Beier, 1951) [NHMW-Zoo-AR 25073]; *P. pallidus* [NHMW-Zoo-AR 25090, NHMW-Zoo-AR 25125]; and *P. salomonis* (Beier, 1935) [NHMW-Zoo-AR 25110]. As mentioned by Harvey (1988), the identification keys to *Paratemnoides* species by Beier (1932a, 1932b) are based generally on the size or thickness of palpal segments and legs. Harvey (1988) applied the character of measurements of leg segments as distinguishing ones for *P. assimilis* and *P. ceylonicus*. Specimens of species mentioned above were examined and compared in this study. Leg segments were measured but the values completely overlapped in all examined species. Considering these results and the fact that the *Paratemnoides* species descriptions are generally not sufficient, a revision of this genus is necessary to clearly set species boundaries.

Currently, *P. ceylonicus* is one of the synonyms of *P. pallidus* (Fig. 2B) (Klausen 2005; WPC 2022). The current synonymy of the two species was justified by no significant difference between *P. ceylonicus* and *P. pallidus* in palpal chela measurements (Klausen 2005). Beier (1932a, 1932b, 1973) supported the existence of *P. ceylonicus* by the presence of minute denticles on the anterior margin of the palpal femur while other palpal segments are smooth.

All examined specimens of *P. ceylonicus* deposited in NHMW possess distinct granulation present on palpal femur as well as on patella just like in *P. pallidus*. The present study supports the synonymization of *P. ceylonicus* with *P. pallidus* suggested by Klausen (2005).

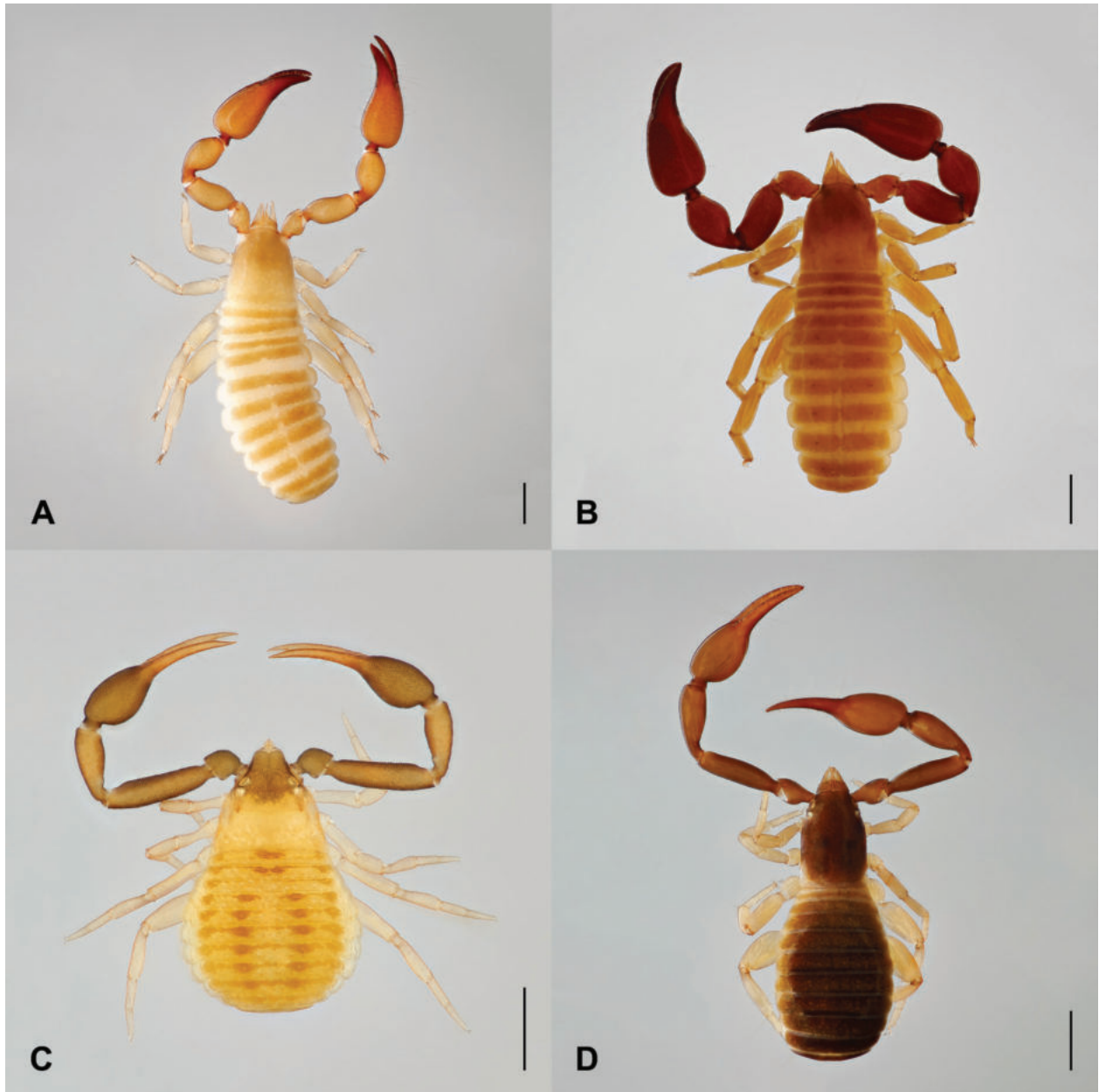


Figure 2. **A** *Paratemnoides assimilis*, female **B** *Paratemnoides pallidus*, male **C** *Geogarypus longidigitatus*, male **D** *Olpium caputi* sp. nov., female. Scale bars: 0.5 mm.

Family Geogarypidae Chamberlin, 1930

Genus *Geogarypus* Chamberlin, 1930

***Geogarypus longidigitatus* (Rainbow, 1897)**

Fig. 2C

Materials examined (Fig. 1). FRENCH POLYNESIA • 1 ♂; Huahine, Motuhionoa [16°46'15"N, 151°00'12"W]; 61 m a.s.l.; 06 Nov. 2020; F. Jacq leg.; *Mangifera indica* and *Talipariti tiliaceum* forest, leaf litter sifting; NHMW 29978. • 1 ♂, 1 deutonymph; Huahine, Motuhionoa [16°46'16"N, 151°00'12"W]; 79 m a.s.l.; 06 Nov. 2020; F. Jacq leg.; *Talipariti tiliaceum* forest, leaf-litter sifting; NHMW 29979.

Measurements (in mm, length/width). ♂. Body length 1.57. Pedipalp: trochanter 0.22/0.16, femur 0.55/0.13, patella 0.40/0.15, chela 0.91/0.23, hand with pedicel 0.44/0.23, fixed finger length 0.51. Carapace 0.53–0.55/0.64.

Identification. *Geogarypus longidigitatus* is remarkably similar to *G. ocellatus* Mahnert, 1978, as both possess the same pattern of carapace coloration, but the palpal patella and chela of *G. ocellatus* are more slender than in *G. longidigitatus* (e.g. patella and chela: *G. longidigitatus* 2.5–2.6× longer than broad and 3.5–4.2× longer than broad vs. *G. ocellatus* 3.0–3.3× longer than broad and 4.1–4.5× longer than broad) (Mahnert 1978b; Harvey 2000). See Harvey (2000) for the complete redescription of *G. longidigitatus* and diagnosis of other geogarypid species. Newly described geogarypids found in the Asian-Australian-Pacific regions differ from *G. longidigitatus* as follows: *G. muchmorei* Novák & Harvey, 2018 differs by its larger area of brown coloration on the carapace and the swollen margin of the chelal hand; *G. klarae* Novák & Harvey, 2018 differs by having a white palpal trochanter and strongly curved teeth on the fixed chelal finger (Novák and Harvey 2018); *G. plusculus* Cullen & Harvey, 2021 and *G. facetus* Cullen & Harvey, 2021 differ by the patchy coloration of the carapace and brighter palpal trochanter and femur (Cullen and Harvey 2021).

Remarks. The species is widely distributed in the Indo-Pacific region (Novák and Harvey 2018; WPC 2022). Harvey (2000) assumed that the wide distribution of the species is also due to human activities.

Family Olpiidae Banks, 1895

Genus *Olpium* L. Koch, 1873

Olpium caputi Krajčovičová & Christophoryová, sp. nov.

<https://zoobank.org/A27FF8CF-E164-4A69-8787-FE60F61300EB>

Figs 2D, 4

Material examined (Fig. 1). **Holotype:** FRENCH POLYNESIA • 1 ♀; Tahiti, Mont Marau Summit [17°36'52"N, 149°31'45"W]; 1450 m a.s.l.; 01 Sept. 2017; F.A. Jacq & T. Ramage leg.; sifting of epiphyte moss on *Pterophylla parviflora* (G.Forst.) Pillon & H.C.Hopkins; NHMW 29980.

Etymology. The species' epithet is a patronym honouring Zuzana Čaputová, the Slovak President. As a female leader, she expresses clear attitudes and supports women as well as scientists. In this manner, we would like to pay tribute to her.

Diagnosis. *Olpium caputi* sp. nov. is most similar to *O. afghanicum* Beier, 1952 and *O. philippinum* Beier, 1967, as all possess a dark brown carapace, pedipalps, and abdomen, and with carapace and abdomen being darker than palpal segments, a carapace without transverse furrows, and similar proportions of the palpal segments (e.g. patella 2.80–3.30× longer than broad, chela with pedicel 3.40–4.00× longer than broad and chelal finger 0.60–0.63 mm long) (Beier 1952, 1967). *Olpium caputi* sp. nov. differs from *O. afghanicum* in having smooth chelal hands and two enlarged setae present on the palpal femur, while in *O. afghanicum* the the chelal hands possess mediobasal dense granulation and only one enlarged seta is present on palpal femur (Beier 1952). *Olpium caputi* sp. nov. differs from *O. philippinum* in having all palpal segments smooth, while *O. philippinum* possesses sparse mediobasal granulation on

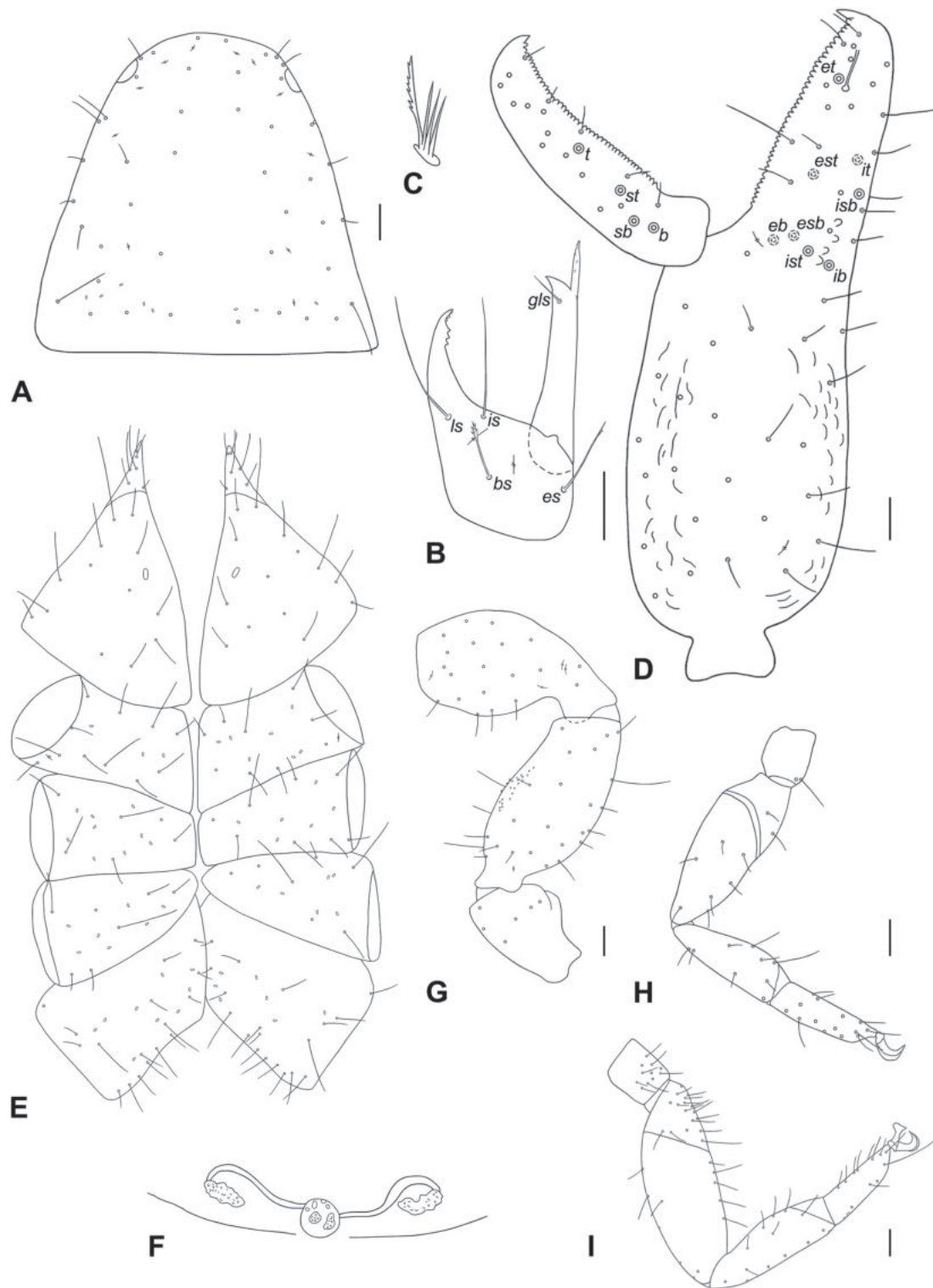


Figure 3. *Paratemnoides assimilis* **A** carapace, dorsal view **B** chelicera with setae pattern, dorsal view **C** rallum **D** palpal chela, dorsal view, showing trichobothriotaxy, teeth and venom apparatus **E** coxal area, ventral view **F** genital area **G** pedipalp, dorsal view (trochanter, femur, and patella) **H** leg I, lateral view **I** leg IV, lateral view. Scale bars: 0.1 mm.

the palpal trochanter and hand. In addition, the palpal femur of *O. caputi* sp. nov. is more slender than in *O. philippinum* (e.g. palpal femur in *O. caputi* sp. nov. 4.11× longer than broad vs that of *O. philippinum* 3.20–3.30× longer than broad) (Beier 1967).

Description. ♀ (Figs 2D, 4). Integument pigmented; carapace, pedipalps, and abdomen dark brown; carapace and abdomen slightly darker than palpal segments; tergites I–II whitish, following tergites brown, markedly darker (Fig. 2D). **Carapace** (Fig. 4A). Carapace 1.33× longer than broad, rectangular without transverse furrows; 4 eyes, the anterior ones with very convex lens, both pairs with tapetum; 25 thin setae, of which 4 anterior and 3 posterior; with 12 lyrifissures. **Chelicera** (Fig. 4B, C). Chelicera 2.08× longer than broad, palm with 5 acuminate setae; fixed finger with 7 teeth; moveable finger with 1 subdistal seta, galea broken apically (Fig. 4B), rallum with 3 blades, distal one serrated (Fig. 4C), serrula exterior with 17 blades. **Pedipalps** (Figs 2D, 4D, G). Pedipalps smooth (Figs 2D, 4G). Trochanter 1.95×, femur 4.11×, patella 2.83×, chela 3.74×, hand with pedicel 1.82× longer than broad. Femur dorsal with 2 elongate setae without enlarged alveoli (Fig. 4G). Venom apparatus very short present in both fixed and moveable fingers terminating in nodus ramosus distal to trichobothrium *et* on fixed finger (Fig. 4D). Fixed chelal finger with 8 trichobothria, moveable chelal finger with 4 trichobothria. Fixed chelal finger with 41 slightly reclined and pointed teeth; moveable chelal finger with 35 small marginal teeth (Fig. 4D). A coupled sensillum (*pc*) closer to *sb* than to *st*. Trichobothria *eb*, *esb*, *ib*, *isb* located on the base of the fixed finger; *est* closer to *ist* than to *it*; *b* and *sb* located on the base of the moveable finger; *st* closer to *sb* than to *t*. For a complete trichobothrial pattern see Fig. 4D. **Coxae** (Fig. 4E). Coxae smooth, all setae acuminate; manducatory processes with 5 setae; palpal coxae with 10–11 setae; pedal coxae I–IV chaetotaxy: 4: 5: 7–8: 14 (1 damaged); for lyrifissures see Fig. 4E. **Abdomen** (Fig. 2D). Tergites longitudinally not divided. Pleural membrane longitudinally striate. **Tergal chaetotaxy I–X**: 2: 4: 5: 4: 4: 4: 4: 6: 10. **Chaetotaxy of sternites II–X**: 7: 4: 4: 6: 8: 6: 6: 9: 10. Genital area very simple with marginal row of 7 acuminate setae on posterior operculum; one pair of lateral cribriform plates and one pair of medial cribriform plates next to each other as on Fig. 4F. **Leg I** (Fig. 4H). Trochanter 1.38×, femur 3.00×, patella 1.91×, tibia 4.43×, tarsus I 3.40×, tarsus II 3.00× deeper than broad. **Leg IV** (Fig. 4I). Trochanter 1.53×, femoropatella 2.87×, tibia 4.36×, tarsus I 2.86×, tarsus II 3.33× deeper than broad. Leg IV with a long tactile seta basally on tarsus I (Fig. 4I). Claws simple, arolium significantly longer than claws (Fig. 4H–I).

Measurements (in mm, length/width or, for legs, length/depth). ♀. Body length 2.28. Pedipalps: trochanter 0.39/0.20, femur 0.74/0.18, patella 0.65/0.23, chela 1.27/0.34, hand with pedicel 0.62/0.34, hand without pedicel 0.54, moveable finger 0.67. Chelicera 0.27/0.13, moveable finger 0.17. Carapace 0.80/0.60. Leg I: trochanter 0.18/0.13, femur 0.30/0.10, patella 0.21/0.11, tibia 0.31/0.07, tarsus I 0.17/0.05, tarsus II 0.15/0.05. Leg IV: trochanter 0.26/0.17, femoropatella 0.66/0.23, tibia 0.48/0.11, tarsus I 0.20/0.07, tarsus II 0.20/0.06.

Distribution and ecology. Currently, this species is known only from the type locality in Tahiti, French Polynesia. The specimen was collected by sifting from epiphyte moss.

Remarks. Dashdamirov and Schawaller (1993) questioned the affiliation of *O. afghanicum* within the genus *Olpium* L. Koch, 1873 based on the following characters: nodus ramosus is distal of trichobothrium *et*, tarsus I is longer than tarsus II, the first tergite and posterior margin of carapace bear four setae. As mentioned in Murthy and Ananthkrishnan (1977), the length of

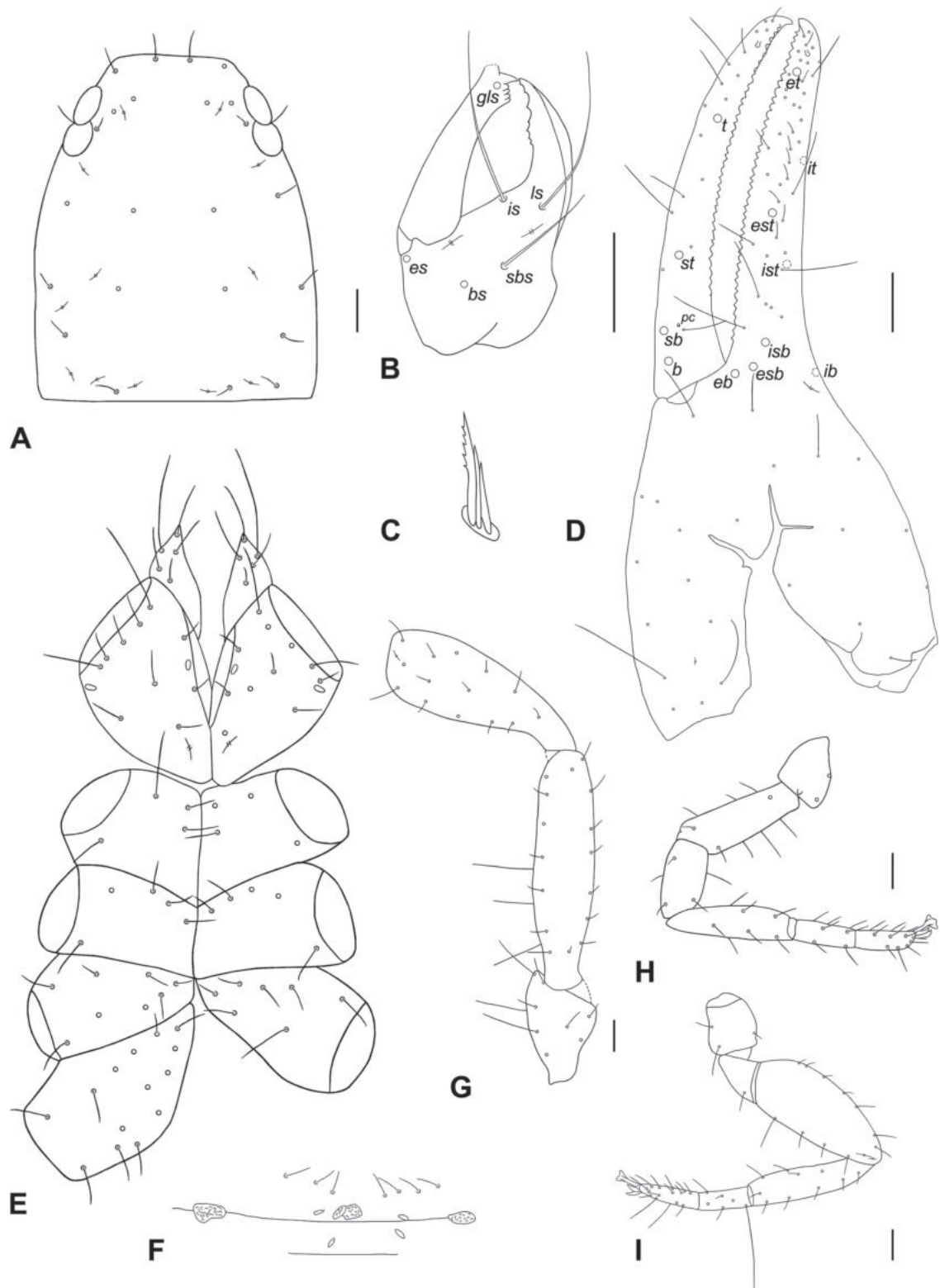


Figure 4. *Olpium caputi* sp. nov. **A** carapace, dorsal view **B** chelicera with setae pattern, dorsal view **C** rallum **D** palpal chela, dorsal view, showing trichobothriotaxy, teeth and venom apparatus **E** coxal area, ventral view **F** genital area **G** pedipalp, dorsal view (trochanter, femur, and patella) **H** leg I, lateral view **I** leg IV, lateral view. Scale bars: 0.1 mm.

nodus ramosus, given by Hoff (1964) for Olpini with *Olpium* as the type genus, cannot be satisfactorily used to distinguish *Olpium* from other genera. As explained by Harvey and Leng (2008), almost all Olpiinae Banks, 1895 possess

short venom ducts not reaching *et* on the fixed chelal finger. The redescrptions of *Olpium pallipes* (Lucas, 1849) and *Olpium kochi* Simon, 1881 show the variability in setae number on the posterior margin of carapace, both species bear 4–5 setae on it (Heurtault 1979; Mahnert 1981). New described *O. caputi* sp. nov. possesses a very short venom apparatus terminating in nodus ramosus distal to trichobothrium *et* and three setae are present on the posterior margin of carapace.

Identification key to pseudoscorpion species from French Polynesia

- 1 Carapace subtriangular, brown in anterior half, posterior half creamy white; eyes situated away from anterior margin of carapace; palpal segments brown: femur 0.46–0.81 mm long; chela with pedicel 0.82–1.24 mm long; moveable finger 0.47–0.70 mm long; anal plate located between tergite and sternite XI..... ***Geogarypus longidigitatus***
- Carapace subrectangular; eyes situated near anterior margin of carapace... **2**
- 2 Spermatheca absent; all body segments smooth without granulation; carapace and abdomen darker than palpal segments; tergites I–II whitish; carapace without transverse furrows; 4 eyes, the anterior ones with very convex lens; palpal femur 4.11× longer than broad and in basal half with 2 trichobothria (enlarged setae); femur I of leg I as long as femur II or longer ***Olpium caputi* sp. nov.**
- Spermatheca present; palpal femur without trichobothria; male sternites without discrete patches of sensory organs and without coxal sacks or ram's horn organs **3**
- 3 Venom apparatus present in moveable finger only; chelal fingers normally with at least one accessory tooth; carapace with indistinct eye spots **4**
- Venom apparatus present in fixed finger only; chelal fingers without accessory teeth; carapace with 2 distinct eye spots **5**
- 4 Small species; palpal femur 0.42–0.44 mm long; palpal chela with pedicel 0.72 mm long; chelal fingers 0.36 mm long; venom apparatus terminating in nodus ramosus at the level of trichobothrium *t*; female spermatheca consisting of 2 separate curved tubes terminating in cylindrical sacks..... ***Americhernes kanaka***
- Large species; palpal femur 0.59–0.74 mm long; palpal chela with pedicel 1.09–1.34 mm long; chelal fingers 0.52–0.67 mm long; venom apparatus terminating in nodus ramosus submedially between trichobothria *t* and *st*; female spermatheca unpaired and T-shaped ***Haplochernes funafutensis***
- 5 Trichobothrium *it* of fixed chelal finger distant from the fingertip at most as distance between *ist* and *isb*; venom apparatus terminating in nodus ramosus slightly distal to trichobothria *est*; palpal segments smooth, except for small and scattered granulations exteriorly on trochanter, interiorly on femur and patella and at the base of chelal fingers; chelal fingers shorter than the width of chelal hand ***Oratemnus samoanus***
- Trichobothrium *it* of fixed chelal finger distant from the fingertip further than distance between *ist* and *isb*; venom apparatus terminating in nodus ramosus slightly proximal to trichobothria *et*; palpal segments smooth, only anterior face of femur with minute denticles; chelal fingers longer than the width of chelal hand ***Paratemnoides assimilis***

Discussion

Much of the Pacific Basin was colonized by animals primarily from New Guinea and adjacent areas via over-water dispersal. Small islands were “stepping stones”, facilitating dispersal across the Pacific (Miller 1996). Munroe (1996) showed that there is a progressive decrease in the number of founding stocks and an increase in the proportion of radiating speciation with distance from Papuan source areas, also known as the “radiation zone” (MacArthur and Wilson 1967). This, and the taxonomic disharmony it induced, led to many free ecological niches and so a strong endemism developed. Ramage (2017) indicated that 61% of French Polynesia native terrestrial arthropods are endemic, which is similar to the flora (62%) and avifauna (64%), but far less than the exceptional level of endemism of the snail fauna (95%).

Two pseudoscorpion species are known to occur only in French Polynesia, *Americhernes kanaka* (WPC 2022) and the newly described *Olpium caputi* sp. nov. They could be considered endemic, but, as pointed out by Chamberlin (1939a), the single island endemism of some pseudoscorpion species is doubtful. Our knowledge about pseudoscorpions in Oceania is still very limited. There are natural ways in which they are distributed such as phoresy and introductions via transport must also be taken into account. Even if the pseudoscorpions were not explicitly undertaking phoresy during the research, it must be considered that some of the populations may have become established after transportation on an aerial host. Pseudoscorpions may also naturally arrive in French Polynesia under the bark of floating trunks or transported by Austronians with root vegetables, as they did with ants (Ramage 2014).

Paratemnoides assimilis was originally described from the Philippines and later discovered on Java and Krakatau Islands (Harvey 1988; WPC 2022). It was collected from various habitats, such as under the bark of a dead tree, in vegetation, in litter, and inside a tent (Harvey 1988). Several specimens presented in the current study were found on the island of Huahine for the first time. The specimens were found in a decaying tree trunk and Malaise trap. *Geogarypus longidigitatus* was originally described from Funafuti, one of the islands of Tuvalu (Rainbow 1897). *Geogarypus longidigitatus*, with its numerous synonyms, is known to have an extremely wide distribution and is also found in various habitats such as in litter and soil, on decaying substrates, in vegetation (moss, fern, grass, epiphyte), under stones, on rock walls, under bark, and in the roadside bush with anthropochorous vegetation (Chamberlin 1939b; Harvey 2000). All specimens presented in this study were found for the first time on the island of Huahine and were collected by leaf-litter sifting.

Acknowledgements

We thank Christoph Hörweg for his kind help with the comparative materials deposited in NHMW and the deposition of the new pseudoscorpion materials and our colleague Alica Christophoryová for technical assistance with figures. We would also like to thank the 2nd Agricultural Sector of the French Polynesian Agricultural Service for its interest in arthropodofauna during its environmental impact assessment. We are grateful to reviewers Catalina Romero-Ortiz and Hsiang-Yun Lin for valuable and constructive comments, which improved the quality of the paper.

Additional information

Conflict of interest

The authors have declared that no competing interests exist.

Ethical statement

No ethical statement was reported.

Funding


The research was financially supported by VEGA Grant 1/0704/20 and by the Slovak Research and Development Agency under Contract No. APVV-19-0076.

Author contributions

Conceptualization: KK, JC. Methodology: KK, TR, FAJ, JC. Resources: FAJ, TR. Visualization: FAJ, JC, KK. Writing – original draft: KK, JC. Writing – review and editing: KK, TR, FAJ, JC.

Author ORCIDs

Katarína Krajčovičová  <https://orcid.org/0000-0003-1303-2434>

Thibault Ramage  <https://orcid.org/0000-0001-5939-7098>

Frédéric A. Jacq  <https://orcid.org/0000-0002-9177-6212>

Jana Christophoryová  <https://orcid.org/0000-0002-3746-1367>

Data availability

All of the data that support the findings of this study are available in the main text.

References

- Beier M (1932a) Revision der Atemnidae (Pseudoscorpionidea). Zoologische Jahrbucher. Abteilung fur Systematik, Ökologie und Geographie der Tiere 62(56): 547–610.
- Beier M (1932b) Pseudoscorpionidea II. Subord. C. Cheliferinea. Tierreich 58: 1–294. <https://doi.org/10.1515/9783111385402>
- Beier M (1952) The 3rd Danish Expedition to Central Asia. Zoological Results 7. Pseudoscorpionidea (Chelicerata) aus Afghanistan. Videnskabelige Meddelelser fra Dansk naturhistorisk Forening i Kjøbenhavn 114: 245–250.
- Beier M (1967) Die Pseudoscorpione der Noona Dan Expedition nach den Philippinen und Bismarck Inseln. Entomologische Meddelelser 35: 315–324.
- Beier M (1973) Pseudoscorpionidea von Ceylon. Entomologica Scandinavica 4: 39–55.
- Chamberlin JC (1931) The arachnid order Chelonethida. Stanford University Publications, Biological Sciences 7(1): 1–284.
- Chamberlin JC (1938) New and little-known false-scorpions from the Pacific and elsewhere (Arachnida - Chelonethida). Annals & Magazine of Natural History 11(2): 259–285. <https://doi.org/10.1080/00222933808526844>
- Chamberlin JC (1939a) Tahitian and other records of *Haplochernes funafutensis* (With) (Arachnida: Chelonethida). Bulletin of the Bernice P. Bishop Museum 142: 203–205.
- Chamberlin JC (1939b) New and little-known false scorpions from the Marquesas Islands (Arachnida: Chelonethida). Bulletin of the Bernice P. Bishop Museum 142: 207–215.

- Cullen CL, Harvey MS (2021) Two new species of the pseudoscorpion genus *Geogarypus* (Pseudoscorpiones: Geogarypidae) from northern Australia. *Records of the Western Australian Museum* 36(1): 71–78. <https://doi.org/10.18195/issn.0312-3162.36.2021.071-078>
- Dashdamirov S, Schawaller W (1993) Pseudoscorpions from Middle Asia, Part 2 (Arachnida: Pseudoscorpiones). *Stuttgarter Beiträge zur Naturkunde, Serie A* 496(14): 1–14.
- Dupon JF, Bonvallet J, Vigneron E, Gay JC, Morhange C, Ollier C, Peugniez G, Reitel B, Yon-Cassat F, Danard M, Laidet D (1993) *Atlas de la Polynésie Française*. Orstom, Paris, 250 pp.
- Gillespie RG (2002) Biogeography of spiders on remote oceanic islands of the Pacific: Archipelagos as stepping stones? *Journal of Biogeography* 29(5–6): 655–662. <https://doi.org/10.1046/j.1365-2699.2002.00714.x>
- Gillespie RG, Claridge EM, Goodacre SL (2008) Biogeography of the fauna of French Polynesia: Diversification within and between a series of hot spot archipelagos. *Philosophical Transactions of the Royal Society of London, Series B, Biological Sciences* 363(1508): 3335–3346. <https://doi.org/10.1098/rstb.2008.0124>
- Harvey MS (1988) Pseudoscorpions from the Krakatau Islands and adjacent regions, Indonesia (Chelicerata: Pseudoscorpionida). *Memoirs of the Museum of Victoria* 49(2): 309–353. <https://doi.org/10.24199/j.mmv.1988.49.13>
- Harvey MS (1990) New pseudoscorpions of the genera *Americhernes* Muchmore and *Cordylochernes* Beier from Australia (Pseudoscorpionida: Chernetidae). *Memoirs of the Museum of Victoria* 50(2): 325–336. <https://doi.org/10.24199/j.mmv.1990.50.06>
- Harvey MS (1992) The phylogeny and classification of the Pseudoscorpionida (Chelicerata: Arachnida). *Invertebrate Systematics* 6(6): 1373–1435. <https://doi.org/10.1071/IT9921373>
- Harvey MS (2000) From Siam to Rapa Nui – the identity and distribution of *Geogarypus longidigitatus* (Rainbow) (Pseudoscorpiones: Geogarypidae). *Bulletin - British Arachnological Society* 11(9): 377–384.
- Harvey MS, Leng MC (2008) The first troglomorphic pseudoscorpion of the family Olpiidae (Pseudoscorpiones), with remarks on the composition of the family. *Records of the Western Australian Museum* 24(4): 387–394. [https://doi.org/10.18195/issn.0312-3162.24\(4\).2008.387-394](https://doi.org/10.18195/issn.0312-3162.24(4).2008.387-394)
- Heurtault J (1979) Complément à la description de *Olpium pallipes* Lucas, 1845, type de la famille Olpiidae (Arachnides, Pseudoscorpions). *Revue Suisse de Zoologie* 86(4): 925–931. <https://doi.org/10.5962/bhl.part.82349>
- Hoff CC (1964) The pseudoscorpions from Jamaica. Part 3. The suborder Diplosphyronida. *Bulletin of the Institute of Jamaica* 10(3): 4–47.
- Judson MLI (2007) A new and endangered species of the pseudoscorpion genus *Lagynochthonius* from a cave in Vietnam, with notes on chelal morphology and the composition of the Tyrannochthoniini (Arachnida, Chelonethi, Chthoniidae). *Zootaxa* 1627(1): 53–68. <https://doi.org/10.11646/zootaxa.1627.1.4>
- Klausen FE (2005) The male genitalia of the family Atemnidae (Pseudoscorpiones). *The Journal of Arachnology* 33(3): 641–662. <https://doi.org/10.1636/H03-6.1>
- MacArthur RH, Wilson EO (1967) *The Theory of Island Biogeography*. Princeton University Press, Princeton, 203 pp.
- Mahnert V (1978a) Pseudoskorpione (ausgenommen Olpiidae, Garypidae) aus Congo-Brazzaville (Arachnida, Pseudoscorpiones). *Folia Entomologica Hungarica* 31(1): 69–133.

- Mahnert V (1978b) Contributions à l'étude de la faune terrestre des îles granitiques de l'archipel des Séchelles. Pseudoscorpiones. *Revue de Zoologie Africaine* 92(4): 867–888.
- Mahnert V (1981) Taxonomische Irrwege: *Olpium savignyi* Simon, *O. kochi* Simon, *O. bicolor* Simon (Pseudoscorpiones). *Folia Entomologica Hungarica* 42(34): 95–99.
- Miller SE (1996) Biogeography of Pacific insects and other terrestrial invertebrates: A status report. In: Keast A, Miller SE (Eds) *The Origin and Evolution of Pacific Island Biotas, New Guinea to Eastern Polynesia: Patterns and Processes*. Academic Publishers, Amsterdam, 463–475.
- Munroe EG (1996) Distributional patterns of Lepidoptera in the Pacific Islands. In: Keast A, Miller SE (Eds) *The Origin and Evolution of Pacific Island Biotas, New Guinea to Eastern Polynesia: Patterns and Processes*. Academic Publishers, Amsterdam, 275–295.
- Murthy VA, Ananthkrishnan TN (1977) Indian Chelonethi. *Oriental Insects Monograph* 4: 1–210.
- Novák J, Harvey MS (2018) New species and records of the pseudoscorpion genus *Geogarypus* (Pseudoscorpiones: Geogarypidae) from India, Sri Lanka and New Guinea. *Zootaxa* 4394(3): 417–427. <https://doi.org/10.11646/zootaxa.4394.3.7>
- Rainbow WJ (1897) The arachnid fauna of Funafuti. *Memoirs of the Australian Museum* 3(2): 105–126. <https://doi.org/10.3853/j.0067-1967.3.1897.491>
- Ramage T (2014) Les Fourmis de Polynésie française (Hymenoptera, Formicidae). *Bulletin de la Société Entomologique de France* 119(2): 145–176. <https://doi.org/10.3406/bsef.2014.29346>
- Ramage T (2017) Checklist of terrestrial and freshwater arthropods of French Polynesia (Chelicerata; Myriapoda; Crustacea; Hexapoda). *Zoosystema* 39(2): 213–225. <https://doi.org/10.5252/z2017n2a3>
- Rein JO (2023) *The Scorpion Files*. Trondheim: Norwegian University of Science and Technology. <https://www.ntnu.no/ub/scorpion-files/> [Accessed on 14.8.2023]
- Roderick G, Gillespie RG (2016) Arthropodes terrestres des îles Marquises: diversité et évolution. In: Galzin R, Duron SD, Meyer JY (Eds) *Biodiversité terrestre et marine des îles Marquises, Polynésie française*. Paris: Société française d'Ichtyologie, 526 pp.
- Vaucel J-A, Larréché S, Paradis C, Courtois A, Pujo J-M, Elenga N, Résière D, Caré W, de Haro L, Gallart J-C, Torrents R, Schmitt C, Chevalier J, Labadie M, Kallel H (2022) French Scorpionism (Mainland and Oversea Territories): Narrative Review of Scorpion Species, Scorpion Venom, and Envenoming Management. *Toxins* 14(10): 719. <https://doi.org/10.3390/toxins14100719>
- WPC (2022) *World Pseudoscorpiones Catalog*. Natural History Museum Bern. <http://wac.nmbe.ch> [Accessed on 14.8.2023]
- WSC (2023) *World Spider Catalog*. Version 24.5. Natural History Museum Bern. <http://wsc.nmbe.ch> [Accessed on 14.8.2023]

Two new species of *Hesperopenna* Medvedev & Dang, 1981 (Coleoptera, Chrysomelidae, Galerucinae) from Singapore

Jan Bezděk¹, David Kopr¹

¹ Mendel University in Brno, Department of Zoology, Fisheries, Hydrobiology and Apiculture, Zemědělská 1, 613 00 Brno, Czech Republic
Corresponding author: Jan Bezděk (bezdek@mendelu.cz)

Abstract

Two new species of *Hesperopenna* Medvedev & Dang, 1981 are described from Singapore: *H. temasek* **sp. nov.** and *H. bakeri* **sp. nov.** The specimens of both new species were collected by Charles Fuller Baker and found in the unidentified Galerucinae material deposited in the National Museum of Natural History, Smithsonian Institution, Washington, DC. *Hesperopenna temasek* **sp. nov.** is diagnosed by the black extreme elytral suture in the basal third, antennae longer than the body, the structure of the penis, and the last abdominal ventrite with two deep U-shaped incisions in females. *Hesperopenna bakeri* **sp. nov.** is diagnosed by the black tibia and first two tarsomeres, and the structure of the penis.

Key words: Charles Fuller Baker, Leaf beetles, Oriental Region, taxonomy



Academic editor: Caroline Chaboo
Received: 29 November 2023
Accepted: 26 January 2024
Published: 19 February 2024

ZooBank: <https://zoobank.org/A419AB2F-74A7-48CD-9F1B-4EC0F45E9847>

Citation: Bezděk J, Kopr D (2024) Two new species of *Hesperopenna* Medvedev & Dang, 1981 (Coleoptera, Chrysomelidae, Galerucinae) from Singapore. ZooKeys 1192: 45–56. <https://doi.org/10.3897/zookeys.1192.116516>

Copyright: © Jan Bezděk & David Kopr.
This is an open access article distributed under terms of the Creative Commons Attribution License ([Attribution 4.0 International – CC BY 4.0](https://creativecommons.org/licenses/by/4.0/)).

Introduction

The genus *Hesperopenna* Medvedev & Dang, 1981 was proposed for a single species *H. flava* Medvedev & Dang, 1981 from Vietnam (Medvedev and Dang 1981). The taxonomic history of *Hesperopenna* is complicated, as the species were placed in several genera. Bezděk (2013) redefined the genus, synonymised the genera *Liroetiella* Kimoto, 1989, *Martinella* Medvedev, 2000 and *Levnmia* Özdikmen, 2008 with *Hesperopenna*, and transferred species dispersed in *Calomicrus* Dillwyn, 1829, *Luperus* Geoffroy, 1762 and *Microlepta* Jacoby, 1886 to *Hesperopenna*. In the same paper (Bezděk 2013) the species of *Hesperopenna* were divided into six species groups based on the structure of male genitalia and external body characters. Meantime, additional new species were described by Medvedev (2013a, b) and Medvedev and Romantsov (2013). Bezděk (2016) revised the *Hesperopenna vietnamica* species group, made additional taxonomical changes in the genus, and pointed out that the classification of species groups is insufficient and re-evaluation is necessary. Recently, one additional species from Halmahera was described (Bezděk 2023).

Hesperopenna species are characterised by a combination of filiform antennae, the anterior margin of pronotum unbordered, the pronotum regularly convex with a shallow oblique impression behind the anterior angles, the procoxal cavities open, the apices of the meso- and metatibiae with a spine. Additionally, metatarsomere I is about as long as two following metatarsomeres combined, the claws are appendiculate, and usually, the aedeagus has a complicated structure (Bezděk 2013, 2016). The dorsum of almost all known species is completely pale; black dorsal coloration can be found only in certain species (see Bezděk 2023). The biology and immature stages of *Hesperopenna* are unknown.

In general appearance, *Hesperopenna* species may resemble some Oriental genera/species of the section Monoleptites (e.g., *Monolepta* Chevrolat, 1836, *Ochrlea* Clark, 1865, *Paleosepharia* Laboissière, 1936, etc.) but the genus can be easily distinguished by the shorter metatarsomere I (typically elongated in Monoleptites). Also, some species of *Erganoides* Jacoby, 1903 are similar mainly to smaller species of *Hesperopenna*. However, the pronotum of *Erganoides* species is regularly convex, without any oblique impression behind anterior angles.

While studying undetermined Galerucinae material borrowed from the USNM, we discovered two new species of *Hesperopenna* from Singapore. The specimens were collected by Charles Fuller Baker (1872–1927), an American entomologist, botanist and agronomist. In 1912 he moved to the Philippines and was Professor and Dean of the College of Agriculture at Los Baños. During his long stay in the Philippines, he left only once and that was for a year's leave of absence in 1917–1918 to become assistant director of the Botanic Gardens at Singapore. According to his long-standing will, the main insect collection was bequeathed to the U.S. National Museum (Essig 1927). The type series of both new species were most likely collected in the years 1917–1918 during his stay in Singapore.

Materials and methods

All measurements were made using an ocular grid mounted on an MBS-10 stereomicroscope (at 16× magnification for the body length and 32× magnification for the remaining measurements). Photographs of specimens were taken with a Canon 800D digital camera with a Canon MP-E 65 mm objective. Images of the same objects at different focal planes were combined using Helicon Focus 8 software. The base distribution map was downloaded from <https://d-maps.com/>. The pictures were edited with Corel Photopaint 12.

Specimens studied herein are deposited at the following institutes and collections:

JBCB Jan Bezděk collection, Brno, Czech Republic;
USNM National Museum of Natural History, Smithsonian Institution, Washington, DC, USA (Alexander S. Konstantinov).

Exact label data are cited for all type specimens of described species; a double slash (//) divides the data on different labels and a single slash (/) divides the data in different rows.

Taxonomy

Hesperopenna temasek Bezděk & Kopr, sp. nov.

<https://zoobank.org/930B1890-E499-4A45-9687-C9B1A0A66D8B>

Figs 1A–D, 2

Type locality. Singapore, approx. 1°17'N, 103°51'E.

Type material. Holotype: ♂ (USNM), “Singapore / Coll. Baker [printed white label]”. **Paratypes:** 4 ♂♂ 5 ♀♀ (USNM, 1 ♂ 1 ♀ in JBCB), same label as holotype; 1 ♂ 1 ♀ (USNM), “Singapore / Coll. Baker [printed white label] // 17369 [handwritten white label]”. The specimens are provided with additional printed red label: “HOLOTYPUS, [or PARATYPUS] / *Hesperopenna* / *temasek* sp. nov., / J. Bezděk & / D. Kopr det. 2023 [printed red label]”.

Description. Body length: ♂♂: 3.6–4.3 mm (holotype 4.3 mm), ♀♀: 3.5–4.3 mm. Body elongate oval, moderately convex, and glabrous. Body brown, except dark apices and outer basal parts of mandibles, furrows around antennal socket and frontal tubercles, extreme elytral suture in basal third, outer extreme margins of epipleura in basal third, and mesepisterna. Antennomeres brown, darkened apical part of each antennomere. Legs with slightly infusate last two tarsomeres.

Male (holotype, Fig. 1A, B). Head with transverse rectangular labrum, with rounded anterior angles, anterior margin emarginated in middle, surface with six pores in transverse row, each bearing long, pale seta. Mandibles slightly enlarged, well visible (Fig. 2I). Anterior part of head flat, lustrous and nearly glabrous, with several setae along anterior margin and close to eyes, anterior margin straight. Interantennal space extremely narrow, 0.28 times as wide as transverse diameter of antennal socket. Interocular space 1.33 times as wide as transverse diameter of eye. Frontal tubercles subtriangular, basal and oblique sides bent, moderately elevated, dull, and separated by thin, shallow groove. Vertex glabrous, lustrous, impunctate, separated from frontal tubercles by widely bent furrow. Antennae filiform, 1.21 times as long as body, length ratios of antennomeres in sequence from first equals 100-19-50-75-69-69-62-62-62-44-56 (100 = 0.8 mm). Antennomeres I–II almost glabrous, with several long setae, III–XI densely covered with short recumbent setae mixed with sparse longer setae.

Pronotum transverse, 1.47 times as wide as long, widest in middle. Surface lustrous, glabrous, densely covered with small fine punctures, moderately convex, with shallow impressions from anterior angles parallel with anterior margin. Anterior margin straight, lateral margins rounded, posterior margin widely rounded. Anterior margin unbordered, lateral and posterior margins distinctly bordered. Anterior angles swollen, posterior angles obtusangulate, pointed, each angle with setigerous pore bearing long seta. Scutellum small, triangular with rounded tip, impunctate, and glabrous.

Elytra 1.35 times as long as wide (measured at widest, in posterior third) and 0.67 times as long as body. Surface glabrous, densely covered with very fine, confused punctures. Humeral calli developed. Epipleura lustrous, glabrous, smooth, widest at anterior third, gradually narrowed towards elytral apex. Macropterous.

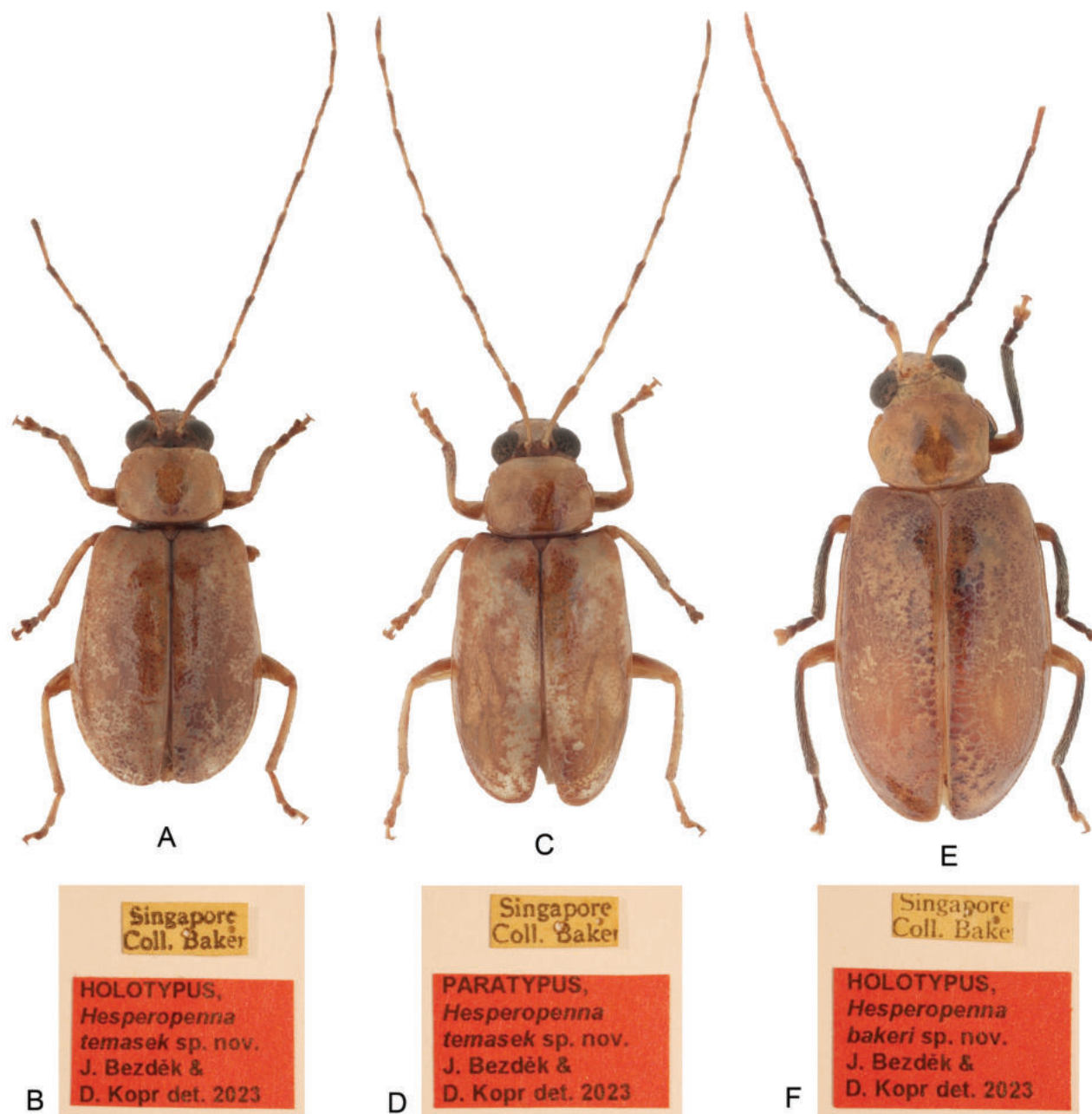


Figure 1. Habitus, dorsal view **A** *Hesperopenna temasek* sp. nov., holotype, male **B** *H. temasek* sp. nov., holotype, labels **C** *H. temasek* sp. nov., paratype, female **D** *H. temasek* sp. nov., paratype, labels **E** *H. bakeri* sp. nov., holotype, male **F** *H. bakeri* sp. nov., holotype, labels.

Procoxal cavities opened behind. Posterior margin of last abdominal ventrite widely concave, surface with distinct transverse impression along posterior margin. Abdomen covered with short sparse setae, posterior margin of last abdominal ventrite with longer setae. All legs densely covered with short recumbent setae. Apices of all tibiae with spine. Protarsomere I elongated triangular, slightly wider than small and triangular protarsomere II, length ratio of protarsomeres I–III and V equals 100-20-20-80 (100 = 0.25 mm). Mesotarsomere I elongated triangular, slightly wider than small and triangular mesotarsomere II, length ratio of mesotarsomeres I–III and V equals 100-50-75-125 (100 = 0.20 mm). Metatarsomere I long, narrow, slightly wider apically, length

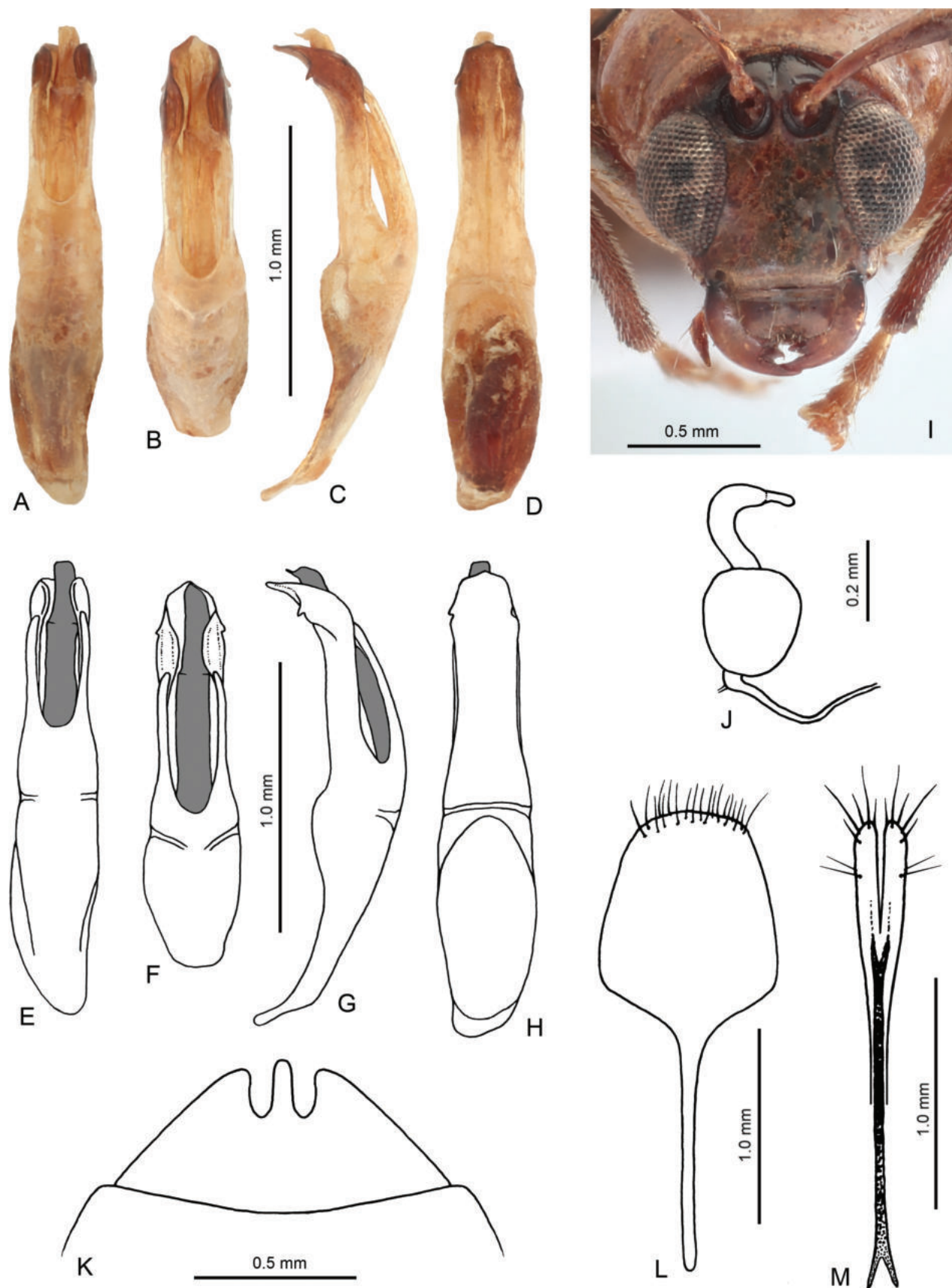


Figure 2. Diagnostic characters of *Hesperopenna temasek* sp. nov. **A** penis, dorsal view **B** penis, apical part **C** penis, lateral view **D** penis, ventral view **E** penis, dorsal view, drawing **F** penis, apical part, drawing **G** penis, lateral view, drawing **H** penis, ventral view, drawing **I** head **J** spermatheca **K** last visible abdominal ventrite, female **L** sternite VIII, female **M** gonocoxae.

ratio of metatarsomeres I–III and V equals 100–29–43–57 (100 = 0.4 mm). Claws appendiculate.

Penis (Fig. 2A–H) elongate, 5.90 times as long as wide, subparallel, with slightly wider basal half. Apical half forming ventral groove-like plate and two narrow dorsolateral processes separated by large and deep U-shaped incision. In lateral view, apical part of ventral plate bent down forming curtain-like plate with very small sharp denticle. Penis with one long robust internal sclerite placed in ventral groove-like plate.

Female (Fig. 1C–D). Last abdominal ventrite with two deep U-shaped incisions separated by narrow subtriangular process (Fig. 2K). Apex of pygidium with small semicircular incision. Spermatheca with spherical nodulus and C-shaped cornu terminating by short narrow appendix (Fig. 2J). Sternite VIII shovel-like, with apical margin moderately rounded, with setae cumulated on and along apical margin, tignum narrow, straight, 1.13 times as long as sternite VIII (Fig. 2L). Gonocoxae long, 8.80 times as long as wide, apical third wider, subparallel, with split apex bearing several long setae, basal two third narrow, base bifurcated (Fig. 2M).

Differential diagnosis. Dark color on dorsum is rare in *Hesperopenna* species and is known in a few species: head in *H. nigriceps* (Kimoto, 2004) from eastern India, head and pronotum in *H. nigricollis* (Kimoto, 1989) from Thailand, head and pronotum in some specimens of *H. bacboensis* (Medvedev, 2013) from Vietnam, head and scutellum in some specimens of *H. thailandica* (Kimoto, 1989) from Thailand, Laos and China (Yunnan), whole elytra in *H. gilolo* Bezděk, 2023 from Halmahera, and, finally, elytra with a black extreme lateral margin in basal half in *H. zofka* Bezděk, 2013 from Indonesia (Java, Bali). *Hesperopenna temasek* sp. nov. has black frontal tubercles and furrows around antennal sockets, extreme elytral suture in basal third, outer extreme margins of epipleura in basal third, and mesepisterna. The antennae are c. 1.20 times as long as body. Most of *Hesperopenna* species have antennae slightly shorter than body or at least slightly longer (c. 1.05 times as long as body). Longer antennae are known in *H. pallida* species group (sensu Bezděk 2013), however this group is awaiting revision. Nevertheless, the penis of *H. temasek* sp. nov. with two narrow dorsolateral processes separated by large and deep U-shaped incision and with very small sharp denticles on apicolateral curtain-like plates, is completely different in comparison with very simple structure of penis in *H. pallida* species group. Mandibles (Fig. 2I) are somewhat enlarged, better visible than in other *Hesperopenna* species.

The females are characterized by the shape of last abdominal ventrite with two deep U-shaped incisions separated by narrow subtriangular process (Fig. 2K). The females of the vast majority of *Hesperopenna* species have the posterior margin of the last abdominal ventrite entire or with one more or less shallow median emargination. The only species with similarly structured last abdominal ventrite in females is *H. nigricollis* (Kimoto, 1989) from Thailand.

Distribution. Singapore.

Etymology. Temasek is an early recorded name of a settlement on the site of modern Singapore. Noun in apposition.

***Hesperopenna bakeri* Bezděk & Kopr, sp. nov.**

<https://zoobank.org/12478282-4E4D-4385-B1FC-3782FCABCBBE>

Figs 1E–F, 3

Type locality. Singapore, approx. 1°17'N, 103°51'E.

Type material. Holotype: ♂ (USNM), “Singapore / Coll. Baker [printed white label]”. **Paratypes:** 2 ♀♀ (USNM), same label as holotype. The specimens are provided with additional printed red label: “HOLOTYPUS, [or PARATYPUS] / *Hesperopenna* / *bakeri* sp. nov., / J. Bezděk & / D. Kopr det. 2023 [printed red label]”.

Description. Body length: ♂: 5.6 mm (holotype), ♀♀: 5.1–5.8 mm. Body elongate oval, moderately convex, and glabrous. Body orange brown, except darkened apices of mandibles. Antennomeres I–II orange, III–VI black, VII dark brown, VIII–XI brown. Legs brown with black tibia and first two tarsomeres.

Male (holotype, Fig. 1E–F). Head with transverse rectangular labrum, with rounded anterior angles, anterior margin straight and shallowly emarginated in middle, surface with six pores in transverse row, each bearing long, pale seta. Anterior part of head slightly convex, lustrous and nearly glabrous, with several setae along anterior margin and close to eyes, anterior margin slightly concave. Interantennal space narrow, 0.71 times as wide as transverse diameter of antennal socket. Interocular space 1.35 times as wide as transverse diameter of eye. Frontal tubercles transverse, outer parts narrow and transverse, subtriangular medially, moderately elevated, lustrous, and separated by thin, shallow groove. Vertex glabrous, lustrous, impunctate, separated from frontal tubercles by shallow bent line. Antennae filiform, 0.80 times as long as body, length ratios of antennomeres in sequence from first equals 100-26-52-87-87-87-87-83-69-83 (100 = 0.6 mm). Antennomeres I–II almost glabrous, with several long setae, III–XI densely covered with short recumbent setae mixed with sparse longer setae.

Pronotum transverse, 1.35 times as wide as long, widest in middle. Surface lustrous, glabrous, covered with indistinct punctures, moderately convex, with shallow impressions from anterior angles parallel with anterior margin. Anterior margin straight, lateral margins rounded, posterior margin moderately rounded. Anterior margin unbordered, lateral and posterior margins distinctly bordered. Anterior angles distinctly swollen, posterior angles obtusely angulate, each angle with setigerous pore bearing long seta. Scutellum small, triangular with rounded apex, impunctate, and glabrous.

Elytra 1.60 times as long as wide (measured at widest, in posterior third) and 0.71 times as long as body. Surface glabrous except very scarce short setae on apical slopes and on lateral and apical margins, densely covered with very small, confused punctures. Humeral calli developed. Epipleura lustrous, glabrous, smooth, widest at anterior third, gradually narrowed towards elytral apex. Macropterous.

Procoxal cavities open behind. Last abdominal ventrite with well visible impressed furrows forming subtriangular plate, posterior margin of last abdominal ventrite nearly straight. Abdomen covered with sparse setae, plate on last abdominal ventrite with longer and denser setae (Fig. 3L). All legs densely covered with short recumbent setae. Apices of meso- and metatibiae with spine. Protarsomere I elongated subtriangular, slightly wider than small and triangular

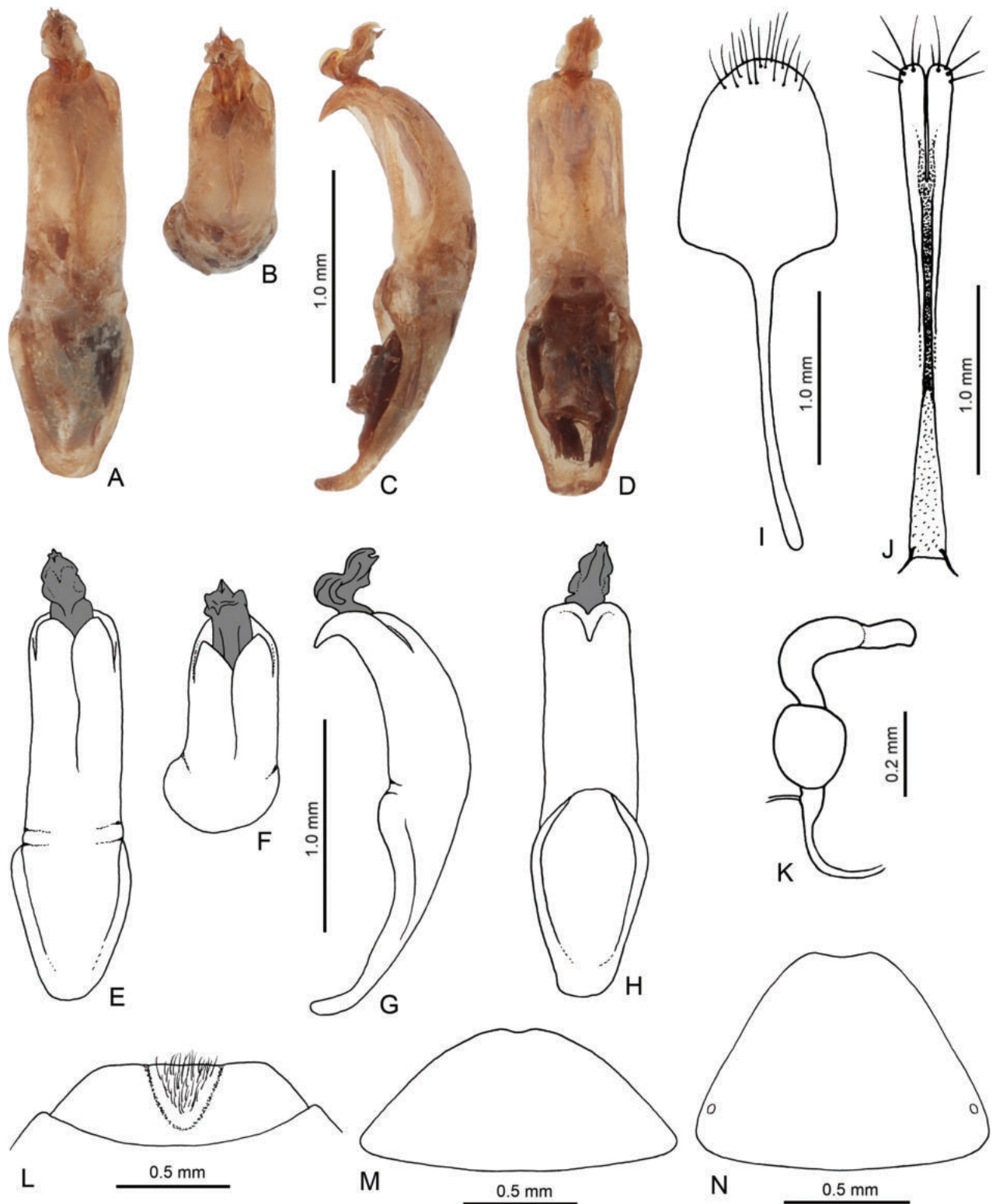


Figure 3. Diagnostic characters of *Hesperopenna bakeri* sp. nov. **A** penis, dorsal view **B** penis, apical part **C** penis, lateral view **D** penis, ventral view **E** penis, dorsal view, drawing **F** penis, apical part, drawing **G** penis, lateral view, drawing **H** penis, ventral view, drawing **I** sternite VIII, female **J** gonocoxae **K** spermatheca **L** last visible abdominal ventrite, male **M** last visible abdominal ventrite, female **N** pygidium, female.

protarsomere II, length ratio of protarsomeres I–III and V equals 100-66-66-111 (100 = 0.20 mm). Mesotarsomere I elongated triangular, as wide as triangular mesotarsomere II, length ratio of mesotarsomeres I–III equals 100-50-41

(100 = 0.25 mm) (mesotarsomere V missing). Metatarsomere I long, narrow, slightly wider apically, length ratio of metatarsomeres I–III and V equals 100-41-35-65 (100 = 0.4 mm). Claws appendiculate.

Penis (Fig. 3A–H) elongate, parallel, 3.90 times as long as wide, dorsal side with two partly overlapping plates anteriorly forming two widely rounded processes. Apex triangular, strongly bent downwards. In lateral view, penis moderately bent. Penis with one long robust internal sclerite with apex bent upwards and covered with complicated structure.

Female. Last abdominal ventrite without impressed furrows forming subtriangular plate, posterior margin widely rounded with very small apical emargination (Fig. 3M). Apex of pygidium with wide shallow emargination (Fig. 3N). Spermatheca with spherical nodulus and C-shaped cornu, narrowed basally, terminated by wide appendix (Fig. 3K). Sternite VIII shovel-like, with widely rounded apical margin, with setae cumulated on and along apical margin, tignum narrow, slightly bent, 1.33 times as long as sternite VIII (Fig. 3I). Gonocoxae long, 9.50 times as long as wide, distinctly narrowed in middle part, with split apex, apical part with several long setae, base with two short thin processes (Fig. 3J).

Differential diagnosis. Having brown legs with black tibia and first two tarsomeres *Hesperopenna bakeri* sp. nov. is similar to *H. tibialis* (Kimoto, 1989) from Laos, Thailand and Peninsular Malaysia, and *H. zofka* Bezděk, 2013 from Indonesia (Java, Bali) from *Hesperopenna medvedevi* species group (see Bezděk 2013), and also to *H. vietnamica* (Medvedev, 2000), and some specimens of *H. thailandica* (Kimoto, 1989) with black tibia from *Hesperopenna vietnamica* species group (see Bezděk 2016). *Hesperopenna tibialis* and *H. zofka* are large species with body length more than 6.8 mm while the body length of *H. bakeri* sp. nov. is 5.6–5.8 mm. *Hesperopenna bakeri* sp. nov. has less transverse pronotum, 1.35 times as wide as long, while pronota of *H. vietnamica* and *H. thailandica* are more transverse, 1.75–1.85 times as wide as long. Penis of *H. bakeri* sp. nov. (Fig. 3A–H) has dorsal side with two wide partly overlapping plates, the apex is triangular, strongly bent downwards, and endophallic sclerite is robust. Penis of *H. tibialis* and *H. zofka* is robust, with two endophallic sclerites (one very large, with spoon-like apex and distinct ridges ventrally, second thin, usually hidden inside the aedeagus – see figs in Bezděk 2013), and that of *H. vietnamica* and *H. thailandica* has two thin lateral processes with very deep incision between them, ventral side of penis apically with hook-like process, and endophallic sclerite thin (see figs in Bezděk 2016).

Distribution. Singapore.

Etymology. Dedicated to Charles Fuller Baker (1872–1927), an American entomologist, botanist and agronomist, who collected the type series.

Discussion

Hesperopenna currently includes 39 species (Nie et al. 2017; Bezděk 2023, present paper). Most known species occur in continental Southeast Asia (Vietnam, Laos, Thailand, Myanmar, Eastern India, and continental Malaysia). Only four species extend into the southernmost parts of the Palearctic Region (Nepal, Bhutan and Yunnan). The occurrence of *Hesperopenna* in the Sunda

Islands is very little studied. Two species are known from Sumatra and one from Java and Bali, but it is assumed that there will be many more species in the Sunda Islands. *Hesperopenna* species are also confirmed in the Philippines and the island of Borneo, with several hitherto undescribed species awaiting the descriptions. The easternmost record of *Hesperopenna* is from Halmahera in the Maluku archipelago (Bezděk 2023). For a distributional map of the genus *Hesperopenna* see Fig. 4.

The depositories of large museums usually contain a large amount of unprocessed and undetermined material (Löbl 2023), often from biotopes that have completely changed their character over the years or disappeared outright. The discovery of more than a hundred-year-old specimens of two new species in museum material is not surprising. Eleven years ago, the average time span between species discovery and description was found to be 21 years (Fontaine et al. 2012), however, it is significantly longer for some insects (Löbl 2023). The existence of completely new species in the depository clearly underlines the importance of natural history museum collections for preserving evidence of global biodiversity. We can only hope that both newly described species will also be re-discovered in the wild, and that this paper does not describe species that are new to science but already extinct (compare e.g., Rossini et al. 2021).



Figure 4. Distributional map of the genus *Hesperopenna*. The countries and regions with confirmed occurrence are colored in grey.

Acknowledgements

We would like to thank Alexander S. Konstantinov (USNM) for the opportunity to study the Galerucinae collection at the Smithsonian Institution. We are also obliged to the three reviewers, Chi-Feng Lee, Maurizio Biondi and Kaniyarikkal D. Prathapan, whose suggestions and additions helped to significantly improve the quality of the manuscript.

Additional information

Conflict of interest

The authors have declared that no competing interests exist.

Ethical statement

No ethical statement was reported.

Funding

No funding was reported.

Author contributions

Conceptualization: JB. Data curation: JB. Investigation: JB. Methodology: JB. Visualization: JB, DK. Writing - original draft: JB. Writing - review and editing: DK.

Author ORCIDs

Jan Bezděk  <https://orcid.org/0000-0003-4358-7211>

David Kopr  <https://orcid.org/0000-0003-2466-9609>

Data availability


All of the data that support the findings of this study are available in the main text.

References

- Bezděk J (2013) Revision of the genus *Hesperopenna* (Coleoptera: Chrysomelidae: Galerucinae). I. Generic redescription, definition of species groups and taxonomy of *H. medvedevi* species group. *Acta Entomologica Musei Nationalis Pragae* 53: 715–746.
- Bezděk J (2016) Revision of the genus *Hesperopenna* Medvedev et Dang, 1981 (Coleoptera: Chrysomelidae: Galerucinae). II. *H. vietnamica* species group and new taxonomical changes. *Studies and Reports. Taxonomical Series* 12: 7–27.
- Bezděk J (2023) *Hesperopenna gilolo* sp. nov., the easternmost record of the genus from Halmahera, Indonesia (Coleoptera: Chrysomelidae: Galerucinae). *Zootaxa* 5277(3): 581–584. <https://doi.org/10.11646/zootaxa.5277.3.10>
- Essig EO (1927) Obituary: Charles Fuller Baker. *Journal of Economic Entomology* 20(5): 748–754. <https://doi.org/10.1093/jee/20.5.748>
- Fontaine B, Perrard A, Bouchet P (2012) 21 years of shelf life between discovery and description of new species. *Current Biology* 22(22): R943–R944. <https://doi.org/10.1016/j.cub.2012.10.029>
- Geoffroy EL (1762) *Histoire abrégée des insectes qui se trouvent aux environs de Paris; dans laquelle ces animaux sont rangés suivant un ordre méthodique. Tome premier.* Durand, Paris, [xxxviii +] 523 pp. [10 pls] <https://doi.org/10.5962/bhl.title.154842>

- Jacoby M (1886) Descriptions of new genera and species of phytophagous Coleoptera from the Indo-Malayan and Austra-Malayan subregions, contained in the Genoa Civic Museum. Third Part. *Annali del Museo Civico di Storia Naturale di Genova* 24: 41–121.
- Kimoto S (1989) Chrysomelidae (Coleoptera) of Thailand, Cambodia, Laos and Vietnam. IV. Galerucinae. *Esakia* 27: 1–241. <https://doi.org/10.5109/2511>
- Kimoto S (2004) New or little known Chrysomelidae (Coleoptera) from Nepal, Bhutan and the northern territories of Indian subcontinent. *Bulletin of the Kitakyushu Museum of Natural History and Human History, Series A* 2: 47–63.
- Löbl I (2023) Assessing Earth's biotic diversity in natural history museums – gone with the wind? *Phegea* 51(2): 50–51. <https://doi.org/10.6084/m9.figshare.22722733>
- Medvedev LN (2000) Chrysomelidae (Coleoptera) of Laos from the collection of the Hungarian Natural History Museum. *Annales Historico-Naturales Musei Nationalis Hungarici* 92: 161–182.
- Medvedev LN (2013a) New species of *Calomicrus* Stephens, 1834 (Chrysomelidae: Galerucinae) from China and Indochina. *Russian Entomological Journal* 22: 37–42.
- Medvedev LN (2013b) New and interesting Chrysomelidae (Insecta: Coleoptera) from the collection of the Naturkundemuseum Erfurt. *Vernate* 32: 415–420.
- Medvedev LN, Dang DT (1981) Novye rody i vidy zhukov-listoedov podsem. Galeruciane (Coleoptera, Chrysomelidae) iz Vietnama [New genera and species of leaf-beetles of the subfamily Galerucinae (Coleoptera, Chrysomelidae) from Vietnam]. *Entomologicheskoe Obozrenie* 60: 629–635.
- Medvedev LN, Romantsov P (2013) New and poorly known Chrysomelidae (Coleoptera) from South-East Asia. *Caucasian Entomological Bulletin* 9(1): 137–140. <https://doi.org/10.23885/1814-3326-2013-9-1-137-140>
- Nie RE, Bezděk J, Yang X-K (2017) How many genera and species of Galerucinae s. str. do we know? Updated statistics (Coleoptera, Chrysomelidae). *ZooKeys* 720: 91–102. <https://doi.org/10.3897/zookeys.720.13517>
- Özdikmen H (2008) Substitute names for some preoccupied leaf beetles genus group names described by L. N. Medvedev (Coleoptera: Chrysomelidae). *Munis Entomology & Zoology* 3(2): 643–647.
- Rossini M, Vaz-de-Mello FZ, Montreuil O, Porch N, Tarasov S (2021) Extinct before discovered? *Epactoides giganteus* sp. nov. (Coleoptera, Scarabaeidae, Scarabaeinae), the first native dung beetle to Réunion island. *ZooKeys* 1061: 75–86. <https://doi.org/10.3897/zookeys.1061.70130>

A new odorous frog species of *Odorrana* (Amphibia, Anura, Ranidae) from Guizhou Province, China

Shi-Ze Li^{1,2*}, Ji-Jun Chen^{3*}, Hai-Jun Su⁴, Jing Liu^{1,4}, Xiu-Jun Tang³, Bin Wang² 

1 Department of Food Science and Engineering, Moutai Institute, Renhuai 564500, China

2 Chengdu Institute of Biology, Chinese Academy of Sciences, Chengdu 610041, China

3 Leigongshan National Nature Reserve Administration, Leishan 557100, China

4 College of Forestry, Guizhou University, Guiyang 550025, China

Corresponding authors: Bin Wang (wangbin@cib.ac.cn); Xiu-Jun Tang (tangxiujun1030@126.com)

Abstract

The frog genus *Odorrana* is distributed across east and southeastern Asia. Based on morphological differences and molecular phylogenetics, a new species of the genus occurring from Leigong Mountain in Guizhou Province, China is described. Phylogenetic analyses based on DNA sequences of the mitochondrial *12S rRNA*, *16S rRNA*, and *ND2* genes supported the new species as an independent lineage. The uncorrected genetic distances between the *12S rRNA*, *16S rRNA*, and *ND2* genes between the new species and its closest congener were 5.0%, 4.9%, and 16.3%, respectively. The new species is distinguished from its congeners by a combination of the following characters: body size moderate (SVL 39.1–49.4 mm in males, 49.7 mm in female); head width larger than head length; tympanum distinctly visible; small rounded granules scattered all over dorsal body and limbs; dorsolateral folds absent; heels overlapping when thighs are positioned at right angles to the body; tibiotarsal articulation reaching the level between eye to nostril when leg stretched forward; vocal sacs absent in male and nuptial pads present on the base of finger I.

Key words: Leigong Mountain, molecular phylogenetic analysis, morphology, new species



Academic editor: Angelica Crottini

Received: 20 October 2023

Accepted: 24 January 2024

Published: 19 February 2024

ZooBank: <https://zoobank.org/FC0F8160-F924-4006-B2DA-86713FB1252B>

Citation: Li S-Z, Chen J-J, Su H-J, Liu J, Tang X-J, Wang B (2024) A new odorous frog species of *Odorrana* (Amphibia, Anura, Ranidae) from Guizhou Province, China. ZooKeys 1192: 57–82. <https://doi.org/10.3897/zookeys.1192.114315>

Copyright: © Shi-Ze Li et al.

This is an open access article distributed under terms of the Creative Commons Attribution License ([Attribution 4.0 International – CC BY 4.0](https://creativecommons.org/licenses/by/4.0/)).

Introduction

The odorous frogs of the genus *Odorrana* Fei, Ye & Huang, 1990 inhabit mountain streams at elevations of about 200–2000 m and can also be found on rocks or branches near the riverbed, ranging from Japan, southern China and Indochina, northeastern India, Myanmar and Thai-Malay Peninsula, Java, Sumatra, and Borneo (Frost 2024). Phylogenetic studies indicate that *Odorrana* is monophyletic (Chen et al. 2013). The genus currently consists of 65 species (Frost 2024), of which 42 occur in China and 27 species are endemic to China (Fei et al. 2012; Amphibia China 2024; Frost 2024).

Systematic arrangements in this genus have been controversial. Ye and Fei (2001) suggested four species groups (*O. andersonii*, *O. kuangwuensis*, *O. schmackeri*, and *O. livida* species groups) based on a morphological study. Fei et al. (2005) established two subgenera (*Odorrana* Fei, Ye & Huang, 1990 and

* These authors have contributed equally to this work.

Bamburana Fei, Ye, Huang, Jiang & Xie, 2005) within *Odorrana*. Molecular phylogenetic studies support the division of species groups within *Odorrana* but not the two subgenera (Che et al. 2007). Subsequently, Fei et al. (2009) divided the Chinese *Odorrana* species into six species groups (*O. tormota*, *O. taiwaniana*, *O. graminea*, *O. margaretae*, *O. schmackeri*, and *O. andersonii* species groups). These divisions have been accepted by some researchers (Pham et al. 2016a, b; Li et al. 2018a) but others have rejected the monophyly of the *O. margaretae*, *O. schmackeri*, and *O. andersonii* species groups (Chen et al. 2013). The species diversity in the genus is also indicated as underestimated in these phylogenetic frameworks.

Guizhou Province is one of the areas of the most abundant amphibians in China, and in the last five years a series of new frog species have been described from this region (Frost 2024; Amphibia China 2024). During fieldwork in Leigongshan Nature Reserve, Leishan County, Guizhou Province, China, between March to October 2023, seven *Odorrana* specimens were collected. Morphologically, these specimens most closely *O. huanggangensis* Chen, Zhou & Zheng, 2010, and *O. wuchuanensis* (Xu, 1983), but differs from these two species by the presence of small, rounded granules scattered all over the dorsal body and limbs, and the vocal sacs are absent in the male. To further distinguish these specimens, we conducted phylogenetic analyses based on mitochondrial DNA and morphological comparisons. All analyses consistently indicated that the specimens from Leigongshan Nature Reserve are a new taxon, described herein as a new species.

Materials and methods

Sampling

Seven specimens (♀ $n = 1$; ♂ $n = 6$) of the unnamed taxon were collected by hand from Leigongshan Nature Reserve, Guizhou Province, China (Fig. 1) and the field work was approved by the Management Office of the Leigongshan Nature Reserve (project number: P5226002023000019). The Animal Care and Use Committee of Guizhou University provided full approval for this research (Number: EAE-GZU-2022-T115). All specimens were fixed in 10% buffered formalin for 10 h, and then later transferred to 75% ethanol. Tissue samples were preserved separately in 95% prior to fixation. Specimens collected in this work were deposited in Moutai Institute (MT), Guizhou Province, China. In addition, 12 tissue samples containing two *Odorrana fengkaiensis* Wang, Lau, Yang, Chen, Liu, Pang & Liu, 2015, one *O. hainanensis* Fei, Ye & Li, 2001, one *O. bacboensis* (Bain, Lathrop, Murphy, Orlov & Ho, 2003), three *O. ichangensis* Chen, 2020, and two *O. hejiangensis* (Deng & Yu, 1992) were used (Table 1).

Molecular data and phylogenetic analyses

DNA was extracted from muscle tissue using a DNA extraction kit from Tiangen Biotech Co., Ltd. (Beijing). All samples were sequenced for three mitochondrial genes, partial 12S ribosomal RNA gene (12S *rRNA*), 16S ribosomal RNA gene (16S *rRNA*), and NADH dehydrogenase subunit 2 (*ND2*). The primers used for 12S *rRNA* were P1 (5'-CCAGGCTTTACTTTATGC-3') and P2 (5'-GCGATTAAGTTGGGTAACGC-3') following Kocher et al. (1989); for 12S *rRNA* were P7 (5'-CGCCTGTTTACCAAAAACAT-3') and P8 (5'-CCGGTCTGAACTCAGATCAC-

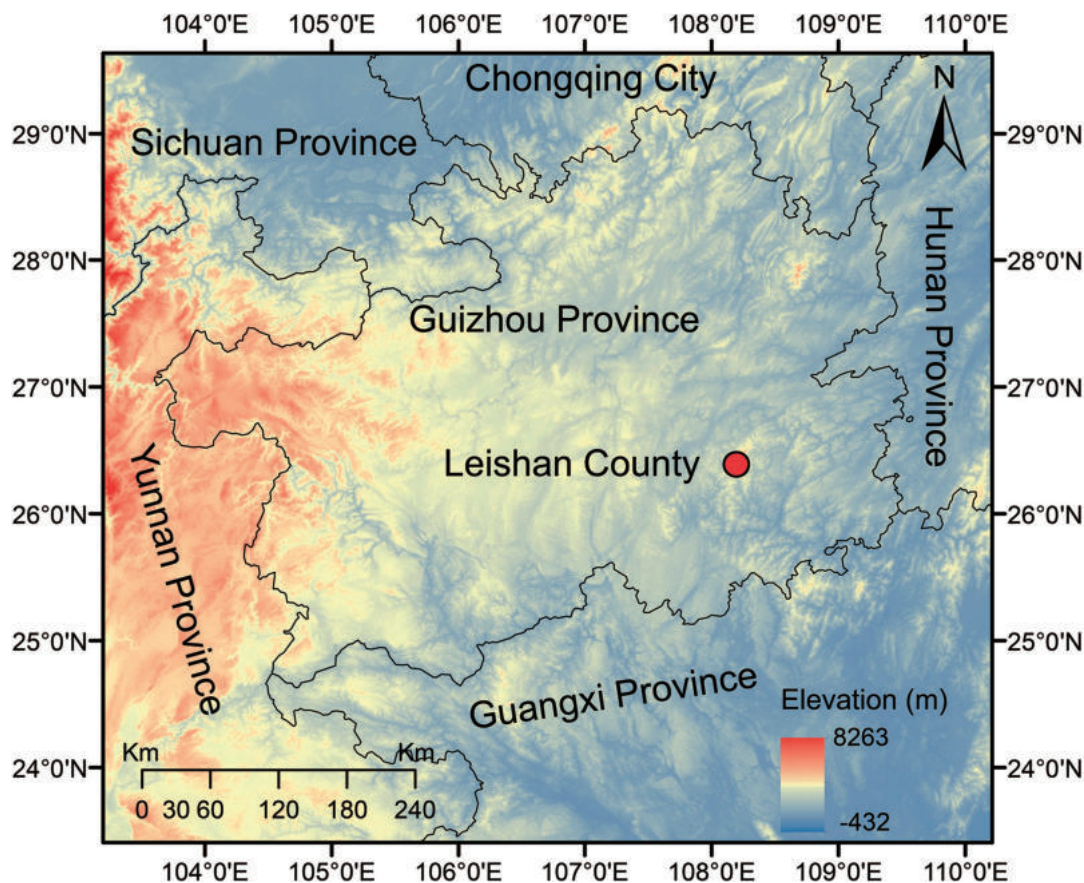


Figure 1. Geographical location of the type locality of *Odorrana leishanensis* sp. nov., Leigongshan Nature Reserve, Leishan County, Guizhou Province, China.

GT') following Simon et al. (1994); and for *ND2* were Gln-LND2 (5'-CCCTTTG-CACTTCCTTTATGC-3') and Ala-HND2 (5'-GGCCTGAGTTGCATTCATG-3') following Li et al. (2015). PCR amplification reactions were performed in a 30 μ l volume contains 1 \times High-Fidelity Master Mix (Chengdu TSINGKE Biological Technology Co. Ltd.) 15 μ l, ddH₂O 10 μ l, 0.5 μ M Forward primer 2 μ l, 0.5 μ M Revers primer 2 μ l and 4.25 μ g/ μ l DNA 1 μ l, reaction with the following cycling conditions: an initial denaturing step at 95 $^{\circ}$ C for 4 min; 36 cycles of denaturing at 95 $^{\circ}$ C for 40 s, annealing at 47 $^{\circ}$ C (for *ND2*)/57 $^{\circ}$ C (for *12S* and *16S*) for 40 s and extending at 72 $^{\circ}$ C for 70 s, and a final extending step of 72 $^{\circ}$ C for 10 min. PCR products were purified with spin columns and then were sequenced with both forward and reverse primers, same as for the PCR. Sequencing was conducted using an ABI Prism 3730 automated DNA sequencer in Chengdu TSINGKE Biological Technology Co. Ltd. (Chengdu, China). All sequences were deposited in GenBank (see Table 1 for GenBank accession numbers). For phylogenetic analyses and genetic divergence analyses, we downloaded available corresponding sequence data for all related species from GenBank according to previous studies (Chen et al 2013; Li et al 2018a; for GenBank accession no. refer to Table 1).

86 Sequences were assembled and aligned using the Clustalw module in BioEdit v. 7.0.9.0 (Hall 1999) with default settings. The datasets were checked by eye and revised manually if necessary. Based on the *12S rRNA*, *16S rRNA*, *ND2*, and *12S rRNA + 16S rRNA + ND2* concatenated dataset, phylogenetic analyses were conducted using maximum likelihood (ML) and Bayesian inference (BI) methods, implemented in PhyML 3.0 (Guindon et al. 2010) and MrBayes

Table 1. Information of samples used in molecular phylogenetic analyses in this study; a slash (/) indicates information absent.

ID	Species	Locality	Voucher number	GenBank accession number			Citation
				12s	16s	ND2	
1	<i>Odorrana leishanensis</i> sp. nov.	Leigongshan Nature Reserve, Leishan, Guizhou, China	MT LS2023080610	OR879770	OR879754	OR863727	this study
2	<i>Odorrana leishanensis</i> sp. nov.	Leigongshan Nature Reserve, Leishan, Guizhou, China	MT LS20230805001	OR879771	OR879755	OR863728	this study
3	<i>Odorrana leishanensis</i> sp. nov.	Leigongshan Nature Reserve, Leishan, Guizhou, China	MT LS20230811024	OR879772	OR879756	OR863729	this study
4	<i>Odorrana leishanensis</i> sp. nov.	Leigongshan Nature Reserve, Leishan, Guizhou, China	MT LS20230729013	OR879773	OR879757	OR863730	this study
5	<i>Odorrana leishanensis</i> sp. nov.	Leigongshan Nature Reserve, Leishan, Guizhou, China	MT LS20230806018	OR879774	OR879758	OR863731	this study
6	<i>Odorrana leishanensis</i> sp. nov.	Leigongshan Nature Reserve, Leishan, Guizhou, China	MT LS20230711020	OR879775	OR879759	OR863732	this study
7	<i>Odorrana leishanensis</i> sp. nov.	Leigongshan Nature Reserve, Leishan, Guizhou, China	MT LS20230717001	OR879776	OR879760	OR863733	this study
8	<i>Odorrana fengkaiensis</i>	Heishiding Nature Reserve, Fengkai, Guangdong, China	SYS a002262	KT315354	KT315375	OR863743	Wang et al. 2015; this study
9	<i>Odorrana fengkaiensis</i>	Heishiding Nature Reserve, Fengkai, Guangdong, China	SYS a002263	KT315355	KT315376	OR863744	Wang et al. 2015; this study
10	<i>Odorrana fengkaiensis</i>	Heishiding Nature Reserve, Fengkai, Guangdong, China	SYS a002273	KT315356	KT315377	/	Wang et al. 2015
11	<i>Odorrana hainanensis</i>	Wuzhishan city, Hainan, China	HNNU0606105	KF184996	KF185032	/	Wang et al. 2015
12	<i>Odorrana hainanensis</i>	Diaoluoshan Forest Park, Lingshui, Hainan, China	SYS a002260	KT315362	KT315383	OR863741	this study
13	<i>Odorrana bacboensis</i>	Bainan village, Napo, Guangxi, China	SYS a001046	KT315364	KT315385	OR863742	this study
14	<i>Odorrana bacboensis</i>	Khe Moi, Nghe An, Vietnam	ROM 13044	AF206099	DQ650569	/	Chen et al. 2005
15	<i>Odorrana bacboensis</i>	Hekou, Yunnan, China	HNNU HK001	KF185008	KF185044	/	Chen et al. 2013
16	<i>Odorrana schmackeri</i>	Songtao, Guizhou, China	MT ST20210622001	OR879782	OR879768	OR863745	this study
17	<i>Odorrana schmackeri</i>	Yichang City, Hubei, China	HNNU090811349	KF185011	KF185047	/	Chen et al. 2013
18	<i>Odorrana schmackeri</i>	Songtao, Guizhou, China	MT ST20210622002	OR879782	OR879769	OR863746	this study
19	<i>Odorrana kweichowensis</i>	Lengshuihe Nature Reserve, Jinsha, Guizhou, China	CIBjs20150803008	MH193538	MH193552	MH193606	Li et al. 2018
20	<i>Odorrana kweichowensis</i>	Lengshuihe Nature Reserve, Jinsha, Guizhou, China	CIBjs20171014001	MH193539	MH193551	MH193605	Li et al. 2018
21	<i>Odorrana sangzhiensis</i>	Sangzhi, Hunan, China	CSUFT 4308220046	MW465705	MW464864	/	Zhang et al. 2021
22	<i>Odorrana sangzhiensis</i>	Sangzhi, Hunan, China	CSUFT 4308220051	MW465701	MW464865	/	Zhang et al. 2021
23	<i>Odorrana sangzhiensis</i>	Sangzhi, Hunan, China	CSUFT 4308220048	MW465702	MW464861	/	Zhang et al. 2021
24	<i>Odorrana ichangensis</i>	Zhijin, Guizhou, China	MT ZJ20210814003	/	OR879766	OR863739	this study
25	<i>Odorrana ichangensis</i>	Zhijin, Guizhou, China	MT ZJ20210814004	/	OR879767	OR863740	this study
26	<i>Odorrana ichangensis</i>	Yichang City, Hubei, China	SYS a005475	OR879781	OR879765	OR863738	this study
27	<i>Odorrana hejiangensis</i>	Chishui, Guizhou, China	MT CS20200605007	OR879779	OR879763	OR863736	this study
28	<i>Odorrana hejiangensis</i>	Chishui, Guizhou, China	MT CS20200605008	OR879780	OR879764	OR863737	this study
29	<i>Odorrana hejiangensis</i>	Hejiang, Sichuan, China	HNNU10071202	KF185016	KF185052	/	Chen et al. 2013
30	<i>Odorrana tianmuis</i>	Lin'an, Zhejiang, China	HNNU707071	KF185004	KF185040	/	Chen et al. 2013
31	<i>Odorrana tianmuis</i>	Lin'an, Zhejiang, China	SYS a002680	OR879777	OR879761	OR863734	this study
32	<i>Odorrana tianmuis</i>	Lin'an, Zhejiang, China	SYS a002681	OR879778	OR879762	OR863735	this study
33	<i>Odorrana huanggangensis</i>	Fanjingshan Nature Reserve, Jiangkou, Guizhou, China	CIBFJS20150502002	MH193532	MH193565	MH193614	Li et al. 2018
34	<i>Odorrana huanggangensis</i>	Leigongshan Nature Reserve, Leishan, Guizhou, China	CIBLS20140818005	MH193530	MH193564	MH193612	Li et al. 2018
35	<i>Odorrana huanggangensis</i>	Wuyishan Nature Reserve, Fujian, China	HNNU0607001	KF185023	KF185059	/	Chen et al. 2013
36	<i>Odorrana versabilis</i>	Leigongshan Nature Reserve, Leishan, Guizhou, China	HNNU003	KF185019	KF185055	/	Chen et al. 2013
37	<i>Odorrana nasuta</i>	Wuzhishan, Hainan, China	HNNU051119	KF185017	KF185053	/	Chen et al. 2013

ID	Species	Locality	Voucher number	GenBank accession number			Citation
				12s	16s	ND2	
38	<i>Odorrana exiliversabilis</i>	Wuyishan, Fujian, China	HNNU0607032	KF185020	KF185056	/	Chen et al. 2013
39	<i>Odorrana yentuensis</i>	Guangxi, China	NHMG1401035	MH665669	MH665675	/	Mo et al. 2015
40	<i>Odorrana nasica</i>	HaTinh, Vietnam	AMNH A161169	DQ283345	DQ283345	/	Frost et al. 2006
41	<i>Odorrana tormota</i>	Huangshan, Anhui, China	AM04005	DQ835616	DQ835616	DQ835616	Su et al. 2007
42	<i>Odorrana narina</i>	Okinawa Island, Japan	/	AB511287	AB511287	AB600990	Kurabayashi et al. 2010
43	<i>Odorrana amamiensis</i>	Tokunoshima, Ryukyu, Japan	KUHE:24635	AB200923	AB200947	AB600991	Matsui et al. 2006
44	<i>Odorrana supranarina</i>	Iriomotejima, Ryukyu	KUHE:12898	AB200926	AB200950	/	Matsui et al. 2006
45	<i>Odorrana swinhoana</i>	Nantou, Taiwan, China	HNNUTW9	KF185010	KF185046	/	Chen et al. 2013
46	<i>Odorrana utsunomiyaorum</i>	Iriomotejima, Ryukyu	KUHE:12896	AB200928	AB200952	/	Matsui et al. 2006
47	<i>Odorrana hosii</i>	Kuala Lumpur, Malaysia	IABHU 21004	AB511284	AB511284	/	Kurabayashi et al. 2010
48	<i>Odorrana graminea</i>	Wuzhishan, Hainan, China	HNNU0606123	KF185002	KF185038	/	Chen et al. 2013
49	<i>Odorrana chloronota</i>	Ha Giang, Vietnam	AMNH A163935	DQ283394	DQ283394	/	Frost et al. 2006
50	<i>Odorrana livida</i>	Prachuap Kirikhan, Thailand	FMNH 263415	KF771294	DQ650613	DQ650546	Stuart et al. 2006b
51	<i>Odorrana leporipes</i>	Shaoguan, Guangdong, China	HNNU10081099	KF185000	KF185036	/	Chen et al. 2013
52	<i>Odorrana aureola</i>	Phu Rua, Loei, Thailand	FMNH 265919	/	DQ650564	DQ650500	Stuart et al. 2006
53	<i>Odorrana morafkai</i>	Tram Lap, Vietnam	ROM 7446	AF206103	AF206484	/	Chen et al. 2005
54	<i>Odorrana banaorum</i>	Tram Lap, Vietnam	ROM 7472	AF206106	AF206487	/	Chen et al. 2005
55	<i>Odorrana junlianensis</i>	Junlian, Sichuan, China	HNNU002JL	KF185022	KF185058	/	Chen et al. 2013
56	<i>Odorrana grahami</i>	Kunming, Yunnan, China	HNNU10081016	KF185015	KF185051	/	Chen et al. 2013
57	<i>Odorrana hmongorum</i>	Lao Cai, Vietnam	ROM 38605	/	EU861556	EU861585	Bain et al. 2009
58	<i>Odorrana daorum</i>	Sa Pa, Vietnam	ROM 19053	AF206101	AF206482	/	Chen et al. 2005
59	<i>Odorrana andersonii</i>	Longchuan County, Yunnan, China	HNNU001YN	KF185021	KF185057	/	Chen et al. 2013
60	<i>Odorrana jingdongensis</i>	Jingdong, Yunnan, China	20070711017	KF185014	KF185050	/	Chen et al. 2013
61	<i>Odorrana margaretae</i>	Mt. Emei, Sichuan, China	HNNU20050032	KF184999	KF185035	/	Chen et al. 2013
62	<i>Odorrana kuangwuensis</i>	Nanjiang, Sichuan, China	HNNU09081185	KF184998	KF185034	/	Chen et al. 2013
63	<i>Odorrana dulongensis</i>	Dulongjiang, Yunnan, China	KIZ035027	/	MW128102	/	Liu et al. 2021
64	<i>Odorrana wuchuanensis</i>	Maolan National Nature Reserve, Libo County, Guizhou, China	GZNU20180608018	MW481342	MW481353	MW481364	Luo et al. 2021
65	<i>Odorrana wuchuanensis</i>	Wuchuan, Guizhou Prov., China	HNNU019L	KF185007	KF185043	/	Chen et al. 2013
66	<i>Odorrana mutschmanni</i>	Cao Bang, Vietnam	IEBR 3725	KU356762	KU356766	/	Pham et al. 2016b
67	<i>Odorrana yizhangensis</i>	Nanling Nature Reserve, Ruyuan County, Guangdong, China	CIBHN201108149	MH193540	MH193560	MH193615	Li et al. 2018
68	<i>Odorrana yizhangensis</i>	Yizhang, Hunan	HNNU10081075	KF185012	KF185048	/	Chen et al. 2013
69	<i>Odorrana lungshengensis</i>	Longsheng, Guangxi	HNNU70028	KF185018	KF185054	/	Chen et al. 2013
70	<i>Odorrana lungshengensis</i>	Leigongshan Nature Reserve, Leishan, Guizhou, China.	CIBLS20140616006	MH193534	MH193554	MH193608	Li et al. 2018
71	<i>Odorrana anlungensis</i>	Anlong, Guizhou, China	HNNU10081109	KF185013	KF185049	/	Chen et al. 2013
72	<i>Odorrana chapaensis</i>	Lai Chau, Vietnam	AMNH A161439	DQ283372	DQ283372	/	Frost et al. 2006
73	<i>Odorrana geminata</i>	Ha Giang, Vietnam	AMNH 163782	/	EU861546	EU861572	Bain et al. 2009
74	<i>Odorrana ishikawae</i>	Amami Island, Japan	IABHU 5275	AB511282	AB511282	AB511282	Kurabayashi et al. 2010
75	<i>Odorrana absita</i>	Xe Kong, Laos	FMNH 258107	/	EU861542	EU861568	Bain et al. 2009
76	<i>Odorrana liboensis</i>	Maolan National Nature Reserve, Libo, Guizhou, China	GZNU20180608007	MW481339	MW481350	/	Luo et al. 2021
77	<i>Odorrana lipuensis</i>	Lipu, Guangxi, China	NHMG1303018	MH665670	MH665676	/	Mo et al. 2015
78	<i>Odorrana concelata</i>	Longlinchang Village, Qingyuan, Guangdong, China	GEP a050	OP137167	OP137161	/	Lin et al. 2022
79	<i>Babina adenopleura</i>	/	A-A-WZ001	NC_018771	NC_018771	NC_018771	Yu et al. 2012
80	<i>Nidirana daunchina</i>	Emeishan, Sichuan, China	HNNU20060103	KF185029	KF185065	/	Chen et al. 2013
81	<i>Amolops loloensis</i>	Shimian, Sichuan, China	SM-ZDTW-01	NC_029250	NC_029250	NC_029250	Xue et al. 2016
82	<i>Amolops ricketti</i>	Wugongshan, Jiangxi, China	AM13988	NC_023949	NC_023949	NC_023949	Li et al. 2016
83	<i>Glandirana tientaiensis</i>	Huangshan, Anhui, China	SCUM0405192CJ	KX269222	KX269222	KX269435	Yuan et al. 2016
84	<i>Sylvirana guentheri</i>	Fuzhou City, Fujian, China	SCUM-H002CJ	KX269219	KX269219	/	Yuan et al. 2016
85	<i>Pelophylax nigromaculata</i>	Hongya, Sichuan, China	SCUM045199CJ	KX269216	KX269216	KX269431	Yuan et al. 2016
86	<i>Rana weiningensis</i>	Weining County, Guizhou, China	SCUM0405171	KX269217	KX269217	KX269432	Yuan et al. 2016

3.12 (Ronquist and Huelsenbeck 2003), respectively, and the best-fit model was obtained by the Bayesian inference criteria (BIC) computed with PartitionFinder 2 (Lanfear et al. 2012). The analysis suggested that the best partition scheme was *12S rRNA/16S rRNA/ND2* genes. We selected GTR+R as the best model for *12S rRNA* and *16S rRNA* and the TN93 + I + G as the best model for the *ND2* gene. For ML analyses conducted in PhyML 3.0, the bootstrap consensus tree inferred from 1000 replicates was used to estimate nodal supports of inferred relationships on phylogenetic trees. For Bayesian analyses conducted in MrBayes 3.12, four Markov chains were run for 50 million generations with sampling every 1000 generations until the trees reach convergence (split frequency < 0.05). The first 25% of trees were removed as the “burn-in” stage followed by calculation of Bayesian posterior probabilities and the 50% majority-rule consensus of the post burn-in trees sampled at stationarity. Finally, uncorrected *p*-distances (1000 replicates) between species based on *12S rRNA* (45 species), *16S rRNA* (51 species), and *ND2* (23 species) were calculated in MEGA 6.06 (Tamura et al. 2013).

Morphological comparisons

Morphological measurements were made with dial calipers to nearest 0.1 mm (Wenzhou Weidu Electronics Co. Ltd., China). Twenty morphometric characters of 76 adults specimens were measured containing seven specimens of the undescribed taxon, 15 *Odorrana hejiangensis*, eight *O. huanggangensis*, 13 *O. ichangensis*, nine *O. kweichowensis* Li, Xu, Lv, Jiang, Wei & Wang, 2018, ten *O. schmackeri* (Boettger, 1892), and 14 *O. wuchuanensis* following Fei et al. (2009) and Li et al. (2018a), abbreviated as follows:

- ED** eye diameter (distance from the anterior corner to the posterior corner of the eye);
- FL** foot length (distance from tarsus to the tip of fourth toe);
- HDL** head length (distance from the tip of the snout to the articulation of jaw);
- HDW** maximum head width (greatest width between the left and right articulations of jaw);
- HLL** hindlimb length (maximum length from the vent to the distal tip of the Toe IV);
- IND** internasal distance (minimum distance between the inner margins of the external nares);
- IOD** interorbital distance (minimum distance between the inner edges of the upper eyelids);
- LAL** length of lower arm and hand (distance from the elbow to the distal end of the Finger IV);
- ML** manus length (distance from tip of third digit to proximal edge of inner palmar tubercle);
- NED** nasal to eye distance (distance between the nasal and the anterior corner of the eye);
- NSD** nasal to snout distance (distance between the nasal the posterior edge of the vent);
- LW** lower arm width (maximum width of the lower arm);
- SVL** snout-vent length (distance from the tip of the snout to the posterior edge of the vent);

- SL** snout length (distance from the tip of the snout to the anterior corner of the eye);
- TFL** length of foot and tarsus (distance from the tibiotarsal articulation to the distal end of the Toe IV);
- THL** thigh length (distance from vent to knee);
- TL** tibia length (distance from knee to tarsus);
- TW** maximal tibia width;
- TYD** maximal tympanum diameter;
- UEW** upper eyelid width (greatest width of the upper eyelid margins measured perpendicular to the anterior-posterior axis).

To reduce the impact of allometry, a size-corrected value from the ratio of each character to SVL was calculated for the following morphometric analyses. Principal component analysis (PCA) of size-corrected variables and simple bivariate scatterplots was used to explore and reflect the morphometric differences between the undescribed taxon and the phylogenetic relationships closely and sympatric species contains *Odorrana hejiangensis*, *O. huanggangensis*, *O. ichangensis*, *O. kweichowensis*, *O. schmackeri*, and *O. wuchuanensis*. One-way analysis of variance (ANOVA) was used to test the significance of differences on morphometric characters between the undescribed taxon and *O. hejiangensis*, *O. huanggangensis*, *O. ichangensis*, *O. kweichowensis*, *O. schmackeri*, and *O. wuchuanensis* in the males. The statistical analyses were performed using SPSS 21.0 (SPSS, Inc., Chicago, IL, USA), and differences were considered to be significant at $p < 0.05$.

Sex was determined by direct observation of calling behavior and the presence of internal vocal sac openings for males, as well as the presence of eggs on the abdomen for females. The presence or absence of nuptial pads/spines was examined by optical microscopy.

We compared the morphological characters of the undescribed taxon with other species of *Odorrana*. Comparative data were obtained from the literature for 65 species of *Odorrana* (all of the authorities of the 65 species were shown in Table 2). For comparison, we examined the type and/or topotype materials for *O. hejiangensis*, *O. huanggangensis*, *O. ichangensis*, *O. kweichowensis*, *O. schmackeri*, and *O. wuchuanensis* (Suppl. material 1).

Results

Phylogenetic analyses

The ML and BI phylogenetic trees were constructed based on *12S rRNA* (400 bp), *16S rRNA* (484 bp), *ND2* (915 bp), and *12S rRNA + 16S rRNA + ND2* concatenated dataset. Both the independent dataset and concatenated dataset of ML and BI analyses resulted in essentially identical topologies with high node supporting values. The specimens of the undescribed taxon were clustered into an independent clade, sharing a sister relationship with the clade containing *Odorrana schmackeri*, *O. kweichowensis*, *O. fengkaiensis*, *O. hainanensis*, *O. bacboensis*, *O. ichangensis*, *O. hejiangensis*, *O. tianmuisi* Chen, Zhou & Zheng, 2010, and *O. huanggangensis* with high node support values (0.99 in BI and 78% in ML, Fig. 2; 0.98 in BI and 92% in ML, Suppl. material 5; 0.80 in BI and 50% in ML, Suppl. material 6; 0.99 in BI and 70% in ML, Suppl. material 7).

Table 2. References for morphological characters for congeners of the genus *Odorrana*.

ID	<i>Odorrana</i> species	Citation
1	<i>O. absita</i> (Stuart & Chan-ard, 2005)	Stuart and Chan-ard 2005
2	<i>O. amamiensis</i> (Matsui, 1994)	Matsui 1994
3	<i>O. andersonii</i> (Boulenger, 1882)	Boulenger 1882
4	<i>O. anlungensis</i> (Liu & Hu, 1973)	Hu et al. 1973
5	<i>O. arunachalensis</i> Saikia, Sinha & Kharkongor, 2017	Saikia et al. 2017
6	<i>O. aureola</i> Stuart, Chuaynkern, Chan-ard & Inger, 2006	Stuart et al. 2006a
7	<i>O. bacboensis</i> (Bain, Lathrop, Murphy, Orlov & Ho, 2003)	Bain et al. 2003; Wang et al. 2015
8	<i>O. banaorum</i> (Bain, Lathrop, Murphy, Orlov & Ho, 2003)	Bain et al. 2003
9	<i>O. bolavensis</i> (Stuart & Bain, 2005)	Stuart and Bain 2005
10	<i>O. cangyuanensis</i> (Yang, 2008)	Yang 2008
11	<i>O. chapaensis</i> (Bourret, 1937)	Bourret 1937
12	<i>O. chloronota</i> (Günther, 1876)	Günther 1876; Che et al. 2020
13	<i>O. concealata</i> Wang, Zeng & Lin, 2022	Lin et al. 2022
14	<i>O. confusa</i> Song, Zhang, Qi, Lyu, Zeng & Wang, 2023	Song et al. 2023
15	<i>O. damingshanensis</i> Chen, Mo, Lin & Qin, 2024	Chen et al. 2024
16	<i>O. dulongensis</i> Liu, Che & Yuan, 2021	Liu et al. 2021
17	<i>O. exiliversabilis</i> Li, Ye & Fei, 2001	Fei et al. 2001b
18	<i>O. fengkaiensis</i> Wang, Lau, Yang, Chen, Liu, Pang & Liu, 2015	Wang et al. 2015
19	<i>O. geminata</i> Bain, Stuart, Nguyen, Che & Rao, 2009	Bain et al. 2009
20	<i>O. gigatympana</i> (Orlov, Ananjeva & Ho, 2006)	Orlov et al. 2006
21	<i>O. grahami</i> (Boulenger, 1917)	Boulenger 1917
22	<i>O. graminea</i> (Boulenger, 1900)	Boulenger 1900
23	<i>O. hainanensis</i> Fei, Ye & Li, 2001	Fei et al. 2001a
24	<i>O. heatwolei</i> (Stuart & Bain, 2005)	Stuart and Bain 2005
25	<i>O. hosii</i> (Boulenger, 1891)	Boulenger 1891
26	<i>O. hejiangensis</i> (Deng & Yu, 1992)	Deng and Yu 1992
27	<i>O. huanggangensis</i> Chen, Zhou & Zheng, 2010	Chen et al. 2010a
28	<i>O. ichangensis</i> Chen, 2020	Shen et al. 2020
29	<i>O. ishikawae</i> (Stejneger, 1901)	Stejneger 1901
30	<i>O. indepressa</i> (Bain & Stuart, 2006)	Bain and Stuart 2006
31	<i>O. jingdongensis</i> Fei, Ye & Li, 2001	Fei et al. 2001a
32	<i>O. junlianensis</i> Huang, Fei & Ye, 2001	Ye and Fei 2001
33	<i>O. khalam</i> (Stuart, Orlov & Chan-ard, 2005)	Stuart and Chan-ard 2005
34	<i>O. kuangwuensis</i> (Liu & Hu, 1966)	Hu et al. 1966
35	<i>O. kweichowensis</i> Li, Xu, Lv, Jiang, Wei & Wang, 2018	Li et al. 2018
36	<i>O. livida</i> (Blyth, 1856)	Blyth 1856
37	<i>O. liboensis</i> Luo, Wang, Xiao, Wang & Zhou, 2021	Luo et al. 2021
38	<i>O. lipuensis</i> Mo, Chen, Wu, Zhang & Zhou, 2015	Mo et al. 2015; Pham et al. 2016a
39	<i>O. leporipes</i> (Werner, 1930)	Werner 1930
40	<i>O. lungshengensis</i> (Liu & Hu, 1962)	Liu and Hu 1962
41	<i>O. macrotympana</i> (Yang, 2008)	Yang 2008
42	<i>O. margaretae</i> (Liu, 1950)	Liu 1950
43	<i>O. mawphlangensis</i> (Pillai & Chanda, 1977)	Pillai and Chanda 1977; Mahony 2008
44	<i>O. mutschmanni</i> Pham, Nguyen, Le, Bonkowski & Ziegler, 2016	Pham et al. 2016a
45	<i>O. monjerai</i> (Matsui & Jaafar, 2006)	Matsui and Jaafar 2006
46	<i>O. morafkai</i> (Bain, Lathrop, Murphy, Orlov & Ho, 2003)	Bain et al. 2003
47	<i>O. nasica</i> (Boulenger, 1903)	Boulenger 1903
48	<i>O. nasuta</i> Li, Ye & Fei, 2001	Fei et al. 2001b
49	<i>O. narina</i> (Stejneger, 1901)	Stejneger 1901
50	<i>O. nanjiangensis</i> Fei, Ye, Xie & Jiang, 2007	Fei et al. 2007a
51	<i>O. orba</i> (Stuart & Bain, 2005)	Stuart and Bain 2005
52	<i>O. sangzhiensis</i> Zhang, Li, Hu & Yang, 2021	Zhang et al. 2021

ID	<i>Odorrana</i> species	Citation
53	<i>O. schmackeri</i> (Boettger, 1892)	Boettger (1892); Shen et al. (2020)
54	<i>O. sinica</i> (Ahl, 1927)	Ahl 1927 "1925"; Bain et al. 2003
55	<i>O. swinhoana</i> (Boulenger, 1903)	Boulenger 1903
56	<i>O. supranarina</i> (Matsui, 1994)	Matsui 1994
57	<i>O. splendida</i> Kuramoto, Satou, Oumi, Kurabayashi & Sumida, 2011	Kuramoto et al. 2011
58	<i>O. tianmuyii</i> Chen, Zhou & Zheng, 2010	Chen et al. 2010b
59	<i>O. tiannanensis</i> (Yang & Li, 1980)	Yang and Li 1980
60	<i>O. tormota</i> (Wu, 1977)	Wu 1977
61	<i>O. utsunomiyaorum</i> (Matsui, 1994)	Matsui 1994
62	<i>O. versabilis</i> (Liu & Hu, 1962)	Liu and Hu 1962
63	<i>O. wuchuanensis</i> (Xu, 1983)	Wu et al. 1983
64	<i>O. yentuensis</i> Tran, Orlov & Nguyen, 2008	Tran et al. 2008; Lu et al. 2016
65	<i>O. yizhangensis</i> Fei, Ye & Jiang, 2007	Fei et al. 2007b

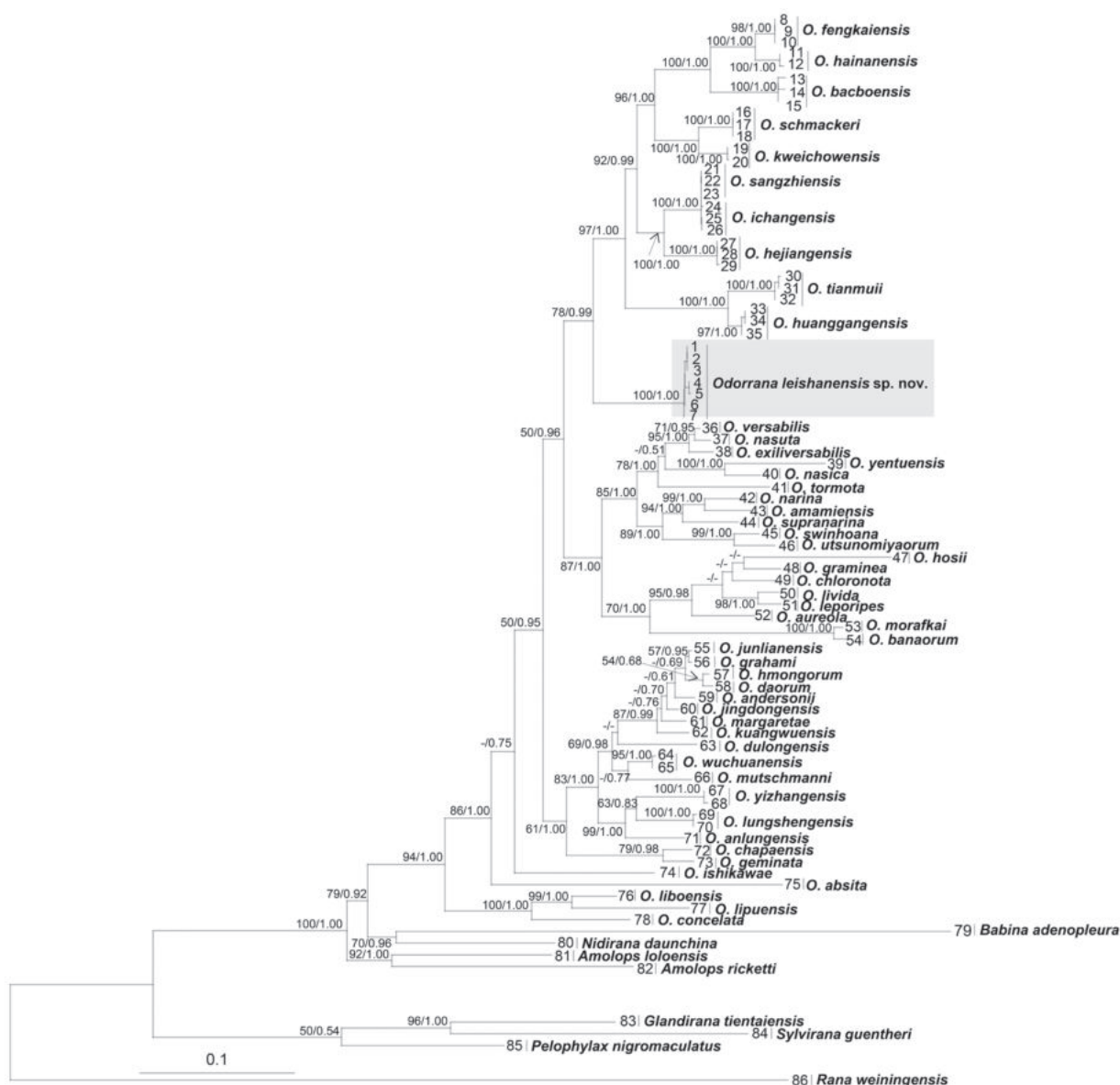


Figure 2. Maximum likelihood (ML) tree of the genus *Odorrana* reconstructed based on the 12S rRNA, 16S rRNA, and ND2 gene sequences. ML bootstrap supports (BS)/Bayesian posterior probability (BPP) are denoted beside each node, and “-” denotes BS < 50% or BPP < 0.60. Samples 1–86 refer to those listed in Table 1.

The mean genetic distance between the undescribed taxon and its closely related species is 5.0%, 4.9%, and 16.3% on 12S, 16S, and ND2, respectively, much higher than that between many pairs of species in the genus *Odorrana* (Suppl. materials 2–4).

Morphological analyses

The results of ANOVA indicated that in male, the undescribed taxon was significantly different from *Odorrana hejiangensis*, *O. huanggangensis*, *O. ichangensis*, *O. kweichowensis*, *O. schmackeri*, and *O. wuchuanensis* in many morphometric characters (all P values < 0.05; Table 3). In PCA for males, the total variation of the first two principal components was 43.3%, on the two-dimensional plots of PC1 vs PC2, the undescribed taxon could be separated from *O. hejiangensis*, *O. huanggangensis*, *O. ichangensis*, *O. kweichowensis*, *O. schmackeri*, and *O. wuchuanensis* (Fig. 3). Detailed morphological comparisons revealed discrete diagnostic characters between the undescribed taxon and its congeners. Therefore, adopt integrative taxonomy approaches with evidence from molecular and morphology to take the decision to describe the unidentified taxon as new species described herein.

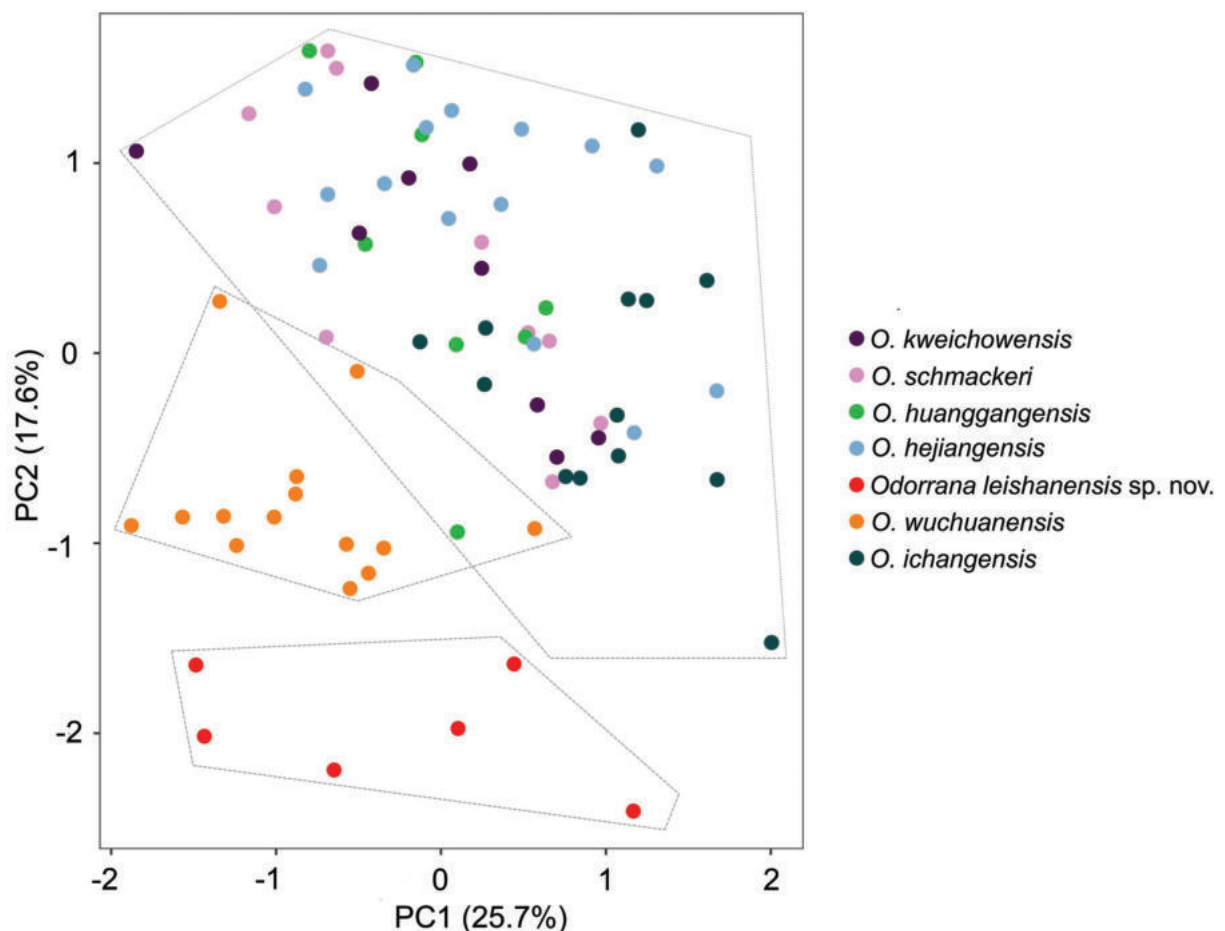


Figure 3. Plots of the first principal component (PC1) versus the second (PC 2) for *Odorrana leishanensis* sp. nov., *O. hejiangensis*, *O. huanggangensis*, *O. ichangensis*, *O. kweichowensis*, *O. schmackeri*, and *O. wuchuanensis* in males from a principal component analysis.

Table 3. The results of the one-way ANOVA with P-values for morphometric comparisons between males of *Odorrana leishanensis* sp. nov., *O. hejiangensis*, *O. huanggangensis*, *O. ichangensis*, *O. kweichowensis*, *O. schmackeri*, and *O. wuchuanensis*.

	OL vs OHG	OL vs OHJ	OL vs OI	OL vs OK	OL vs OS	OL vs OW
SVL	0.841	0.000**	0.006**	0.193	0.193	0.000**
HDL	0.001**	0.020*	0.000**	0.003**	0.003**	0.001**
HDW	0.643	0.967	0.599	0.469	0.469	0.000**
SL	0.192	0.577	0.044*	0.495	0.495	0.011*
NED	0.364	0.313	0.185	0.394	0.394	0.094
NSD	0.002**	0.067	0.011*	0.145	0.145	0.002**
IND	0.054	0.000**	0.000**	0.000**	0.000**	0.157
ED	0.005**	0.015*	0.067	0.015*	0.015*	0.128
IOD	0.164	0.002**	0.586	0.016*	0.016*	0.409
UEW	0.006**	0.018*	0.223	0.009**	0.009**	0.934
TYD	0.000**	0.000**	0.000**	0.000**	0.000**	0.000**
LAL	0.016*	0.007**	0.000**	0.001**	0.001**	0.000**
LW	0.163	0.000**	0.007**	0.001**	0.001**	0.009**
ML	0.801	0.237	0.000**	0.029*	0.029*	0.852
HLL	0.197	0.022*	0.001**	0.230	0.230	0.660
THL	0.406	0.021*	0.020*	0.745	0.745	0.450
TL	0.524	0.224	0.283	0.173	0.173	0.049*
TW	0.272	0.000**	0.005**	0.036*	0.036*	0.414
FL	0.003**	0.007**	0.036*	0.025*	0.025*	0.001**
TFL	0.505	0.812	0.343	0.583	0.583	0.622

Notes: OL, *Odorrana leishanensis* sp. nov.; OHG, *O. huanggangensis*; OHJ, *O. hejiangensis*; OI, *O. ichangensis*; OK, *O. kweichowensis*; OS, *O. schmackeri*; OW, *O. wuchuanensis*. Significance level: * $p < 0.05$; ** $p < 0.01$. Abbreviations for the morphometric characters refer to Materials and methods section.

Taxonomic accounts

Odorrana leishanensis sp. nov.

<https://zoobank.org/D51EC9FE-C269-4189-9815-AB65D3FBE0B6>

Figs 4–6

Material examined. Holotype. MT LS20230729013, adult male, collected by Jing Liu on 29 July 2023 in the Leigongshan Nature Reserve (26.3833°N, 108.1967°E; elevation 1830 m a.s.l.), Leishan County, Guizhou Province, CHINA.

Paratype. Two males MT LS20230711020 and MT LS20230717001, collected by Jing Liu on 11 and 17 July 2023; one male MT LS20230805001 collected by Chaobo Feng on 5 August 2023; two males MT LS20230806010, MT LS20230806018 and one female MT LS20230811024 collected by Shize Li on 6 and 8 August 2023 from the same place as holotype.

Diagnosis. *Odorrana leishanensis* sp. nov. can be distinguished from its congeners by the following characters: (1) body size moderate (SVL♂ ($n = 6$) = 39.1–49.4 mm, SVL♀ ($n = 1$) = 49.7 mm in female); (2) head width larger than head length; (3) tympanum distinctly visible; (4) small rounded granules scattered all over dorsal body and limbs; (5) dorsolateral folds absent; (6) heels overlapping when thighs are positioned at right angles to the body; tibiotarsal articulation reaching the level between eye to nostril when leg stretched forward; (7) vocal sacs in male absent, and nuptial pads in male present on base of finger I.

Description of holotype (Figs 4, 5). Adult male, body size moderate (SVL 49.4 mm); head width larger than head length (HDW/HDL = 1.14); snout short, rounded in dorsal view, projecting beyond lower jaw; eye large and convex, ED 0.73 SL; nostril rounded, closer to tip of snout than to eye; internasal distance larger than interorbital distance; tympanum distinct, approximately 0.68 ED; vomerine teeth on well-developed ridges; tongue deeply notched posteriorly; pupil horizontally oval; vocal sac absent.

Forelimbs slender (LW/SVL = 0.09); lower arm and hand not reach one-second of body length (LAL/SVL = 0.42); fingers slender, relative finger lengths II < I < IV < III; finger tips on I–IV dilated to wide cordiform disks with circum-marginal grooves, without webbing and lateral fringes; subarticular tubercle prominent; supernumerary tubercle indistinct; inner metacarpal tubercle oval, elongate; outer metacarpal tubercles absent; light yellow glandular nuptial pad on finger I.

Hindlimbs long; tibio-tarsal articulation reaching between eye to nostril when hindlimb adpressed along the side of the body; heels overlapped; tibia longer than thigh length; toes slender, relative lengths I < II < III < V < IV; toes entirely webbed; tips of toes expanded into disc with circummarginal grooves; outer metatarsal tubercle absent; inner metatarsal tubercle present.

Dorsal rough, there are small, rounded granules scattered all over dorsal body and limbs, ventral surfaces of the head, body, and limbs smooth; weak supratympanic fold from the posterior edge of the eye to the posterior edge of the tympanum; dorsolateral folds absent.

Coloration of holotype in life (Fig. 4). Dorsum grass-green with a small amount of brown spots; flanks pale yellow with several black spots; dorsal surfaces of

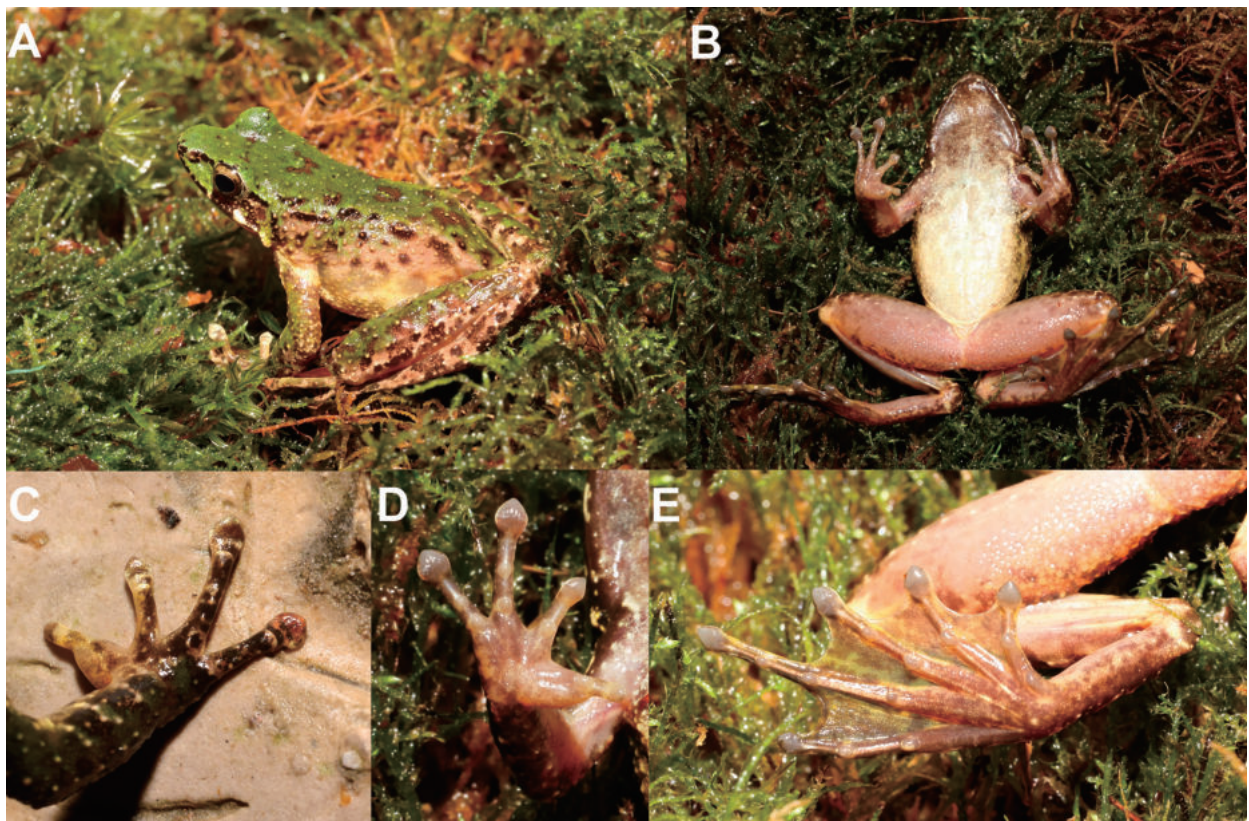


Figure 4. Photographs of the holotype MTL20230729013 of *Odorrana leishanensis* sp. nov. in life **A** dorsal view **B** ventral view **C** dorsal view of hand **D** ventral view of hand **E** ventral view of foot.

anterior forelimbs pale yellow, anterior forelimbs olive-brown, with black bands and irregular grass-green spots; dorsal surfaces of hindlimbs grass-green with black bands; upper jaw with a ring of brown spots; lower jaw yellow with black spots; grass-green and black spotted mosaic on the loreal region; tympanum brown-black; ventral surface of throat and chest brown, belly pale yellow.

Coloration of holotype in preservation (Fig. 5). After three months in 75% ethanol, the dorsal surface of the body faded to dark olive; the dorsal surface of the head changed to darker; the transverse bands on limbs and digits were not distinct; ventral surface of throat brown, gradually dark brown on chest, the belly was pale yellow; palm color faded to white.

Variation. Morphological measurements of all specimens are presented in Table 4 and Suppl. material 1. All specimens were very similar in morphology and color pattern, but in MT LS20230805001 the skin from the corner of the eye to the base of the thigh was noticeably pale brown with green patches mixed in and the flank of the ventral surface was white with dark brown spots (Fig. 6A, B); in MT LS20230806010 the dorsum was green and the ventral surface of the throat and chest darker (Fig. 6C, D); in MT LS20230811024 the granulation on the dorsolateral surface was covered with black spots and the ventral surface of the throat and chest were white with darker spots (Fig. 6E, F).

Secondary sexual characters. Adult females slightly larger than adult males; adult males lack vocal sacs. During breeding season, pale yellow glandular nuptial pads in males present on finger I (Figs 4C, 5D).

Comparisons. The molecular phylogenetic analyses placed the new species in an independent clade and sharing a sister relationship with the clade

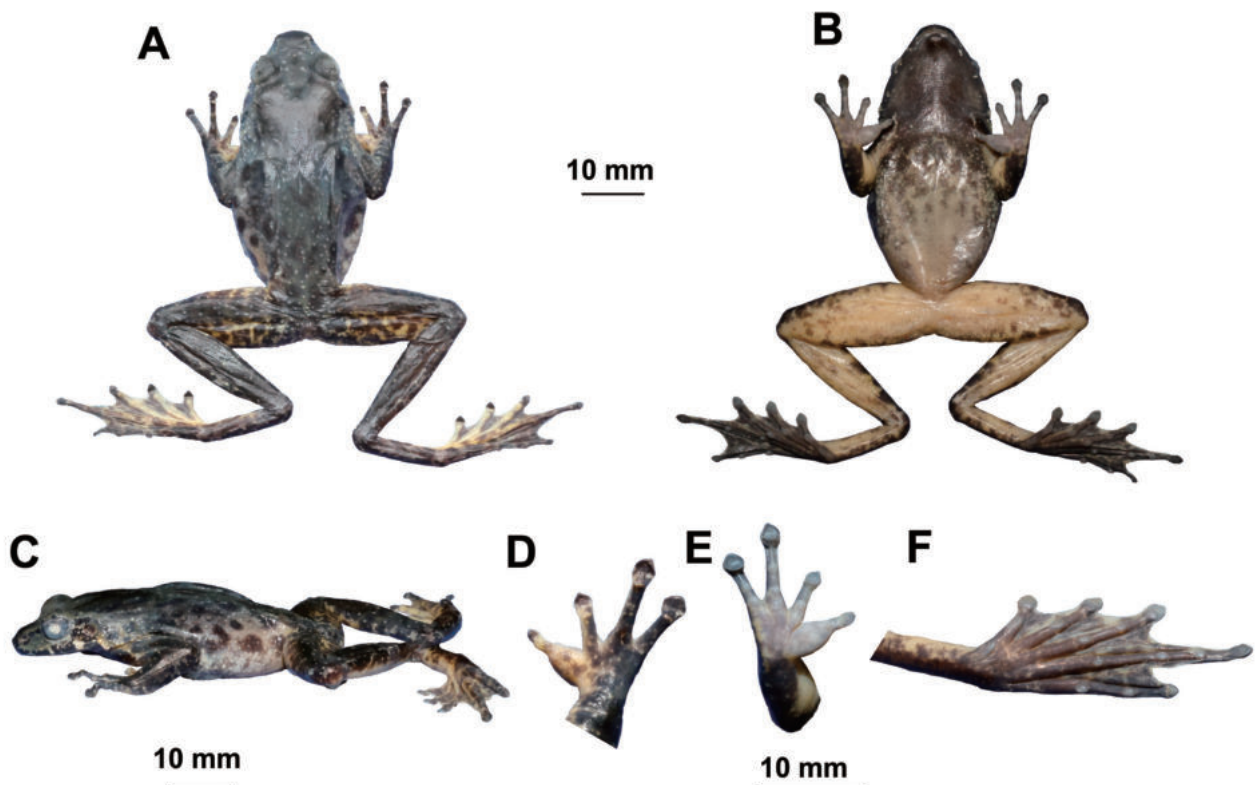


Figure 5. The holotype specimen MTL20230729013 of *Odorrana leishanensis* sp. nov. (preserved) in **A** dorsal view **B** ventral view **C** lateral view **D** dorsal view of hand **E** ventral view of hand **F** ventral view of foot.

Table 4. Measurements of the adult specimens of *Odorrana leishanensis* sp. nov. Units are given in mm. See abbreviations for the morphological characters in Materials and methods section.

Character	Holotype	Males (n = 6)		Female (n = 1)
		Range	Mean ± SD	
SVL	49.43	39.1–49.4	42.3 ± 4.0	49.7
HDL	15.13	11.6–17.8	13.7 ± 2.2	17.2
HDW	17.23	13.3–17.2	14.6 ± 1.4	17.7
SL	6.73	5.6–6.7	6.2 ± 0.5	7.7
NED	3.57	2.4–3.6	3.2 ± 0.4	4.1
NSD	2.92	1.6–2.9	2.4 ± 0.5	3.4
IND	6.02	4.8–6.0	5.3 ± 0.5	6.3
ED	4.94	4.1–4.9	4.5 ± 0.3	5.8
IOD	3.76	3.4–4.4	4.0 ± 0.3	5.1
UEW	4.04	2.9–4.0	3.4 ± 0.4	4.8
TYD	3.36	2.3–3.4	2.5 ± 0.4	2.5
LAL	20.52	17.4–20.5	18.7 ± 1.2	24.6
LW	4.38	2.9–4.4	3.3 ± 0.6	4.7
ML	12.19	10.5–12.2	11.3 ± 0.6	14.9
HLL	82.28	67.8–82.3	72.3 ± 5.2	87.3
THL	24.57	19.9–24.6	21.2 ± 1.7	28.3
TL	27.65	22.8–27.7	24.5 ± 1.75	29.7
TW	5.77	3.5–5.8	4.4 ± 0.7	6.9
TFL	38.43	31.3–38.4	33.8 ± 2.6	39.6
FL	26.66	22.7–26.7	23.9 ± 1.5	28.2

composed of *O. schmackeri*, *O. kweichowensis*, *O. fengkaiensis*, *O. hainanensis*, *O. bacboensis*, *O. ichangensis*, *O. hejiangensis*, *O. tianmii*, and *O. huanggangensis*. *Odorrana leishanensis* sp. nov. differs from the aforementioned species by having a similar body size in males and females, SVL♂ = 39.1–49.4 mm, ♀ = 49.7 mm (vs female size larger than males); vocal sac in males absent (vs present).

Odorrana leishanensis sp. nov. differs from *O. amamiensis*, *O. andersonii*, *O. aureola*, *O. bacboensis*, *O. chapaensis*, *O. chloronota*, *O. damingshanensis*, *O. geminata*, *O. grahmi*, *O. ishikawae*, *O. indeprensa*, *O. jingdongensis*, *O. junlianensis*, *O. kuangwuensis*, *O. leporipes*, *O. lungshengensis*, *O. mutschmanni*, *O. nanjiangensis*, *O. narina*, *O. splendida*, *O. supranarina*, *O. tiannanensis*, *O. versabilis*, and *O. wuchuanensis* in having a medium body size (maximum SVL < 50.0 mm in males vs minimum SVL > 50.0 mm in all other species).

Odorrana leishanensis sp. nov. differs from *O. absita*, *O. amamiensis*, *O. andersonii*, *O. anlungensis*, *O. aureola*, *O. bacboensis*, *O. banaorum*, *O. bolavensis*, *O. chapaensis*, *O. chloronota*, *O. dulongensis*, *O. fengkaiensis*, *O. geminata*, *O. grahmi*, *O. graminea*, *O. hainanensis*, *O. heatwolei*, *O. hejiangensis*, *O. hosii*, *O. huanggangensis*, *O. ichangensis*, *O. indeprensa*, *O. jingdongensis*, *O. junlianensis*, *O. khalam*, *O. kuangwuensis*, *O. kweichowensis*, *O. liboensis*, *O. livida*, *O. lungshengensis*, *O. macrotympa*, *O. margaretae*, *O. monjerai*, *O. morafkai*, *O. mutschmanni*, *O. nanjiangensis*, *O. narina*, *O. orba*, *O. sangzhiensis*, *O. schmackeri*, *O. sinica*, *O. splendida*, *O. supranarina*, *O. swinhoana*, *O. tiannanensis*, *O. tormota*, *O. versabilis*, *O. wuchuanensis*, *O. yentuensis*, *O.*

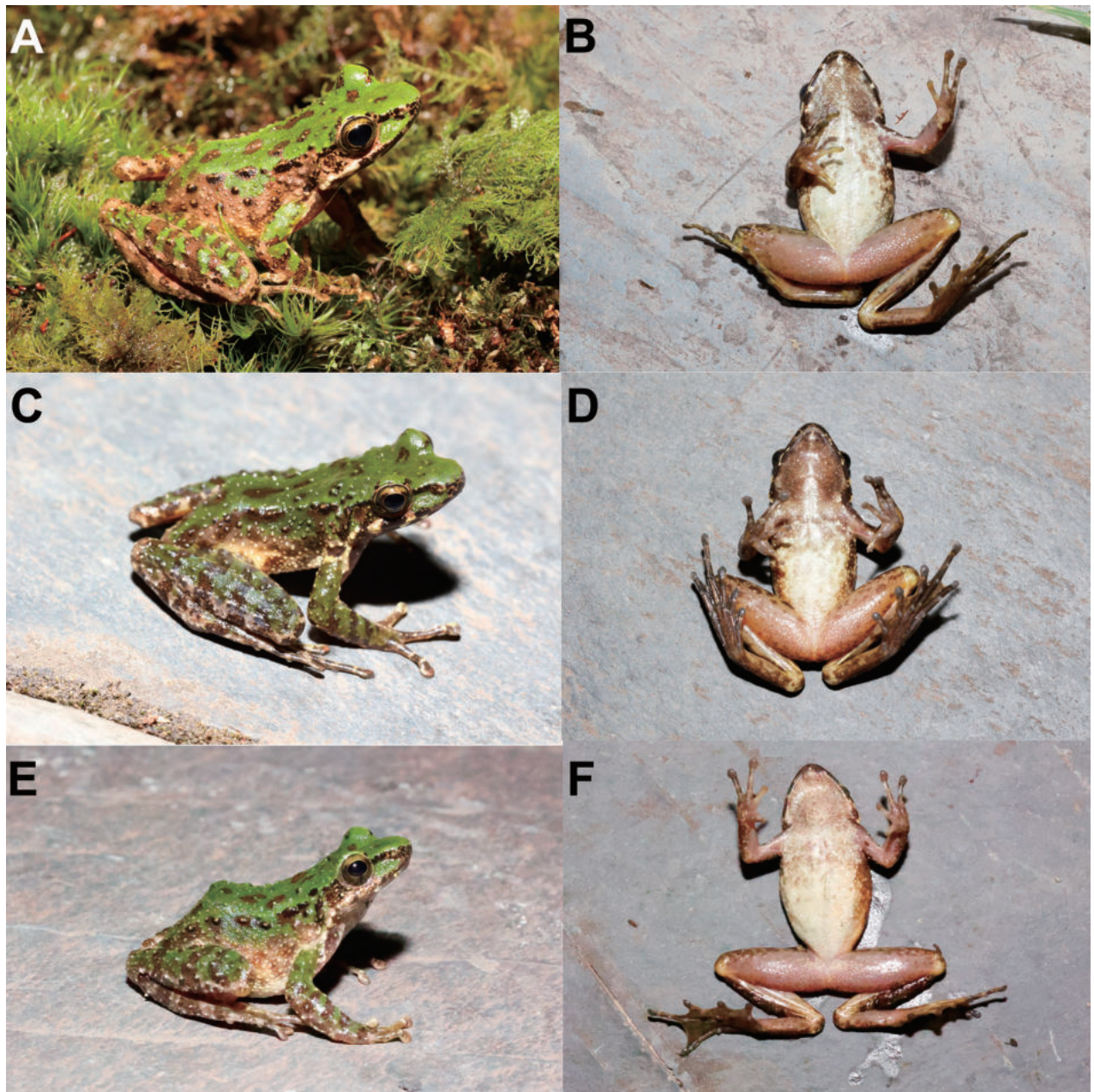


Figure 6. Color variation in *Odorrana leishanensis* sp. nov. **A** dorsolateral view of the male specimen MTL20230805001 **B** ventral view of the male specimen MTL20230805001 **C** dorsolateral view of the male specimen LS20230806010 **D** ventral view of the male specimen MTL20230806010 **E** dorsolateral view of the female specimen LS20230811024 **F** ventral view of the female specimen MTL20230811024.

yizhangensis, and *O. yunnanensis* by having medium female body size (SVL < 50.0 mm vs minimum SVL > 50.0 mm in the other species).

Odorrana leishanensis sp. nov. differs from *O. absita*, *O. amamiensis*, *O. banaorum*, *O. bolavensis*, *O. chloronota*, *O. confusa*, *O. damingshanensis*, *O. exiliversabilis*, *O. gigatympa*, *O. graminea*, *O. heatwolei*, *O. hosii*, *O. khalam*, *O. leporipes*, *O. livida*, *O. macrotympana*, *O. margaretae*, *O. monjerai*, *O. narina*, *O. nasica*, *O. nasuta*, *O. orba*, *O. supranarina*, *O. tormota*, *O. utsunomiyaorum*, *O. versabilis* and *O. yentuensis* by lacking dorsolateral folds (vs present in the other species).

Odorrana leishanensis sp. nov. differs from *O. bacboensis*, *O. jingdongensis*, *O. lungshengensis*, *O. margaretae*, *O. mutschmanni*, *O. nanjiangensis*, *O. narina*,

O. orba, *O. sinica*, *O. swinhoana*, *O. tormota*, and *O. yizhangensis* by the tibio-tarsal articulation reaching to between the eye and the nostril when the leg is stretched forward (vs reaching the tip of the snout), from *O. nasica* and *O. nasuta* (vs reaching the tip of the snout or a little beyond), from *O. hainanensis* (vs reaching the tip of the snout or the anterior corner of eye), from *O. junlianensis* (vs reaching the tip of the snout or between the nostril and the snout), from *O. cangyuanensis*, *O. exiliversabilis*, *O. fengkaiensis*, *O. gigatympana*, *O. grahami*, *O. graminea*, *O. tiannanensis*, *O. versabilis*, and *O. yentuensis* (vs reaching to or beyond the tip of the snout), from *O. amamiensis* (vs reaching far beyond the tip of the snout), from *O. anlungensis*, *O. huanggangensis*, *O. kuangwuensis*, *O. macrotympana*, *O. wuchuanensis*, and *O. ichangensis* (vs reaching the nostril or beyond the tip of the snout), from *O. lipuensis*, *O. splendida*, and *O. supranarina* (vs reaching the anterior corner of the eye), and from *O. utsunomiyaorum* (vs reaching between the anterior corner of the eye and the nostril).

Odorrana leishanensis sp. nov. differs from *O. absita*, *O. amamiensis*, *O. andersonii*, *O. anlungensis*, *O. aureola*, *O. bacboensis*, *O. banaorum*, *O. bolavensis*, *O. cangyuanensis*, *O. chapaensis*, *O. chloronota*, *O. dulongensis*, *O. exiliversabilis*, *O. fengkaiensis*, *O. geminata*, *O. gigatympana*, *O. grahami*, *O. graminea*, *O. hainanensis*, *O. heatwolei*, *O. hejiangensis*, *O. huanggangensis*, *O. ichangensis*, *O. indepressa*, *O. ishikawae*, *O. jingdongensis*, *O. junlianensis*, *O. khalam*, *O. kweichowensis*, *O. lungshengensis*, *O. macrotympana*, *O. morafkai*, *O. nanjiangensis*, *O. nasica*, *O. nasuta*, *O. orba*, *O. sinica*, *O. swinhoana*, *O. tianmuyii*, *O. tiannanensis*, *O. tormota*, *O. utsunomiyaorum*, *O. versabilis*, *O. yentuensis* and *O. yizhangensis* by vocal sacs absent in male (vs present in the other species).

The congeners *O. graminea*, *O. huanggangensis*, and *O. lungshengensis* have sympatric distribution with *Odorrana leishanensis* sp. nov. (Fei et al. 2012; Amphibia China 2024). The new species can be distinguished from these species by a series of morphological characters as follows. This new species differs from *O. graminea* by the presence of vocal sacs in male and dorsolateral folds absent (vs vocal sacs in male and dorsolateral folds present in the latter) and small, rounded but rough dorsal granules scattered all over dorsal body and limbs (vs dorsum smooth in the latter). It differs from *O. huanggangensis* and *O. lungshengensis* by vocal sacs in male absent (vs vocal sacs present in male in the latter) and small, rounded but rough dorsal granules scattered all over dorsal body and limbs (vs dorsum smooth the other species).

Distribution and habitats. At present, *Odorrana leishanensis* sp. nov. is only known from Leigongshan National Nature Reserve, Leishan County, Guizhou Province, China. The population inhabits mountain forest at elevations between 1600–1800 m and is often found on bamboo and encountered in forest nearby streams (Fig. 7). *Boulenophrys leishanensis* Li, Xu, Liu, Jiang, Wei & Wang, 2018, *B. spinata* Liu & Hu, 1973, *O. lungshengensis* Liu & Hu, 1962, *Leptobrachella wulingensis* Qian, Xia, Cao, Xiao & Yang, 2020, *Paramesotriton caudopunctatus* Liu & Hu, 1973 and *Leptobrachium leishanensis* Liu & Hu, 1973, were also found in the type locality of the new species.

Etymology. The specific epithet *leishanensis* refers to the distribution of this species, Leishan County, Guizhou Province, China. We propose the common English name “Leishan Odorous Frog” and the Chinese name as “Lei Shan Chou Wa (雷山臭蛙)” for this species.



Figure 7. Habitats of *Odorrana leishanensis* sp. nov. at the type locality, Leishan County, Guizhou Province, China (inset: the holotype on bush stems beside the stream).

Discussion

In recent years, new species of *Odorrana* have been discovered almost every year (Frost 2024). Within the genus, *O. schmackeri* has been considered as the most widespread species in China, covering Henan, Sichuan, Chongqing, Guizhou, Hubei, Anhui, Jiangsu, Zhejiang, Hunan, Fujian, Guangdong, and Guangxi provinces (Fei et al. 2012). In recent years *O. schmackeri* was indicated as a complex of species, probably containing some cryptic species (Chen et al. 2013; Li et al. 2015; Zhu 2016), and have been described one after another (Wang et al. 2015; Li et al. 2018a; Shen et al. 2020; Zhang et al. 2021). Molecular phylogenetic analyses indicated that *Odorrana leishanensis* sp. nov. was revealed as the sister to the clade corresponding to the *O. schmackeri* complex, and is morphologically distinct from the latter (vocal sacs absent, and smaller body size in female). This may indicate that the new species has probably experienced an independent evolutionary history.

Leigong Mountain in Guizhou Province, China is the main summit of the Miaoling mountain range. Since the 1980s, many scholars have investigated the amphibians in this area and several species were described, i.e., *Paramesotriton caudopunctatus* (Liu & Hu, 1973), *Boulenophrys spinata*, *Leptobranchium leishanense* (Liu & Hu, 1973), *B. leishanensis*, and *Nidirana leishanensis* Li, Wei, Xu, Cui, Fei, Jiang, Liu & Wang, 2019. Among them, *B. leishanensis* and *N. leishanensis* had previously been misidentified as *B. minor* (Stejneger, 1926) and *N. adenopleura* (Boulenger, 1909) (Hu et al. 1973; Li et al. 2018b; Li et al. 2019). From 2014 to July 2023 we conducted several surveys in this region but the new species has only just been discovered, with only seven adult specimens found in a small area at elevations of 1600–1800 m. Therefore, we infer that the population of the new species is small, and we recommend classifying the

new species as vulnerable (VU) according to the evaluation criteria of the IUCN Red List of threatened Species (IUCN 2012). Future research should focus on determining the distribution and elevational range of the species.

Acknowledgements

We thank Prof. Yingyong Wang and Dr Zhitong Lyu for the tissue samples of some species and thanks Chaobo Feng, Tuo Shen, Junjian Zhou and Lyu Zhou for their help in collecting data and specimens.

Additional information

Conflict of interest

The authors have declared that no competing interests exist.

Ethical statement

No ethical statement was reported.

Funding

This work was supported by the Projects from the National Natural Science Foundation of China (Nos. 32270498, 31960099, 32260136, and 32070426), the West Light Foundation of The Chinese Academy of Sciences (Grant No. 2021XBZG_XBQNXZ_A_006), Guizhou Provincial Science and Technology Projects (Nos. ZK[2022]540), Forestry Science and Technology Research Project of Guizhou Forestry Department (No. [2020]13, [2020]04); Guizhou Provincial Department of Education Youth Science and Technology Talents Growth Project (No. KY[2020]234), and High-level personnel research start-up funding projects of Moutai Institute (Nos. mygccrc[2022]055, mygccrc[2022]067, mygccrc[2022]083); Survey of Amphibian and Reptile Resources in Leigongshan Nature Reserve (P5226002023000019).

Author contributions

Investigation: JL, JJC. Methodology: HJS. Project administration: XJT. Visualization: BW. Writing – original draft: SZL.

Author ORCIDs

Bin Wang  <https://orcid.org/0000-0001-6036-5579>

Data availability

All of the data that support the findings of this study are available in the main text or Supplementary Information.

References

- Ahl E (1927 [1925]) Über vernachlässigte Merkmale bei Fröschen. Sitzungsberichte der Gesellschaft Naturforschender Freunde zu Berlin, 40–47.
- Amphibia China (2024) The database of Chinese amphibians. Electronic Database. Kunming Institute of Zoology (CAS), Kunming, Yunnan. <http://www.amphibiachina.org/> [Accessed 24 January 2024]
- Bain RH, Stuart BL (2006 [2005]) A new species of cascade frog (Amphibia: Ranidae) from Thailand, with new data on *Rana banaorum* and *Rana morafkai*.

- The Natural History Bulletin of the Siam Society 53(1): 3–16. [https://doi.org/10.1643/0045-8511\(2006\)006\[0043:TNISOC\]2.0.CO;2](https://doi.org/10.1643/0045-8511(2006)006[0043:TNISOC]2.0.CO;2)
- Bain RH, Lathrop A, Murphy RW, Orlov NL, Cuc HT (2003) Cryptic species of a cascade frog from Southeast Asia: Taxonomic revisions and descriptions of six new species. *American Museum Novitates* 3417: 1–60. [https://doi.org/10.1206/0003-0082\(2003\)417<0001:CSOACF>2.0.CO;2](https://doi.org/10.1206/0003-0082(2003)417<0001:CSOACF>2.0.CO;2)
- Bain RH, Stuart BL, Nguyen TQ, Che J, Rao DQ (2009) A new *Odorrana* (Amphibia: Ranidae) from Vietnam and China. *Copeia* 2(2): 348–362. <https://doi.org/10.1643/CH-07-195>
- Blyth E (1856) Report for October Meeting, 1855. *Journal of the Asiatic Society of Bengal* 24: 711–723.
- Boettger O (1892) Katalog der Batrachier-Sammlung im Museum der Senckenbergischen Naturforschenden Gesellschaft in Frankfurt am Main. Gebrüder Knauer, Frankfurt am Main, 11 pp.
- Boulenger GA (1882) Catalogue of the Batrachia Salientias. Ecaudata in the collection of the British Museum, London, 55 pp.
- Boulenger GA (1891) On new or little-known Indian and Malayan reptiles and batrachians. *Annals & Magazine of Natural History* 8(46): 288–292. <https://doi.org/10.1080/00222939109460437>
- Boulenger GA (1900) On the reptiles, batrachians, and fishes collected by the late Mr. John Whitehead in the interior of Hainan. *Proceedings of the Zoological Society of London* 1899: 956–962.
- Boulenger GA (1903) Descriptions of new batrachians in the British Museum. *Annals & Magazine of Natural History* 12(71): 552–557. <https://doi.org/10.1080/00222930308678892>
- Boulenger GA (1917) Descriptions of new frogs of the genus *Rana*. *Annals & Magazine of Natural History* 20(120): 413–418. <https://doi.org/10.1080/00222931709487029>
- Bourret R (1937) Notes herpétologiques sur l'Indochine française. XIV. Les batraciens de la collection du Laboratoire des Sciences naturelles de l'Université. Descriptions de quinze espèces ou variétés nouvelles. *Annexe au Bulletin Général de l'Instruction Publique* 4: 5–56.
- Che J, Pang JF, Zhao H, Wu GF, Zhao EM, Zhang YP (2007) Phylogeny of Raninae (Anura: Ranidae) inferred from mitochondrial and nuclear sequences. *Molecular Phylogenetics and Evolution* 43(1): 1–13. <https://doi.org/10.1016/j.ympev.2006.11.032>
- Che J, Jiang K, Yan F, Zhang YP (2020) *Amphibians and Reptiles in Tibet – Diversity and Evolution*. Science Press, Beijing, 238–243.
- Chen LQ, Murphy RW, Lathrop A, Ngo A, Orlov NL, Ho CT, Somorjai I (2005) Taxonomic chaos in Asian ranid frogs: An initial phylogenetic resolution. *The Herpetological Journal* 15: 231–243.
- Chen XH, Zhou KY, Zheng GM (2010a) A new species of the genus *Odorrana* from China (Anura, Ranidae). *Dong Wu Fen Lei Xue Bao* 35(1): 206–211.
- Chen XH, Zhou KY, Zheng GM (2010b) A new species of odorous frog from China (Anura: Ranidae). *Journal of Beijing Normal University* 46(5): 606–609.
- Chen XH, Chen Z, Jiang JP, Qiao L, Lu YQ, Zhou KY, Zheng GM, Zhai XF, Liu JX (2013) Molecular phylogeny and diversification of the genus *Odorrana* (Amphibia, Anura, Ranidae) inferred from two mitochondrial genes. *Molecular Phylogenetics and Evolution* 69(3): 1196–1202. <https://doi.org/10.1016/j.ympev.2013.07.023>
- Chen WC, Mo YM, Lin L, Qin K (2024) A new species of *Odorrana* Fei, Ye & Huang, 1990 (Amphibia, Anura, Ranidae) from central Guangxi, China with a discussion

- of the taxonomy of *Odorrana* (*Bamburana*). *ZooKeys* 1190: 131–152. <https://doi.org/10.3897/zookeys.1190.109886>
- Deng QX, Yu ZW (1992) A new species of the genus *Rana* from China. *Journal of Sichuan Teacher College* 13(4): 323–326.
- Fei L, Ye CY, Huang YZ (1990) Key to Chinese Amphibians. Publishing House for Scientific and Technological Literature, Chongqing, 364 pp.
- Fei L, Ye CY, Li C (2001a) Descriptions of two new species of the genus *Odorrana* in China (Anura: Ranidae). *Dong Wu Fen Lei Xue Bao* 26(1): 108–114.
- Fei L, Ye CY, Li C (2001b) Taxonomic studies of *Odorrana versabilis* in China II. Descriptions of two new species (Amphibia: Ranidae). *Dong Wu Fen Lei Xue Bao* 26(4): 601–607.
- Fei L, Ye CY, Jiang JP, Xie F, Huang YZ (2005) An Illustrated Key to Chinese Amphibians. Sichuan Publishing House of Science and Technology, Chongqing, 123 pp.
- Fei L, Ye CY, Jiang JP (2007a) A new Ranidae frog species China *Odorrana* (*Odorrana*) *yizhangensis* (Ranidae: Anura). *Dong Wu Fen Lei Xue Bao* 32(4): 989–992.
- Fei L, Ye CY, Xie F, Jiang JP (2007b) A new Ranidae frog species from Sichuan, China *Odorrana* (*Odorrana*) *nanjiangensis* (Ranidae: Anura). *Zoological Research* 28(5): 551–555.
- Fei L, Hu SQ, Ye CY, Huang YZ (2009) *Fauna Sinica. Amphibia* (Vol. 2) Anura. Science Press, Beijing, 957 pp.
- Fei L, Ye CY, Jiang JP (2012) *Colored Atlas of Chinese Amphibians and Their Distributions*. Sichuan Publishing House of Science & Technology, Chengdu, 619 pp.
- Frost DR (2024) *Amphibian Species of the World: an Online Reference*. Version 6.1. Electronic Database. American Museum of Natural History, New York. <http://research.amnh.org/herpetology/amphibia/index.html> [Accessed 24 January 2024]
- Frost DR, Grant T, Faivovich J, Bain RH, Haas A, Haddad CFB, de Sá RO, Channing A, Wilkinson M, Donnellan SC, Raxworthy CJ, Campbell JA, Blotto BL, Moler PE, Drewes RC, Nussbaum RA, Lynch JD, Green DM, Wheeler WC (2006) The amphibian tree of life. *Bulletin of the American Museum of Natural History* 297: 1–370. [https://doi.org/10.1206/0003-0090\(2006\)297\[0001:TATOL\]2.0.CO;2](https://doi.org/10.1206/0003-0090(2006)297[0001:TATOL]2.0.CO;2)
- Guindon S, Dufayard JF, Lefort V, Anisimova M, Hordijk W, Gascuel O (2010) New algorithms and methods to estimate maximum-likelihood phylogenies: assessing the performance of PhyML 3.0. *Systematic Biology* 59(3): 07–321. <https://doi.org/10.1093/sysbio/syq010>
- Günther A (1876) Tird report on collections of Indian reptiles obtained by the British Museum. *Proceedings of the Zoological Society of London* 1875: 567–577.
- Hall TA (1999) BIOEDIT: A user-friendly biological sequence alignment editor and analysis program for Windows 95/98/NT. *Nucleic Acids Symposium Series* 41(41): 95–98.
- Hu SX, Zhao EM, Liu CZ (1966) A herpetological survey of the Tsinling and Ta-pa shan Regions. *Acta Zoologica Sinica* 18(1): 57–89.
- Hu SX, Zhao EM, Liu CZ (1973) A survey of amphibians and reptiles in Kweichow Province, including a herpetofauna analysis. *Acta Zoologica Sinica* 19(2): 149–171.
- IUCN (2012) *IUCN Red List Categories and Criteria: Version 3.1, (2nd edn.)*. Cambridge, Gland, 16 pp.
- Kocher TD, Thomas WK, Meyer A, Edwards SV, Paabo S, Villablanca FX, Wilson AC (1989) Dynamics of mitochondrial DNA evolution in mammals: Amplification and sequencing with conserved Primers. *Proceedings of the National Academy of Sciences of the United States of America* 86(16): 6169–6200. <https://doi.org/10.1073/pnas.86.16.6196>
- Kurabayashi A, Natsuhiko Y, Naoki S, Yoko H, Shohei O, Tamotsu F, Masayuki S (2010) Complete mitochondrial DNA sequence of the endangered frog *Odorrana ishikawae*

- (family Ranidae) and unexpected diversity of mt gene arrangements in ranids. *Molecular Phylogenetics and Evolution* 56(2): 543–553. <https://doi.org/10.1016/j.ympev.2010.01.022>
- Kuramoto M, Satou N, Oumi S, Kurabayashi A, Sumida M (2011) Inter-and intra-Island divergence in *Odorrana ishikawae* (Anura, Ranidae) of the Ryukyu Archipelago of Japan, with description of a new species. *Zootaxa* 2767(1): 25–40. <https://doi.org/10.11646/zootaxa.2767.1.3>
- Lanfear R, Calcott B, Ho SYW, Guindon S (2012) PartitionFinder: Combined selection of partitioning schemes and substitution models for phylogenetic analyses. *Molecular Biology and Evolution* 29(6): 1695–1701. <https://doi.org/10.1093/molbev/mss020>
- Li YM, Wu XY, Zhang HB, Yan P, Xue H, Wu XB (2015) Vicariance and its impact on the molecular ecology of a Chinese Ranid frog species-complex (*Odorrana schmackeri*, Ranidae). *PLOS ONE* 10(9): e0138757. <https://doi.org/10.1371/journal.pone.0138757>
- Li YM, Wu XY, Zhang HB, Yan P, Xue H, Wu XB (2016) The complete mitochondrial genome of *Amolops ricketti* (Amphibia, Anura, Ranidae). *Mitochondrial DNA. Part A, DNA Mapping, Sequencing, and Analysis* 27(1): 242–243. <https://doi.org/10.3109/19401736.2014.883606>
- Li SZ, Xu N, Lv JC, Jiang JP, Wei G, Wang B (2018a) A new species of the odorous frog genus *Odorrana* (Amphibia, Anura, Ranidae) from southwestern China. *PeerJ* 6: e5695. <https://doi.org/10.7717/peerj.5695>
- Li SZ, Xu N, Liu J, Jiang JP, Wei G, Wang B (2018b) A new species of the Asian toad genus *Megophrys* sensu lato (Amphibia: Anura: Megophryidae) from Guizhou Province, China. *Asian Herpetological Research* 9(4): 224–239. <https://doi.org/10.16373/j.cnki.ahr.180072>
- Li SZ, Wei G, Xu N, Cui JG, Fei L, Jiang JP, Liu J, Wang B (2019) A new species of the Asian music frog genus *Nidirana* (Amphibia, Anura, Ranidae) from Southwestern China. *PeerJ* 7: e7157. <https://doi.org/10.7717/peerj.7157>
- Lin SS, Li YH, Su HL, Yi H, Pan Z, Sun YJ, Zeng ZC, Wang J (2022) Discovery of a new limestone karst-restricted odorous frog from northern Guangdong, China (Anura, Ranidae, *Odorrana*). *ZooKeys* 1120: 47–66. <https://doi.org/10.3897/zookeys.1120.87067>
- Liu CZ (1950) Amphibians of western China. *Fieldiana. Zoology Memoirs* 2: 1–400. <https://doi.org/10.5962/bhl.part.4737>
- Liu CZ, Hu SQ (1962) A survey of amphibians and reptiles in Guangxi Province. *Acta Zoologica Sinica* 14: 73–104.
- Liu XL, He YH, Wang YF, Beukema W, Hou SB, Li YC, Che J, Yuan ZY (2021) A new frog species of the genus *Odorrana* (Anura: Ranidae) from Yunnan, China. *Zootaxa* 4908(2): 263–275. <https://doi.org/10.11646/zootaxa.4908.2.7>
- Luo T, Wang SW, Xiao N, Wang YL, Zhou J (2021) A new species of odorous frog genus *Odorrana* (Anura, Ranidae) from southern Guizhou Province, China. *Asian Herpetological Research* 12(4): 381–398. <https://doi.org/10.16373/j.cnki.ahr.200122>
- Mahony S (2008) Redescription and generic reallocation of *Rana mawphlangensis* Pillai & Chanda, 1977 (Amphibia: Ranidae). *Hamadryad Madras* 33(1): 1–12.
- Matsui M (1994) A taxonomic study of the *Rana narina* complex, with descriptions of three new species (Amphibia: Ranidae). *Zoological Journal of the Linnean Society* 111(4): 385–415. <https://doi.org/10.1111/j.1096-3642.1994.tb01489.x>
- Matsui M, Jaafar I (2006) A new cascade frog of the subgenus *Odorrana* from peninsular Malaysia. *Zoological Science* 23(7): 647–651. <https://doi.org/10.2108/zsj.23.647>
- Matsui M, Tomohiko S, Hidetoshi OT, Tanaka U (2005) Multiple invasions of the Ryukyu Archipelago by Oriental frogs of the subgenus *Odorrana* with phylogenetic

- reassessment of the related subgenera of the genus *Rana*. *Molecular Phylogenetics and Evolution* 37(3): 733–742. <https://doi.org/10.1016/j.ympev.2005.04.030>
- Mo YM, Chen WC, Wu HY, Zhang W, Zhou SC (2015) A new species of *Odorrana* inhabiting complete darkness in a karst cave in Guangxi, China. *Asian Herpetological Research* 6(1): 11–17. <https://doi.org/10.16373/j.cnki.ahr.140054>
- Orlov NL, Natalia B, Cuc HT (2006) A new cascade frog (Amphibia: Ranidae) from central Vietnam. *Russian Journal of Herpetology* 13(2): 155–163.
- Pham CT, Nguyen TQ, Bernardes M, Nguyen TT, Ziegler T (2016a) First records of *Bufo gargarizans* Cantor, 1842 and *Odorrana lipuensis* Mo, Chen, Wu, Zhang et Zhou, 2015 (Anura: Bufonidae, Ranidae) from Vietnam. *Russian Journal of Herpetology* 23(2): 103–107.
- Pham CT, Nguyen TQ, Le MD, Bonkowski M, Ziegler T (2016b) A new species of *Odorrana* (Amphibia: Anura: Ranidae) from Vietnam. *Zootaxa* 4084(3): 421–435. <https://doi.org/10.11646/zootaxa.4084.3.7>
- Pillai RS, Chanda SK (1977) Two new species of frogs (Ranidae) from Khasi Hills, India. *Journal of the Bombay Natural History Society* 74: 136–140.
- Ronquist FR, Huelsenbeck JP (2003) MrBayes3: Bayesian phylogenetic inference under mixed models. *Bioinformatics* 19(12): 1572–1574. <https://doi.org/10.1093/bioinformatics/btg180>
- Saikia B, Sinha B, Kharkongor IJ (2017) *Odorrana arunachalensis*: A new species of Cascade Frog (Anura: Ranidae) from Talle Valley Wildlife Sanctuary, Arunachal Pradesh, India. *Journal of Bioresources* 4: 30–41.
- Shen HJ, Zhu YJ, Li Z, Chen Z, Chen XH (2020) Reevaluation of the holotype of *Odorrana schmackeri* Boettger, 1892 (Amphibia: Anura: Ranidae) and characterization of one cryptic species in *O. schmackeri* sensu lato through integrative approaches. *Asian Herpetological Research* 11(4): 297–311. <https://doi.org/10.16373/j.cnki.ahr.200097>
- Simon C, Frati F, Beckenbach A, Crespi B, Liu H, Flook P (1994) Evolution, weighting and phylogenetic utility of mitochondrial gene sequences and a compilation of conserved polymerase chain reaction primers. *Annals of the Entomological Society of America* 87(6): 651–701. <https://doi.org/10.1093/aesa/87.6.651>
- Song HM, Zhang SY, Qi S, Lyu ZT, Zeng ZC, Zhu YH, Huang MH, Luan FC, Shu ZF, Gong Y, Liu ZF, Wang YY (2023) Redefinition of the *Odorrana versabilis* Group, with a New Species from China (Anura, Ranidae, *Odorrana*). *Asian Herpetological Research* 14(4): 283–299. <https://doi.org/10.3724/ahr.2095-0357.2023.0019>
- Stejneger L (1901) Diagnoses of eight new batrachians and reptiles from the Riu Kiu Archipelago, Japan. *Proceedings of the Biological Society of Washington* 14: 189–191.
- Stuart BL, Bain RH (2005) Tree new species of spinule-bearing frogs allied to *Rana megatympanum* Bain, Lathrop, Murphy, Orlov & Ho, 2003 from Laos and Vietnam. *Herpetologica* 61(4): 478–492. <https://doi.org/10.1655/05-06.1>
- Stuart BL, Chanard T (2005) Two new *Huia* (Amphibia: Ranidae) from Laos and Thailand. *Copeia* 2005(2): 279–289. <https://doi.org/10.1643/CH-04-137R3>
- Stuart BL, Chuaynkern Y, Chan-ard T, Inger RF (2006a) Tree new species of frogs and a new tadpole from eastern Thailand. *Fieldiana. Zoology* 111: 1–19. [https://doi.org/10.3158/0015-0754\(2006\)187\[1:TNSOFA\]2.0.CO;2](https://doi.org/10.3158/0015-0754(2006)187[1:TNSOFA]2.0.CO;2)
- Stuart BL, Inger RF, Voris HK (2006b) High level of cryptic species diversity revealed by sympatric lineages of Southeast Asian forest frogs. *Biology Letters* 2(3): 470–474. <https://doi.org/10.1098/rsbl.2006.0505>

- Su X, Wu XB, Yan P, Cao SY, Hu YL (2007) Rearrangement of a mitochondrial tRNA gene of the concave-eared torrent frog, *Amolops tormotus*. *Gene* 394(1–2): 25–34. <https://doi.org/10.1016/j.gene.2007.01.022>
- Tamura K, Stecher G, Peterson D, Fiipski A, Kumar S (2013) MEGA6: Molecular evolutionary genetics analysis, version 6.0. *Molecular Biology and Evolution* 30(12): 2725–2729. <https://doi.org/10.1093/molbev/mst197>
- Tran TT, Orlov NL, Nguyen TT (2008) A new species of Cascade frog of *Odorrana* Fei, Yi et Huang, 1990 genus (Amphibia: Anura: Ranidae) from Bac Giang Province (Yen Tu Mountain Range, northeast Vietnam). *Russian Journal of Herpetology* 15: 212–224.
- Wang YY, Lau N, Yang JH, Chen GL, Liu ZY, Pang H, Liu Y (2015) A new species of the genus *Odorrana* (Amphibia: Ranidae) and the first record of *Odorrana bacboensis* from China. *Zootaxa* 3999(2): 235–254. <https://doi.org/10.11646/zootaxa.3999.2.4>
- Werner F (1930) *Rana leporipes*, a new species of frog from South China, with field notes by R. Mell. *Lingnan Science Journal* 9: 45–47.
- Wu GF (1977) A new species of frogs from Huang-Shan, Anhui, *Amolops tormotus* Wu. *Dong Wu Xue Bao* 23: 113–115.
- Wu L, Xu RH, Dong Q, Li DJ, Liu JS (1983) A new species of *Rana* and records of amphibians from Guizhou province. *Dong Wu Fen Lei Xue Bao* 29(1): 66–70.
- Xue R, Liu JB, Yu JJ, Yang JD (2016) The complete mitogenome of *Amolops loloensis* and related phylogenetic relationship among Ranidae. *Mitochondrial DNA. Part A, DNA Mapping, Sequencing, and Analysis* 27(6): 4629–4630. <https://doi.org/10.3109/19401736.2015.1101589>
- Yang DT (2008) *Amphibia and Reptilia of Yunnan*. Yunnan Science and Technology Press, Kunming, 65–81.
- Yang DT, Li SM (1980) A new species of the genus *Rana* from Yunnan. *Zoological Research* 1(2): 261–264.
- Ye CY, Fei L (2001) Phylogeny of genus *Odorrana* (Amphibian: Ranidae) in China. *Dong Wu Fen Lei Xue Bao* 47(5): 528–534.
- Yu DN, Zhang JY, Zheng RQ (2012) The complete mitochondrial genome of *Babina adenopleura* (Anura: Ranidae). *Mitochondrial DNA* 23(6): 423–425. <https://doi.org/10.3109/19401736.2012.710214>
- Yuan ZY, Zhou WW, Chen X, Poyarkov N, Chen HM, Liaw NHJ, Chou WH, Matzke H, Iizuka K, Min MS, Kuzmin S, Zhang YP, Che J (2016) Spatiotemporal Diversification of the True Frogs (Genus *Rana*): A Historical Framework for a Widely Studied Group of Model Organisms. *Systematic Biology* 65(5): syw055. <https://doi.org/10.1093/sysbio/syw055>
- Zhang B, Li Y, Hu K, Li P, Gu Z, Xiao N, Yang D (2021) A new species of *Odorrana* (Anura, Ranidae) from Hunan Province, China. *ZooKeys* 1024: 91–115. <https://doi.org/10.3897/zookeys.1024.56399>
- Zhu YJ (2016) Genetic Differentiation of *Odorrana schmackeri* Species Complex. Henan Normal University, Henan.

Supplementary material 1

Measurements of the adult specimens of *Odorrana leishanensis* sp. nov., *O. hejiangensis*, *O. huanggangensis*, *O. ichangensis*, *O. kweichowensis*, *O. schmackeri*, and *O. wuchuanensis*

Authors: Shi-Ze Li, Ji-Jun Chen, Hai-Jun Su, Jing Liu, Xiu-Jun Tang, Bin Wang

Data type: xlsx

Explanation note: Units in mm. See abbreviations for the morphological characters in Materials and methods section.

Copyright notice: This dataset is made available under the Open Database License (<http://opendatacommons.org/licenses/odbl/1.0/>). The Open Database License (ODbL) is a license agreement intended to allow users to freely share, modify, and use this Dataset while maintaining this same freedom for others, provided that the original source and author(s) are credited.

Link: <https://doi.org/10.3897/zookeys.1192.114315.suppl1>

Supplementary material 2

Uncorrected *p*-distances between the *Odorrana* species based on the 12S *rRNA* gene sequences

Authors: Shi-Ze Li, Ji-Jun Chen, Hai-Jun Su, Jing Liu, Xiu-Jun Tang, Bin Wang

Data type: xlsx

Copyright notice: This dataset is made available under the Open Database License (<http://opendatacommons.org/licenses/odbl/1.0/>). The Open Database License (ODbL) is a license agreement intended to allow users to freely share, modify, and use this Dataset while maintaining this same freedom for others, provided that the original source and author(s) are credited.

Link: <https://doi.org/10.3897/zookeys.1192.114315.suppl2>

Supplementary material 3

Uncorrected *p*-distances between the *Odorrana* species based on the 16S *rRNA* gene sequences

Authors: Shi-Ze Li, Ji-Jun Chen, Hai-Jun Su, Jing Liu, Xiu-Jun Tang, Bin Wang

Data type: xlsx

Copyright notice: This dataset is made available under the Open Database License (<http://opendatacommons.org/licenses/odbl/1.0/>). The Open Database License (ODbL) is a license agreement intended to allow users to freely share, modify, and use this Dataset while maintaining this same freedom for others, provided that the original source and author(s) are credited.

Link: <https://doi.org/10.3897/zookeys.1192.114315.suppl3>

Supplementary material 4

Uncorrected *p*-distances between the *Odorrana* species based on the *ND2* gene sequences

Authors: Shi-Ze Li, Ji-Jun Chen, Hai-Jun Su, Jing Liu, Xiu-Jun Tang, Bin Wang

Data type: xls

Copyright notice: This dataset is made available under the Open Database License (<http://opendatacommons.org/licenses/odbl/1.0/>). The Open Database License (ODbL) is a license agreement intended to allow users to freely share, modify, and use this Dataset while maintaining this same freedom for others, provided that the original source and author(s) are credited.

Link: <https://doi.org/10.3897/zookeys.1192.114315.suppl4>

Supplementary material 5

Maximum likelihood (ML) tree of the genus *Odorrana* reconstructed based on the *12S rRNA* gene sequences

Authors: Shi-Ze Li, Ji-Jun Chen, Hai-Jun Su, Jing Liu, Xiu-Jun Tang, Bin Wang

Data type: jpg

Explanation note: ML bootstrap supports (BS)/Bayesian posterior probability (BPP) are denoted beside each node, and “-” denotes BS < 50% or BPP < 0.60. Samples 1–86 refer to those listed in Table 1.

Copyright notice: This dataset is made available under the Open Database License (<http://opendatacommons.org/licenses/odbl/1.0/>). The Open Database License (ODbL) is a license agreement intended to allow users to freely share, modify, and use this Dataset while maintaining this same freedom for others, provided that the original source and author(s) are credited.

Link: <https://doi.org/10.3897/zookeys.1192.114315.suppl5>

Supplementary material 6

Maximum likelihood (ML) tree of the genus *Odorrana* reconstructed based on the *16S rRNA* gene sequences

Authors: Shi-Ze Li, Ji-Jun Chen, Hai-Jun Su, Jing Liu, Xiu-Jun Tang, Bin Wang

Data type: jpg

Explanation note: ML bootstrap supports (BS)/Bayesian posterior probability (BPP) are denoted beside each node, and “-” denotes BS < 50% or BPP < 0.60. Samples 1–86 refer to those listed in Table 1.

Copyright notice: This dataset is made available under the Open Database License (<http://opendatacommons.org/licenses/odbl/1.0/>). The Open Database License (ODbL) is a license agreement intended to allow users to freely share, modify, and use this Dataset while maintaining this same freedom for others, provided that the original source and author(s) are credited.

Link: <https://doi.org/10.3897/zookeys.1192.114315.suppl6>

Supplementary material 7

Maximum likelihood (ML) tree of the genus *Odorrana* reconstructed based on the *ND2* gene sequences

Authors: Shi-Ze Li, Ji-Jun Chen, Hai-Jun Su, Jing Liu, Xiu-Jun Tang, Bin Wang









Data type: jpg

Explanation note: ML bootstrap supports (BS)/Bayesian posterior probability (BPP) were denoted beside each node, and “-” denotes BS < 50% or BPP < 0.60. Samples 1–86 refer to those listed in Table 1.

Copyright notice: This dataset is made available under the Open Database License (<http://opendatacommons.org/licenses/odbl/1.0/>). The Open Database License (ODbL) is a license agreement intended to allow users to freely share, modify, and use this Dataset while maintaining this same freedom for others, provided that the original source and author(s) are credited.

Link: <https://doi.org/10.3897/zookeys.1192.114315.suppl7>

A new species of the *Cyrtodactylus chauquangensis* species group (Squamata, Gekkonidae) from Lao Cai Province, Vietnam

Tung Thanh Tran¹, Quyen Hanh Do², Cuong The Pham^{2,3}, Tien Quang Phan², Hanh Thi Ngo^{4,5,6}, Minh Duc Le^{4,7,8}, Thomas Ziegler^{5,6}, Truong Quang Nguyen^{2,3}

1 Vinh Phuc College, Phuc Yen City, Vinh Phuc Province, Vietnam

2 Institute of Ecology and Biological Resources, Vietnam Academy of Science and Technology, 18 Hoang Quoc Viet Road, Hanoi, Vietnam

3 Graduate University of Science and Technology, Vietnam Academy of Science and Technology, 18 Hoang Quoc Viet Road, Cau Giay, Hanoi, Vietnam

4 Central Institute for Natural Resources and Environmental Studies, Vietnam National University, 19 Le Thanh Tong, Hanoi, Vietnam

5 Cologne Zoo, Riehler Straße 173, 50735, Cologne, Germany

6 Institute of Zoology, University of Cologne, Zùlpicher Straße 47b, 50674, Cologne, Germany

7 Faculty of Environmental Sciences, Hanoi University of Science, Vietnam National University, 334 Nguyen Trai Road, Hanoi, Vietnam

8 Department of Herpetology, American Museum of Natural History, Central Park West at 79th Street, New York, New York 10024, USA

Corresponding author: Truong Quang Nguyen (nqt2@yahoo.com)

Abstract

We describe a new species of the genus *Cyrtodactylus* based on five adult specimens from Bac Ha District, Lao Cai Province, northern Vietnam. *Cyrtodactylus luci* **sp. nov.** is distinguished from the remaining Indochinese bent-toed geckos by a combination of the following morphological characteristics: medium size (SVL up to 89.5 mm); dorsal tubercles in 17–19 irregular transverse rows; ventral scales in 32–34 longitudinal rows at midbody; precloacal pores present in both sexes, 9 or 10 in males, 8 or 9 in females; 12–15 enlarged femoral scales on each thigh; femoral pores 9–12 in males, 5–10 in females; postcloacal tubercles 2–4; lamellae under toe IV 21–23; dorsal pattern consisting of 5 or 6 irregular dark bands, a thin neckband without V-shape or triangle shape in the middle, top of head with dark brown blotches; subcaudal scales transversely enlarged. Molecular phylogenetic analyses recovered the new species as the sister taxon to *C. gulinqingensis* from Yunnan Province, China, with strong support from all analyses and the two taxa are separated by approximately 8.87–9.22% genetic divergence based on a fragment of the mitochondrial ND2 gene. This is the first representative of *Cyrtodactylus* known from Lao Cai Province.

Key words: *Cyrtodactylus luci* sp. nov., gecko, molecular phylogeny, morphology, ND2 gene, taxonomy

Introduction

The *Cyrtodactylus chauquangensis* species group is broadly distributed in the northern Indochina-Burma region, from northern Thailand and Laos to north central and northwestern Vietnam and to southwestern China (Uetz et al. 2023). Taxa within the group are almost exclusively adapted to karst ecosystems. Le et al. (2016) suggested that the group included at least ten species. Grismer et al. (2021a, 2021b) provided a taxonomic review and analyzed phylogenetic relationships of 17 species and one undescribed form from northern Thailand.



Academic editor: Anthony Herrel

Received: 10 December 2023

Accepted: 1 February 2024

Published: 19 February 2024

ZooBank: <https://zoobank.org/9AE17751-35AF-4665-AA7C-C3906D68808F>

Citation: Tran TT, Do QH, Pham CT, Phan TQ, Ngo HT, Le MD, Ziegler T, Nguyen TQ (2024) A new species of the *Cyrtodactylus chauquangensis* species group (Squamata, Gekkonidae) from Lao Cai Province, Vietnam. ZooKeys 1192: 83–102. <https://doi.org/10.3897/zookeys.1192.117135>

Copyright: © Tung Thanh Tran et al. This is an open access article distributed under terms of the Creative Commons Attribution License ([Attribution 4.0 International – CC BY 4.0](https://creativecommons.org/licenses/by/4.0/)).

The group currently contains 23 recognized species with several taxa recently discovered from Yunnan Province, southern China (Grismer et al. 2021a, 2021b, 2021c; Liu and Rao 2021, 2022).

Lao Cai Province is located in the border area between Vietnam and China with an international borderline of 203 km (Portal of Lao Cai Province 2023). Although Lao Cai contains an area of limestone forest (Portal of Lao Cai Province 2023), no representative of *Cyrtodactylus* has been known from this province so far. On the other hand, members of the genus have been recorded in several neighboring forests, including six species from Yunnan Province of China (*Cyrtodactylus dianxiensis* Liu & Rao, 2021, *C. gulinqingensis* Liu, Li, Hou, Orlov & Ananjeva, 2021, *C. hekouensis* Zhang, Liu, Bernstein, Wang & Yuan, 2021, *C. menglianensis* Liu & Rao, 2022, *C. wayakonei* Nguyen, Kingsada, Rösler, Auer & Ziegler, 2010, *C. zhenkangensis* Liu & Rao, 2021) and five other species reported from Vietnam: one species from Lai Chau (*C. martini* Ngo, 2011) and four species from Son La (*C. bichnganae* Ngo & Grismer, 2010, *C. otai* Nguyen, Le, Pham, Ngo, Hoang, Pham & Ziegler, 2015, *C. sonlaensis* Nguyen, Pham, Ziegler, Ngo & Le, 2017 and *C. taybacensis* Pham, Le, Ngo, Ziegler & Nguyen, 2019).

During our recent field trip in northern Vietnam, we collected five specimens of an unnamed gekkonid species from Bac Ha District, Lao Cai Province, which can be assigned to the *Cyrtodactylus chauquangensis* group based on molecular data. However, the population from Lao Cai Province can be distinguished from congeners by morphological differences and genetic divergence. Therefore, we describe it as a new species in the following.

Materials and methods

Sampling

Field surveys were conducted in Bac Ha District, Lao Cai Province, Vietnam in June 2022 and October 2023 (Fig. 1). After being photographed in life, specimens were anesthetized and euthanized in a closed vessel with a piece of cotton wool containing ethyl acetate (Simmons 2002), fixed in 85% ethanol and subsequently stored in 70% ethanol. Specimens were subsequently deposited in the collections of the Institute of Ecology and Biological Resources (IEBR), Hanoi, Vietnam.

Molecular data and phylogenetic analyses

DNA was extracted using DNeasy Blood and Tissue kit (Qiagen, Germany) following manufacturer's instructions. Extracted DNA was amplified by HotStar Taq Mastermix (Qiagen, Germany) with 21 µl volume (10 µl of mastermix, 5 µl of water, 2 µl of each primer at 10 pmol and 2 µl of DNA). PCR conditions were: 95 °C for 15 min to active the taq; with 40 cycles at 95 °C for 30 s, 52 °C for 45 s, 72 °C for 60 s; and the final extension at 72 °C for 6 min. A fragment of the mitochondrial gene, NADH dehydrogenase subunit 2 (ND2), was amplified using the primer pair MetF1 (5'-AAGCTTTCGGGCCCATACC-3') and COIR1 (5'-AGRGTGCCAATGTCTTTGTGRTT-3') (Arevalo et al. 1994; Macey et al. 1997). PCR products were visualized using electrophoresis through a 2% agarose gel stained with ethidium bromide. Successful amplifications were purified to eliminate PCR components using GeneJET™ PCR Purification kit (ThermoFischer



Figure 1. Type locality of *Cyrtodactylus luci* sp. nov. in Lao Cai Province (red circle), Vietnam.

Scientific, Lithuania). Purified PCR products were sent to FirstBase (Malaysia) for sequencing in both directions. We included two samples of the newly discovered population from Lao Cai Province, one of *Cyrtodactylus bichnganae*, one of *C. bobrovi*, one of *C. cucphuongensis*, one of *C. huongsonensis*, one of *C. ngoiensis*, one of *C. sonlaensis*, one of *C. taybacensis*, and one of *C. vilaphongi* along with all available GenBank sequences of these species and other members of the *Cyrtodactylus chauquangensis* group. Two species, *C. hontreensis* and *C. septimontium*, of the *C. intermedius* group, were selected as outgroups (Grismer et al. 2021b). In the end, we were able to incorporate all ingroup taxa (Table 1).

After sequences were aligned by Clustal X v.2.1 (Thompson et al. 1997), data were analyzed using maximum likelihood (ML) as implemented in IQ-TREE (Nguyen et al. 2015), maximum parsimony (MP) implemented in PAUP*4.0b10 (Swofford 2001) and Bayesian inference (BI) as implemented in MrBayes v.3.2.7

Table 1. Species of *Cyrtodactylus* used in the phylogenetic analysis including localities and GenBank accession numbers of the mitochondrial NADH dehydrogenase subunit 2 (ND2) fragment gene (–: data unavailable).

Species	Locality	Museum number/ Field number	Accession number	Reference
<i>C. auribalteatus</i>	Cambodia: Phnom Aural Wildlife Sanctuary, Kampong Speu Province	–	AP018116	Areesirisuk et al. 2018
<i>Cyrtodactylus luci</i> sp. nov.	Vietnam: Coc Ly Commune, Bac Ha District, Lao Cai Province	IEBR R.5240	PP253960	This study
<i>Cyrtodactylus luci</i> sp. nov.	Vietnam: Coc Ly Commune, Bac Ha District, Lao Cai Province	IEBR R.5241	PP253059	This study
<i>C. bichnganae</i>	Vietnam: Son La City, Son La Province	UNS 0473	MF169953	Brennan et al. 2017
<i>C. bichnganae</i>	Vietnam: Son La City, Son La Province	TBU PAT250	PP253951	This study
<i>C. bobrovi</i>	Vietnam: Ngoc Son – Ngo Luong NR, Lac Son District, Hoa Binh Province	IEBR A.2015.29	MT953471	Grismer et al. 2020
<i>C. bobrovi</i>	Vietnam: Tan Lac, Hoa Binh Province	HB.2015.73	PP253953	This study
<i>C. chauquangensis</i>	Vietnam: Quy Hop District, Nghe An Province	NA 2016.1	MT953475	Grismer et al. 2020
<i>C. cucphuongensis</i>	Vietnam: Cuc Phuong NP, Ninh Binh Province	CP 17.02	MT953477	Grismer et al. 2020
<i>C. cucphuongensis</i>	Vietnam: Cuc Phuong NP, Ninh Binh Province	NHQ.17.71	PP253954	This study
<i>C. doisuthep</i>	Thailand: Doi Phrabart abbey, Chiang Dao District, Chiang Mai Province	AUP–00777	MT497801	Chomdej et al. 2021
<i>C. doisuthep</i>	Thailand: Doi Suthep Mt., Chiang Mai Province	AUP–00774	MT550626	Chomdej et al. 2020
<i>C. dumnuui</i>	Thailand: Chiang Dao, Chiang Mai Province	AUP 00768	MW713972	Grismer et al. 2021
<i>C. erythrosp</i>	Thailand: Coral Cave, Pang Mapha District, Mae Hong Son Province	AUP–00771	MT497806	Chomdej et al. 2021
<i>C. erythrosp</i>	Thailand: Moe Cham Pae, Mae Hong Son	AUP 00772	MW713958	Grismer et al. 2021b
<i>C. gulinqingensis</i>	China: Gulinqing NR, Maguan County, Wenshan Prefecture, Yunnan Province	KIZ 061813	MZ782150	Liu et al. 2021
<i>C. gulinqingensis</i>	China: Gulinqing NR, Maguan County, Wenshan Prefecture, Yunnan Province	KIZ 061816	MZ782152	Liu et al. 2021
<i>C. gulinqingensis</i>	China: Gulinqing NR, Maguan County, Wenshan Prefecture, Yunnan Province	KIZ 061817	MZ782153	Liu et al. 2021
<i>C. houaphanensis</i>	Laos: near Viengxai, Houaphan Province	IEBR A.2013.109	MW792067	Grismer et al. 2021b
<i>C. huongsonensis</i>	Vietnam: Huong Son, My Duc District, Hanoi City	IEBR A.2011.3A	MT953481	Grismer et al. 2020
<i>C. huongsonensis</i>	Vietnam: Lac Thuy, Hoa Binh Province	HB.2016.44	PP253957	This study
<i>C. hontreensis</i>	Vietnam: Hon Tre Island, Kien Hai District, Kien Giang Province	LSUHC8583	JX440539	Wood et al. 2012
<i>C. martini</i>	Vietnam: Lai Chau Town, Lai Chau Province	UNS 0471	MF169968	Brennan et al. 2017
<i>C. menglianensis</i>	China: Menglian County, Puer City, Yunnan Province	KIZ20210714	OM296043	Liu and Rao 2022
<i>C. menglianensis</i>	China: Menglian County, Puer City, Yunnan Province	KIZ20210716	OM296044	Liu and Rao 2022
<i>C. ngoiensis</i>	Laos: Ngoi District, Luang Prabang Province	IEBR A.20213.100	MW792066	Grismer et al. 2021b
<i>C. ngoiensis</i>	Laos: Ngoi District, Luang Prabang Province	AT2012.1	PP253956	This study
<i>C. otai</i>	Vietnam: Xuan Nha NR, Van Ho District, Son La Province	TBU 2017.2	MT953486	Grismer et al. 2020
<i>C. puhuensis</i>	Vietnam: Pu Hu Nature Reserve, Thanh Hoa Province	ND 01.15	MT953489	Grismer et al. 2020
<i>C. septimontium</i>	Vietnam: Co To Mountain, An Giang Province	NAP 05321	MH940237	Murdoch et al. 2019
<i>C. sonlaensis</i>	Vietnam: Muong Bang Commune, Phu Yen District, Son La Province	IEBR A.2017.1	MT953492	Grismer et al. 2020
<i>C. sonlaensis</i>	Vietnam: Muong Bang Commune, Phu Yen District, Son La Province	IEBR A.2017.2	PP253958	This study
<i>C. soni</i>	Vietnam: Van Long Wetland NR, Gia Vien District, Ninh Binh Province	IEBR R.2016.4	MT953491	Grismer et al. 2020
<i>C. spelaeus</i>	Laos: Kasi District, Vientiane Province	HLM 0315	MW713962	Grismer et al. 2021b
<i>C. taybacensis</i>	Vietnam: Ca Nang Commune, Quynh Nhai District, Son La Province	IEBR 4379	MT953495	Grismer et al. 2020
<i>C. taybacensis</i>	Vietnam: Ta Ma Commune, Tuan Giao District, Dien Bien Province	DB2021.1	PP253952	This study
<i>C. vilaphongi</i>	Laos: Luang Prabang District, Luang Prabang Province	NUOL R–2013.5	PP253955	This study
<i>C. vilaphongi</i>	Laos: Luang Prabang District, Luang Prabang Province	IEBR A.2013.13	MT953497	Grismer et al. 2021b
<i>C. wayakonei</i>	Laos: Ban Nam Eng, Vieng Phoukha District, Luang Nam Tha Province	ZFMK 91016	MT953498	Grismer et al. 2020
<i>C. zhenkangensis</i>	China: Zhenkang County, Lincang City, Yunnan Province	KIZL2020047	MW792062	Grismer et al. 2021b

(Ronquist et al. 2012). For the MP analysis, heuristic analysis was conducted with 100 random taxon addition replicates using tree-bisection and reconnection (TBR) branch-swapping algorithm, with no upper limit set for the maximum number of trees saved. Bootstrap support (BP) was calculated using 1000 pseudo-replicates and 100 random taxon addition replicates. All characters

were equally weighted and unordered. For the ML analysis, we used IQ-TREE v.1.6.8 (Nguyen et al. 2015) with a single model and 10000 ultrafast bootstrap replications (UFB). The optimal model for nucleotide evolution was determined using jModelTest v.1.2.4 (Darriba et al. 2012).

For the BI analysis, we used the optimal model determined by jModelTest with parameters estimated by MrBayes v.3.2.7. Two independent analyses with four Markov chains (one cold and three heated) were run simultaneously for 10^7 generations with a random starting tree and sampled every 1000 generations. Loglikelihood scores of sample points were plotted against generation time to detect stationarity of the Markov chains. Trees generated prior to stationarity were removed from the final analyses using the burn-in function. The posterior probability values (PP) for all nodes in the final majority rule consensus tree were provided. We regard $BP \geq 70\%$ and UFB and PP of $\geq 95\%$ as strong support and values of $< 70\%$ and $< 95\%$, respectively, as weak support (Hillis and Bull 1993; Ronquist et al. 2012; Minh et al. 2013).

The optimal model for nucleotide evolution was set to GTR+I+G for ML and BI analysis. The cut-off point for the burn-in function was set to 60, or 0.6% of the total number of trees generated, in the Bayesian analysis, as -lnL scores reached stationarity after 60,000 generations in both runs. Uncorrected pairwise divergences were calculated in PAUP*4.0b10.

Morphological characters

Measurements were taken with a digital calliper to the nearest 0.1 mm. Abbreviations are as follows: **SVL**: snout-vent length, measured from tip of snout to vent; **TaL**: tail length, measured from vent to tip of tail (* = regenerated); **HL**: head length, measured from tip of snout to retroarticular process of jaw; **HW**: head width, maximum width of head; **HH**: head height, from occiput to underside of jaws; **OrbD**: orbital diameter, greatest diameter of orbit; **SE**: snout to eye distance, from tip of snout to anterior-most point of eye; **EE**: eye to ear distance, from anterior edge of ear opening to posterior corner of eye; **NE**: nares to eye distance, from anterior-most point of eye to posterior-most point of nostril; **ED**: ear length, longest dimension of ear; **ForeaL**: forearm length, from base of palm to tip of elbow; **CrusL**: crus length, from base of heel to knee; **TrunkL**: trunk length, distance from axilla to groin measured from posterior edge of forelimb insertion to anterior edge of hindlimb insertion; **BW**: body width, the widest distance of body; **Internar**: internarial distance, distance between nares; **Interorb**: interorbital distance, shortest distance between left and right supraciliary scale rows.

Scale counts were taken as follows: **SL**: supralabials, counted from the first labial scale to corner of mouth; **IL**: infralabials, counted from the first labial scale to corner of mouth; **N**: nasal scales surrounding nare; **IN**: postrostrals or internasals; **PM**: postmentals; **GST**: granular scales surrounding dorsal tubercles; **V**: ventral scales in longitudinal rows at midbody; **SLB**: number of scales along the midbody from mental to anterior edge of cloaca; **FP**: femoral pores; **PP**: precloacal pores; **PAT**: postcloacal tubercles; **TubR**: tubercle, number of dorsal longitudinal rows of tubercles at midbody between the lateral folds; **EFS**: enlarged femoral scales, number of enlarged femoral scale beneath each thigh; **NSF IV**: number of subdigital lamellae on the fourth finger; **NST IV**: number of subdigital lamellae on the fourth toe. Bilateral scale counts were given as left/right; above sea level (asl).

Multiple Factor Analysis (MFA)

The MFA was also applied in this study using morphometric and meristic characteristics, including SVL, HL, HW, HH, OrbD, SE, EE, ED, Foreal, CrusL, TrunkL, Internar, Interorb and SL, IL, GST, V, TubR, EFS, FP, PP, PAT, NSF IV, NST IV. Other morphological characteristics were not used due to the limitation of available morphometric and meristic data or incomplete sampling (regenerated tail). All statistical analyses were performed using R Core Team (2023). The MFA used six quantitative groups – “SVL”, “Head” (including HL, HW, HH), “Eye” (consist of OrbD, SE, EE, ED), “FT” (including Foreal and CrusL), “TrunkL”, “Inter” (consist of Internar and Interorb) and eight qualitative groups – “SpeciesInfor” (including Name of species and ID), “SL-IL” (consist of SL and IL in both sides), “GST_PAT_TubR” (including GST, PAT in both sides and TubR), “V”, “EFS” in both sides, “FP” in both sides, “PP”, “LIV” (consist of NSF IV and NST IV in left side). To remove the effects of allometry, morphometric data were also normalized to adjust raw data of morphometrics through the `allom()` function in R package `GroupStruct` (available at [heep://github.com/chankinonn/GroupStruct](https://github.com/chankinonn/GroupStruct)). Accordingly, the allometric formula is $X_{adj} = \log_{10}(X) - \beta[\log_{10}(SVL) - \log_{10}(SVL_{mean})]$, where X_{adj} = adjusted value; X = measured value; β = unstandardized regression coefficient for each population and SVL_{mean} = overall average SVL of two populations (Thorpe 1975, 1983; Turan 1999; Leonart et al. 2000; Grismer et al. 2021a; Chan and Grismer 2022). The ordination test was performed using packages `Factoextra` (Kassambara and Mundt 2017) and `FactoMineR` (Le et al. 2008) in the software R. The approach was applied to identify active groups and to explain phenotypic variance by estimating the first two Dim values-eigenvalue proportions. Similar coded colors in the MFA scatter plot, surrounded with convex hulls, were presented to visualize the phenotypic spaces of the new species and the most closely related species from China, namely *Cyrtodactylus gulinqingensis* Liu, Li, Hou, Orlov & Ananjeva, 2021; spaces were shown within a spatial coordinate of dimension axes (Dim1 and Dim2). To evaluate the overlap, the loadings of Dim1 and Dim2 of each *Cyrtodactylus* individual were extracted to identify the difference between the two species using the T-test. For all the tests, we applied a significance level of $p < 0.05$.

Results

Phylogenetic analysis

The matrix of molecular data contained 1300 aligned characters, of which 580 were parsimony informative. The MP analysis produced a single most parsimonious tree (tree length = 2359, consistency index = 0.49, retention index = 0.66). Tree topologies from three analyses, ML, MP, and BI were similar and the *Cyrtodactylus* from Bac Ha District, Lao Cai Province was recovered with strong statistical support in all analyses as the sister taxon to *C. gulinqingensis* (BP = 94%; UBP = 100%; PP = 1.00) (Fig. 2). In terms of genetic divergences, the new species is separated from *C. gulinqingensis* by 8.87–9.22% based on a fragment of the mitochondrial ND2 gene. Genetically, it is also significantly divergent from other species within the *C. chauquangensis* group with a pairwise divergence of 12.32–23.85% (Suppl. material 1).

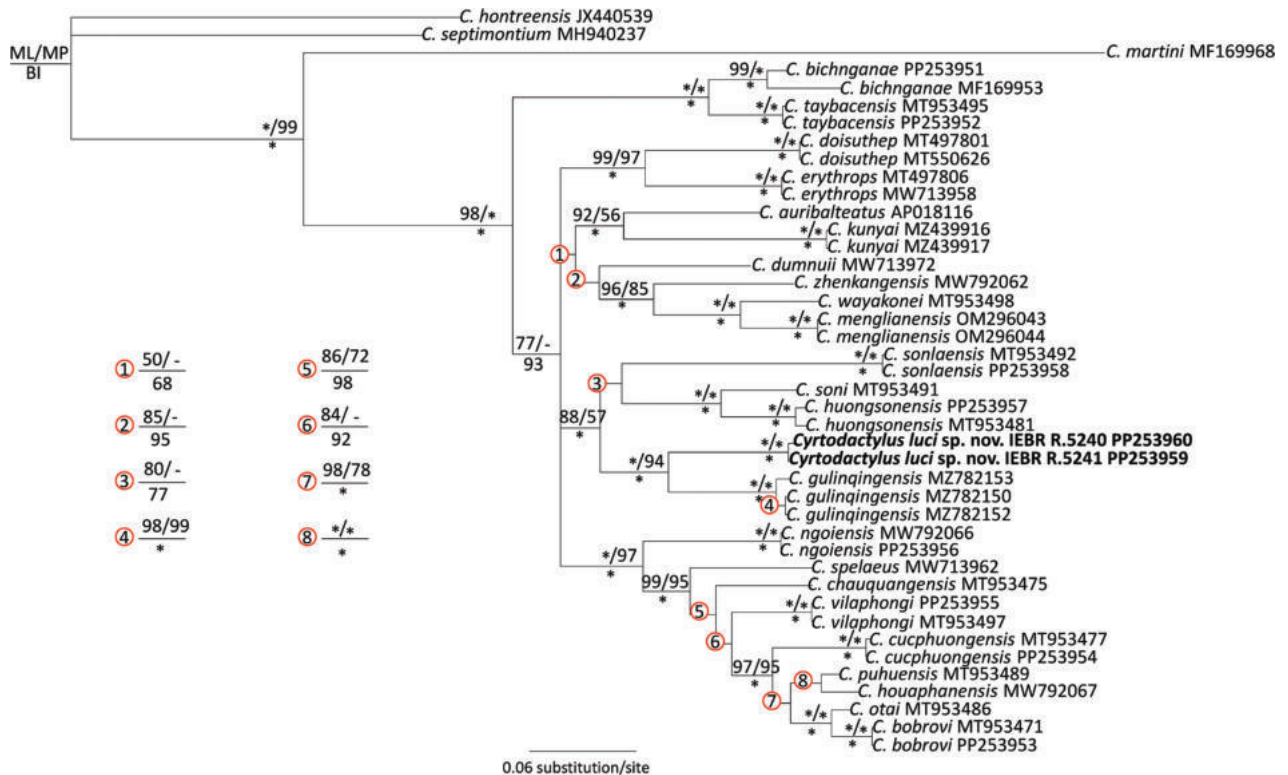


Figure 2. Phylogram based on the Bayesian analysis. Number above and below branches are ML/MP bootstrap and ultrafast bootstrap values and Bayesian posterior probabilities ($\geq 50\%$), respectively. Asterisk and hyphen denote 100% and $> 50\%$ values, respectively.

Morphological analysis

Morphologically, the new species from Bac Ha District, Lao Cai Province is closely similar to *C. gulinqingensis* from Yunnan Province, China, however, they plotted separately from each other in MFA (Fig. 3A) and there was a significant difference between two species ($p < 0.05$). The MFA also identified the data set of SVL, Head, Eye, FT, TrunkL, Inter, SL-IL, GST_PAT_TubR, V, EFS, FP, PP as active groups (Fig. 3B). The Eye, FT, Head, Inter, SVL and Trunk groups were the most important in both the first and second multi-factorial dimensions (Fig. 3C, D).

Taxonomy

Cyrtodactylus luci sp. nov.

<https://zoobank.org/B03559F4-9C45-4991-8A74-5C346FCD6C37>

Figs 4, 5

Type material. Holotype. IEBR R.5237 (Field number BH-LC 2022.5), adult male, collected by T.T. Tran, T.Q. Phan and N.H. Nguyen on 30 June 2022, in limestone karst forest near Tham Phuc Village (22°29.514'N, 104°12.416'E, at an elevation of 677 m a.s.l.), Coc Ly Commune, Bac Ha District, Lao Cai Province, Vietnam. **Paratypes.** IEBR R.5238 (Field number BH-LC 2022.1), IEBR R.5239 (Field number BH-LC 2022.3), adult males and IEBR R.5240, R.5241 (Field numbers BH-LC 2022.2, 2022.4), adult females, bear the same collection data as the holotype.

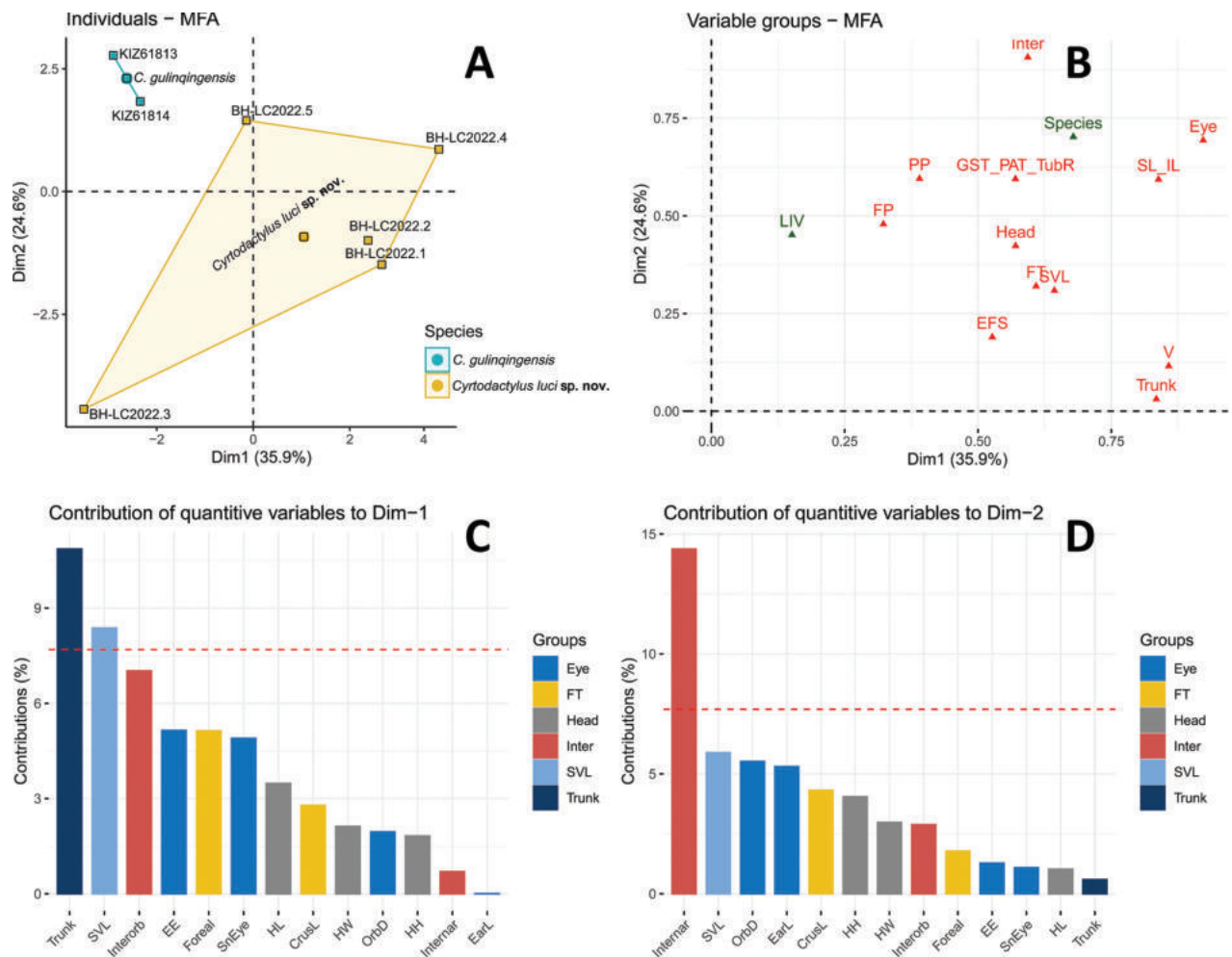


Figure 3. **A** MFA of *Cyrtodactylus luci* sp. nov. from Vietnam and *C. gulinqingensis* from China **B** scatterplot the groups of all variables for Dim1 and Dim2 axes in the MFA, green triangles as inactive groups of variables, red triangles as active groups of variables **C** bar plot of groups' contribution to the first axes (Dim1) in the MFA **D** bar plot of groups' contribution to the second axes (Dim2) in the MFA.

Diagnosis. The new species can be distinguished from other members of the genus *Cyrtodactylus* by a combination of the following characteristics: Size medium (SVL up to 89.5 mm); dorsal tubercles in 17–19 irregular transverse rows; ventral scales in 32–34 longitudinal rows at midbody; precloacal pores present in both sexual, 9 or 10 in males, 8 or 9 in females; 12–15 enlarged femoral scales on each thigh; femoral pores 9–12 in males, 5–10 in females; post-cloacal tubercles 2–4; lamellae under toe IV 21–23; dorsal pattern consisting of 5 or 6 irregular dark bands, a discontinuous thin neckband without V-shape or triangle shape in the middle, dorsal head surface with dark brown blotches; subcaudal scales transversely enlarged.

Description of holotype. Adult male, snout-vent length (SVL) 86.3 mm; body relatively short (TrunkL/SVL 0.4); head distinct from neck, moderately long (HL/SVL 0.28), relatively wide (HW/HL 0.69), slightly depressed (HH/HL 0.41); eye slightly large (OrbD/HL 0.24), pupils vertical; upper eyelid fringe with spinous scales; ear opening below the postocular stripes, obliquely directed and oval, small in size (ED/HL 0.06); two enlarged supranasals, separated from each other anteriorly by one internasal; nares oval, surrounded by supranasal, ros-

tral, first supralabial and three postnasals; loreal region and frontal concave; snout long (SE/HL 0.41), round anteriorly, longer than diameter of orbit (OrbD/SE 0.58); snout scales small, round, granular, larger than those in frontal and parietal regions; rostral wider than high with a medial suture, bordered by first supralabial on each side, nostrils, two supranasals and one internasal; mental triangular, wider than high; postmentals two, enlarged, in contact posteriorly, bordered by mental anteriorly, first infralabial laterally, and an enlarged chin scale posteriorly; supralabials 11/10; infralabials 11/10.

Dorsal scales granular; dorsal tubercles round, keeled, conical, four or five times larger than the size of adjoining scales, each surrounded by 10 granular scales, tubercles forming 17 irregular longitudinal rows at midbody; ventral scales smooth, medial scales 2–3 times larger than dorsal granules, round, subimbricate, largest posteriorly, in 32 longitudinal rows at midbody; lateral folds present, without interspersed tubercles; gular region with homogeneous smooth scales; ventral scales between mental and cloacal slit 170; precloacal groove absent; three rows of enlarged scales present in posterior region of pore-bearing scales; ten precloacal pores arranged in a chevron; 12 or 13 enlarged femoral scales beneath thighs continuous with pore-bearing precloacal scales; femoral pores present on each enlarged femoral scales (except one on right thigh), 24 in total; precloacal pores large, horizontal elongated, positioned in posterior margin of scales; femoral pores small, round, positioned in the center of scales.

Fore and hind limbs moderately slender (ForeaL/SVL 0.16, CrusL/SVL 0.19); dorsal surface of forelimbs covered by few slightly developed tubercles; fingers and toes lacking distinct webbing; subdigital lamellae: finger I 12, finger II 16, finger III 17, finger IV 20, finger V 18, toe I 12, toe II 17, toe III 20, toe IV 21, toe V 20.

Tail regenerated, 104.5 mm in length (generated part 19.5 mm); longer than snout-vent length (TaL/SVL: 1.21); postcloacal tubercles 4/4; subcaudals on original part of tail distinctly transversely enlarged, flat, smooth.

Coloration in life. Ground color of dorsal surface of head, neck, body, limbs and tail light brown. Dorsal surface of head with some dark brown blotches; labial region brown with yellowish cream stripes; skin above the eye gray; eyelid with light yellow color; iris yellow copper with black marking; pupil vertical, elliptical, black; nuchal loop dark brown, discontinuous, extending from posterior corner of eye to the neck; tubercles on head, limbs, dorsum light brown to yellow; dorsum with five irregularly-shaped transversal bands and additional irregular smaller blotches; upper surface of limbs with irregular brown marks; six dark brown irregular bands on original part of tail while regenerated part of tail dark gray; chin, throat, chest, belly, lower limbs and ventral surface of tail cream.

Coloration in preservative. The overall color scheme slightly fades in 70% alcohol; yellow color disappeared in preservation while main characteristics are still clearly discernible; dorsal ground color of head, neck, body, limbs and tail grayish brown; color of chin, throat, chest, belly and lower limbs did not change noticeably in preservation.

Sexual dimorphism and variation. The males differ from females in the shape of precloacal pores (larger in males), and the presence of hemipenial swellings at the tail base. For other morphological characteristics see Table 2, Figs 4, 5.

Distribution. *Cyrtodactylus luci* sp. nov. is currently known only from the type locality in Bac Ha District, Lao Cai Province, Vietnam (Fig. 1).

Etymology. The species was named after the zoologist from the Vietnam National Museum of Nature, Vietnam Academy of Science and Technology, late Associate Professor Doctor Luc Van Pham, who contributed greatly to the biodiversity study in Vietnam. For the common names, we suggest Luc's Bent-toed Gecko (English) and Thạch sùng ngón lợc (Vietnamese).



Figure 4. Male holotype of *Cyrtodactylus luci* sp. nov. (IEBR R.5237) in life. Photo: T.Q. Phan.



Figure 5. Female paratype of *Cyrtodactylus luci* sp. nov. (IEBR R.5241) in life. Photo: T.Q. Phan.

Natural history. The bent-toed geckos were collected between 19:00 and 22:00, both on limestone cliffs and on trees, about 1.0–1.8 m above the ground. The surrounding habitat was secondary karst forest of medium and small hardwoods mixed with shrubs and vines (Fig. 6). Air temperature was 25.9 °C and relative humidity was 92%.

Comparisons. *Cyrtodactylus luci* sp. nov. is distinguishable from all other members of the *C. chauquangensis* species group by a unique combination of morphological characteristics.

Cyrtodactylus luci sp. nov. differs from *C. auribalteatus* Sumontha, Panitvong & Deen, 2010 by having fewer ventral scale rows (32–34 vs. 38–40 in *C. auribalteatus*), more enlarged femoral scales on each side (12–15 vs. 5–7 in *C. auribalteatus*), more femoral pores on each side in males (9–12 vs. 4 or 5 in *C. auribalteatus*), the presence of femoral pores on each side in females (5–10 vs.

Table 2. Measurements (in mm) and morphological characteristics (abbreviations as in Material and methods) of the type series of *Cyrtodactylus luci* sp. nov. (* = regenerated or broken tail); bilateral meristic characteristics are given as (left/right).

Characters	IEBR R.5237	IEBR R.5238	IEBR R.5239	IEBR R.5240	IEBR R.5241	Min–Max
	(Holotype)	(Paratype)	(Paratype)	(Paratype)	(Paratype)	
Sex	M	M	M	F	F	
SVL	86.3	88.7	71.7	87.1	89.5	71.7–89.5
TaL	104.5*	107.7	86.2	84.2*	84.1*	86.2–107.7
HL	24.5	24.0	20.3	24.6	25.2	20.3–25.2
HW	16.9	16.6	12.8	17.4	17.4	12.8–17.4
HH	10.1	9.8	7.1	9.7	10.6	7.1–10.6
OrbD	5.9	4.9	4.7	5.1	4.8	4.7–5.9
SE	10.2	10.0	8.4	10.6	10.8	8.4–10.8
EE	6.5	6.6	5.5	6.6	7.2	5.5–7.2
NE	7.5	7.9	6.0	7.7	8.7	6.0–8.7
ED	1.4	1.6	1.9	1.8	1.3	1.4–1.9
ForeaL	14.2	14.2	11.5	14.1	14.4	11.5–14.4
CrusL	16.3	17.2	13.5	16.7	16.8	13.5–17.2
TrunkL	34.4	39.7	31.5	39.7	42.1	31.5–42.1
BW	13.8	14.0	9.4	17.6	19.2	9.4–19.2
Internar	2.8	2.5	2.0	2.7	3.0	2.0–3.0
Interorb	6.9	7.3	5.2	7.6	7.8	5.2–7.8
SL	11/10	11/11	10//10	11/10	11/9	9–11
IL	11/10	12/12	11/13	11/10	9/12	9–13
N	4/4	4/4	4/4	4/4	4/5	4–5
IN	1	1	1	1	1	1
PM	2	3	2	2	2	2
GST	10/10/10	10/10/10	10/9/10	10/10/10	10/10/10	9–10
V	32	34	32	34	34	32–34
SLB	170	171	169	171	166	166–171
FP	12/12	10/9	11/12	10/10	7/5	9–12 in males 5–10 in females
PP	10	9	9	8	9	9–10 in males 8–9 in females
PAT	3/3	4/2	3/3	4/3	3/3	2–4
TubR	17	17	17	19	18	17–19
EFS	13/12	14/15	14/14	13/13	17/15	12–15
NSF IV	18	21	20	19	20	18–21
NST IV	21	23	23	21	23	21–23

absent in *C. auribalteatus*), more precloacal pores in males (9 or 10 vs. 6 in *C. auribalteatus*), the presence of precloacal pores in females (8 or 9 vs. absent in *C. auribalteatus*) and fewer dorsal tubercle rows (17–19 vs. 22–24 in *C. auribalteatus*); from *C. bichnganae* Ngo & Grismer, 2010 by having a smaller size (SVL 71.7–89.5 mm vs. 95.3–99.9 mm in *C. bichnganae*), more ventral scale rows (32–34 vs. 30 or 31 in *C. bichnganae*), more femoral pores on each side in females (5–10 vs. 1 in *C. bichnganae*), and more lamellae under toe IV (21–23 vs. 16–20 in *C. bichnganae*); from *C. bobrovi* Nguyen, Le, Pham, Ngo, Hoang, Pham & Ziegler, 2015 by having fewer ventral scale rows (32–34 vs. 40–45 in *C. bobrovi*), the presence of enlarged femoral scales on each side (12–15 vs. absent in *C. bobrovi*), the presence of femoral pores on each side in males (9–12 vs. absent in *C. bobrovi*) and in females (5–10 vs. absent in *C. bobrovi*), more precloacal pores in males (9 or 10 vs. 5 in *C. bobrovi*), the presence of precloacal pores in females (8 or 9 vs. absent in *C. bobrovi*), and the presence of transversely enlarged subcaudal plates (vs. absent in *C. bobrovi*); from *C. chauquangensis* Hoang, Orlov, Ananjeva, Johns, Hoang & Dau, 2007 by having a smaller size (SVL 71.7–89.5 mm vs. 91.0–99.3 mm in *C. chauquangensis*), fewer ventral scale rows (32–34 vs. 36–38 in *C. chauquangensis*), the presence of enlarged femoral scales on each side (12–15 vs. absent in *C. chauquangensis*), the presence of femoral pores on each side in males (9–12 vs. absent in *C. chauquangensis*) and also in females (5–10 vs. absent in *C. chauquangensis*), more precloacal pores in males (9 or 10 vs. 6 or 7 in *C. chauquangensis*) and also in females (8 or 9 vs. 6 or 7 in *C. chauquangensis*); from *C. cucphuongsensis* Ngo & Chan, 2011 by having fewer ventral scale rows (32–34 vs. 42 in *C. cucphuongsensis*), the presence of femoral pores on each side in males (9–12 vs. absent in *C. cucphuongsensis*) and in females (5–10 vs. absent in *C. cucphuongsensis*) and the presence of precloacal pores in males (9–10 vs. absent in *C. cucphuongsensis*); from *C. doisuthep* Kunya, Panmongkol, Pauwels, Sumontha, Meewasana, Bunkhwamdi & Dangsri, 2015 by the presence of femoral pores on each side in males (9–12 vs. absent in *C. doisuthep*) and in females (5–10 vs. absent in *C. doisuthep*), more precloacal pores in males (9 or 10 vs. 5 or 6 in *C. doisuthep*) and also in females (8 or 9 vs. absent in *C. doisuthep*); from *C. dumnuii* Bauer, Kunya, Sumontha, Niyomwan, Pauwels, Chanhome & Kunya, 2010 by having fewer ventral scale rows (32–34 vs. 40 in *C. dumnuii*), more femoral pores on each side in males (9–12 vs. 6–7 in *C. dumnuii*) and in females (5–10 vs. absent in *C. dumnuii*), more precloacal pores in males (9 or 10 vs. 5 or 6 in *C. dumnuii*) and also in females (8 or 9 vs. 0–7 in *C. dumnuii*) and more lamellae under toe IV (21–23 vs. 19 in *C. dumnuii*); from *C. erythropros* Bauer, Kunya, Sumontha, Niyomwan, Panitvong, Pauwels, Chanhome & Kunya, 2009 by having more ventral scale rows (32–34 vs. 28 in *C. erythropros*), more lamellae under finger IV (18–21 vs. 16 in *C. erythropros*), more lamellae under toe IV (21–23 vs. 20 in *C. erythropros*) and differences in dorsal color pattern (banded vs. blotched in *C. erythropros*); from *C. gulinqingensis* Liu, Li, Hou, Orlov & Ananjeva, 2021 by having more dorsal tubercle rows (17–19 vs. 14–16 in *C. gulinqingensis*), fewer femoral pores on each side in males (9–12 vs. 13–15 in *C. gulinqingensis*) and in females (5–10 vs. 1–3 in *C. gulinqingensis*) and fewer precloacal pores in females (8 or 9 vs. 7 in *C. gulinqingensis*); from *C. houaphanensis* Schneider, Luu, Sitthivong, Teynié, Le, Nguyen & Ziegler, 2020 by having fewer ventral scale rows (32–34 vs. 35 in *C. houaphanensis*), the presence of enlarged femoral scales on each side (12–15 vs. absent in *C. houaphanensis*), the presence of femoral pores on each

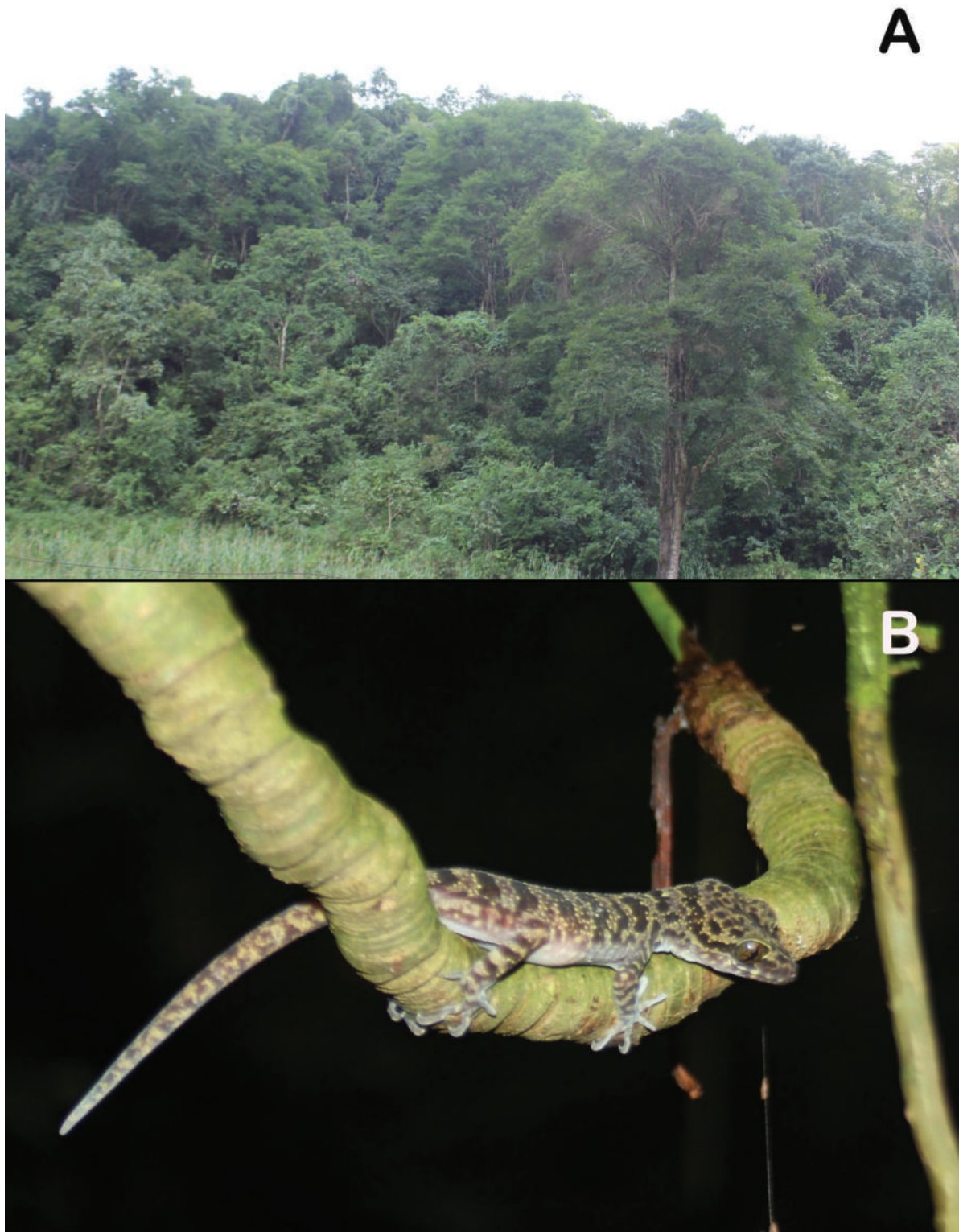


Figure 6. **A** macrohabitat **B** microhabitat of *Cyrtodactylus luci* sp. nov. Coc Ly Commune, Bac Ha District, Lao Cai Province, Vietnam. Photo: T.Q. Phan.

side in males (9–12 vs. absent in *C. houaphanensis*) and in females (5–10 vs. absent in *C. houaphanensis*) and more precloacal pores in males (9 or 10 vs. 6 in *C. houaphanensis*); from *C. huongsonensis* Luu, Nguyen, Do & Ziegler, 2011 by having fewer ventral scale rows (32–34 vs. 41–48 in *C. huongsonensis*), more

enlarged femoral scales on each side (12–15 vs. 7–9 in *C. huongsonensis*) and more precloacal pores in males (9 or 10 vs. 6 in *C. huongsonensis*); from *C. martini* Ngo, 2011 by having fewer ventral scale rows (32–34 vs. 39–43 in *C. martini*), more precloacal pores in males (9 or 10 vs. 4 in *C. martini*), the presence of precloacal pores in females (8 or 9 vs. absent in *C. martini*) and the presence of transversely enlarged subcaudal plates (vs. absent in *C. martini*); from *C. menglianensis* Liu & Rao, 2022 by having more ventral scale rows (32–34 vs. 26–29 in *C. menglianensis*), the presence of enlarged femoral scales on each side (12–15 vs. absent in *C. menglianensis*), the presence of femoral pores on each side in males (9–12 vs. absent in *C. menglianensis*) and in females (5–10 vs. absent in *C. menglianensis*), more precloacal pores in males (9 or 10 vs. 7 in *C. menglianensis*) and the presence of precloacal pores in females (8 or 9 vs. absent in *C. menglianensis*); from *C. ngoiensis* Schneider, Luu, Sitthivong, Teynié, Le, Nguyen & Ziegler, 2020 by having fewer ventral scale rows (32–34 vs. 38–43 in *C. ngoiensis*), more enlarged femoral scales on each side (12–15 vs. 7–10 in *C. ngoiensis*), more femoral pores on each side in males (9–12 vs. 7 in *C. ngoiensis*) and in females (5–10 vs. absent in *C. ngoiensis*), more precloacal pores in males (9 or 10 vs. 7 in *C. ngoiensis*) and in females (8 or 9 vs. 7 in *C. ngoiensis*) and more lamellae under toe IV (21–23 vs. 19–20 in *C. ngoiensis*); from *C. otai* Nguyen, Le, Pham, Ngo, Hoang, Pham & Ziegler, 2015 by having fewer ventral scale rows (32–34 vs. 38–43 in *C. otai*), the presence of enlarged femoral scales on each side (12–15 vs. absent in *C. otai*), the presence of femoral pores on each side in males (9–12 vs. absent in *C. otai*) and in females (5–10 vs. absent in *C. otai*), more precloacal pores in males (9 or 10 vs. 7 or 8 in *C. otai*), the presence of precloacal pores in females (8 or 9 vs. absent in *C. otai*), and the presence of transversely enlarged subcaudal plates (vs. absent in *C. otai*); from *C. puhuensis* Nguyen, Yang, Le, Nguyen, Orlov, Hoang, Nguyen, Jin, Rao, Hoang, Che, Murphy & Zhang, 2014 by having fewer ventral scale rows (32–34 vs. 36 in *C. puhuensis*), the presence of femoral pores on each side in males (9–12 vs. absent in *C. puhuensis*) and in females (5–10 vs. absent in *C. puhuensis*), and more precloacal pores in males (9 or 10 vs. 5 in *C. puhuensis*); from *C. soni* Le, Nguyen, Le & Ziegler, 2016 by having fewer ventral scale rows (32–34 vs. 41–45 in *C. soni*), more dorsal tubercle rows (17–19 vs. 10–13 in *C. soni*), more enlarged femoral scales on each side (12–15 vs. 8–11 in *C. soni*), more femoral pores on each side in males (9–12 vs. 6–8 in *C. soni*), and more precloacal pores in males (9 or 10 vs. 6 or 7 in *C. soni*); from *C. sonlaensis* Nguyen, Pham, Ziegler, Ngo & Le, 2017 by having more dorsal tubercle rows (17–19 vs. 13–15 in *C. sonlaensis*), fewer femoral pores on each side in males (9–12 vs. 14–15 in *C. sonlaensis*), the presence of femoral pores on each side in females (5–10 vs. absent in *C. sonlaensis*), more precloacal pores in males (9 or 10 vs. 8 in *C. sonlaensis*) and the presence of precloacal pores in females (8 or 9 vs. absent in *C. sonlaensis*); from *C. spelaeus* Nazarov, Poyakov, Orlov, Nguyen, Milto, Martynov, Konstantinov & Chulisov, 2014 by having fewer ventral scale rows (32–34 vs. 36–39 in *C. spelaeus*), the presence of enlarged femoral scales on each side (12–15 vs. absent in *C. spelaeus*), the presence of femoral pores on each side in males (9–12 vs. absent in *C. spelaeus*) and in females (5–10 vs. absent in *C. spelaeus*) and differences in dorsal color pattern (banded vs. blotched in *C. spelaeus*); from *C. taybacensis* Pham, Le, Ngo, Ziegler & Nguyen, 2019 by having more dorsal tubercle rows (17–19 vs. 13–16 in *C. taybacensis*), the presence of femoral pores on each side in males (9–12 vs. absent in *C. taybacensis*)

and in females (5–10 vs. absent in *C. taybacensis*), fewer precloacal pores in males (9 or 10 vs. 11–13 in *C. taybacensis*) and more lamellae under toe IV (21–23 vs. 16–20 in *C. taybacensis*); from *C. vilaphongi* Schneider, Nguyen, Le, Nophaseud, Bonkowski & Ziegler, 2014 by having more dorsal tubercle rows (17–19 vs. 15–16 in *C. vilaphongi*), the presence of enlarged femoral scales on each side (12–15 vs. absent in *C. vilaphongi*), the presence of femoral pores on each side in females (5–10 vs. absent in *C. vilaphongi*) and in females (8 or 9 vs. absent in *C. vilaphongi*), more lamellae under toe IV (21–23 vs. 18–20 in *C. vilaphongi*), and the presence of transversely enlarged subcaudal plates (vs. absent in *C. vilaphongi*); from *C. wayakonei* Nguyen, Kingsada, Rosler, Auer & Ziegler, 2010 by the presence of enlarged femoral scales on each side (12–15 vs. absent in *C. wayakonei*), the presence of femoral pores on each side in males (9–12 vs. absent in *C. wayakonei*) and in females (5–10 vs. absent in *C. wayakonei*), more precloacal pores in males (9 or 10 vs. 6–8 in *C. wayakonei*) and in females (8 or 9 vs. 7 in *C. wayakonei*), and more lamellae under toe IV (21–23 vs. 19–20 in *C. wayakonei*); from *C. zhenkangensis* Liu & Rao, 2021 by having fewer dorsal tubercle rows (17–19 vs. 20–24 in *C. zhenkangensis*), more femoral pores on each side in males (9–12 vs. 2–5 in *C. zhenkangensis*) and in females (5–10 vs. 0–3 in *C. zhenkangensis*) and the presence of dark-colored nuchal loop (vs. absent in *C. zhenkangensis*).

Discussion

The new species from Bac Ha District, Lao Cai Province, is most similar to *Cyrtodactylus gulinqingensis*, a recently described species from Muguang County, Wenshan Prefecture, Yunnan Province of China (Liu et al. 2021). In terms of geographic distribution, the type locality of *C. luci* is approximately 40 km distant from that of its sister species in China. However, they are distinguished from each other by morphological differences as well as a genetic divergence of 8.87–9.22% (ND2 gene).

Our tree topology (Fig. 2) is similar to that reported in Grismer et al. (2021b). However, while *C. auribalteatus* is recovered as a member of the clade including *C. dumnuui*, *C. wayakonei* and other taxa in this study, it is grouped with the lineage consisting of *C. sonlaensis*, *C. huongsonensis* and *C. soni* in Grismer et al. (2021b). According to our phylogenetic analyses, the new species and *C. gulinqingensis* from Yunnan cluster with the latter clade with strong nodal support provided only by BI (Fig. 2). In addition to *C. luci* and *C. gulinqingensis*, the other species in the group occur in Son La (*C. sonlaensis*) and Ninh Binh (*C. soni*) provinces and the suburb of Ha Noi City (*C. huongsonensis*), northwestern Vietnam.

In the *Cyrtodactylus chauquangensis* group, except for *C. doisuthep*, a species known from dry evergreen and deciduous dipterocarp forests in Thailand (Kunya et al. 2014), all 23 remaining species are karst dwellers, comprising three species from Yunnan Province of China, five species from northern Laos, four species from northern Thailand, and 12 species from northern Vietnam (Uetz et al. 2023, this study). In terms of altitudinal distribution range, the members of this species group are found at elevations from 17 m (*C. soni*) to 1660 m (*C. doisuthep*) but most of them occur at elevations between 300 and 800 m a.s.l. (Kunya et al. 2015; Le et al. 2016). The new species is the 24th species of the *C. chauquangensis* group, the first species from Lao Cai Province and the eastern side of the Red River in Vietnam, and the 53rd species of *Cyrtodactylus* known from Vietnam (Ngo et al. 2022; Uetz et al. 2023).

Acknowledgements

We are grateful to the directorate of the Forest Protection Department of Lao Cai Province for supporting our field work. We thank N.H. Nguyen (Hanoi) for his assistance in the field and T.A. Tran (Hanoi) for providing the map. For the fruitful collaboration within joint research projects, we cordially thank A.H. Le (IEBR, Hanoi), as well as T. Pagel and C. Landsberg (Cologne Zoo). Many thanks to L.L. Grismer (La Sierra) and V.Q. Luu (Hanoi) for their helpful comments on our manuscript.

Additional information

Conflict of interest

The authors have declared that no competing interests exist.

Ethical statement

No ethical statement was reported.

Funding

This research is funded by the National Foundation for Science and Technology Development (NAFOSTED, Grant No. 106.05-2021.19). Doctoral research of HT Ngo in Germany is funded by the German Academic Exchange Service (DAAD).

Author contributions


Conceptualization: TQN. Data curation: TQP, HTN, QHD, CTP, TTT. Formal analysis: HTN, CTP, MDL, QHD. Funding acquisition: TQN. Investigation: TQP, TTT. Methodology: MDL, TZ, TQN. Supervision: TQN, TZ. Writing - original draft: HTN, TQN, QHD. Writing - review and editing: MDL, HTN, TZ, CTP, TQP, TTT, TQN.

Author ORCIDs

Tung Thanh Tran  <https://orcid.org/0000-0001-7648-1179>

Quyen Hanh Do  <https://orcid.org/0000-0002-9437-4673>

Cuong The Pham  <https://orcid.org/0000-0001-5158-4526>

Tien Quang Phan  <https://orcid.org/0000-0002-2738-5364>

Hanh Thi Ngo  <https://orcid.org/0000-0002-5283-6243>

Minh Duc Le  <https://orcid.org/0000-0002-2953-2815>

Thomas Ziegler  <https://orcid.org/0000-0002-4797-609X>

Truong Quang Nguyen  <https://orcid.org/0000-0002-6601-0880>

Data availability

All of the data that support the findings of this study are available in the main text or Supplementary Information.

References

Areesirisuk P, Muangmai N, Kunya K, Singchat W, Sillapaprayoon S, Lapbenjakul S, Thapana W, Kantachumpoo A, Baicharoen S, Rerkamnuyachoke B, Peyachoknagul S, Han K, Srikulnath K (2018) Characterization of five complete *Cyrtodactylus* mitogenome structures reveals low structural diversity and conservation of repeated sequences in the lineage. PeerJ 6: e6121. <https://doi.org/10.7717/peerj.6121>

- Arevalo E, Davis SK, Sites JW (1994) Mitochondrial DNA sequence divergence and phylogenetic relationships among eight chromosome races of the *Sceloporus grammicus* complex (Phrynosomatidae) in central Mexico. *Systematic Biology* 43(3): 387–418. <https://doi.org/10.1093/sysbio/43.3.387>
- Bauer AM, Kunya K, Sumontha M, Niyomwan P, Panitvong N, Pauwels OSG, Chanhome L, Kunya T (2009) *Cyrtodactylus erythrops* (Squamata: Gekkonidae), a new cave-dwelling gecko from Mae Hong Son Province, Thailand. *Zootaxa* 3811(1): 251–261. <https://doi.org/10.11646/zootaxa.2124.1.4>
- Bauer A, Kunya K, Sumontha M, Niyomwan P, Pauwels OSG, Chanhome L, Kunya T (2010) *Cyrtodactylus dumnuui* (Squamata: Gekkonidae), a new cave-dwelling gecko from Chiang Mai Province, Thailand. *Zootaxa* 2570(1): 41–50. <https://doi.org/10.11646/zootaxa.2570.1.2>
- Brennan IG, Bauer AM, Ngo TV, Wang YY, Wang WZ, Zhang YP, Murphy RW (2017) Barcoding utility in a mega-diverse, cross-continental genus: Keeping pace with *Cyrtodactylus* geckos. *Scientific Reports* 7(1): e5592. <https://doi.org/10.1038/s41598-017-05261-9>
- Chan KO, Grismer LL (2022) GroupStruct: An R package for allometric size correction. *Zootaxa* 5124(4): 471–482. <https://doi.org/10.11646/zootaxa.5124.4.4>
- Chomdej S, Pradit W, Suwannapoom C, Pawangkhanant P, Nganvongpanit K, Poyarkov NA, Che J, Gao Y, Gong S (2021) Phylogenetic analyses of distantly related clades of bent-toed geckos (genus *Cyrtodactylus*) reveal an unprecedented amount of cryptic diversity in northern and western Thailand. *Scientific Reports* 11(1): 2328. <https://doi.org/10.1038/s41598-020-70640-8>
- Darriba D, Taboada GL, Doallo R, Posada D (2012) jmodelTest 2: More models, new heuristics and high-performance computing. *Nature Methods* 9(8): e772. <https://doi.org/10.1038/nmeth.2109>
- Grismer LL, Wood Jr PL, Le MD, Grismer JL (2020) Evolution of habitat preference in 243 species of Bent-toed geckos (Genus *Cyrtodactylus* Gray, 1827) with a discussion of karst habitat conservation. *Ecology and Evolution* 10(24): 13717–13730. <https://doi.org/10.1002/ece3.6961>
- Grismer LL, Suwannapoom C, Pawangkhanant P, Nazarov RA, Yushchenko PV, Naiduangchan M, Le MD, Luu VQ, Poyarkov NA (2021a) A new cryptic arboreal species of the *Cyrtodactylus brevipalmatus* group (Squamata: Gekkonidae) from the uplands of western Thailand. *Vertebrate Zoology* 71: 723–746. <https://doi.org/10.3897/vz.71.e76069>
- Grismer LL, Wood Jr PL, Poyarkov NA, Le MD, Kraus F, Agarwal I, Oliver PM, Nguyen SN, Nguyen TQ, Karunarathna S, Welton LJ, Stuart BL, Luu VQ, Bauer AM, O'Connell KA, Quah ESH, Chan KO, Ziegler T, Ngo H, Nazarov RA, Aowphol A, Chomdej S, Suwannapoom C, Siler CD, Anuar S, Ngo TV, Grismer JL (2021b) Phylogenetic partitioning of the third-largest vertebrate genus in the world, *Cyrtodactylus* Gray, 1827 (Reptilia; Squamata; Gekkonidae) and its relevance to taxonomy and conservation. *Vertebrate Zoology* 71: 101–154. <https://doi.org/10.3897/vertebrate-zoology.71.e59307>
- Grismer LL, Wood Jr PL, Poyarkov NA, Le MD, Karunarathna S, Chomdej S, Suwannapoom C, Qi S, Liu S, Che J, Quah E, Kraus F, Oliver P, Riyanto A, Pauwels O, Grismer J (2021c) Karstic landscapes are foci of species diversity in the world's third-largest vertebrate genus *Cyrtodactylus* Gray, 1827 (Reptilia: Squamata; Gekkonidae). *Diversity* 13(5): 1–15. <https://doi.org/10.3390/d13050183>
- Hillis DM, Bull JJ (1993) An empirical test of bootstrapping as a method for assessing confidence in phylogenetic analysis. *Systematic Biology* 42(2): 182–192. <https://doi.org/10.1093/sysbio/42.2.182>

- Hoang QX, Orlov NL, Ananjeva NB, Johns AG, Hoang TN, Dau VQ (2007) Description of a new species of the genus *Cyrtodactylus* Gray, 1827 (Squamata: Sauria: Gekkonidae) from the karst of North Central Vietnam. *Russian Journal of Herpetology* 14: 98–106.
- Kassambara A, Mundt F (2017) Factoextra: extract and visualize the result of multivariate data analyses. [r package, version 1.0.5.999]
- Kunya K, Panmongkol A, Pauwels O, Sumontha M, Meewasana J, Bunkhwamdi W, Dangsri S (2014) A new forest-dwelling Bent-toed Gecko (Squamata: Gekkonidae: *Cyrtodactylus*) from Doi Suthep, Chiang Mai Province, northern Thailand. *Zootaxa* 3811(2): 251–261. <https://doi.org/10.11646/zootaxa.3811.2.6>
- Kunya K, Sumontha M, Panitvong N, Dongkumfu W, Sirisamphan T, Pauwels O (2015) A new forest-dwelling Bent-toed Gecko (Squamata: Gekkonidae: *Cyrtodactylus*) from Doi Inthanon, Chiang Mai Province, northern Thailand. *Zootaxa* 3905: 573–584. <https://doi.org/10.11646/zootaxa.3905.4.9>
- Le S, Josse J, Husson F (2008) FactoMiner: A Package for Multivariate Analysis. *Journal of Statistical Software* 25(1): 1–18. <https://doi.org/10.18637/jss.v025.i01>
- Le DT, Nguyen TQ, Le MD, Ziegler T (2016) A new species of *Cyrtodactylus* (Squamata: Gekkonidae) from Ninh Binh Province, Vietnam. *Zootaxa* 4162(2): 268–282. <https://doi.org/10.11646/zootaxa.4162.2.4>
- Liu S, Rao DQ (2021) A new species of *Cyrtodactylus* Gray, 1827 (Squamata, Gekkonidae) from Yunnan, China. *ZooKeys* 1021: 109–126. <https://doi.org/10.3897/zookeys.1021.60402>
- Liu S, Rao D (2022) A new species of *Cyrtodactylus* Gray, 1827 (Squamata, Gekkonidae) from southwestern Yunnan, China. *ZooKeys* 1084: 83–100. <https://doi.org/10.3897/zookeys.1084.72868>
- Liu S, Li Q, Hou M, Orlov NL, Ananjeva NB (2021) A new species of *Cyrtodactylus* Gray (Squamata, Gekkonidae) from southern Yunnan, China. *Russian Journal of Herpetology* 28(4): 185–196. <https://doi.org/10.30906/1026-2296-2021-28-4-185-196>
- Lleonart J, Salat J, Torres GJ (2000) Removing allometric effects of body size in morphological analysis. *Journal of Theoretical Biology* 205(1): 85–93. <https://doi.org/10.1006/jtbi.2000.2043>
- Luu VQ, Nguyen TQ, Do HQ, Ziegler T (2011) A new *Cyrtodactylus* (Squamata: Gekkonidae) from Huong Son limestone forest, Hanoi, northern Vietnam. *Zootaxa* 3129(1): 39–50. <https://doi.org/10.11646/zootaxa.3129.1.3>
- Macey JR, Larson A, Ananjeva NB, Fang Z, Papenfuss TJ (1997) Two novel gene orders and the role of light-strand replication in rearrangement of the vertebrate mitochondrial genome. *Molecular Biology and Evolution* 14(1): 91–104. <https://doi.org/10.1093/oxfordjournals.molbev.a025706>
- Minh BQ, Nguyen MAT, von Haeseler A (2013) Ultrafast approximation for phylogenetic bootstrap. *Molecular Biology and Evolution* 30(5): 1188–1195. <https://doi.org/10.1093/molbev/mst024>
- Murdoch ML, Grismer LL, Wood Jr PL, Thy N, Poyarkov NA, Tri NV, Aowphol A, Pauwels OSB, Grismer JL (2019) Six new species of the *Cyrtodactylus intermedius* complex (Squamata: Gekkonidae) from the Cardamom Mountains and associated highlands of Southeast Asia. *Zootaxa* 4554(1): 1–62. <https://doi.org/10.11646/zootaxa.4554.1.1>
- Nazarov RA, Poyarkov Jr NA, Orlov NL, Nguyen SN, Milto KD, Martynov AA, Konstantinov EL, Chulisov AS (2014) A review of genus *Cyrtodactylus* (Reptilia: Sauria: Gekkonidae) in fauna of Laos with description of four new species. *Trudy Zoologicheskogo Instituta* 318(4): 391–423. <https://doi.org/10.31610/trudyzin/2014.318.4.391>

- Ngo TV (2011) *Cyrtodactylus martini*, another new karst-dwelling *Cyrtodactylus* Gray, 1827 (Squamata: Gekkonidae) from Northwestern Vietnam. *Zootaxa* 2834(1): 33–46. <https://doi.org/10.11646/zootaxa.2834.1.3>
- Ngo TV, Chan KO (2011) A new karstic cave-dwelling *Cyrtodactylus* Gray (Squamata: Gekkonidae) from northern Vietnam. *Zootaxa* 3125: 51–63.
- Ngo TV, Grismer LL (2010) A new karst dwelling *Cyrtodactylus* (Squamata: Gekkonidae) from Son La Province, northwestern Vietnam. *Hamadryad* 35: 84–95. <https://doi.org/10.11646/zootaxa.3835.1.4>
- Ngo HT, Do QH, Pham CT, Luu VQ, Grismer LL, Ziegler T, Nguyen VTH, Nguyen TQ, Le MD (2022) How many more species are out there? Current taxonomy substantially underestimates the diversity of bent-toed geckos (genus *Cyrtodactylus*) in Laos and Vietnam. *ZooKeys* 1097: 135–152. <https://doi.org/10.3897/zookeys.1097.78127>
- Nguyen TQ, Kingsada P, Rösler H, Auer M, Ziegler T (2010) A new species of *Cyrtodactylus* (Squamata: Gekkonidae) from northern Laos. *Zootaxa* 2652(1): 1–16. <https://doi.org/10.11646/zootaxa.2652.1.1>
- Nguyen SN, Yang JX, Le NTT, Nguyen LT, Orlov NL, Hoang CV, Nguyen TQ, Jin J-Q, Rao D-Q, Hoang TN, Che J, Murphy RW, Zhang YP (2014) DNA barcoding of Vietnamese bent-toed geckos (Squamata: Gekkonidae: *Cyrtodactylus*) and the description of a new species. *Zootaxa* 3784(1): 48–66. <https://doi.org/10.11646/zootaxa.3784.1.2>
- Nguyen TQ, Le MD, Pham AV, Ngo HN, Hoang CV, Pham CT, Ziegler T (2015) Two new species of *Cyrtodactylus* (Squamata: Gekkonidae) from the karst forest of Hoa Binh Province, Vietnam. *Zootaxa* 3985(3): 375–390. <https://doi.org/10.11646/zootaxa.3985.3.3>
- Nguyen TQ, Pham AV, Ziegler T, Ngo HT, Le MD (2017) A new species of *Cyrtodactylus* (Squamata: Gekkonidae) and the first record of *C. otai* from Son La Province, Vietnam. *Zootaxa* 4341(1): 25–40. <https://doi.org/10.11646/zootaxa.4341.1.2>
- Pham AV, Le MD, Ngo HT, Ziegler T, Nguyen TQ (2019) A new species of *Cyrtodactylus* (Squamata: Gekkonidae) from northwestern Vietnam. *Zootaxa* 4544(1): 360–380. <https://doi.org/10.11646/zootaxa.4544.3.3>
- Portal of Lao Cai Province (2023) Portal of Lao Cai Province. <https://www.laocai.gov.vn>
- R Core Team (2023) R: A language and environment for statistical computing. R Foundation for Statistical Computing, Vienna. <https://www.R-project.org/>
- Ronquist F, Teslenko M, van der Mark P, Ayres DL, Darling A, Höhna S, Larget B, Liu L, Suchard MA, Huelsenbeck JP (2012) MrBayes 3.2: Efficient Bayesian phylogenetic inference and model choice across a large model space. *Systematic Biology* 61(3): 539–542. <https://doi.org/10.1093/sysbio/sys029>
- Schneider N, Nguyen TQ, Le MD, Nophaseud L, Bonkowski M, Ziegler T (2014) A new species of *Cyrtodactylus* (Squamata: Gekkonidae) from the karst forest of northern Laos. *Zootaxa* 3835(1): 80–96. <https://doi.org/10.11646/zootaxa.3835.1.4>
- Schneider N, Luu VQ, Sitthivong S, Teynie A, Le MD, Nguyen TQ, Ziegler T (2020) Two new species of *Cyrtodactylus* (Squamata: Gekkonidae) from northern Laos, including new finding and expanded diagnosis of *C. bansocensis*. *Zootaxa* 4822(4): 503–530. <https://doi.org/10.11646/zootaxa.4822.4.3>
- Simmons JE (2002) Herpetological collecting and collections management. Revised edition. Society for the Study of Amphibians and Reptiles, Herpetological Circular 31: 1–153.
- Sumontha M, Panitvong N, Deen G (2010) *Cyrtodactylus auribalteatus* (Squamata: Gekkonidae), a new cave-dwelling gecko from Phitsanulok Province, Thailand. *Zootaxa* 2370(1): 53–64. <https://doi.org/10.11646/zootaxa.2370.1.3>

- Swofford DL (2001) PAUP*. Phylogenetic Analysis Using Parsimony (*and Other Methods). Version 4. Sinauer Associates, Sunderland, Massachusetts. [program]
- Thompson JD, Gibson TJ, Plewniak F, Jeanmougin F, Higgins DG (1997) The ClustalX windows interface: Flexible strategies for multiple sequence alignment aided by quality analysis tools. *Nucleic Acids Research* 25(24): 4876–4882. <https://doi.org/10.1093/nar/25.24.4876>
- Thorpe RS (1975) Quantitative handling of characters useful in snake systematics with particular reference to intraspecific variation in the Ringed Snake *Natrix natrix* (L.). *Biological Journal of the Linnean Society, Linnean Society of London* 7(1): 27–43. <https://doi.org/10.1111/j.1095-8312.1975.tb00732.x>
- Thorpe RS (1983) A review of the numerical methods for recognizing and analysing racial differentiation. In: Felsenstein J (Ed.) *Numerical Taxonomy*. NATO ASI Series, Vol. 1. Springer, Berlin, Heidelberg, 404–423. https://doi.org/10.1007/978-3-642-69024-2_43
- Turan C (1999) A note on the examination of morphometric differentiation among fish populations: The Truss System. *Turkish Journal of Zoology* 23: 259–263.
- Uetz P, Hallermann J, Hosek J [Eds] (2023) *The Reptile Database*. <http://www.reptile-database.org> [Accessed 01 October 2023]
- Wood Jr PL, Heinicke MP, Jackman TR, Bauer AM (2012) Phylogeny of bent-toed geckos (*Cyrtodactylus*) reveals a west to east pattern of diversification. *Molecular Phylogenetics and Evolution* 65(3): 992–1003. <https://doi.org/10.1016/j.ympev.2012.08.025>

Supplementary material 1

Pair-wise genetic distance between samples used in this study

Authors: Tung Thanh Tran, Quyen Hanh Do, Cuong The Pham, Tien Quang Phan, Hanh Thi Ngo, Minh Duc Le, Thomas Ziegler, Truong Quang Nguyen

Data type: xlsx

Copyright notice: This dataset is made available under the Open Database License (<http://opendatacommons.org/licenses/odbl/1.0/>). The Open Database License (ODbL) is a license agreement intended to allow users to freely share, modify, and use this Dataset while maintaining this same freedom for others, provided that the original source and author(s) are credited.

Link: <https://doi.org/10.3897/zookeys.1192.117135.suppl1>

A crane fly of the genus *Gynoplistia* Macquart (Diptera, Limoniidae) from the early Miocene of New Zealand

André Nel¹, Uwe Kaulfuss²

1 Institut de Systématique, Évolution, Biodiversité (ISYEB), UMR 7205, Muséum national d'Histoire naturelle, CNRS, Sorbonne Université, EPHE, Université des Antilles, 75005 Paris, France

2 Georg-August-University, Department of Animal Evolution and Biodiversity, Untere Karspüle 2, 37073 Göttingen, Germany

Corresponding author: Uwe Kaulfuss (uwe.kaulfuss@uni-goettingen.de)

Abstract

The first fossil limoniid fly from the Miocene Fossil-Lagerstätte of Foulden Maar in New Zealand is described on the basis of an isolated well-preserved wing. The specimen is tentatively attributed to a new species *Gynoplistia fouldensensis* **sp. nov.** in the large extant genus *Gynoplistia*, which is well diversified in the country. It is the second fossil record of this genus, the first one being an isolated wing from the Cretaceous Weald Clay Formation in the United Kingdom.

Key words: Australasia, Fossil-Lagerstätte, Foulden Maar, Insecta, Tipuloidea

Introduction

Limoniid flies are very frequent in the fossil record, with 468 species distributed in 48 genera (Alroy 1998). They are supposed to be among the oldest known Diptera, with a fossil record dating back to the Triassic (Krzemiński and Krzemińska 2003; Kopeć et al. 2020). However, they remain quite difficult to study because of the lack of information on the body structures in many fossils. Nevertheless, many Cretaceous and Cenozoic fossils are attributed to extant genera, suggesting an impressive morphological stability through time for the whole family.

The fossil limoniids from Australasia are very poorly known, with two “limoniid indet.” briefly described and figured by Jell and Duncan (1986: figs 49, 50) and Jell (2004: figured on p. 104), one undescribed Miocene record (McCurry et al. 2022), and one Upper Jurassic genus and species described to date from Australia (Oberprieler et al. 2015). Thus, each new fossil is welcome to increase our knowledge on the past history of these flies in this region.

Limoniids are frequently encountered in the Miocene lacustrine sediments and amber from Europe, China, Russia, Sumatra, Mexico, and Dominican Republic (e.g., Gentilini 1984; Wu et al. 2019; Ngô-Muller et al. 2021).



Academic editor: Pavel Starkevich
Received: 9 November 2023
Accepted: 15 January 2024
Published: 20 February 2024

ZooBank: <https://zoobank.org/2D3C1BDA-5897-4ABF-AE02-F4AAE81A69B9>

Citation: Nel A, Kaulfuss U (2024) A crane fly of the genus *Gynoplistia* Macquart (Diptera, Limoniidae) from the early Miocene of New Zealand. ZooKeys 1192: 103–110. <https://doi.org/10.3897/zookeys.1192.115536>

Copyright: © André Nel & Uwe Kaulfuss. This is an open access article distributed under terms of the Creative Commons Attribution License ([Attribution 4.0 International – CC BY 4.0](https://creativecommons.org/licenses/by/4.0/)).

Here we describe a new limoniid species based on an isolated wing from the early Miocene of New Zealand, we tentatively attribute it to the genus *Gynoplistia* Macquart, 1835. With 319 extant species, this genus is very speciose and distributed all over the world (Oosterbroek 2024). Nevertheless, the only previously fossil known was *Gynoplistia* (?) *mitchelli* Jarzembowski, 1991, described on the basis of an isolated wing from the Early Cretaceous of the United Kingdom (Jarzembowski 1991).

Materials and methods

The single specimen described herein was collected at the Foulden Maar Fossil-Lagerstätte (Fig. 1) near Middlemarch, Otago, southern New Zealand (45.5269°S, 170.2191°E) in a diatomite mining pit, which is registered as I43/f8503 in the New Zealand Fossil Record File (GNS Science and Geoscience Society of New Zealand 2003). The varved and highly fossiliferous diatomite at the fossil site represents the latest uppermost *Rhoipites waimumuensis* (Couper, 1923) to lower early *Proteacidites isopogiformis* Couper, 1960 pollen zones, corresponding to New Zealand local stages late Waitakian-early Otaian (earliest Miocene, Aquitanian) (Mildenhall et al. 2014). Geological setting and palaeoecology of the fossil site are summarised by Lindqvist and Lee (2009), Lee et al. (2016, 2022), and Kaulfuss (2017).

The specimen was studied and photographed with a Nikon SMZ1000 stereomicroscope with attached Canon T3 camera. Wetting the specimen with ethanol revealed venational details of the wing and enhanced the contrast between the diatomite matrix and the fossil.

Photographs were stacked and enhanced in Photoshop CS5.1 (Adobe Systems Inc.) and the drawing of the wing was prepared from photographs using CorelDraw. We follow the wing venation terminology of de Jong (2017).

Wing nomenclature: CuA, cubitus anterior; CuP, cubitus posterior; A, anal vein; d, discal medial cell; M₁, M₂, M₃, M₄, branches of median vein; m1, cell between M₁ and M₂; Rs, posterior branch of radius; R₁, R₂, R₃, R₄, R₅, apical branches of radius; r-m, crossvein between R₅ and M₁₊₂; Sc, subcostal vein.

Systematic palaeontology

Order Diptera Linnaeus, 1758

Family Limoniidae Rondani, 1856

Genus *Gynoplistia* Macquart, 1835

***Gynoplistia fouldensensis* sp. nov.**

<https://zoobank.org/E23FB30B-A2E1-477E-B47C-DC875723A096>

Fig. 2

Type material. Holotype: NEW ZEALAND • sex unknown; an isolated wing; near Middlemarch, Otago; Foulden Maar Fossil-Lagerstätte; 45.5269°S, 170.2191°E; Geology Museum, Department of Geology, University of Otago (OU); OU46615.

Locality and horizon. Foulden Maar diatomite, near Middlemarch, Otago, New Zealand; earliest Miocene, Aquitanian.

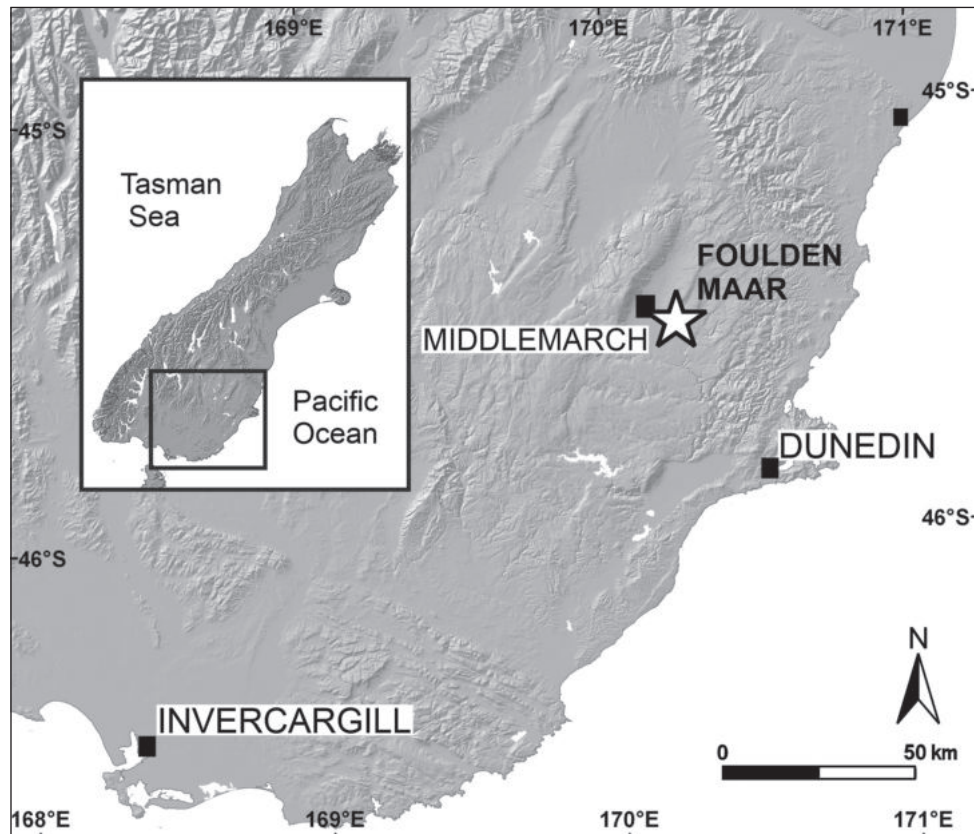


Figure 1. Map of the South Island of New Zealand showing the location of the Foulden Maar fossil site.

Diagnosis. The wing venation of the new species strongly resembles that of the fossil *G. (?) mitchelli* in the shape of the radial and median veins. Still, *G. fouldensensis* sp. nov. but can be differentiated by the shape of discal cell and crossvein between M_3 and M_4 being more distal than basal part of M_3 .

Description. Wing 8.8 mm long, 3.2 mm wide, with brown tinge, a series of white spots in anterior part and five series of transverse darker spots, veins black; Sc long, ending into C, extending far distal beyond fork of Rs, Sc-r just before tip of Sc; part of R_5 basal to r-m elongate and oblique, R_5 straight, reaching wing apex, 1.5 as long as Rs, R_{2+3+4} 0.9 mm long; R_2 beyond fork of R_3 and $R_{4'}$; R_3 3.0 mm long, slightly undulate; R_4 3.4 mm long, straight; no supernumerary crossveins in cells r3, r4, and r5; r-m and m-cu not aligned, r-m situated a short distance past base of discal medial cell, m-cu situated midway between base and apex of discal medial cell; fork of vein M_{3+4} in apical section of discal medial cell; discal medial cell 1.4 mm long, 0.7 mm wide, closed; cell m1 present, c. 1.2 mm long; vein CuA straight; anal vein straight.

Etymology. Named after the type locality Foulden Maar (Otago, New Zealand).

Discussion. This wing corresponds to that of a Limoniidae because of the following characters (after de Jong 2017): well-developed CuP and anal vein; anal vein nearly straight; apex of vein Sc well developed; apices of R_1 and R_3 well separated; fork of vein M_{3+4} in apical section of discal medial cell; crossvein m-cu far removed from fork of $M_{3+4'}$; vein CuA straight. It is quite delicate to attribute an isolated fossil wing of Limoniidae to a genus because many genera are separated on the basis of body characters.

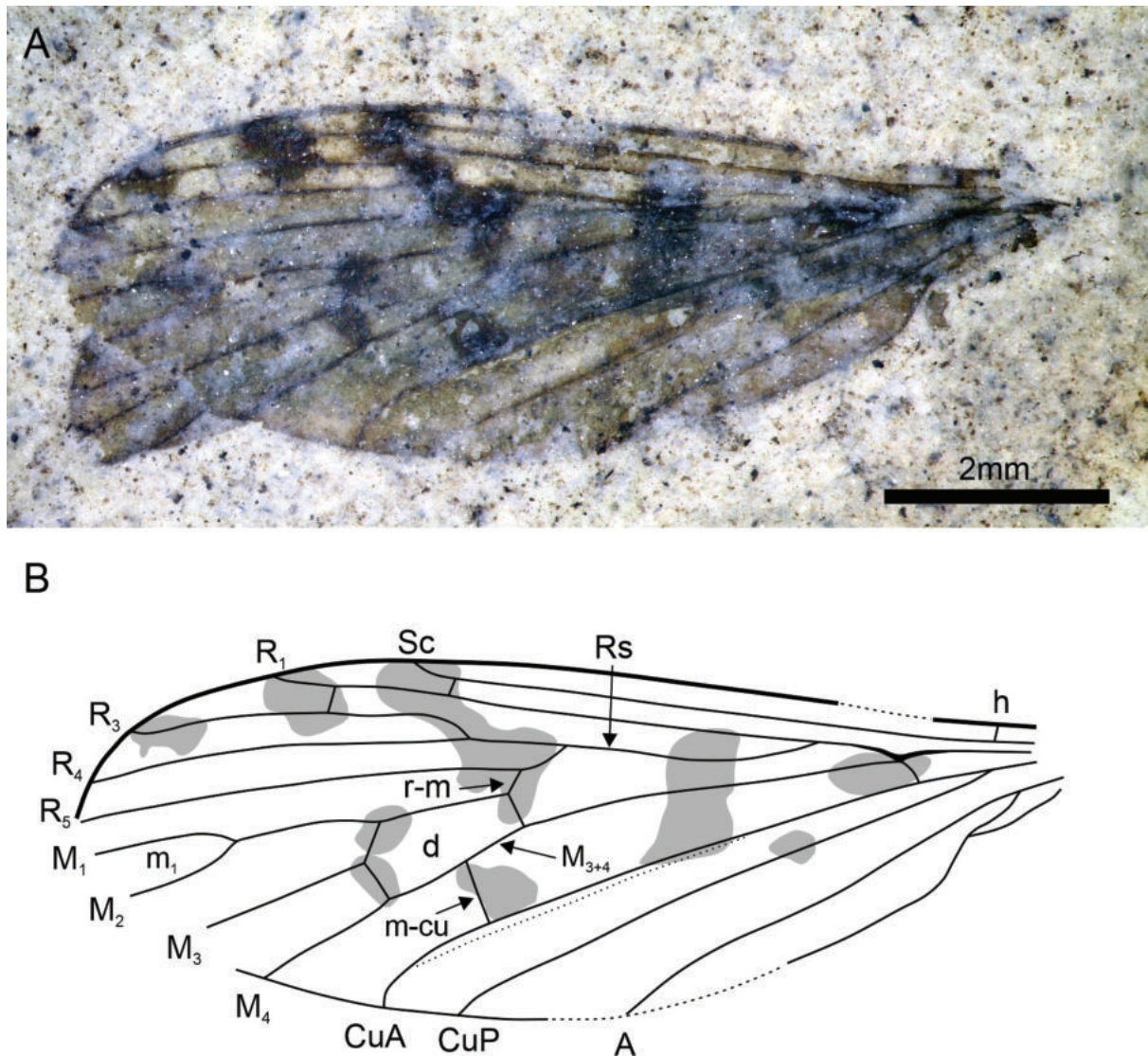


Figure 2. *Gynoplistia fouldensis* sp. nov., holotype, OU46615 **A** wing photograph **B** interpretative drawing of wing. Scale bar: 2 mm.

The combination of characters “cell m1 present, part of R_5 basal to r-m elongate and oblique, and forked R_{2+3+4} ” is encountered in some species of the genera *Gynoplistia*, *Pseudolimnophila* Alexander, 1919, *Hexatoma* Latreille, 1809 (*sensu lato*), and *Pilaria* Sintenis, 1889. The Australasian species of *Epiphragma* Osten Sacken, 1860 also have a cell m1 and a forked R_{2+3+4} , but their part of R_5 basal r-m is very short, unlike in the new fossil.

Hexatoma (*sensu lato*) forms a morphology-based phylogenetic clade with *Pseudolimnophila*, *Pilaria*, and *Ulomorpha* (Ribeiro 2008).

Pseudolimnophila and *Ulomorpha* are unknown in the Australasian/Oceanian region. *Pilaria* is represented by *P. brooksi* Alexander, 1953 in this region. This species has no cell m1 (Alexander 1953).

Hexatoma is currently divided into six subgenera (Podenas et al. 2022). The new fossil would fall in the subgenus *Eriocera* Macquart, 1838 because of the following characters: radial sector with three branches, medial cell distal, supernumerary crossveins missing in cells r3, r4, and r5, vein Sc reaching wing margin beyond Rs branching point, R_2 beyond fork of R_3 and R_4 (Podenas et al. 2022).

Following Oosterbroek (2024), *Hexatoma* is represented in the Australasian region only by five species of the subgenus *Eriocera*, which are *Hexatoma (Eriocera) aperta* (Alexander, 1920), *H. (E.) atra* (Doleschall, 1859), *H. (E.) australiensis* (Alexander, 1920), *H. (E.) metallica* (Schiner, 1868), and *H. (E.) setifera* (Alexander, 1931). The new fossil differs from all these species in the presence of cell m1. Also, *H. (Eriocera) metallica* differs from the new fossil in the uniformly infusate wing and aligned r-m and m-cu (Billingham and Theischinger 2022). *Hexatoma (E.) australiensis* also has wings with a “pale brown suffusion”, and R_{2+3+4} “equal to or a little shorter than R_3 alone” versus much shorter in the new fossil (Alexander 1920: 104). *Hexatoma (E.) aperta* has “brownish gray” wings and *H. (E.) setifera* a blackish tinge, and both have an opened discal medial cell (Alexander 1920: 105, 1931: 166). *Hexatoma (E.) atra* has R_3 only slightly longer than R_{2+3+4} , and m-cu is situated close to base of the discal medial cell (Edwards 1921). Thus, the new fossil is not similar to any of these species.

Unlike the genera previously mentioned, *Gynoplistia* is very diverse in New Zealand, with 108 species listed by Oosterbroek (2024). Some representatives of this genus have patterns of wing coloration with colored bands and spots, very close to that of *G. fouldensis* sp. nov. Theischinger (1993) proposed a revision of the Australian species of *Gynoplistia*. Affinities with the subgenus *Cerozodia* Westwood, 1835 are excluded because of the vein Sc ending into C in the new fossil. The wing venation would rather fit with that of a species of the subgenera *Xenolimnophila* Alexander, 1922 or *Gynoplistia* for the narrow elongate cell r3, the oblique basal part of R_5 , the presence of cell m1, the vein m-cu not aligned with r-m, and the wing coloration with spots and bands (Theischinger 1993: figs 9b, 11b). The New Zealand species of *Gynoplistia* also have wing coloration with spots and bands, but many have a basal part of R_5 clearly less oblique than in the new fossil (e.g., Edwards 1923: pl. 30; Alexander 1939: pl. 28, fig. 1).

It is noteworthy that the wing venation of the fossil *G. (?) mitchelli* strongly resembles that of *G. fouldensis* sp. nov., especially in the shape of the radial and median veins, but with an important difference in the shape of the discal cell, that is, the crossvein between M_3 and M_4 is more distal than basal part of M_3 in the new fossil versus the contrary in *G. (?) mitchelli* (Jarzembowski 1991: fig. 14). Indeed, the discal cell of *G. (?) mitchelli* resembles that of the *H. (Eriocera)* spp.

Conclusion

This study of a new fossil wing illustrates the difficulties encountered when describing a fossil Limoniidae on the sole basis of wing characters. In this case at least two genera could be candidates for an attribution, even if we prefer the genus *Gynoplistia* rather than *Hexatoma* mostly because of the pattern of wing coloration. Also the attribution of this Miocene fossil species to *Gynoplistia* is unsurprising because this genus is nowadays very diverse in New Zealand, whereas *Hexatoma* remains unknown from this country.

Acknowledgements

We thank Dr Daubian Santos and Dr Wieslaw Krzemiński for their useful comments on the first version of the paper. We thank the Gibson family at Foulden Hills for kindly permitting access to the fossil site.

Additional information

Conflict of interest

The authors have declared that no competing interests exist.

Ethical statement

No ethical statement was reported.

Funding

This work was funded by the German Research Foundation (project 429296833).

Author contributions

All authors have contributed equally.

Author ORCIDs

André Nel  <https://orcid.org/0000-0002-4241-7651>

Uwe Kaulfuss  <https://orcid.org/0009-0007-6858-8612>

Data availability

All of the data that support the findings of this study are available in the main text.




References

- Alexander CP (1919) The crane-flies of New York. Part 1. Distribution and taxonomy of the adult flies. *Memoirs of the Cornell University. Agriculture Experimental Station* 25: 767–993.
- Alexander CP (1920) New or little-known Australian crane-flies (Tipulidae, Diptera). *Proceedings of the Royal Society of Queensland* 32: 92–109. <https://doi.org/10.5962/p.272125>
- Alexander CP (1931) New or little-known Tipulidae (Diptera). XLIX. Australasian species. *Annals and Magazine of Natural History (Series 10)* 8: 145–166. <https://doi.org/10.1080/00222933108673374>
- Alexander CP (1939) New or little-known Tipulidae from New Zealand (Order Diptera). Part III. *Records of the Canterbury Museum* 4: 219–230.
- Alexander CP (1953) New or little-known Tipulidae (Diptera). XCVI. Oriental-Australasian species. *Annals and Magazine of Natural History (Series 12)* 6: 898–914. <https://doi.org/10.1080/00222935308654506>
- Alroy J (1998) *Fossilworks: Gateway to the Paleobiology Database*. <http://www.fossilworks.org/> [Accessed on 06.11.2023]
- Billingham ZD, Theischinger G (2022) New and poorly known species of crane flies (Diptera: Limoniidae) from New South Wales, Australia. *Records of the Australian Museum* 74(1): 19–40. <https://doi.org/10.3853/j.2201-4349.74.2022.1775>
- de Jong H (2017) 14. Limoniidae and Tipulidae (crane flies). In: Kirk-Spriggs AH, Sinclair BJ (Eds) *Manual of Afrotropical Diptera*. Vol. 2. Nematoceros Diptera and lower Brachycera. Suricata 5. South African National Biodiversity Institute, Pretoria, 427–477.
- Doleschall CL (1859) Derde bijdrage tot de kennis der dipteren fauna van Nederlandsch Indie. *Natuurkundig Tijdschrift voor Nederlandsch Indie* 17: 73–128.
- Edwards FW (1921) The Old-World species of *Eriocera* in the British Museum Collection (Diptera, Tipulidae). *Annals and Magazine of Natural History (Series 9)* 8: 67–99. <https://doi.org/10.1080/00222932108632559>

- Edwards FW (1923) A preliminary revision of the crane-flies of New Zealand (Anisopodidae, Tanyderidae, Tipulidae). Transactions (Proceedings) of the New Zealand Institute 54: 265–352.
- Gentilini G (1984) Limoniidae and Trichoceridae (Diptera: Nematocera) from the Upper Miocene of Monte Castellaro (Pesaro, Central Italy). Bolletino del Museo Civico di Storia Naturale di Verona 11: 171–190.
- GNS Science and Geoscience Society of New Zealand (2003) New Zealand Fossil Record File [43/f8503]. GNS Science. <https://doi.org/10.21420/JQQB-NK89>
- Jarzewowski EA (1991) New insects from the Weald clay of the Weald. Proceedings of the Geologists' Association 102: 93–108. [https://doi.org/10.1016/S0016-7878\(08\)80069-7](https://doi.org/10.1016/S0016-7878(08)80069-7)
- Jell PA (2004) The fossil insects of Australia. Memoirs of the Queensland Museum 50(1): 1–124.
- Jell PA, Duncan PM (1986) Invertebrates, mainly insects, from the freshwater, Lower Cretaceous, Koonwarra fossil bed, (Korumburra Group), South Gippsland, Victoria. In: Jell PW, Roberts J (Eds) Plants and invertebrates from the Lower Cretaceous Koonwarra fossil bed, South Gippsland, Victoria. Memoir 3 of the Association of the Australasian Palaeontologists, Sydney, 111–205.
- Kaulfuss U (2017) Crater stratigraphy and the post-eruptive evolution of Foulden Maar, southern New Zealand. New Zealand Journal of Geology and Geophysics 60(4): 410–432. <https://doi.org/10.1080/00288306.2017.1365733>
- Kopeć K, Skibińska K, Soszyńska-Maj A (2020) Two new Mesozoic species of Tipulomorpha (Diptera) from the Teete locality, Russia. Palaeoentomology 3(5): 466–472. <https://doi.org/10.11646/palaeoentomology.3.5.4>
- Krzemiński W, Krzemińska E (2003) Triassic Diptera: descriptions, revisions and phylogenetic relations. Acta Zoologica Cracoviensia 46(suppl. – Fossil Insects): 153–184.
- Latreille PA (1809) Genera crustaceorum et insectorum secundum ordinem naturalem in familias disposita, iconibus exemplisque plurimis explicata. Tomus Quartus et Ultimus. Parisii et Argentorati [= Paris and Strasbourg]: A. Koenig, 399 pp.
- Lee DE, Kaulfuss U, Conran JG, Bannister JM, Lindqvist JK (2016) Biodiversity and palaeoecology of Foulden Maar: an early Miocene Konservat-Lagerstätte deposit in southern New Zealand. Alcheringa: an Australian Journal of Palaeontology 40: 525–541. <https://doi.org/10.1080/03115518.2016.1206321>
- Lee DE, Kaulfuss U, Conran JG (2022) Fossil treasures of Foulden Maar. Window into Miocene Zealandia. Otago University Press, Dunedin, 216 pp.
- Lindqvist JK, Lee DE (2009) High-frequency paleoclimate signals from Foulden Maar, Waipiata Volcanic Field, southern New Zealand: An Early Miocene varved lacustrine diatomite deposit. Sedimentary Geology 222(1–2): 98–110. <https://doi.org/10.1016/j.sedgeo.2009.07.009>
- Linnaeus C (1758) Systema Naturae per Regna Tria Naturae, Secundum Clases, Ordines, Genera, Species, cum Characteribus, Differentiis, Synonymies, Locis. Tomus I. Editio decima, reformata. Impensis Direct, Laurentii Salvii, Holmiae, 824 pp. <https://doi.org/10.5962/bhl.title.542>
- Macquart P-J-M (1835) Histoire naturelle des Insectes. Diptères, Ouvrage accompagné de planches. Tome deuxième. N.E. Roret, Paris, 1–703 + 1–8. <https://doi.org/10.5962/bhl.title.14274>
- McCurry MR, Cantrill DJ, Smith PM, Beattie R, Dettmann M, Baranov V, Magee C, Nguyen JMT, Forster MA, Hinde J, Pogson R, Wang H, Marjo CE, Vasconcelos P, Frese M (2022) A Lagerstätte from Australia provides insight into the nature of Miocene

- mesic ecosystems. *Science Advances* 8(1): eabm1406. <https://doi.org/10.1126/sciadv.abm1406>
- Mildenhall DC, Kennedy EM, Lee DE, Kaulfuss U, Bannister JM, Fox B, Conran JG (2014) Palynology of the early Miocene Foulden Maar, Otago, New Zealand: Diversity following destruction. *Review of Palaeobotany and Palynology* 204: 27–42. <https://doi.org/10.1016/j.revpalbo.2014.02.003>
- Ngô-Muller V, Garrouste R, Pouillon J-M, Christophersen V, Christophersen A, Nel A (2021) The first representative of the fly genus *Trentepohlia* subgenus *Mongoma* in amber from the Miocene of Sumatra (Diptera: Limoniidae). *Historical Biology* 33(2): 254–257. <https://doi.org/10.1080/08912963.2019.1610948>
- Oberprieler SK, Krzemiński W, Hinde J, Yeates DK (2015) First crane fly from the Upper Jurassic of Australia (Diptera: Limoniidae). *Zootaxa* 4021(1): 178–186. <https://doi.org/10.11646/zootaxa.4021.1.8>
- Oosterbroek P (2024) Catalogue of the Craneflies of the World (CCW). <https://ccw.naturalis.nl/index.php> [Accessed on 08.01.2024]
- Osten Sacken CR (1860) New genera and species of North American Tipulidae with short palpi, with an attempt at a new classification of the tribe. *Proceedings of the Academy of Natural Sciences of Philadelphia* 11: 197–254.
- Podenas S, Park S-J, Byun H-W, Podeniene V (2022) *Hexatoma* crane flies (Diptera, Limoniidae) of Korea. *ZooKeys* 1105: 165–208. <https://doi.org/10.3897/zookeys.1105.82495>
- Ribeiro G (2008) Phylogeny of the Limnophilinae (Limoniidae) and early evolution of the Tipulomorpha (Diptera). *Invertebrate Systematics* 22(6): 627–694. <https://doi.org/10.1071/IS08017>
- Rondani C (1856) *Dipterologiae Italicae Prodrumus*. Vol. 1: Genera Italica ordinis dipterorum ordinatim disposita et distincta et in familias et stirpes aggregata. A. Stocch [sic], Parmae [= Parma], 228 pp. <https://doi.org/10.5962/bhl.title.8160>
- Schiner JR (1868) *Reise der österreichischen Fregatte Novara um die Erde in den Jahren 1857, 1858, 1859 unter den Befehlen des Commodore B. von Wüllerstorff-Urbair*. Zoologischer Theil. K. Gerold's, Sohn, Wien, 388 pp.
- Sintenis F (1889) Vierten Bericht über Livländische Tipuliden und *Dixa*. *Sitzungsberichte der Naturforscher-Gesellschaft bei der Universität Dorpat* 8: 393–398.
- Theischinger G (1993) The Limoniinae (Diptera, Tipulidae) of Australia. 3. The genus *Gynoplistia* Macquart. *Stapfia* 29: 1–106.
- Wu S, Krzemiński W, Soszyńska-Maj A, Ren D (2019) New fossil representative of the genus *Helius* (Diptera, Limoniidae) from the little known and newly discovered locality Caergen Village of northeastern Tibetan Plateau (China). *Palaeontologia Electronica* 22.1.2A: 1–8. <https://doi.org/10.26879/817>

Two new species of the hyperdiverse geometrid moth genus *Eois* (Lepidoptera, Geometridae, Larentiinae) from Ecuador, with descriptions of early stages

Lydia M. Doan¹, James S. Miller^{2†}, John W. Brown³, Matthew L. Forister¹, Lee A. Dyer^{1,4}

¹ Department of Biology, Ecology, Evolution and Conservation of Biology, University of Nevada, Reno, NV 89557, USA

² Entomology Department, American Museum of Natural History, New York, NY, 10024, USA

³ Entomology Department, National Museum of Natural History, Smithsonian Institution, Washington, DC, 20560, USA

⁴ INABIO – Instituto Nacional de Biodiversidad, Quito, Ecuador

Corresponding author: Lee A. Dyer (ldyer@unr.edu)

Abstract

The hyperdiverse geometrid genus *Eois* Hübner, estimated to encompass more than 1,000 species, is among the most species-rich genera in all of Lepidoptera. While the genus has attracted considerable attention from ecologists and evolutionary biologists in recent decades, limited progress has been made on its alpha taxonomy. This contribution focuses on the Olivacea clade, whose monophyly has been recognized previously through molecular analyses. We attempt to define the clade from a morphological perspective and recognize the following species based on morphology and genomic data: *E. olivacea* (Felder & Roggenhofer); *E. pseudolivacea* Doan, **sp. nov.**; *E. auruda* (Dognin), **stat. rev.**; *E. beebei* (Fletcher, 1952), **stat. rev.**; *E. boliviensis* (Dognin), **stat. rev.**; and *E. parumsimii* Doan, **sp. nov.** Descriptions and illustrations of the immature stages of *E. pseudolivacea* reared from *Piper* (Piperaceae) in Ecuador are provided.

Key words: COI, genitalia, morphology, Neotropics, *olivacea* species group, *Piper*, taxonomy



Academic editor: Axel Hausmann

Received: 16 August 2023

Accepted: 4 January 2024

Published: 21 February 2024

ZooBank: <https://zoobank.org/94FB491F-B5A5-4514-A1EF-062B6A216D11>

Citation: Doan LM, Miller JS, Brown JW, Forister ML, Dyer LA (2024) Two new species of the hyperdiverse geometrid moth genus *Eois* (Lepidoptera, Geometridae, Larentiinae) from Ecuador, with descriptions of early stages. ZooKeys 1192: 111–140. <https://doi.org/10.3897/zookeys.1192.111275>

Copyright: © Lydia M. Doan et al.
This is an open access article distributed under terms of the Creative Commons Attribution License (Attribution 4.0 International – CC BY 4.0).

Introduction

Larentiinae is the second largest subfamily of the highly diverse and worldwide family Geometridae, commonly known as geometers, loopers, or inch worms owing to the unusual gait of the caterpillars. Larentiines are primarily denizens of temperate regions, with more than 6,200 described species. However, the larentiine genus *Eois* Hübner is strictly tropical, and 83% of the described species are restricted to the Neotropics (Brehm et al. 2005; Strutzenberger et al. 2010, 2011, 2017; Brehm et al. 2011; Öunap et al. 2016). The genus is comprised of 267 formally described species: 220 in the Neotropics (Moraes et al. 2021a, b), 30 in Southeast Asia, and 17 in Africa (Herbulot 2000; De Prins and De Prins 2023). Remarkably, it is estimated that an additional 1,000 or more Neotropical species of *Eois* remain to be described (Brehm et al. 2011; Strutzenberger et al. 2017; Moraes et al. 2021a, b). If these estimates are correct, the genus is among the most species-rich in all of Lepidoptera. Based on Lepidoptera inven-

† deceased.

tories in Central and South America, *Eois* appears to reach its greatest diversity in high elevation (higher than 2,000 m) habitats of the eastern Andes (Brehm et al. 2005; Brehm et al. 2011; Öunap et al. 2016).

Species of *Eois* are generally small, with wingspans of 12–20 mm. Wing shape and pattern are diverse, featuring ground colors of yellows, greens, or browns, some with finely reticulated networks of lines, some with spots or bands, and others nearly uniform in color (Moraes et al. 2021a). Larvae are mostly green, with brown, red, or black spots or bands; others are completely dark (Brehm et al. 2011: fig. 6; also see <http://caterpillars.org>). In some clades, larvae are elongate and transparent greenish, whereas in others they are stout and brightly colored; one species even appears to mimic bird-droppings (Brehm et al. 2011). The larvae exhibit a typical geometrid ground plan, with slender bodies, the absence of prolegs on abdominal segments 3–5, and slight modifications to the basic setal pattern found in other larentiines (McGuffin 1958).

The majority of *Eois* species were described between 1891 and 1920; but the first species was named by Hübner in 1818 and the most recent by Moraes in 2021 (Parsons et al. 1999; Moraes et al. 2021a, b). While progress on the taxonomy of the genus has been slow since the 1950s, during the past two decades *Eois* has experienced a resurgence in attention from ecologists and evolutionary biologists focused on the interactions of *Eois* immatures with their host plants and associated parasitoids (e.g., Dyer and Palmer 2004; Connahs et al. 2009; Brehm et al. 2011; Strutzenberger and Fiedler 2011; Strutzenberger et al. 2012; Seifert et al. 2015). *Eois* larvae are specialized feeders on shrubs and vines of Piperaceae (mostly *Piper*), and their diversification mirrors the substantial diversification of their larval hosts (Rodriguez-Castaneda et al. 2010; Jahner et al. 2017). Strutzenberger et al. (2010) indicate that *Eois* larvae also feed on Chlorantaceae, but out of more than 10,000 rearing records from Costa Rica, Ecuador, Brazil, Peru, and Argentina (Dyer et al. 2007; Forister et al. 2015; Salcido et al. 2022, and Janzen/Hallwachs databases, Dyer et al. databases), there are fewer than 300 records of this plant family.

A preliminary molecular phylogeny of the genus based on the mitochondrial gene cytochrome oxidase subunit 1 (COI; 1220 bp) and the nuclear gene elongation factor 1 alpha (Ef-1a; 1066 bp), evaluating 142 taxa, was presented by Strutzenberger et al. (2010), and this was followed by a checklist of the Neotropical species compiled by Brehm et al. (2011). A second analysis by Strutzenberger et al. (2017) using the same genes and a total of 221 *Eois* species, confirmed and reinforced their previous findings. The most recent molecular study of the genus by Moraes et al. (2021b) suggests that *Eois* potentially harbors an unparalleled array of cryptic diversity. Taken together, these molecular studies provide a preliminary phylogenetic framework for taxonomic progress at the species level, through the identification of many well-defined clades that can now be investigated based on their monophyly.

In each of the molecular studies, a well-defined “Olivacea Clade” was recognized that is rich in undescribed species from South America, primarily Ecuador (Strutzenberger et al. 2010, 2017; Moraes et al. 2021b), and this is supported by the large number of BINs represented in BOLD (Barcode of Life Database). Thus, we concentrate here on the Olivacea clade as a productive and diverse locus for the discovery and description of new species within the enormous undescribed diversity of the genus *Eois*. We utilize extensive morphological characters in this

work, rather than molecular data, acknowledging that molecular identification has become an important part of modern taxonomy, sometimes in the form of a short section of mitochondrial DNA. The utilization of a single molecular marker (or “barcode”) has a number of issues (Taylor and Harris 2012, Mallo and Posada 2016) that are especially problematic in rapidly diversifying and under-documented lineages (Meyer and Paulay 2005). Genomic resolution, essential to the future of taxonomy, has been used in *Eois* (Jahner et al. 2017), and we expect that our work here helps lay the foundation for such studies moving forward. Also, the focus here is on describing two commonly reared species in Ecuador that have been and continue to be important in ecological and evolutionary studies (Dyer et al. 2007; Wilson et al. 2012; Forister et al. 2015; Glassmire et al. 2016; Jahner et al. 2017; Salcido et al. 2022; Sudta et al. 2022).

Materials and methods

Specimens examined

The bulk of the material used in this treatment is from two sources: the type collection of the National Museum of Natural History, Washington, D.C. (**USNM**), and an inventory of the caterpillars at Yanayacu Biological Station, Napo Province, Ecuador (Miller and Dyer 2009; Sudta et al. 2022). The Yanayacu site is located at 2200 m elevation in the Quijos Valley, Napo Province, in the Andes Mountains of northeastern Ecuador. The station lies just south of the equator (00°35.9'S, 77°53.4'W) in one of the world's last remaining unexplored regions of high-elevation cloud forest. The survey has run continuously from 2001 to present.

At Yanayacu, caterpillars were discovered in the field primarily using visual searches. Larvae were taken to the laboratory where they were placed in plastic bags that were coded, imaged, tagged, and hung on clothes lines. Periodically, observational notes were taken on the larvae, and additional host material was added as needed. When an adult moth or butterfly, or sometimes its parasitoid, emerged, it was preserved and labeled. Each specimen received a unique voucher number in the form of a serial number (e.g., 15328), with time of year, elevation, latitude and longitude, host plant, and other data. In the text, we use “**r.f.**” (reared from) to denote larval host plants. Some specimens were preserved in alcohol and examined for setal patterns and other important larval characters such that a general description of shared characters among *Eois* larvae from this location is possible. Adults were collected at light traps at Yanayacu throughout the study period, and immatures and adults were collected at sites across the Neotropics (Forister et al. 2015; Salcido et al. 2022), and there was no overlap with the reared material from Yanayacu.

Morphological data

We utilized a morphological species concept to delineate and describe the newly discovered species. Our approach focused on the examination of morphological characters, with an emphasis on the male and female genitalia. We used a matrix comprising 107 morphological characters to assess variation among individuals and delineate species (see Appendix 1). The data matrix included 37 binary and 70 multi-state characters: 16 external features (wings

and other appendages), 58 male genitalia characters, and 33 female genitalia characters. The matrix was based on identified specimens in the collection of the University of Nevada, Reno (**UNR**); the Natural History Museum, London (**NHMUK**); the McGuire Center for Lepidoptera and Biodiversity, Florida Museum of Natural History, Gainesville, Florida (**AME**); and the National Museum of Natural History, Smithsonian Institution, Washington, DC (**USNM**; all USNM specimens are labelled with a unique USNM ENT barcode label, the numbers of which are given in the text).

In our results below, we also include redescriptions of three previously described species of the Olivacea Clade, which are based only on males. We present the first published illustrations of the adults and genitalia of *E. auruda* and *E. boliviensis*, and contemporary illustrations of *E. beebei*; those in the original publication of the latter are of poor quality.

Based on previously published data, the extensive BOLD database, and our own personal experience, species of *Eois* exhibit narrow geographic ranges, with none of the described species documented thus far beyond the limits of a single country. This distributional feature adds support to the morphological hypothesis that *E. olivacea* (described from Colombia), *E. boliviensis* (described from Bolivia), *E. beebei* (described from Venezuela), and *E. auruda* (described from Ecuador) are unlikely to be conspecific. Hence, these taxa are returned to species-level.

Dissections and photography

Dissection methods followed those presented by Robinson (1976), except all parts were slide mounted using Euparal rather than Canada balsam. Initially, we attempted to evert the vesica, teasing it out with a 000 pin, but owing to the small size of the phallus, the process frequently inflicted more damage than the value of viewing features of the everted vesica. Also in the male genitalia, a membranous region surrounding the phallus typically supports a dense field of small spines. Although we attempted to leave the membrane in situ, more often it was detached with the phallus. For mated females, any spermatophores and associated material were removed.

Images of adults and genitalia were captured using a 65 mm lens attached to a Canon EOS 40D digital SLR camera (Canon U.S.A., Lake Success, NY) mounted on a Visionary Digital BK Lab System (Visionary Digital, Palmyra, VA). Multiple images were stacked using Helicon Focus software and subsequently enhanced using Adobe PhotoShop and GIMP 2.10 software. Plates were constructed in Adobe Photoshop CC 2020 (v. 21. 0).

Terminology

Descriptions of morphology and wing maculation are based on the examination of specimens using a Zeiss Stemi 2000-C stereomicroscope with SCHOTT EasyLED ring-light illuminator. Forewing length was measured to the nearest 0.5 mm using an optical micrometer. Terms for genital structures and forewing pattern elements follow Holloway (1997) and Viidalepp (2011). However, an unusual structure in the male genitalia of members of several clades of *Eois* appears to lack a term. It is a membranous, flat, lateral flap of variable size and

length attached to the sides of the tegumen and/or transtilla, which supports long, fine male scent scales. We suggest the term “lacina” for these structures and use that term throughout the manuscript. Viidalepp (2011) indicates that “The paired, heavily sclerotized, long and tapered projections from the posterior side of tegumen, which are the peculiarity of two species of the genus *Solitanea* Djakonov (the tribe Solitaneini Leraut) can be identified neither with *socii* nor with *gnathos*.” Although we are uncertain of the homology of lacina with the structures in *Solitanea*, they appear to occupy the same position in the male genitalia.

Abbreviations for morphological structures in the text are as follows: **Tg7** = tergum 7; **Tg8** = tergum 8; **St7** = sternum 7; **St8** = sternum 8; **PVP** = post-vaginal plate; **DB** = ductus bursae; **DS** = ductus seminalis; **CB** = corpus bursae.

For the older type material (i.e., *E. auruda*, *E. boliviensis*, and *E. beebei*), we provide latitude, longitude, and elevation based on the locality data from the specimen label. Therefore, owing to the often imprecise nature of these label data, these parameters represent estimates only.

Results

The Olivacea clade

The Olivacea clade was first recognized by Strutzenberger et al. (2010) based on an analysis of 142 morphospecies of *Eois*, employing sequence data from two genes: COI (1220 bp) and Ef-1a (1060 bp). Sixteen morphospecies linked together to form the clade, all of which were assumed to be undescribed. The monophyly of the clade was subsequently confirmed by Strutzenberger et al. (2017) based on considerably broader taxon sampling ($n = 221$ morphospecies) but with the same genes, expanding the number of morphospecies in the clade to 23. A recent molecular study by Moraes et al. (2021a, b) found support for an *olivacea* species group, but not for the clade; however, their study was based entirely on the mitochondrial gene COI.

A preliminary genomic study of four species of *Eois* in the Olivacea Clade, all of which are undescribed, represented by 137 samples (Doan 2023), is the subject of ongoing work and a forthcoming publication. Similarly, a morphological analysis is in progress, based on a subset of *Eois* species (94 taxa and 107 morphological characters), and this will contribute to the delineation of the Olivacea Clade (Doan 2023).

Brehm et al. (2011: 1093) noted that all species belonging to the clade “have a green ground color and yellowish fringes...” They also commented that the caterpillars “show particularly contrasting patterns, including bright and dark spots dorsally...and pink spots laterally...in some species, whereas others exhibit merely some pale patches...” (Brehm et al. 2011: 1094–1095). They concluded that all species of the clade feed on species of *Piper* (Piperaceae). They further recognized that conspicuous morphological differences could be found even among closely related species within the group. For example, the male genitalia of some taxa possess numerous stout cornuti in the vesica, whereas others lack them altogether. Within the Olivacea Clade as defined by Strutzenberger et al. (2010, 2017), there appears to be three species complexes: an *E. olivacea* complex, an *E. goodmanii* complex, and an *E. muscosa* complex (although the last is represented by a single morphospecies). Although the first two species

complexes were recognized as monophyletic by Moraes et al. (2021b), they were included as part of a larger clade, and *muscosa* was not included in their study. We focus our current efforts on the *E. olivacea* species complex. However, because diagnostic morphological characters to separate the *E. olivacea* species complex from the *E. goodmanii* species complex are yet to be discovered, one or more of the species treated herein may belong to the latter.

***Eois olivacea* species complex**

Remark. As currently defined, the *E. olivacea* species complex includes *E. olivacea* (Felder and Rogenhofer 1875) (TL: Bogotá, Colombia; type in NHMUK), *E. beebei* (Fletcher, 1952) (TL: Rancho Grande near Maracay, Venezuela; type in NHMUK), *E. auruda* (Dognin, 1900) (TL: Loja, Ecuador; type in USNM), and *E. boliviensis* (Dognin, 1900) (TL: Bolivia, type in USNM), along with nearly a dozen undescribed morphospecies treated by Strutzenberger et al. (2017). BOLD (Barcode of Life Database) includes 27 BINs, mostly from Ecuador, with many fewer from Peru and Colombia, that likely represent species in the *olivacea* species complex. Herein, we describe two new species based nearly entirely on morphology of the adults. We also provide superficial descriptions and illustrations of the egg, larva, and pupa of *E. pseudolivacea*.

To minimize redundancy in the species descriptions, we first provide a general diagnosis and description of the *E. olivacea* species complex, which includes features shared by all the included taxa. In the individual species descriptions that follow, we include diagnoses and descriptions that include details of the features treated broadly in the general description of the complex.

Diagnosis. Ovum (Fig. 1). The eggs are uniformly cream colored, oval, and flattened without sculpturing, and are deposited horizontally (i.e., not upright). They are laid singly on a leaf, but infrequently multiple eggs, as many as 12, can be found on a single leaf.

Larva (Figs 2, 3). The caterpillars are typical of those of Larentiinae. The head is rounded with a standard arrangement of stemmata, a spinneret that is long and pointed but not extending beyond the labium, and a retinaculum on each mandible. The thoracic prolegs each have 6–8 setae. Abdominal segments 1–5 are approximately twice as long as those posterior to A5. There are no ridges, bumps, swollen segments, scoli, or filaments. Abdominal segments exhibit typical larentiine chaetotaxy with a few exceptions: A2–A7 lack the extra L seta found in temperate larentiines, and A1 has an arrangement of setae that includes two D setae, three L setae, two SV setae, and one V seta. All spiracles are round with a single seta immediately dorsal. The abdomen bears prolegs only on A6 and A10; each A6 proleg has 5 setae, and A10 prolegs have 6 setae each. Crochets are biordinal and arranged in two groups that surround a large pad in a hemi-ellipse. There are paired paraprocts on A10, and the anal shield is rounded. Larvae scrape the bottoms of leaves, leaving characteristic windows of upper epidermal tissue on the host leaf.

Pupa (Fig. 4). The pupae of *Eois* are similar to those of other geometrids; they are 45–55 mm in length and dark brown. They are attached to the undersides of leaves by the hooked spines of the cremaster.

Imago. Adults of the *E. olivacea* species complex all share extremely similar wing color and pattern, with a pale yellowish to pale gray-green ground color,



Figures 1–4. Early stages of *Eois pseudolivacea* from Ecuador 1 egg 2 second instar larva 3 fifth instar larva 4 pupa.

usually with one to three faint, jagged or wavy, narrow, whitish fasciae (i.e., antemedial, medial, and postmedial lines) extending from the costa to the hind margin of the forewing and continuing across the hindwing. The postmedial fascia is usually well defined, whereas the submedian and median fasciae are often reduced or lacking altogether (especially in worn specimens). The outer margin of the wings (termen) bears an extremely narrow line of red-brown to maroon scales, and the fringe is bright yellow throughout, in contrast to the wing ground color and the terminal line. There usually is a small brown dot near the apex of the discal cell in both the forewing and hindwing, but the dot is occasionally weakly expressed or absent.

On the head, the chaetosemata are represented by small, rounded patches posterior to the bases of the antennae, connected by a narrow, continuous row of setae located in a naked region near the posterior margin of the head, typical of members of the tribe Asthenini (Viidalepp 2011). The male genitalia are characterized by the absence of an uncus, with the semi-sclerotized scaphium occupying this position; the dorsal part of the tegumen narrow; the presence of lacina; and a patch of spines in the membrane surrounding the phallus, often arranged in two longitudinal rows. The vesica in all species examined bears a small, variable, semicircular plate with a saw-toothed margin (or field) around the curved side. Clusters of large, elongate cornuti are present in the vesica of a few species but absent in most. All these morphological features appear to be shared with members of the *E. goodmanii* and *E. muscosa* species complexes.

Members of the *E. goodmanii* species complex are superficially similar to those of the *olivacea* complex, but the wing ground color is usually a darker green or darker gray-green; the postmedial line is ill-defined and either dark

rather than pale, extremely faint, or absent altogether; and the fringe is interrupted by brown patches rather than entirely yellow. Members of the *muscosa* species complex are superficially dissimilar to the other two groups, with the pale green forewing lacking medial and antemedial lines: instead with the inner two-thirds of the wing featuring a large, ill-defined patch of pale brown scales, and the fringe not contrasting with the forewing ground color.

Description. Male. Head: Scales of frons smooth appressed, fawn brown; scales of vertex slightly paler; vertex between bases of antennae with narrow, transverse band of snow-white scales, separating fawn brown scales of frons from paler scales of vertex. Ocellus absent. Chaetosema a rounded patch posterior to base of antenna, with narrow continuous row across vertex in naked region near posterior margin of head. Compound eye large, comprising greater than 0.66 of head. Antenna cylindrical, bipectinate in males, with long, slender rami biciliate to tip, rami absent in distal 0.25 of antenna; dorsum of flagellomeres with white scales. Labial palpus with segment 2 approximately 0.5 length of segment 1; segment 3 short, approximately 0.25 as long as segment 1; length of all segments combined 0.5–0.7 × diameter of compound eye.

Thorax: Concolorous with forewing dorsum ground color. Legs long, slender, densely covered in scales, usually concolorous with thorax; tibia of mid- and hindlegs with conspicuous tibial spurs, midtibia with one, hind tibia with two, approximately 0.25 length of tarsomere 1; sclerotized tips of tibial spurs simple, elongated. Forewing broadly triangular, length 1.2 × width at termen, outer margin evenly convex, with discal cell less than 0.5 wing length, accessory cell long, originating from distal costal margin of discal cell. Ground color variable from pale yellow to pale greenish gray; antemedial line usually faint, wavy, ill defined, ivory; medial line either extremely faint or lacking altogether; postmedial line usually well defined, wavy, ivory, angled perpendicularly toward costa beyond M_3 ; region from postmedial line to termen sometimes with a faint, narrow, zigzag, ivory line; discal spot usually well defined, somewhat oblong-round, red-brown; costal region usually faintly tinged pale pinkish brown, irregularly marked with small cream blotches; termen with narrow, dark red-brown line, concolorous with discal spot, variable from nearly straight to conspicuously scalloped. Fringe pale yellow. Forewing underside usually ivory, suffused with faint reddish brown, darkest in costal portion, with or without trace of dorsal pattern; discal spot round, orange-brown, faint to absent. Fringe pale yellow. Hindwing concolorous with forewing; antemedial line ill defined, ivory; postmedial line well defined, wavy, ivory; termen and fringe as in forewing. Hindwing underside ivory to yellowish gray, with ill-defined pattern similar to upperside; discal spot faint. Hindwing rounded, outer margin evenly convex, with discal cell approximately 0.33 as long as wing, M_3 and CuA_1 stalked; frenulum with one thick spine in male, 6–8 weaker spines in female.

Abdomen: Concolorous with thorax, usually with narrow row of white to cream scales at posterior end of each segment. Slender, extending beyond anal angle of hindwing. Tg8 somewhat narrower posteriorly; St8 slightly tapered posteriorly; St8 equal in width to St7; Tg8 roughly equal in width to Tg7; St8 equal in width to Tg7; posterior margin of St8 with shallow, U-shaped mesal excavation. Genitalia with uncus absent; tegumen narrow, dorsal part band-like, with arms forming rounded dorsal arch; lacina of variable size and shape from lateral margins of tegumen or transtilla; junction of tegumen and vinculum forming a

shallow angle. Anal tube (scaphium) long, with ventral surface bearing a long, relatively wide, sclerotized band. Saccus shallow with transverse dorsal margin at base of valva; ventral margin forming small, transverse-ovoid pocket. Transstilla weakly sclerotized, distinctly bilobed. Membrane surrounding phallus with one or two variable fields of short spines. Juxta gradually narrowing dorsally with wide dorsal margin and U-shaped mesal excavation. Area between phallus and juxta simple. Valva elongate-subrectangular to rounded, with dorsal and ventral margins roughly parallel, but ventral margin variably constricted near middle, with patch of long, fine setae at constriction; costa long, narrow, band-like, extending to apex. Apex of valva with fine, hair-like setae, similar to those covering remainder of valva; sacculus narrow, lightly sclerotized, 0.3–0.5 as long as valva, ventral margin contiguous with ventral margin of valva, without secondary group of robust setae near apex of sacculus; inner margin of sacculus lacking row of setae. Phallus usually about as long as valva, wide, with broad distal opening, narrowed basally, with rounded base; apex developed into blade-like ventral process. Vesica with at least one semicircular plate with a saw-toothed margin; cornuti variable: two clusters of fine short cornuti, a single group of large, spine-like cornuti, or cornuti absent altogether; base of vesica minutely scobinate with a pair of narrow, curved scobinate sclerites.

Female. Head: Essentially as described for male, but antenna filiform, lacking rami.

Thorax: Essentially as described for male.

Abdomen: Essentially as described for male. Genitalia with papillae anales narrow to roughly triangular, distal portion rounded. Tg8 either narrow, quadrate, or U-shape, with transverse posterior margin, bearing transverse striations. Dorsal membrane between Tg8 and papillae anales simple, with a small membranous invagination. Posterior apophyses longer than anterior apophyses. Ostium forming a large, dorso-ventrally compressed, vase-like structure. Region between ostium and ductus bursae broadly membranous, bearing a ventral appendix. Ductus bursae narrow, lightly sclerotized with lateral margins rolled upward, ductus U-shaped in cross-section. Ductus bursae arising from a small, narrow appendix at base of corpus bursae ventrally, curving to right. Corpus bursae oblong with variable lateral band of long spines; rounded anteriorly, membranous, continuous with remainder of corpus. Signum horn-like with base partially protruding beyond outer wall on left side of corpus bursae. Internal part of signum comprised of long, curved spines. Narrow, strap-like, spinose sclerite arising from signum, wrapping around corpus bursae; remainder of corpus bursae beyond signum smooth and simple. Corpus bursae often composed of two parts, with smooth distal portion broadly attached to remainder of corpus.

Few members of the species complex can be distinguished reliably based on facies alone. However, structures of the male and female genitalia provide morphological characters for separating these similar-looking adults. The species complex can be divided into two subgroups based on the arrangement and size of the cornuti in the vesica of the male phallus: Group I species have either one or two small patches of small cornuti (usually less than 0.15 the length of the phallus) or lack them altogether; and Group II species have one or two patches of large, elongate, robust cornuti that are >0.25 the length of the phallus (Doan 2023). We treat only Group I species here.

***Eois olivacea* (Felder & Rogenhofer, 1875)**

Figs 5–7

Jodis olivacea Felder & Rogenhofer, 1875: pl. 128, fig. 13.

Eois olivacea: Parsons et al. 1999: 279; Brehm et al. 2011: 1106.

Type material examined. *Holotype* ♂, COLOMBIA, Bogota [ca 2630 m] (NHMUK).

Additional specimens examined. COLOMBIA: Fasaogasuga, [1770 m], [no date] (1♂), Dognin Collection, USNM slide 154,479, USNM ENT 01906870 (USNM).

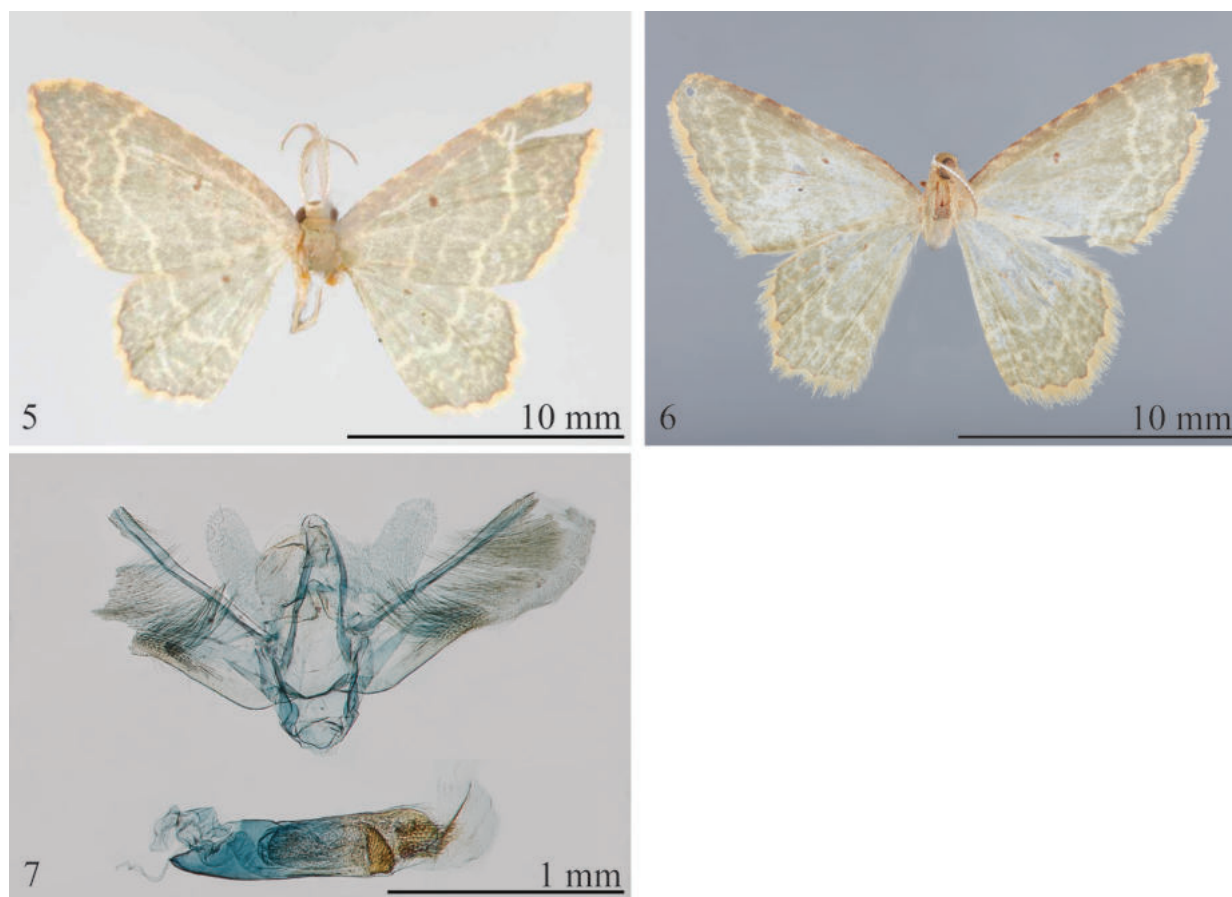
Remarks and diagnosis. The holotype male of this species (Fig. 1) lacks an abdomen; hence, comparisons of the genitalia to congeners is impossible. However, among several candidates from Colombia (USNM) that are potential conspecifics of *E. olivacea*, a male from Fasaogasuga possesses the distinctive jagged line midway between the postmedial line and the termen of the forewing that is characteristic of the type of *E. olivacea* (Fig. 5). Hence, we provisionally assign that specimen to *E. olivacea*. The question may be resolved through molecular analyses that are beyond the scope of this contribution. In the redescription below, details of external features are based on the holotype, and those of the genitalia are based on the putative conspecific. Although the genitalia of the specimen from Fasaogasuga are damaged, the important characters are intact.

If our association is correct, *E. olivacea* has the simplest vesica of any member of the complex, with the possible exception of *E. beebei*, with a single semi-circular plate bearing teeth along the curved margin. The lacina of *E. olivacea* are shorter than those of *E. pseudolivacea*.

Redescription. Male. Head: Essentially as described for species complex. **Thorax:** Essentially as described for species complex, except forewing length 9.0 mm ($n = 1$); forewing ground color pale gray-green; antemedial and medial lines faint, postmedial line well defined, ivory; distinctive, ivory, zigzag line midway between postmedial line and termen; discal spot small; costal region lightly tinged pale pinkish brown, irregularly and faintly marked with small cream blotches; termen with narrow, dark red-brown line, concolorous with discal spot, consisting of uninterrupted series of inward-directed scallops. Forewing underside as described for species complex. Hindwing concolorous with forewing, with antemedial line ill defined, postmedial line well defined; termen and fringe as in forewing. **Abdomen:** Genitalia (Fig. 7) with tegumen slender, lacina broad basally, upcurved, narrower and somewhat parallel-sided in distal 0.5, rounded apically; valva subrectangular, slightly constricted near middle with patch of long fine setae at constriction, sacculus well defined, terminating at constriction of valva, outer margin weakly angled subbasally; phallusca as long as valva; vesica with semicircular, saw-toothed plate, lacking large cornuti; membrane surrounding phallus with a pair of dorsal fields of short spines.

Female. Unknown.

Distribution and biology. This species is known from the holotype from near Bogotá and a second specimen from Fasaogasuga, Colombia. The early stages remain unknown.



Figures 5–7. *Eois olivacea* adult and male genitalia 5 holotype upperside (NHMUK) 6 *E. cf. olivacea* from Colombia upperside (USNM) 7 male genitalia of “surrogate” *E. olivacea*, USNM slide 154,479.

***Eois pseudolivacea* Doan, sp. nov.**

<https://zoobank.org/E3FD5A8C-2186-4512-957A-1B9BCFAF790E>

Figs 8–11

Type material. Holotype ♂, ECUADOR, Napo, Yanayacu Biological Station, 2163 m, 00°35'0.9"S, 077°53'0.4"W, Mar 2010, r.f. 46067, Earthwatch, slide 69575 (UNR).

Paratypes (5♂, 6♀). ECUADOR: Napo: Yanayacu Biological Station, 2066.8 m, 00°34'0.001"S, 77°52'.001"W, Jun 2013, r.f. 75714, 75718 (2♂), July 2013, r.f. 78585, 78550, 78563 (1♂, 2♀), Sept 2014, r.f. 86500 (1♀), Aug 2015, r.f. 88081 (1♂), Earthwatch (UNR). ECUADOR: Napo: Yanayacu Biological Station, 2096.6 m, 00°35'7.02"S, 77°52'31.379"W, Oct 2013, r.f. 80578, 80648, 80696 (3♀), Earthwatch (UNR). [no further locality data] r.f. B1409 (1♂), Earthwatch (UNR).

Remarks and diagnosis. *Eois pseudolivacea* is described from Ecuador, where it occurs in sympatry with several very similar congeners. Superficially, *E. pseudolivacea* is nearly indistinguishable from other members of the species complex (Figs 8, 9). However, the male genitalia (Fig. 10) are easily recognized by the length of the lacina, which is nearly as long as the valva.

Description. Male. Head: Essentially as described for species complex. **Thorax:** Essentially as described for the species complex, except forewing length 9.5 mm ($n = 12$); forewing ground color pale moss; antemedial line faint,

ivory, uniform in width throughout; medial line faint, wavy, ivory; postmedial line prominent, well defined, wavy, ivory, perpendicularly angled toward costa beyond M_3 ; region from postmedial line to termen with two narrow, wavy, ivory lines; discal spot well defined, round, red-brown; costal margin banded cream and dark red-brown; termen with narrow, dark red-brown line, concolorous with discal spot. Fringe pale yellow. Forewing underside ivory, suffused with faint reddish brown, with faint trace of dorsal pattern; discal spot round, orange-brown, faint to absent. Fringe pale yellow. Hindwing concolorous with forewing; antemedial line ivory; postmedial line wavy, cream, perpendicularly angled toward costa beyond CuA. Hindwing underside with pattern similar to upperside, with faint red-brown antemedial and postmedial lines, region from postmedial line to termen with two, wavy, red-brown lines; discal spot faint. **Abdomen:** Genitalia (Fig. 10) with lacina nearly as long as valva, somewhat parallel-sided; membrane surrounding phallobase bearing large dorsal field of short spines arranged in two longitudinal rows; vesica bilobed, each lobe with distal group of small spine-like cornuti.

Female. Head and Thorax: Essentially as described for male, but antenna slightly narrower, lacking rami. **Abdomen:** Genitalia (Fig. 11) with papillae anales narrow; ductus bursae narrow; corpus bursae oblong, with large, curved, spinelike signum located laterally on left side.



Figures 8–11. *Eois pseudolivacea* adult and genitalia **8** holotype upperside (UNR) **9** holotype underside (UNR) **10** male genitalia, slide 69575 (UNR); arrow indicates elongate lacina **11** female genitalia, slide 86478 (UNR).

Distribution and biology. This species is known only from Napo Province, Ecuador. It was reared from larvae discovered on *Piper lanceifolium* ($n = 456$) and *P. baezanum* ($n = 49$).

The eggs, larvae, and pupae of *E. pseudolivacea* have all the general characteristics described above for *Eois* with no modifications (Figs 1–4). First and second instars are similarly colored, with a clear beige head capsule, yellowish green thorax, abdomen, pinacula, and setae. The thoracic legs and prolegs are clear. Instars 3–5 have this same color pattern but also have paired broad cream patches subdorsally, extending across all segments from T2 to A8; A9 and A10 are usually pale cream colored, pinacula are chalky white with brown setae, and mandibles are dark brown. A thin white lateral stripe connects all spiracles. Pupae are usually pressed along major leaf veins on the underside of the leaf.

Etymology. The species name refers to the superficial similarity of this species to *E. olivacea*.

***Eois auruda* (Dognin, 1900)**

Figs 12–14

Amaurinia auruda Dognin, 1900: 443.

Eois auruda: Parsons et al. 1999: 279; Brehm et al. 2011: 1106.

Type material examined. **Holotype** ♂, ECUADOR, [Loja Province], environs de Loja, 1889, Dognin Collection, USNM type 32227, USNM ENT 01906872 (USMN). **Paratype** (1♂). ECUADOR, Loja, valley of Zamora [00°35.9'S, 77°53'W, 2163 m], May 1886, USNM slide 154,179, USNM ENT 01906873 (USMN).

Additional material examined. ECUADOR: [Loja Province], Environs de Loja, 1891 (1♂), USNM slide 154,650, USNM ENT 01906874 (USNM).

Remarks and diagnosis. *Eois auruda* was described by Dognin based on two males from “Loja et vallée de Zamora, Equateur.” One specimen is clearly labelled “type” and the other “co-type.” Superficially, *E. auruda* is paler yellowish orange than the pale green of most members of the species complex, and the maroon scallops of the termen are weakly interrupted by yellowish brown (Fig. 12). In the male genitalia (Fig. 14), the membrane surrounding the phallus has a smaller dorsal field of short spines than in related species.

Description. Male. Head: Essentially as described for complex. **Thorax:** Essentially as described for complex, except forewing length 9.0–10.0 mm ($n = 3$). Forewing ground color pale yellowish green; postmedial line prominent throughout; antemedial line faint; discal spot, small, round, faint, reddish brown; costal region slightly tinged with pale brown; termen with dark maroon scalloped line, concolorous with discal spot; fringe two-toned, mostly pale yellow with small incursions of red and/or brown between veins M_2 and M_3 . Forewing underside pale yellow, suffused with pale reddish brown, with faint indication of upper surface markings; antemedial line absent. Discal spot round, faint to absent, orange-brown; termen with dark orange-brown line. Hindwing ground color brownish pale yellowish green; antemedial line absent or very faint; postmedial line well defined; region between postmedial line and termen with several extremely faint, interrupted wavy, pale-yellow lines; discal spot well defined, red-brown. Fringe two-toned, mostly yellow, interrupted by pale red veins M_2 and



Figures 12–14. *Eois auruda* 12 holotype upperside (USNM) 13 holotype underside (USNM) 14 male genitalia, USNM slide 154,179.

M₃. Hindwing underside with pattern and coloration similar to forewing underside, but with pale pinkish tint, especially in costal region. **Abdomen:** Essentially as described for genus. Genitalia (Fig. 14) with tegumen slender, lacina broad basally, upcurved, somewhat parallel-sided in distal 0.5; valva subrectangular, slightly constricted near middle with patch of long fine setae, sacculus well defined, rounded subbasally, terminating at constriction of valva; phallus long, broad; vesica with semicircular, saw-toothed plate, lacking large cornuti; membrane surrounding phallus with very small dorsal field of short spines.

Female. Unknown.

Distribution and biology. This species is known from three specimens from Loja Province, Ecuador, collected before the turn of the twentieth century.

***Eois beebei* Fletcher, 1952, stat. rev.**

Figs 15, 16

Racheospila beebei Fletcher, 1952: 101.

Eois beebei: Parsons et al. 1999: 279; Brehm et al. 2011: 1106.

Type material examined. *Holotype* ♂, VENEZUELA, Rancho Grande near Maracay, W. Beebe, No. 481604 (NHMUK).



Figures 15, 16. *Eois beebei* 15 holotype upperside (NHMUK) 16 male genitalia (NHMUK).

Remarks and diagnosis. Fletcher (1952) described this species from a single male collected by William Beebe at Rancho Grande (now known as Henri Pittier National Park), in the Venezuelan Coastal Range, an historically well-known collecting locality. Fletcher's description is somewhat outdated, as is his rather crude drawing of the male genitalia. The species was treated as a synonym of *E. olivacea* by Parsons et al. (1999), without the benefit of a comparison of the genitalia with those of the latter.

As in many members of Group I, the phallus of *E. beebei* has a large, conspicuous, scobinate plate with a saw-toothed edge situated near the distal end of the vesica, but lacks long cornuti (Fig. 16). The species can be distinguished from *E. olivacea* by the shorter and narrower valvae, and from *E. pseudolivacea* by the shorter lacina.

Redescription. Male. Head: Frons and vertex pale pinkish buff with distinct white bar between bases of antennae; labial palpus pale pinkish buff, length ~ 0.5 diameter of compound eye; pectinations of antenna ~ 4 × as long as the diameter of the shaft. **Thorax:** Pale olive; forewing ground color pale olive, anterior 0.5 irrorate with pale grayish brown, costa lightly irrorated with cream-brown, post-medial fascia white, discal spot fuscous. Fringe chalcedony yellow. Forewing undersurface white, glossy; discal spot minute. **Abdomen:** Pale olive, each segment edged posteriorly with white. Male genitalia (Fig. 16) with top of tegumen broadly rounded; lacina supporting long androconial scales; valva subrectangular with distinct sacculus along venter of basal 0.5. Phallus with weakly sclerotized patch near apex; vesica with two scobinate plates in apical 0.5, lacking elongate cornuti.

Female. Unknown.

Distribution and biology. Known only from the type locality.

Eois boliviensis (Dognin, 1900)

Figs 17–19

Thalassodes boliviensis Dognin, 1900: 215.

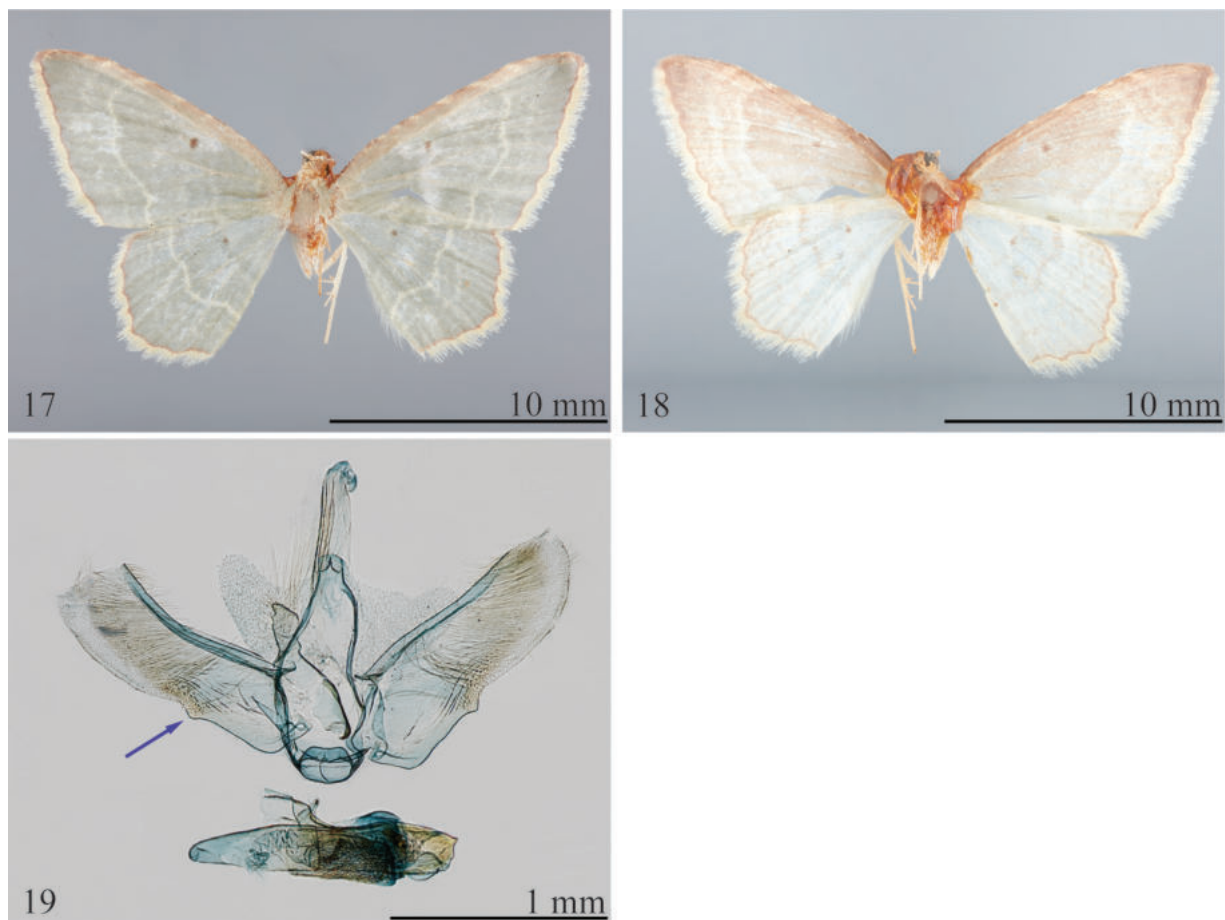
Eois boliviensis: Parsons et al. 1999: 275; Brehm et al. 2011: 1105.

Type material examined. Holotype ♂, BOLIVIA, [no additional data], USNM slide 154,454, USNM ENT 01906882 (USNM).

Remarks and diagnosis. Dognin (1900) described this species from a single male from Bolivia, without a specific locality. There are two additional specimens in the USNM from the Dognin collection identified by him as *boliviensis*. This species was transferred to *Amurinia*, now considered a synonym of *Eois*, and later treated as *Eois* by Parsons et al. (1999) and Brehm et al. (2011).

Eois boliviensis is superficially similar to other members of the species group, but the ground color is a distinctive darker gray-green (Fig. 17). The male genitalia (Fig. 19) are also typical of other species, with a coarsely toothed, scobinate plate near the distal end of the vesica, and the absence of long cornuti. The species can be distinguished from all other members of the species complex by the small, free, triangular lobe at the distal end of the sacculus~ 0.33 the distance from the base to the apex of the valva (Fig. 19), the relatively smaller toothed plate in the vesica, and the reduced patch of spines in the membranous region surrounding the phallus in the male genitalia.

Redescription. Male. Head: Frons and vertex pale green, with white bar between bases of antennae; labial palpus pale grayish green. **Thorax:** Essentially as described for species complex, except forewing length 10.0 mm ($n = 1$); forewing ground color gray-green, with straw colored, wavy, postmedial line; small spot in cell, red-brown; terminal line more wavy than scalloped, reddish brown; fringe straw. Underside pale gray-green, entirely suffused with pale reddish brown. Hindwing ground color and postmedial line concolorous with those



Figures 17–19. *Eois boliviensis* **17** holotype upperside (USNM) **18** holotype underside (USNM) **19** male genitalia, USNM slide 154,454; arrow indicates sacculus with small triangular process at termination.

of forewing. Underside pale grayish green, with pinkish tint in costal region.

Abdomen: Pale green. Male genitalia (Fig. 19) with tegumen arms joined dorsally forming a weakly bilobed process; lacina broad in basal 0.4, narrower and weakly attenuate in distal 0.6 with rounded outer margin, bearing long, hair-like androconial scales; valva elongate-subrectangular, $\sim 3 \times$ longer than wide, parallel-sided, with rounded outer margin; sacculus angled subbasally, with small triangular process at termination, ~ 0.33 distance from base to apex of valva; phallus ca as long as valva, attenuate basally, somewhat truncate apically; membrane surrounding phallus with broad, weakly developed field of spines; vesica with small, coarsely toothed plate in apical 0.5, lacking elongate cornuti.

Female. Unknown.

Distribution and biology. *Eois boliviensis* is known from three specimens collected in Bolivia without additional locality data. Nothing is known of the biology.

***Eois parumsimii* Doan, sp. nov.**

<https://zoobank.org/4A65A58B-A430-4E22-A1F0-79D75A7267F8>

Figs 20–23

Type material. Holotype ♂, ECUADOR, Napo, Yanayacu Biological Station, 2113.9 m, 00°35'48.998"S, 77°53'17.998"W, Nov 2012, r.f. 71361, Earthwatch (UNR).

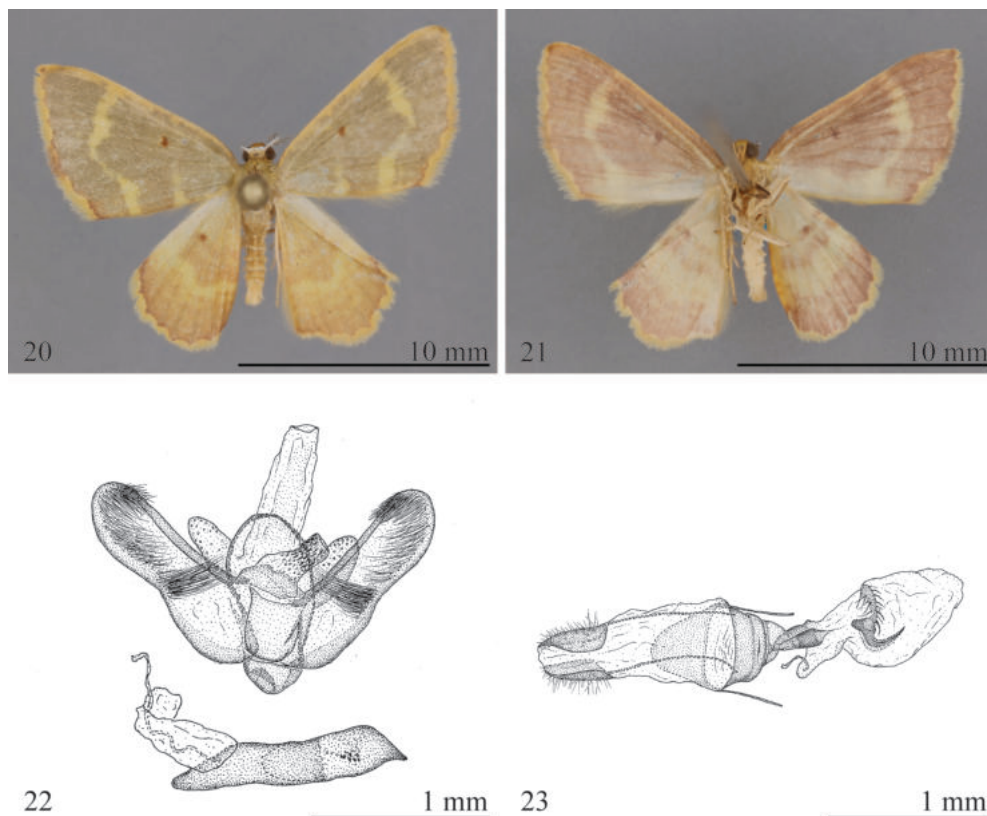
Paratypes (5♂, 2♀). ECUADOR: Napo: Yanayacu Biological Station, 2066.8 m, 00°34'0.001"S, 77°52'0.001"W, Feb 2005, r.f. 1673, 1674 (2♂), Sept 2010, r.f. 51792 (1♂), Earthwatch (UNR); 2188.4 m, 00°35'54"S, 77°53'44.34"W, Nov 2005, r.f. 9442 (1♂), Earthwatch (UNR); 1240.7 m, 00°43'38.798"S, 77°46'22"W, Jun 2014, r.f. 84256 (1♀), Earthwatch (UNR); 1871.9 m, 00°31'31.2"S, 77°52'35.399"W, Aug 2014, r.f. 85960, 85963 (1♂, 1♀), Earthwatch (UNR).

Diagnosis. This species is described from specimens reared from larvae collected at Yanayacu Biological Station in Ecuador. Externally, *E. parumsimii* is distinct from all of species in the genus, with a much broader, yellow, postmedial line on a pale pinkish gray ground color (Fig. 20). The male genitalia of *E. parumsimii* can be distinguished from those of other members of the complex by the following combination of character states: the ventral margin of the sacculus forming a blunt conical pocket (vs a small, transverse-ovoid pocket in most other species); and the membrane surrounding the phallus with a large dorsal field of short spines arranged in a series of longitudinal rows (vs arranged in two longitudinal rows most other in species). The female genitalia of *E. parumsimii* have short, trapezoidal papillae anales, whereas the papillae anales are slenderer in most other species; and the signum is located laterally on the left side of the corpus bursae, whereas it located ventrally in many other species of the complex.

Description. Male. Head: Essentially as described for species complex. **Thorax:** Essentially as described for species complex, except forewing length 8.0–9.0 mm ($n = 8$); ground color manzanilla olive, anterior portion of antemedial line very faint, posterior portion prominent, pale yellow; postmedial line well defined, wavy, pale yellow; discal spot well defined, red brown; basal 0.66 of costal margin concolorous with ground color, distal portion with clay-brown markings; termen with slender clay-brown line; fringe two-toned, mostly pale yellow, with red-brown incursion between veins M_2 and M_3 . Forewing underside ground color pale yellow, suffused with red-brown, inverse to dorsal pattern; antemedial line absent; postmedial line

prominent, width variable, but broader near costa and posterior margin; discal spot round, faint, clay-brown; termen clay brown. Fringe pale yellow. Hindwing upperside ground color clay-brown; antemedial line faint; postmedial line wavy, pale yellow; discal spot round, well defined, orange-brown; termen clay-brown. Fringe pale yellow. Hindwing with pattern similar to forewing, with prominent pale yellow antemedial and postmedial lines and faint discal spot. **Abdomen:** Genitalia (Fig. 22) with tegumen arms forming rounded triangular dorsal arch, curving slightly posterad; ventral margin of saccus forming a blunt conical pocket; transtilla slender, V-shaped; juxta wide basally, abruptly narrowed in distal 0.33 with acute dorsal part; dorsal margin of juxta narrow, truncate, with a small down-curved lip; valva subrectangular, weakly constricted on ventral margin near distal end of sacculus; a brush of bristle-like setae near apex, contrasting with remaining setae; setae at apex of sacculus longer than width of valva; ventral margin of sacculus bowed outward; base of phallus narrow, horn-shaped, membrane surrounding phallus with large dorsal field of short spines arranged in longitudinal rows; phallus ca as long as valva; vesica bifurcated distally with two appendices, one with distal group of spine-like cornuti, the other at base of vesica with a single, large scobinate plate.

Female. Head and Thorax: Essentially as described for male except lacking rami on antenna. **Abdomen:** Genitalia (Fig. 23) with papillae anales short, trapezoidal. Dorsal membrane between Tg8 and papillae anales bearing a large dorsal sac. Ductus bursae wide; ductus seminalis arising from elongate, triangular appendix at base of corpus bursae; Corpus bursae oblong, without mesal constriction, distal appendix absent; signum wing-shaped with serrate lateral margins, located laterally on left side of corpus bursae, internal part horn-like.



Figures 20–23. *Eois parumsimii* 20 holotype upperside (UNR) 21 holotype underside (UNR) 22 male genitalia, slide 75819 (UNR) 23 female genitalia, slide 75961 (UNR).

Biology and distribution. This species is known only from Napo Province, Ecuador. Adults were reared from larvae ($n = 25$) discovered in the field on *Piper baezanum*, which is a threatened species endemic to Ecuador (Santiana and Pitman 2004).

The eggs, larvae, and pupae of *E. parumsimii* have all the same general characteristics described above for *Eois* with no modifications (Figs 1–4) and are difficult to distinguish from those of *E. pseudolivacea*. All larval instars (until the prepupal stage) are similarly colored, with a translucent beige head capsule, pale green thorax and abdomen, translucent pinacula, and paired subdorsal yellow spots on all segments from T2–A6. Abdominal segments are separated by slight constrictions. The prothoracic legs and abdominal prolegs are tan. The prepupa is translucent.

Etymology. The species epithet *parumsimii* is a patronym for Michael Lumibao, who is the partner and long-time supporter of the first author; the name is derived from his Chinese zodiac animal.

Acknowledgements

We are indebted to Gunnar Brehm for sharing his collection of images of the type specimens of most species of *Eois*. We thank the dozens of volunteers that participated in Earthwatch teams from 2001 to 2019 for their assistance collecting and rearing larvae. We thank Goeff Martin and David Lees (NHMUK) for providing images of the genitalia of *Eois beebei*. Finally, we thank Patrick Strutzenberger, J. Bolling Sullivan, and Gunnar Brehm for providing helpful reviews of the manuscript that increased its quality and clarity. We are grateful to INABIO for the long-term loans to UNR of all type specimens of *E. pseudolivacea* Doan and *E. parumsimii* Doan.

Additional information

Conflict of interest

The authors have declared that no competing interests exist.

Ethical statement

No ethical statement was reported.

Funding

Funding from the National Science Foundation included grants DEB 1442103, DEB 2114793 and EN 2133818.

Author contributions

Dissections, identifications, and imaging were completed by LMD, JSM, and JWB. Funding was to LAD and MLF. All authors contributed to conceiving and writing the manuscript.

Author ORCIDs

Lydia M. Doan  <https://orcid.org/0000-0002-7039-8814>

John W. Brown  <https://orcid.org/0000-0001-5610-9855>

Matthew L. Forister  <https://orcid.org/0000-0003-2765-4779>

Lee A. Dyer  <https://orcid.org/0000-0002-0867-8874>

Data availability

All of the data that support the findings of this study are available in the main text.

References

- Brehm G, Pitkin LM, Hilt N, Fiedler K (2005) Montane Andean rain forests are a global diversity hotspot of geometrid moths. *Journal of Biogeography* 32(9): 1621–1627. <https://doi.org/10.1111/j.1365-2699.2005.01304.x>
- Brehm G, Bodner F, Strutzenberger P, Hünefeld F, Fiedler K (2011) Neotropical *Eois* (Lepidoptera: Geometridae): checklist, biogeography, diversity, and description patterns. *Annals of the Entomological Society of America* 104(6): 1091–1107. <https://doi.org/10.1603/AN10050>
- Connahs H, Rodríguez-Castañeda G, Walters T, Walla T, Dyer L (2009) Geographic variation in host-specificity and parasitoid pressure of an herbivore (Geometridae) associated with the tropical genus *Piper* (Piperaceae). *Journal of Insect Science* 9(28): 28. <https://doi.org/10.1673/031.009.2801>
- De Prins J, De Prins W (2023) Afromoths online database of Afrotropical moth species (Lepidoptera). <https://www.afromoths.net/>
- Doan LM (2023) It's the shape that matters! The diverse world of genitalia: A taxonomic and evolutionary exploration of the neotropical genus *Eois* Hübner (Lepidoptera: Geometridae: Larentiinae). Unpublished PhD dissertation, University of Nevada, Reno.
- Dognin P (1900) Heterocereres Nouveau de L'Amérique du Sud. *Annales de la Société Entomologique de Belgique* 44: 213–233.
- Dyer LA, Palmer AD [Eds] (2004) *Piper: a model genus for studies of phytochemistry, ecology, and evolution*. Kluwer Academic/Plenum Publishers, New York, 214 pp. <https://doi.org/10.1007/978-0-387-30599-8>
- Dyer LA, Singer MS, Lill JT, Stireman III JO, Gentry GL, Marquis RJ, Ricklefs RE, Greeney HF, Wagner DL, Morais HC, Diniz IR, Kursar TA, Coley PD (2007) Host specificity of Lepidoptera in tropical and temperate forests. *Nature* 448(7154): 696–699. <https://doi.org/10.1038/nature05884>
- Felder R, Rogenhofer AF (1875) In: Felder C, Felder R, Rogenhofer AF (Eds) *Reise der österreichischen Fregatte Novara um die Erde in den Jahren 1857, 1858, 1859 unter den Behilfen des Commodore B. von Wüllerstorff-Urbair. Zoologischer Theil. Zweiter Band. Zweite Abtheilung: Lepidoptera. Aus der Kaiserlich-Königlichen Hof- und Staatsdruckerei, Vienna, 20 pp. [+ pls 108–140]*
- Fletcher DS (1952) Four new species of Geometridae (moths) from Rancho Grande, North-central Venezuela. *Zoologica (New York)* 37(10): 101–105. <https://doi.org/10.5962/p.190383>
- Forister ML, Novotny V, Panorska AK, Baje L, Basset Y, Butterill PT, Cizek L, Coley PD, Dem F, Diniz IR, Drozd P, Fox M, Glassmire A, Hazen R, Hrcek J, Jahner JP, Kama O, Kozubowski TJ, Kursar TA, Lewis OT, Lill J, Marquis RJ, Miller SE, Morais HC, Murakami M, Nickel H, Pardikes N, Ricklefs RE, Singer MS, Smilanich AM, Stireman JO, Villamarín-Cortez S, Vodka S, Volf M, Wagner DL, Walla T, Weiblen GD, Dyer LA (2015) Global distribution of diet breadth in insect herbivores. *Proceedings of the National Academy of Sciences of the United States of America* 112(2): 442–447. <https://doi.org/10.1073/pnas.1423042112>
- Glassmire AE, Jeffrey CS, Forister ML, Parchman TL, Nice CC, Jahner JP, Wilson JS, Walla TR, Richards LA, Smilanich AM, Leonard MD, Morrison CR, Simbaña W, Salagaje LA, Dodson CD, Miller JS, Tepe EJ, Villamarín-Cortez S, Dyer LA (2016) Intraspecific

- phytochemical variation shapes community and population structure for specialist caterpillars. *The New Phytologist* 212(1): 208–219. <https://doi.org/10.1111/nph.14038>
- Herbulot C (2000) Sept nouveaux Geometridae africains (Lepidoptera). *Bulletin de la Societe Entomologique de Mulhouse* 56: 21–26.
- Holloway JD (1997) The moths of Borneo, Part 10: Family Geometridae, subfamilies Sterrhinae and Larentiinae. *Malayan Nature Journal* 51: 1–242.
- Jahner JP, Forister ML, Parchman TL, Smilanich AM, Miller JS, Wilson JS, Walla TR, Tepe EJ, Richards LA, Quijano-Abril MA, Glassmire AE, Dyer LA (2017) Host conservatism, geography, and elevation in the evolution of a Neotropical moth radiation. *Evolution* 71(12): 2885–2900. <https://doi.org/10.1111/evo.13377>
- Mallo D, Posada D (2016) Multilocus inference of species trees and DNA barcoding. *Philosophical Transactions of the Royal Society of London, Series B, Biological Sciences* 371(1702): 20150335. <https://doi.org/10.1098/rstb.2015.0335>
- McGuffin WC (1958) Larvae of the Nearctic Larentiinae (Lepidoptera: Geometridae). *Canadian Entomologist* 90: 1–104. <https://doi.org/10.4039/entm9008fv>
- Meyer CP, Paulay G (2005) DNA barcoding: Error rates based on comprehensive sampling. *PLOS Biology* 3(12): e422. <https://doi.org/10.1371/journal.pbio.0030422>
- Miller JS, Dyer LA (2009) Special feature: Diversity of insect-plant interactions in the eastern Andes of Ecuador. *Journal of Insect Science* 9(26): 26. <https://doi.org/10.1673/031.009.2601>
- Moraes SS, Montebello Y, Stanton MA, Yamaguchi LF, Kato MJ, Freitas AV (2021a) Description of three new species of Geometridae (Lepidoptera) using species delimitation in an integrative taxonomy approach for a cryptic species complex. *PeerJ* 9: e11304. <https://doi.org/10.7717/peerj.11304>
- Moraes SS, Murillo-Ramos L, Machado PA, Ghanavi HR, Magaldi LM, Silva-Brandão KL, Kato MJ, Freitas AVL, Wahlberg N (2021b) A double-edged sword: Unrecognized cryptic diversity and taxonomic impediment in *Eois* (Lepidoptera, Geometridae). *Zoologica Scripta* 50(5): 633–646. <https://doi.org/10.1111/zsc.12488>
- Õunap E, Viidalepp J, Truuverk A (2016) Phylogeny of the subfamily Larentiinae (Lepidoptera: Geometridae): Integrating molecular data and traditional classifications. *Systematic Entomology*, 41(4): 824–843. <https://doi.org/10.1111/syen.12195>
- Parsons M, Scoble MJ, Honey MR, Pitkin LM, Pitkin BR (1999) The catalogue. In: Scoble MJ (Ed.) *Geometrid moths of the world: catalogue*. Commonwealth Scientific and Industrial Research Organization, Collingwood, Australia. <https://doi.org/10.1071/9780643101050>
- Robinson GS (1976) The preparation of slides of Lepidoptera genitalia with special reference to the Microlepidoptera. *Entomologist's Gazette* 27: 127–132.
- Rodriguez-Castaneda G, Dyer LA, Brehm G, Connahs H, Forkner RE, Walla TR (2010) Tropical forests are not flat: How mountains affect herbivore diversity. *Ecology Letters* 13(11): 1348–1357. <https://doi.org/10.1111/j.1461-0248.2010.01525.x>
- Salcido DM, Sudta C, Dyer LA (2022) Plant-caterpillar-parasitoid natural history studies over decades and across large geographic gradients provide insight into specialization, interaction diversity, and global change. Chapter 19. In: Marquis RJ, Koptur S (Eds) *Caterpillars in the middle*. Springer Nature, Berlin, 662 pp.
- Santiana J, Pitman N (2004) *Piper baezanum*. IUCN Red List of Threatened Species 2004: e.T45817A11017241. <https://doi.org/10.2305/IUCN.UK.2004.RLTS.T45817A11017241.en>
- Seifert CL, Bodner F, Brehm G, Fiedler K (2015) Host plant associations and parasitism of South Ecuadorian *Eois* species (Lepidoptera: Geometridae) feeding on *Peperomia* (Piperaceae). *Journal of Insect Science* 15(1): 119. <https://doi.org/10.1093/jisesa/iev098>

- Strutzenberger P, Fiedler K (2011) Temporal patterns of diversification in Andean *Eois*, a species-rich clade of moths (Lepidoptera, Geometridae). *Journal of Evolutionary Biology* 24(4): 919–925. <https://doi.org/10.1111/j.1420-9101.2010.02216.x>
- Strutzenberger P, Brehm G, Bodner F, Fiedler K (2010) Molecular phylogeny of *Eois* (Lepidoptera, Geometridae): Evolution of wing patterns and host plant use in a species-rich group of Neotropical moths. *Zoologica Scripta* 39(6): 603–620. <https://doi.org/10.1111/j.1463-6409.2010.00440.x>
- Strutzenberger P, Brehm G, Fiedler K (2011) DNA barcoding-based species delimitation increases species count of *Eois* (Geometridae) moths in a well-studied tropical mountain forest by up to 50%. *Insect Science* 18(3): 349–362. <https://doi.org/10.1111/j.1744-7917.2010.01366.x>
- Strutzenberger P, Brehm G, Fiedler K (2012) DNA Barcode sequencing from old type specimens as a tool in taxonomy: A case study in the diverse genus *Eois* (Lepidoptera: Geometridae). *PLOS ONE* 7(11): e49710. <https://doi.org/10.1371/journal.pone.0049710>
- Strutzenberger P, Brehm G, Gottsberger B, Bodner F, Seifert CL, Fiedler K (2017) Diversification rates, host plant shifts and an updated molecular phylogeny of Andean *Eois* moths (Lepidoptera: Geometridae). *PLOS ONE* 12(12): e0188430. <https://doi.org/10.1371/journal.pone.0188430>
- Sudta C, Salcido DM, Forister ML, Walla TR, Villamarín-Cortez S, Dyer LA (2022) Jack-of-all-trades paradigm meets long-term data: Generalist herbivores are more widespread and locally less abundant. *Ecology Letters* 25(4): 948–957. <https://doi.org/10.1111/ele.13972>
- Taylor HR, Harris WE (2012) An emergent science on the brink of irrelevance: A review of the past 8 years of DNA barcoding. *Molecular Ecology Resources* 12(3): 377–388. <https://doi.org/10.1111/j.1755-0998.2012.03119.x>
- Viidalepp J (2011) A morphological review of tribes in Larentiinae (Lepidoptera: Geometridae). *Zootaxa* 3136(1): 1–44. <https://doi.org/10.11646/zootaxa.3136.1.1>
- Wilson JS, Forister ML, Dyer LA, O'Connor JM, Burls K, Feldman CR, Jaramillo MA, Miller JS, Rodríguez-Castañeda G, Tepe EJ, Whitfield JB, Young B (2012) Host conservatism, host shifts and diversification across three trophic levels in two Neotropical forests. *Journal of Evolutionary Biology* 25(3): 532–546. <https://doi.org/10.1111/j.1420-9101.2011.02446.x>

Appendix 1

Adult morphological characters in *Eois*

This appendix contains additional methodology of *Eois* species identification, complete with a morphological guide based off of 94 *Eois* and 5 outgroup *Eois* species, as well as character matrix of species *E. parumsimii* and *E. pseudolivacea* (Table A1). The guide includes 107 characters (37 binary and 70 multi-state), with 16 external characters (characters 1–16), 58 male-only characters (characters 17–75), and 33 female-only characters (characters 76–107).

Methodology, terminology, and abbreviations

Examination of specimens was performed under a Zeiss Stemi 2000-C stereomicroscope with SCHOTT EasyLED ring-light illuminator. Species were identified through the examination of photos of holotype or type photos (Brehm

unpublished data) and their genitalia. Terminology for genital structures and components of forewing pattern follow Holloway (1997) and Viidalepp (2011). With the exception of an unusual structure in the male genitalia of members of the several clades of *Eois*, that appears to lack a term. It is a flat, membranous, lateral flap of variable size and length attached to the sides of the tegumen and/or transtilla, which supports long, fine male scent scales or androconia. The term “lacina” is suggested for these structures.

In the guide below, brief descriptions of each morphological character are followed by a number/score, or character state, in brackets (e.g. [1], [2], [3], etc.) which denotes variation of that character. Scores of 0, unless otherwise stated, are character states commonly observed in the outgroup taxa.

Abbreviations for morphological structures in the guide are as follows: **Lp1** = labial palpus segment 1; **Lp2** = labial palpus segment 2; **Lp3** = labial palpus segment 3; **FW** = forewing; **HW** = hindwing; **Tg7** = tergum 7; **Tg8** = tergum 8; **St7** = sternum 7; **St8** = sternum 8; **PVP** = postvaginal plate; **DB** = ductus bursae; **DS** = ductus seminalis; **CB** = corpus bursae.

External characters of both genders

1. Scales between antennal bases concolorous with vertex of head [0]; a transverse band of snowy white scales located between antennal bases [1]; a narrow band of creamy yellow scales between antennal bases [2].
2. Dorsum of antennal shaft/flagellum concolorous with remainder of head [0]; dorsum of antennal shaft white [1]; each antennal annulation mostly brown, edged with lighter scales [2]; dorsum of antennal shaft with alternating rings of light brown and creamy yellow scales [3]; each antennal annulation a mixture of brown and cream-colored scales [4]; mesal surface of antennal shaft white, lateral surface brown [5].
3. Labial palpus segment 2 roughly half as long as Lp1 [0]; Lp2 roughly equal in length to, or slightly longer than, Lp1 [1]; Lp2 over twice as long as Lp1 [2].
4. Labial palpus segment 3 small, approximately $\frac{1}{4}$ as long as Lp1 [0]; Lp3 somewhat elongate, nearly $\frac{1}{2}$ as long as Lp1 [1].
5. Forewing lacking shiny scales [0]; forewing with patches of glossy, metallic scales, especially grouped within dark-patterned areas [1].
6. Forewing lacking a spot near apex of discal cell [0]; FW with a small brown spot near apex of discal cell [1].
7. Hind wing lacking a spot near apex of discal cell [0]; HW with a brown spot near apex of discal cell [1].
8. Forewing discal cell at least $\frac{1}{2}$ wing length [0]; FW discal cell much shorter than $\frac{1}{2}$ wing length [1].
9. Hind wing discal cell at least $\frac{1}{2}$ as long as wing, M3 and CuA1 veins arising separately from corner of cell [0]; HW discal cell short, approximately $\frac{1}{3}$ as long as wing, M3 and CuA1 stalked [1].
10. Forewing accessory cell present, moderate in length [0]; accessory cell present, long [1]; FW accessory cell absent [2].
11. Forewing outer margin evenly convex [0]; FW outer margin with a projection at apex of vein CuA1 [1].
12. Hindwing outer margin evenly convex [0]; HW outer margin with a projection at apex of vein M3 [1].

13. Male forewing shorter than female FW **[0]**; male forewing longer than female FW **[1]**.
14. Sclerotized tips of tibial spurs short and delicate, simple **[0]**; sclerotized tips of tibial spurs elongate, simple **[1]**; sclerotized tips of tibial spurs extremely long, with blade-like lateral margins **[2]**; sclerotized tips of tibial spurs minute **[3]**.
15. Ventral margin of tibial spur simple **[0]**; each tibial spur with a sclerotized, scaleless seam running along ventral surface **[1]**.
16. Dorsum of abdomen a single, uniform color **[0]**; abdominal dorsum yellow with a reddish stripe on the posterior margin of each segment **[1]**; abdominal dorsum yellow with a wide transverse stripe on segments 3+4 and a second stripe on 7+8 **[2]**; abdominal dorsum with a single spot on anterior margin of each segment **[3]**; abdominal dorsum pink with a yellow mesal spot on segment 2 and one on segment 3 **[4]**; abdomen yellowish, with a brown dorsal spot on segment 2 **[5]**.

Male-Only Characters

17. Each antennal annulation, exclusive of rami, roughly cylindrical **[0]**; antenna fasciculate **[1]**.
18. Antenna bipectinate nearly to apex, rami becoming gradually shorter distally **[0]**; antenna bipectinate in basal $\frac{3}{4}$, simple in distal $\frac{1}{4}$ **[1]**; antenna bipectinate in basal $\frac{2}{3}$, simple in distal $\frac{1}{3}$ **[2]**; rami absent, antenna ciliate **[3]**.
19. Rami of antenna relatively short **[0]**; rami of antenna long and thin **[1]**; rami extremely short and flattened, apices bearing long bristles **[2]**; rami absent **[?]**.
20. Tergum 8 roughly rectangular **[0]**; Tg8 somewhat narrower posteriorly **[1]**; tergum 8 strongly tapered posteriorly **[2]**.
21. Tergum 8 roughly equal in width to Tg7 **[0]**; Tg8 much narrower than Tg7 **[1]**.
22. Posterior margin of tergum 8 simple **[0]**; posterior margin of tergum 8 bearing a row of golden, bristle-like scales **[1]**; posterior margin of Tg8 with a small, somewhat sclerotized upturned flange **[2]**.
23. Sternum 8 roughly rectangular **[0]**; sternum 8 slightly tapered posteriorly **[1]**; sternum 8 strongly tapered posteriorly **[2]**.
24. Sternum 8 equal in width to St7 **[0]**; Sternum 8 much narrower than St7 **[1]**.
25. Posterior margin of St8 transverse **[0]**; posterior margin of St8 with a shallow, U-shaped mesal excavation **[1]**; posterior margin of St8 with a deep, V-shaped mesal excavation **[2]**; St8 asymmetrical, divided into two asymmetrical parts **[3]**.
26. Posterolateral angles of St8 simple **[0]**; posterolateral angles of St8 acute **[1]**; posterolateral angles of St8 forming elongate prongs **[2]**.
27. Uncus present **[0]**; uncus absent **[1]**.
28. Lateral portion of tegumen arms narrow **[0]**; lateral portion of tegumen arms extremely wide **[1]**.
29. Junction of tegumen and vinculum forming a shallow angle **[0]**; junction of tegumen and vinculum forming a deep notch **[1]**.
30. Dorsal part of tegumen, where arms meet at midline, relatively wide **[0]**; dorsal part of tegumen, where arms meet at midline, narrow, band-like **[1]**; dorsal part of tegumen extremely narrow **[2]**.

31. Dorsal portion of tegumen, where arms meet at midline, forming a rounded arch **[0]**; tegumen arms forming a somewhat triangular dorsal arch, curving slightly backward **[1]**; tegumen arms forming a narrow dorsal arch, curving strongly backward **[2]**.
32. Arms of tegumen fully sclerotized, androconia absent **[0]**; each arm of tegumen with a membranous section along posterior margin, this bearing a set of long androconia **[1]**; androconia on arms of tegumen attached to a short lacina (< ½ as long as valva) **[2]**; androconia of tegumen attached to a long lacina, nearly ½ as long as valva **[3]**; lacina at least ⅔ as long as valva **[4]**.
33. Anal tube short, with a short longitudinal ventral sclerite **[0]**; anal tube long, ventral surface bearing a long, relatively wide sclerotized band **[1]**; anal tube extremely long, extending nearly to apex of valvae, ventral surface bearing a narrow longitudinal band **[2]**.
34. Surface of sclerite below anal tube simple **[0]**; sclerite below anal tube with a longitudinal furrow **[1]**.
35. Region of membrane below saccus simple **[0]**; region of membrane below saccus with a small pocket, bearing a set of spatulate androconia **[1]**.
36. Saccus deep, dorsal margin partially enclosing bases of valvae **[0]**; saccus shallow, dorsal margin transverse, valva bases exposed **[1]**.
37. Ventral margin of saccus broadly triangular **[0]**; ventral margin of saccus gently curved, band-like **[1]**; ventral margin of saccus forming a small, transverse-ovoid pocket **[2]**; ventral margin of saccus forming a blunt conical pocket **[3]**; ventral margin of saccus forming an acute, triangular pocket **[4]**; ventral margin of saccus quadrate **[5]**.
38. Transtillar arms meet at midline to form a small U-shaped structure, pointing anteriorly **[0]**; transtillar arms forming a large, shelf-like, U-shaped structure anteriorly **[1]**; transtillar arms forming a small, V-shaped structure **[2]**.
39. Transtillar arms lacking projections (most *Eois*) **[0]**; each transtillar arm bearing an elongate, setose process (“labides”) (outgroup character) **[1]**; transtillar absent **[?]**.
40. Area of manica posterior to tegumen simple **[0]**; area of manica posterior to tegumen bearing a pocket of long, bristle-like scales **[1]**.
41. Sclerite connecting base of valval costa to dorsum of juxta relatively narrow, simple **[0]**; sclerite connecting base of valval costa to juxta wide, elbowed **[1]**.
42. Membrane surrounding phallus base simple **[0]**; membrane surrounding phallus base bearing a small dorsal field of anteriorly-directed spines **[1]**; membrane surrounding phallus base with a large dorsal field of spines **[2]**.
43. Spines surrounding phallus base short **[0]**; spines surrounding phallus base relatively long **[1]**; spines surrounding phallus base extremely robust, thorn-like **[2]**; two lengths of spines surrounding phallus base **[3]**; spines absent at phallus base (outgroup characteristic) **[?]**.
44. A uniform field of spines surrounding phallus base **[0]**; spines in membrane surrounding phallus base arranged in a series of longitudinal rows **[1]**; spines surrounding phallus base arranged in two longitudinal rows **[2]**; a small group of lateral spines on either side of phallus, in addition to larger dorsal group **[3]**; spines absent at phallus base (outgroup characteristic) **[?]**.
45. Region of manica dorsal to spine-field simple **[0]**; region of manica dorsal to spine-field bearing a thin, Y-shaped sclerite **[1]**.

46. Juxta narrow at base [0]; juxta wide at base [1].
47. Outer surface of juxta slightly convex or flat [0]; juxta bearing a pair of lateral depressions [1].
48. Juxta gradually narrowing dorsally [0]; juxta abruptly narrowing in upper third [1].
49. Dorsal margin of juxta relatively wide, with a V-shaped or U-shaped mesal excavation [0]; dorsal margin of juxta narrow but truncate, with a small down-curved lip [1]; dorsal part of juxta acute [2]; dorsal margin of juxta forming a sclerotized, down-curved, horn-like structure [3].
50. Area between phallus and juxta simple [0]; a narrow, rod-like sclerite located between juxta and phallus [1].
51. Costa of valva narrow and band-like [0]; costa extremely narrow, rod-like [1]; costa relatively wide [2]; dorsal margin of valva membranous, costa apparently absent [3].
52. Costa long, extending nearly to valva apex [0]; costa somewhat shortened, falling well short of valva apex [1].
53. Dorsal margin of costa simple [0]; dorsal margin of costa bearing a short, elbow-like process near apex [1]; dorsal margin of costa bearing a pair of large thorn-like processes [2].
54. Valva relatively wide, dorsal and ventral margins roughly parallel [0]; valve wide, expanded toward apex [1]; valva extremely wide, forming a large oval [2]; valva abruptly narrowing toward apex [3].
55. Valva apex rounded [0]; valva apex slightly acute, triangular [1]; valva apex strongly acute, apex blade-like [2].
56. Inner surface of valva bearing setae for nearly its entire length [0]; inner surface of valva naked in basal half [1].
57. Apex of valva with fine, hair-like setae, similar to those covering remainder of valva [0]; valva with a brush of bristle-like or spine-like setae near apex, contrasting with remaining setae [1].
58. Inner surface of valva covered with hair-like setae only [0]; inner surface of valva covered with hair-like setae and pedicellate scales [1].
59. Valva without an isolated set of long setae near apex of sacculus [0]; ventral margin of valva with a secondary group of robust setae near apex of sacculus [1]; setae at apex of sacculus extremely long, longer than width of valva [2].
60. Valva lacking a row of setae along inner margin of sacculus [0]; valva with a group of long, hair-like setae along inner margin of sacculus [1]; valva with a dense group of bristle-like setae along inner margin of sacculus [2].
61. Sacculus heavily sclerotized [0]; sacculus lightly sclerotized [1]; area of sacculus membranous, sacculus apparently absent [2].
62. Sacculus approximately $\frac{1}{2}$ as long as valva [0]; sacculus long, extending $\frac{2}{3}$ or more the length of valva [1]; sacculus short, less than $\frac{1}{2}$ as long as valva [2]; sacculus absent [?].
63. Sacculus relatively narrow [0]; sacculus wide [1]; sacculus an extremely broad, somewhat ovoid triangle [2]; sacculus apparently comprising a thin, sclerotized rod [3]; sacculus absent [?].
64. Ventral margin of sacculus roughly parallel to ventral margin of valva [0]; ventral margin of sacculus bowed outward [1]; ventral margin of sacculus with an elbow at base [2].

65. Ventral margin of valva smoothly contiguous with outer margin of sacculus [0]; a shallow excavation formed along ventral margin of valva near sacculus apex [1]; a pronounced notch formed along ventral margin of valva near sacculus apex [2].
66. Apex of sacculus simple [0]; sacculus bearing an apical spine [1]; sacculus bearing a transverse, apical flange [2]; sacculus with an acute, angled process at apex [3]; apex of sacculus bearing a large, spatulate process [4]; sacculus absent [?].
67. Phallus moderate in width, distal opening narrow [0]; phallus wide, distal opening wide [1]; phallus narrow [2].
68. Phallus moderate in length [0]; phallus elongate [1]; phallus short [2].
69. Base of phallus gradually narrowing anteriorly, rounded [0]; phallus base broadly rounded [1]; base of phallus narrow, somewhat horn-shaped [2].
70. Phallus base simple [0]; phallus base bearing a dorsal vertical flange [1].
71. Apex of phallus simple [0]; apex of phallus bearing a hook-like ventral process [1]; apex of phallus forming a large, blade-like ventral process [2]; apex of phallus bearing a prominent, spatulate ventral process [3]; apex of phallus bearing a narrow, acute ventral process [4].
72. Vesica comprising a single tube [0]; vesica bifurcate, comprising two appendices [1].
73. Vesica lacking spine-like cornuti [0]; vesica bearing a single distal group of one or more coarse, spine-like cornuti [1]; vesica with two distal groups of spine-like cornuti [2]; vesica with a single, tiny nub-like distal cornutus [3]; distal group of spine-like cornuti on vesica short, together forming a ratchet-like structure [4]; vesica bearing spine-like cornuti on dorsal appendix, and minute denticles on ventral appendix [5].
74. Main duct of vesica simple at base [0]; main duct of vesica minutely scobinate at base [1]; main duct of vesica with a patch of spines near base [2]; main duct of vesica with a thorn-like process at base [3].
75. Vesica lacking scobinate sclerites at base [0]; vesica with a pair of narrow, curved scobinate sclerites at base [1]; scobinate sclerites large [2]; vesica with a single, large scobinate sclerite at base [3].

Female-only characters

76. Antenna ciliate [0]; antenna bipectinate [1]; antennal cilia long and bristle-like [2].
77. Tergum 8 triangular, posterior margin gradually narrowed [0]; tergum 8 broadly triangular [1]; tergum 8 quadrate, posterior margin transverse [2]; tergum 8 a narrow, U-shaped band [3].
78. Ventral surface of A8 in area of postvaginal plate membranous or lightly sclerotized, PVP apparently absent [0]; postvaginal plate present, simple [1]; postvaginal plate large, somewhat quadrate [2]; postvaginal plate short, strap-like [3]; postvaginal plate convex [4]; postvaginal plate a triangle, tapering posteriorly [5].
79. Region of postvaginal plate smooth [0]; region of PVP bearing transverse striations [1].
80. Anterior apophyses shorter than posterior apophyses [0]; anterior apophyses elongate, equal in length to posterior apophyses [1].

81. Ostium large and funnel-shaped **[0]**; ostium forming a large, dorso-ventrally compressed, vase-like structure **[1]**; ostium comprising a narrow, transverse band **[2]**; ostium forming a large, concave structure, its dorsal wall striate **[3]**; region of ostium membranous **[4]**.
82. Region between ostium and ductus bursae moderate in length **[0]**; region between ostium and DB long **[1]**; region between ostium and ductus bursae short **[2]**; no membranous region between ostium and ductus bursae **[3]**.
83. Region between ostium and ductus bursae simple **[0]**; region between ostium and ductus bursae broadly membranous **[1]**; region between ostium and ductus bursae spiculate **[2]**; region between ostium and ductus bursae sclerotized **[3]**. region between ostium and ductus bursae absent **[?]**.
84. Region between ostium and ductus bursae simple **[0]**; region between ostium and ductus bursae bearing a ventral appendix **[1]**; region between ostium and ductus bursae bearing a small knob-like ventral process **[2]**; region between ostium and ductus bursae absent **[?]**.
85. Ductus bursae moderate in length **[0]**; ductus bursae short **[1]**; ductus bursae elongate **[2]**; ductus bursae apparently absent **[3]**.
86. Ductus bursae relatively narrow **[0]**; ductus bursae wide **[1]**; ductus bursae extremely narrow **[2]**; ductus bursae absent **[?]**.
87. Ductus bursae heavily sclerotized **[0]**; ductus bursae lightly sclerotized **[1]**; ductus bursae membranous **[2]**; ductus bursae absent **[?]**.
88. Lateral margins of ductus bursae simple **[0]**; lateral margins of ductus bursae rolled upward, ductus U-shaped in cross section **[1]**; lateral margins of ductus bursae rolled strongly inward, meeting near mid-line **[2]**; ductus bursae absent **[?]**.
89. Ductus seminalis arising from a small narrow appendix at base of CB **[0]**; DS arising from an elongate, triangular appendix at base of CB **[1]**; DS arising from a large, sac-like appendix at base of CB **[2]**.
90. Ductus seminalis arising ventrally and curling to moth's right **[0]**; ductus seminalis arising laterally on right side **[1]**; ductus seminalis arising dorsally and curling to the left **[2]**; DS arising laterally on left side and curling right **[3]**.
91. Base of corpus bursae spineless **[0]**; base of corpus bursae bearing a group of internal spines immediately beyond ductus seminalis **[1]**; base of corpus bursae bearing an irregular, sclerotized plate **[2]**.
92. Area of corpus bursae basal to signum mostly membranous **[0]**; area of CB basal to signum bearing longitudinal striae **[1]**; area of CB basal to signum sclerotized **[2]**.
93. Base of corpus bursae rounded, contiguous with remainder of corpus **[0]**; base of corpus bursae forming a separate neck-like constriction **[1]**.
94. Surface of corpus bursae lacking a covering of internal spicules (most of ingroup *Eois*) **[0]**; entire surface of corpus bursae with a dense covering of internal spicules (most of outgroup) **[1]**; basal 2/3 of corpus bursae covered with internal spicules **[2]**.
95. Signum comprising an ovoid patch of short spines **[0]**; signum horn-like, its base partially protruding from CB **[1]**; horn seemingly reduced, barely projecting above surface of bursa **[2]**; signum absent **[3]**.

96. Signum located ventrally [0]; signum located laterally on right side of CB [1]; signum located laterally on left side of CB [2]; signum located dorsally [3]; signum absent [?].
97. Internal part of horn-like signum narrow, curved, dentate along lateral margin [0]; internal part of horn-like signum wing-shaped, lateral margins serrate [1]; internal part of horn-like signum spatulate, lateral margins smooth [2]; internal part of horn-like signum forming a huge, claw-like structure [3]; internal part of horn-like signum comprised of long, curved spines [4]; internal part of horn-like signum smooth, horn-like [5]; horn-like signum absent [?].
98. Corpus bursae lacking a sclerotized crescent surrounding signum (both outgroup, most ingroup *Eois*) [0]; a sclerotized crescent, variable in size, present in CB membrane surrounding signum [1].
99. Corpus bursae without a sclerite arising from signum [0]; a spinose sclerite arising from signum, sclerite narrow, strap-like, wrapping around CB [1]; spinose sclerite becoming broad and plate-like [2]; signum sclerite a large ovoid plate, its outer margin bordered with long, curved spines [3]; signum sclerite reduced, thin, spines few or absent [4]; signum sclerite short, covered with a mass of fine internal bristles [5].
100. Central area of corpus bursae simple, without modifications beyond signum [0]; central area of CB with a large melanized area, covered in longitudinal striae [1]; area of CB beyond signum sclerite with an inset, well-defined rugose area [2]; central area of CB with a rugose, transverse fold [3]; corpus bursae with a smooth, inset sclerite in addition to signum sclerite [4]; central area of CB with a single, dentate pocket [5]; central area of CB bearing a pair of deep, spinose pockets [6]; central area of corpus bursae with a transverse sclerotized band [7]; central area of CB broadly sclerotized [8].
101. Corpus bursae single-parted, distal appendix absent [0]; CB composed of two parts, distal portion broadly attached to remainder of corpus [1]; CB composed of two parts, distal appendix with a relatively narrow, cylindrical attachment to remainder of corpus [2]; secondary appendix with a narrow, neck-like attachment to CB [3].
102. Distal appendix of corpus bursae smooth [0]; distal appendix of corpus bursae minutely wrinkled [1]; membrane of distal appendix delicate, fragile [2]; distal appendix absent [?].
103. Dorsal membrane between Tg8 and papillae anales simple, with a small membranous invagination [0]; membrane between Tg8 and papillae anales bearing a large dorsal sac [1].
104. Papillae anales roughly triangular in shape, distal portion rounded [0]; papillae anales elongate, distal portion rounded or acute [1]; papillae anales short, trapezoidal [2]; papillae anales sickle-shaped, acute at apex [3]; papillae anales extremely narrow [4].
105. Papillae anales lacking an apical hook [0]; papillae anales with a tiny apical hook [1].
106. Papillae anales evenly setose, bristles absent [0]; base of papillae anales with a series of longitudinal striae, a few scattered bristles present [1]; base of papillae anales heavily striate, with a dorsal corona of long, down-curved bristles [2].
107. Surface of papillae anales simple [0]; surface of papillae anales covered with a series of longitudinal striae [1].

Table A1. Character matrix of morphological character states of species *E. parumsimii* and *E. pseudolivacea* from a larger *Eois* data matrix.

Char. #	<i>E. parumsimii</i>	<i>E. pseudolivacea</i>	Char. #	<i>E. parumsimii</i>	<i>E. pseudolivacea</i>	Char. #	<i>E. parumsimii</i>	<i>E. pseudolivacea</i>
1	1	1	41	0	0	81	1	1
2	1	1	42	2	2	82	0	0
3	0	0	43	0	0	83	1	1
4	0	0	44	1	2	84	1	1
5	0	0	45	0	0	85	0	0
6	1	1	46	1	1	86	1	0
7	1	1	47	0	0	87	1	1
8	1	1	48	1	1	88	1	1
9	1	1	49	1	1	89	1	1
10	1	1	50	0	0	90	0	0
11	0	0	51	0	0	91	0	0
12	0	0	52	0	0	92	0	0
13	0	0	53	0	0	93	0	0
14	1	1	54	0	0	94	0	0
15	0	0	55	0	0	95	1	1
16	0	0	56	0	0	96	2	2
17	0	0	57	1	1	97	1	1
18	1	1	58	0	0	98	0	0
19	1	1	59	2	2	99	1	1
20	1	1	60	0	0	100	0	0
21	1	1	61	1	1	101	0	0
22	0	0	62	0	0	102	?	?
23	1	1	63	0	0	103	1	1
24	1	1	64	1	1	104	2	4
25	1	1	65	1	1	105	0	0
26	0	0	66	0	0	106	0	0
27	1	1	67	1	1	107	0	0
28	0	0	68	0	0			
29	0	0	69	2	2			
30	2	2	70	0	0			
31	1	1	71	2	2			
32	4	4	72	1	1			
33	1	1	73	1	2			
34	0	0	74	1	1			
35	0	0	75	3	3			
36	1	1	76	0	0			
37	3	2	77	2	2			
38	2	2	78	0	0			
39	0	0	79	1	1			
40	0	0	80	0	0			

Eleven species of jumping spiders from Sichuan, Xizang, and Yunnan, China (Araneae, Salticidae)

Cheng Wang¹, Xiaoqi Mi¹, Shuqiang Li²

¹ Guizhou Provincial Key Laboratory for Biodiversity Conservation and Utilization in the Fanjing Mountain Region, Tongren University, Tongren, Guizhou 554300, China

² Institute of Zoology, Chinese Academy of Sciences, Beijing 100101, China

Corresponding author: Shuqiang Li (lisq@ioz.ac.cn)

Abstract

Ten new species of jumping spiders are described from China, including *Attulus jimani* sp. nov. (♂♀) from Yunnan, *Colaxes cibagou* sp. nov. (♂♀), *Epeus pengi* sp. nov. (♂♀), *Evarcha zayu* sp. nov. (♂♀), *Icius zang* sp. nov. (♂♀), *Pancorius nyingchi* sp. nov. (♂♀), *Stertinus liqingae* sp. nov. (♂♀), and *Synagelides medog* sp. nov. (♀) from Xizang, *S. tianquan* sp. nov. (♂♀), and *Yaginumaella erlang* sp. nov. (♂♀) from Sichuan. The hitherto unknown female of *Phintella longapophysis* Lei & Peng, 2013 is described for the first time. Diagnostic photos and the distributional maps for all species are provided. Four new combinations are proposed: *Epeus dilucidus* (Próchniewicz, 1990), **comb. nov.**, and *E. guangxi* (Peng & Li, 2002), **comb. nov.** transferred from *Plexippoides* Prószyński, 1984, *Phintella sufflava* (Jastrzębski, 2009), **comb. nov.** transferred from *Carrhotus* Thorell, 1891, and *Yaginumaella armata* (Jastrzębski, 2011), **comb. nov.** transferred from *Pancorius* Simon, 1902.

Key words: New combination, salticid, southwestern China, taxonomy



Academic editor: Dimitar Dimitrov
Received: 23 October 2023
Accepted: 5 February 2024
Published: 21 February 2024

ZooBank: <https://zoobank.org/406CD197-9BA6-4F38-B519-2F8AD3DCBA1C>

Citation: Wang C, Mi X, Li S (2024) Eleven species of jumping spiders from Sichuan, Xizang, and Yunnan, China (Araneae, Salticidae). ZooKeys 1192: 141–178. <https://doi.org/10.3897/zookeys.1192.114589>

Copyright: © Cheng Wang et al. This is an open access article distributed under terms of the Creative Commons Attribution License ([Attribution 4.0 International – CC BY 4.0](https://creativecommons.org/licenses/by/4.0/)).

Introduction

With the series of taxonomic studies conducted, the knowledge of the family Salticidae Blackwall, 1841 from China has significantly increased, and the recorded species number has exceeded 720, which is higher than Brazil, the most species-richest country worldwide (Metzner 2024; WSC 2024). However, the Chinese jumping spider remains a poor species survey, and in the light of prospection by Li (2020), the species number could reach ca 1500.

Sichuan, Xizang, and Yunnan are the three bordered provinces in southwestern China. They partly belong to the Hengduan Mountains and Himalayan Mountains, which have been the centre of diversification for several spider groups and have presented a very high species diversity of jumping spiders, especially Yunnan, where at least 235 species are documented, far exceeding the number of salticid species known from Vietnam (161), Japan (150), and about 2/3 the species number known from India (364), and 3/5 known from Indonesia (397) (Wang and Li 2021; Li and Lin 2024; Metzner 2024; WSC 2024).

In our recent examination of jumping spider specimens collected from those three provinces, ten species were recognized as new to science, and the unknown females of *Phintella longapophysis* Lei & Peng, 2013 were also found. This work aims to describe the new species, the unknown female of *P. longapophysis* and propose four new combinations in other salticids.

Material and methods

Specimens were collected by beating shrubs or hand collecting. They were preserved in 80% or absolute ethanol. Specimens are deposited in the Institute of Zoology, Chinese Academy of Sciences in Beijing (IZCAS), China, and Tongren University (TRU) in Tongren, China. The specimens were examined with an Olympus SZX10 stereomicroscope. After dissection, the vulva was cleared in trypsin enzyme solution before examination and imaging. Images of the copulatory organs and habitus were taken with a Kuy Nice CCD mounted on an Olympus BX43 compound microscope. Compound focus images were generated using Helicon Focus v. 6.7.1. Drawings of the paths of copulatory ducts were generated by Adobe Illustrator CC 2018. All measurements are given in millimetres. Leg measurements are given as total length (femur, patella, tibia, metatarsus, tarsus). Abbreviations used in the text and figures are as follows:

ALE anterior lateral eye; **AME** anterior median eye; **AERW** anterior eye row width; **AR** atrial ridge; **AS** anterior chamber of spermatheca; **At** atrium; **CD** copulatory duct; **CO** copulatory opening; **E** embolus; **EFL** eye field length; **FD** fertilization duct; **H** epigynal hood; **LP** lamellar process; **MA** median apophysis; **MS** median septum; **PCA** prolateral cymbial apophysis; **PERW** posterior eye row width; **PL** posterior lobe; **PLE** posterior lateral eye; **PS** posterior chamber of spermatheca; **RCA** retrolateral cymbial apophysis; **RTA** retrolateral tibial apophysis; **S** spermatheca; **SD** sperm duct; **TF** tegular flap.

Institutional abbreviations: **IZCAS** Institute of Zoology, Chinese Academy of Sciences; **TRU** Tongren University.

Taxonomy

Family Salticidae Blackwall, 1841

Genus *Attulus* Simon, 1889

Type species. *Attus helveolus* Simon, 1871.

Comments. *Attulus* is placed in the Subtribe Sitticina Simon, 1901, together with five other genera (Maddison et al. 2020; Metzner 2024) and represented by 59 nominal species widely distributed in Eurasia (WSC 2024). It can be easily distinguished from other genera of the Subtribe except *Sittisax* Prószyński, 2017 based on the long fourth legs and absence of retromarginal cheliceral teeth (Maddison et al. 2020), and it can be distinguished from *Sittisax* by the tube-shaped, folded spermathecae.

***Attulus jimani* sp. nov.**

<https://zoobank.org/0DA85789-371E-4548-A0C6-C7391BF8FD63>

Figs 1, 2, 22A

Type material. *Holotype* ♂ (IZCAS-Ar44763), CHINA: Yunnan: Deqen County (28°27.88'N, 98°54.98'E, ca 3350 m), 5 Jun. 1994, J. He leg. *Paratypes* 4♂2♀ (IZCAS-Ar44764–44769), same data as for holotype.

Etymology. The specific name is after the collector, Jiman He; noun (name) in genitive case.

Diagnosis. The male of *Attulus jimani* sp. nov. resembles that of *A. dubatolovi* (Logunov & Rakov, 1998) in the general shape of palp, especially the RTA, but it differs as follows: 1) embolus originating at ca 8:30 o'clock position (Fig. 1A, B), versus about 6 o'clock position in *A. dubatolovi* (Logunov and Rakov 1998: fig. 74); 2) RTA blunt apically in retrolateral view (Fig. 1C), versus sharply pointed in *A. dubatolovi* (Logunov and Rakov 1998: fig. 75). The female of *A. jimani* sp. nov. closely resembles that of *A. clavator* (Schenkel, 1936) in the general shape of epigyne and vulva, but it can be distinguished by the spermatheca having an elongated anterior chamber, and a transversely extending posterior chamber, and by the absence of markings on the dorsum of abdomen (Fig. 2B, E), versus the spermatheca having a spherical anterior chamber, and posterolaterally extending posterior chamber, and the presence of a pair of oval spots on the dorsum of abdomen in *A. clavator* (Peng 2020: fig. 302a, e). The female also somewhat resembles that of *A. nitidus* (Hu, 2001) but is readily distinguished by the median septum, which is separated from epigastric furrow about one-third its length and almost equal in width anteromedially (Fig. 2A), versus at least half its length, and widened anteriorly in *A. nitidus* (Hu 2001: fig. 266-3).

Description. Male (Figs 1, 2C, D, F, G). Total length 4.81. Carapace 2.45 long, 1.86 wide. Abdomen 2.50 long, 1.93 wide. Eye sizes and inter-distances: AME 0.37, ALE 0.24, PLE 0.20, AERW 1.40, PERW 1.33, EFL 0.90. **Legs:** I 6.21 (1.75, 1.13, 1.60, 1.15, 0.58), II 4.86 (1.45, 0.88, 1.18, 0.85, 0.50), III 3.91 (1.15, 0.60, 0.93, 0.78, 0.45), IV 5.49 (1.75, 0.78, 1.25, 1.08, 0.63). Carapace dark brown, covered with dense setae on the elevated cephalon; fovea dark, longitudinal. Chelicerae red-brown to dark brown, each with three teeth on promargin. Endites widened at distal half, with pale antero-inner areas. Labium dark, tapered, with dark grey anterior margin. Sternum red-brown to dark brown, about 1.5 times longer than wide. Legs red-brown to dark brown. Abdomen oval, dorsum dark brown, without distinct markings, with three pairs of muscle depressions medially, covered with pale, thin setae; venter grey-brown, covered with dense thin setae.

Palp (Fig. 1A–C): tibia slightly wider than long, with flat and broad RTA almost shovel-shaped in ventral view; cymbium less than 1.5 times longer than wide, setose; bulb flat, almost oval; embolus originating at ca 8:30 o'clock position of bulb, widened at base, and followed by the slender remaining portion slightly curved and ending with blunt tip.

Female (Fig. 2A, B, E). Total length 5.06. Carapace 2.35 long, 1.82 wide. Abdomen 2.78 long, 2.23 wide. Eye sizes and inter-distances: AME 0.38, ALE 0.25, PLE 0.20, AERW 1.39, PERW 1.39, EFL 0.86. **Legs:** I 4.18 (1.25, 0.83, 1.00, 0.65, 0.45), II 3.81 (1.13, 0.75, 0.88, 0.60, 0.45), III 3.72 (1.13, 0.63, 0.83, 0.68, 0.45), IV 5.46



Figure 1. Male palp of *Attulus jimani* sp. nov., holotype **A** prolateral **B** ventral **C** retrolateral. Scale bars: 0.1 mm.

(1.80, 0.70, 1.38, 1.08, 0.50). **Habitus** (Fig. 2E) similar to that of the male except paler in colour.

Epigyne and vulva (Fig. 2A, B): wider than long, atrium irregular, posteromedially located, separated by the arch-bridge-shaped median septum; copulatory openings almost half-round, situated at the lateral sides of the base of median septum, far away from each other about 1/3 the epigynal width; copulatory ducts anterolaterally extending before strongly curved about 150° at distal end; spermathecae divided into two elongated chambers, the posterior chamber transversely extending.

Distribution. Known only from the type locality in Yunnan, China (Fig. 22A).

Genus *Colaxes* Simon, 1900

Type species. *Colaxes nitidiventris* Simon, 1900.

Comments. *Colaxes* is a rather poorly known genus, which is placed in the tribe Ballini Banks, 1892 together with 21 other genera, and only contains four endemic species recorded from India and Sri Lanka (Maddison 2015; Metzner 2024; WSC 2024). The genus was diagnosed by Benjamin (2004) for the following: 1) the presence of dark markings on the laterals of the abdomen and the absence of markings on the lateral sides of legs I–IV; 2) the presence of only

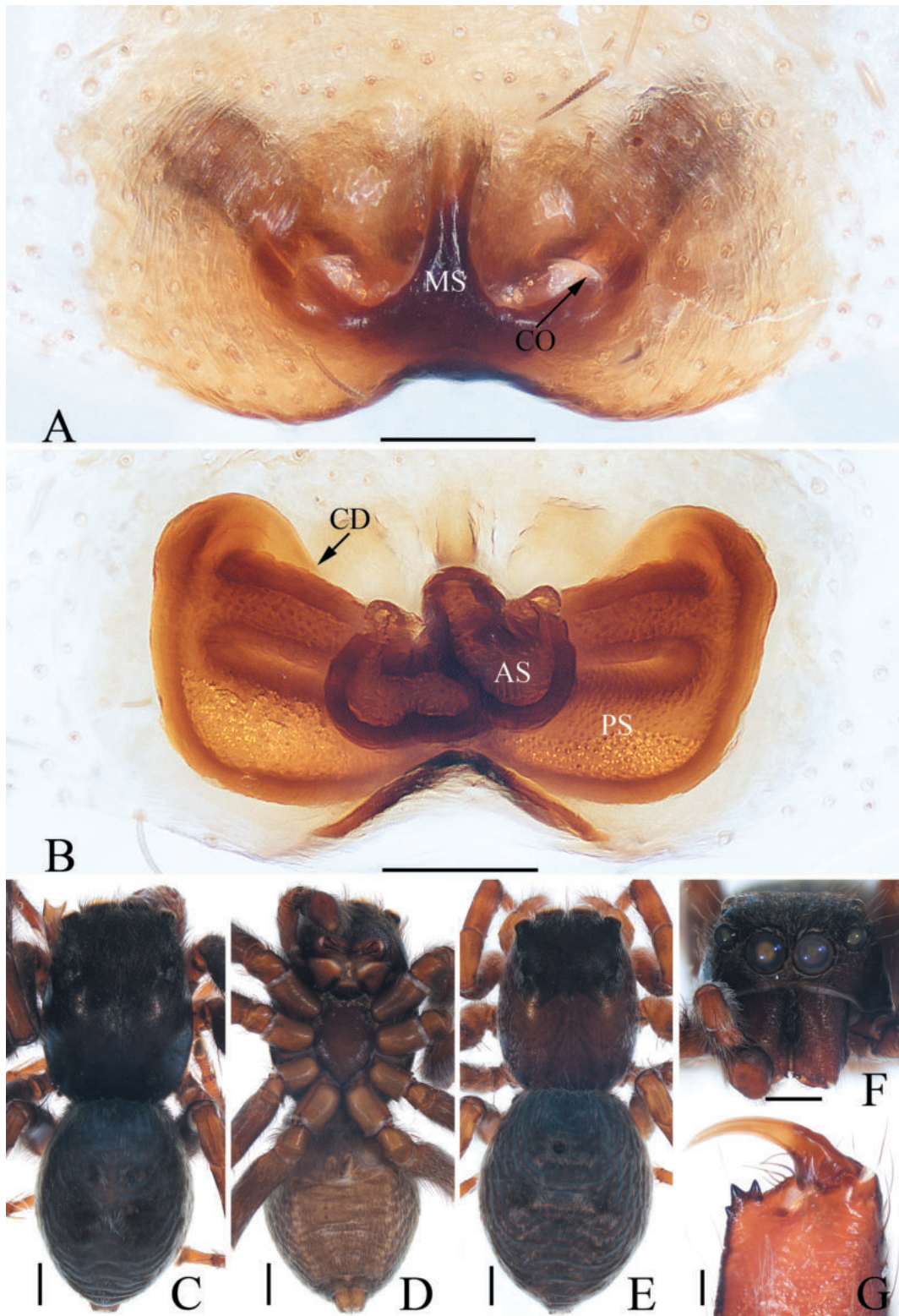


Figure 2. *Attulus jimani* sp. nov., male holotype and female paratype **A** epigyne, ventral **B** vulva, dorsal **C** holotype habitus, dorsal **D** ditto, ventral **E** female paratype habitus, dorsal **F** holotype carapace, frontal **G** holotype chelicera, posterior. Scale bars: 0.1 mm (**A, B, G**); 0.5 mm (**C–F**).

four spines on tibia I (except for *Ballus* C. L. Koch, 1850); and 3) absence of leaf-like setae ventrally on tibiae I (except for *Cynapes* Simon, 1900 and *Ballus*). However, the mentioned diagnosis was doubted by Paul et al. (2020), who also

pointed out that the taxonomic validity of *Colaxes* requires further investigation. It is worth noting that Paul et al. (2020) were not concerned about the absence of leaf-like setae ventrally on tibiae I, an essential character in Benjamin's taxonomic study of the tribe Ballini in 2004. According to this character, *Colaxes* can be easily distinguished from Asian Ballini genera except *Ballus*, *Copocrossa* Simon, 1901, and *Mantisatta* Warburton, 1900.

Moreover, *Colaxes* can be distinguished from *Ballus* by the carapace, which is longer than wide, but wider than long in the latter (Benjamin 2004), and it can be distinguished from *Copocrossa*, and *Mantisatta* by lacking much-developed leg I (see the colour habitus photos of *Copocrossa tenuilineata* (Simon, 1900) and *Mantisatta trucidans* Warburton, 1900 in Metzner 2024). However, a proper definition of the genus can't be provided because the genotype is relatively poorly known, and members are rather diverse in habitus and copulatory organs. The below new species might not be true *Colaxes*. However, we still decided to temporarily assign it to the genus because it lacks leaf-like setae ventrally on tibiae I, shares similar copulatory organs with the known member, *C. horton* Benjamin, 2004, and is geographically adjacent to the genotype.

***Colaxes cibagou* sp. nov.**

<https://zoobank.org/3E3387C2-5AA8-4A75-B079-EDA98189747C>

Figs 3, 4, 22B

Type material. *Holotype* ♂ (TRU-XZ-JS-0001), CHINA: Xizang: Zayu County, Cibagou National Nature Reserve (28°41.43'N, 97°2.86'E, ca 2570 m), 26 Jun. 2023, C. Wang leg. *Paratypes* 2♂1♀ (TRU-XZ-JS-0002–0004), same data as for holotype; 3♂2♀ (TRU-XZ-JS-0005–0009), same locality as for holotype, 13 Aug. 2003, C. Wang & H. Yao leg.

Etymology. The species name is a noun derived from the type locality: Cibagou National Nature Reserve.

Diagnosis. *Colaxes cibagou* sp. nov. can be easily distinguished from other congeners by the wide embolic coils, which are equal to about four-fifths the bulb width in diameter, the male cheliceral promarginal fissidental tooth, and the presence of hood structure formed by the anterior portion of the epigynal median septum (Figs 3A, 4A, G), versus embolic coils less than two-thirds the bulb width in diameter, two or three male cheliceral promarginal teeth, and the absence of similar hood structure in *Colaxes* (for illustrations, see Metzner 2024).

Description. Male (Figs 3, 4C, D, F–H). Total length 3.66. Carapace 1.55 long, 1.23 wide. Abdomen 2.21 long, 1.02 wide. Eye sizes and inter-distances: AME 0.34, ALE 0.17, PLE 0.13, AERW 0.96, PERW 1.04, EFL 0.62. **Legs:** I 3.37 (1.08, 0.55, 0.83, 0.63, 0.28), II 2.28 (0.70, 0.38, 0.50, 0.45, 0.25), III 2.29 (0.70, 0.33, 0.50, 0.48, 0.28), IV 2.82 (0.88, 0.38, 0.63, 0.63, 0.30). Carapace sub-square, yellow except the eye bases black, without distinct markings, covered with pale thin setae on face and bilateral sides of eye field; fovea indistinct. Chelicerae dark yellow, each with promarginal fissidental tooth with two or three cusps, and two retromarginal teeth separated by fissidental tooth with two cusps. Endites paler than chelicerae and widened distally. Labium yellow to brown, the antero-submarginal portions pale. Sternum shield-shaped, covered with thin setae. Legs pale to red-brown; legs I strongest, with slightly inflated femora,

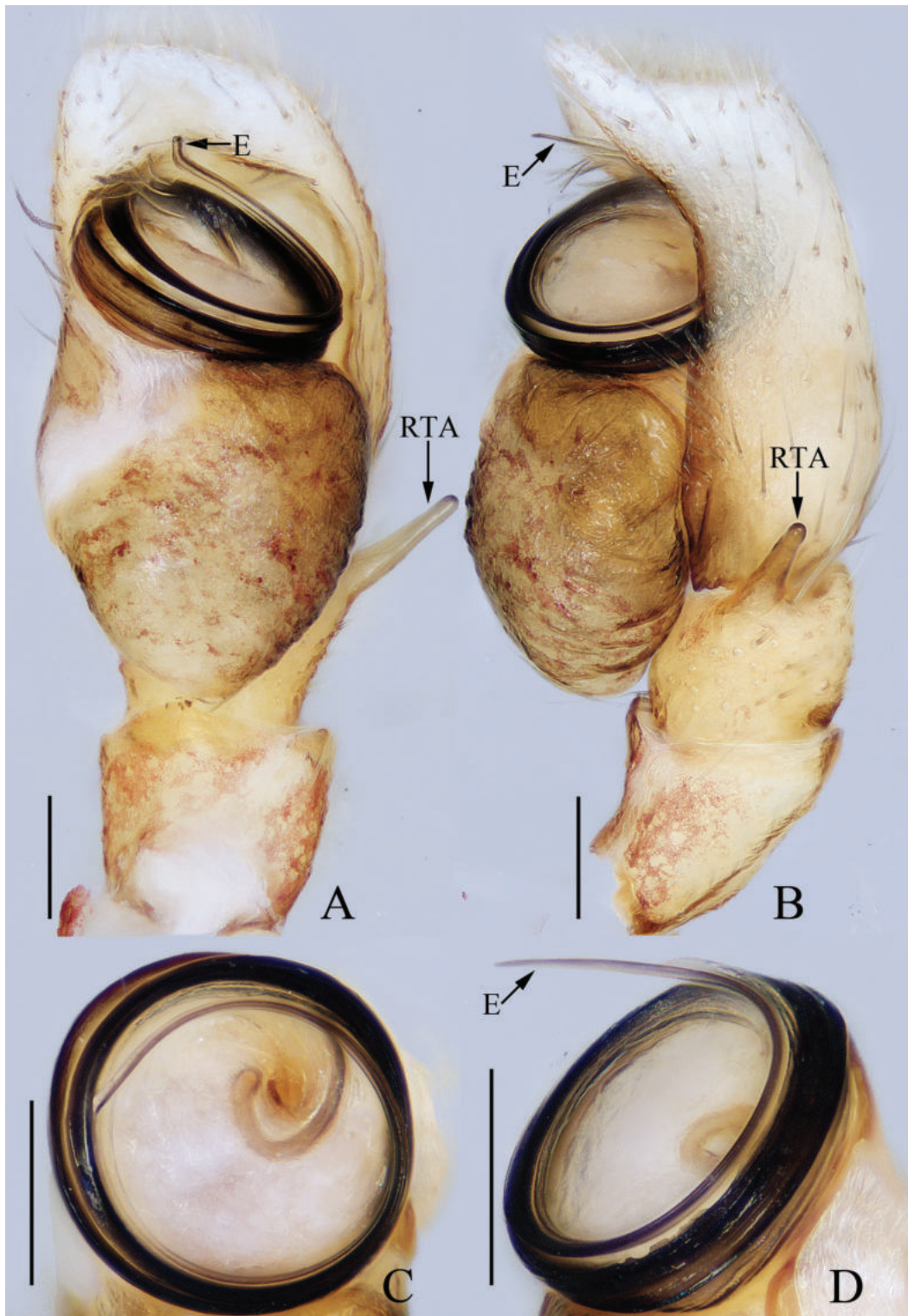


Figure 3. *Colaxes cibagou* sp. nov., holotype (A, B) and male paratype (C, D) A palp, ventral B ditto, retrolateral C embolus, anteroventral D ditto, retrolateral. Scale bars: 0.1 mm.

and five and four ventral spines on tibiae and metatarsi, respectively. Abdomen elongated, dorsum pale to dark brown, with narrow, longitudinal, anteromedian, dark brown stripes followed by four chevron markings, covered with dense silver spots laterally, and prominent scutum extending across the whole surface; venter grey, with broad, green-brown, median longitudinal band.

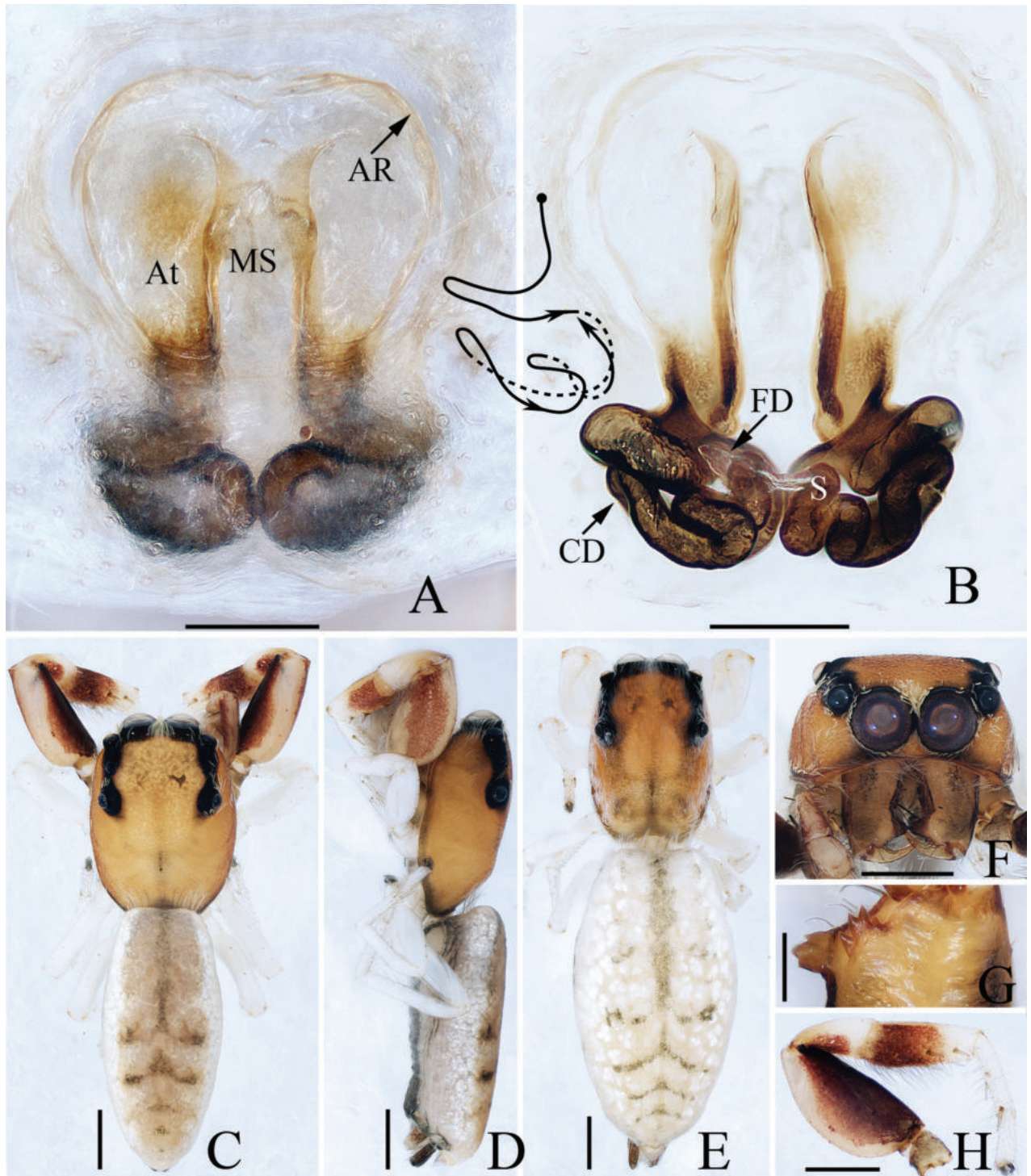


Figure 4. *Colaxes cibagou* sp. nov., male holotype and female paratype **A** epigyne, ventral **B** vulva, dorsal **C** holotype habitus, dorsal **D** ditto, lateral **E** female paratype habitus, dorsal **F** holotype carapace, frontal **G** holotype chelicera, posterior **H** leg I of holotype, proximal. Scale bars: 0.1 mm (**A, B, G**); 0.5 mm (**C–F, H**).

Palp (Fig. 3A–D): tibia slightly wider than long, with straight, antero-retrolaterally extended RTA tapered to blunt tip; cymbium about 1.5 times longer than wide; bulb swollen, slightly narrowed medio-posteriorly; embolus long, arising at the anterior portion of bulb, coiled more than twice, with blunt tip.

Female (Fig. 4A, B, E). Total length 4.51. Carapace 1.62 long, 1.17 wide. Abdomen 2.81 long, 1.55 wide. Eye sizes and inter-distances: AME 0.34, ALE 0.17,

PLE 0.13, AERW 0.96, PERW 1.06, EFL 0.60. **Legs:** I 2.62 (0.80, 0.48, 0.63, 0.43, 0.28), II 2.06 (0.58, 0.38, 0.50, 0.35, 0.25), III 2.14 (0.70, 0.33, 0.43, 0.43, 0.25), IV 2.77 (0.88, 0.33, 0.70, 0.58, 0.28). **Habitus** (Fig. 4E) similar to that of male except the less-developed legs I, the absence of abdomen dorsal scutum, and two cheliceral promarginal teeth.

Epigyne and vulva (Fig. 4A, B): longer than wide; atrium oval, with invert U-shaped anterior ridge, and separated by broad median septum, which forms pair of hood structures at anterior portion; copulatory openings located at the lowest portions of atrium, slit-shaped, separated from each other about 1.5 times their width; copulatory ducts long, forming complicated coils; spermathecae indistinct; fertilization ducts lamellar, extending anterolaterally.

Distribution. Known only from the type locality in Yunnan, China (Fig. 22B).

Comments. The unpublished molecular evidence has supported the pairing.

Genus *Epeus* Peckham & Peckham, 1886

Type species. *Evenus tener* Simon, 1877.

Comments. *Epeus*, one of the members of the subtribe Plexippina Simon, 1901 (Maddison 2015), contains 19 species distributed mainly in East, South, and Southeast Asia (WSC 2024). The genus has always been considered to be closely related to *Plexippoides* Prószyński, 1984 and a relatively comprehensive comparison of those two genera was provided by Logunov (2021), who summarized seven characters to distinguish *Epeus* and *Plexippoides*. However, the conclusion could not be perfect. Those two genera share similar palpal structure, especially in having a cluster of setae antero-retrolateral to the bulb on cavity, the presence of tegular lobe, and the sclerotized RCA; however, *Epeus* can be distinguished from *Plexippoides* by the following: 1) the slender body, covered with sparse setae on carapace (for illustrations, see Metzner 2024), versus rather dumpy body, setose on carapace in *Plexippoides* (Logunov 2021: figs 1, 6, 9, 14, 45, 50); 2) the most anterior margin of bulb cavity is far away from cymbial tip at least ca. one-third the cymbial length (for illustrations, see Metzner 2024), versus close to cymbial tip no more than one-third the cymbial length in *Plexippoides* (Logunov 2021: figs 17, 23, 28); 3) the weakly sclerotized copulatory ducts run posteriorly and form multi-loops (Patoleta et al. 2020), but sclerotized copulatory ducts do not form similar loops in *Plexippoides* (Logunov 2021: figs 33, 37, 41). *P. guangxi* and *P. dilucidus* have slender bodies, and their most anterior margin of bulb cavity is far away from cymbial tip more than one-third the cymbial length (Peng and Li 2002: fig. 3A, C; Próchniewicz 1990: figs 22, 23, 26). Based on that, they are being transferred.

Epeus pengi sp. nov.

<https://zoobank.org/812997F9-7D51-426E-938B-C0548CC3E819>

Figs 5, 6, 22B

Type material. **Holotype** ♂ (TRU-XZ-JS-0010), CHINA: Xizang: Bowo County, 318 National Highway, nearby the 102 Tunnel (30°4.41'N, 95°7.99'E, ca 2160 m), 30 Jun. 2023, C. Wang leg. **Paratypes** 1 ♀ (TRU-XZ-JS-0011), same data as for

holotype; 3 ♀ (TRU-XZ-JS-0012–0014), Zayu County, Cibagou National Nature Reserve (28°34.07'N, 97°5.44'E, ca 1620 m), 22 Jun. 2023, C. Wang leg.

Etymology. The species name is a patronym in honour of Prof. Xianjin Peng, who has significantly contributed to the taxonomy of Chinese salticids; noun (name) in genitive case.

Diagnosis. The male of *Epeus pengi* sp. nov. closely resembles that of *E. dilucidus* (Próchniewicz, 1990) comb. nov. in the general shape of palp, but it can be distinguished as follows: 1) RTA crossed with RCA in ventral view (Fig. 5B), versus not crossed in *E. dilucidus* (Próchniewicz 1990: figs 21, 25); 2) RCA only slightly curved in ventral view (Fig. 5B), versus curved about 90° in *E. dilucidus* (Próchniewicz 1990: figs 21, 25). The male also somewhat resembles that of *E. guangxi* (Peng & Li, 2002), comb. nov. in having a similar palp, but can be easily distinguished by the lack of brushes on the femora and tibiae of legs I (Fig. 6J), versus the presence of brushes formed by greyish-black long bristles ventrally and dorsally on the tibiae and metatarsi of legs I (see the description of Peng and Li 2002). The female is almost indistinguishable from *E. bicuspidatus* (Song, Gu & Chen, 1988) both in habitus and copulatory organs, but can be distinguished by the thicker copulatory ducts, which do not extend beyond the copulatory openings (Fig. 6A–D), versus thinner copulatory ducts, extending beyond the copulatory openings in *E. bicuspidatus* (Meng et al. 2015: figs 11–14).

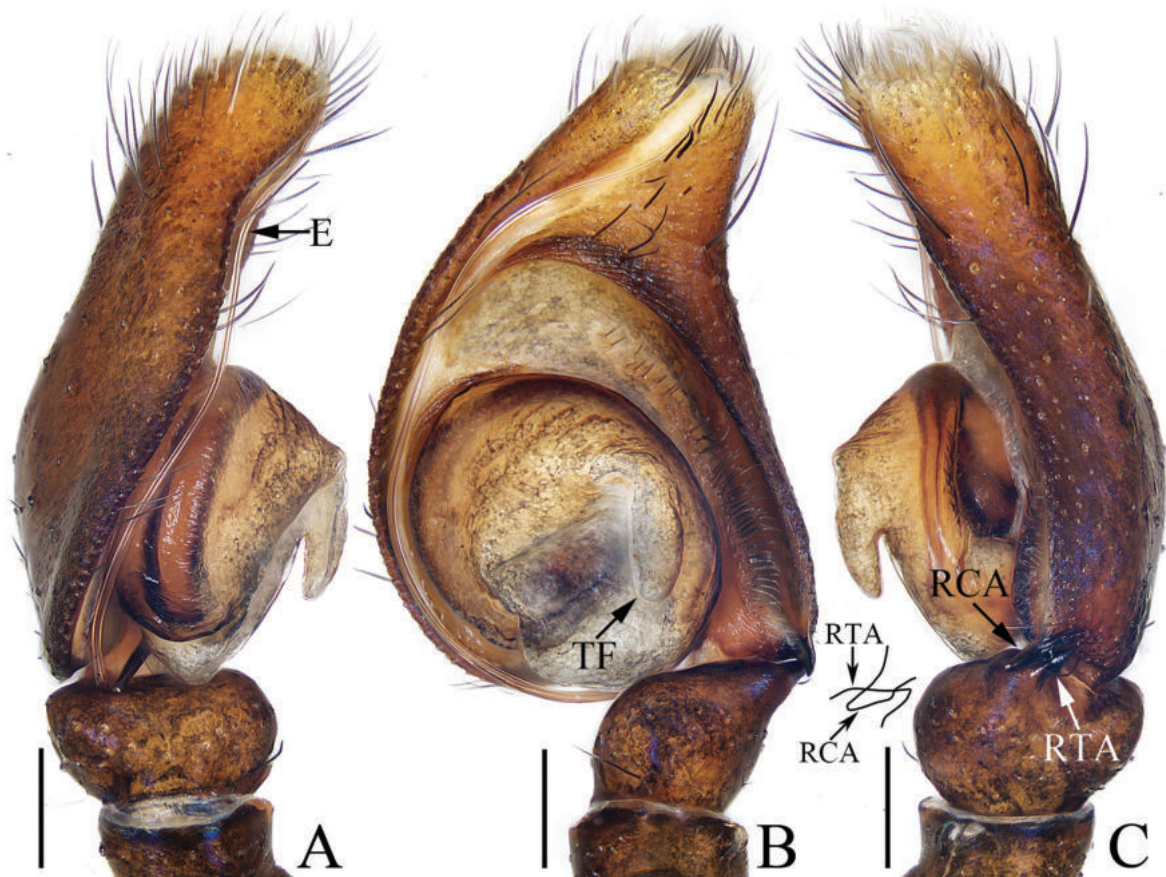


Figure 5. Male palp of *Epeus pengi* sp. nov., holotype A prolateral B ventral C retrolateral. Scale bars: 0.2 mm.

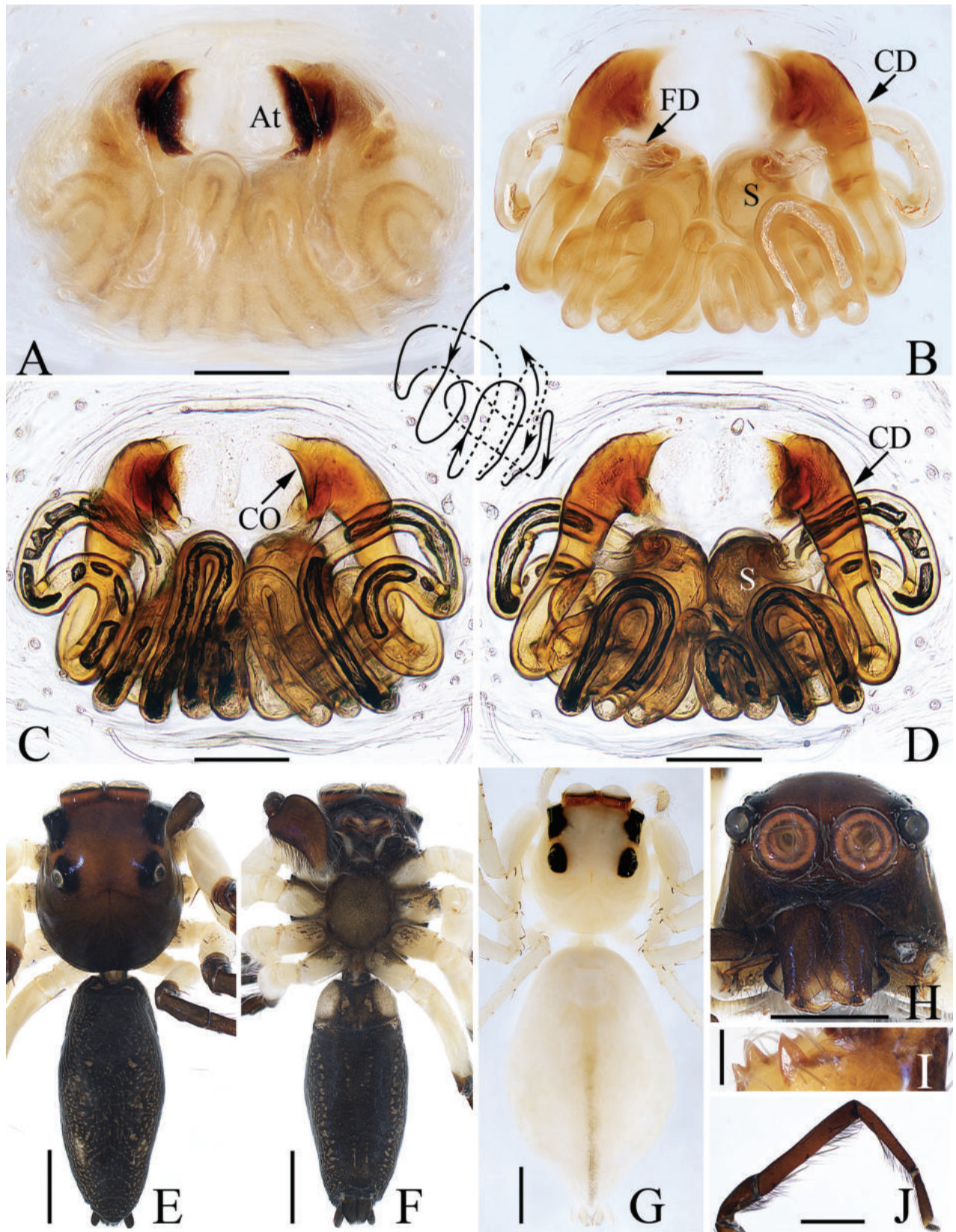


Figure 6. *Epeus pengi* sp. nov., male holotype and female paratype **A, C** epigyne, ventral **B, D** vulva, dorsal **E** holotype habitus, dorsal **F** ditto, ventral **G** female paratype habitus, dorsal **H** holotype carapace, frontal **I** holotype chelicera, posterior **J** leg I of holotype, prolateral. Scale bars: 0.1 mm (**A–D, I**); 1.0 mm (**E–H, J**).

Description. Male (Figs 5, 6E, F, H–J). Total length 5.84. Carapace 2.35 long, 2.00 wide. Abdomen 3.39 long, 1.45 wide. Eye sizes and inter-distances: AME 0.60, ALE 0.30, PLE 0.27, AERW 1.74, PERW 1.61, EFL 1.16. **Legs:** I 7.90 (2.35, 1.00, 2.20, 1.50, 0.85), II 7.70 (2.35, 1.00, 2.00, 1.50, 0.85), III 8.70 (2.65, 1.00, 2.00, 2.05, 1.00), IV 8.50 (2.40, 0.85, 2.00, 2.25, 1.00). Carapace orange-brown to dark, with sub-square, elevated cephalon, and sloped thorax with half round margin; fovea dark red, longitudinal. Chelicerae red-brown, each with two pro-marginal teeth and one retromarginal tooth. Endites sub-square, with pale inner portions. Labium near linguiform, with pale anterior portion. Sternum dark brown, mingled with green, slightly longer than wide, legs pale to red-brown. Abdomen elongated, dorsum dark brown, spotted; venter coloured as dorsum.

Palp (Fig. 5A–C): tibia swollen in retrolateral view, with short, strongly sclerotized RTA widened at base, and with pointed tip directed towards about 1: 30 o'clock position in retrolateral view; cymbium about 1.5 times longer than wide in ventral view, bearing cluster of dark setae retrolateral to the bulb on cavity, and with base-retrolateral apophysis tapered to relatively pointed tip; bulb swollen, almost round, with posteriorly extended tegular flap originating at the antero-retrolateral submargin; embolus originating at ca 5 o'clock position of bulb, flagelliform, extending ca half circle along the bulb and then antero-retrolaterally extending to the cymbial tip.

Female (Fig. 6A–D, G). Total length 7.17. Carapace 2.21 long, 2.08 wide. Abdomen 4.58 long, 3.04 wide. Eye sizes and inter-distances: AME 0.58, ALE 0.25, PLE 0.21, AERW 1.73, PERW 1.58, EFL 1.17. **Legs:** I 6.90 (2.00, 1.00, 1.85, 1.30, 0.75), II 6.90 (2.15, 1.00, 1.75, 1.25, 0.75), III 7.95 (2.50, 1.00, 1.75, 1.85, 0.85), IV 7.80 (2.25, 0.85, 1.85, 2.00, 0.85). Carapace and abdomen (Fig. 6G) pale yellow; dorsum of abdomen with narrow, longitudinal stripe extending antero-medially to the terminus.

Epigyne and vulva (Fig. 6A–D): wider than long, with anterior, oval atrium; copulatory openings anterolaterally located, with C-shaped margins; copulatory ducts long, slightly widened at base, forming complicated coils; spermathecae almost spherical, touched, medially located; fertilization ducts originating from anterior portions of spermathecae, extending transversely.

Distribution. Known only from the type locality in Xizang, China (Fig. 22B).

Genus *Evarcha* Simon, 1902

Type species. *Araneus falcatus* Clerck, 1757.

Comments. *Evarcha*, one of the largest genera of the subtribe Plexippina Simon, 1901 (Maddison 2015), contains 92 worldwide distributed species (WSC 2024). The genus has a vast diversity in genital morphology: embolus ranging from short, stout and compact to very long and filamentous, tegulum ranging from rounded to more complex shapes bearing outgrowths, insemination ducts ranging from broad and membranous to thin and tube-shaped might indicate it is more of a 'hold all' genus harbouring unrelated species (Kanesharatnam and Benjamin 2021). Based on the above, a valid definition of the genus could not be proposed. We assigned the new species to the genus because it shares copulatory organs similar to some known species, such as *E. laetabunda* (C. L. Koch, 1846) and *E. michailovi* Logunov, 1992.

***Evarcha zayu* sp. nov.**

<https://zoobank.org/FE6BE80E-C2DD-41A2-8927-FEAD4441BF44>

Figs 7, 8, 22A

Type material. *Holotype* ♂ (IZCAS-Ar44770), CHINA: Xizang: Zayu County, Zhuwagen Township (28°40.27'N, 97°27.15'E, ca 2330 m), 18–19 Jul. 1994, S. Wu leg. *Paratypes* 3♀ (IZCAS-Ar44771–773), same data as for holotype.

Etymology. The species name is a noun derived from the type locality: Zayu County.

Diagnosis. *Evarcha zayu* sp. nov. closely resembles *E. laetabunda* (C. L. Koch, 1846) in having very similar copulatory organs, but can be distinguished as follows: 1) RTA bifurcated with two rami in retrolateral view (Fig. 7C), versus not bifurcated in *E. laetabunda* (Logunov 1992: fig. 2B); 2) median septum almost square (Fig. 8A), versus almost triangular in *E. laetabunda* (Logunov 1992: fig. 3A). The species also somewhat resembles *E. michailovi* Logunov, 1992 in the general shape of copulatory organs, but it differs as follows: 1) RTA bifurcated with two rami in retrolateral view (Fig. 7C), versus not bifurcated in *E. michailovi* (Logunov 1992: fig. 2D); 2) median septum about half the atrial length (Fig. 8A), versus less than one-third the atrial length in *E. michailovi* (Logunov 1992: fig. 3C).

Description. **Male** (Figs 7, 8C, D, F, G). Total length 5.03. Carapace 2.35 long, 2.00 wide. Abdomen 2.62 long, 1.71 wide. Eye sizes and inter-distances: AME 0.44, ALE 0.26, PLE 0.25, AERW 1.62, PERW 1.50, EFL 1.00. **Legs:** I 5.84 (1.63, 1.08, 1.48, 1.00, 0.65), II 4.41 (1.33, 0.83, 1.00, 0.75, 0.50), III 5.62 (1.83, 0.95, 1.13, 1.08, 0.63), IV 4.88 (1.50, 0.65, 1.00, 1.10, 0.63). Carapace red-brown to dark brown,

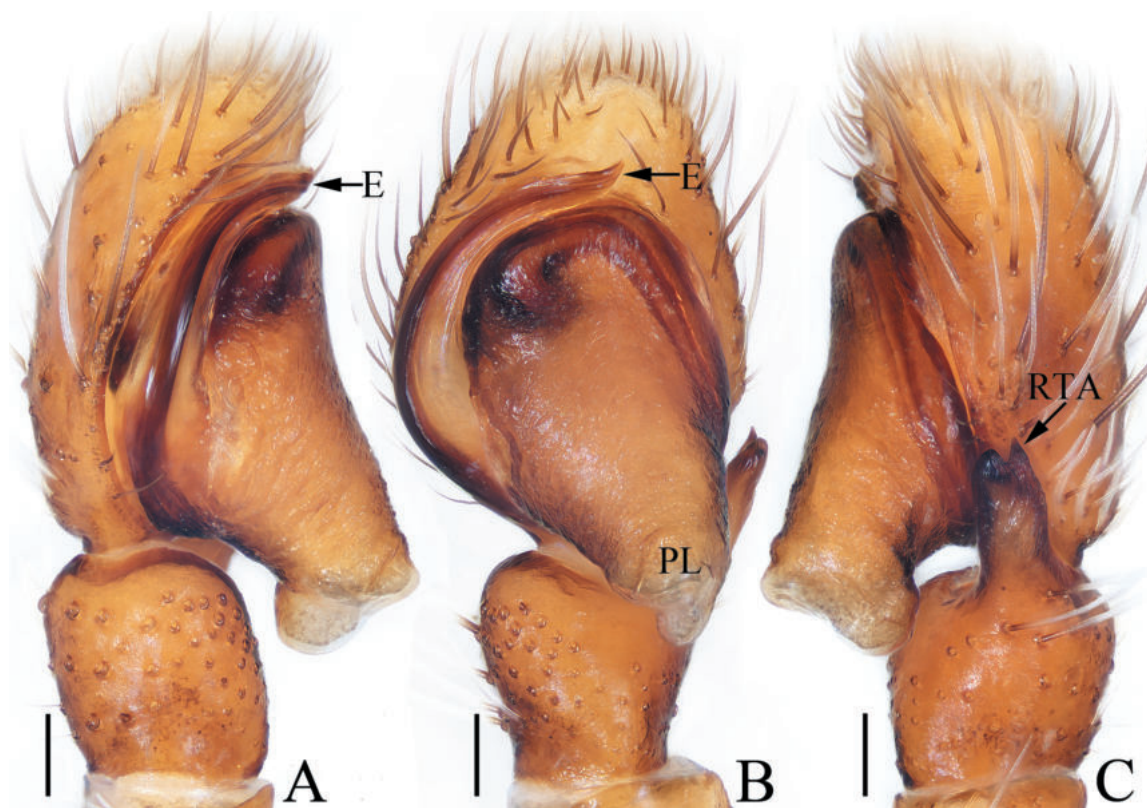


Figure 7. Male palp of *Evarcha zayu* sp. nov., holotype **A** prolateral **B** ventral **C** retrolateral. Scale bars: 0.1 mm.

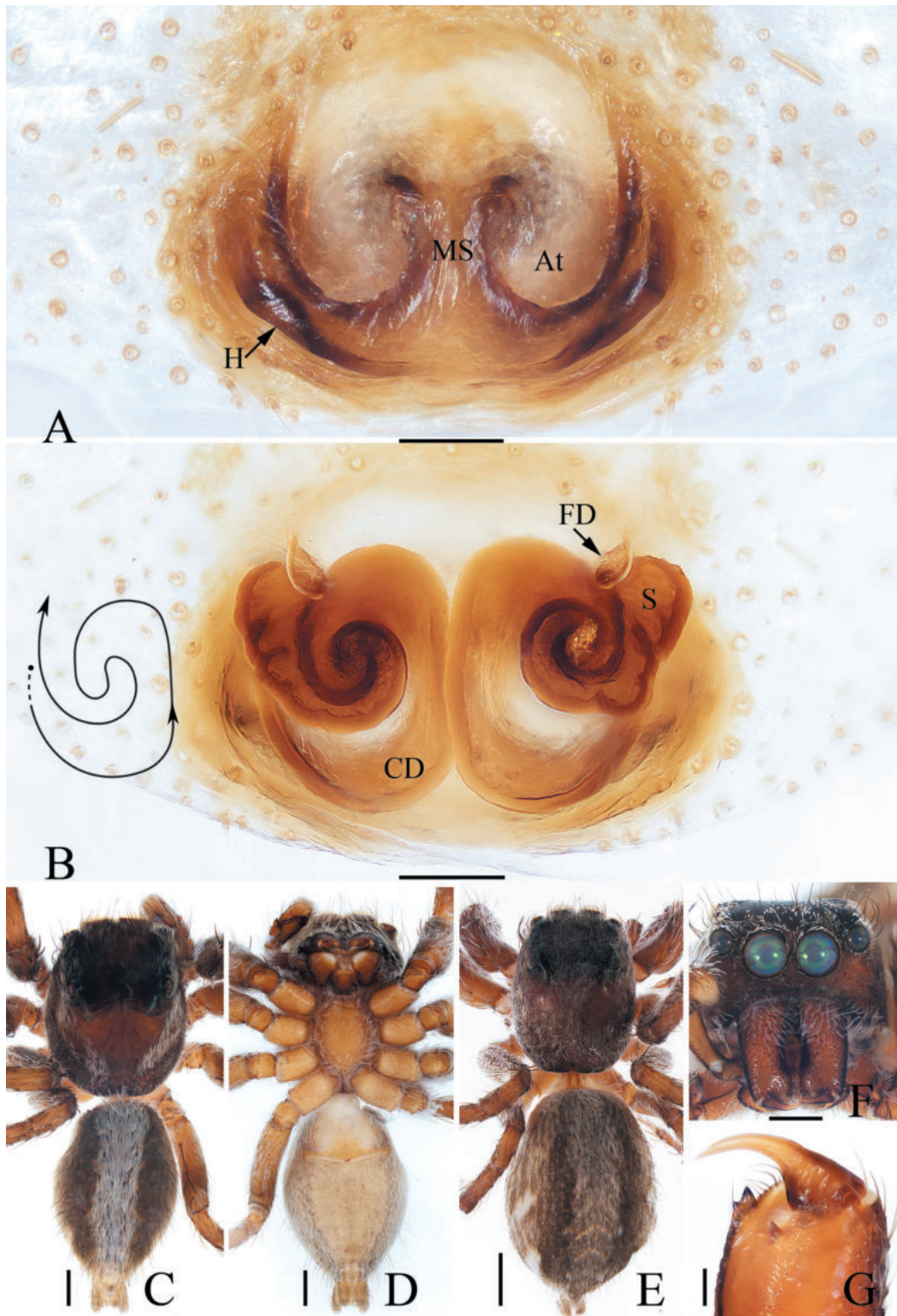


Figure 8. *Evarcha zayu* sp. nov., male holotype and female paratype **A** epigyne, ventral **B** vulva, dorsal **C** holotype habitus, dorsal **D** ditto, ventral **E** female paratype habitus, dorsal **F** holotype carapace, frontal **G** holotype chelicera, posterior. Scale bars: 0.1 mm (**A**, **B**, **G**); 0.5 mm (**C**, **D**, **F**); 1.0 mm (**E**).

covered with dense white and dark setae; fovea longitudinal, dark. Chelicerae red-brown, each with two promarginal teeth and one retromarginal tooth, with small dark tubercle bearing pale scale-like setae on base half of anterior surface. En-

dites slightly longer than wide, and widened distally, with pale distal inner portions. Labium almost linguiform. Sternum somewhat longer than wide, with straight anterior margin, covered with dense pale setae sub-marginally. Legs yellow to dark brown, setose. Abdomen sub-oval, dorsum pale to brown, covered with sparse, dark, long setae laterally, and broad, central, longitudinal, pale setal band about 1/3 the abdominal width, extending across the surface; venter pale grey.

Palp (Fig. 7A–C): tibia slightly wider than long in retrolateral view, with straight, anteriorly extended RTA bifurcated distally into sclerotized ventral ramus and apically pointed dorsal ramus; cymbium longer than wide, covered with long setae; bulb swollen medio-posteriorly, with well-developed posterior lobe extending postero-dorsally at terminus; embolus broad, originating at ca 6 o'clock position of bulb, curved ca half circle along the prolateral side of bulb, with notably pointed tip.

Female (Fig. 8A, B, E). Total length 7.28. Carapace 3.00 long, 2.36 wide. Abdomen 4.04 long, 2.84 wide. Eye sizes and inter-distances: AME 0.52, ALE 0.28, PLE 0.24, AERW 1.72, PERW 1.72, EFL 1.12. **Legs**: I 5.71 (1.70, 1.20, 1.33, 0.85, 0.63), II 5.66 (1.75, 1.20, 1.25, 0.83, 0.63), III 7.11 (2.38, 1.25, 1.38, 1.35, 0.75), IV 6.61 (2.00, 1.00, 1.38, 1.40, 0.83). **Habitus** (Fig. 8E) similar to that of male except darker in colour and without white setae on carapace.

Epigyne and vulva (Fig. 8A, B): slightly wider than long, with pair of postero-lateral hoods; atrium big, almost oval, separated by sub-square median septum about half the atrial length; copulatory ducts long, curved into U-shape antero-medially, and forming coils distally; spermathecae elongated; fertilization ducts extending anterolaterally.

Distribution. Known only from the type locality in Xizang, China (Fig. 22A).

Genus *Icius* Simon, 1876

Type species. *Icelus notabilis* C. L. Koch, 1846.

Comments. *Icius*, belongs to the tribe Chrysillini Simon, 1901, and is represented by 38 nominal species widely distributed from all over the world (WSC 2024). Like *Evarcha*, the genus might be more of a 'hold all' genus harbouring unrelated species. We assigned the below new species to the genus because it shares very similar habitus and relatively consistent copulatory organs with the generotype, *I. hamatus* (C. L. Koch, 1846). The generic position of the new species needs further attention. It is worth mentioning that the specimens described as *Icius hamatus* and *Phintella versicolor* in Hu (2001) are misidentified (the misidentification of *Icius hamatus* was documented by WSC 2024), and they are most closely related to *Icius zang* sp. nov. morphologically.

Icius zang sp. nov.

<https://zoobank.org/B0386D54-4320-432A-B7E4-DDC694A01EEC>

Figs 9, 10, 22A

Type material. **Holotype** ♂ (IZCAS-Ar44774), CHINA: Xizang: Lhasa City (29°39.11'N, 91°6.78'E, ca 3660 m), 26 Aug. 2001, X. Peng leg. **Paratypes** 3♂3♀ (IZCAS-Ar44775–44780), same data as for holotype.

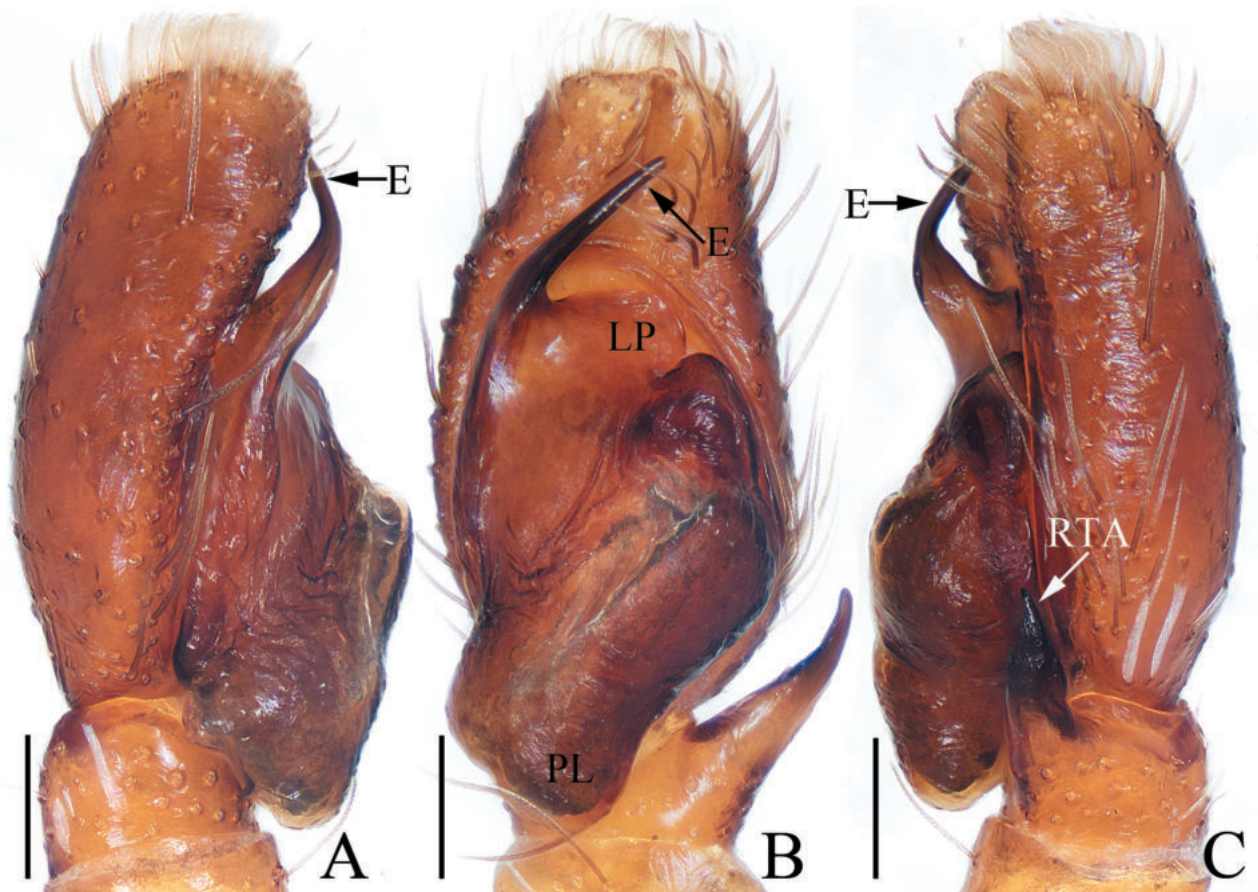


Figure 9. Male palp of *Icius zang* sp. nov., holotype **A** prolateral **B** ventral **C** retrolateral. Scale bars: 0.1 mm.

Etymology. The specific name is after one of the most popular minorities (Zang) in Xizang, China; noun.

Diagnosis. *Icius zang* sp. nov. resembles that of *I. hamatus* (C. L. Koch, 1846) in having similar habitus and the general shape of copulatory organs but can be easily distinguished by the presence of only one tibial apophysis and the pair of epigynal hoods (Figs 9B, C, 10A, B) versus two tibial apophyses and only one epigynal hood in *I. hamatus* (Peng 2020: fig. 123a–d).

Description. Male (Figs 9, 10C, D, F, G). Total length 4.53. Carapace 2.05 long, 1.55 wide. Abdomen 2.40 long, 1.75 wide. Eye sizes and inter-distances: AME 0.36, ALE 0.19, PLE 0.19, AERW 1.13, PERW 1.18, EFL 0.80. **Legs:** I 4.15 (1.30, 0.75, 1.00, 0.70, 0.40), II 3.04 (0.90, 0.55, 0.68, 0.53, 0.38), III 3.06 (0.90, 0.50, 0.68, 0.60, 0.38), IV 3.65 (1.13, 0.53, 0.78, 0.78, 0.43). Carapace red-brown, setose, with scale-like setal bands on anterior and lateral margins; fovea longitudinal. Chelicerae red-brown, each with two promarginal teeth and one retromarginal tooth. Endites longer than wide, widened distally. Labium almost linguiform. Sternum ca 1.5 times longer than wide, covered with long pale thin setae. Legs yellow to red-brown, setose. Abdomen oval, dorsum dark brown, with pair of longitudinal, setal pale stripes laterally; venter pale brown to brown.

Palp (Fig. 9A–C): tibia wider than long; RTA slightly broadened anteromedially and slightly curved towards bulb distally, with pointed tip; cymbium ca two times as long as wide; bulb swollen medio-posteriorly, with blunt posterior lobe; embolus originating at antero-prolateral portion of bulb, curved medially and blunt apically, accompanied by half-round lamellar process near the base.

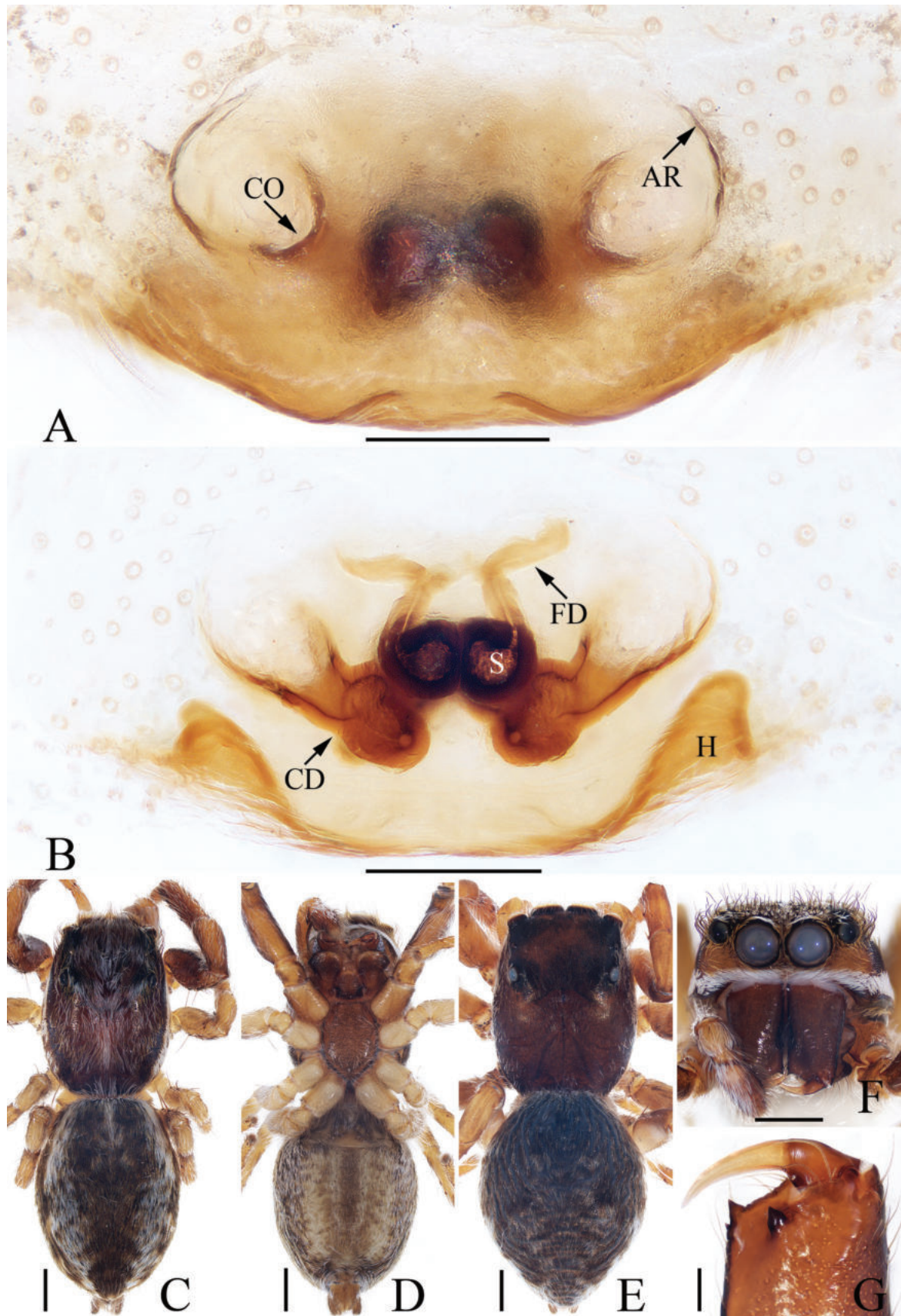


Figure 10. *Icius zang* sp. nov., male holotype and female paratype **A** epigyne, ventral **B** vulva, dorsal **C** holotype habitus, dorsal **D** ditto, ventral **E** female paratype habitus, dorsal **F** holotype carapace, frontal **G** holotype chelicera, posterior. Scale bars: 0.1 mm (**A**, **B**, **G**); 0.5 mm (**C**–**F**).

Female (Fig. 10A, B, E). Total length 4.82. Carapace 2.36 long, 1.77 wide. Abdomen 2.67 long, 2.05 wide. Eye sizes and inter-distances: AME 0.41, ALE 0.26, PLE 0.19, AERW 1.41, PERW 1.36, EFL 0.85. **Legs:** I 4.11 (1.25, 0.83, 0.95, 0.63, 0.45), II 3.79 (1.18, 0.75, 0.83, 0.58, 0.45), III 3.61 (1.15, 0.63, 0.70, 0.70, 0.43), IV 5.48 (1.75, 0.78, 1.35, 1.05, 0.55). **Habitus** (Fig. 10E) similar to that of male but without dense setae, white scale-like setal marginal bands on carapace, and pair of longitudinal, pale setal bands on abdomen.

Epigyne and vulva (Fig. 10A, B): wider than long, with pair of posterolateral hoods; atrium large, anterior located, with C-shaped lateral ridges; copulatory openings almost half round, open laterally; copulatory ducts thick, strongly curved medially; spermathecae almost spherical, touching; fertilization ducts originating from the lateral-anterior portion of spermathecae.

Distribution. Known only from the type locality in Xizang, China (Fig. 22A).

Genus *Pancorius* Simon, 1902

Type species. *Ergane dentichelis* Simon, 1899.

Comments. *Pancorius*, contains 45 species mainly distributed in East, South, and Southeast Asia (WSC 2024). The genus is distinguishable from closely related genera *Colopsus* Simon, 1902, *Evarcha*, *Hyllus* C. L. Koch, 1846 by sandy brown habitus with pale white central and lateral carapace bands, serrated longitudinal abdominal band, simple palp with rounded or oval bulb, short embolus, single RTA with pointed tip, epigyne with sizeable central pocket, comparably small membranous window and multi-chambered spermathecae (Kane-sharatnam and Benjamin 2021). The below-described new species is placed in the genus because it generally resembles that of most species. However, it is worth mentioning that it is specific for having a very long embolus originating from the median portion of the bulb's prolateral side and with a membranous portion at base that may indicate its generic position needs further attention.

Pancorius nyingchi sp. nov.

<https://zoobank.org/4AE822ED-CEB6-4956-B132-D8DBFB7466AA>

Figs 11, 12, 22A

Type material. **Holotype** ♂ (TRU-XZ-JS-0015), CHINA: Xizang: Zayu County, Cibagou National Nature Reserve (28°41.43'N, 97°2.86'E, ca 2570 m), 23 Jun. 2023, C. Wang leg. **Paratypes** 8♂10♀ (TRU-XZ-JS-0016–0033), same data as for holotype; 5♂3♀ (TRU-XZ-JS-0034–0041), Bowo County, 318 National Highway, nearby the 102 Tunnel (30°4.41'N, 95°7.99'E, ca 2160 m), 30 Jun. 2023, C. Wang leg.; 5♂3♀ (TRU-XZ-JS-0042–0049), Medog County, Renqingbengsi Scenic Area (29°18.10'N, 95°21.29'E, ca 2040), 18 Aug. 2023, C. Wang and H. Yao leg.

Etymology. The species name is a noun in apposition derived from Nyingchi City. The type localities Zayu, Bowo, Medog belong to the municipal administration of Nyingchi.

Diagnosis. *Pancorius nyingchi* sp. nov. resembles *P. manipuriensis* (Biswas & Biswas, 2004) in the general shape of copulatory organs, but it can be easily

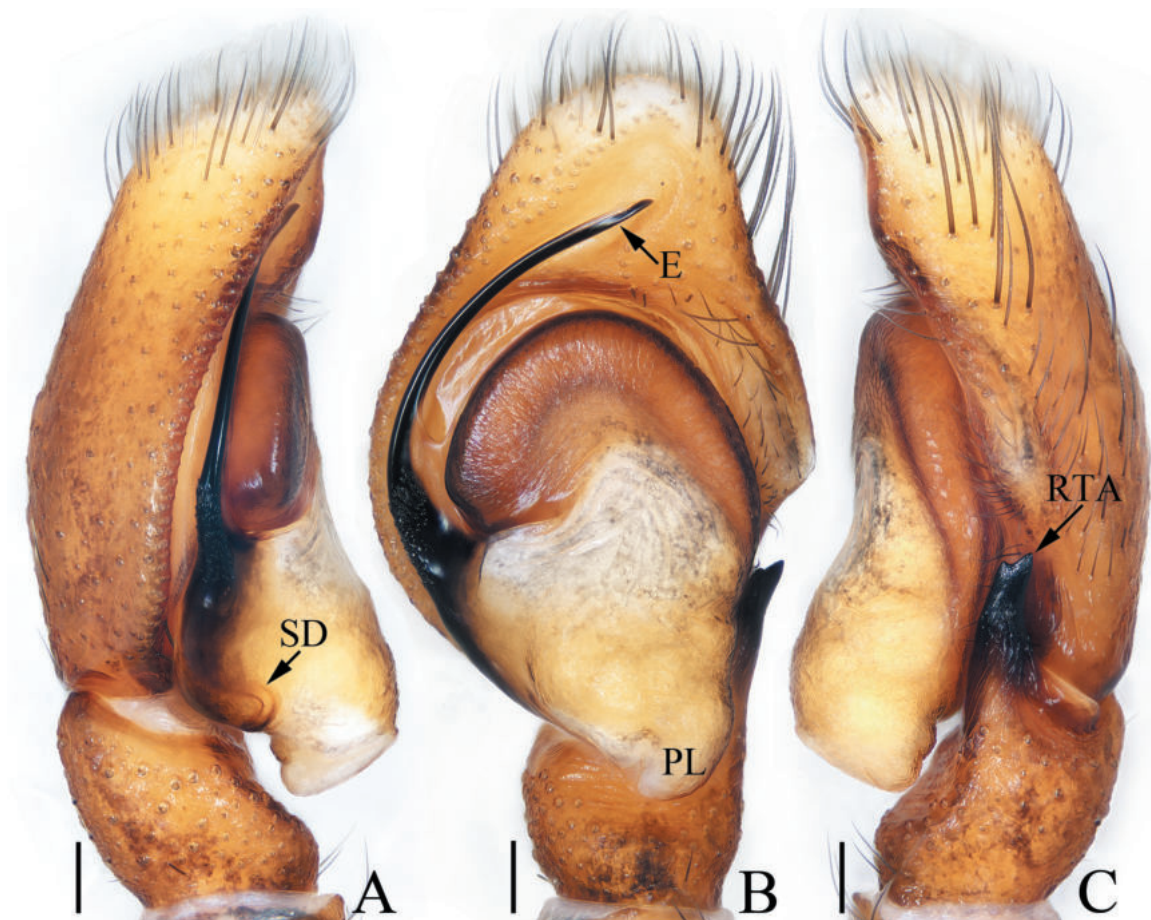


Figure 11. Male palp of *Pancorius nyingchi* sp. nov., holotype **A** prolateral **B** ventral **C** retrolateral. Scale bars: 0.1 mm.

distinguished as follows: 1) embolus originating at ca 9:00 o'clock position of bulb (Fig. 11A, B), versus ca 10:30 o'clock position of bulb in *P. manipuriensis* (Caleb 2023: fig. 15); 2) embolus is almost as long as bulb (Fig. 11B), versus less than half the bulb length in *P. manipuriensis* (Caleb 2023: fig. 15); 3) epigyne with a single hood (Fig. 12A), versus a pair of hoods in *P. manipuriensis* (Caleb 2023: figs 21, 22)

Description. Male (Figs 11, 12C, D, F, G). Total length 6.30. Carapace 2.83 long, 2.26 wide. Abdomen 3.30 long, 2.17 wide. Eye sizes and inter-distances: AME 0.62, ALE 0.38, PLE 0.33, AERW 1.96, PERW 1.91, EFL 1.17. **Legs:** I 7.30 (2.05, 1.30, 1.90, 1.30, 0.75), II 5.70 (1.75, 1.15, 1.30, 0.90, 0.60), III 6.20 (2.00, 1.00, 1.25, 1.25, 0.70), IV 6.35 (1.90, 1.00, 1.40, 1.40, 0.65). Carapace red-brown to dark brown, with two clusters of lateral, white setae, and big, red-brown area on thorax; fovea longitudinal, dark. Chelicerae red-brown, each with two promarginal teeth and one retromarginal tooth. Endites dark brown, with pale inner-distal portions. Labium coloured same as endites, with pale anterior margin bearing several dark setae. Sternum dark brown, longer than wide, with straight anterior margin. Legs yellow to dark brown, with three and two pairs of ventral spines on tibiae and metatarsi I, respectively. Abdomen elongated, dorsum dark brown, dotted, with pair of anterolateral pale stripes, two pairs of median muscle depressions, and longitudinal, central pale band extending from middle to the terminus; venter pale bilaterally, with broad, dark brown band bearing two pairs of longitudinal, dotted lines.

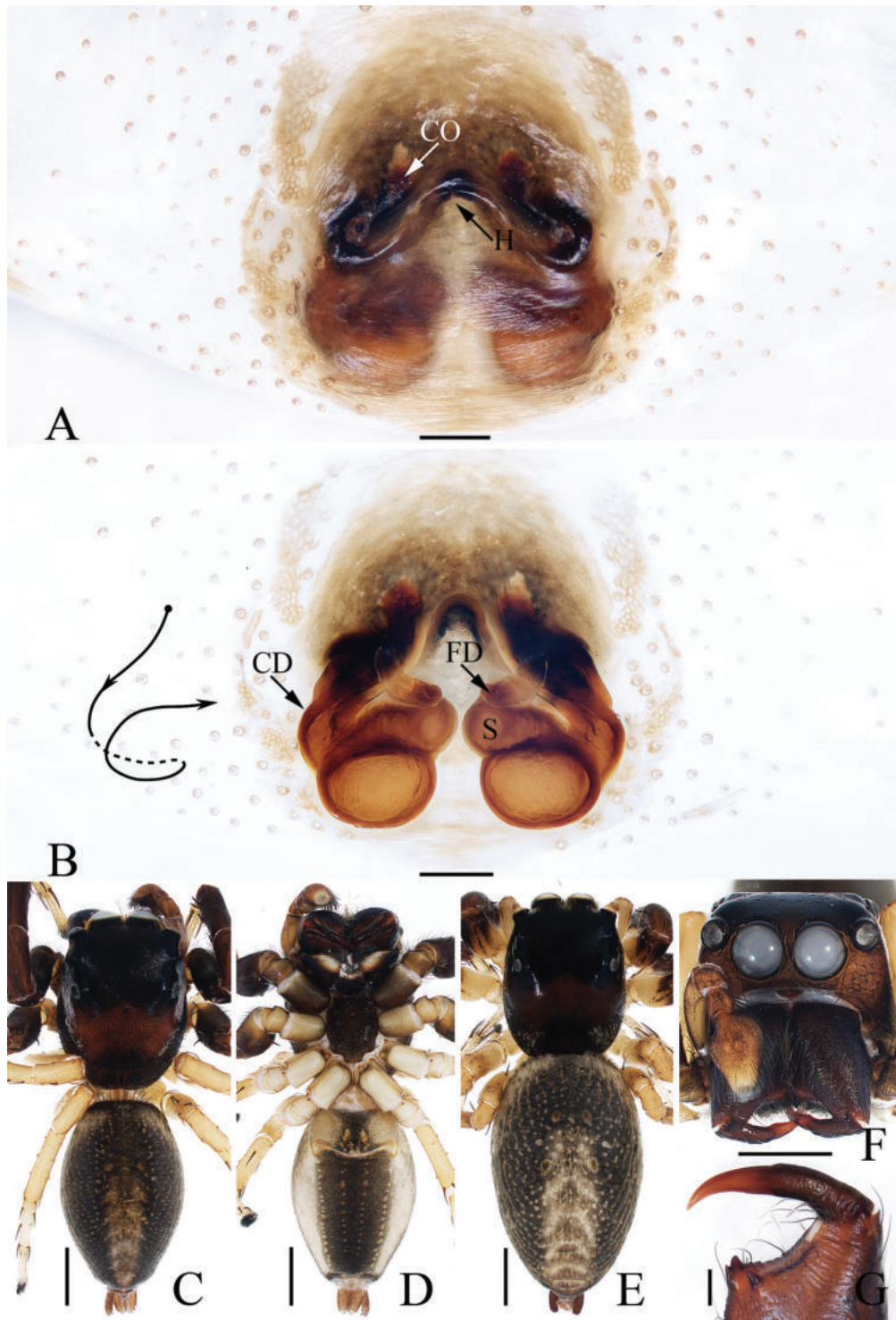


Figure 12. *Pancorius nyingchi* sp. nov., male holotype and female paratype **A** epigyne, ventral **B** vulva, dorsal **C** holotype habitus, dorsal **D** ditto, ventral **E** female paratype habitus, dorsal **F** holotype carapace, frontal **G** holotype chelicera, posterior. Scale bars: 0.1 mm (**A**, **B**); 0.2 (**G**); 1.0 mm (**C**–**F**).

Palp (Fig. 11A–C): tibia wider than long, with strongly sclerotized RTA almost equal in length with tibia, bifurcated with two small sub-triangular rami distally; cymbium about 1.5 times as long as wide; bulb flat, with posterior lobe extending postero-prolaterally; embolus strongly sclerotized, widened

at base, curved around the prolateral margin of bulb into C-shape, with noticeably pointed tip.

Female (Fig. 12A, B, E). Total length 6.84. Carapace 2.71 long, 2.22 wide. Abdomen 4.31 long, 2.67 wide. Eye sizes and inter-distances: AME 0.62, ALE 0.36, PLE 0.31, AERW 1.87, PERW 1.87, EFL 1.11. **Legs:** I 5.05 (1.50, 1.00, 1.20, 0.75, 0.60), II 4.85 (1.50, 1.00, 1.05, 0.70, 0.60), III 5.80 (1.90, 0.95, 1.20, 1.10, 0.65), IV 6.00 (1.90, 0.95, 1.30, 1.20, 0.65). **Habitus** (Fig. 12E) similar to that of male.

Epigyne and vulva (Fig. 12A, B): longer than wide, with downward opened, antero-central hood; copulatory openings slit-shaped, anterolaterally located; copulatory ducts curved and twisted; spermathecae indistinct; fertilization ducts lamellar, anterolaterally extending.

Distribution. Known only from the type locality in Xizang, China (Fig. 22A).

Genus *Phintella* Strand, 1906

Type species. *Phintella typica* Strand, 1906.

Comments. *Phintella*, one of the species-richest genera of the tribe Chrysillini Simon, 1901, contains 72 species mainly distributed in Asia and Africa (WSC 2024). The genus is diverse in habitus and copulatory organs, which indicates it should be split or at least should be further divided into groups. *Phintella longapophysis* is a convincing sample. It is sexual dimorphism in habitus, with hook-shaped distal apophysis on endites and distal-retrolateral tegular lobe (Figs 13B, 14C–E) that are different from the generotype and its congeners, which without sexual dimorphism, lacks the hook-shaped distal apophysis on endites, and with the lamellar process instead of distal-retrolateral tegular lobe (for illustration, see Metzner 2024).

Moreover, *Phintella sufflava* (Jastrzębski, 2009), comb. nov. is transferred because it shares a similar epigyne and vulva with *P. longapophysis* Lei & Peng, 2013. In the following, we considered *P. longapophysis* Lei & Peng, 2013 as a valid species rather than a synonym of the latter because the examined female specimens consistently have spherical spermathecae, which is different from *P. sufflava*. However, we cannot confirm whether the difference is due to interspecific differences or intraspecific variations. So, the status of the two mentioned species needs further confirmation.

Phintella longapophysis Lei & Peng, 2013

Figs 13, 14, 22A

Phintella longapophysis Lei & Peng, 2013: 100, figs 1, 2a–c (male holotype, not examined).

Material examined. 7♂9♀ (TRU-XZ-JS-0050–0065), CHINA: Xizang: Zayu County, Cibagou National Nature Reserve (28°41.43'N, 97°2.86'E, ca 2570 m), 23 Jun. 2023, C. Wang leg.; 3♂2♀ (TRU-XZ-JS-0066–0070), Bowo County, 318 National Highway, nearby the 102 Tunnel (30°4.41'N, 95°7.99'E, ca 2160 m), 30 Jun. 2023, C. Wang leg.

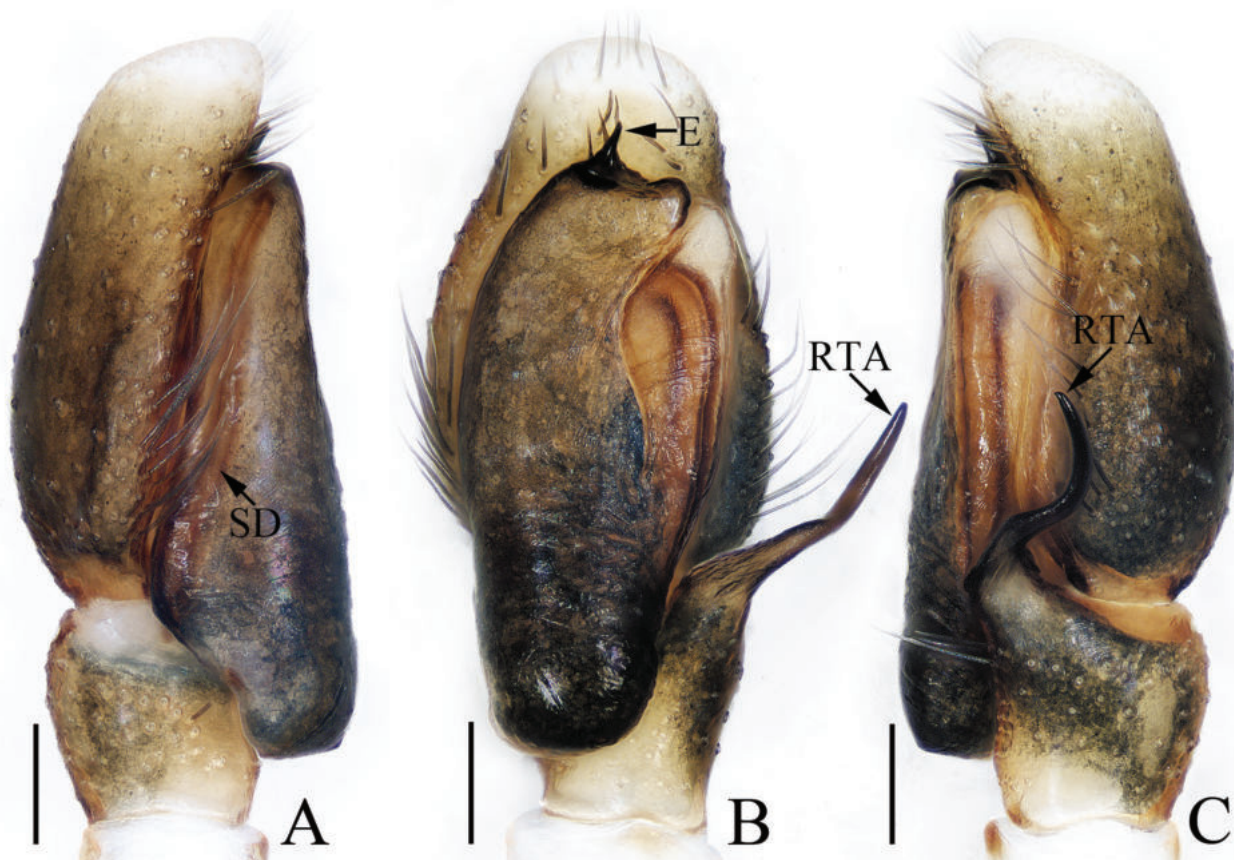


Figure 13. Male palp of *Phintella longapophysis* Lei & Peng, 2013 **A** prolateral **B** ventral **C** retrolateral. Scale bars: 0.1 mm.

Diagnosis. The male was thoroughly diagnosed by Lei and Peng (2013). The female of this species closely resembles that of *P. sufflava* (Jastrzębski, 2009), comb. nov. in having very similar epigyne and vulva, but it can be distinguished by the spherical spermathecae (Fig. 14B) versus sub-square spermathecae in *P. sufflava* (Jastrzębski 2009: fig. 4).

Description. Male (Figs 13, 14C, D, F, G). See Lei and Peng (2013).

Female (Fig. 14A, B, E). Total length 4.06. Carapace 1.56 long, 1.10 wide. Abdomen 2.48 long, 1.24 wide. Eye sizes and inter-distances: AME 0.36, ALE 0.20, PLE 0.19, AERW 1.04, PERW 1.08, EFL 0.84. **Legs:** I 2.63 (0.75, 0.50, 0.63, 0.45, 0.30), II 2.40 (0.75, 0.40, 0.55, 0.40, 0.30), III 2.91 (0.95, 0.40, 0.58, 0.65, 0.33), IV 3.45 (1.13, 0.43, 0.78, 0.78, 0.33). Carapace yellow to green-brown, covered with white scale-like setae on eyes base; fovea longitudinal, short. Chelicerae pale yellow, with two promarginal teeth and one retromarginal tooth smaller than males in size. Legs pale, with three and two pairs of ventral spines on tibiae and metatarsi I, respectively. Abdomen oval, dorsum pale to brown, with irregular brown patches; venter pale.

Epigyne and vulva (Fig. 14A, B): wider than long, with posterior concave; copulatory openings anterior located, almost C-shaped, close to each other; copulatory ducts almost straight, connected to the anterior margins of spherical spermathecae; fertilization ducts originating from the inner-anterior portions of spermathecae.

Distribution. China (Yunnan, Xizang) (Fig. 22A).

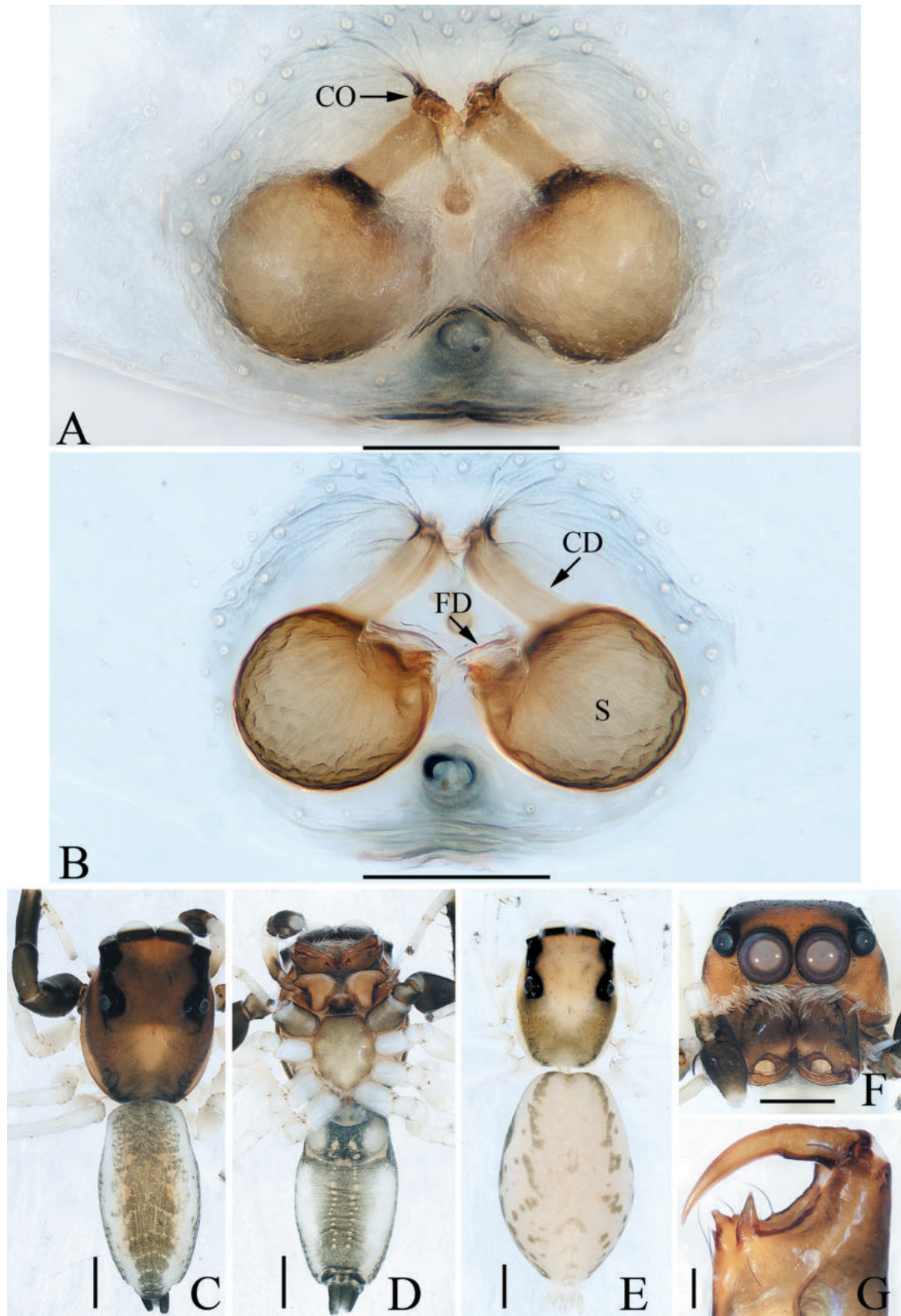


Figure 14. *Phintella longapophysis* Lei & Peng, 2013 A epigyne, ventral B vulva, dorsal C male habitus, dorsal D ditto, ventral E female habitus, dorsal F male carapace, frontal G male chelicera, posterior. Scale bars: 0.1 mm (A, B, G); 0.5 mm (C–F).

Genus *Stertinius* Simon, 1890

Type species. *Stertinius dentichelis* Simon, 1890.

Comments. *Stertinius*, is represented by 15 nominal species mainly distributed from East and Southeast Asia (WSC 2024). The genus is poorly defined because the generotype lacks diagnostic drawings, and most of its species were assigned because they present similar habitus and copulatory organs with other known congeners (Prószyński and Deeleman-Reinhold 2013). Based on the above, we assigned the new species to the genus because it generally harbors similar habitus and copulatory organs to *S. ryukyuensis* Suguro, 2020.

Stertinius liqingae sp. nov.

<https://zoobank.org/F6859C70-B45F-4F4B-9875-4369CB957F2D>

Figs 15, 16, 22B

Type material. **Holotype** ♂ (TRU-XZ-JS-0071), CHINA: Xizang: Zayu County, Cibagou National Nature Reserve (28°41.43'N, 97°2.86'E, ca 2570 m), 23 Jun. 2023, C. Wang leg. **Paratypes** 7♂8♀ (TRU-XZ-JS-0072–0086), same data as for holotype; 5♂3♀ (TRU-XZ-JS-0087–0094), Bowo County, 318 National Highway, nearby the 102 tunnel (30°4.41'N, 95°7.99'E, ca 2160 m), 30 Jun. 2023, C. Wang leg.

Etymology. The specific name is a patronym of Miss Liqing Fan, who helped us collect specimens in Cibagou National Nature Reserve; noun (name) in genitive case.

Diagnosis. *Stertinius liqingae* sp. nov. resembles that of *S. ryukyuensis* Suguro, 2020 in having similar habitus, palpal, and vulva structure, but can be distinguished by: 1) embolus about two times greater than the largest diameter of sperm duct (Fig. 15B), versus more than three times greater than the largest diameter of sperm duct in *S. ryukyuensis* (Suguro 2020: fig. 9); 2) RTA blunt apically in retrolateral view (Fig. 15C), versus pointed in *S. ryukyuensis* (Suguro 2020: fig. 10); 3) epigyne with a triangular hood (Fig. 16A, B), versus absent in *S. ryukyuensis* (Suguro 2020: fig. 12). The male also somewhat resembles that of *Simaetha pengi* Wang & Li, 2020 in having similar palpal structure, but is easily distinguished as follows: 1) embolus not curved distally (Fig. 15B), versus curved towards prolaterally in *S. pengi* (Wang and Li 2020: fig. 13C); 2) RTA almost triangular in retrolateral view (Fig. 15C), versus almost bar-shaped in *S. pengi* (Wang and Li 2020: fig. 13B).

Description. Male (Figs 15, 16D, E, G, H). Total length 2.59. Carapace 1.38 long, 1.25 wide. Abdomen 1.51 long, 1.13 wide. Eye sizes and inter-distances: AME 0.28, ALE 0.15, PLE 0.14, AERW 1.03, PERW 1.16, EFL 0.70. **Legs:** I 2.72 (0.88, 0.58, 0.58, 0.40, 0.28), II 1.94 (0.60, 0.38, 0.38, 0.30, 0.28), III 1.74 (0.53, 0.28, 0.35, 0.30, 0.28), IV 2.12 (0.68, 0.33, 0.43, 0.38, 0.30). Carapace almost oval, jacinth to dark brown, setose, with big, irregular dark and brown patches on cephalon; fovea indistinct. Chelicerae yellow to brown, each with two pro-marginal teeth and one retromarginal pillar-shaped tooth. Endites longer than wide, with straight distal margins. Labium coloured same as endites, bearing several dark setae at anterior margin. Sternum slightly longer than wide. Legs setose, pale to brown, legs I strongest, with enlarged femora, and two pairs

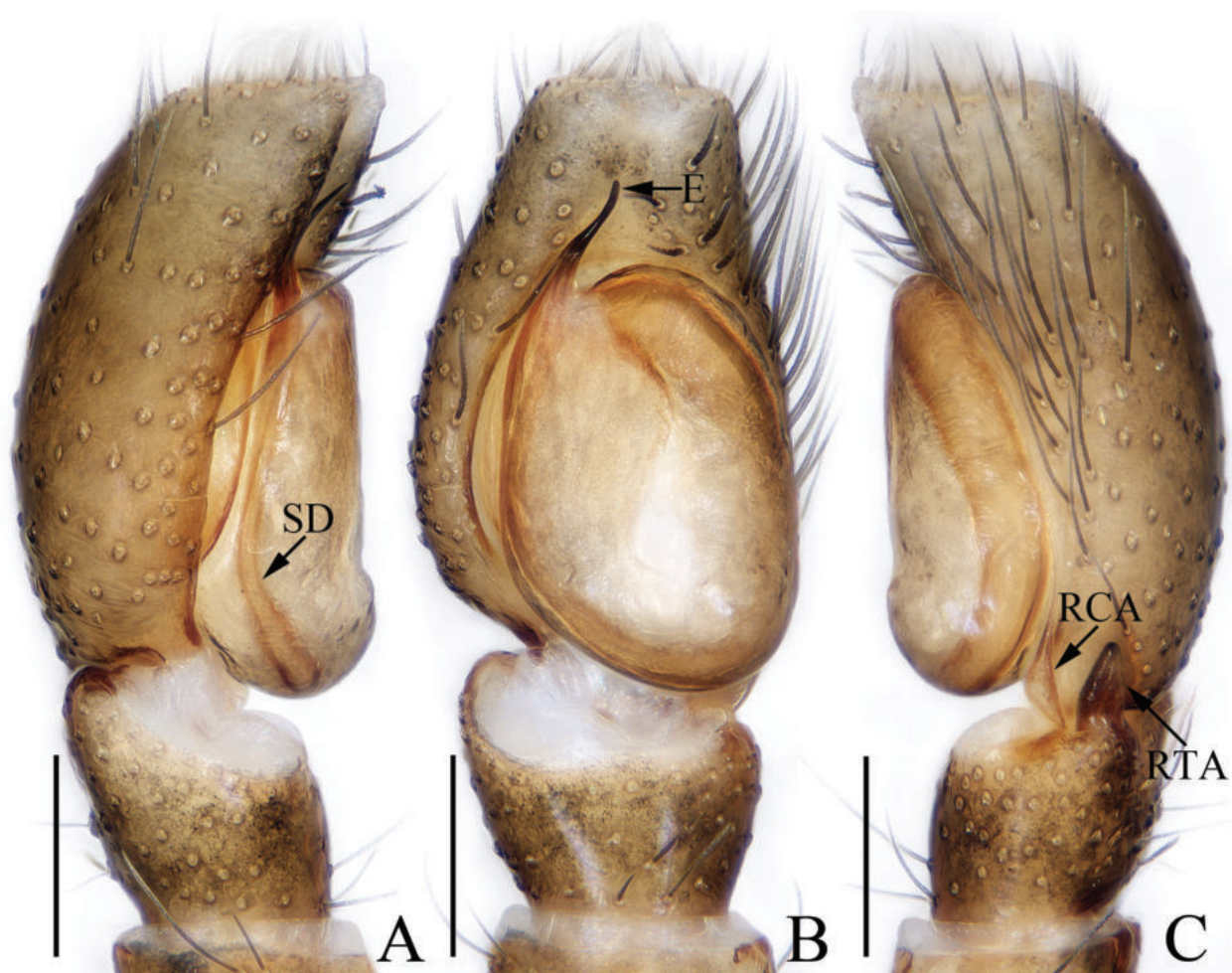


Figure 15. Male palp of *Sertinius liqingae* sp. nov., holotype **A** prolateral **B** ventral **C** retrolateral. Scale bars: 0.1 mm.

of ventral spines on tibia and metatarsi, respectively. Abdomen oval, dorsum brown to dark brown, with irregular pale and dark brown patches, and three pairs of muscle depressions medially; venter pale to brown.

Palp (Fig. 15A–C): tibia wider than long, with straight, tapered, upward extending RTA blunt apically; cymbium ca 1.5 times longer than wide, with lamellar base-retrolateral apophysis; bulb oval, flat; embolus short, originating from ca 10:30 o'clock position of bulb, slightly curved medio-distally and with blunt tip.

Female (Fig. 16A–C, F). Total length 2.84. Carapace 1.16 long, 1.01 wide. Abdomen 1.79 long, 1.27 wide. Eye sizes and inter-distances: AME 0.27, ALE 0.14, PLE 0.13, AERW 0.85, PERW 1.00, EFL 0.58. **Legs**: I 1.96 (0.68, 0.40, 0.40, 0.28, 0.20), II 1.60 (0.50, 0.35, 0.30, 0.25, 0.20), III 1.53 (0.50, 0.28, 0.30, 0.25, 0.20), IV 1.99 (0.63, 0.35, 0.43, 0.33, 0.25). **Habitus** (Fig. 16F) similar to that of male except the smaller retromarginal cheliceral tooth and without indistinct pale and pale patches on dorsum of abdomen.

Epigyne and vulva (Fig. 16A–C): wider than long, with central hood between copulatory openings; copulatory openings oval, bilateral to epigynal hood; copulatory ducts short; spermathecae divided into the anterior elliptical chamber and posterior sub-spherical chamber; fertilization ducts originating from the median of the inner portion of posterior chambers, antero-transversely extending.

Distribution. Known only from the type locality in Xizang, China (Fig. 22B).

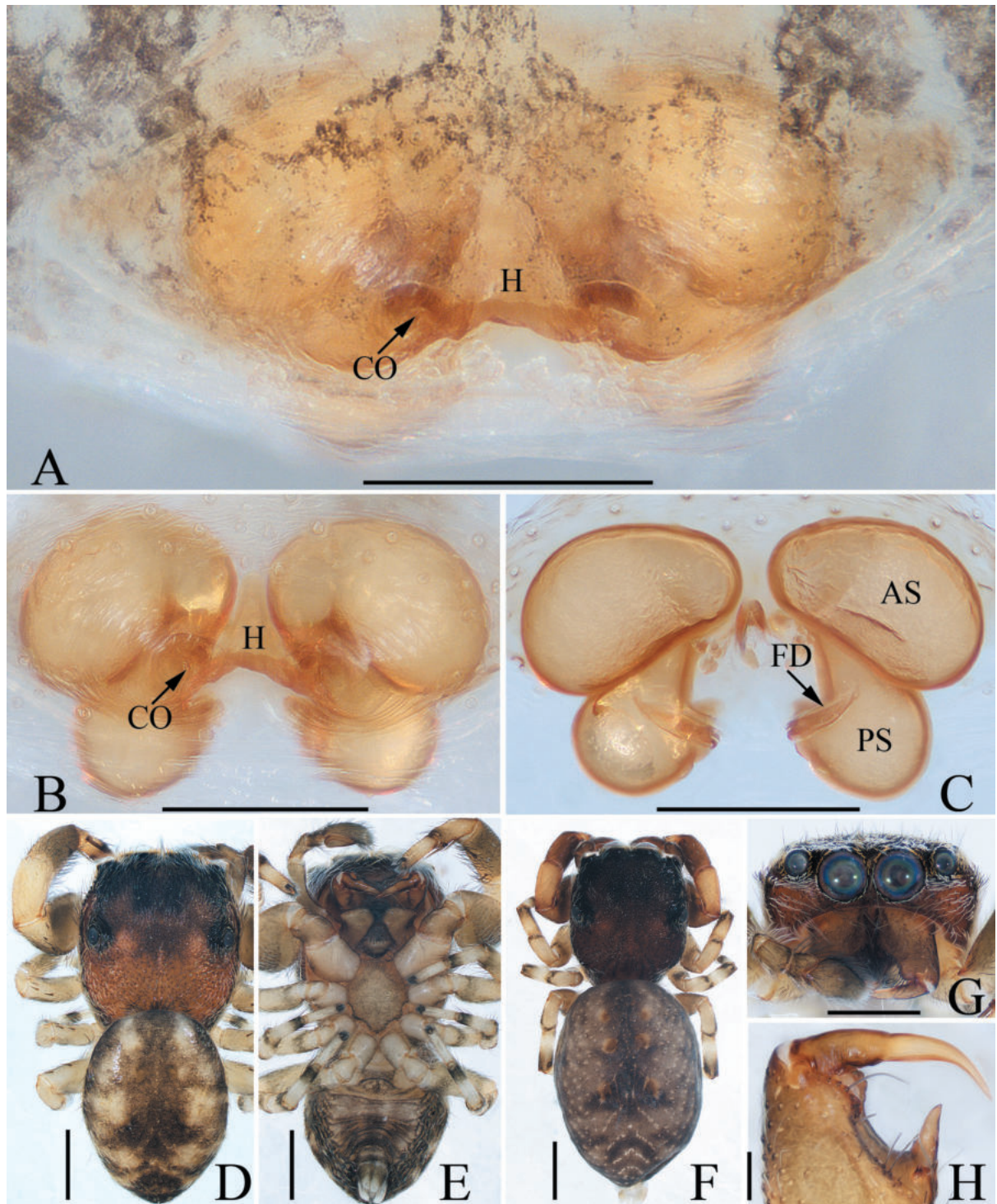


Figure 16. *Sertinius liqingae* sp. nov., male holotype and female paratype **A, B** epigyne, ventral **C** vulva, dorsal **D** holotype habitus, dorsal **E** ditto, ventral **F** female paratype habitus, dorsal **G** holotype carapace, frontal **H** holotype chelicera, posterior. Scale bars: 0.1 mm (**A–C, H**); 0.5 mm (**D–G**).

Genus *Synagelides* Strand, 1906

Type species. *Synagelides agoriformis* Strand, 1906.

Comments. *Synagelides*, contains 72 ant-like species distributed in East, South, and Southeast Asia (WSC 2024). The genus is closely similar to *Pseudosynagelides* Žabka, 1991 in habitus and copulatory organs, but it can be distin-

guished from it by the following: 1) the presence of triangular femoral apophysis of palp (for illustration, see Metzner 2024), versus absent in *Pseudosynagelides* (Žabka 1991: figs 9D, 16D); 2) the tegular median apophysis is retrolateral to embolus (for illustration, see Metzner 2024), but prolateral to embolus in *Pseudosynagelides* (Žabka 1991: figs 9B, C, 12A, C, E). It is worth mentioning that *Synagelides* could be much more diverse than its currently known (Wang et al. 2023), and the genus still needs much taxonomic attention, especially the cavaleriei group (see Bohdanowicz 1987), which shares very similar copulatory organs that made it very hard to identify.

***Synagelides medog* sp. nov.**

<https://zoobank.org/8562AA17-4961-4A70-A222-E39906DF21F7>

Figs 17, 22A

Type material. *Holotype* ♀ (TRU-XZ-JS-0095), CHINA: Xizang: Medog County, Renqingbenshi scenic area (29°18.10'N, 95°21.29'E, ca 2040 m), 18 Aug. 2023, C. Wang and H. Yao leg. *Paratypes* 2♀ (TRU-XZ-JS-0096–0097), same data as for holotype.

Etymology. The species name is a noun derived from the type locality: Medog County.

Diagnosis. *Synagelides medog* sp. nov. resembles that of *S. furcatoides* Li, Cheng, Wang, Yang & Peng, 2023 and *S. montiformis* Li, Cheng, Wang, Yang & Peng, 2023 in having similar epigyne and vulva, but can be easily distinguished by the absence of epigynal hood, and mediolaterally located atrial ridge (Fig. 17A–D), versus the presence of epigynal hood, and with the posteriorly located atrial ridge in *S. furcatoides* and *S. montiformis* (Li et al. 2023: figs 4, 5, 13, 26, 34).

Description. Female (Fig. 17A–I). Total length 4.06. Carapace 1.56 long, 1.10 wide. Abdomen 2.48 long, 1.24 wide. Eye sizes and inter-distances: AME 0.36, ALE 0.20, PLE 0.19, AERW 1.04, PERW 1.08, EFL 0.84. **Legs:** I 3.49 (1.13, 0.88, 0.75, 0.45, 0.28), II 2.55 (0.80, 0.40, 0.60, 0.50, 0.25), III 2.78 (0.83, 0.40, 0.65, 0.65, 0.25), IV 3.97 (1.13, 0.53, 1.00, 0.98, 0.33). Carapace almost square, red-brown to dark brown, spotted on eyes field and covered with thin setae anteriorly; fovea hollow. Chelicerae yellow, each with two promarginal teeth and one retromarginal tooth. Endites almost square, with pale inner portions bearing dense brown setae. Labium coloured same as endites. Sternum almost shield-shaped, longer than wide. Legs yellow to brown, with two pairs of ventral spines on tibiae and metatarsi I, respectively. Abdomen elongated, dorsum dark, without indistinct markings; venter paler than dorsum, with pair of dotted lines centrally.

Epigyne and vulva (Fig. 17A–D): wider than long; atrium big, oval, posteriorly located, with pair of arc-shaped, anterolateral ridges; copulatory openings oval, posterolaterally located on atrium, separated from each other by more than their width; copulatory ducts long, slightly curved into C-shaped at anterior half and then posterior extending to connect with the postero-lateral portions of oval spermathecae, with short accessory glands located at the anterior portions of the posterior half; fertilization ducts originating from the antero-inner portion of spermathecae, antero-transversely extending.

Male. Unknown.

Distribution. Known only from the type locality in Xizang, China (Fig. 22B).

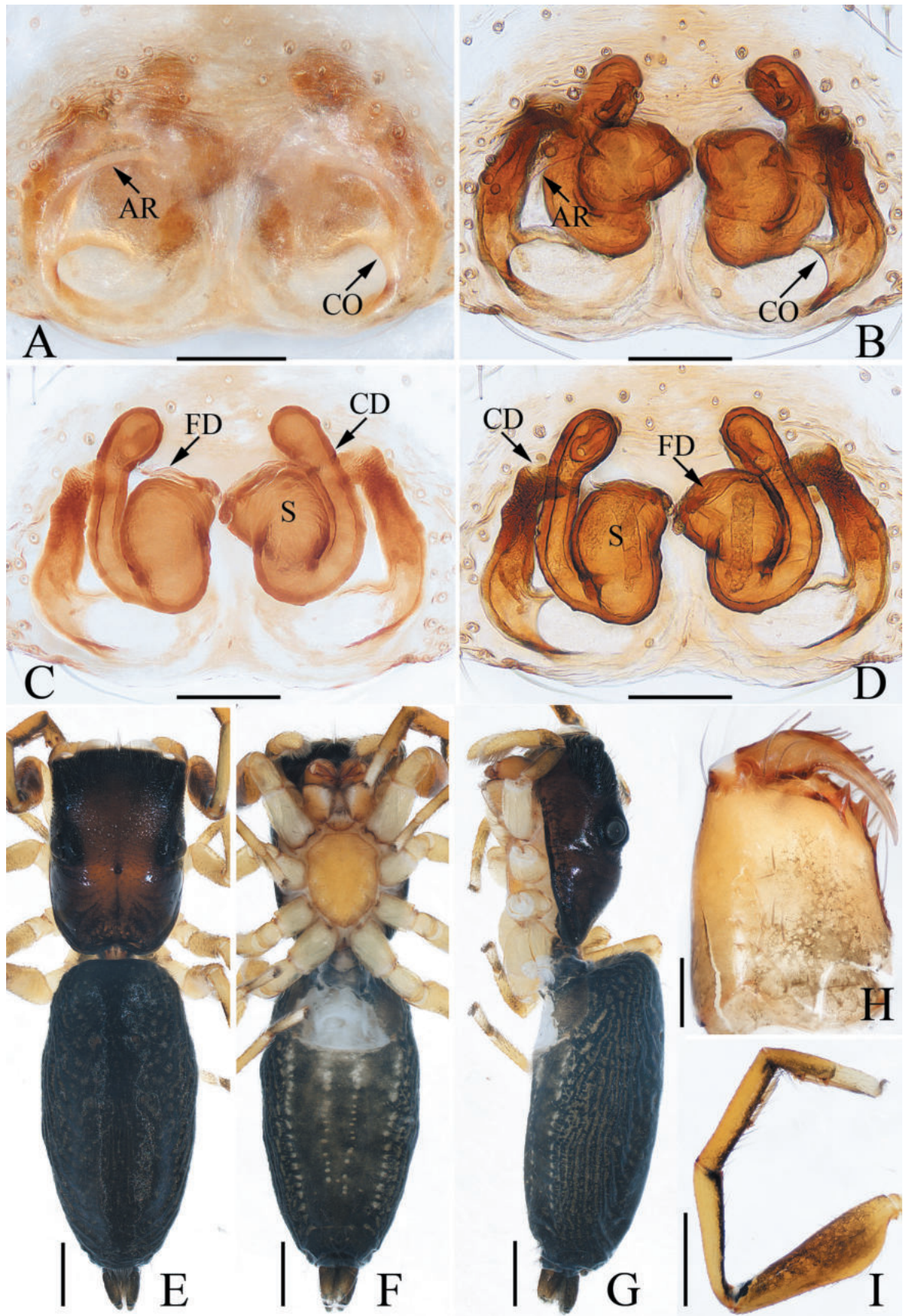


Figure 17. *Synagelides medog* sp. nov., holotype A, B epigyne, ventral C, D vulva dorsal E habitus dorsal F ditto, ventral G ditto, lateral H chelicera, posterior I leg I, prolateral. Scale bars: 0.1 mm (A–D, H); 0.5 mm (E–G, I).

***Synagelides tianquan* sp. nov.**

<https://zoobank.org/EF1AA08D-17B0-4172-B4FF-F872EB7902C4>

Figs 18, 19, 22A

Type material. *Holotype* ♂ (IZCAS-Ar44781), CHINA: Sichuan: Tianquan County (30°2.89'N, 102°45.93'E, ca 730), 7 Jul. 2004, S. Li leg. *Paratype* 1 ♀ (IZCAS-Ar44782), same data as for holotype.

Etymology. The species name is a noun in apposition derived from the type locality.

Diagnosis. *Synagelides tianquan* sp. nov. resembles that of *S. emangou* Liu, 2022 and *S. zhaoi* Peng, Li & Chen, 2003 in the general shape of copulatory organs, especially the inverted cup-shaped epigynal hood, but can be readily distinguished as follows: 1) cymbium lacking a flap apophysis (Fig. 18D), versus presence of a big flap apophysis dorsally in *S. emangou* and *S. zhaoi* (Liu et al. 2022: fig. 1C, E–G; Peng 2020: fig. 336c–e); 2) spermathecae curved toward anterior side bilaterally (Fig. 19B), versus not curved in *S. emangou* and *S. zhaoi* (Liu et al. 2022: fig. 2D; Peng 2020: fig. 336g); 3) copulatory ducts strongly curved anteromedially (Fig. 19B), versus almost straight in *S. emangou* and *S. zhaoi* (Liu et al. 2022: fig. 2D; Peng 2020: fig. 336g).

Description. Male (Figs 18, 19C, D, F, G). Total length 2.80. Carapace 1.41 long, 1.05 wide. Abdomen 1.41 long, 0.89 wide. Eye sizes and inter-distances: AME 0.33, ALE 0.20, PLE 0.19, AERW 0.99, PERW 1.07, EFL 0.88. **Legs:** I 3.97 (1.28, 1.03, 0.93, 0.43, 0.30), II 2.36 (0.70, 0.38, 0.55, 0.48, 0.25), III 2.38 (0.70, 0.35, 0.50, 0.58, 0.25), IV 3.33 (1.00, 0.43, 0.80, 0.80, 0.30). Carapace sub-square, red-brown to dark brown, with elevated cephalon and sloped thorax, covered with thin setae; fovea oval, hollowed. Chelicerae pale yellow, each with two promarginal teeth and one retromarginal tooth. Endites almost square, bearing dense pale setae at distal-inner portions. Labium coloured same as endites. Sternum almost shield-shaped, less than 1.5 times longer than wide. Legs yellow to red-yellow, with four and two pairs of ventral spines on tibiae and metatarsi I, respectively. Abdomen elongate-oval, dorsum brown, with two pairs of median muscle depressions, and five transverse pale setal stripes anteriorly and medially, covered by anterior jacinth scutum; venter brown, with pale central area.

Palp (Fig. 18A–D): femur longer than wide, with medio-prolateral, triangular apophysis; patella enlarged; tibia short; RTA weakly sclerotized and broadened base-medially, followed by the acutely narrowed, strongly sclerotized remainder with rather blunt tip directed towards anteroventral side; cymbium longer than wide, with irregular dorsal apophysis and strongly sclerotized prolateral apophysis blunt at terminus; bulb swollen; embolus flat, forming half disc at base and with blunt tip; median apophysis large, irregular.

Female (Fig. 19A, B, E). Total length 3.47. Carapace 1.43 long, 1.04 wide. Abdomen 1.96 long, 1.27 wide. Eye sizes and inter-distances: AME 0.35, ALE 0.20, PLE 0.19, AERW 1.00, PERW 1.10, EFL 0.86. **Legs:** I 3.29 (1.03, 0.78, 0.85, 0.38, 0.25), II 2.31 (0.70, 0.38, 0.53, 0.45, 0.25), III 2.39 (0.73, 0.38, 0.45, 0.58, 0.25), IV 3.44 (1.00, 0.48, 0.88, 0.80, 0.28). **Habitus** (Fig. 19E) similar to that of male except paler in color and without setal stripes and scutum on the dorsum of abdomen.

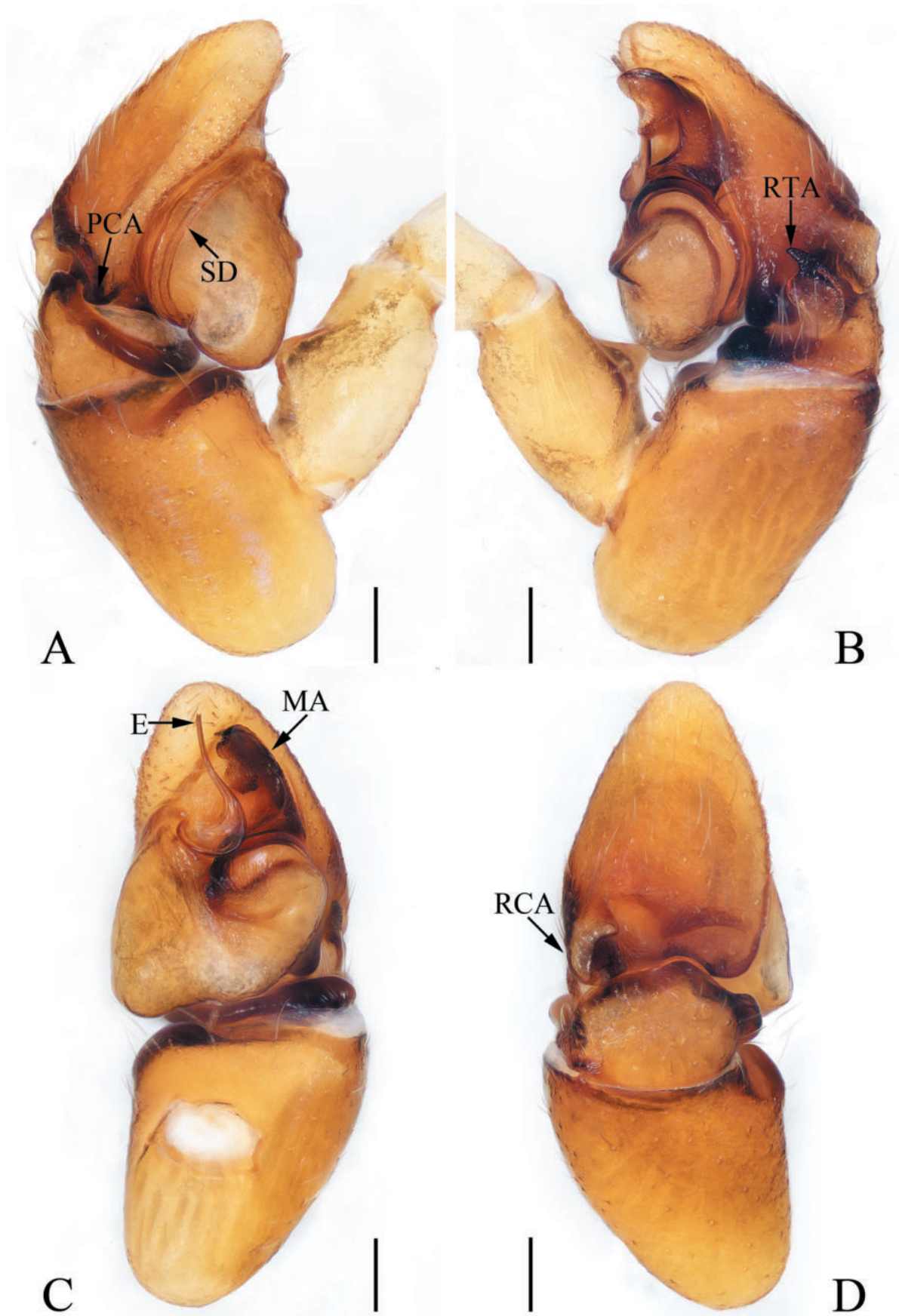


Figure 18. Male palp of *Synagelides tianquan* sp. nov., holotype A prolateral B retrolateral C ventral D dorsal. Scale bars: 0.1 mm.

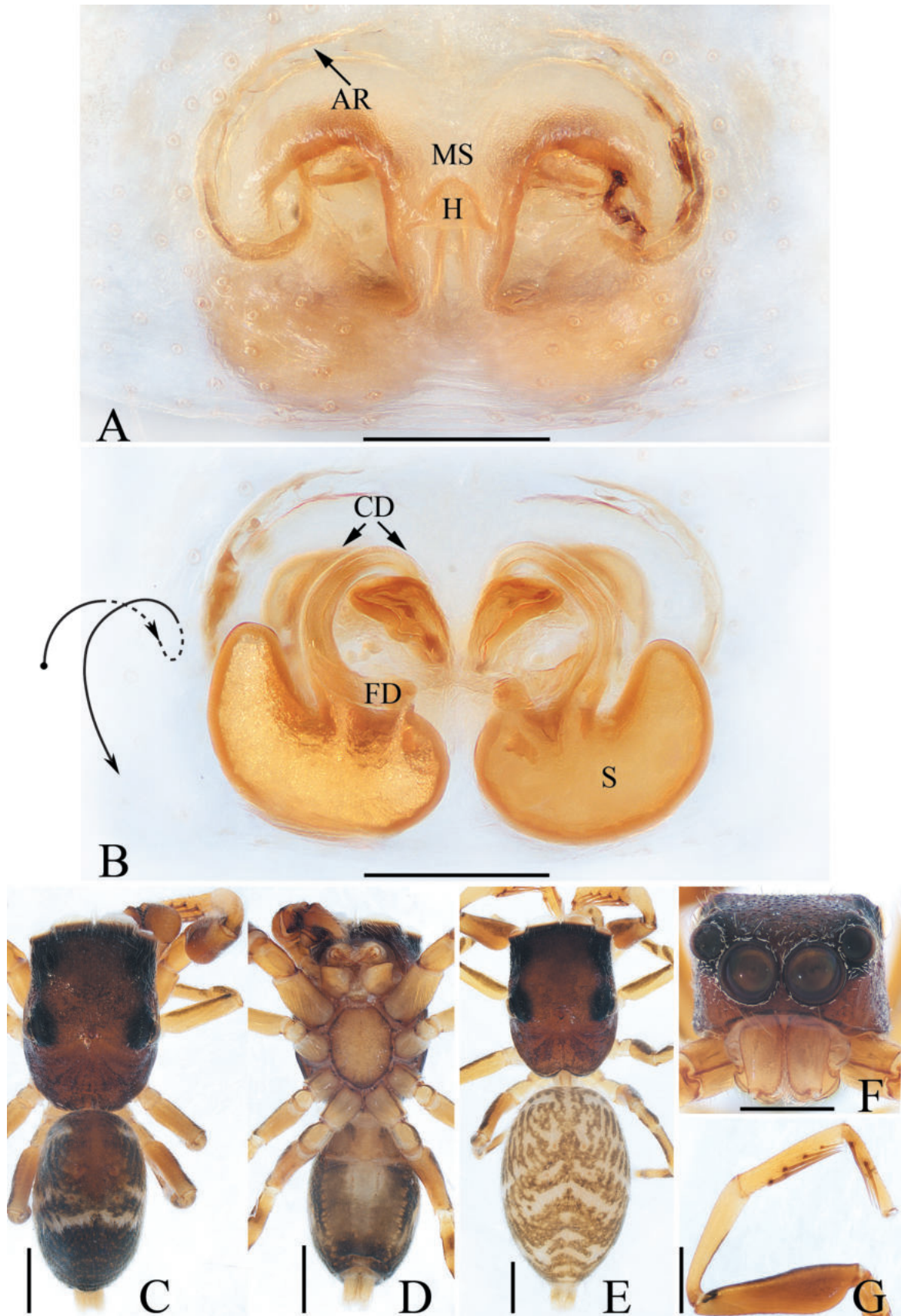


Figure 19. *Synagelides tianquan* sp. nov., male holotype and female paratype **A** epigyne, ventral **B** vulva, dorsal **C** holotype habitus, dorsal **D** ditto, ventral **E** female paratype habitus, dorsal **F** holotype carapace, frontal **G** leg I of holotype, prolateral. Scale bars: 0.1 mm (**A**, **B**); 0.5 mm (**C**–**G**).

Epigyne and vulva (Fig. 19A, B): wider than long; atrium oval, anterior located, with pair of lateral ridges, and separated by the big, irregular median septum bearing triangular epigynal hood opening downward; copulatory openings beneath the anterolateral portions of median septum; copulatory ducts slender, strongly curved at the position of anterior 1/3; spermathecae boat-shaped, close to each other; fertilization ducts originating from the inner-anterior margins of spermathecae, extending transversely.

Distribution. Known only from the type locality in Sichuan, China (Fig. 22B).

Genus *Yaginumaella* Prószyński, 1979

Type species. *Pellenes ususudi* Yaginuma, 1972.

Comments. *Yaginumaella*, one of the members of the subtribe Plexippina Simon, 1901 (Maddison 2015), contains 14 species mainly distributed in East Asia (WSC 2024). The genus has always been considered to be closely related to *Ptocasius* Simon, 1885 (Li et al. 2018; Patoleta et al. 2020), and has even been considered as a synonym of the latter unofficially (e.g. Žabka 1985). One of the influential studies of the two genera is Patoleta et al. (2020), who transferred 37 species of *Yaginumaella* into *Ptocasius* based on the similarities in copulatory organs structures. However, this work has not discussed the difference in habitus patterns (see Li et al. 2018). And now, the generic position of species for these two genera is controversial. Herein, we adopt the view of Li et al. (2018) and assign the new species to *Yaginumaella*.

Yaginumaella armata (Jastrzębski, 2011), comb. nov. is transferred because it shares a similar habitus and palpal structure to *Yaginumaella* rather than *Pancorius*, given that the embolus originates at the bulb's base but antero-apically in *Pancorius*. Moreover, the described female of *Y. armata* (new materials collected from Gyirong County, Xizang, were examined by us) is likely mismatched and may belong to a member of the tribe Chrysillini.

Yaginumaella erlang sp. nov.

<https://zoobank.org/AF2DDE2B-5598-41FC-BC67-7BAB8E458136>

Figs 20, 21, 22B

Type material. **Holotype** ♂ (IZCAS-Ar44783), CHINA: Sichuan: Tianquan County, Erlangshan National Nature Reserve (30°10.17'N, 102°26.94'E, ca 760 m), 10 Dec. 2004, Z.T. Zhang leg. **Paratypes** 2♂2♀ (IZCAS-Ar44784-44787), same data as for holotype.

Etymology. The species name is a noun derived from the type locality: Erlang Mountain National Nature Reserve.

Diagnosis. *Yaginumaella erlang* sp. nov. resembles that of *Ptocasius pseudoflexus* (Liu, Yang & Peng, 2016) in general shape of palp, but can be distinguished as follows: 1) RTA curved medially, and with a pointed tip in retrolateral view (Fig. 20C), versus curved distally, and with a rather blunt tip in *P. pseudoflexus* (Liu et al. 2016: figs 15, 16); 2) copulatory ducts extending straight at base in dorsal view (Fig. 21B), versus curved in *P. pseudoflexus* (Liu et al. 2016: figs 15, 16).

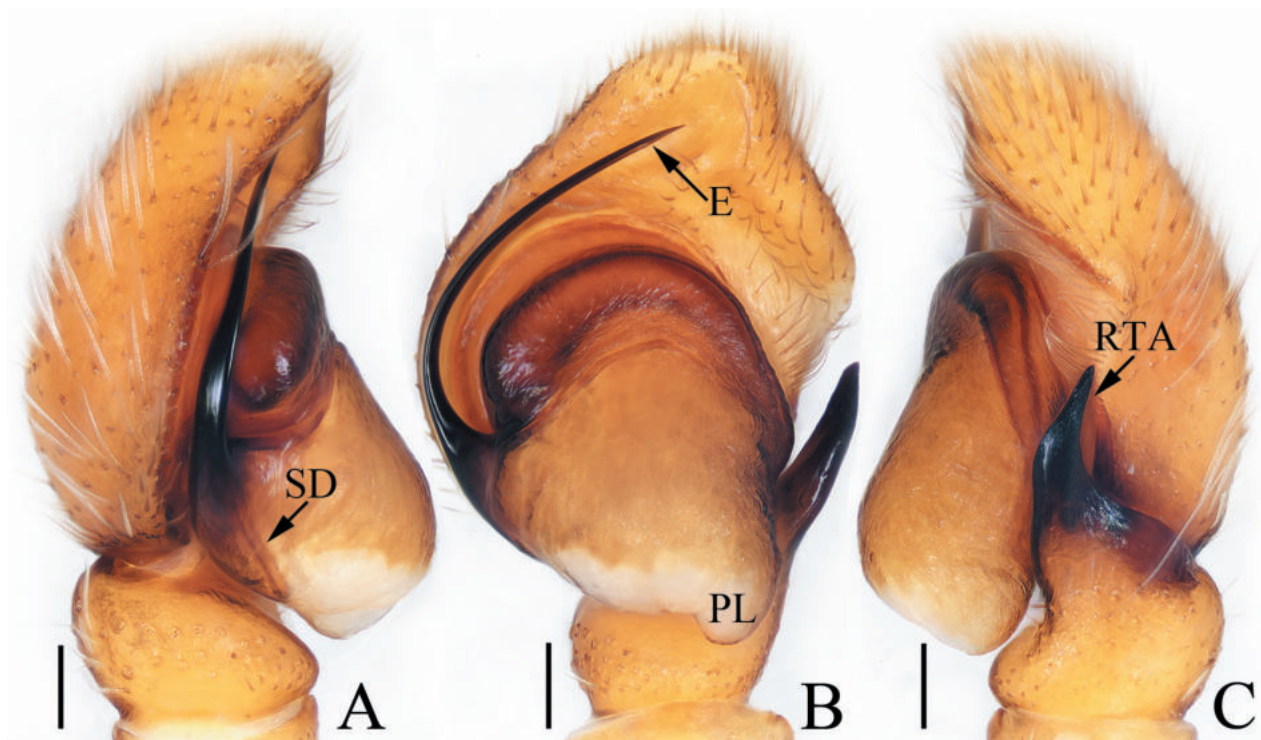


Figure 20. Male palp of *Yaginumaella erlang* sp. nov., holotype **A** prolateral **B** ventral **C** retrolateral. Scale bars: 0.1 mm.

Description. Male (Figs 20, 21C, D, F, G). Total length 4.27. Carapace 2.11 long, 1.60 wide. Abdomen 2.22 long, 1.36 wide. Eye sizes and inter-distances: AME 0.44, ALE 0.25, PLE 0.22, AERW 1.40, PERW 1.38, EFL 0.91. **Legs:** I 4.30 (1.30, 0.75, 1.05, 0.70, 0.50), II 3.95 (1.25, 0.75, 0.85, 0.60, 0.50), III 4.25 (1.35, 0.65, 0.90, 0.85, 0.50), IV 4.55 (1.45, 0.65, 0.90, 1.05, 0.50). Carapace red-brown, setose, with longitudinal, central orange-yellow band extending from the middle of eyes field to the posterior margin, and pair of orange-yellow lateral bands; fovea dark red, longitudinal. Chelicerae yellow to brown, each with two promarginal teeth and one retromarginal tooth. Endites paler than chelicerae, slightly widened distally. Labium linguiform, with paler anterior portion. Sternum about 1.5 times longer than wide, tapered at posterior half. Legs pale to dark yellow, with dark stripes prolaterally on femora I, and three and two pairs of ventral spines on tibia and metatarsi I, respectively. Abdomen elongate-oval, dorsum yellow to dark brown, dotted bilaterally, with longitudinal yellow band about one-third the abdominal width; venter pale to dark brown, with longitudinal, central, dark brown band.

Palp (Fig. 20A–C): tibia wider than long, with strongly sclerotized RTA broadened at base, slightly curved medially, and pointed apically; cymbium setose; bulb swollen medio-posteriorly, with small posterior lobe extending postero-prolaterally and blunt at terminus; embolus strongly sclerotized, originating at ca 9 o'clock position of bulb, curved into C-shape base-medially, and with pointed tip directed towards about 2 o'clock position.

Female (Fig. 21A, B, E). Total length 4.99. Carapace 2.08 long, 1.60 wide. Abdomen 2.70 long, 1.82 wide. Eye sizes and inter-distances: AME 0.45, ALE 0.27, PLE 0.23, AERW 1.45, PERW 1.43, EFL 0.99. **Legs:** I 3.80 (1.15, 0.70, 0.85, 0.65, 0.45), II 3.55 (1.15, 0.65, 0.75, 0.55, 0.45), III 4.15 (1.25, 0.65, 0.85, 0.90, 0.50), IV 4.55 (1.40, 0.70, 0.95, 1.00, 0.50). **Habitus** (Fig. 21E) similar to that of male except slightly darker in color.

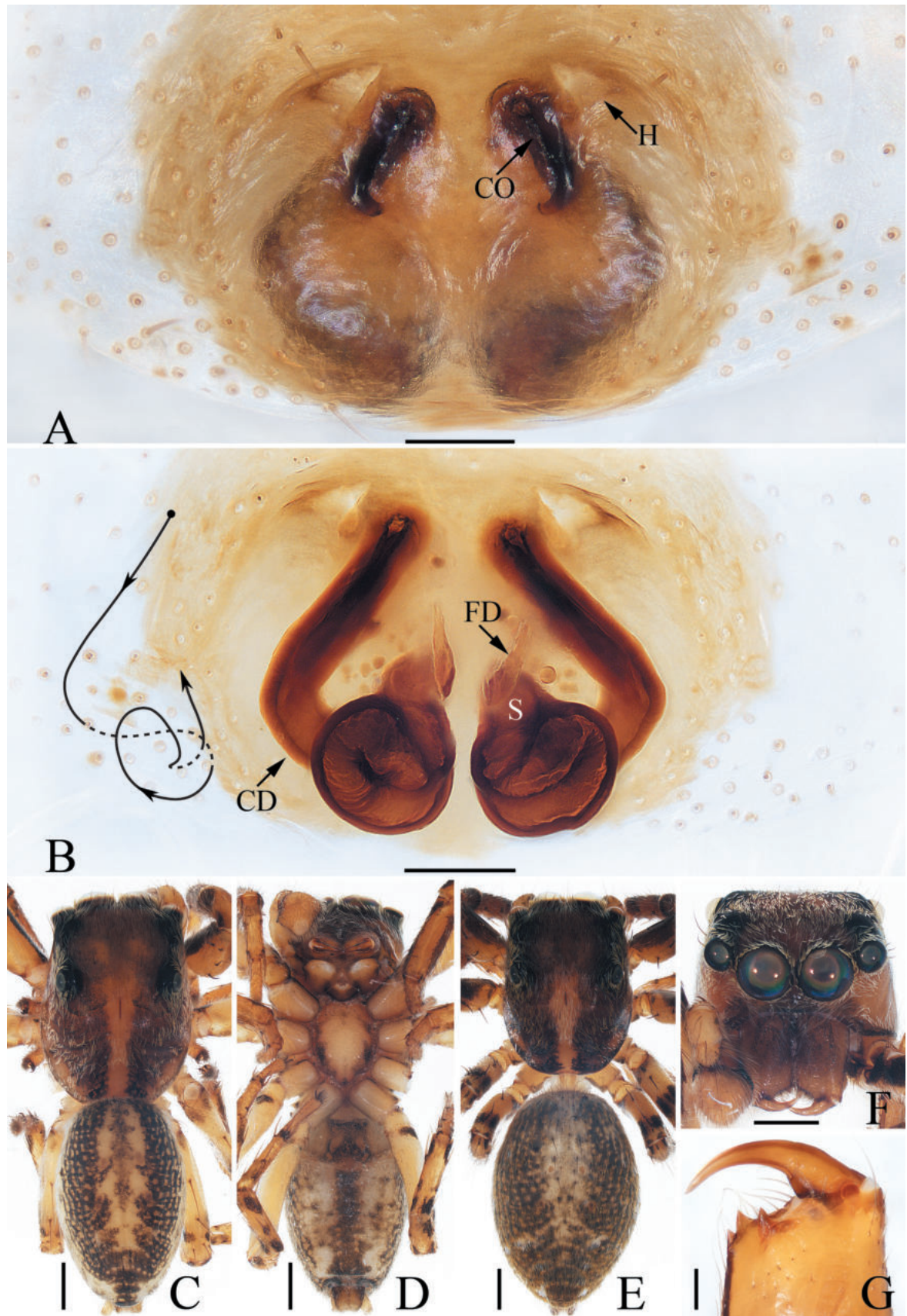


Figure 21. *Yaginumaella erlang* sp. nov., male holotype and female paratype **A** epigyne, ventral **B** vulva, dorsal **C** holotype habitus, dorsal **D** ditto, ventral **E** female paratype habitus, dorsal **F** holotype carapace, frontal **G** holotype chelicera, posterior. Scale bars: 0.1 mm (**A**, **B**, **G**); 0.5 mm (**C**–**F**).

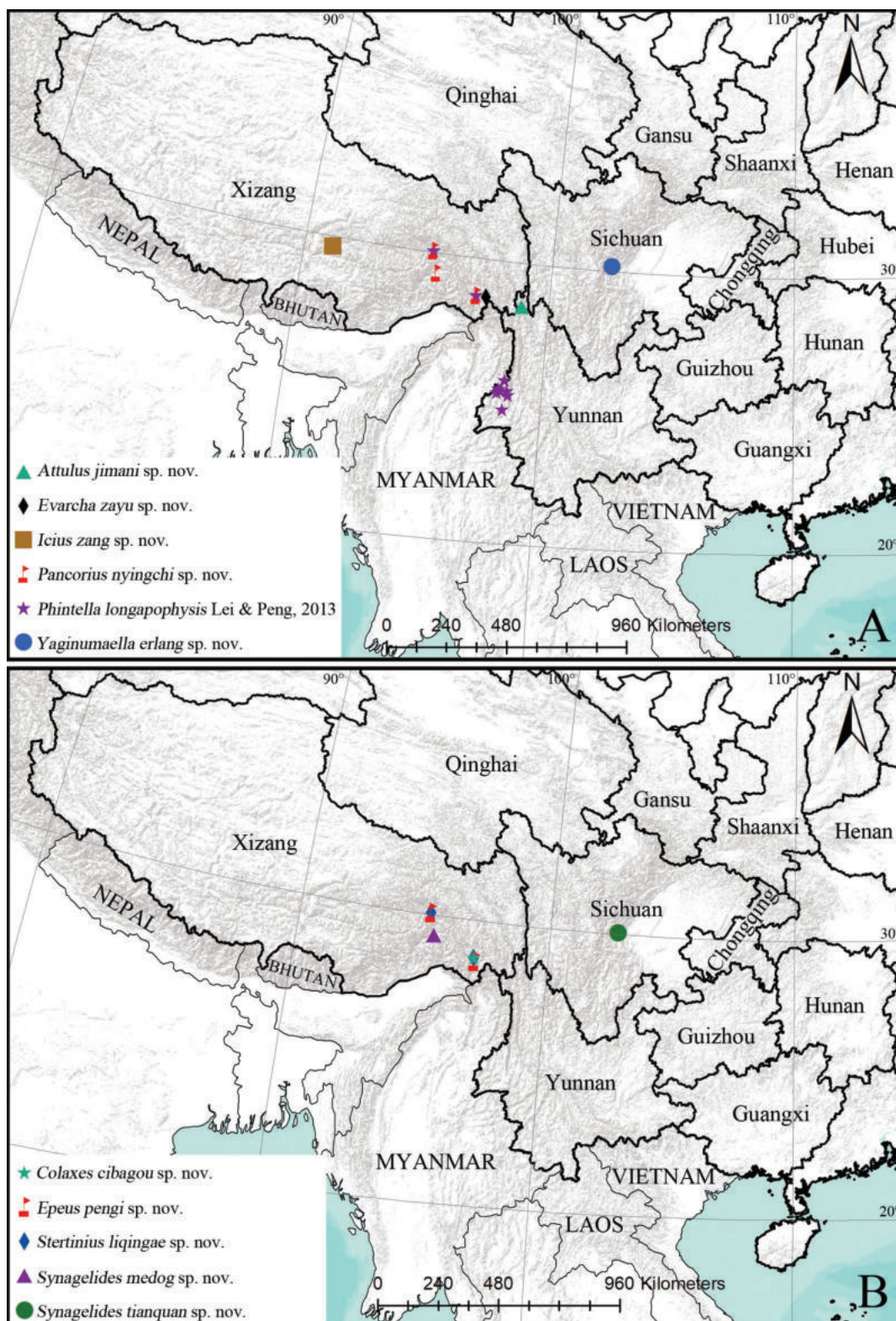


Figure 22. Distributional records of the described species.

Epigyne and vulva (Fig. 21A, B): slightly wider than long, with pair of anterior or sub-triangular hoods open postero-laterally, and anterolateral to copulatory openings; copulatory openings slit-shaped; copulatory ducts long, curved, and twisted; spermathecae indistinct; fertilization ducts lamellar.

Distribution. Known only from the type locality in Sichuan, China (Fig. 22A).

Acknowledgments

The manuscript benefited greatly from comments by Dimitar Dimitrov, Suresh Benjamin, and one anonymous reviewer. The English was checked by Dani Sherwood (UK). Xianjin Peng, Jiman He, Zhengtian Zhang, and Hong Yao helped with fieldwork.

Additional information

Conflict of interest

The authors have declared that no competing interests exist.

Ethical statement

No ethical statement was reported.

Funding

This research was supported by the Scientific Monitoring of Cibagou National Nature Reserve Project, the Scientific Monitoring of Yarlung Zangbo Grand Canyon National Nature Reserve Project, the National Natural Science Foundation of China (NSFC-32200369), the Science and Technology Project Foundation of Guizhou Province ([2020]1Z014), the Key Laboratory Project of Guizhou Province ([2020]2003), the Open Project of Ministry of Education Key Laboratory for Ecology of Tropical Islands, Hainan Normal University, China ([HNSF-OP-202201]), and the Doctoral Research Foundation of Tongren University (trxyDH2102).

Author contributions

SL designed the study. CW and XM performed morphological species identification. CW finished the species descriptions and took the photos. CW and SL drafted and revised the manuscript. All authors read and approved the final version of the manuscript.

Author ORCIDs

Cheng Wang  <http://orcid.org/0000-0003-1831-0579>

Xiaoqi Mi  <https://orcid.org/0000-0003-1744-3855>

Shuqiang Li  <https://orcid.org/0000-0002-3290-5416>

Data availability

All of the data that support the findings of this study are available in the main text.

References

- Benjamin SP (2004) Taxonomic revision and phylogenetic hypothesis for the jumping spider subfamily Ballinae (Araneae, Salticidae). *Zoological Journal of the Linnean Society* 142(1): 1–82. <https://doi.org/10.1111/j.1096-3642.2004.00123.x>
- Bohdanowicz A (1987) Salticidae from the Nepal Himalayas: The genus *Synagelides* Bösenberg & Strand, 1906. *Courier Forschungsinstitut Senckenberg* 93: 65–86.
- Caleb JTD (2023) Deciphering mysteries: On the identity of five enigmatic jumping spiders from northeast India, China and Philippines (Araneae, Salticidae). *Zootaxa* 5230(3): 391–400. <https://doi.org/10.11646/zootaxa.5230.3.8>

- Hu JL (2001) Spiders in Qinghai-Tibet Plateau of China. Henan Science and Technology Publishing House, 658 pp.
- Jastrzębski P (2009) Salticidae from the Himalaya. New species of the genus *Carrhotus* Thorell, 1891 (Araneae: Salticidae). *Genus* 20: 533–537.
- Jastrzębski P (2011) Salticidae from the Himalayas. The genus *Pancorius* Simon, 1892 (Arachnida: Araneae). *Genus* 22: 181–190.
- Kanesharatnam N, Benjamin S (2021) Phylogenetic relationships and systematics of the jumping spider genus *Colopsus* with the description of eight new species from Sri Lanka (Araneae: Salticidae). *Journal of Natural History* 54(43–44): 2763–2814. <https://doi.org/10.1080/00222933.2020.1869335>
- Lei H, Peng XJ (2013) Five new species of the genus *Phintella* (Araneae: Salticidae) from China. *Oriental Insects* 47(1): 99–110. <https://doi.org/10.1080/00305316.2013.783747>
- Li S (2020) Spider taxonomy for an advanced China. *Zoological Systematics* 45(2): 73–77. <https://doi.org/10.11865/zs.202011>
- Li S, Lin Y (2024) Challenges confronting spider taxonomy in Asia. *Zoological Systematics* 49(1): 1–3.
- Li D, Wang C, Irfan M, Peng XJ (2018) Two new species of *Yaginumaella* (Araneae, Salticidae) from Wuling Mountain, China. *European Journal of Taxonomy* 488(488): 1–10. <https://doi.org/10.5852/ejt.2018.488>
- Li B, Cheng Y, Wang Q, Yang SF, Peng XJ (2023) Three new species of the genus *Synagelides* Strand, 1906 (Araneae, Salticidae) from Yunnan, China. *Zootaxa* 5258(2): 211–223. <https://doi.org/10.11646/zootaxa.5258.2.3>
- Liu W, Yang SF, Peng XJ (2016) Two new species of *Yaginumaella* Prószyński, 1976 from Yunnan, China (Araneae, Salticidae). *ZooKeys* 620: 57–66. <https://doi.org/10.3897/zookeys.620.7895>
- Liu KK, Zhao ZY, Xiao YH, Peng XJ (2022) Five new species of *Synagelides* Strand, 1906 from China (Araneae, Salticidae). *ZooKeys* 1102: 59–82. <https://doi.org/10.3897/zookeys.1102.76800>
- Logunov DV (1992) The spider family Salticidae (Araneae) from Tuva. II. An annotated check list of species. *Arthropoda Selecta* 1(2): 47–71.
- Logunov DV (2021) On three species of *Plexippoides* Prószyński, 1984 (Araneae: Salticidae) from the Mediterranean, the Middle East, and Central Asia, with notes on a taxonomic validity of the genus. *Arachnology* 18(7): 766–777. <https://doi.org/10.13156/arac.2020.18.7.766>
- Logunov DV, Rakov SY (1998) Miscellaneous notes on Middle Asian jumping spiders (Aranei: Salticidae). *Arthropoda Selecta* 7: 117–144.
- Maddison WP (2015) A phylogenetic classification of jumping spiders (Araneae: Salticidae). *The Journal of Arachnology* 43(3): 231–292. <https://doi.org/10.1636/arac-43-03-231-292>
- Maddison WP, Maddison DR, Derkarabetian S, Hedin M (2020) Sitticine jumping spiders: Phylogeny, classification, and chromosomes (Araneae, Salticidae, Sitticini). *ZooKeys* 925: 1–54. <https://doi.org/10.3897/zookeys.925.39691>
- Meng XW, Zhang ZS, Shi AM (2015) Description of two unknown females of *Epeus* Peckham & Peckham from China (Araneae: Salticidae). *Zootaxa* 3955(1): 147–150. <https://doi.org/10.11646/zootaxa.3955.1.11>
- Metzner H (2024) Jumping spiders (Arachnida: Araneae: Salticidae) of the world. <https://www.jumping-spiders.com> [Accessed 17 January 2024]

- Patoleta BM, Gardzińska J, Żabka M (2020) Salticidae (Arachnida, Araneae) of Thailand: New species and records of *Epeus* Peckham & Peckham, 1886 and *Ptocasius* Simon, 1885. *PeerJ* 8(e9352): 1–23. <https://doi.org/10.7717/peerj.9352>
- Paul J, Prajapati DA, Joseph MM, Sebastian PA (2020) Description of a new species of *Colaxes* Simon, 1900 (Araneae: Salticidae: Ballinae) from the tropical montane cloud forests of Western Ghats, India. *Arthropoda Selecta* 29(2): 244–250. <https://doi.org/10.15298/arthscl.29.2.10>
- Peng XJ (2020) *Fauna Sinica, Invertebrata* 53, Arachnida: Araneae: Salticidae. Science Press, Beijing, 612 pp.
- Peng XJ, Li S (2002) A review of the genus *Epeus* Peckham & Peckham (Araneae: Salticidae) from China. *Oriental Insects* 36(1): 385–392. <https://doi.org/10.1080/00305316.2002.10417336>
- Próchniewicz M (1990) Salticidae aus Nepal und Bhutan. Genera *Telamonia* Thorell 1887 und *Plexippoides* Prószyński 1976 (Arachnida: Araneae). *Senckenbergiana Biologica* 70: 151–160.
- Prószyński J, Deeleman-Reinhold CL (2013) Description of some Salticidae (Araneae) from the Malay Archipelago. III. Salticidae of Borneo, with comments on adjacent territories. *Arthropoda Selecta* 22(2): 113–144. <https://doi.org/10.15298/arthscl.22.2.02>
- Suguro T (2020) Japanese spiders of the genus *Stertinius* (Araneae: Salticidae). *Acta Arachnologica* 69(1): 55–60. <https://doi.org/10.2476/asjaa.69.55>
- Wang C, Li S (2021) On ten species of jumping spiders from Xishuangbanna, China (Araneae, Salticidae). *ZooKeys* 1062: 123–155. <https://doi.org/10.3897/zookeys.1062.72531>
- Wang C, Mi XQ, Wang WH, Gan JH, Irfan M, Zhong Y, Peng XJ (2023) Notes on twenty-nine species of jumping spiders from South China (Araneae: Salticidae). *European Journal of Taxonomy* 902: 1–91. <https://doi.org/10.5852/ejt.2023.902.2319>
- World Spider Catalog (2024) World Spider Catalog. Version 24.5. Natural History Museum Bern. <https://doi.org/10.24436/2> [Accessed on: 17 January 2024]
- Żabka M (1985) Systematic and zoogeographic study on the family Salticidae (Araneae) from Vietnam. *Annales Zoologici, Warszawa* 39: 197–485.
- Żabka M (1991) Salticidae (Arachnida: Araneae) of Oriental, Australian and Pacific regions, VII. *Mopsolodes*, *Abracadabrella* and *Pseudosynagelides* new genera from Australia. *Memoirs of the Queensland Museum* 30: 621–644.

A new feather mite species of the genus *Mycterialges* Gaud & Atyeo, 1981 (Acari, Xolalgidae) from the Oriental Stork, *Ciconia boyciana* (Ciconiiformes, Ciconiidae) in Korea

Jeong Hun Shim¹, Yeong-Deok Han², Sukyung Kim³, Dongsoo Ha³, Yongun Shin⁴, Soo Hyung Eo¹

1 Department of Forest Science, Kongju National University, Yesan, Republic of Korea

2 Research Center for Endangered Species, National Institute of Ecology, Yeongyang, Republic of Korea

3 Eco-institute for Oriental Stork, Korea National University of Education, Cheongju, Republic of Korea

4 Natural Heritage Division, Cultural Heritage Administration, Deajeon, Republic of Korea

Corresponding author: Soo Hyung Eo (eosh@kongju.ac.kr)



Academic editor: Vladimir Pesic

Received: 15 November 2023

Accepted: 25 January 2024

Published: 21 February 2024

ZooBank: <https://zoobank.org/3F5C9BBE-BA35-4E1C-ADAF-EB5CECE3883F>

Citation: Shim JH, Han Y-D, Kim S, Ha D, Shin Y, Eo SH (2024) A new feather mite species of the genus *Mycterialges* Gaud & Atyeo, 1981 (Acari, Xolalgidae) from the Oriental Stork, *Ciconia boyciana* (Ciconiiformes, Ciconiidae) in Korea. ZooKeys 1192: 179–196. <https://doi.org/10.3897/zookeys.1192.115749>

Copyright: © Jeong Hun Shim et al. This is an open access article distributed under terms of the Creative Commons Attribution License ([Attribution 4.0 International – CC BY 4.0](https://creativecommons.org/licenses/by/4.0/)).

Abstract

A new feather mite species, *Mycterialges boycianae* sp. nov. (Xolalgidae), was identified from the Oriental Stork, *Ciconia boyciana* Swinhoe, 1873, in Korea. Males of *M. boycianae* sp. nov. are distinguished from *Mycterialges mesomorphus* Gaud & Atyeo, 1981, in having a single triangular prodorsal shield, sinuous margins of the opisthosoma located between setae e2 and h2 on the hysteronotal shield, an oval-shaped epiandrum without posterior extensions, a shorter tibia + tarsus IV than femoragenu IV, and an absent ambulacral disc of leg IV. Females differ in having a prodorsal shield with a posterior margin that is blunt-angular, and a concave posterior margin of the hysteronotal shield with posterior extensions. This study presents the first record of the feather mite genus *Mycterialges* in birds of the genus *Ciconia* (Ciconiidae). Additionally, we determined the phylogenetic relationship among Ingrassiinae using the mitochondrial cytochrome c oxidase subunit (COI).

Key words: Analgoidea, Astigmata, COI, ectosymbionts, Ingrassiinae, systematics, taxonomy

Introduction

Feather mites (Astigmata) belong to two superfamilies (Analgoidea and Pterolichoidea), most of which are permanent ectosymbionts. These mites live on specific feathers and microsites on feathers, primarily consuming fungi and bacteria (Doña et al. 2019). They are mainly transmitted vertically from parents to offspring (Doña et al. 2017), and because of these characteristics, they exhibit high host specificity (OConnor 1982; Gaud and Atyeo 1996; Dabert and Mironov 1999; Proctor 2003). Feather mites living on endangered birds could be at risk of extinction due to their high host specificity, as a decrease in the host population could affect them (Waki et al. 2023). For example, *Compressalgae nipponiae* Dubinin, 1950 (Pterolichoidea: Caudiferidae), which is associated with the Crested Ibis *Nipponia nippon* (Temminck, 1835), disappeared due to the extirpation of its native host *N. nippon* in Japan. Consequently, this mite

was registered as “Extinct” in the Red List of the Ministry of the Environment, Japan in 2020 (Waki and Shimano 2020; Waki et al. 2023).

The genus *Mycterialges* Gaud & Atyeo, 1981 is distinguished from other genera in the family Xolalgidae Dubinin, 1953 (Analgoidea) by the number of setae on the anterior tarsi, ambularcal disc shape, male opisthosomal lobes structure and legs IV, and the female’s epigynum form (Gaud and Atyeo 1981a, 1996). This genus is associated with birds of Ciconiidae; only two species of this genus have been reported (Gaud and Atyeo 1981a, 1996; Gaud 1982). The first discovered type species was *Mycterialges mesomorphus* Gaud & Atyeo, 1981, which was recorded in the Wood Stork, *Mycteria americana* Linnaeus, 1758 in North America. Another species was found in the Saddle-billed Stork, *Ephippiorhynchus senegalensis* (Shaw, 1800) in Africa, but it has not yet been accurately described (Gaud 1982).

The family Ciconiidae consists of 20 species in six genera, which are found on all continents except Antarctica. In Korea, two species of the genus *Ciconia* occur: the Black Stork, *Ciconia nigra* (Linnaeus, 1758) and the Oriental Stork, *Ciconia boyciana* Swinhoe, 1873. Both species are observed as winter visitors and are designated as “Endangered Species Level I” by the Korea Ministry of Environment (BirdLife International 2017, 2018; Lee et al. 2020; Gill et al. 2023; NIBR 2023). Among them, *C. boyciana* has become extirpated from Korea’s breeding population since the 1970s due to overfishing, habitat destruction, and food shortages (Sonobe and Izawa 1987; Chan 1991; Collar et al. 2001; Cheong 2005). In Korea, efforts have been made to restore a breeding population of *C. boyciana* since 1996 by importing Oriental Storks from Germany, Russia and Japan to increase their population. Since 2007, storks have been released into the wild to restore the breeding population (Park et al. 2011; Son et al. 2011; Eco-Institute for Oriental Stork 2023).

Research on the migration routes and nest selection of *C. boyciana* has mainly been conducted in East Asia (Shimazaki et al. 2004; Cheng et al. 2023). However, despite active research on the behavior and ecology of the Oriental Storks, research on ectosymbionts has not been actively conducted. *Pelargolichus orientalis* Waki, Mironov & Shimano, 2023 is the only known feather mite of *C. boyciana*. This mite was previously identified as *Pelargolichus didactylus* (Trouessart, 1885) (Dubinin 1956). However, Pérez and Atyeo (1992) identified mites in the Oriental Stork as a different species within the genus *Pelargolichus*, which was later described as *P. orientalis* by Waki et al. (2023). Except for this mite, little is known about other mites associated with Oriental Storks. Since 1996, ecological research has been conducted on the feeding behavior, reintroduction suitability, and habitat of Oriental Storks (Cheong 2005; Sung et al. 2008; Kim 2009; Ha 2019). Recently, we started research on ectosymbionts that can affect the host while interacting with storks.

This study reports a new species of feather mite of the genus *Mycterialges* found on captive *C. boyciana* in Korea. We provide information on the external morphology of the newly discovered feather mite species. In addition, we used the mitochondrial DNA (mtDNA) cytochrome c oxidase subunit I (COI) sequence information to determine the phylogenetic relationship between the new species and known closely related species.

Material and methods

Sampling and characterization

Feather mite sampling from three captive *C. boyciana* individuals was conducted in the same cage at Yesan Oriental Stork Park in Korea in October 2022, with permission from the Cultural Heritage Administration of Korea (B0030104016624). To minimize stress during the investigation, the storks were blindfolded and immobilized by the keepers; the procedure was completed within a maximum of five minutes for each individual. A new species of feather mites was identified from the wing and body feathers of the birds. The mites were carefully removed from the feathers using tweezers, and the collected mites were preserved in 95% ethanol solution. The specimens were mounted on microscope slides using a polyvinyl alcohol mounting medium (BioQuip, California, USA) after clearing with 10% lactic acid (Downs 1943; Han et al. 2016). Specimens were examined using a Dhyana 400DC camera (TUCSEN, Fuzhou, Fujian, China), Leica DM 2000 microscope (Leica, Wetzlar, Germany) with a drawing tube.

Descriptions of a new species followed the standard formats proposed for mites of the subfamily Ingrassiinae Gaud and Atyeo 1981 (Mironov and Proctor 2008; Stefan et al. 2013; Hernandez and Pedroso 2017; Han et al. 2021; Mironov and Hribar 2023). General morphological terms followed Gaud and Atyeo (1996) with minor corrections for coxal setation by Norton (1998). The classification and names of the birds followed those described by Gill et al. (2023). All measurements are in micrometres (μm).

DNA sequencing and molecular analysis

Genomic DNA was extracted from three specimens of the new feather mite using the DNeasy Blood and Tissue Kit (QIAGEN, Hilden, Germany). The COI barcode fragment was amplified using primer set, bcdF05 (5'-TTTTCTACHAAY-CATAAAGATATTGC-3') and bcdR04 (5'-TATAAACYTCDGGATGNCCAAAAAA-3') (Dabert et al. 2008). Polymerase chain reaction (PCR) was conducted following the protocol of A-star *Taq* DNA Polymerase (BIOFACT, Daejeon, Korea). The cycle conditions were as follows: 5 min at 95 °C; 40 cycles at 95 °C for 15 sec, 50 °C for 30 sec, and 72 °C for 60 sec; and a final extension at 72 °C for 5 min (Dabert et al. 2008; Han et al. 2021).

Sequence editing including assembly, alignment, and trimming, was performed using the GENEIOUS v.10.2.5 software (Kearse et al. 2012). We obtained a 635–683 bp fragment sequence of the COI gene from three individuals per mite species. Subsequently, the sequences of these three specimens were used for phylogenetic analysis, together with 17 COI regions of the subfamily Ingrassiinae obtained from the National Center for Biotechnology Information (NCBI). In addition, we collected data from the NCBI on one individual of the subfamily Xolalgininae Dubinin, 1953 (Gaud and Atyeo 1981a, b, 1996). The samples were aligned using GENEIOUS and the COI fragment was trimmed to 548 bp. A phylogenetic tree was constructed using COI fragments of the 21 feather mites (Table 1) and generated using the maximum-likelihood (ML) algorithm in PhyML v.3.0 (Guindon et al. 2010). To calculate nucleotide substitution, we used the Hasegawa-Kishino-Yano-1985 (HKY85) + gamma distribution and

Table 1. Feather mites used for the phylogenetic analysis in this study (COI barcode fragment).

Mite subfamily	Mite species	Host species	Sample source	GenBank accession No.	Reference
Xolalginae (outgroup)	<i>Xolalgoides</i> sp.	<i>Vireo hypochryseus</i>	Mexico	KU203107	Klimov et al. 2017
Ingrassiinae	<i>Analloptes</i> sp.	<i>Xiporhynchus flavigaster</i>		KU203108	
	<i>Glaucalges</i> sp.	<i>Tyto alba</i>	Germany	EU271955	Dabert et al. 2008
				EU271956	
	<i>Glaucalges attenuatus</i>	<i>Asio otus</i>		EU271957	
				EU271958	
	<i>Ingrassia</i> sp.	–	–	EU271954	Unpublished
		–	–	GQ864347	Dabert et al. 2010
	<i>Ingrassia chionis</i>	<i>Chionis albus</i>	Antarctica	MZ489649	Han et al. 2021
				MZ489650	
	<i>Ingrassia oceanodromae</i>	–	–	OL685164	Unpublished
	<i>Ingrassia philomachi</i>	<i>Calidris pugnax</i>	Kazakhstan	KU203104	Klimov et al. 2017
	<i>Ingrassia veligera</i>	<i>Tringa glareola</i>	Korea	MK031706	Han and Min 2019
	<i>Ingrassiella</i> sp.	<i>Catharus fuscater</i>	Peru	KU203102	Klimov et al. 2017
	<i>Metingrassia pelecani</i>	–	–	MG407963	Unpublished
		–	–	MG408765	
	–	–	MG410544		
<i>Mycterialges boyciana</i> sp. nov.	<i>Ciconia boyciana</i>	Korea	OR802170	This study	
			OR802171		
			OR802172		
<i>Vingrassia velata</i>	<i>Anas crecca</i>	Russia	KU203105	Klimov et al. 2017	

invariant site (G+) model, which was selected as the best model based on Smart Model Selection (SMS) (Lefort et al. 2017). The reliability of the tree was tested using 1000 bootstrap replicates (Felsenstein 1985).

Results

Systematics

Superfamily Analgoidea Trouessart & Mégnin, 1884

Family Xolalgidae Dubinin, 1953

Subfamily Ingrassiinae Gaud & Atyeo, 1981

Genus *Mycterialges* Gaud & Atyeo, 1981

Type species. *Mycterialges mesomorphus* Gaud & Atyeo, 1981, by original designation.

Remarks. To date, the genus *Mycterialges* has included only one described species, *M. mesomorphus*, found on the Wood Stork, *Mycteria americana* (Ciconiiformes: Ciconiidae), in Florida, USA (Gaud and Atyeo 1981a). In the review of feather mites associated with ciconiiforms in Africa, Gaud (1982) recognized one more *Mycterialges* species from the Saddle-billed Stork, *Ephippiorhynchus senegalensis* in Uganda. This unnamed species known only from a single male was illustrated but has never been formally described.

***Mycterialges boyciana* Shim, Han & Eo, sp. nov.**

<https://zoobank.org/FAEA2BCB-5781-4E20-B15B-5B46F77DCC34>

Type material. Male *holotype* (Prof. Eo lab, Kongju National University no. ESH_Em00001), and two male and three female *paratypes* (Prof. Eo lab no. ESH_Em00002-ESH_Em00006) from wing coverts and plumages of *Ciconia boyciana* (Ciconiiformes: Ciconiidae), Korea, Chungcheongnam-do, Yesan-gun, Yesan Oriental Stork Park, 36°32'32"N, 126°48'08"E, 17 October 2022, coll. by Shim JH and Han Y.-D.

Description. Male (holotype, range for 2 paratypes in parentheses) (Figs 1, 2, 5A–E). Length of idiosoma from anterior end to bases of setae *h3* 460 (465–470), greatest width 200 (210–220), length of hysterosoma 290 (285–300). Lateral margins of subcapitulum lateral margins with small tooth-like extensions. Prodorsal shield: narrow triangular plate occupying median part of prodorsum, posterior margin slightly convex and almost extending to level of scapular setae *se*, 81 (78–79) in length along midline, 45 (43–45) in width in posterior part (Fig. 1). Setae *se* separated by 75 (74–76), setae *si* situated slightly posterior to level of setae *se*. Scapular shields wide, with inner margin almost straight. Setae *c2* represented by macrosetae, 370 (280–290) long, situated on soft tegument. Humeral shields well developed, fused ventrally with epimerites III. Humeral setae *cp* 390 (290–310) long, situated on posterior margins; setae *c3* filiform, 93 (62–71) long, situated ventrally on anterior margin of humeral shields. Hyteronotal shield: anterior margin straight, anterior angles represented by narrow finger-like extensions anterior to setae *d1*, lateral margins with rounded convexities posterior to level of setae *cp*, length of shield from tips of anterior extensions to bases of setae *h3* 280 (270–275) (Fig. 1). Setae *d2* represented by macrosetae, 350 (270–345) in length. Opisthosoma nearly as wide as one-third of anterior part of hysterosoma, lateral margins of opisthosoma between levels of setae *e2* and *h2* shallowly concave, width at level of setae *h2* 53 (45–52). Supranal concavity circular, separated from the terminal cleft. Terminal cleft small angular, 12 (12–13) long. Opisthosomal lobes fused to each other in basal part and separated by median sclerotized septum, free parts of lobes represented by short and rounded convexities on posterior margin of opisthosoma. Setae *ps1* situated at level of setae *h2*. Distance between dorsal setae: *c2:e1* 140 (130–140), *e1:d2* 48 (43–49), *d2:h3* 100 (95–100), *h3:h3* 27 (26–29), *ps1:ps1* 14 (15).

Epimerites I fused into a Y with stem about 2/3 the length of epimerites. Coxal fields I–II open; coxal fields III almost closed, with small gap in anterior end. Coxal fields IV completely sclerotized, with posterolateral angles fused with lateral margins of hysteronotal shields. Setae *4a* and *4b* situated on inner margins of sclerotized coxal fields IV. Coxal setae *4b* posterior to level of setae *3a*. Genital apparatus 21 (20–21) long and 19 (18–20) wide, with base situated at level of anterior margin of trochanters IV. Paragenital apodemes fused into large teardrop-shaped sclerite 72 (72–78) long and 30 (27–32) wide, encircling genital apparatus and setae *g*. Genital papillae situated on anterior part of fused paragenital apodemes. Opisthoventral shields fused to each other at midline forming entire shield flanking anal field posterolaterally. Diameter of adanal suckers 7 (7–8). Distance between ventral setae: *4b:4b* 30 (38–43), *4b:3a* 21 (17–18), *4b:g* 95 (81–86), *g:ps3* 37 (40–41), *ps3:h3* 70 (62–72).

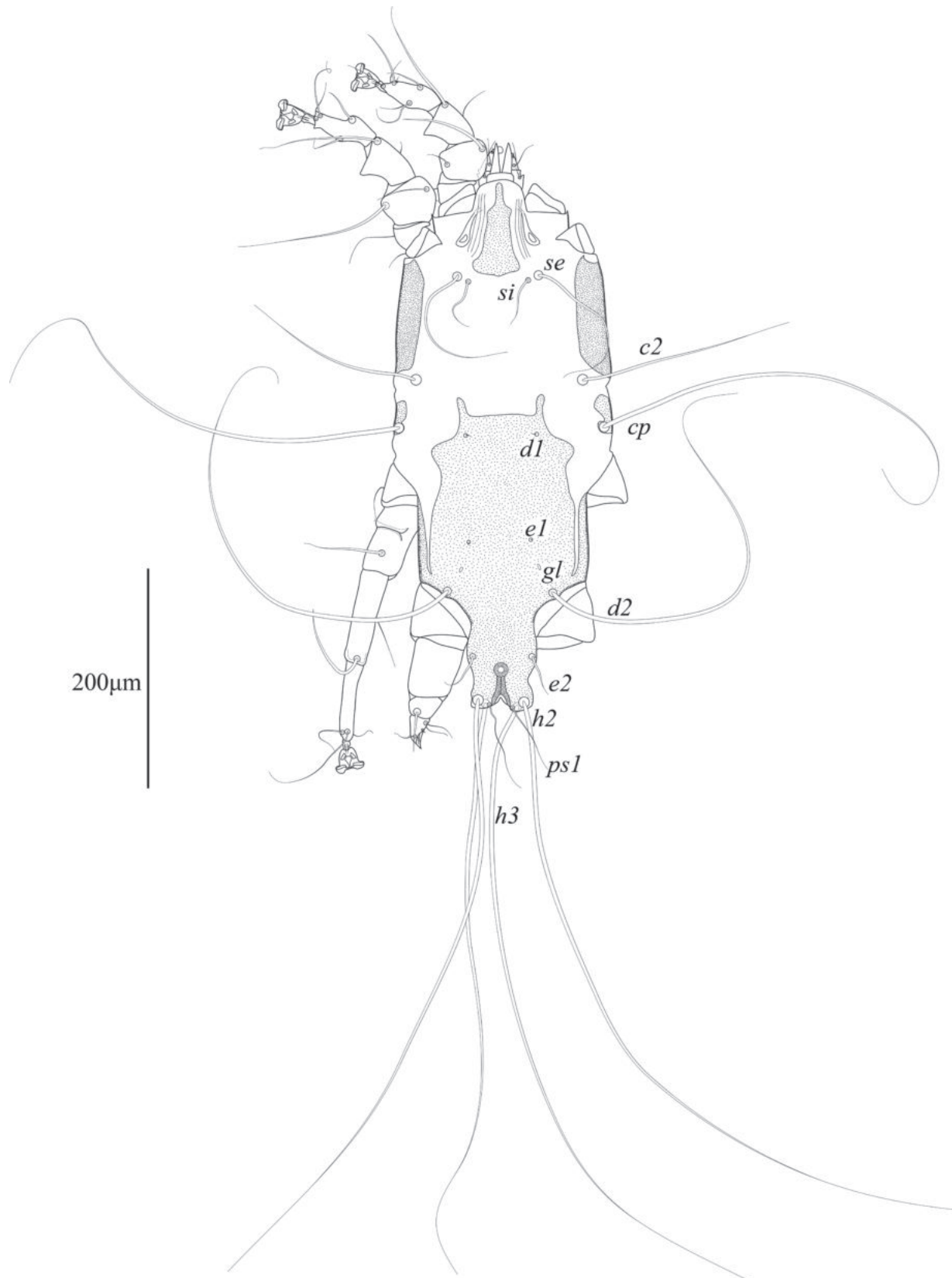


Figure 1. *Mycterialges boyciana* sp. nov., male dorsal view.

Tarsi I, II without apico-dorsal extension. Ventral setae *la*, *s* of tarsi I and setae *la*, *wa* and *s* of tarsi II absent. Tibia I, II with spine-like ventral processes. Leg IV short and thickened, with tibia and tarsus extending beyond lobar apices.

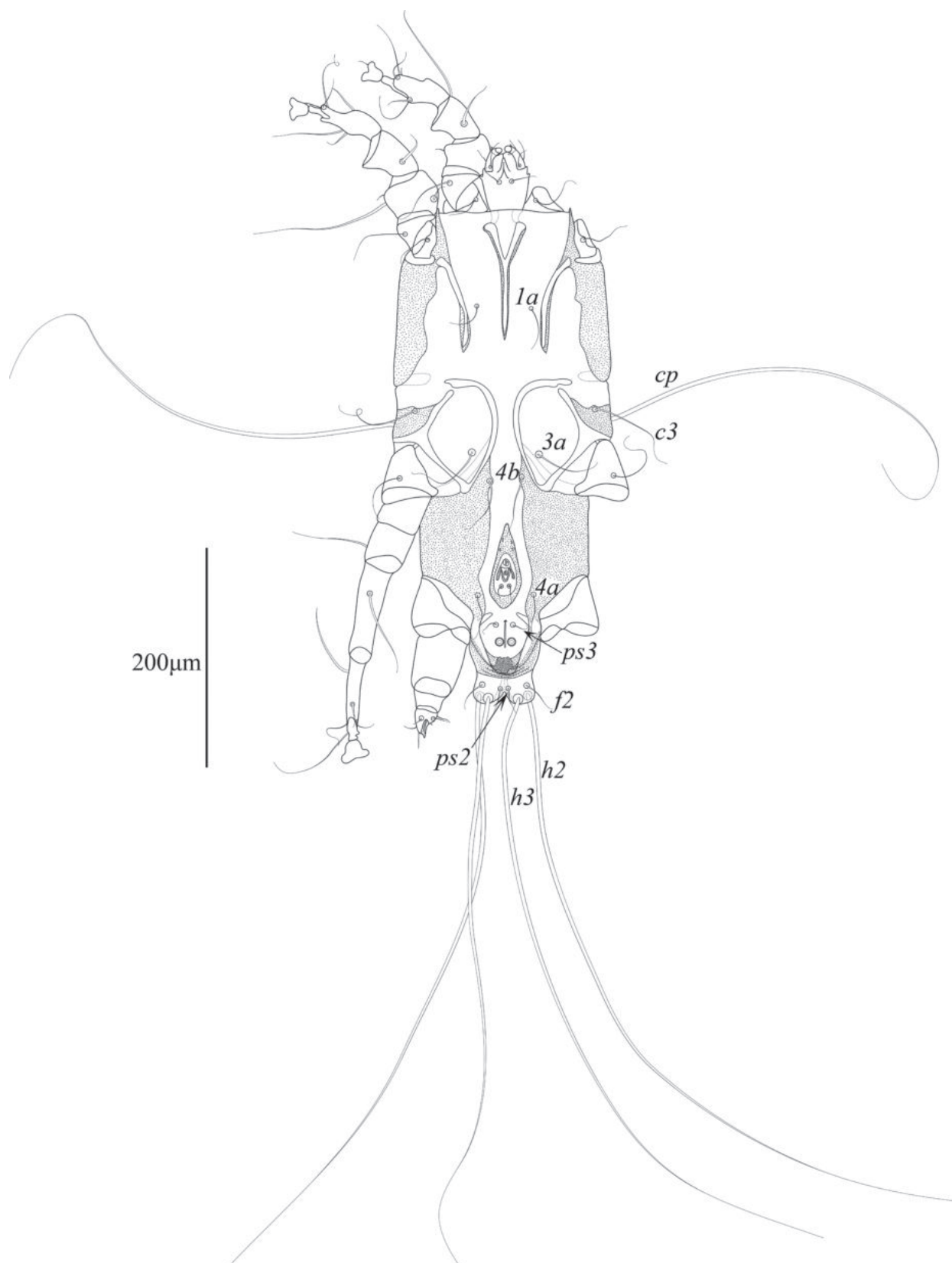


Figure 2. *Mycterialges boyciana* sp. nov., male ventral view.

Length of tibia IV along external margin 19 (18–22). Tarsus IV conical, 25 (24–26) long, ambulacral disc absent, ambulacral stalk acute apically, setae *d* and *e* of tarsus IV filiform and spine, respectively. Length of solenidia: σ I 90

(64–77), σ II 47 (43–46), σ III 68 (63–64), ϕ I 100 (93–94), ϕ II 105 (77–90), ϕ III 87 (83–88), ϕ IV 33 (32–32).

Female. (Range for 3 paratypes) (Figs 3, 4, 5F, G). Length of idiosoma from anterior end to bases of setae *h3* 425–440, greatest width 190–200, length of hysterosoma 270–275. Subcapitulum shaped as in male. Prodorsal shield: shaped almost as in male, except posterior margin blunt-angular and extending beyond level of setae *si*, 85–92 long, 58–62 wide (Fig. 3). Setae *se* separated by 85–88. Scapular shields more narrow than in male. Humeral shields not developed. Setae *c2* short filiform, situated on soft tegument. Setae *cp* situated ventrally on soft tegument, 135–150 long. Hysteronotal shield: large longitudinal plate occupying median part of hysterosoma; anterior margins almost straight, extending to or beyond level of setae *cp*; lateral margins slightly concave; posterior margin deeply concave, posterior angles encompassing bases of setae *e2*; greatest length 185–190, greatest width 74–83. Setae *d1*, *e1* and *e2* situated on hysteronotal shield, setae *d2* situated on striated tegument. Distance between dorsal setae: *c2:d2* 92–95, *d2:e2* 112–118, *e2:h3* 50–55, *d2:d2* 91–93, *e2:e2* 71–75, *h2:h2* 59–65, *h3:h3* 49–50.

Epimerites I fused into a Y, stem about half as long as epimerites. Epigynum shaped as thick bow-shaped transverse bulk with a pair of acute posterior branches, 29–34 long, 56–63 wide. Apodemes of oviporus long, posterior ends extending to midlevel of trochanters III (Fig. 4). Seta *4a* situated on epigynum. Setae *4b*, *g*, *3a*, and *4a* short filiform, not exceeding length of femorogenua III, IV. Setae *h3* slightly shorter than setae *h2*.

Legs I, II as in the male. Leg IV with distal half of tarsus extending beyond posterior end of opisthosoma. Tarsi III, IV without apical spines. Length of tarsi III and IV 73–75 and 81–84, respectively. Lengths of solienidia: σ I 67–71, σ II 24–33, σ III 49–52, ϕ III 57–67, ϕ IV 91–100 (Fig. 5F, G).

Differential diagnosis. The genus *Mycterialges* has included only the type species, *Mycterialges mesomorphus*, and one additional undescribed species (Gaud and Atyeo 1981a; Gaud 1982). The new species *Mycterialges boyciana* sp. nov. differs from *M. mesomorphus* by a number of characters: in males of *M. boyciana*, the prodorsal shield consists of a single triangular plate, the anterior part of the hysteronotal shield is widened and has a pair of narrow extensions, the paragenital apodemes are fused into a large teardrop sclerite encompassing genital apparatus, the legs IV are much shorter than legs III, and tibia + tarsus IV are shorter than femoragenu IV, tarsus IV is conical and ambulacral disc of tarsus IV is absent; in females, the posterior margin of prodorsal shield is blunt-angular and extends slightly beyond the level of setae *si*, the hysteronotal shield is as wide as the prodorsal shield and its posterior margin is deeply concave, setae *e2* are situated on the posterior corners of the hysteronotal shield, and setae *g* and *3a* are situated on the same transverse level. In males of *M. mesomorphus*, the prodorsal shield consists of two plates (triangular anterior parts and trapezoidal posterior part), the anterior part of the hysteronotal shield is narrowed and without extensions, the paragenital apodemes are fused into ovate sclerites around genital apparatus and with a pair of posterior projections, the legs IV are almost as long as legs III, and tibia + tarsus IV are much longer than femoragenu IV, tarsus IV has a claw-like apical process, and ambulacral disc of tarsus IV is narrowly lanceolate; in females, the posterior margin of prodorsal shield is straight and does not extend to the level

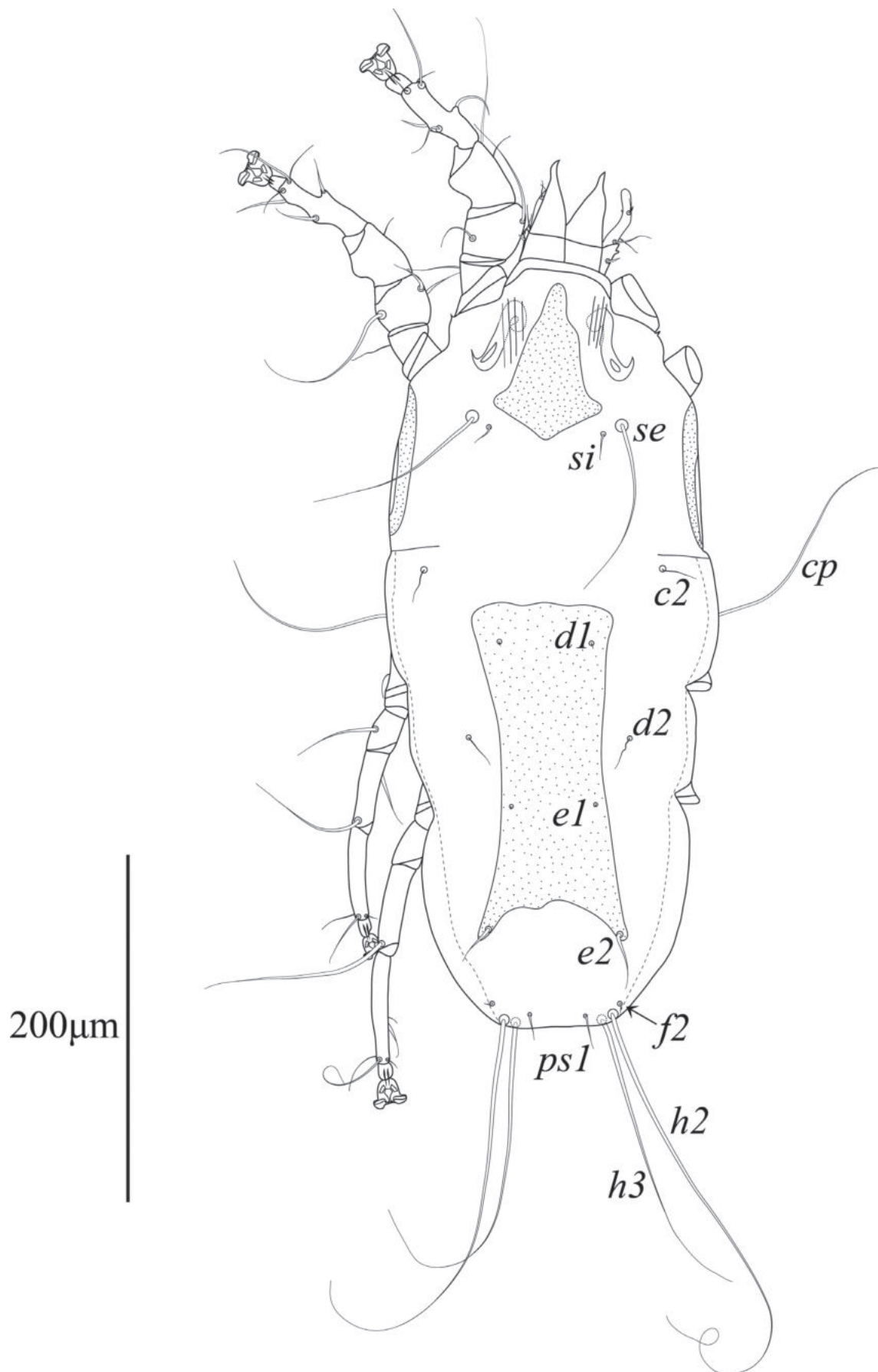


Figure 3. *Mycterialges boyciana* sp. nov., female dorsal view.

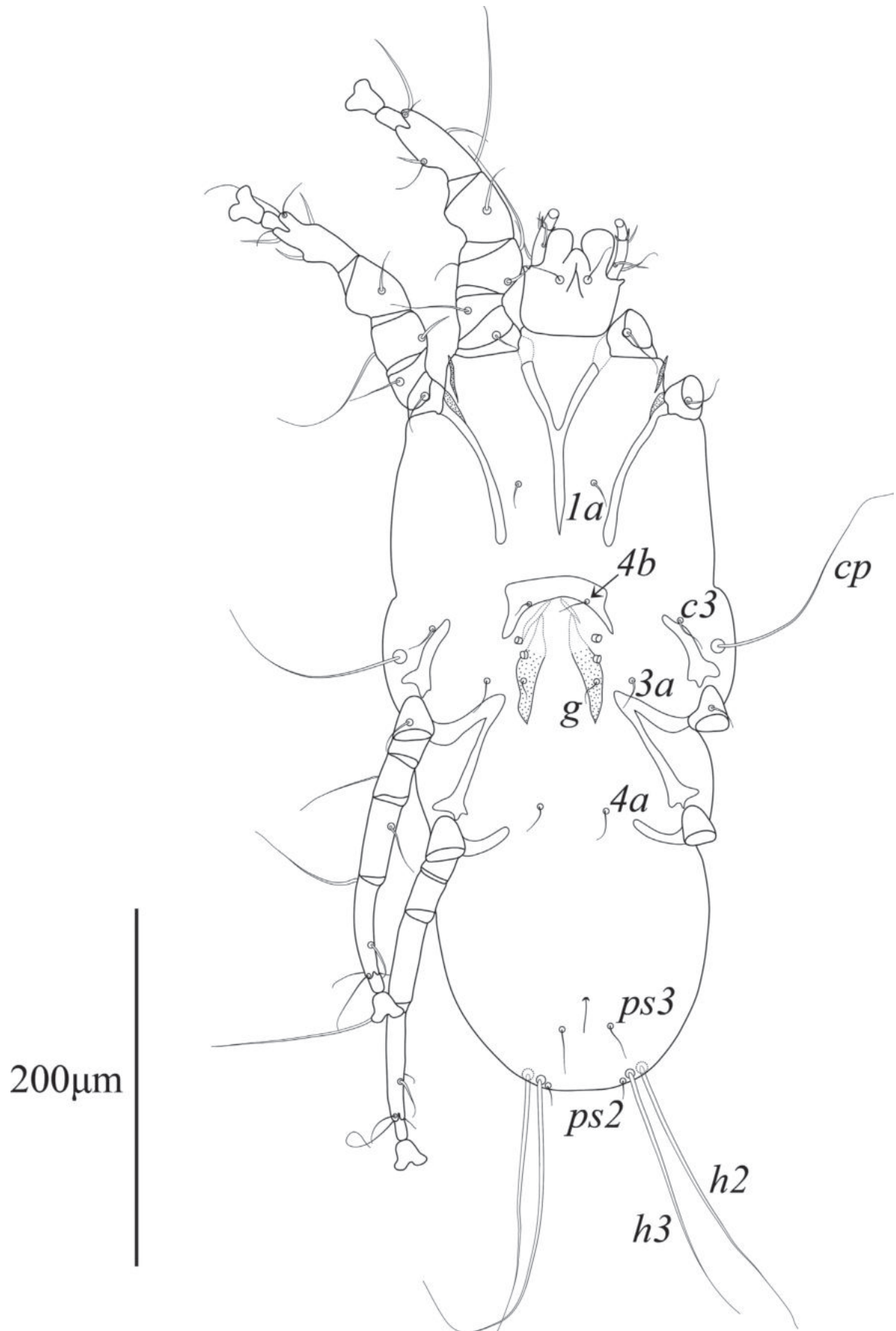


Figure 4. *Mycterialges boyciana* sp. nov., female ventral view.

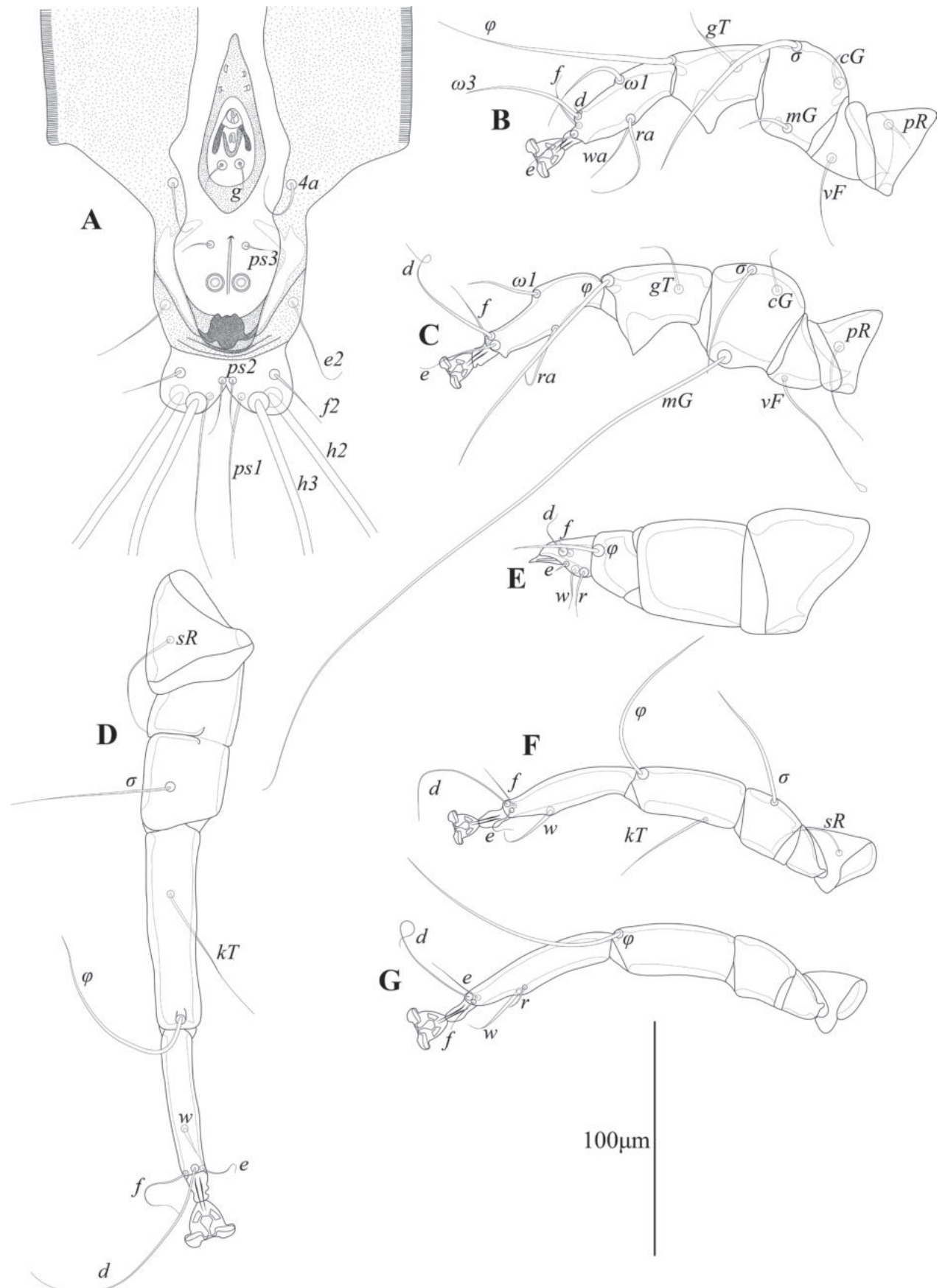


Figure 5. *Mycterialges boyciana* sp. nov., details, ventral view **A** opisthoma of male, dorsal view **B** leg I of male **C** leg II of male **D** leg III of male **E** leg IV of male **F** tibia and tarsus III of female **G** tibia and tarsus IV of female.

of setae *si*, the hysteronotal shield is narrow, approximately half as wide as the prodorsal shield and its posterior margin is straight, setae *e2* are situated on the soft tegument at the level of the posterior margin of the hysteronotal shield, and setae *g* are anterior to level of setae *3a*. Actually, *M. mycterialges* sp. nov. is much more similar to the unnamed *Mycterialges* species, known only from male and illustrated but not described (Gaud 1982: fig. 6a, b), in sharing the following features: the prodorsal shield is triangular, the anterior end of the hysteronotal shield has a pair of narrow extensions, legs IV are much shorter than legs III, and tibia+tarsus IV are shorter than femoragenu IV, tarsus IV is conical, and ambulacral disc of pretarsus IV is absent. Males of *M. boyciana* differs from those of the unnamed *Mycterialges* species in the following features: setae *d2* are represented by macrosetae extending beyond the posterior margin of opisthosoma, setae *cp* are situated on the humeral shields, and the paragenital apodemes fused into the teardrop-shaped sclerite free from epimerites IV. In the male of the unnamed *Mycterialges* species, setae *d2* extend to midlevel between setae *e2* and *h2*, setae *cp* are situated on striated tegument, and the paragenital apodemes fused into the teardrop-shaped sclerite are fused with the inner tips of epimerites IV.

Etymology. The specific name is taken from the species epithet of the type host and is a noun in the genitive case.

Phylogenetic relationships based on mtDNA COI

The ML phylogenetic tree of the COI barcode fragment showed *Mycterialges boyciana* sp. nov. to be grouped within the subfamily Ingrassiinae clade with three individuals of *M. boyciana*, exhibiting 93.7% bootstrap support for this grouping. Among the COI sequences collected from NCBI, the genus *Glaucalges* formed the clade closest to *M. boyciana* (Fig. 6). The genetic distance between *M. boyciana* and *Glaucalges* species was estimated to be ~16.1–16.2%.

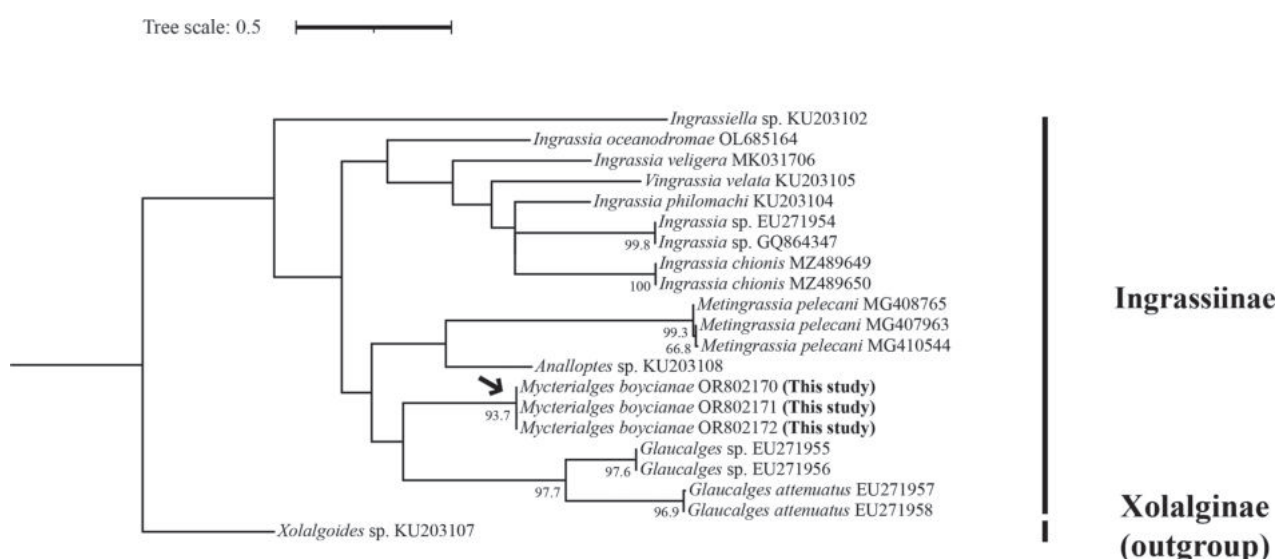


Figure 6. Maximum-likelihood phylogenetic tree of COI barcode fragment for members of the subfamily Ingrassiinae. Bootstrap percentages of more than 50% are shown. Scale bars indicate the number of substitutions per nucleotide site. The subfamily Xolalgininae is the outgroup taxon.

Discussion

This study describes a new feather mite species, *Mycterialges boyciana* sp. nov. found on the wings and body of captive *Ciconia boyciana* at the Yesan Oriental Stork Park in Korea. The genus *Mycterialges* has the following features: in both sexes, tarsi I, II only have two and one ventral setae, respectively, and the ambulacral disc is inverted triangle-shaped with a concave middle; in males, the opisthosomal lobes are fused and bluntly rounded, leg IV is hypertrophied; in females, the epigynum is short and straight (Gaud and Atyeo 1981a, 1996). *Mycterialges boyciana* has all these main characteristics (Figs 1–5), but exhibits significant variation from the type species in the legs IV. In the case of the type species *M. mesomorphus*, the male legs IV are hypertrophied, but not to the terminal width, and there is an ambulacrum (Gaud and Atyeo 1981a). In contrast, legs IV of *M. boyciana* and *M. sp.* (Gaud and Atyeo 1981a, 1996), are hypertrophied to the extent of the terminal width, have a femorogenu that combines the femur and genu, and have a claw instead of an ambulacrum (Figs 1–2, 5) (Gaud and Atyeo 1996). Despite these significant differences, no other species have been identified in *Mycterialges* apart from the type species so far. Therefore, we have included the newly discovered feather mite in *Mycterialges* based on the form of *M. sp.*, despite the lack of precise identification by Gaud and Atyeo (1981a, 1996). We observed that the mites discovered in the genus *Mycterialges* exhibit significant differences in legs IV, thus suggesting that there is a need to redefine this genus.

We showed the phylogenetic relationship of Ingrassiinae using the COI barcode fragment (Fig. 6). However, despite gathering all available Ingrassiinae data from the NCBI, our tree could only provide minimal information. This is due to the fact that, while the Ingrassiinae consists of 16 genera and 106 species (Gaud and Atyeo 1981a; Mironov and Galloway 2002; Mironov et al. 2005; Dabert et al. 2008; Constantinescu et al. 2013; Stefan et al. 2013; Hernandez 2014; Li and Zhang 2016; Mironov et al. 2017; Hernandez and Pedrosa 2017; Han et al. 2021; Hernandez and Brito 2022), our tree data includes only seven genera and 12 species, some of which have not been accurately described. Therefore, it is necessary to collect more data on mites to obtain more accurate results (Maddison and Knowles 2006; Knowles and Klimov 2011).

Finally, we discuss the situations faced by *M. boyciana*. This mite's host, *C. boyciana*, is not only an endangered species in Korea, but is also listed as an 'Endangered' (EN) species on the International Union for Conservation Nature (IUCN) Red List (BirdLife International 2018). Moreover, the nesting sites of the Oriental Stork are extremely limited and confined to parts of Russia and China (Zhou et al. 2013; BirdLife International 2018). Given its high host specificity, this situation could be extinction-threatening for *M. boyciana*, a permanent ectosymbiont (O'Connor 1982; Doña et al. 2019). Therefore, we believe that it is necessary to investigate the distribution, biology, ecology, and conservation status of feather mites, including *M. boyciana*, to confirm whether ectosymbionts are at risk of extinction.

Acknowledgements

The authors would like to express their gratitude to Junhee Hyeon, Youngjun Kim, Byungho Yoon, and Sangrim Park from Yesan Oriental Stork Park, and Nayoung Koh and other members of the Eo Lab, who assisted with the sampling.

Additional information

Conflict of interest

The authors have declared that no competing interests exist.

Ethical statement

No ethical statement was reported.

Funding

This research was supported by the reintroduction project of Oriental Stork funded by the Cultural Heritage Administration and Yesan County and a grant from the Kongju National University, Republic of Korea, in 2020.

Author contributions

Funding acquisition: YS. Investigation: YDH, JHS. Methodology: JHS, YDH. Project administration: SK, SHE, DH. Supervision: SHE. Writing – original draft: JHS. Writing – review and editing: SHE, YDH.

Author ORCIDs

Jeong Hun Shim  <https://orcid.org/0009-0000-1858-7725>

Yeong-Deok Han  <https://orcid.org/0000-0002-6625-8966>

Sukyung Kim  <https://orcid.org/0000-0003-3545-0282>

Dongsoo Ha  <https://orcid.org/0000-0002-1943-9190>

Yongun Shin  <https://orcid.org/0000-0001-7491-994X>

Soo Hyung Eo  <https://orcid.org/0000-0001-6719-1612>

Data availability

All of the data that support the findings of this study are available in the main text.

References

- BirdLife International (2017) *Ciconia nigra* (amended version of 2016 assessment). The IUCN Red List of Threatened Species 2017: e.T22697669A111747857. <https://doi.org/10.2305/IUCN.UK.2017-1.RLTS.T22697669A111747857.en> [Accessed on: 2023-9-17]
- BirdLife International (2018) *Ciconia boyciana*. The IUCN Red List of Threatened Species 2018: e.T22697695A131942061. <https://doi.org/10.2305/IUCN.UK.2018-2.RLTS.T22697695A131942061.en> [Accessed on: 2023-9-17]
- Chan S (1991) The history and current status of the Oriental White Stork. Hong Kong bird report 1990: 128–148.
- Cheng L, Zhou L, Yu C, Wei Z, Li C (2023) Flexible nest site selection of the endangered Oriental Storks (*Ciconia boyciana*): Trade-off from adaptive strategies. Avian Research 14: e100088. <https://doi.org/10.1016/j.avrs.2023.100088>
- Cheong S (2005) Development of propagation-husbandry techniques and behavioral ecology of the oriental white stork (*Ciconia boyciana*) in captivity: for the future reintroduction and conservation in Korea. Unpublished PhD thesis, Biology Dept., University of Education (Educators), Korea. [In Korean]

- Collar NJ, Andreev AV, Chan S, Crosby NJ, Subramanya S, Tobias JA (2001) Threatened birds of Asia: The birdlife international red data book. Birdlife international, Cambridge, 194–222.
- Constantinescu IC, Chișamera GABRIEL, Pocora V, Stanciu C, Adam COSTICĂ (2013) Two new species of feather mites (Acarina: Analgoidea) from the Moustached Warbler, *Acrocephalus melanopogon* (Passeriformes, Acrocephalidae) in Romania. *Zootaxa* 3709(3): 267–276. <https://doi.org/10.11646/zootaxa.3709.3.5>
- Dabert J, Mironov SV (1999) Origin and evolution of feather mites (Astigmata). *Experimental & Applied Acarology* 23(6): 437–454. <https://doi.org/10.1023/A:1006180705101>
- Dabert J, Ehrnsberger R, Dabert M (2008) *Glaucalgus tytonis* sp. n. (Analgoidea, Xolalgidae) from the barn owl *Tyto alba* (Strigiformes, Tytonidae): Compiling morphology with DNA barcode data for taxon descriptions in mites (Acari). *Zootaxa* 1719: 41–52.
- Dabert M, Witalinski W, Kazmierski A, Olszanowski Z, Dabert J (2010) Molecular phylogeny of acariform mites (Acari, Arachnida): Strong conflict between phylogenetic signal and long-branch attraction artifacts. *Molecular Phylogenetics and Evolution* 56(1): 222–241. <https://doi.org/10.1016/j.ympev.2009.12.020>
- Doña J, Potti J, Hera I, Blanco G, Frias O, Jovani R (2017) Vertical transmission in feather mites: Insights into its adaptive value. *Ecological Entomology* 42(4): 492–499. <https://doi.org/10.1111/een.12408>
- Doña J, Proctor H, Serrano D, Johnson KP, Oploo AOV, Huguet-Tapia JC, Ascunce MS, Jovani R (2019) Feather mites play a role in cleaning host feathers: New insights from DNA metabarcoding and microscopy. *Molecular Ecology* 28(2): 203–218. <https://doi.org/10.1111/mec.14581>
- Downs WG (1943) Polyvinyl alcohol: A medium for mounting and clearing biological specimens. *Science* 97(2528): e2528. <https://doi.org/10.1126/science.97.2528.539>
- Dubinin VB (1956) Feather Mites (Analgoidea). Part III. Family Pterolichidae. *Fauna SSSR. Paukoobraznye* 6: 1–813. [In Russian]
- Eco-Institute for Oriental Stork (2023) Stork Monitoring Data Base. <https://storkdb.net/> [Accessed on: 2023-9-17]
- Felsenstein J (1985) Confidence limits on phylogenies: An approach using the bootstrap. *Evolution; International Journal of Organic Evolution* 39(4): 783–791. <https://doi.org/10.2307/2408678>
- Gaud J (1982) Acariens Sarcoptiformes plumicoles des oiseaux Ciconiiformes d'Afrique. II: parasites des Ciconiidae, Scopidae et Pheonicopteridae. *Revue zoologique Africaine* 96: 335–357.
- Gaud J, Atyeo WT (1981a) The feather mite family Xolalgidae, Dubinin, new status (feather mites, Sarcoptiforms, Analgoidea)-The subfamily Ingrassiinae, n. sub-fam. *Acarologia* 22: 63–79.
- Gaud J, Atyeo WT (1981b) The feather mite family Xolalgidae, Dubinin. 2. The subfamilies Xolalginae and Zumptiinae, n. sub-fam. *Acarologia* 22: 313–324.
- Gaud J, Atyeo WT (1996) Feather mites of the world (Acarina, Astigmata): The supraspecific taxa. *Annales du Musée Royal de l'Afrique Centrale, Sciences Zoologiques* 277: 1–193. [(Pt. 1, text), 1–436 (Pt. 2, illustrations)]
- Gill F, Donsker D, Rasmussen P [Eds] (2023) IOC World Bird List (v. 13.2). <https://www.worldbirdnames.org/> [Accessed on: 2023-9-17]
- Guindon S, Dufayard JF, Lefort V, Anisimova M, Hordijk W, Gascuel O (2010) New algorithms and methods to estimate maximum-likelihood phylogenies: Assessing

- the performance of PhyML 3.0. *Systematic Biology* 59(3): 307–321. <https://doi.org/10.1093/sysbio/syq010>
- Ha DS (2019) A study on the analysis and prediction of the habitat types of reintroduction oriental stork (*Ciconia boyciana*). Unpublished PhD thesis, Biology Dept., University of Education (Educators), Korea. [In Korean]
- Han YD, Min GS (2019) Three feather mites (Acari: Sarcoptiformes: Astigmata) isolated from *Tringa glareola* in South Korea. *Journal of Species Research* 8: 215–224. <https://doi.org/10.12651/JSR.2019.8.2.215>
- Han YD, Song JH, Min GS (2016) New record of two feather mites (Acari: Sarcoptiformes: Astigmata) from Korea. *Journal of Species Research* 5(3): 324–332. <https://doi.org/10.12651/JSR.2016.5.3.324>
- Han YD, Mironov SV, Kim JH, Min GS (2021) Feather mites (Acariformes, Astigmata) from marine birds of the Barton Peninsula (King George Island, Antarctica), with descriptions of two new species. *ZooKeys* 1061: 109–130. <https://doi.org/10.3897/zookeys.1061.71212>
- Hernandes FA (2014) The feather mites of nightjars (Aves: Caprimulgidae), with descriptions of two new species from Brazil (Acari: Xolalgidae, Gabuciniidae). *Folia Parasitologica* 61(2): 173–181. <https://doi.org/10.14411/fp.2014.024>
- Hernandes FA, Brito G (2022) Feather mites (Acariformes: Astigmata) of the brown noddy, *Anous stolidus* (L.) (Charadriiformes: Laridae), with description of two new species from Brazil. *Acarologia* 62(2): 317–331. <https://doi.org/10.24349/rblu-98ly>
- Hernandes FA, Pedroso LGA (2017) Two new feather mites of the genus *Protonyssus* Trouessart, 1916 (Acariformes: Xolalgidae) from Brazilian parakeets (Psittacidae), with a key to species. *International Journal of Acarology* 43(3): 204–211. <https://doi.org/10.1080/01647954.2016.1250815>
- Kearse M, Moir R, Wilson A, Stones-Havas S, Cheung M, Sturrock S, Buxton S, Cooper A, Markowitz S, Duran C, Thierer T, Ashton B, Meintjes P, Drummond A (2012) Geneious basic: An integrated and extendable desktop software platform for the organization and analysis of sequence data. *Bioinformatics* 28(12): 1647–1649. <https://doi.org/10.1093/bioinformatics/bts199>
- Kim SK (2009) Habitat suitability assessment for the reintroduction of oriental white stork (*Ciconia boyciana*): A GIS-based multi-criteria evaluation approach. Unpublished PhD thesis, Biology Dept., University of Education (Educators), Korea. [In Korean]
- Klimov PB, Mironov SV, OConnor BM (2017) Detecting ancient codispersals and host shifts by double dating of host and parasite phylogenies: Application in proctophylloid feather mites associated with passerine birds. *Evolution; International Journal of Organic Evolution* 71(10): 2381–2397. <https://doi.org/10.1111/evo.13309>
- Knowles LL, Klimov PB (2011) Estimating phylogenetic relationships despite discordant gene trees across loci: the species tree of a diverse species group of feather mites (Acari: Proctophylloidae). *Parasitology* 138(13): 1750–1759. <https://doi.org/10.1017/S003118201100031X>
- Lee WS, Koo TH, Park JY (2020) A Field Guide to the Birds of Korea (2nd revised edn.). LG Evergreen Foundation, 328 pp.
- Lefort V, Longueville JE, Gascuel O (2017) SMS: Smart model selection in PhyML. *Molecular Biology and Evolution* 34(9): 2422–2424. <https://doi.org/10.1093/molbev/msx149>
- Li GY, Zhang ZQ (2016) Hotspots of mite new species discovery: Sarcoptiformes (2013–2015). *Zootaxa* 4208(2): 101–126. <https://doi.org/10.11646/zootaxa.4208.2.1>
- Maddison WP, Knowles LL (2006) Inferring phylogeny despite incomplete lineage sorting. *Systematic Biology* 55(1): 21–30. <https://doi.org/10.1080/10635150500354928>

- Mironov SV, Galloway TD (2002) Four new species of feather mites (Acari: Analgoidea). *Canadian Entomologist* 134(5): 605–618. <https://doi.org/10.4039/Ent134605-5>
- Mironov SV, Hribar LJ (2023) A new feather mite of the genus *Xolalgoides* (Acariformes: Xolalgidae) from the Northern Mockingbird, *Mimus polyglottos* (Passeriformes: Mimidae). *Acarologia* 63(2): 569–579. <https://doi.org/10.24349/0ju0-uugu>
- Mironov SV, Proctor HC (2008) The probable association of feather mites of the genus *Ingrassia* (Analgoidea: Xolalgidae) with the blue penguin *Eudyptula minor* (Aves: Sphenisciformes) in Australia. *The Journal of Parasitology* 94(6): 1243–1248. <https://doi.org/10.1645/GE-1579.1>
- Mironov SV, Dabert J, Ehrnsberger R (2005) Six new feather mite species (Acari: Astigmata) from the carolina parakeet *Conuropsis carolinensis* (Psittaciformes: Psittacidae), an extinct parrot of North America. *Journal of Natural History* 39(24): 2257–2278. <https://doi.org/10.1080/00222930400014155>
- Mironov SV, Ehrnsberger R, Dabert J (2017) Feather mites of the genera *Dubininia* and *Cacatualges* (Acari: Xolalgidae) associated with parrots (Aves: Psittaciformes) of the Old World. *Zootaxa* 4272(4): 451–490. <https://doi.org/10.11646/zootaxa.4272.4.1>
- NIBR (National Institute of Biological Resources) (2023) Species of National Institute of Biological Resources. National Institute of Biological Resources. <https://species.nibr.go.kr/> [Accessed on: 2023-7-13]
- Norton R (1998) Morphological evidence for the evolutionary origin of Astigmata (Acari: Acariformes). *Experimental & Applied Acarology* 22(10): 559–594. <https://doi.org/10.1023/A:1006135509248>
- OConnor BM, OConnor BM (1982) Evolutionary ecology of astigmatid mites. *Annual Review of Entomology* 27(1): 385–409. <https://doi.org/10.1146/annurev.en.27.010182.002125>
- Park SR, Yoon J, Kim SK (2011) Captive propagation, habitat restoration, and re-introduction of oriental white storks (*Ciconia boyciana*) extirpated in South Korea. *Reintroduction* 1: 31–36.
- Pérez TM, Atyeo WT (1992) A review of the Xoloptoidinae (Acari, Pterolichidae) and the description of a new genus. *Entomologische Mitteilungen aus dem Zoologischen Museum Hamburg* 10: 209–220.
- Proctor HC (2003) Feather mites (Acari: Astigmata): ecology, behavior and evolution. *Annual Review of Entomology* 48(1): 185–209. <https://doi.org/10.1146/annurev.ento.48.091801.112725>
- Shimazaki H, Tamura M, Higuchi H (2004) Migration routes and important stopover sites of endangered oriental white storks (*Ciconia boyciana*), as revealed by satellite tracking. *Memoirs of National Institute of Polar Research* 58: 162–178.
- Son JK, Sung HC, Kang B (2011) The study on the selection of suitable site for palustrine wetland creation at habitat restoration areas for Oriental stork (*Ciconia boyciana*). *Korean Wetlands Society* 13: 95–104.
- Sonobe K, Izawa N (1987) Endangered bird species in the Korean peninsula. *Museum of Korean Nature and Wild Bird Soc. Japan*, 75 pp.
- Stefan LM, Gomez-Diaz E, Mironov SV (2013) Three new species of the feather mite subfamily Ingrassiinae (Acariformes: Xolalgidae) from shearwaters and petrels (Procellariiformes: Procellariidae). *Zootaxa* 3682(1): 105–120. <https://doi.org/10.11646/zootaxa.3682.1.4>
- Sung HC, Cheong SW, Kim JH, Kim SK, Park SR (2008) A case study of foraging time budget and habitat selection of oriental white storks (*Ciconia boyciana*) in natural state. *Korean Journal of Environmental Biology* 26: 121–127.

- Waki T, Shimano S (2020) A report of infection in the crested ibis *Nipponia nippon* with feather mites in current Japan. *Nihon Dani Gakkaishi* 29(1): 1–8. <https://doi.org/10.2300/acari.29.1>
- Waki T, Mironov SV, Nakajima A, Shimano S (2023) A new feather mite of the genus *Pelargolichus* (Acariformes: Pterolichidae) from the Oriental White Stork *Ciconia boyciana* (Ciconiiformes: Ciconiidae) in Japan. *Systematic and Applied Acarology* 28: 471–482. <https://doi.org/10.11158/saa.28.3.5>
- Zhou L, Xue W, Zhu S, Shan K, Chen J (2013) Foraging habitat use of oriental white stork (*Ciconia boyciana*) recently breeding in China. *Zoological Science* 30(7): 559–564. <https://doi.org/10.2108/zsj.30.559>

New stenurothripid thrips from mid-Cretaceous Kachin amber (Thysanoptera, Stenurothripidae)

Dawei Guo¹, Michael S. Engel^{2,3,4}, Chungkun Shih^{1,5}, Dong Ren¹

¹ College of Life Sciences, Capital Normal University, Beijing 100048, China

² Division of Invertebrate Zoology, American Museum of Natural History, Central Park West at 79th Street, New York, NY 10024-5192, USA

³ Facultad de Ciencias Biológicas, Universidad Nacional Mayor de San Marcos, Lima, Peru

⁴ Departamento de Entomología, Museo de Historia Natural, Universidad Nacional Mayor de San Marcos, Av. Arenales 1256 Jesús María, Lima, Peru

⁵ Department of Paleobiology, National Museum of Natural History, Smithsonian Institution, Washington, DC 20013-7012, USA

Corresponding author: Dong Ren (rendong@cnu.edu.cn)

Abstract

Hitherto, only two species of the thysanopteran suborder Terebrantia have been reported from mid-Cretaceous Kachin amber (Myanmar). This is here expanded through the discovery of two new genera and species, described and figured as *Parallelothrips separatus* **gen. et sp. nov.** and *Didymothrips abdominalis* **gen. et sp. nov.**, both of the family Stenurothripidae. Both taxa have key apomorphies of the Stenurothripidae, allowing for a confident assignment as to family. Both species have characteristic comb-like anteromarginal setae, which are discussed along with structural differences between the two sexes. Cycad pollen was found on the thrips' bodies, providing further evidence that Thysanoptera were pollinators of gymnosperms during the mid-Cretaceous.

Key words: Cenomanian, new genus, new species, pollinating insects, taxonomy, Thysanoptera



Academic editor: Elison F. B. Lima

Received: 23 December 2023

Accepted: 31 January 2024

Published: 21 February 2024

ZooBank: <https://zoobank.org/E6DAB213-FCA6-4BD3-AA45-04CD5850DE17>

Citation: Guo D, Engel MS, Shih C, Ren D (2024) New stenurothripid thrips from mid-Cretaceous Kachin amber (Thysanoptera, Stenurothripidae). ZooKeys 1192: 197–212. <https://doi.org/10.3897/zookeys.1192.117754>

Copyright: © Dawei Guo et al.

This is an open access article distributed under the terms of the CC0 Public Domain Dedication.

Introduction

Thrips, order Thysanoptera, comprise a group of small paraneopteran insects with piercing asymmetrical mouthparts, often a characteristic pretarsal bladder, and bearing simplified, linear wings with reduced or absent venation and fringe cilia on the margins. The right mandible of thrips was lost in their evolution, with the left mandible forming a unique asymmetrical feeding tube with the maxillary stylets. The order comprises more than 6600 species, classified into 14 families and 857 genera, with 187 species and 70 genera known only from the fossil record (ThripsWiki 2023).

Thysanoptera is divided into two extant suborders: the reciprocally monophyletic Terebrantia Haliday, 1836 and Tubulifera Haliday, 1836 (Grimaldi and Engel 2005; Buckman et al. 2013; Johnson et al. 2018). These clades are principally distinguished by the form of the tenth abdominal segment, but also by their wing structure (Ulitzka 2022), behavior and development. Tubulifera, as their name suggests, have an elongate, tubular tenth segment and lay eggs on the plant's surface, while Terebrantia have a sawlike ovipositor and lay eggs within plant tissue. In addition, Tubulifera have three "pupal" stages, while Terebrantia have two.

Some thrips are important pollinators, and occupied such a role even prior to the rise of angiosperms (Willmer 2011). The earliest record of thrips pollination is from Albian amber, approximately 110–105 million years ago (Peñalver et al. 2012). Thrips feed on pollen or other plant tissues and lay eggs within or on the same plants, and their larvae also feed on the flowers (Bailey 1949); in many species adults transport pollen between plants, thereby completing the plants' reproduction. Today thrips pollination can lead to higher fruiting success in many plants (Garcia-Fayos and Goldarazena 2008; Eliyahu et al. 2015), and instances of thrips-host plant coevolution have been documented (Brookes et al. 2015). Notable examples of thrips pollination include cycads that attract small pollinators such as thrips and weevils, which can enter their ovulate cones while larger insects are excluded (Terry 2001). Indeed, some flowers emit different odors or regulate their temperature to either attract thrips or encourage them to depart from the plant (Terry et al. 2007).

Up to now, species of Thysanoptera recorded from the Cretaceous include the families of Aeolothripidae, Melanthripidae, Merothripidae, Rohrthripidae, Stenurothripidae and Thripidae, and nearly all of these are based on specimens included in amber and more than half of those from the mid-Cretaceous of Kachin, Myanmar (Table 1). Among fossil insect species reported from Kachin amber, the orders Coleoptera (532 species), Hymenoptera (344 species), Diptera (253 species), and Hemiptera (224 species) account for the greatest numbers (Ross 2023), while only 19 species in seven genera from three families have been reported for Thysanoptera (Ulitzka 2018, 2019, 2022; Tong et al. 2019).

Stenurothripidae Bagnall, 1923 are a rather small family of Terebrantia, which includes six extant species and 19 extinct species, among which about half of the species were found in Baltic amber (ThripsWiki 2023). The most significant feature of this family is the antenna with nine antennomeres and a broad-based conical sensorium on antennomeres III and IV (Peñalver and Nel 2010; Nel et al. 2012). Extant genera of this family were once placed in Adiheterothripidae (Bhatti 2006), but the family was subsequently resurrected and removed from synonymy (Peñalver and Nel 2010).

Herein we document two new genera and species of Stenurothripidae, *Paralelothrips separatus* and *Didymothrips abdominalis*, from mid-Cretaceous Kachin amber, enriching the number of species of Thysanoptera from the fossil record. We also discuss their potential interactions with cycads, enlarging the available evidence of gymnosperm pollination by Thysanoptera during the Cretaceous.

Materials and methods

The amber fossils studied here were collected from the state of Kachin (Hukawng Valley) of northern Myanmar, located at 26°21'33.41"N, 96°43'11.88"E (Guo et al. 2017). Previous studies have recovered an earliest Cenomanian age for the deposit, approximately 98.79±0.62 Ma (Shi et al. 2012). The amber specimens mentioned in this study were acquired by Mr. Fangyuan Xia before 2015 and donated to us in 2016; both are deposited in the Key Lab of Insect Evolution and Environmental Changes, College of Life Sciences, Capital Normal University, Beijing, China (CNUB, Curator: Dong Ren). The amber specimen is labeled with year of acquisition (e.g., 2016) and specimen accession number (e.g., 116) following the prefix "CNU-THY-MA".

Table 1. Checklist of thrips reported from Cretaceous amber, with locality and reference indicated.

Suborder	Family	Genus species	Locality	Reference
Tubulifera	†Rohrthripidae	† <i>Rohrthrips burmiticus</i>	Kachin amber	Ullitzka 2018
		† <i>Rohrthrips libanicus</i>	Lebanese amber	Nel et al. 2010
		† <i>Rohrthrips breviceps</i>	Kachin amber	Ullitzka 2019
		† <i>Rohrthrips jiewenae</i>	Kachin amber	Ullitzka 2019
		† <i>Rohrthrips maryae</i>	Kachin amber	Ullitzka 2019
		† <i>Rohrthrips schizovenatus</i>	Kachin amber	Ullitzka 2019
		† <i>Rohrthrips patrickmuelleri</i>	Kachin amber	Ullitzka 2019
		† <i>Rohrthrips brachyvenis</i>	Kachin amber	Ullitzka 2022
		† <i>Rohrthrips multihamuli</i>	Kachin amber	Ullitzka 2022
		† <i>Rohrthrips pandemicus</i>	Kachin amber	Ullitzka 2022
		† <i>Rohrthrips rhamphorhynchus</i>	Kachin amber	Ullitzka 2022
		† <i>Rohrthrips setiger</i>	Kachin amber	Ullitzka 2022
		† <i>Sesquithrips markpankowskii</i>	Kachin amber	Ullitzka 2022
		† <i>Sesquithrips rostratus</i>	Kachin amber	Ullitzka 2022
		† <i>Adstrictubothrips mirapterus</i>	Kachin amber	Ullitzka 2022
		† <i>Gemineurothrips microcephalus</i>	Kachin amber	Ullitzka 2022
		† <i>Gemineurothrips peculiaris</i>	Kachin amber	Ullitzka 2022
		† <i>Paralleloalathrips bivenatus</i>	Kachin amber	Ullitzka 2022
Terebrantia	Aeolothripidae	† <i>Cretothrips antiquus</i>	New Jersey amber	Grimaldi et al. 2004
	Melanthripidae	† <i>Gymnopollistrips maior</i>	Spanish amber	Peñalver et al. 2012
		† <i>Gymnopollistrips minor</i>	Spanish amber	Peñalver et al. 2012
	Merothripidae	† <i>Jezzinotrips cretacicus</i>	Lebanese amber	zur Strassen 1973
		† <i>Myanmarothrips pankowskiorum</i>	Kachin amber	Ullitzka 2018
	Thripidae	† <i>Tethystrips hispanicus</i>	Spanish amber	Nel et al. 2010
		† <i>Tethystrips libanicus</i>	Lebanese amber	Nel et al. 2010
	Stenurothripidae	† <i>Cenomanithrips primus</i>	Kachin amber	Tong et al. 2019
		† <i>Exitelothrips mesozoicus</i>	Lebanese amber	zur Strassen 1973
		† <i>Neocomothrips hennigianus</i>	Lebanese amber	zur Strassen 1973
		† <i>Progonothrips horridus</i>	Lebanese amber	zur Strassen 1973
		† <i>Rhetinotrips elegans</i>	Lebanese amber	zur Strassen 1973
		† <i>Scaphothrips antennatus</i>	Lebanese amber	zur Strassen 1973
† <i>Scudderthrips sucinus</i>		Lebanese amber	zur Strassen 1973	
† <i>Hispanothrips utrillensis</i>		Spanish amber	Peñalver and Nel 2010	

So as to obtain a better view of specimens, the amber pieces were prepared through a series of steps: initially cut using a razor blade, followed by grinding with Emery papers of different grain sizes, and finally polished with polishing powder. For the current pieces, we produced thin slices, with a thickness of no more than 2 mm.

Specimens were examined and photographed using a Nikon SMZ25 microscope with a Nikon DS-Ri2 digital camera system, illuminated by two or more white-light-LED incident illuminators. White papers were employed as diffusers to prevent reflections on the amber's surface, and papers with different colors

were put under each piece along with transmitting light to create a stronger contrast with the inclusions (as described by Ullitzka 2015). Source images were stacked in Helicon Focus 8 software. Line drawings were prepared with Adobe Illustrator CC 2022 and Adobe Photoshop CC 2020 software.

Systematic paleontology

Family Stenurothripidae Bagnall, 1923

Parallelothrips Guo, Engel, Shih & Ren, gen. nov.

<https://zoobank.org/889D330E-E93A-4171-A53A-0A3A3F45B90C>

Type species. *Parallelothrips separatus* Guo, Engel, Shih & Ren, sp. nov.

Etymology. The new generic name is a combination of the Ancient Greek adjective *παράλληλος* (*parállēlos*, meaning, “parallel”) and the Ancient Greek noun *θρίψ* (*thrips*, meaning, “woodworm”). The name refers to the two parallel rows of marginal setae on the pronotum. The gender of the name is masculine.

Diagnosis. Antenna (Fig. 1) with nine antennomeres, antennomeres III and IV asymmetrical inverse cone-shaped, stouter than distal antennomeres, each with a broad-based conical sensorium. Head (Fig. 1C) dorsally with transverse striations basally, cheek rounded behind compound eye. Compound eye prolonged ventrally. Pronotum wider than head, with striate sculpture basally, studded with regular rows of setae on both anterior and posterior margins, posteroangular setae long and stout. Mesonotum (Fig. 1C) not adjoined to pronotum, with distinct separation between segments. Fore wing (Fig. 2A) narrow, with two longitudinal veins and two crossveins visible, wing surface covered with microtrichia (Fig. 2B), fringe cilia of posterior margin longer than those of anterior margin and slightly undulate, wavy duplicated cilia present around wing tip. Hind wing (Fig. 2C) nearly transparent, surface covered with microtrichia, with one distinct longitudinal vein. Abdomen 10-segmented, about as wide as thorax at widest point, with some strong setae near apex; female segments VIII–X coniform, male (Fig. 3D) segment X rounded.

Parallelothrips separatus Guo, Engel, Shih & Ren, sp. nov.

<https://zoobank.org/B65E3843-59B7-48F1-9757-82F56AD5E1C6>

Figs 1–3

Type materials. *Holotype* male (CNU-THY-MA2016116) and *paratype* female (CNU-THY-MA2016117), both as inclusions in Kachin amber piece CNU006122.

Etymology. The specific epithet is the Latin participle *sēparātus*, meaning “divided” or “separated” and referring to the distance between the pronotum and mesonotum of the holotype.

Diagnosis. As for the genus (*vide supra*).

Description. *Holotype male* (CNU-THY-MA2016116). Body, legs, as well as antennae and wing veins uniformly dark brown, right compound eye and wings partly hidden by a shiny reflective layer of air. Antenna (Fig. 1A, C) curved laterally; body fully extended, right forewing spread, some fringe cilia from anterior margin fractured (Fig. 2A); legs (Fig. 1B) extended except right mid and hind legs folded under body.

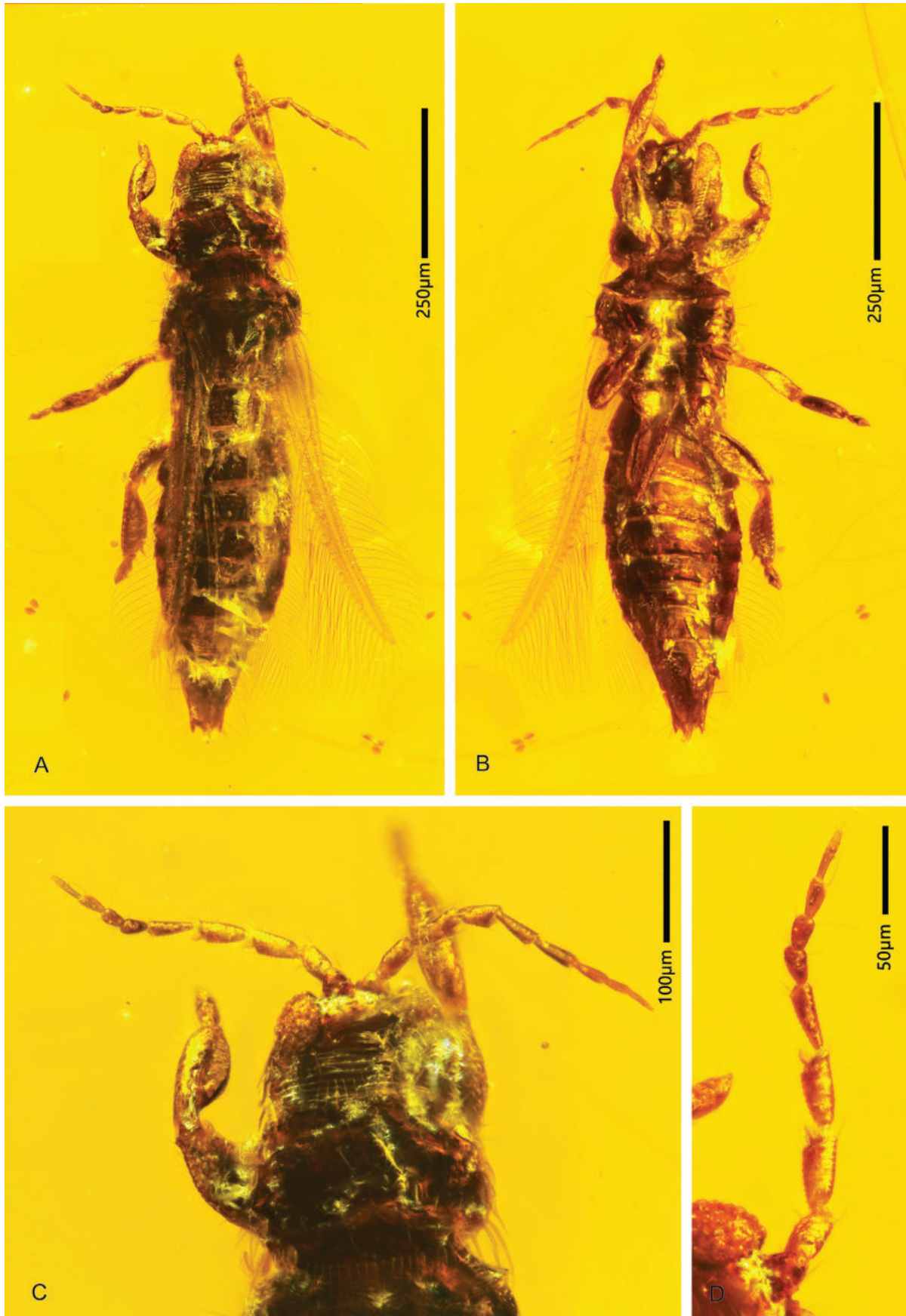


Figure 1. *Parallelothrips separatus* gen. et sp. nov.; holotype male (CNU-THY-MA2016116) **A** dorsal view **B** ventral view **C** head and pronotum, dorsal view **D** left antenna, conical sensorium present on antennomeres III–IV.

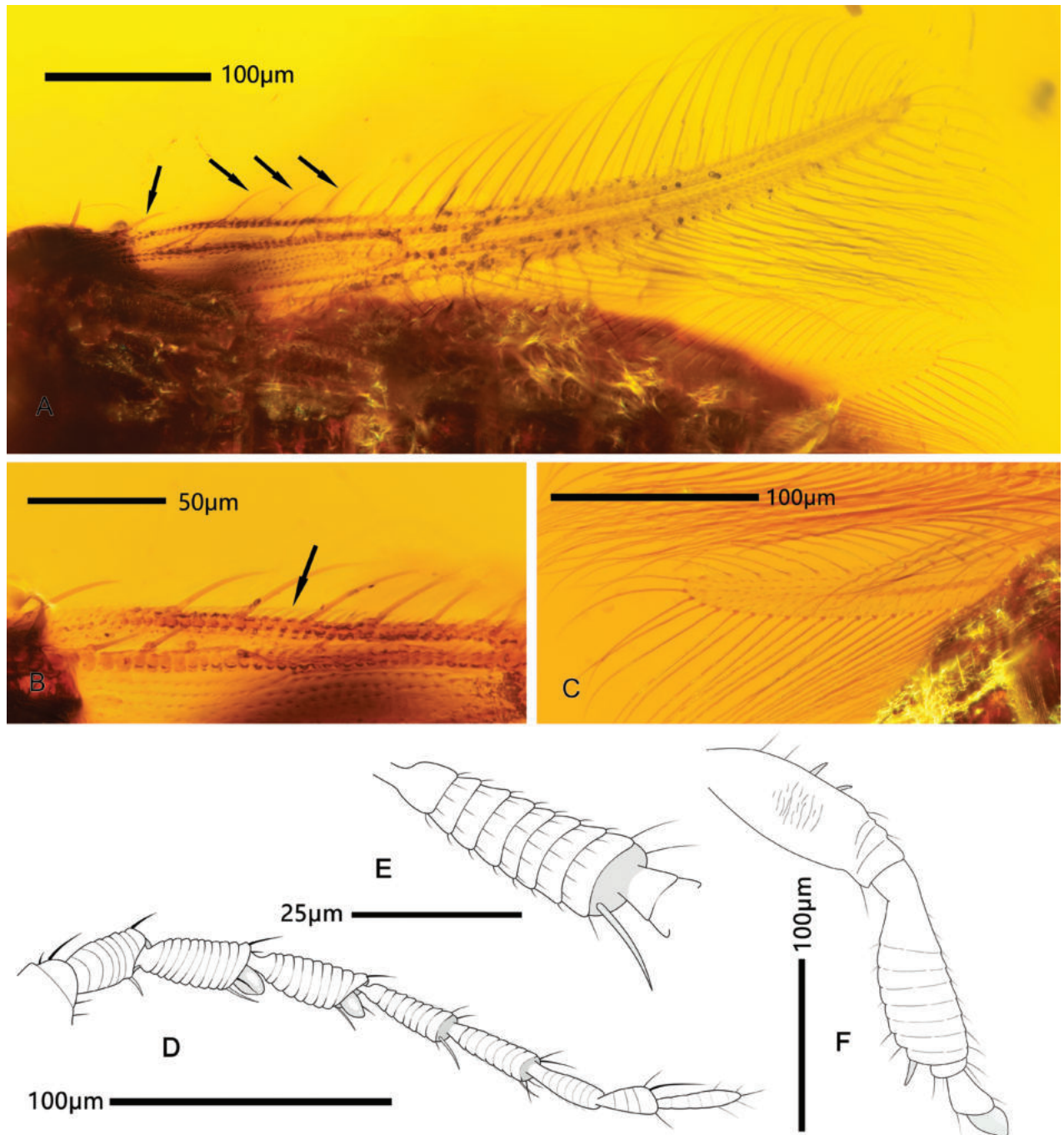


Figure 2. *Parallelothrips separatus* gen. et sp. nov.; holotype male (CNU-THY-MA2016116) **A** right fore wing, dorsal view, the foremost fringe cilium lacks a corresponding anteromarginal setae (indicated by black arrows) **B** microtrichia of anterior wing margin **C** surface of hind wing, covered with microtrichia **D** ventral view of left antenna **E** antennomere V, showing rounded annulation sculpture and microtrichia **F** dorsal view of hind leg (from metafemur onward).

Head (Fig. 1C) wider than long, dorsally sculptured with transverse striations at base, cheeks rounded behind compound eyes. Compound eye (Fig. 1C) large, with dozens of large ommatidia, front margin protruding over base of antenna, postocular setae as well as ocellar setae short and pointed, directing backward; median ocellus directed forwards, lateral ocelli close to compound eyes. Antenna (Figs 1D, 2D) with nine antennomeres, antennomeres II–IX rounded with transversal annulation, furnished with several microtrichia (Fig. 2E); antennomeres

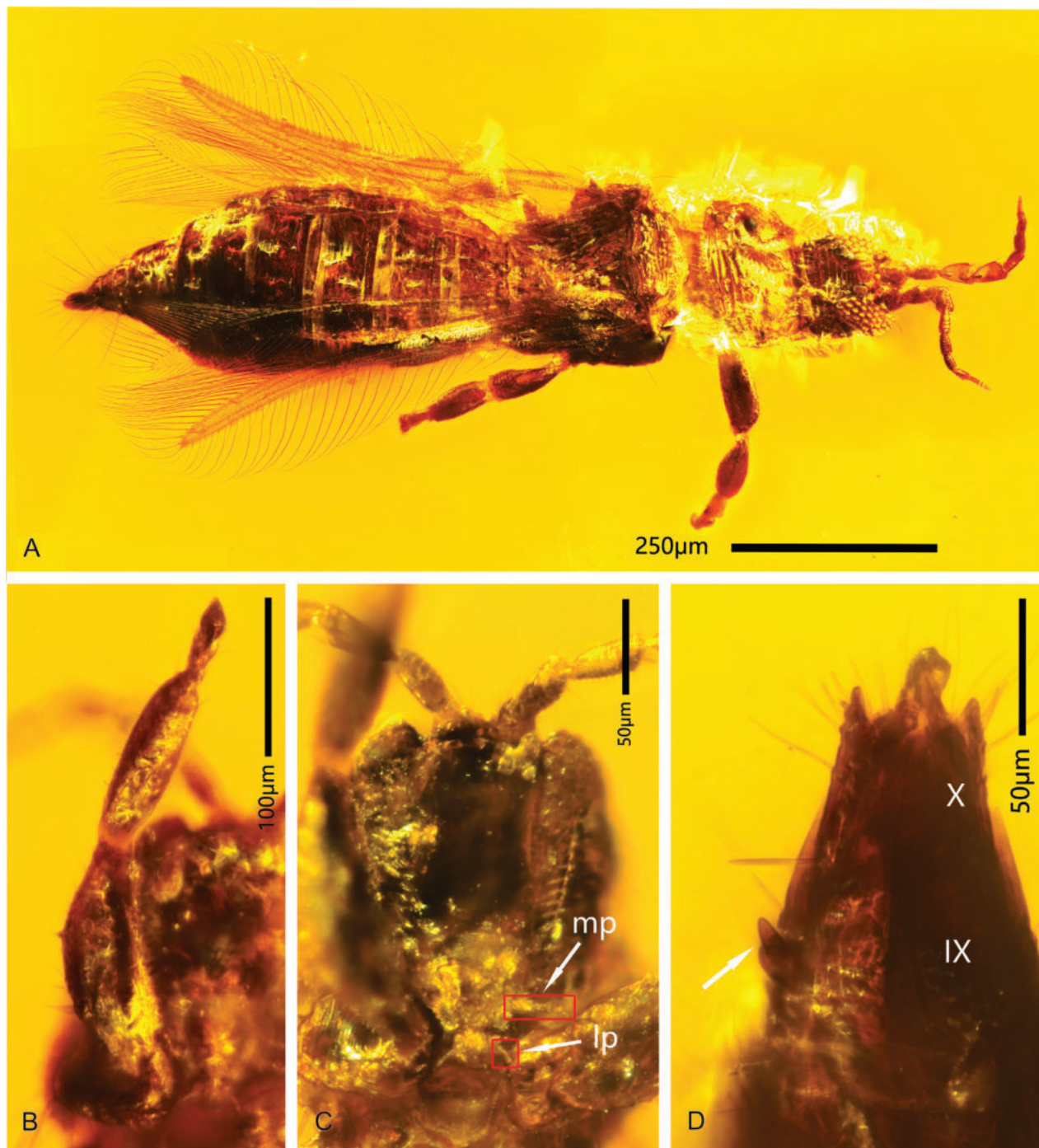


Figure 3. *Parallelothrips separatus* gen. et sp. nov. **A** female (CNU-THY-MA2016117), dorsal view **B** fore leg of male (CNU-YHY-MA2016116), vesicle cone-shaped at the tip **C** mouth cone (CNU-THY-MA2016116), mp indicated: maxillary palpus, lp indicated: labial palpus **D** distal abdominal segments of male (CNU-THY-MA2016116), spine on segment IX (indicated by a white arrow).

I–IV stouter than distal antennomeres; I broadened basally, III–IV symmetrical inverse cone-shaped and both having a conical sensorium with a broad base; sense cone simple, at least one inner on antennomeres II–VI. Mouth cone (Fig. 3C) short; maxillary palps stout, trimerous; labial palps short and slender.

Pronotum (Fig. 1C) wider than long, dorsally sculptured with transverse striations, lateral margin rounded, tightly adjoined to head; anteromarginal and

posteromarginal setae comb-like; anteroangular setae not visible, posteroangular setae long and stout. Mesonotum fan-shaped; sculptured with transverse striations, slightly separated from pronotum. Metanotum sculptured with light longitudinal striations. Fore wing (Fig. 2A) narrow, slightly wider at basal third, distally slightly bent forwards. Wing venation pale in color, anterior vein ending at apex, with seven small setae; posterior vein with six setae distributed evenly, ending near wing tip, one crossvein (r-m) present between them, other above it; membrane (Fig. 2B) covered with microtrichia. Fringe cilia fine and long, those located near duplicated cilia slightly undulate; wavy duplicated cilia present near apex and apical part of posterior wing margin, stouter than other cilia. Anteromarginal setae long and fine, running parallel to direction of fringe cilia and spaced in pairs; foremost fringe cilia lack paired anteromarginal setae, and position of first fringe cilium quiet distant, near base of wing (Fig. 2A). Some microtrichia densely arranged along anterior wing margin, extending from base to apex (Fig. 2B). Clavus with a pair of setiform processes at tip. Hind wing (Fig. 2C) almost transparent, membrane covered with microtrichia, with one longitudinal vein ending nearly at wing apex; fringe cilia from posterior margin longer than that of anterior margin, and both straight. Legs (Figs 2F, 3B) furnished with many microtrichia, hind leg (Fig. 2F) with two spines on femora and a stout spine at the end of tibiae, tarsi dimerous, no hamus present, vesicles cone-shaped.

Abdomen with ten segments, dorsally sculptured with lines of transverse striations; some small setae present on posterior margin of each segment; segment I partly hidden by metanotum, not narrower than thorax at basal segments, slightly bent upwards at apex; with a pair of spines and a pair of short stout setae on segment IX (Fig. 3D); segment X round, pleurite protrudes on both sides, aedeagus protrudes medioapically.

Paratype female (CNU-THY-MA2016117, Fig. 3A). Body, antennae, and legs uniformly dark brown, wing surface as well as veins and fringe cilia light brown. Body slightly inclined to left, antennae curved to both sides, pronotum bent downwards, abdomen extended; wings spread; right fore and mid legs spread, other legs bent under head and body.

Nearly identical to male (CNU-THY-MA2016116) in size, but lighter in color. Compound eye protruding over front margin of head, ocellus large. Forewing narrow, duplicated cilia extending from mid-wing to tip, clearly undulate near apex. Fore legs with femora stout, mid and hind legs slender; vesicles rounded at apex of each tarsus. Abdomen slenderer than thorax and gradually broadening before segment VI; latero-tergites protruding on segments III–VI; segments VIII–X cone-shaped, curved downwards, narrow and elongate; surrounded with several long and strong setae apically.

Measurements. Male CNU-THY-MA2016116 (in microns): Body length 946 (antennae not included). Head, length 108; width 155. Eye, length 43; width 44. Prothorax, length 74; width 203. Anteromarginal setae, length 17; posteromarginal setae, length 24; posteroangular setae, length 54. Pterothorax, length 146; largest width 215. Abdomen, length 548; largest width 205 (segment V). Antenna, length 285; lengths of segments: I 20, II 38, III 43, IV 44, V 33, VI 37, VII 25 VIII 16, IX 29. Forewing, length 555, width 40 at crossvein. Hind wing, length 554, largest width 29. Fore leg, length 341; mid leg, length 336; hind leg, length 340.

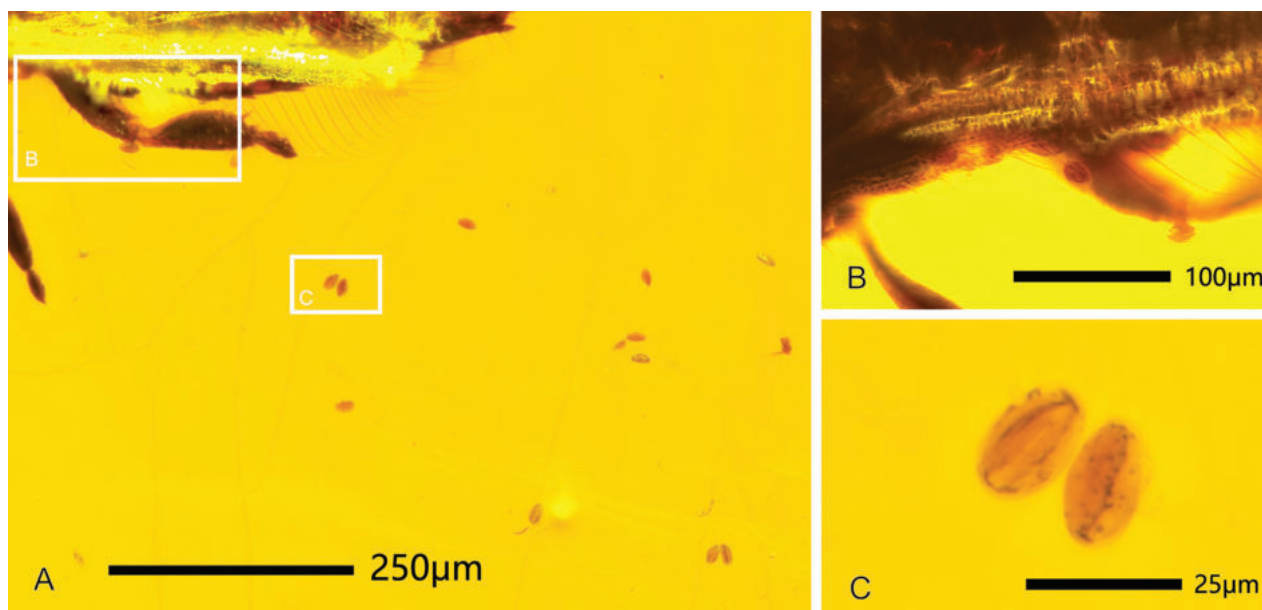


Figure 4. Cycad pollen found in the CNU-THY-MA2016116 **A** pollen distributed around the thrips **B** pollen attached on the fringe cilia and legs **C** enlarged details of the cycad pollen.

Female CNU-THY-MA2016117 (in microns): Body length 1010 (antennae not included). Head, length 110; width 122. Eyes, length 61; width 49. Hind ocelli, diameter 8. Prothorax, length 110; width 161. Anteromarginal setae, length 19; posteromarginal setae, length 19; posteroangular setae, length 61. Pterothorax, length 206; largest width 222. Abdomen, length 553; largest width 231 (segment V). Antenna, length 236; lengths of segments: I 22, II 32, III 43, IV 34, V 30, VI 22, VII 14, VIII 13, IX 26. Forewing, length 580, width 31 at crossvein. Hind wing, length 599, largest width 26. Fore leg, length 254.

Syninclusions. Some cycad pollen (Fig. 4) was found around and on the body of the male.

***Didymothrips* Guo, Engel, Shih & Ren, gen. nov.**

<https://zoobank.org/C96F2CBF-450D-414F-9E91-AE4CCF232309>

Type species. *Didymothrips abdominalis* Guo, Engel, Shih & Ren, sp. nov.

Etymology. The new generic name is a combination of the Ancient Greek *Δίδυμοι* (*Dídymoi*, the original Greek name for the later Roman Gemini) and the Ancient Greek noun *θρίψ* (*thrips*, meaning, “woodworm”). The name refers to the anteromarginal and posteromarginal setae of the pronotum. The gender of the name is masculine.

Diagnosis. Antenna (Fig. 5A) with nine antennomeres, cone-shaped sensorium present on inverted-triangle shaped antennomeres III–VI. Head (Fig. 5C) dorsally sculptured with transverse striations; compound eye protruding in front of the front margin. Pronotum (Fig. 5C) about as wide as the head, sculptured with transverse striate, furnished with some sparse microtrichia; anteromarginal and posteromarginal setae of pronotum long and comb-like, two pairs of long posteroangular setae present. Mesonotum partly hidden by pronotum and its posteromarginal setae. Forewing (Fig. 5D) narrow, slightly bent forwards and membrane covered with

microtrichia; two parallel longitudinal wing veins furnished with several stout setae, crossveins not developed. Fringe cilia long and undulate, duplicated cilia present at distal part of posterior wing margin. Abdomen 10-segmented, showing differences between the male and the female; female (Fig. 5A, B) generally with a flat and wide abdomen with pointed terminal direct backward or slightly downward, while male (Fig. 5A) with a short and thick abdomen with terminal not pointed.

***Didymothrips abdominalis* Guo, Engel, Shih & Ren, sp. nov.**

<https://zoobank.org/B9768AC0-4906-4E12-A555-2C3F6A0712EB>

Fig. 5

Type materials. *Holotype* female (CNU-THY-MA2016102/1) and *paratype* male CNU-THY-MA2016102/2 (Fig. 5A), inclusions in Kachin amber piece CNU009269; as well as a paratype female CNU-THY-MA2016118 (Fig. 5B) in Kachin amber piece CNU009461.

Etymology. The specific epithet is from the Latin adjective *abdōminālis*, meaning “abdominal” and referring to the wide abdomen of the species.

Diagnosis. As for the genus (*vide supra*).

Description. *Holotype female* (CNU-THY-MA2016102/1). Body (Fig. 5A) uniformly dark brown, antennae and wing veins light brown, posterior half of pronotum transparent. Antennae (Fig. 5C) bent towards sides, legs spread under body, forewing (Fig. 5A) overlapping body, right hind wing partly covered by forewing, left hind wing almost completely covered by fore wing except apex.

Head (Fig. 5C) wider than long, dorsally sculptured with transverse striations. Cheek nearly straight, slightly diverging posteriorly. A pair of short ocellar setae located behind lateral ocelli; two pairs of postocular setae close to compound eyes. Ocelli rather large, median ocellus near middle of base of antenna, interocellar setae long and direct upward; lateral ocelli located close to compound eye. Compound eye (Fig. 5C) protruding in front of anterior margin of head, with many large ommatidia. Antenna (Fig. 5C) with nine antennomeres; I inverse funnel-shaped, II oval, III–IV inverted-triangle shaped, V–IX elongate club-shaped, II–IX with a pedicle at base. Conical sensorium present on antennomere III but not visible on IV. Mouth cone difficult to observe.

Pronotum (Fig. 5C) wider than long, trapezoidal, tightly adjoined with head; dorsally with transverse sculpture and some sparse setae; anteromarginal and posteromarginal setae long and comb-like; posteroangular setae long and pointed. Mesonotum (Fig. 5A) triangular; dorsally with some transverse striations, partly covered by pronotum. Metanotum dorsally furnished with some stout setae and longitudinal lines, slightly bent upwards. Forewing (Fig. 5D) narrow, slightly bent forwards at apex; two longitudinal veins light in color and parallel, anterior vein ending at apex, with strong setae; posterior vein reaching 4/5 of wing length; two crossveins visible close to each other between anterior wing margin and longitudinal veins at basal third; membrane furnished with many microtrichia. Fringe cilia straight on anterior margin but undulate and a little longer on posterior margin; duplicated cilia undulate (Fig. 5D). Clavus with pair of setiform processes at tip. Hind wing transparent, one longitudinal vein nearly reaching apex, some microtrichia present at apex of wing. Legs long and slender, femora of fore legs slightly enlarged, protarsus without a hamus.

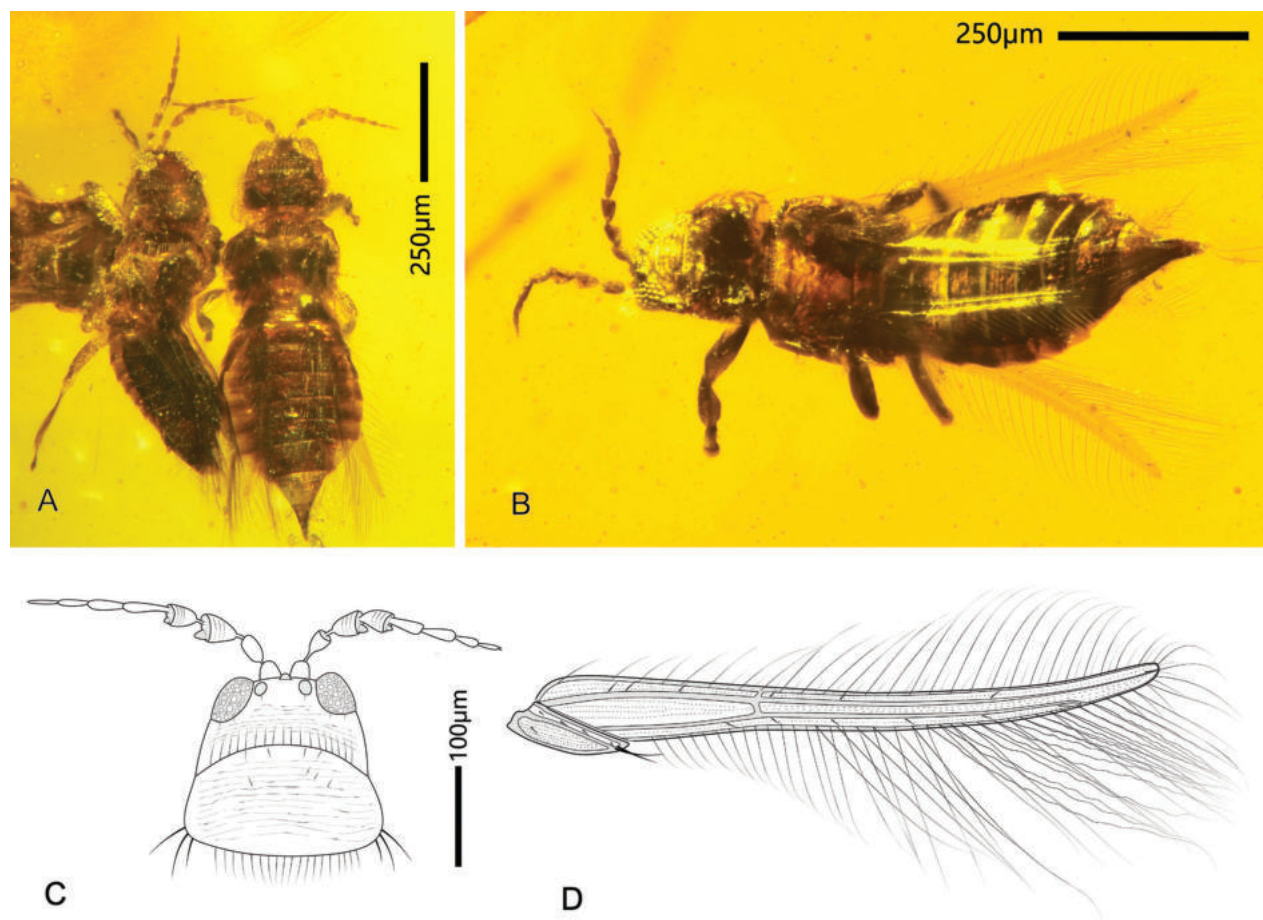


Figure 5. *Didymothrips abdominalis* gen. et sp. nov. **A** holotype female (right) (CNU-THY-MA2016102/1) and paratype male (left) (CNU-THY-MA2016102/2), dorsal view **B** paratype female (CNU-THY-MA2016118), dorsal view **C** head, antenna and pronotum of CNU-THY-MA2016102/1 **D** forewing of CNU-THY-MA2016102/1.

Abdomen (Fig. 5A) flat and broad, dorsally sculptured with transverse striations; abdominal tergite I hidden by metanotum, wider than thorax at middle part, widest at segments V–VI, rapidly tapering in width along segments VIII–X; segment X conically shaped, surrounded with some long straight setae, directed posteriorly.

Paratype male (CNU-THY-MA2016102/2, Fig. 5A). Body, legs, and antennae uniformly dark brown, fore wing membrane light brown. Body not fully extended, with head slightly bent downwards and abdomen bent upwards; fore and mid legs recurved under body, blocked by a female thrips (CNU-THY-MA2016102/1), hind legs fully extended; wings overlapping body.

Similar to female in color and most body structures, but smaller and much slender in size. Antenna stouter than female; abdomen short and thick, generally slightly bent upwards, not wider than thorax, edges between different segments distinct, somewhat conical process present on segment IX, segment X round, with two pleurites connected by membrane.

Measurements. Female CNU-THY-MA2016102/1 (in microns): Body length 799 (antenna not included). Head, length 72; width 166. Eye, length 50; width 33. Hind ocelli, diameter 12; distance between the hind ocelli 43. Prothorax, length 134; width 168. Anteromarginal setae, length 24; posteromarginal setae, length 26. Pterothorax, length 169; largest width 250. Abdomen, length 567;

largest width 308 (segment V). Antenna, length 262; lengths of segments: I 17, II 33, III 35, IV 37, V 37, VI 33, VII 23, VIII 21, IX 26. Forewing, length 562, width 33 at crossvein. Hind wing, length 551.

Male CNU-THY-MA2016102/2 (in microns): Body length 745 (antenna not included). Head, length 90; width 138. Eye, length 58; width 48. Hind ocelli, diameter 12; distance between the hind ocelli 32. Ocellar setae, length 34. Postocular setae, length 30. Prothorax, length 125; width 185. Anteromarginal setae, length 24; posteromarginal setae, length 26. Pterothorax, length 148; largest width 226. Abdomen, length 379; largest width 221 (segment V). Antenna, length 266; lengths of segments: I 16, II 38, III 37, IV 33, V 31, VI 34, VII 25, VIII 25, IX 27. Forewing, length 604, width 37 at crossvein.

Syninclusions. 168 *Stenurothrips* specimens are preserved in the amber CNU-THY-MA2016102, together with a cicadid (Hemiptera), a nematoceran (Diptera), and an apocritan wasp (Hymenoptera). Two stenurothripids, an unnamed species of Thripidae, and an aphid are contained in CNU-THY-MA2016118.

Discussion

Schliephake (1990) characterized Stenurothripidae as: antenna with nine antennomeres, all antennomeres freely connected; conical sensorium with a broad base present on antennomeres III and IV; fore wing covered with microtrichia, two longitudinal veins nearly reaching the tip of the wing margin; usually with three to four crossveins between the longitudinal veins or between them and the marginal vein; fringe cilia wavy (for most fossil species) or straight (for extant species) on the posterior margin of the fore wing; and distal tarsomere with a hook-shaped tooth (hamus) ventrally (Schliephake 1990). The fossil specimens from the three Kachin amber pieces (CNU006122, CNU009269 and CNU009461) share most of the characters listed above except that they lack the tarsal hamus, and only two crossveins in the forewing are visible, but are otherwise most consistent with Stenurothripidae.

The two new genera established here have characteristic comb-like anteromarginal setae (Figs 1C, 5C) on the pronotum, which are yet to be found elsewhere in the family and, therefore, are considered apomorphies of these new genera. In addition, they are distinguished from other stenurothripid genera as follows: *Stenurothrips* have an elongate tenth abdominal segment, which is not the case in the two new genera; the new genera have narrow wings whereas *Exitelothrips*, *Neocomothrips* and *Progonothrips* have broad wings; the genera *Oligothrips* and *Hispanothrips* have a hamus present on the protrasus, which is absent in the two new genera. Note that *Rhethinotrips* and *Progonothrips*, both from Lebanese amber, should perhaps be classified in their own subfamily distinct from other Stenurothripidae.

It is tempting to classify the species here into a single genus with anteromarginal pronotal setae were it not for the considerable differences in their overall morphology. For example, in the female the head of *Parallelotrips* is narrower than the pronotum, while the head of *Didymothrips* is about as wide as the pronotum and they are closely adjoined. The mesonotum of *Parallelotrips* is not closely adjoined to the pronotum, and only the middle part of the anterior margin protrudes forward, whereas they are closer in *Didymothrips* with the mesonotum partly hidden by the pronotum. The legs (Figs 3A, B, 5A) of

Parallelothrips and *Didymothrips* are significantly different, with the latter thinner and not showing any sexual dimorphism. *Parallelothrips* has a slender abdomen with an elongate cone-shape at the end, only a little wider than the thorax, while *Didymothrips* has a broad and flat abdomen with a stout cone-shape tip, much wider than the thorax. The differences between the males are even more significant; males of *Parallelothrips* are similar to females in body size and shape, except for the last three abdominal segments while the males of *Didymothrips* (Fig. 5A) are obviously smaller than their females, with abdomen more slender and thicker. Significant distinctions in body structures are used here to establish two separate, but likely closely related, genera, enriching the known diversity of thrips from Kachin amber.

As we have males and females of both new species, we were able to document sexual dimorphism for both cases. In *Parallelothrips separatus*, females and males differ in the form of their legs as well as the shape of the abdominal apex, while in *Didymothrips abdominalis* the differences between the two sexes are mainly reflected in the abdominal form.

All of the thrips currently documented from Kachin amber have nine antennomeres, a condition considered plesiomorphic for crown-Thysanoptera (Mound et al. 1980). According to a phylogenetic estimation based on morphology (Nel et al. 2014), Stenurothripidae and Thripidae are closely related as they share the following characters: both have narrow wings with M emerging from R proximally or near to the RA-RP fork and the ovipositor is straight or downcurved (Nel et al. 2012). The most recognizable feature of Stenurothripidae is the presence of the broad-based conical sensorium on antennomeres III and IV, which cannot be observed in all of our specimens due to preservation but can be sufficiently discerned in enough individuals to indicate they are Stenurothripidae.

Compared to extant Stenurothripidae, the new species have simple wing venation (Figs 2A, 5D) and fewer crossveins; the wavy duplicated cilia on the forewing are present around the margin of the wing apex and extend to the middle of the posterior wing margin. These cilia extend apically, and each forms a pair with a normal fringe; this situation is similar to other thrips documented from mid-Cretaceous Kachin amber inclusions.

The pollen grains (Fig. 4) around the thrips in CNU-THY-MA2016116 are tiny (average 21.0 μm long and 12.6 μm wide) with a spindle to ovoid shape, along with a smooth surface and a groove medially, and decorated with a few small dark spots laterally (likely pits or punctures). The medial groove is as long as the pollen grain and the depth can reach up to half of the thickness, slightly wider at both ends and narrower medially (Fig. 4C). These characteristics suggest that the pollen grains are from the gymnosperm form-genus *Cycadopites*.

The pollination efficiency of thrips depends mainly on two aspects, the ability to carry pollen, which is determined by the number of setae on the body, and the overall mobility of the animal related to the presence or absence of wings (Lewis 1973). In contrast with *Gymnopollisthrips* (Peñalver et al. 2012), there are no specialized ring setae on the new species, while *Parallelothrips* has many setae on its body, legs, and antennae, and a greater number of anteromarginal bristles and duplicated cilia present on the forewing, which could enhance the capture and transport of pollen grains. Indeed, in most of the specimens of *P. separatus* the posterior margin of the pronotum is not closely adjoined to the anterior margin of the mesonotum and some pollen grains were found

affixed to the posteromarginal and posteroangular setae extending between the two sides (Fig. 5B), suggesting that this structure was likely specialized for the transport of pollen grains.

Here we document two new genera of Thysanoptera from mid-Cretaceous Kachin amber, expanding the known diversity of the order and the family Stenurothripidae, in particular. Currently, Stenurothripidae have been found in the Cretaceous from Lebanon, Spain, and Myanmar, demonstrating their wide distribution at the time. These genera were likely pollinators of gymnosperms during the mid-Cretaceous.

Acknowledgements

We are grateful to Yanchen Zhao, Jiajia Wang, Qi Feng, Yurong Jiang, Xiaotian Liu, Ziqiang Xu and Mao Zhang (Capital Normal University) for their help and technical support. We are grateful for the constructive comments from Dr Manfred R. Ulitzka.

Additional information

Conflict of interest

The authors have declared that no competing interests exist.

Ethical statement

No ethical statement was reported.

Funding

This research was supported by grants from National Natural Science Foundation of China [No. 32020103006] and Support Project of High-level Teachers in Beijing Municipal Universities [No: BPHR20220114].

Author contributions

Dawei Guo: data curation, formal analysis, methodology, writing-original draft. Michael S. Engel: formal analysis, writing-review and editing. Chungkun Shih: writing - review and editing. Dong Ren: methodology, resources, writing-review, supervision.

Author ORCIDs

Dawei Guo  <https://orcid.org/0009-0009-4349-5545>

Michael S. Engel  <https://orcid.org/0000-0003-3067-077X>

Chungkun Shih  <https://orcid.org/0000-0002-3434-2477>

Dong Ren  <https://orcid.org/0000-0001-8660-0901>

Data availability

All of the data that support the findings of this study are available in the main text.




References

- Bailey SF (1949) The genus *Orothrips* Moulton (Thysanoptera: Orothripini). *The Pan-Pacific Entomologist* 25: 104–112.
- Bhatti JS (2006) The classification of Terebrantia (Insecta) into families. *Oriental Insects* 40(1): 339–375. <https://doi.org/10.1080/00305316.2006.10417487>

- Brookes DR, Hereward JP, Terry LI, Walter GH (2015) Evolutionary dynamics of a cycad obligate pollination mutualism – Pattern and process in extant *Macrozamia* cycads and their specialist thrips pollinators. *Molecular Phylogenetics and Evolution* 93: 83–93. <https://doi.org/10.1016/j.ympev.2015.07.003>
- Buckman RS, Mound LA, Whiting MF (2013) Phylogeny of thrips (Insecta: Thysanoptera) based on five molecular loci. *Systematic Entomology* 38(1): 123–133. <https://doi.org/10.1111/j.1365-3113.2012.00650.x>
- Eliyahu D, McCall AC, Lauck M, Trakhtenbrot A, Bronstein JL (2015) Minute pollinators: The role of thrips (Thysanoptera) as pollinators of pointleaf manzanita, *Arctostaphylos pungens* (Ericaceae). *Journal of Pollination Ecology* 16: 64–71. [https://doi.org/10.26786/1920-7603\(2015\)10](https://doi.org/10.26786/1920-7603(2015)10)
- Garcia-Fayos P, Goldarazena A (2008) The role of thrips in pollination of *Arctostaphylos uva-ursi*. *International Journal of Plant Sciences* 169(6): 776–781. <https://doi.org/10.1086/588068>
- Grimaldi D, Engel MS (2005) *Evolution of the Insects*. Cambridge University Press, Cambridge, 755 pp.
- Grimaldi D, Shmakov A, Fraser N (2004) Mesozoic thrips and early evolution of the order Thysanoptera (Insecta). *Journal of Paleontology* 78(5): 941–952. [https://doi.org/10.1666/0022-3360\(2004\)078<0941:MTAEEO>2.0.CO;2](https://doi.org/10.1666/0022-3360(2004)078<0941:MTAEEO>2.0.CO;2)
- Guo M, Xing L, Wang B, Zhang W, Wang S, Shi A, Bai M (2017) A catalogue of burmite inclusions. *Zoological Systematics* 42(3): 249–379. <https://doi.org/10.11865/zs.201715>
- Johnson KP, Dietrich CH, Friedrich F, Beutel RG, Wipfler B, Peters RS, Allen JM, Petersen M, Donath A, Walden KKO, Kozlov AM, Podsiadlowski L, Mayer C, Meusemann K, Vasilikopoulos A, Waterhouse RM, Cameron SL, Weirauch C, Swanson DR, Percy DM, Hardy NB, Terry I, Liu S, Zhou X, Misof B, Robertson HM, Yoshizawa K (2018) Phylogenomics and the evolution of hemipteroid insects. *Proceedings of the National Academy of Sciences of the United States of America* 115(50): 12775–12780. <https://doi.org/10.1073/pnas.1815820115>
- Lewis T (1973) *Thrips, their biology, ecology and economic importance*. Academic Press, New York, 324 pp. <https://doi.org/10.2307/3870>
- Mound LA, Heming BS, Palmer JM (1980) Phylogenetic relationships between the families of recent Thysanoptera. *Zoological Journal of the Linnean Society* 69(2): 111–141. <https://doi.org/10.1111/j.1096-3642.1980.tb01934.x>
- Nel P, Peñalver E, Azar D, Hodebert G, Nel A (2010) Modern thrips families Thripidae and Phlaeothripidae in early Cretaceous amber (Insecta: Thysanoptera). *Annales de la Société Entomologique de France* 46(1–2): 154–163. <https://doi.org/10.1080/00379271.2010.10697651>
- Nel P, Azar D, Prokop J, Roques P, Hodebert G, Nel A (2012) From Carboniferous to Recent: Wing venation enlightens evolution of thysanopteran lineage. *Journal of Systematic Palaeontology* 10(2): 385–399. <https://doi.org/10.1080/14772019.2011.598578>
- Nel P, Retana-Salazar AP, Azar D, Nel A, Huang DY (2014) Redefining the Thripida (Insecta: Paraneoptera). *Journal of Systematic Palaeontology* 12(7): 865–878. <https://doi.org/10.1080/14772019.2013.841781>
- Peñalver E, Nel P (2010) *Hispanothrips* from Early Cretaceous Spanish amber, a new genus of the resurrected family Stenurothripidae (Insecta: Thysanoptera). *Annales de la Société Entomologique de France* 46(1–2): 138–147. <https://doi.org/10.1080/00379271.2010.10697649>

- Peñalver E, Labandeira CC, Barrón E, Delclòs X, Nel P, Nel A, Tafforeau P, Soriano C (2012) Thrips pollination of Mesozoic gymnosperms. *Proceedings of the National Academy of Sciences of the United States of America* 109(22): 8623–8628. <https://doi.org/10.1073/pnas.1120499109>
- Ross AJ (2023) Burmese (Myanmar) amber taxa, on-line supplement v.2023.1. 30 pp. <http://www.nms.ac.uk/explore/stories/natural-world/burmese-amber/>
- Schliephake G (1990) Beiträge zur Kenntnis fossiler Fransenflügler (Thysanoptera) aus dem Bernstein des Tertiär. 1. Beitrag: Stenurothripidae. *Zoology (Delhi)* 2: 163–184. <https://doi.org/10.1007/BF02985981>
- Shi GH, Grimaldi DA, Harlow GE, Wang J, Wang J, Yang MC, Lei WY, Li QL, Li XH (2012) Age constraint on Myanmar amber based on U-Pb dating of zircons. *Cretaceous Research* 37: 155–163. <https://doi.org/10.1016/j.cretres.2012.03.014>
- Terry I (2001) Thrips and weevils as dual, specialist pollinators of the Australian cycad *Macrozamia communis* (Zamiaceae). *International Journal of Plant Sciences* 162(6): 1293–1305. <https://doi.org/10.1086/321929>
- Terry I, Walter GH, Moore C, Roemer R, Hull C (2007) Odor-mediated push–pull pollination in cycads. *Science* 318(5847): 70. <https://doi.org/10.1126/science.1145147>
- ThripsWiki (2023) ThripsWiki – providing information on the World’s thrips. http://thrips.info/wiki/Main_Page [Accessed 22 Mar 2023]
- Tong T, Shih CK, Ren D (2019) A new genus and species of Stenurothripidae (Insecta: Thysanoptera: Terebrantia) from mid-Cretaceous Myanmar amber. *Cretaceous Research* 100: 184–191. <https://doi.org/10.1016/j.cretres.2019.03.005>
- Ulitzka MR (2015) Two new species of Aeolothripidae from Baltic Tertiary amber (Insecta: Thysanoptera). *Palaeodiversity* 8: 89–94. <https://www.researchgate.net/publication/286418745>
- Ulitzka MR (2018) A first survey of Cretaceous thrips from Burmese amber including the establishment of a new family of Tubulifera (Insecta: Thysanoptera). *Zootaxa* 4486(4): 548–558. <https://doi.org/10.11646/zootaxa.4486.4.8>
- Ulitzka MR (2019) Five new species of *Rohrthrips* (Thysanoptera: Rohrthripidae) from Burmese amber, and the evolution of Tubulifera wings. *Zootaxa* 4585(1): 27–40. <https://doi.org/10.11646/zootaxa.4585.1.2>
- Ulitzka MR (2022) New genera and species of Rohrthripidae (Thysanoptera: Tubulifera) from Burmese Cretaceous amber. *Zootaxa* 5162(1): 1–36. <https://doi.org/10.11646/zootaxa.5162.1.1>
- Willmer P (2011) *Pollination and floral ecology*. Princeton University Press, Princeton, 778 pp. <https://doi.org/10.1515/9781400838943>
- zur Strassen R (1973) Fossile Fransenflügler aus mesozoischem Bernstein des Libanon (Insecta: Thysanoptera). *Stuttgarter Beiträge zur Naturkunde A* 256: 1–51.

A new species of *Raorchestes* (Anura, Rhacophoridae) from Yunnan Province, China

Lingyun Du^{1,2}, Yuhan Xu^{1,2}, Shuo Liu³, Guohua Yu^{1,2}

1 Key Laboratory of Ecology of Rare and Endangered Species and Environmental Protection, Guangxi Normal University, Ministry of Education, Guilin 541004, China

2 Guangxi Key Laboratory of Rare and Endangered Animal Ecology, College of Life Science, Guangxi Normal University, Guilin 541004, China

3 Kunming Natural History Museum of Zoology, Kunming Institute of Zoology, Chinese Academy of Sciences, Kunming 650223, China

Corresponding authors: Guohua Yu (yugh2018@126.com); Shuo Liu (liushuo@mail.kiz.ac.cn)

Abstract

A new bush frog species is described from Yunnan, China, based on phylogenetic analyses, species delimitation analyses, and morphological comparisons. *Raorchestes hekouensis* sp. nov. is distinguished from all other congeners by a combination of 11 morphological characters. The new species brings the current number of *Raorchestes* species in China to ten, nine of which are distributed in Yunnan. Molecular analyses supported an unnamed lineage previously recorded as “*Raorchestes gryllus*” in northern Vietnam. Further studies including additional samples are necessary to clarify the species diversity and boundaries of *Raorchestes* in China and Indochina.

Key words: Indochina, “*Raorchestes gryllus*”, *Raorchestes hekouensis* sp. nov., species diversity, taxonomy



Academic editor: Angelica Crottini

Received: 8 May 2023

Accepted: 5 January 2024

Published: 22 February 2024

ZooBank: <https://zoobank.org/OA4E2531-A55E-4F94-A479-D051D8A84256>

Citation: Du L, Xu Y, Liu S, Yu G (2024) A new species of *Raorchestes* (Anura, Rhacophoridae) from Yunnan Province, China. ZooKeys 1192: 213–235. <https://doi.org/10.3897/zookeys.1192.106013>

Copyright: © Lingyun Du et al.

This is an open access article distributed under terms of the Creative Commons Attribution License ([Attribution 4.0 International – CC BY 4.0](https://creativecommons.org/licenses/by/4.0/)).

Introduction

The genus *Raorchestes* Biju, Shouche, Dubois, Dutta & Bossuyt, 2010, which currently contains 76 species (Frost 2023), is one of the most speciose genera within the family Rhacophoridae. Members of *Raorchestes* are characterized by a small body size (15–45 mm), lack of vomerine teeth, transparent/translucent vocal sac when calling, and direct development (Biju et al. 2010; Vijayakumar et al. 2014). *Raorchestes* is widely distributed in South and Southeast Asia, from India to Nepal, Myanmar, Thailand, and Laos to southwestern China, Vietnam, Cambodia, and West Malaysia (Frost 2023).

Most *Raorchestes* species were initially assigned to the genus *Philautus* Gistel, 1848 (Bossuyt and Dubois 2001); however, Yu et al. (2009) and Li et al. (2009) revealed that frogs traditionally classified in *Philautus* consisted of two groups rather than being a monophylum, and Li et al. (2009) proposed the name *Pseudophilautus* Laurent, 1943 for the group primarily distributed on the Indian subcontinent, which itself consists of two reciprocally monophyletic groups, i.e., a radiation with notably large diversity in the Western Ghats of India and a radiation with large diversity in Sri Lanka. Biju et al. (2010) later erected the genus *Raorchestes* for the clade with substantial diversity in the

Western Ghats to distinguish it from *Pseudophilautus* sensu stricto, a clade of 80 species largely restricted to Sri Lanka (Biju et al. 2010; Meegaskumbura et al. 2019). Based on phylogenetic analysis, Li et al. (2013) suggested that *Raorchestes* and *Pseudophilautus* formed a sister group of *Kurixalus* Ye, Fei & Dubois, 1999; however, more recent studies based on wider genus-level sampling suggested *Raorchestes* is sister to *Pseudophilautus* (Vijayakumar et al. 2014; Chan et al. 2018; Garg et al. 2021) or the clade composed of *Raorchestes* and *Pseudophilautus* is sister to *Mercurana* Abraham, Pyron, Ansil, Zachariah & Zachariah, 2013 (Meegaskumbura et al. 2019).

As one of the most diverse groups in the Rhacophoridae family, *Raorchestes* frogs form a distinct radiation with more than 80% of the known species distributed in South Asia, especially in India. As such, most research attention has been paid to the taxonomy and evolution of Indian *Raorchestes*. For examples, Vijayakumar et al. (2014) reported on *Raorchestes* relationships within the Western Ghats, naming nine species and recognizing 15 clades within the Western Ghats complex; Vijayakumar et al. (2016) revealed that geological processes, Quaternary glaciations, and ecological gradients drove diversification of *Raorchestes* frogs in the Western Ghats; and Garg et al. (2021) named five species in the Western Ghats and delimited *Raorchestes* into 16 species groups.

The diversity of *Raorchestes* in southwestern China, Indochina, the Himalayas, and northeastern India is markedly lower than that in the Western Ghats. To date, only 16 species are known from these areas, including *R. andersoni* (Ahl, 1927), *R. annandalii* (Boulenger, 1906), *R. cangyuanensis* Wu, Suwannapoom, Xu, Murphy & Che, 2019, *R. dulongensis* Wu, Liu, Gao, Wang, Li, Zhou, Yuan & Che, 2021, *R. gryllus* (Smith, 1924), *R. hillisi* Jiang, Ren, Guo, Wang & Li, 2020, *R. huanglianshan* Jiang, Wang, Ren & Li, 2020, *R. longchuanensis* (Yang & Li, 1978), *R. malipoensis* Huang, Liu, Du, Bernstein, Liu, Yang, Yu & Wu, 2023, *R. manipurensis* (Mathew & Sen, 2009), *R. menglaensis* (Kou, 1990), *R. parvulus* (Boulenger, 1893), *R. rezakhani* Al-Razi, Maria & Muzaffar, 2020, *R. sahai* (Sarkar & Ray, 2006), *R. shillongensis* (Pillai & Chanda, 1973), and *R. yadongensis* Zhang, Shu, Liu, Dong & Guo, 2022 (Frost 2023). Of these 16 species, nine are known in China (i.e., *R. andersoni*, *R. cangyuanensis*, *R. dulongensis*, *R. hillisi*, *R. huanglianshan*, *R. longchuanensis*, *R. malipoensis*, *R. menglaensis*, and *R. yadongensis*), all from the border areas of Yunnan, except for *R. yadongensis*, which is only known from southern Tibet (Zhang et al. 2022). Moreover, the distribution of the *R. andersoni* is also recorded in southern Medog, Tibet (e.g., Chen et al. 2020; Fei et al. 2012), *R. andersoni* was originally described “on level marshy flats on the banks of the Nam-poung [= Nanben River] in the centre of the Kakhien Hills”, Yingjiang County, Yunnan, China by Anderson (1878), and it was once recognized as *Theلودerma andersoni* by Li et al. (2009). However, Hou et al. (2017) suggested that it possibly belonged to *Raorchestes* on the basis of morphological similarities to *Philautus longchuanensis*, subsequently Chen et al. (2020) transferred *T. andersoni* (Ahl, 1927) to the genus *Raorchestes* based on the molecular evidence. *Raorchestes parvulus* was originally described from Karin Bia-po in Myanmar by Boulenger (1893) and previously recorded from China by Yu et al. (2019) based on specimens from Menglun, Yunnan. However, Jiang et al.

(2020) considered that the record of *R. parvulus* from Yunnan was misidentified and revised it to *R. menglaensis*.

Six *Raorchestes* species are known from Southeast Asia, i.e., *R. parvulus* (Boulenger, 1893), *R. gryllus*, *R. menglaensis*, *R. huanglianshan*, *R. longchuanensis*, and *R. malipoensis* (Frost 2023). However, the taxonomic status of *R. gryllus* is problematic. This species was originally described from Langbian Plateau in Lam Dong Province, southern Vietnam, and has been widely reported in Vietnam (Lam Dong, Dak Lak, Gia Lai, and Kon Tum, Lao Cai, Cao Bang, Vinh Phu, and Bac Thai) and Laos (Sepian, Boloven Highlands, Champasak Province) (Bourret 1937, 1939, 1942; Orlov et al. 2002, 2012; Teynié et al. 2004; Nguyen et al. 2009). Biju et al. (2010) confirmed the affiliation of *R. gryllus* with the genus *Raorchestes* based on molecular data from Li et al. (2009). However, those specimens used in Li et al. (2009) were collected from Pac Ban, Tuyen Quang, northern Vietnam, and Orlov et al. (2012) considered records of *R. gryllus* in this region to be highly improbable. Furthermore, the species contains a series of tubercles along the outer side of the forearm and foot, and a dermal projection on the snout (Smith 1924), very similar to members of *Kurixalus*, and differing in egg capsule appearance from other *Raorchestes* species, with thick and semi-transparent eggs in *R. gryllus* compared to transparent eggs in other *Raorchestes* species (Orlov et al. 2012).

Recently, Poyarkov et al. (2021) suggested the transfer of *R. gryllus* to *Kurixalus* based on unpublished molecular data of specimens from the type locality and unpublished morphological data from type material, implying that the so-called "*R. gryllus*" specimens from northern Vietnam used in previous phylogenetic analyses (e.g., Li et al. 2009, 2013; Nguyen et al. 2014; Wu et al. 2019) are not actually true *K. gryllus*, but represent an unnamed species. Moreover, Huang et al. (2023) considered that the specimen of *R. UI ROM30288* from Pac Ban, Tuyen Quang, northern Vietnam was misidentified and revised it to *R. malipoensis*. This suggests that other records of the species from Vietnam and Laos need further examination.

Yunnan Province harbors the highest amphibian species diversity in China (AmphibiaChina, 2022), with many new species described in recent years (e.g., Gan et al. 2020; Liu et al. 2021; Wang et al. 2022). During recent field surveys in Hekou, Yunnan, China, we collected eight specimens of *Raorchestes*. Morphological comparison and phylogenetic analysis indicated that these specimens could be distinguished from all other members of the genus *Raorchestes*, except for the *R. UI ROM 38828* from northern Vietnam in molecular analysis, indicating that the eight specimens from Hekou and the ROM38828 specimen from northern Vietnam represent a new species.

Materials and methods

Sampling

Field surveys were conducted in March 2019 and April 2023 at Liangzi village, Hekou, Yunnan, China (Fig. 1). Specimens were euthanized, fixed, and preserved in 75% ethanol. Liver tissues were taken and preserved in 99% ethanol. Voucher specimens and tissue samples were deposited at Guangxi Normal University (GXNU), China.

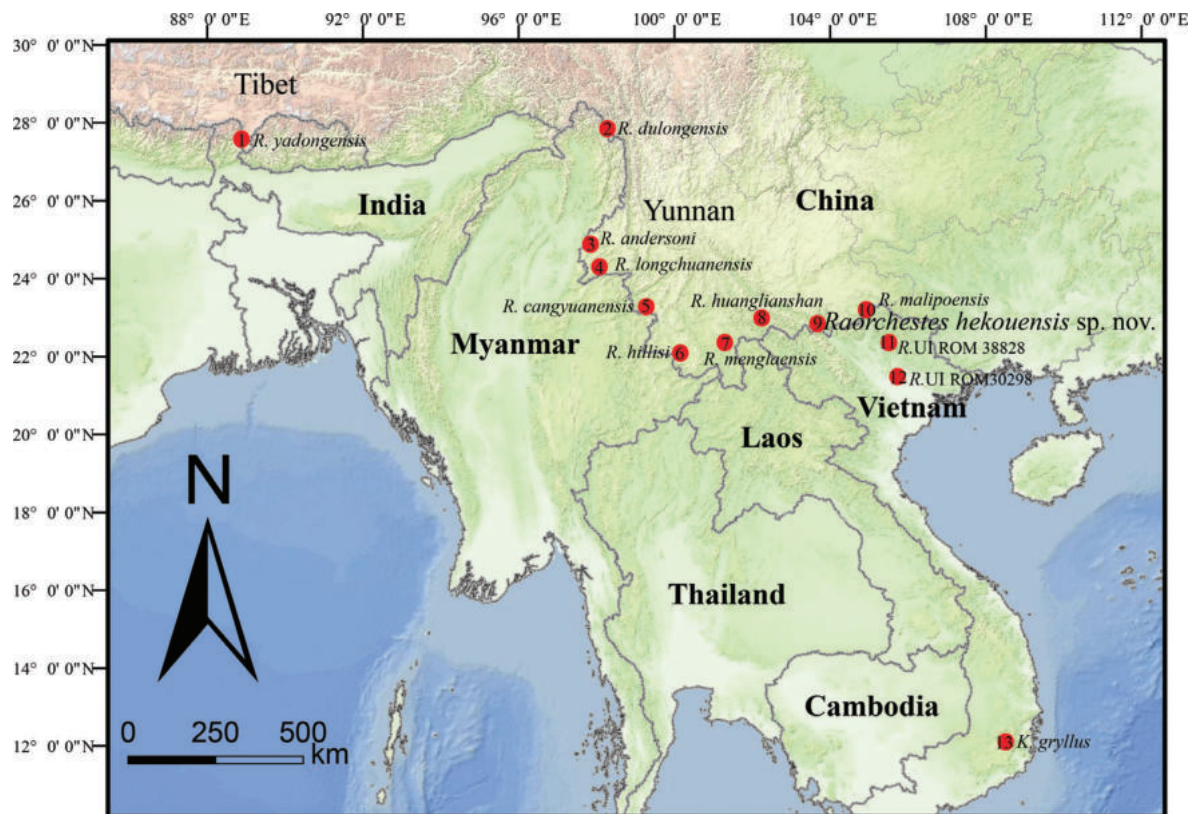


Figure 1. Map showing type localities of *Raorchestes* species originally described from China (1–10), type locality of *K. gryllus* in Vietnam (13), and collection sites of *R. UI* used in this study (11, 12). *Raorchestes hekouensis* sp. nov. is known from the type locality (9) and Pac Ban, Tuyen Quang, Vietnam (11).

Morphology and morphometrics

All measurements were made with slide calipers to the nearest 0.1 mm. Morphological characters and measurements followed Du et al. (2020) and included: snout-vent length (**SVL**); head length (**HL**); head width (**HW**); snout length (**SL**); internarial distance (**INS**); interorbital distance (**IOS**); maximum transverse distance of upper eyelid (**UEW**); eye diameter (**ED**); tympanum diameter (**TD**); eye-nostril distance (**EN**); length of lower arm and hand (**LAHL**); tibia length (**TIL**); length of foot and tarsus (**TFL**); foot length (**FL**). Morphological measurements of the specimens are given in Table 1. Males and females were identified based on the presence of an external single subgular vocal sac or sac slit opening. Comparative data on the morphology of other *Raorchestes* species were obtained from previous publications (Boulenger 1893, 1906; Smith 1924; Pillai and Chanda 1973; Yang and Li 1978; Kou 1990; Bossuyt and Dubois 2001; Sarkar and Ray 2006; Fei et al. 2009, 2012; Mathew and Sen 2009; Orlov et al. 2012; Wu et al. 2019, 2021; Al-Razi et al. 2020; Che et al. 2020; Jiang et al. 2020; Zhang et al. 2022; Huang et al. 2023).

DNA sequencing

We extracted genomic DNA from liver tissues stored in 99% ethanol following standard protocols (Vences et al. 2012). We amplified and sequenced the mitochondrial 16S ribosomal RNA (16S) genes using the primer pair L2188 (Matsui et al. 2006) and 16H1 (Hedges, 1994). Polymerase chain reaction (PCR) amplifications were performed in a 50- μ L reaction volume, with an initial denaturing

Table 1. Measurements (in mm) of *Raorchestes hekouensis* sp. nov. specimens from Liangzi, Hekou, Yunnan. Holotype is marked with an asterisk (*).

Catalog No.	Adults					Sub-adults		
	GXNU YU000159*	GXNU YU000536	GXNU YU000537	GXNU YU000538	GXNU YU000160	GXNU YU000153	GXNU YU000154	GXNU YU000156
Sex	Male	Male	Male	Male	Female	Male	Female	Female
SVL	17.5	17.8	16.7	16.1	21.1	14.5	12.5	12.9
HL	6.1	5.8	5.7	5.6	7.2	5.1	4.1	4.5
HW	6.9	7.1	6.1	6.1	7.6	5.3	4.9	4.5
SL	2.4	1.7	1.6	1.9	2.8	1.7	1.3	1.6
INS	2.2	2.4	2.1	2.3	2.6	2.0	1.6	1.8
IOS	2.4	2.8	2.3	2.1	2.7	2.0	1.7	1.8
UEW	1.9	1.7	1.9	1.5	2.1	1.2	1.1	1.7
ED	2.5	3.1	2.7	2.4	3.0	2.3	2.0	2.0
TD	1.3	1.1	1.3	1.2	1.4	0.7	0.5	0.8
DNE	1.5	1.2	1.3	1.3	1.8	1.2	1.0	1.0
LAHL	8.5	7.4	7.9	7.1	10.1	6.9	5.8	6.0
TIL	9.2	8.8	8.4	7.8	10.6	7.7	6.1	6.1
TFL	11.4	11.0	10.4	8.9	13.6	8.8	7.8	7.5
FL	6.6	6.6	5.7	5.4	8.1	5.1	4.1	4.1

step at 95 °C for 4 min, 35 cycles of denaturing at 94 °C for 1 min, annealing at 51 °C for 1 min, and extension at 72 °C for 1 min, with a final extension step of 72 °C for 10 min. Sequencing was conducted using the corresponding PCR primers. All new sequences were deposited in GenBank under accession numbers ON986419–ON986422, OQ029526, OQ859106 and OQ859107 (Table 2).

Phylogenetic analysis and species delimitation

To examine the phylogenetic position of the specimens collected from Hekou, Yunnan, China, we reconstructed phylogenetic trees of the genus *Raorchestes* based on sequences of the 16S rRNA (16S) genes. Furthermore, 35 homologous sequences of other *Raorchestes* species were obtained from GenBank (Table 2). *Pseudophilautus kani* (Biju & Bossuyt, 2009) and *Pseudophilautus amboli* (Biju & Bossuyt, 2009) were selected as outgroups based on Wu et al. (2021). All sequences were aligned in MEGA v. 7.0 (Kumar et al. 2016) using the ClustalW tool and both ends of the sequence were trimmed to minimize missing characters.

Phylogenetic relationships were inferred based on maximum likelihood (ML) and Bayesian inference (BI) analyses. BI analysis was conducted in MrBayes v. 3.2.6 (Ronquist et al. 2012). The best-fitting model (GTR + I + G) was chosen using the Akaike Information Criterion (AIC) in JModelTest v. 2.1.10 (Darriba et al. 2012). Four Monte Carlo Markov chains were started from a random tree. The chains were run for three million generations and sampled every 100 generations, with the first 25% of sampled trees discarded as burn-in. The remaining trees were used to create a consensus tree and to estimate Bayesian posterior probabilities (BPP). ML analysis was performed using RAxML v. 8.2.10 (Stamatakis 2014) under the GTR + I + G model. Tree searches were performed 100 times with 1000 bootstrap (BS) replicates to assess node support. Nodes with BPP \geq 0.95 and BS \geq 70 were considered well supported. Additionally, uncorrected pairwise genetic distances (p -distances) between species in 16S rRNA sequences were calculated using MEGA v. 7.0. (Kumar et al. 2016).

Table 2. Information on voucher numbers, localities, and GenBank accession numbers for all specimens used in this study.

Species	Locality	Voucher No.	16S	Reference
<i>Raorchestes hekouensis</i> sp. nov.	Hekou, Yunnan, China	GXNU YU000153	ON986419	This study
<i>Raorchestes hekouensis</i> sp. nov.	Hekou, Yunnan, China	GXNU YU000154	OQ029526	This study
<i>Raorchestes hekouensis</i> sp. nov.	Pac Ban, Tuyen Quang, Vietnam	ROM 38828	KC465838	Li et al. (2013)
<i>Raorchestes hekouensis</i> sp. nov.	Hekou, Yunnan, China	GXNU YU000156	ON986420	This study
<i>Raorchestes hekouensis</i> sp. nov.	Hekou, Yunnan, China	GXNU YU000159	ON986421	This study
<i>Raorchestes hekouensis</i> sp. nov.	Hekou, Yunnan, China	GXNU YU000160	ON986422	This study
<i>Raorchestes hekouensis</i> sp. nov.	Hekou, Yunnan, China	GXNU YU000536	OQ859106	This study
<i>Raorchestes hekouensis</i> sp. nov.	Hekou, Yunnan, China	GXNU YU000537	OQ859107	This study
<i>Raorchestes andersoni</i>	Medog, Tibet, China	KIZYPX16167	MW023609	Chen et al. (2020)
<i>Raorchestes andersoni</i>	Medog, Tibet, China	KIZ014104	MW023610	Chen et al. (2020)
<i>Raorchestes annandalii</i>	Nepal	CDZMTU419	MT983169	Khatiwada et al. (2021)
<i>Raorchestes agasthyaensis</i>	Western Ghats, India	CESF492	JX092723	Vijayakumar et al. (2014)
<i>Raorchestes archeos</i>	Agasthyamalai Massif, Western Ghats, India	CESF1190	JX092675	Vijayakumar et al. (2014)
<i>Raorchestes cangyuanensis</i>	Cangyuan, Yunnan, China	KIZ 015855	MN475866	Wu et al. (2019)
<i>Raorchestes cangyuanensis</i>	Cangyuan, Yunnan, China	KIZ 015856	MN475867	Wu et al. (2019)
<i>Raorchestes crustai</i>	Elivalmalai Massif, Western Ghats, India	CESF1199	JX092677	Vijayakumar et al. (2014)
<i>Raorchestes chromasynchysi</i>	Western Ghats, India	CESF1127	JX092667	Vijayakumar et al. (2014)
<i>Raorchestes dulongensis</i>	Qinlangdang, Yunnan, China	KIZ 035082	MW537814	Wu et al. (2019)
<i>Raorchestes dulongensis</i>	Qinlangdang, Yunnan, China	KIZ0 35125	MW537815	Wu et al. (2019)
<i>Raorchestes ghatei</i>	Western Ghats, India	CESF1262	JX092687	Vijayakumar et al. (2014)
<i>Raorchestes UI</i>	Tam Dao, Vinh Phuc, Vietnam	ROM 30298	MN475869	Wu et al. (2019)
<i>Raorchestes hillisi</i>	Xiding, Yunnan, China	CIB116329	MT488412	Jiang et al. (2020)
<i>Raorchestes hillisi</i>	Xiding, Yunnan, China	CIB116330	MT488413	Jiang et al. (2020)
<i>Raorchestes huanglianshan</i>	Lvchun, Yunnan, China	CIB116353	MT488415	Jiang et al. (2020)
<i>Raorchestes huanglianshan</i>	Lvchun, Yunnan, China	CIB116354	MT488417	Jiang et al. (2020)
<i>Raorchestes leucolatus</i>	Elivalmalai Massif, Western Ghats, India	CESF1147	JX092669	Vijayakumar et al. (2014)
<i>Raorchestes longchuanensis</i>	Gongdong, Yunnan, China	KIZ 048468	MN475870	Wu et al. (2019)
<i>Raorchestes longchuanensis</i>	Gongdong, Yunnan, China	KIZ048492	MN475871	Wu et al. (2019)
<i>Raorchestes malipoensis</i>	Pac Ban, Tuyen Quan, Vietnam	ROM30288	GQ285674	Li et al. (2009)
<i>Raorchestes malipoensis</i>	Malipo, Yunnan, China	GXNU 000339	ON128245	Huang et al. (2023)
<i>Raorchestes menglaensis</i>	Zhushihe, Yunnan, China	CIB116338	MT488403	Jiang et al. (2020)
<i>Raorchestes menglaensis</i>	Zhushihe, Yunnan, China	CIB116340	MT488404	Jiang et al. (2020)
<i>Raorchestes parvulus</i>	Pulau Langkawi, Malaysia	LSUHC 7596	MH590202	Chan et al. (2018)
<i>Raorchestes parvulus</i>	Gunung Stong, Malaysia	LSUHC 11118	MH590201	Chan et al. (2018)
<i>Raorchestes rezakhani</i>	Maulovibazar, Bangladesh	JnUZool-A0319	MN072374	Al-Razi et al. (2020)
<i>Raorchestes shillongensis</i>	Malki forest, Shilong, Meghalaya, India	R2	MG980283	Unpublished
<i>Raorchestes</i> sp. 1	India	CESF420	JX092712	Vijayakumar et al. (2014)
<i>Raorchestes tuberothumerus</i>	Western Ghats, India	0073PhiTub	EU450004	Biju and Bossuyt, (2009)
<i>Raorchestes uthamani</i>	Western Ghats, India	CESF483	JX092722	Vijayakumar et al. (2014)
<i>Raorchestes yadongensis</i>	Yadong, Xizang, China	YBU 21222	OP345440	Zhang et al. (2022)
<i>Raorchestes yadongensis</i>	Yadong, Xizang, China	YBU 21223	OP345441	Zhang et al. (2022)
<i>Pseudophilautus kani</i>	Western Ghats, India	CESF497	JX092724	Vijayakumar et al. (2014)
<i>Pseudophilautus amboli</i>	Western Ghats, India	BNHS4399	EU450025	Biju and Bossuyt (2009)

We used two approaches, i.e., the Bayesian Poisson Tree Processes (bPTP; Zhang et al. 2013) and Assemble Species by Automatic Partitioning (ASAP; Puillandre et al. 2021), to delimit species boundaries. The bPTP method was run on the bPTP server (<http://species.h-its.org/>) using the tree generated by Bayesian phylogenetic analysis and default parameters. For the ASAP method, the simple distance (p -distance) model was used and the partitioning with the lowest ASAP score was selected as the best, as per Puillandre et al. (2021).

Results

Phylogenetic analysis and genetic divergence

The obtained sequence alignment was 552 bp long and included 211 variable sites and 152 parsimony informative sites. Phylogenetic analysis (Fig. 2) revealed that the specimens from Hekou, Yunnan, China, *R. malipoensis* and *R. UI* from northern Vietnam formed a monophyletic group, which itself contained three distinct branches, one consisting of the specimens from Hekou and a specimen of *R. UI* from Pac Ban, Tuyen Quang, Vietnam (ROM 38828) with strong support (BPP = 100, BS = 100) and short internal branch lengths, one consisting only of *R. UI* from Tam Dao, Vinh Phuc, Vietnam (ROM 30298), and one consisting of the recently named bush frog species *R. malipoensis*, which included a specimen previously mistaken of "*R. gryllus*" from Pac Ban, Tuyen Quang, Vietnam (ROM 30288). The clade containing specimens from Hekou was recovered as the sister to *R. malipoensis* with strong support. The bPTP analysis delimited the three lineages into three candidate species (Fig. 3). The ASAP analysis identified 10 partitions (Fig. 3) and the best partition (score = 2.5) also grouped the three lineages into three candidate species. The 16S *p*-distances between the clade consisting of Hekou specimens and the other *Raorchestes* lineages included in this study ranged from 2.5% (*R. malipoensis*) to 12.9% (*R. archeos*), greater than the divergence between *R. hillisi* and *R. yadongensis* (2.0%; Table 3).

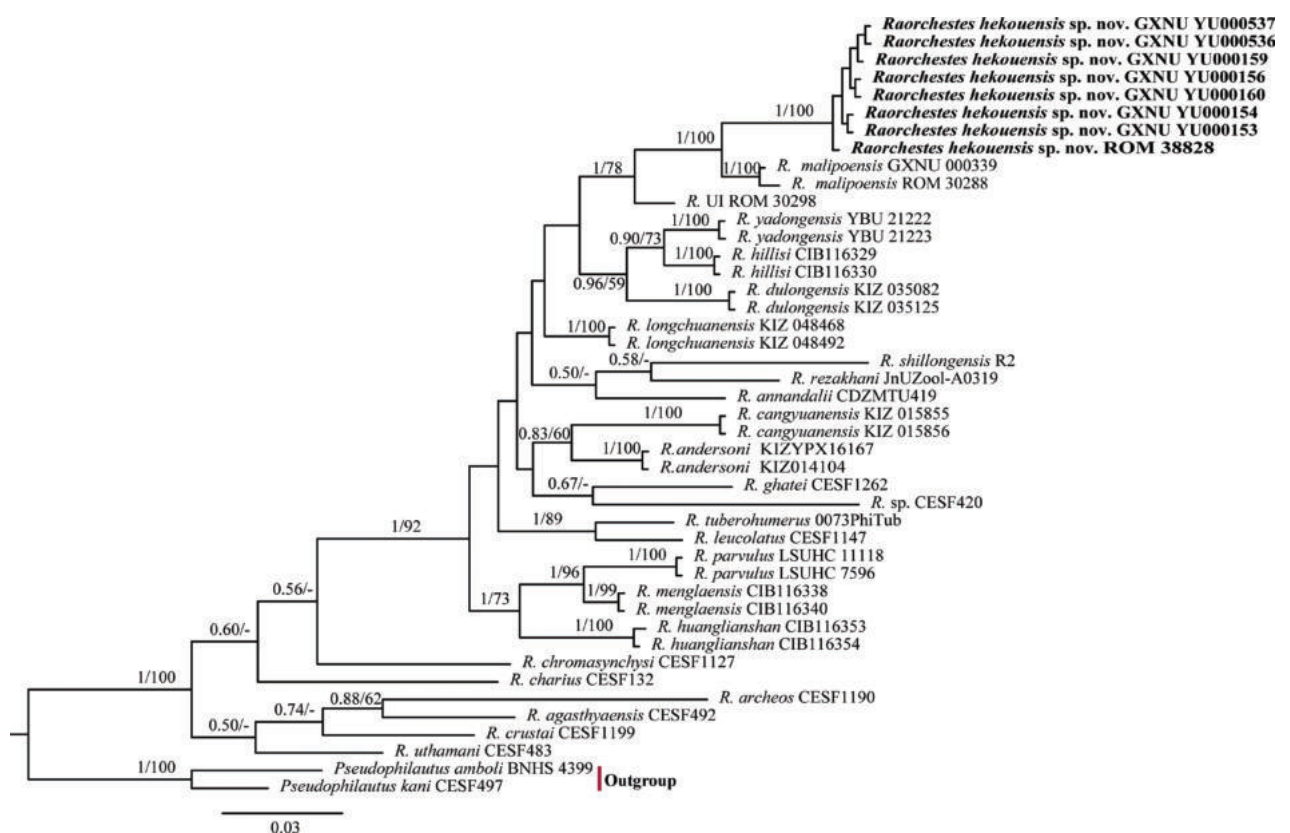


Figure 2. Bayesian phylogram of *Raorchestes parvulus* group estimated from 16S rRNA showing placement of *Raorchestes hekouensis* sp. nov. Nodal support values are shown above branches as Bayesian posterior probability (BPP) / ML bootstrap support (BS), and the symbol “-” indicates value below 50.

Table 3. Uncorrected p-distance (%) in 16S rRNA sequences of *Raorchestes* species used in this study.

ID	Species	1	2	3	4	5	6	7	8	9	10	11	12	13	14	15	16	17	18	19	20	21	22	23	24	25
1	<i>R. hekouensis</i> sp. nov.																									
2	<i>R. malipoensis</i>	2.5																								
3	<i>R. UIROM30298</i>	3.7	2.9																							
4	<i>R. longchuanensis</i>	4.1	3.5	3.2																						
5	<i>R. rezakhani</i>	5.3	5.0	4.6	4.8																					
6	<i>R. andersoni</i>	5.4	4.9	4.9	4.4	5.2																				
7	<i>R. tuberohumerus</i>	6.0	6.2	5.4	5.3	6.6	6.5																			
8	<i>R. menglaensis</i>	6.0	5.5	4.7	4.4	6.7	5.9	5.5																		
9	<i>R. annandalli</i>	6.1	5.7	5.3	4.6	5.1	4.4	7.0	6.4																	
10	<i>R. hillisi</i>	6.1	5.2	3.5	4.5	5.2	5.3	5.6	5.5	5.5																
11	<i>R. parvulus</i>	6.1	6.8	6.9	5.2	8.2	6.7	7.3	2.5	6.5	7.3															
12	<i>R. dulongensis</i>	6.2	5.7	3.7	3.9	5.6	4.8	6.8	5.8	5.9	3.7	7.5														
13	<i>R. leucolatus</i>	6.6	6.1	5.9	5.1	7.3	6.2	3.3	5.3	6.4	6.5	5.9	7.3													
14	<i>R. yadongensis</i>	6.7	5.1	3.9	4.4	6.0	4.9	5.5	5.5	5.3	2.0	6.7	3.7	5.7												
15	<i>R. ghatei</i>	7.1	6.7	5.2	5.4	5.7	5.0	5.7	6.5	5.9	5.7	7.7	5.8	4.9	5.2											
16	<i>R. cangyuanensis</i>	7.6	6.6	5.8	5.8	6.5	4.4	7.3	5.8	6.0	6.2	7.6	6.4	6.9	5.4	6.5										
17	<i>R. huanglianshan</i>	7.6	6.8	6.0	5.5	6.3	6.3	7.1	4.7	6.7	5.8	5.5	6.1	7.0	5.6	6.9	6.4									
18	<i>R. sp 1</i>	8.5	8.0	7.2	6.3	7.0	8.1	8.1	9.0	7.6	8.1	10.6	7.8	8.0	8.0	7.7	9.7	9.9								
19	<i>R. uthamani</i>	8.7	7.9	8.6	8.2	9.0	8.3	8.9	8.6	9.2	8.5	8.6	8.8	6.8	8.3	9.1	9.9	9.0	11.5							
20	<i>R. shillongensis</i>	8.9	8.0	7.3	6.8	5.8	7.3	8.5	8.0	7.0	7.9	9.2	7.7	7.8	7.5	8.4	9.8	8.2	7.4	10.6						
21	<i>R. charius</i>	9.2	9.3	9.1	8.4	8.6	8.9	7.8	8.1	10.1	9.2	8.9	9.7	8.0	8.9	8.5	9.8	7.7	10.9	7.9	10.4					
22	<i>R. agasthyaensis</i>	9.7	9.3	9.3	9.4	9.6	9.3	9.1	9.0	11.0	8.5	9.4	9.4	7.8	9.0	10.4	10.9	9.9	12.5	6.8	11.9	9.2				
23	<i>R. chromasyachysi</i>	9.8	9.1	9.1	7.4	8.8	7.8	9.4	8.7	9.7	8.5	9.1	8.0	7.8	7.4	7.2	8.8	8.6	10.3	5.7	9.5	7.1	7.3			
24	<i>R. crustai</i>	12.6	11.4	10.3	11.6	10.6	10.7	10.4	10.7	12.8	9.6	11.4	10.3	9.4	9.1	10.2	11.8	10.4	14.7	5.3	13.0	7.9	6.2	9.5		
25	<i>R. archeos</i>	12.9	11.2	12.5	12.2	12.1	12.4	12.6	11.3	12.2	11.1	11.8	12.6	11.8	10.1	13.5	12.8	11.7	14.7	9.1	15.8	10.1	8.2	10.1	9.2	

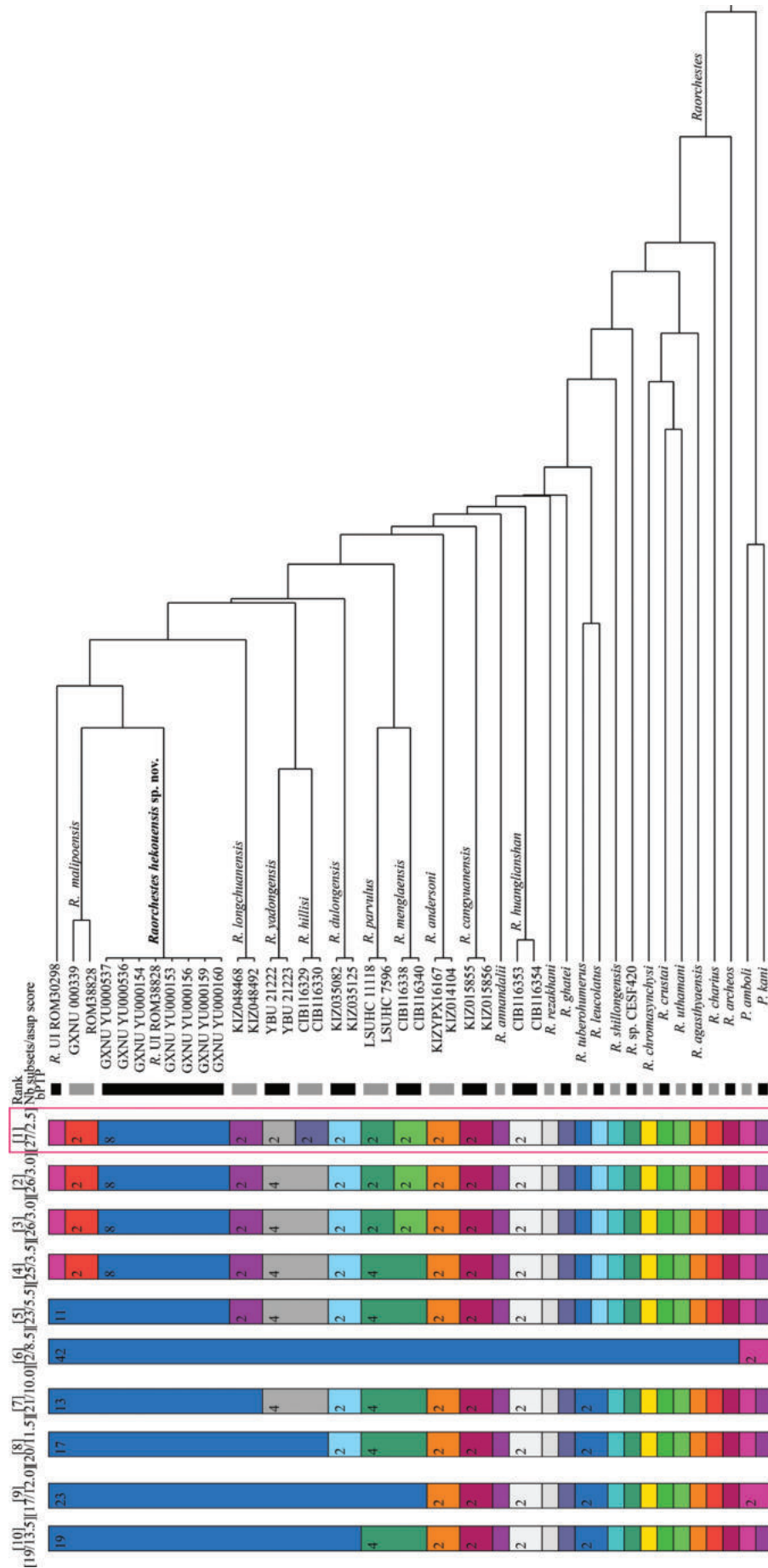


Figure 3. ASAP species delimitation with *Raorchestes* based on 16S sequences. ASAP analysis generated 10 partitions and ranked them using the lowest ASAP score as the best option, and the best partition is highlighted in red. Black and gray vertical bars indicate results of bPTP species delimitation.

Taxonomic account

Raorchestes hekouensis sp. nov.

<https://zoobank.org/4175879C-5620-49B0-B016-8489657C6069>

Table 1, Figs 4–8

Chresonymy. *Raorchestes gryllus* (Li et al. 2013).

Type material. Holotype. GXNU YU000159, adult male, collected on 25 March 2019 by Shuo Liu from Liangzi, Hekou, Yunnan, China (22°49'N, 103°44'E, 1200 m a.s.l.; Fig. 1).

Paratypes. Adult female (GXNU YU000160), three sub-adults (GXNU YU000153, GXNU YU000154, and GXNU YU000156) with the same collection information as the holotype, and three adult males (GXNU YU000536, GXNU YU000537 and GXNU YU000538) collected at the same locality as the holotype on 4 April 2023 by Lingyun Du and Shuo Liu.

Etymology. The specific epithet *hekouensis* is named after the type locality, Hekou County, Yunnan, China. We suggest “Hekou bush frog” as its English common name, and “Hé Kǒu Guàn Shù Wā (河口灌树蛙)” as its Chinese common name.

Diagnosis. *Raorchestes hekouensis* sp. nov. is distinguished from all other relevant congeners by a combination of the following characters: (1) small body size (male SLV 16.1–17.5 mm, $n = 4$; female 21.1 mm, $n = 1$); (2) tympanum distinct; (3) tips of all fingers and toes expanded into discs with circummarginal grooves; (4) rudimentary webbing on toes; (5) all fingers and toes with lateral dermal fringes; (6) inner metacarpal tubercle present and outer metacarpal tubercle indistinct; (7) heels meeting when limbs held at right angles to body; (8) discs of fingers and toes yellow; (9) male with external single subgular vocal sac; (10) distinct X-shaped dark brown marking on back; (11) inner metatarsal tubercle oval, outer metatarsal tubercle absent.

Description of holotype. GXNU YU000159, adult male, body size small (SVL 17.5 mm); head wider than long (HW = 6.9 mm, HL = 6.1 mm); snout rounded in profile, projecting beyond lower jaw, snout length almost equal to diameter of eye (SL = 2.4 mm; ED = 2.5 mm); canthus rostralis rounded, loreal region slightly concave; internarial distance slightly less than interorbital distance, and wider than maximum width of upper eyelid (INS = 2.2 mm; IOS = 2.4 mm; UEW = 1.9 mm); tympanum distinct (TD = 1.3 mm); tongue pyriform, with deep notch at posterior tip; vomerine teeth absent; temporal fold distinct; dorsolateral fold absent. Length of forelimb and hand slightly shorter than half of snout-vent length (LAHL = 8.5 mm, SVL = 17.5); relative fingers lengths: I < II < IV < III; tips of all four fingers expanded into discs with circummarginal grooves; lateral dermal fringes on all fingers; subarticular tubercles distinct, rounded; supernumerary tubercles absent; no webbing between fingers; inner metacarpal tubercle present, outer metacarpal tubercle indistinct; nuptial pads present on first and second fingers in male. Hindlimbs relatively slender, thigh length (TIL = 9.2) shorter than tibia length (TL = 11.4), but greater than foot length (FL = 6.6); tibiotarsal articulation reaching anterior of eye when hindlimb stretched alongside body; heels meeting when limbs held at right angles to body; relative toe lengths: I < II < III < V < IV; tips of toes with well-developed discs with circummarginal grooves; all toes with lateral dermal fringes; subarticular tubercles distinct,

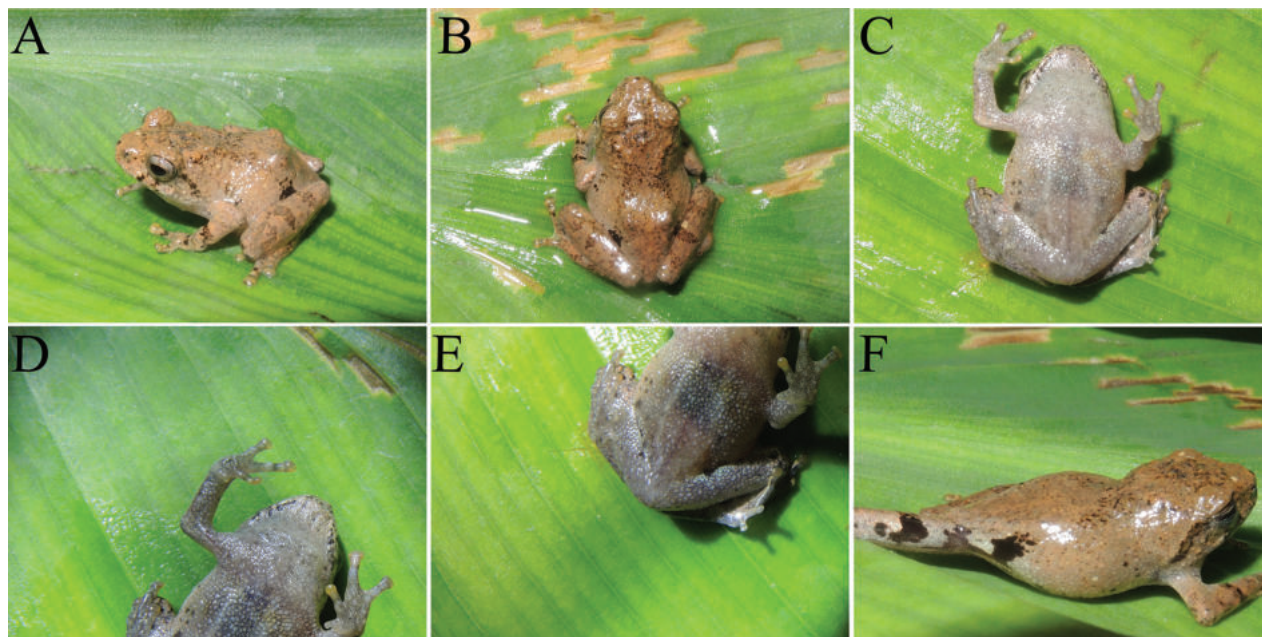


Figure 4. Photographs of holotype of *Raorchestes hekouensis* sp. nov. (GXNU YU000159) in life. Lateral view (A), dorsal view (B), ventral view (C), fingers (D), toes (E), crotch (F).

rounded; supernumerary tubercles absent; rudimentary webbing between toes; inner metatarsal tubercle rounded, outer metatarsal tubercle absent. Dorsal surfaces rough, dorsum, dorsal surface of limbs, snout, between eyes, and upper eyelid shagreened with numerous tubercles; flank of body, dorsal part of forelimbs, thighs, and tibia relatively smooth, scattered with sparse granules; throat, chest, and ventral surfaces of forelimbs smooth; abdomen, underside of thigh, and around vent with granules; dorsolateral folds absent; dorsal, dorsal surface of limbs and around vent with several beige patches.

Coloration of holotype in life. Dorsal surface yellowish brown, with distinct dark brown X-shaped marking on back; blackish line between eyes; tea-brown spots on both sides of lower jaw; dorsal side of limbs with several brown bands; flank near crotch with distinct black region between two creamy white patches, thighs with similar black patch near groin, next to another creamy white patch; ventral surface of throat, chest, ventral side of limbs, and belly opaque creamy white with small black spots and white tubercles; finger and toe discs yellow (Fig. 4).

Coloration of holotype in preservative. Dorsal color changed to grayish brown; forelimbs and hindlimbs with black-brown bands; patches or spots blackish brown; abdomen and ventral sides of limbs still milky white with several small black spots (Fig. 5).

Male secondary sexual characteristics. Adult male with nuptial pads on dorsal surface of first and second fingers and external single subgular vocal sac with slit-like opening at posterior of jaw. White lineae masculinae visible on ventral body.

Variation. Specimen GXNU YU000160 significantly has more black spots on the abdomen and near the cloaca (Fig. 6), specimen GXNU YU000156 differs from the other seven type specimens (GXNU YU000159, GXNU YU000160, GXNU YU000153, GXNU YU000154, GXNU YU000536, GXNU YU000537, and GXNU YU000538) by pale yellow mid-dorsal vertebral stripe from snout to vent,

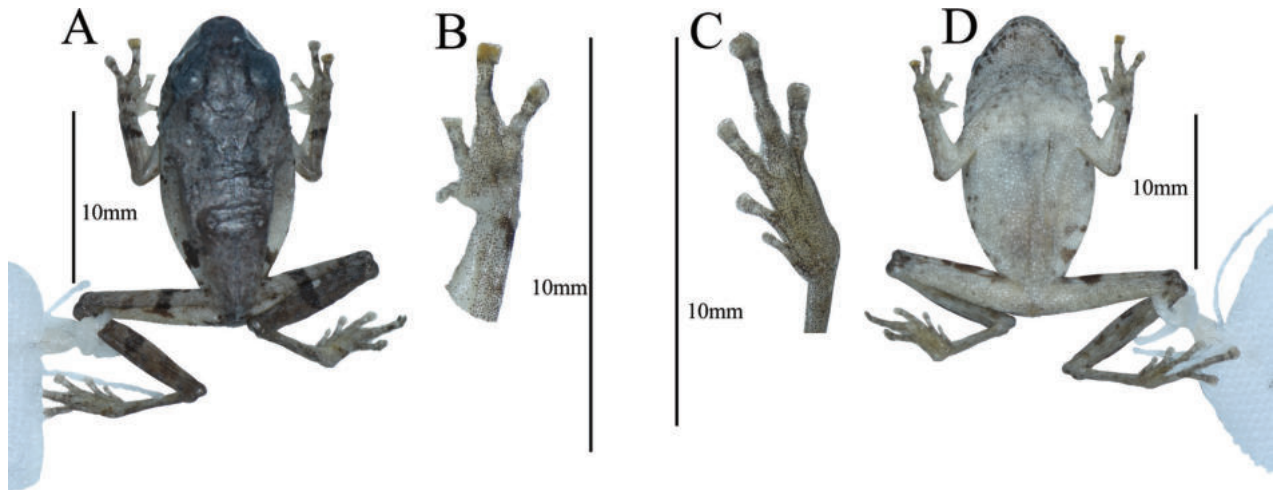


Figure 5. Photographs of *Raorchestes hekouensis* sp. nov. holotype (GXNU YU000159) in preservative, dorsal view (A), ventral view of hand (B), ventral view of foot (C), ventral view (D).

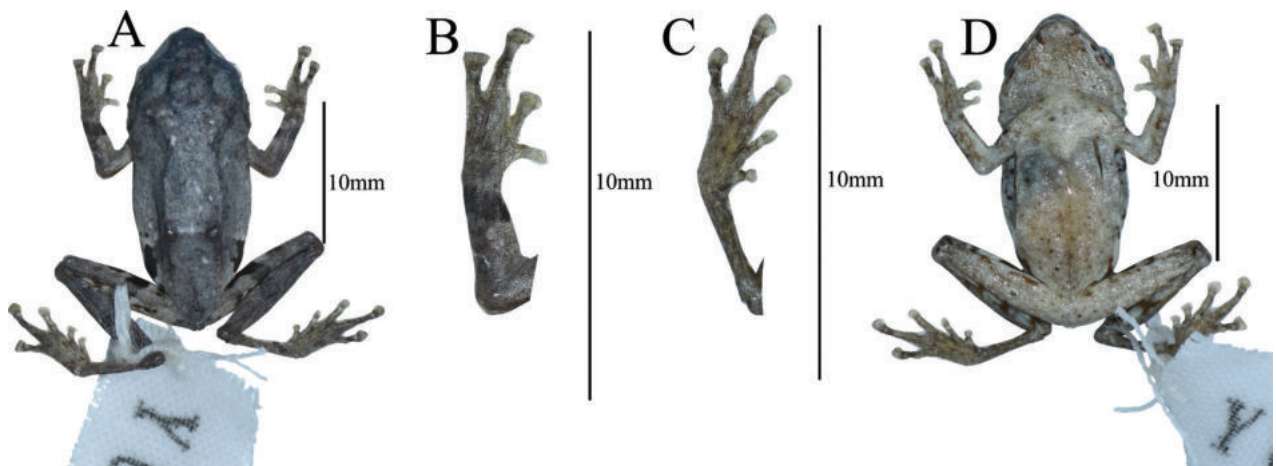


Figure 6. Photographs of *Raorchestes hekouensis* sp. nov. paratype (GXNU YU000160) in preservative, dorsal view (A), dorsal view of hand (B), ventral view of foot (C), ventral view (D).

pale yellow stripe along hindlimbs crossing at vent region, mid-ventral stripe from snout to vent and stripe along forelimbs crossing at breast region (Fig. 7), and the specimen GXNU YU000537 has distinctly darker ground color on the dorsal side, especially on the head (Fig. 8).

Distribution. Currently known from the type locality, Hekou County, Yunnan Province, China, and Bac Pan, Tuyen Quang, Vietnam.

Habitat. In Yunnan, *Raorchestes hekouensis* sp. nov. was found in shrubs and herbs on the edge of a small stream near the road at an elevation of ca 1200 m a.s.l. (Fig. 9) on the nights of 25 March 2019 and 4 April 2023. There were many herbaceous plants near the stream, such as *Ageratina adenophora*. No male was heard calling and no eggs were observed during our surveys in late March, but there were males calling during our surveys in April. Therefore, the breeding season for this species starts in April.

Remarks. *Raorchestes hekouensis* sp. nov. is assigned to the genus *Raorchestes* based on its molecular phylogenetic position and the following morphological characters: relatively small body size (SVL 15.0–45.0 mm); absence of vomerine teeth; large transparent/translucent vocal sac. Due to the

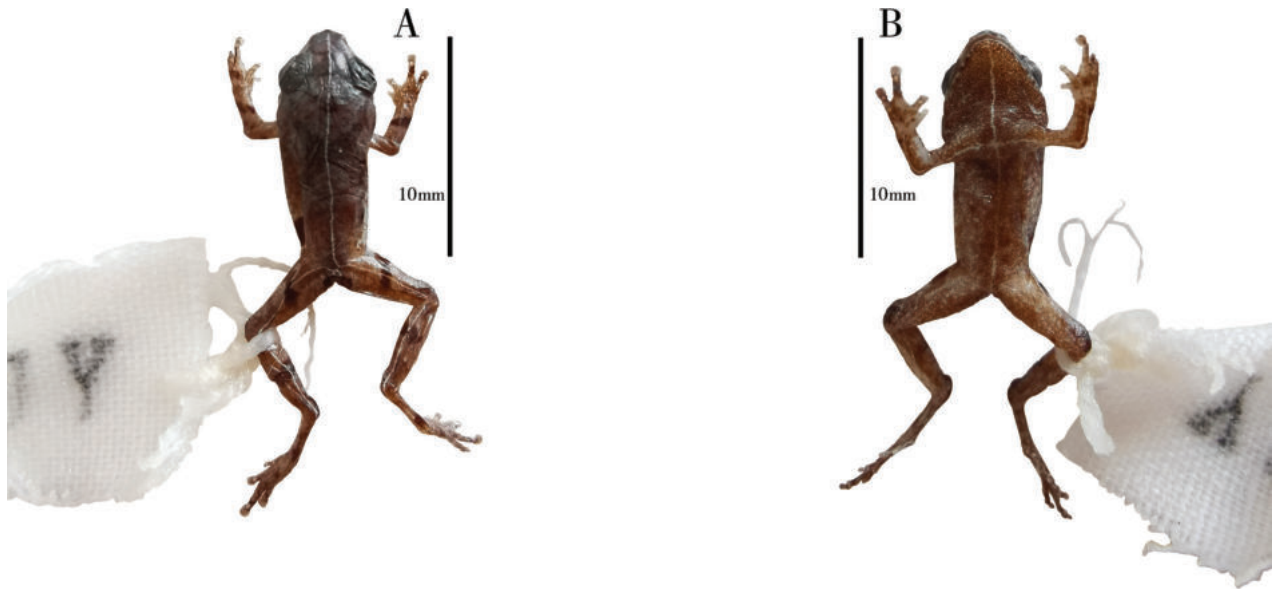


Figure 7. Photographs of *Raorchestes hekouensis* sp. nov. paratype (GXNU YU000156) in preservative, dorsal view (A), and ventral view (B).

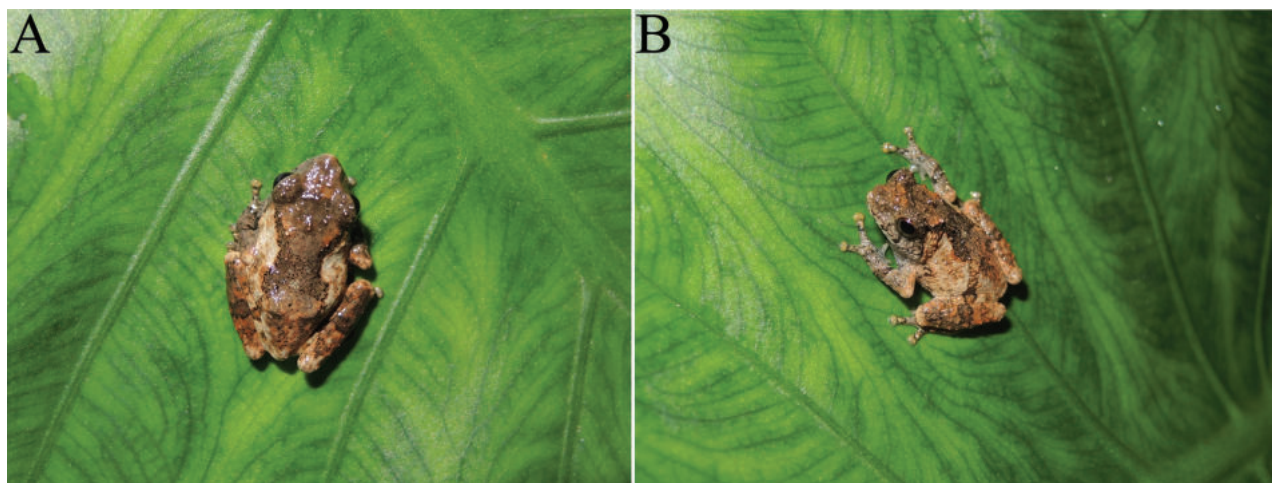


Figure 8. Photographs of *Raorchestes hekouensis* sp. nov. paratype (GXNU YU000537) in life, dorsal view (A), and lateral view (B).

close phylogenetic relationship and distribution (Figs 1, 2), we compared the new species with 16 recognized congeners distributed in Southeast Asia, southwestern China, the Himalayas, and northeastern India, as mentioned above. *Raorchestes hekouensis* sp. nov. is distinguished from all other 16 congeners by a unique combination of characters. A detailed morphological comparison table of currently known *Raorchestes* species from China is provided (Table 4).

Raorchestes gryllus is still considered a member of *Raorchestes* in Frost (2023), although Poyarkov et al. (2021) suggested that it should be transferred to the genus *Kurixalus*. *Raorchestes hekouensis* sp. nov. can be distinguished from *K. gryllus* based on the following characters: no webbing between fingers (vs rudimentary webbing between fingers), rudimentary webbing between toes (vs little more than half webbed), heel with no pointed appendage (vs heel with small, pointed appendage), snout rounded (vs snout pointed with dermal tip), and series of tubercles along outer side of forearm and foot absent (vs present).

Table 4. Morphological comparison among currently known species of *Raorchestes* in China (? = unknown).

Character	<i>Raorchestes hekouensis</i> sp. nov.	<i>R. cangyuanensis</i>	<i>R. dulongensis</i>	<i>R. menglaensis</i>	<i>R. longchuanensis</i>	<i>R. huanglianshan</i>	<i>R. hillisi</i>	<i>R. andersoni</i>	<i>R. yadongensis</i>	<i>R. malipoensis</i>
SVL of adult male (mm)	16.1–17.5	16.1–20.0	15.0–19.0	15.0–21.6	17.8–21.2	17.0–19.6	15.9–17.7	24.0	17.8–24.1	14.6–19.3
HDL/HDW	HDL < HDW	HDL < HDW	HDL > HDW	HDL ≈ HDW	HDL ≈ HDW	HDL ≤ HDW	HDL > HDW	HDL < HDW	HDL < HDW	HDL < HDW
Tympanum	Indistinct	Indistinct	Distinct	Indistinct	Distinct	Distinct	Distinct	Distinct	Distinct	Distinct
Nuptial pad	Present	Present	Absent	Present	Present	Present	Present	?	Present	Present
Vocal sac	External single subgular vocal sac	External single subgular vocal sac	External single subgular vocal sac	Internal single subgular vocal sac	External single subgular vocal sac	External single subgular vocal sac	External single subgular vocal sac	Internal single subgular vocal sac	External single subgular vocal sac	External single subgular vocal sac
Finger web	Absent	Absent	Absent	Absent	Absent	Absent	Absent	Absent	Rudimentary	Absent
Toe web	Rudimentary	Rudimentary	Rudimentary	Rudimentary or 1/4	1/4 webbing	Rudimentary, except between toe I and toe II	Rudimentary, except between toe I and toe II	Rudimentary or 1/3	Rudimentary	Rudimentary
Outer metatarsal tubercle	Absent	Absent	Absent	Present	Absent	Absent	Absent	Absent	Absent	Absent
Relative toe lengths	I < II < III < V < IV	I < II < V < III < IV	I < II < V < III < IV	I < II < III ≤ V < IV	I < II < III = V < IV	I < II < III < V < IV	I < II < III < V < IV	I < II < III ≤ V < IV	I < II < III < V < IV	I < II < V < III < IV
Reference	This study; Li et al. (2013)	Wu et al. (2019)	Wu et al. (2020)	Kou 1990; Jiang et al. (2020)	Yang and Li 1987; Fei et al. (2009)	Jiang et al. (2020)	Jiang et al. (2020)	Anderson 1978; Fei et al. (2009); Che et al. (2020)	Zhang et al. (2022)	Huang et al. (2023)



Figure 9. Habitat at type locality of *Raorchestes hekouensis* sp. nov. at Liangzi Village, Hekou, Yunnan, China.

Raorchestes hekouensis sp. nov. differs from *R. malipoensis* by inner metacarpal tubercle present, outer metacarpal tubercle indistinct (vs inner and outer metacarpal tubercle indistinct), heels meeting when limbs held at right angles to body (vs heels not meeting when limbs held at right angles to body); and relative toe lengths: $I < II < III < V < IV$ (vs $I < II < V < III < IV$). *Raorchestes hekouensis* sp. nov. is distinguishable from *R. huanglianshan* by supernumerary tubercles absent (vs present) and lateral dermal fringes on all fingers and toes present (vs absent). *Raorchestes hekouensis* sp. nov. differs from *R. parvulus* by length of lower arm and hand slightly shorter than half of body size (vs longer than half of body size) and supernumerary tubercles absent (vs present on third finger). *Raorchestes hekouensis* sp. nov. differs from *R. menglaensis* by external single subgular vocal sac in adult male (vs internal single subgular vocal sac), tympanum distinct in male (vs indistinct), and lateral dermal fringes on all fingers and toes present (vs absent). *Raorchestes hekouensis* sp. nov. differs from *R. cangyuanensis* by tympanum distinct in male (vs indistinct) and relative toe lengths: $I < II < III < V < IV$ (vs $I < II < V < III < IV$). *Raorchestes hekouensis* sp. nov. differs from *R. hillisi* by head wider than long (vs head longer than wide) and lateral dermal fringes on all fingers and toes present (vs fingers lacking lateral dermal fringes and toes with weak lateral dermal fringes, except outside of toe I and both sides of toe II). *Raorchestes hekouensis* sp. nov. differs from *R. dulongensis* by head wider than long (vs head longer than wide), snout rounded (vs pointed), relative toe lengths: $I < II < III < V < IV$ (vs $I < II < V < III < IV$), and nuptial pad present (vs absent). *Raorchestes hekouensis* sp. nov. differs from *R. longchuanensis* by head wider than long (vs head length almost equal to width) and lateral dermal fringes on all fingers and toes (vs lateral dermal fringes only on fingers I and II and no lateral dermal fringes on toes). *Raorchestes hekouensis* sp. nov. differs from *R. andersoni* by tibiotarsal articulation reaching anterior of eye (vs tibiotarsal articulation



Figure 10. *Kurixalus gryllus* from Dak Lak Province (Chu Yang Sin National Park) and Lam Dong Province (Bidoup-Nui Ba National Park) in southern Vietnam (sourced from Orlov et al. 2012).

reaching tip of snout), ventral surface of throat, chest, and belly opaque creamy white, with small black spots (vs chest and belly yellowish, with brown punctuations), and flank near crotch with distinct black region between two creamy white patches (vs irregular large black patch on groin, extending to half of side, with two yellow patches). *Raorchestes hekouensis* sp. nov. differs from *R. yadongensis* by lacking webbing between fingers (vs fingers with rudimentary webbing) and tibiotarsal articulation reaching anterior of eye when adpressed (vs tibiotarsal articulation reaching tip of snout when adpressed).

Raorchestes hekouensis sp. nov. differs from *R. rezakhani* by nuptial pad present (vs absent), dermal fringes present on fingers (vs absent), rudimentary webbing between toes (vs webbing moderate, formula: I2-2⁺II1^{3/4}-2⁺III1^{1/2}-3IV2^{3/4}-2⁻V), and inner metacarpal and inner metatarsal tubercles present (vs absent). *Raorchestes hekouensis* sp. nov. differs from *R. annandalii* by snout rounded (vs pointed), supernumerary tubercles in toes absent (vs present), and inner metatarsal tubercle present (vs absent). *Raorchestes hekouensis* sp. nov. differs from *R. shillongensis* by inner metatarsal tubercles distinct, outer metatarsal tubercle absent (vs inner metatarsal tubercle indistinct, outer metatarsal tubercle present), and relative toe lengths: I < II < III < V < IV (vs I ≤ II < V ≤ III < IV). *Raorchestes hekouensis* sp. nov. differs from *R. sahai* by rudimentary webbing between toes (vs nearly half-webbed in toes) and mid-dorsal line absent (vs dark narrow line originating from interorbital region and extending posteriorly to hindmost part of body). *Raorchestes hekouensis* sp. nov. differs from *R. manipurensis* by rudimentary webbing between toes (vs almost 2/3 webbing in toes) and webbing between fingers absent (vs present).

Key to *Raorchestes* species in China

- 1 Fingers with rudimentary webbing *R. yadongensis*
- Fingers without webbing..... 2
- 2 Tympanum indistinct 3
- Tympanum distinct 4
- 3 Fingers and toes with lateral dermal fringes *R. cangyuanensis*
- Fingers and toes lacking lateral dermal fringes *R. menglaensis*
- 4 Internal single subgular vocal sac..... *R. andersoni*
- External single subgular vocal sac..... 5
- 5 Nuptial pad absent *R. dulongensis*
- Nuptial pad present..... 6
- 6 Toes with one-fourth webbing..... *R. longchuanensis*
- Toes not with one-fourth webbing 7
- 7 Fingers with lateral dermal fringe..... 8
- Fingers lacking lateral dermal fringe..... 9
- 8 relative toe lengths: I < II < III < V < IV..... *Raorchestes hekouensis* sp. nov.
- relative toe lengths: I < II < V < III < IV *R. malipoensis*
- 9 Toes lacking lateral dermal fringe *R. huanglianshan*
- Toes with weak lateral dermal fringes, except outside of toe I and both sides of toe II *R. hillisi*

Discussion

The small body size, morphological conservativeness, and remarkably similar characters in the *Raorchestes* genus have resulted in ambiguities in taxonomy and distribution (Jiang et al. 2020), necessitating the application of molecular identification (Orlov et al. 2012). Morphologically, the types and topotypes of *Kurixalus gryllus* are very similar to other members of the genus due to the series of tubercles along the outer side of the forearm and feet, small pointed appendage on the heel, and pointed snout with a dermal tip (Smith 1924; Orlov et al. 2012; Poyarkov et al. 2021), with wide variation in living color patterns of *K. gryllus* from the type locality shown to be very similar to that seen in *Kurixalus motokawai* and *Kurixalus banaensis* (Nguyen, 2015; see Fig. 10). Therefore, we agree with Poyarkov et al. (2021) that “*R. gryllus*” from the type locality should be reassigned to *Kurixalus*. We also consider that the samples of so-called “*R. gryllus*” from northern Vietnam used in the present study (ROM 38828 and ROM 30298) are not conspecific with *K. gryllus* from the type locality as they are phylogenetically nested within the genus *Raorchestes* (Fig. 2).

Our results showed that the *R. UI* ROM 38828 from northern Vietnam clustered with *Raorchestes hekouensis* sp. nov. with a short branch length, indicating that *R. UI* ROM 38828 belonged to the new species (Fig. 2), and recently Huang et al. (2023) revised the specimen ROM 30288 from northern Vietnam, which had been recorded as *R. gryllus*, to *R. malipoensis* so the taxonomic status of the *R. UI* specimen from northern Vietnam (ROM 30298) needs further confirmation. The genetic divergences between *R. malipoensis*, *R. UI* ROM 30298, and *Raorchestes hekouensis* sp. nov. were greater than the divergence between *R. hillisi* and *R. yadongensis* (Table 3), and species delimitations grouped them into three different candidate species (Fig. 3), indicating that the clade comprised of ROM

30298 likely represented an unnamed species, pending further morphological study. Of note, both the ROM 38828 and ROM 30288 specimens were collected from Pac Ban, Tuyen Quang, Vietnam, suggesting the coexistence of *R. malipoensis* and the new species *Raorchestes hekouensis* sp. nov. in that region, which means the records of *Raorchestes* from that region also need verification.

In this study, we used distance-based (ASAP) and tree-based (bPTP) delimitation methods, and the two different species delimitation methods give the same results. The ASAP analysis divides species based on pairwise genetic distance, but it can provide a score for each partitioning result for users to refer to and select partitioning results. The difference is that bPTP delimits species using non-hypermetric phylogenies, and estimates speciation events in terms of a number of substitutions; therefore, it only requires a standard phylogenetic tree as input. The combination of both methods confirms the species delimitation and helps overcome the constraints of each approach (Carstens et al. 2013).

With the description of the new species, there are now ten *Raorchestes* species known from China, all of which occur in Yunnan except for *R. yadongensis*, which is only known from southern Tibet, China (Zhang et al. 2022). Recently Garg et al. (2021) assigned the *Raorchestes* species into 16 species groups and the clade containing species from Southeast and East Asia (e.g., *R. parvulus*, *R. menglaensis*, *R. cangyuanensis*) was placed in the *R. parvulus* species group. Based on Garg et al. (2021) and our phylogenetic results, the new species also belongs to the *R. parvulus* group. The continuous discovery of new *Raorchestes* species from Yunnan in recent years (Wu et al. 2019, 2021; Jiang et al. 2020; Huang et al. 2023; this study) indicates that *Raorchestes* diversity is seriously underestimated in Yunnan. We expect that more *Raorchestes* species will be found from southern Yunnan given the unnamed lineage in adjacent northern Vietnam mentioned above, from Tam Dao, Vinh Phuc (ROM 30298). Therefore, further studies employing a wider range of *Raorchestes* samples across its distribution are necessary to clarify the species boundary in Yunnan.

Due to the placement of "*R. gryllus*" sensu stricto in *Kurixalus*, the number of recognized *Raorchestes* species known from Southeast Asia is decreased to five, including *R. parvulus*, *R. longchuanensis*, *R. menglaensis*, *R. malipoensis*, and *R. huanglianshan* based on recent studies (Poyarkov et al. 2021; Jiang et al. 2020; Wu et al. 2022; Huang et al. 2023); our results revealed the existence of an additional but unnamed lineage in northern Vietnam. Previous phylogenetic analyses have also revealed that nominal *R. parvulus*, which is widely reported across Indochina (Frost 2023), also contains multiple clades that do not form a monophyly (Chan et al. 2018; Wu et al. 2019; Yu et al. 2019; Jiang et al. 2020), indicating that multiple cryptic species may exist within the species. Therefore, *Raorchestes* species diversity in Southeast Asia may be highly underestimated.

Acknowledgements

We thank Qiumei Mo and Mr. Hong Hui for assistance during fieldwork.

Additional information

Conflict of interest

The authors have declared that no competing interests exist.

Ethical statement

No ethical statement was reported.

Funding

This work was supported by grants from the National Natural Science Foundation of China (32060114, 31872212), Key Laboratory of Ecology of Rare and Endangered Species and Environmental Protection (Guangxi Normal University), Ministry of Education (ERESEP2022Z04), and Guangxi Key Laboratory of Rare and Endangered Animal Ecology, Guangxi Normal University (19-A-01-06).

Author contributions

Conceptualization: GY, SL. Formal analysis: LD, YX. Investigation: SL, LD. Software: YX. Writing - original draft: YX, LD.

Author ORCIDs

Lingyun Du  <https://orcid.org/0000-0002-5761-4017>

Shuo Liu  <https://orcid.org/0000-0001-7825-3006>

Guohua Yu  <https://orcid.org/0000-0002-0220-6550>

Data availability

All of the data that support the findings of this study are available in the main text.

References

- Abraham RK, Pyron RA, Ansil BR, Zachariah A, Zachariah A (2013) Two novel genera and one new species of treefrog (Anura: Rhacophoridae) highlight cryptic diversity in the Western Ghats of India. *Zootaxa* 3640(2): 177–189. <https://doi.org/10.11646/zootaxa.3640.2.3>
- Ahl E (1927) Zur Systematik der asiatischen arten der froschgattung Rhacophorus. *Sitzungsberichte der Gesellschaft Naturforschender Freunde zu Berlin* 1927: 35–47.
- Al-Razi H, Maria M, Muzaffar SB (2020) A new species of cryptic Bush frog (Anura, Rhacophoridae, *Raorchestes*) from northeastern Bangladesh. *ZooKeys* 927: 127–151. <https://doi.org/10.3897/zookeys.927.48733>
- AmphibiaChina (2022) The database of Chinese amphibians. Kunming Institute of Zoology (CAS), Kunming, Yunnan, China. <http://www.amphibiachina.org/>
- Anderson J (1878) Anatomical and zoological researches: Comprising an account of the zoological results of the two expeditions to Western Yunnan in 1868 and 1875. Vol 1. Bernard Quaritch, London, 703–860 + 969–975. [index] <https://doi.org/10.5962/bhl.title.50434>
- Biju SD, Bossuyt F (2009) Systematics and phylogeny of *Philautus* Gistel, 1848 (Anura, Rhacophoridae) in the Western Ghats of India, with descriptions of 12 new species. *Zoological Journal of the Linnean Society* 9(155): 374–444. <https://doi.org/10.1111/j.1096-3642.2008.00466.x>
- Biju SD, Shouche Y, Dubois A, Dutta SK, Bossuyt F (2010) A ground-dwelling rhacophorid frog from the highest mountain peak of the Western Ghats of India. *Current Science* 98(8): 1119–1125.
- Bossuyt F, Dubois A (2001) A review of the frog genus *Philautus* Gistel, 1848 (Amphibia, Anura, Ranidae, Rhacophorinae). *Zeylanica* 6(1): 1–112.

- Boulenger GA (1893) Concluding report on the reptiles and batrachians obtained in Burma by Signor L. Fea dealing with the collection made in Pegu and the Karin Hills in 1887–88. *Annali del Museo Civico di Storia Naturale di Genova* 2(13): 304–347.
- Boulenger GA (1906) Description of two Indian frogs. *Journal of the Asiatic Society of Bengal* 2(2): 385–386.
- Bourret R (1937) Notes herpétologiques sur L'Indochine Française. XIV. Les Batraciens de la Collection du Laboratoire des Sciences naturelles de l'Université. Descriptions de quinze espèces ou variétés nouvelles. *Annexe au Bulletin Général de l'Instruction Publique Hanoi* 4: 5–56.
- Bourret R (1939) Notes herpétologiques sur L'Indochine Française XVII. Reptiles et batraciens reçus au Laboratoire des Sciences Naturelles de l'Université au cours de l'année 1938. Descriptions de trois espèces Nouvelles. *Annexe au Bulletin Général de l'Instruction Publique Hanoi* 6: 13–34.
- Bourret R (1942) *Les Batraciens de L'Indochine*. Hanoi: Institut Océanographique de l'Indochine, 517 pp.
- Carstens BC, Pelletier TA, Reid N, Satler JD (2013) How to fail at species delimitation. *Molecular Ecology* 22(17): 4369–4383. <https://doi.org/10.1111/mec.12413>
- Chan KO, Grismer LL, Brown RM (2018) Comprehensive multi-locus phylogeny of Old World tree frogs (Anura: Rhacophoridae) reveals taxonomic uncertainties and potential cases of over- and underestimation of species diversity. *Molecular Phylogenetics and Evolution* 127: 1010–1019. <https://doi.org/10.1016/j.ympev.2018.07.005>
- Che J, Jiang K, Yan F, Zhang YP (2020) *Amphibians and Reptiles in Tibet-Diversity and Evolution*. Science Press, Beijing, 803 pp. [In Chinese]
- Chen JM, Prendini E, Wu YH, Zhang BL, Suwannapoom C, Chen HM, Jin JQ, Lemmon EM, Lemmon AR, Stuart BL, Raxworthy CJ, Murphy RW, Yuan ZY, Che J (2020) An integrative phylogenomic approach illuminates the evolutionary history of Old World tree frog (Anura: Rhacophoridae). *Molecular Phylogenetics and Evolution* 145: 106724. <https://doi.org/10.1016/j.ympev.2019.106724>
- Darriba D, Taboada GL, Doallo R, Posada D (2012) jModelTest 2: More models, new heuristics and parallel computing. *Nature Methods* 9(8): 772. <https://doi.org/10.1038/nmeth.2109>
- Du LN, Liu S, Hou M, Yu GH (2020) First record of *Theلودerma pyaukkya* Dever, 2017 (Anura: Rhacophoridae) in China, with range extension of *Theلودerma moloch* (Annandale, 1912) to Yunnan. *Zoological Research* 41(5): 576–580. <https://doi.org/10.24272/j.issn.2095-8137.2020.083>
- Fei L, Hu SQ, Ye CY, Huang YZ (2009) *Fauna Sinica. Amphibia Vol. 2 Anura*. Science Press, Beijing, 957 pp. [In Chinese]
- Fei L, Ye CY, Jiang JP (2012) *Colored Atlas of Chinese Amphibians and Their Distributions*. Sichuan Publishing House of Science and Technology, Chengdu. [In Chinese]
- Frost DR (2023) *Amphibian Species of the World: and Online Reference. Version 6.1*. American Museum of Natural History, New York, USA. <https://amphibiansoftheworld.amnh.org/> [Accessed 5 May 2023]
- Gan YL, Yu GH, Wu ZJ (2020) A new species of the genus *Amolops* (Anura: Ranidae) from Yunnan, China. *Zoological Research* 41(2): 188–193. <https://doi.org/10.24272/j.issn.2095-8137.2020.018>
- Garg S, Suyesh R, Das S, Bee MA, Biju SD (2021) An integrative approach to infer systematic relationships and define species groups in the shrub frog genus *Raorchestes*, with description of five new species from the Western Ghats, India. *PeerJ* 9: e10791. <https://doi.org/10.7717/peerj.10791>

- Hedges SB (1994) Molecular evidence for the origin of birds. *Proceedings of the National Academy of Sciences of the United States of America* 91(7): 2621–2624. <https://doi.org/10.1073/pnas.91.7.2621>
- Hou M, Yu GH, Chen HM, Liao CL, Zhang L, Chen J, Li PP, Orlov NL (2017) The taxonomic status and distribution range of six *Theلودerma* species (Anura: Rhacophoridae) with a new record in China. *Russian Journal of Herpetology* 24(2): 99–127. <https://doi.org/10.30906/1026-2296-2019-24-2-99-127>
- Huang JK, Liu XL, Du LY, Bernstein JM, Liu S, Yang Y, Yu GH, Wu ZJ (2023) A new species of Bush frog (Anura, Rhacophoridae, *Raorchestes*) from southeastern Yunnan, China. *ZooKeys* 1151: 47–65. <https://doi.org/10.3897/zookeys.1151.95616>
- Jiang K, Ren JL, Wang J, Guo JF, Wang Z, Liu YH, Jiang DC, Li JT (2020) Taxonomic revision of *Raorchestes menglaensis* (Kou, 1990) (Amphibia: Anura), with descriptions of two new species from Yunnan, China. *Asian Herpetological Research* 11(4): 263–281. <https://doi.org/10.16373/j.cnki.ahr.200018>
- Khatiwada JR, Wang B, Zhao T, Xie F, Jiang JP (2021) An integrative taxonomy of amphibians of Nepal: An updated status and distribution. *Asian Herpetological Research* 12(1): 1–35. <https://doi.org/10.16373/j.cnki.ahr.200050>
- Kou ZT (1990) A new species of genus *Philautus* (Amphibia: Rhacophoridae) from Yunnan, China. In: *From Water onto Land*. China Forestry Press, Beijing, 210–212. [In Chinese]
- Kumar S, Stecher G, Tamura K (2016) MEGA7: Molecular Evolutionary Genetics Analysis Version 7.0 for Bigger Datasets. *Molecular Biology and Evolution* 33(7): 1870–1874. <https://doi.org/10.1093/molbev/msw054>
- Laurent RF (1943) Contribution a l'osteologie et a la systematique des rhacophorides non Africains. *Bulletin du Musée Royal d'Histoire Naturelle de Belgique* 19: 1–16.
- Li JT, Che J, Murphy RW, Zhao H, Zhao EM, Rao DQ, Zhang YP (2009) New insights to the molecular phylogenetics and generic assessment in the Rhacophoridae (Amphibia: Anura) based on five nuclear and three mitochondrial genes, with comments on the evolution of reproduction. *Molecular Phylogenetics and Evolution* 53(2): 509–522. <https://doi.org/10.1016/j.ympev.2009.06.023>
- Li JT, Li Y, Klaus S, Rao DQ, Hillis DM, Zhang YP (2013) Diversification of rhacophorid frogs provides evidence for accelerated faunal exchange between India and Eurasia during the Oligocene. *Proceedings of the National Academy of Sciences of the United States of America* 110(9): 3441–3446. <https://doi.org/10.1073/pnas.1300881110>
- Liu XL, He YH, Wang YF, Beukema W, Hou SB, Li YC, Che J, Yuan ZY (2021) A new frog species of the genus *Odorrana* (Anura: Ranidae) from Yunnan, China. *Zootaxa* 4908(2): 263–275. <https://doi.org/10.11646/zootaxa.4908.2.7>
- Mathew R, Sen N (2009) Studies on little known amphibians of Northeast India. *Records of the Zoological Survey of India. Occasional Papers* 293: 1–64.
- Matsui M, Shimada T, Liu WZ, Maryati M, Khonsue W, Orlov N (2006) Phylogenetic relationships of oriental torrent frogs in the genus *Amolops* and its allies (Amphibia, Anura, Ranidae). *Molecular Phylogenetics and Evolution* 38(3): 659–666. <https://doi.org/10.1016/j.ympev.2005.11.019>
- Meegaskumbura M, Senevirathne G, Manamendra-Arachchi K, Pethiyagoda R, Hanken J, Schneider CJ (2019) Diversification of shrub frogs (Rhacophoridae, Pseudophilautus) in Sri Lanka—timing and geographic context. *Molecular Phylogenetics and Evolution* 132(8): 14–24. <https://doi.org/10.1016/j.ympev.2018.11.004>
- Nguyen TT (2015) Systematic study of the rhacophorid frogs in Vietnam. Dissertation. Kyoto University.

- Nguyen SV, Ho CT, Nguyen TQ (2009) Herpetofauna of Vietnam. Edition Chimaira, Frankfurt am Main, 768 pp.
- Nguyen TT, Matsui M, Duc HM (2014) A new tree frog of the genus *Kurixalus* (Anura: Rhacophoridae) from Vietnam. *Current Herpetology* 33(2): 101–111. <https://doi.org/10.5358/hsj.33.101>
- Orlov NL, Murphy RW, Ananjeva NB, Ryabov SA, Ho CT (2002) Herpetofauna of Vietnam, a checklist. Part 1. Amphibia. *Russian Journal of Herpetology* 9: 81–104.
- Orlov NL, Poyarkov AN, Vassilieva AB, Ananjeva NB, Nguyen TT, Sang NV, Geissler P (2012) Taxonomic notes on rhacophorid frogs (Rhacophorinae: Rhacophoridae: Anura) of southern part of Annamite Mountains (Truong Son, Vietnam), with description of three new species. *Russian Journal of Herpetology* 19(1): 23–64.
- Pillai RS, Chanda SK (1973) *Philautus shillongensis*, a new frog (Ranidae) from Meghalaya, India. *Proceedings of the Indian Academy of Sciences. Section B, Biological Sciences* 78(1): 30–36. <https://doi.org/10.1007/BF03045421>
- Poyarkov NA, Nguyen TV, Popov ES, Geissler P, Pawangkhanant P, Thy N, Suwannapoom C, Orlov NL (2021) Recent progress in taxonomic studies, biogeographic analysis, and revised checklist of amphibians in Indochina. *Russian Journal of Herpetology* 28(3): 1–110. <https://doi.org/10.30906/1026-2296-2021-28-3A-1-110>
- Puillandre N, Brouillet S, Achaz G (2021) ASAP: Assemble species by automatic partitioning. *Molecular Ecology Resources* 21(2): 609–620. <https://doi.org/10.1111/1755-0998.13281>
- Ronquist F, Teslenko M, van der Mark P, Ayres DL, Darling A, Höhna S, Larget B, Liu L, Suchard MA, Huelsenbeck JP (2012) MrBayes 3.2: Efficient Bayesian phylogenetic inference and model choice across a large mod space. *Systematic Biology* 61(3): 539–542. <https://doi.org/10.1093/sysbio/sys029>
- Sarkar AK, Ray S (2006) Amphibia. *Zoological Survey of India, Fauna of Arunachal Pradesh. State Fauna Series* 13 (1): 285–316.
- Smith MA (1924) New tree-frogs from Indo-China and the Malay Peninsula. 94. *Proceedings of the Zoological Society of London, London*, 225–234. <https://doi.org/10.1111/j.1096-3642.1924.tb01499.x>
- Stamatakis A (2014) RAxML version 8: A tool for phylogenetic analysis and post-analysis of large phylogenies. *Bioinformatics (Oxford, England)* 30(9): 1312–1313. <https://doi.org/10.1093/bioinformatics/btu033>
- Teynié A, David P, Ohler A, Luanglath K (2004) Notes on a collection of amphibians and reptiles from southern Laos, with a discussion of the occurrence of Indo-Malayan species. *Hamadryad. Madras* 29: 33–62.
- Vences M, Nagy ZT, Sonet G, Verheyen E (2012) DNA barcoding Amphibians and reptiles. In: Kress WJ, Erickson DL (Eds) *DNA Barcodes: Methods and Protocols, Methods in Molecular Biology*, Springer Science + Business Media, LLC, 79–108. https://doi.org/10.1007/978-1-61779-591-6_5
- Vijayakumar SP, Dinesh KP, Prabhu MV, Shanker K (2014) Lineage delimitation and description of nine new species of bush frogs (Anura: *Raorchestes*, Rhacophoridae) from the Western Ghats Escarpment. *Zootaxa* 3893(4): 451–488. <https://doi.org/10.11646/zootaxa.3893.4.1>
- Vijayakumar SP, Menezes RC, Jayarajan A, Shanker K (2016) Glaciations, gradients, and geography: multiple drivers of diversification of bush frogs in the Western Ghats Escarpment. *Proceedings of the Royal Society B, Biological Sciences* 283(1836): 20161011. <https://doi.org/10.1098/rspb.2016.1011>

- Wang J, Li J, Du LY, Hou M, Yu GH (2022) A cryptic species of the *Amolops ricketti* species group (Anura, Ranidae) from China-Vietnam border regions. *ZooKeys* 1112: 139–159. <https://doi.org/10.3897/zookeys.1112.82551>
- Wu YH, Suwannapoom C, Xu K, Chen JM, Jin JQ, Chen HM, Murphy RW, Che J (2019) A new species of the genus *Raorchestes* (Anura: Rhacophoridae) from Yunnan Province, China. *Zoological Research* 40(6): 558–563. <https://doi.org/10.24272/j.issn.2095-8137.2019.066>
- Wu YH, Liu XL, Gao W, Wang YF, Li YC, Zhou WW, Yuan ZY, Che J (2021) Description of a new species of Bush frog (Anura: Rhacophoridae: *Raorchestes*) from north-western Yunnan, China. *Zootaxa* 4941(2): 239–258. <https://doi.org/10.11646/zootaxa.4941.2.5>
- Wu YH, Suwannapoom C, Poyarkov Jr NA, Gao W, Karuno AP, Yuan ZY, Che J (2022) First record of *Kurixalus odontotarsus* (Ye et Fei, 1993) and *Raorchestes longchuanensis* (Yang et Li, 1978) (Anura: Rhacophoridae) Thailand. *Russian Journal of Herpetology* 29(1): 1–18. <https://doi.org/10.30906/1026-2296-2022-29-1-1-18>
- Yang DT, Li SM (1978) In: Yang DT, Su CY, Li SM (Eds) *Amphibians and Reptiles of Gaoligongshan*, Kunming 8: 37–38. [In Chinese]
- Yu GH, Rao DQ, Zhang MW, Yang JX (2009) Re-examination of the phylogeny of Rhacophoridae (Anura) based on mitochondrial and nuclear DNA. *Molecular Phylogenetics and Evolution* 50(3): 571–579. <https://doi.org/10.1016/j.ympev.2008.11.023>
- Yu GH, Liu S, Hou M, Li S, Yang JX (2019) Extension in distribution of *Raorchestes parvulus* (Boulenger, 1893) (Anura: Rhacophoridae) to China. *Zootaxa* 4577(2): 381–391. <https://doi.org/10.11646/zootaxa.4577.2.10>
- Zhang JJ, Kapli P, Pavlidis P, Stamatakis A (2013) A general species delimitation method with applications to phylogenetic placements. *Bioinformatics* 29(22): 2869–2876. <https://doi.org/10.1093/bioinformatics/btt499>
- Zhang HE, Shu GC, Shu FU, Li KE, Liu Q, Wu YY, Dong BJ, Guo P (2022) A new species of bush frog (Anura, Rhacophoridae, *Raorchestes*) from southern Xizang, China. *Zootaxa* 5195(2): 125–142. <https://doi.org/10.11646/zootaxa.5195.2.2>

The mitochondrial genome of *Hua aristarchorum* (Heude, 1889) (Gastropoda, Cerithioidea, Semisulcospiridae) and its phylogenetic implications

Yibin Xu^{1*}, Sheng Zeng^{2*}, Yuanzheng Meng², Deyuan Yang^{2,3}, Shengchang Yang²

¹ Key Laboratory of Cultivation and High-value Utilization of Marine Organisms in Fujian Province, Fisheries Research Institute of Fujian, Xiamen, China

² College of the Environment and Ecology, Xiamen University, Xiamen, China

³ National Taiwan Ocean University, Keelung, Taiwan

Corresponding authors: Yibin Xu (3208871@qq.com); Deyuan Yang (deyuanyang92@163.com); Shengchang Yang (scyang@xmu.edu.cn)

Abstract

Research on complete mitochondrial genomes can help in understanding the molecular evolution and phylogenetic relationships of various species. In this study, the complete mitogenome of *Hua aristarchorum* was characterized to supplement the limited mitogenomic information on the genus *Hua*. Three distinct assembly methods, GetOrganelle, NovoPlasty and SPAdes, were used to ensure reliable assembly. The 15,691 bp mitogenome contains 37 genes and an AT-rich region. Notably, the cytochrome c oxidase subunit I (*COX1*) gene, commonly used for species identification, appears to be slow-evolving and less variable, which may suggest the inclusion of rapidly evolving genes (NADH dehydrogenase subunit 6 [*ND6*] or NADH dehydrogenase subunit 2 [*ND2*]) as markers in diagnostic, detection, and population genetic studies of Cerithioidea. Moreover, we identified the unreliability of annotations (e.g., the absence of annotations for NADH dehydrogenase subunit 4L [*ND4L*] in NC_037771) and potential misidentifications (NC_023364) in public databases, which indicate that data from public databases should be manually curated in future research. Phylogenetic analyses of Cerithioidea based on different datasets generated identical trees using maximum likelihood and Bayesian inference methods. The results confirm that Semisulcospiridae is closely related to Pleuroceridae. The sequences of Semisulcospiridae clustered into three clades, of which *H. aristarchorum* is one; *H. aristarchorum* is sister to the other two clades. The findings of this study will contribute to a better understanding of the characteristics of the *H. aristarchorum* mitogenome and the phylogenetic relationships of Semisulcospiridae. The inclusion of further mitochondrial genome sequences will improve knowledge of the phylogeny and origin of Cerithioidea.

Key words: 16S rRNA, *COX1*, mitogenome, phylogenetic analysis, semisulcospirid gastropods

Introduction

The typical animal mitochondrial genome (mt) is a closed-circular molecule ranging from 14 to 20 kilobases (kb) in length and contains 13 protein-coding genes (PCGs), 22 transfer RNA genes (tRNAs), two ribosomal RNA genes (rRNAs), 12S



Academic editor: Frank Köhler

Received: 27 November 2023

Accepted: 19 January 2024

Published: 22 February 2024

ZooBank: <https://zoobank.org/D180BEA5-2BFC-4F2C-BEAF-6DA92CF90A2C>

Citation: Xu Y, Zeng S, Meng Y, Yang D, Yang S (2024) The mitochondrial genome of *Hua aristarchorum* (Heude, 1889) (Gastropoda, Cerithioidea, Semisulcospiridae) and its phylogenetic implications.

ZooKeys 1192: 237–255. <https://doi.org/10.3897/zookeys.1192.116269>

Copyright: © Yibin Xu et al.

This is an open access article distributed under terms of the Creative Commons Attribution License (Attribution 4.0 International – CC BY 4.0).

* These authors contributed equally to this work.

and 16S), and a non-coding region (NCR) (Boore 1999). mtDNA is widely used to identify common species and investigate genetic relationships and phylogenetic patterns due to its simple structure, abundant copies, rapid evolutionary rate, and ease of isolation (Mabuchi et al. 2014). However, the absence of complete mitochondrial genome sequences in species belonging to the genus *Hua* creates a gap in molecular biology, potentially resulting in an incomplete understanding of the genus's phylogenetic relationships and population history.

Semisulcospiridae Morrison, 1952 is a family of freshwater benthic gastropods comprising more than 50 species from four genera (Liu et al. 1993; Du et al. 2019a, 2019b; Lydeard and Cummings 2019). Semisulcospiridae is mainly distributed in East Asia and North America, with most members of this family (43 species from three genera) reported in China (Du et al. 2019a, 2019b). *Hua* S.-F. Chen, 1943 is a genus of freshwater gastropods belonging to Semisulcospiridae, comprising 16 species (Du et al. 2019a, 2019b; Lydeard and Cummings 2019; Strong et al. 2022). This genus is endemic to southwest China and northern Vietnam, and is commonly observed in clean and well-oxygenated water bodies, such as streams, springs, oligotrophic lakes and rivers (Liu et al. 1979). They are commonly used as environmental indicators. Many species of this genus are narrowly distributed; for example, they are found only in certain springs (Du et al. 2019a; Du and Yang 2023). Due to the eutrophication of water bodies, they face the risk of extinction (Strong and Köhler 2009; Du et al. 2019a, 2019b). Moreover, semisulcospirids have been extensively studied for their role as intermediate hosts of some trematodes, such as *Paragonimus* (Davis et al. 1994). *Hua aristacchorum* (Heude, 1888) is a medium-sized species commonly found in the lakes and rivers of southwestern China. As a well-known representative of *Hua* (Du et al. 2019a), mitogenomic data obtained for this species will provide valuable information on the taxonomy of Semisulcospiridae.

Heude (1889) studied freshwater snails of the middle and lower Yangtze River and named 24 species under the genus *Melania* Lamarck, 1799, including *Melania aristacchorum* Heude, 1888, the original combination of *Hua aristacchorum*. The genus *Hua* was originally named by Chen (1943), and includes 25 species (five species were named by Heude, as mentioned before), together with the genus *Wanga* S.-F. Chen, 1943, which includes eight species (Chen et al. 2023; Du and Yang 2023). The shells of the genus *Hua* are smooth, whereas those of the genus *Wanga* have sculptures. Chen designated *Melania telonaria* Heude, 1888 as the type species of the genus *Hua*, and *Melania henriettae* Gray, 1834 as the type species of the genus *Wanga*.

Because so many names have been applied and morphological polymorphisms have been observed in freshwater Cerithioidea (Davis 1972; Minton et al. 2008), the validity of these taxa is doubtful. After the introduction of molecular biology, a portion of this mystery seemed to have been solved. Köhler and Glaubrecht (2001) revised the genus *Brotia* H. Adams, 1866, and proposed the genus *Wanga* as a synonym of the genus *Brotia*, because the type species of *Wanga*, *Melania henriettae*, belongs to *Brotia*. Strong and Köhler (2009) raised Semisulcospirinae from a subfamily of Pleuroceridae into an independent family through the morphological and molecular analysis of '*Melania*' *jacqueti* Dautzenberg & H. Fischer, 1906, and placed the species into *Hua*. Du et al. (2019a, 2019b) revised the semisulcospirid species in China according to 16S rRNA and COX1 genes, and reproductive organs, and demonstrated that there are

three genera of Semisulcospiridae in China (*Semisulcospira* O. Boettger, 1886, *Koreoleptoxis* J. B. Burch & Y. Jung, 1988 and *Hua*). In these two studies, *Melania aristarchorum* was reclassified as *Hua*.

Previous taxonomic studies on mollusks based on molecular biology have commonly used mitochondrial genes, specifically *COX1*, for species identification, estimation of differentiation rates, and detection of new species (Köhler et al. 2010b; Zhang et al. 2015; Köhler 2017; Aksenova et al. 2018; Du et al. 2019a; Du et al. 2019b; Du and Yang 2019; Wiggering et al. 2019; Yang and Yu 2019; Liang et al. 2022; Wilke et al. 2023; Zhang et al. 2023). Zhang et al. (2018) reported that *COX1* is one of the most conserved PCGs in the mitochondrial genome. Therefore, some species that differ significantly in morphology exhibit only slight differences in their *COX1* gene expression (Köhler et al. 2010a; Du et al. 2019a). Du et al. (2019a) reported that the *p*-distance between *Hua aubryana* (Heude, 1889) and *H. tchangsii* L.-N. Du, Köhler, G.-H. Yu, X.-Y. Chen & J.-X. Yang, 2019 was only 0.9%. Therefore, *COX1* is limited in terms of species identification and phylogenetic studies. To address this problem, complete mitogenome sequencing or the exploration of other mitochondrial PCGs is required.

Materials and methods

Specimen collection and identification

The studied specimen was collected in the Panlong River, Kunming City, Yunnan Province, China (25°7'14"N, 102°44'50"E). This species is not included on the endangered list of the International Union for Conservation of Nature (<https://www.iucnredlist.org/>). The specimen was fixed and preserved in 100% ethanol. Tissues were preserved at -20 °C in a refrigerator, and the voucher specimen (No. RTM13) was deposited at the College of the Environment and Ecology, Xiamen University.

A morphological examination and DNA sequence blast confirmed the specimen to be *Hua aristarchorum*. Morphological identification was performed as previously described (Chen 1943; Du et al. 2019a, 2019b). Identifying characteristics were: medium-sized shell, ovate, with four to five whorls; sculpture variable, consisting of four spiral lirae at the base of the shell, three to four spiral lirae on the upper part of the body whorl, and 12 to 13 axial ribs. The mt *COX1* and 16S rRNA sequences were compared with those in the GenBank database using a BLAST search. Fourteen sequences of 16S rRNA and 12 sequences of *COX1* exhibited an identity of over 99% (16S, GenBank accession No. MK251661, named *H. aristarchorum*) and 99.74% (*COX1*, GenBank accession No. MK251736; *H. aristarchorum*). These 26 sequences corresponded to that of 14 specimens from Huize County and Songming County, Yunnan Province, China (Du et al. 2019b).

DNA extraction, mitogenome sequencing and assembly

Muscle tissue (1 mm³) was clipped from the foot of the specimen for DNA extraction. A TIANamp Genomic DNA Kit (TIANGEN, Beijing, China) was used to extract whole genomic DNA. The mitogenome of *H. aristarchorum* was sequenced using an Illumina Truseq™ DNA Sample Preparation Kit (Illumina, San Diego, CA, USA) with paired reads measuring 150 bp in length. Quality control of raw genomic data was assessed using FastQC v.0.11.5 (Andrews 2010).

Quality trimming and data filtering were performed using fastp v.0.23.2 (Chen et al. 2018). Trimmed reads containing unpaired reads, more than 5% unknown nucleotides, and more than 50% bases with Q-value ≤ 20 were discarded. To evaluate the consistency of the assembly results, GetOrganelle v.1.7.7.0 (Jin et al. 2020), NovoPlasty v.4.3.1 (Dierckxsens et al. 2017) and SPAdes v.3.15.5 (Bankevich et al. 2012) were used.

Mitogenome annotation and sequence analyses

The mitogenome was annotated using the MitoZ annotation module (Meng et al. 2019). The results of the annotation were loaded into Geneious v.2021.0.3 (Kearse et al. 2012) and checked manually with the view of open reading frames (ORFs). Transfer RNA genes were plotted according to the secondary structure predicted by MitoZ v.3.6 (Meng et al. 2019) and MITOS2 (Bernt et al. 2013). The NCR region was determined using the adjacent genes.

The final mitogenome sequence was visualized using the visualization sub-command in MitoZ v.3.6 (Meng et al. 2019), and clean reads were mapped to the gene map (Fig. 1) to show the coverage depth and GC content. Base composition and relative synonymous codon usage (RSCU) were determined using MEGA X (Kumar et al. 2018).

Strand asymmetries were calculated using the following formulae (Perna and Kocher 1995): AT-skew = $(A-T) / (A+T)$; GC-skew = $(G-C) / (G+C)$. DnaSP v.6.0 (Rozas et al. 2017) was used to estimate the nucleotide diversity (π) in a sliding window analysis (a sliding window of 100 bp and a step size of 20 bp) and non-synonymous (K_a) / synonymous (K_s) substitution rates of Semisulcospiridae. To investigate the gene order arrangement of the mitogenome sequence, we re-annotated sequences from Semisulcospiridae using our annotation method.

Phylogenetic analysis

The newly sequenced mitogenome of *H. aristarchorum* and all available Cerithioidea mitogenomes from GenBank (two sequences without annotation: *Batillaria cumingii* MT323103 and *Batillaria zonalis* MT363252; one sequence without ND4L: *Semisulcospira coreana* NC_037771) (25 September, 2023) and two outgroup species (Table 1) were used for the phylogenetic analysis using PhyloSuite v.1.2.3 (Zhang et al. 2020). Phylogenetic trees were constructed using three types of datasets: (1) amino acid sequences of the 13 PCGs (AA); (2) all codon positions of the 13 PCGs (PCG123); and (3) the 13 PCGs, excluding the third codon position (PCG12).

The extracted PCGs of these sequences were aligned using MAFFT v.7.313 (Katoh and Standley 2013), wherein amino acid sequences were aligned using the normal mode and nucleotide sequences were aligned using the codon model. Gblocks v.0.91 (Castresana 2000) was used to remove ambiguously aligned sequences with default settings (for the length after Gblocks, see Suppl. material 1: table S1).

ModelFinder v.2.2.0 (Kalyaanamoorthy et al. 2017) was used to select the best substitution models of maximum likelihood (ML) and Bayesian inference (BI) analyses. The GTR+F+I+G4 model was selected as the best-fitting model for both ML and BI analyses in the PCG123 and PCG12 datasets;

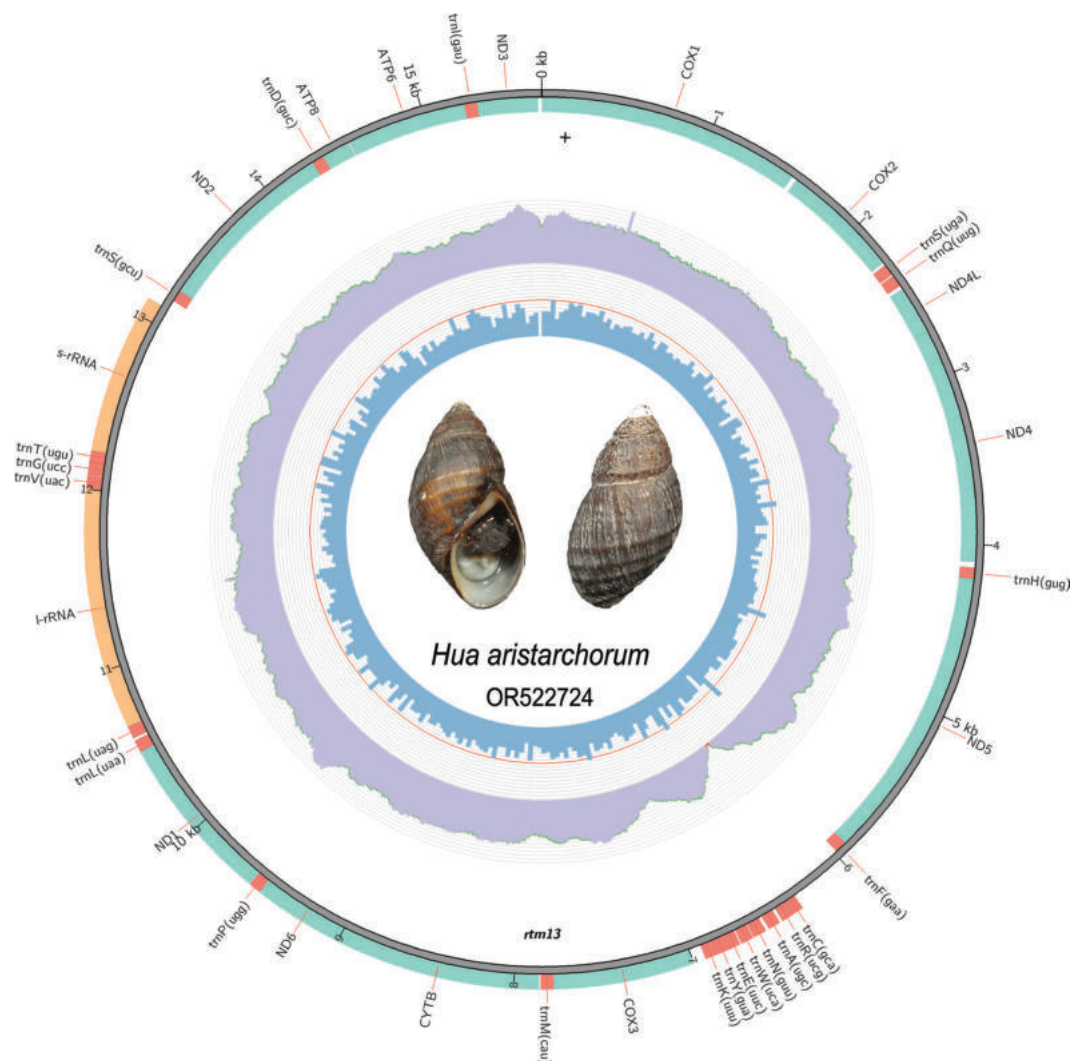


Figure 1. Gene map of the *H. aristarchorum* mitogenome. The photo in the middle is the studied specimen of *H. aristarchorum* (photograph by Yuanzheng Meng). The innermost and middle circles depict the GC content and distribution of the sequencing depth, respectively. The outermost circle represents the arrangement of genes: inner genes from the forward strand, and outer genes from the reverse strand, with the protein-coding genes (PCGs) in green, ribosomal RNAs (rRNAs) in orange, and transfer RNA genes (tRNAs) in red.

LG+F+I+G4 and mtMAM+F+I+G4 were selected for the AA dataset, under ML and BI respectively.

ML analysis was performed in IQ-TREE v.2.2.2 (Nguyen et al. 2015) under an Edge-linked partition model for 20,000 ultrafast bootstraps. BI analysis was performed using MrBayes v.3.2.7a (Ronquist et al. 2012), with two parallel runs for 2,000,000 generations. Finally, iTOL v.6 (Letunic and Bork 2016) was used to visualize the ML and BI trees.

Results and discussion

Mitogenome organization

The mitogenome assembly results using GetOrganelle, NovoPlasty and SPAdes were 15,691, 15,675, and 15,694 bp with an average coverage of 125, 59, and 77, respectively. The only difference between the three methods was the length

Table 1. List of 23 species and two outgroups used for phylogenetic analysis.

Species	Family	Length (bp)	A + T (%)	Accession No.	Reference
<i>Alviniconcha boucheti</i>	Outgroups	15981	67.7	MT123331	(Lee et al. 2020)
<i>Epitonium scalare</i>	Outgroups	15140	69.4	MK251987	(Guo et al. 2019)
<i>Batillaria zonalis</i>	Batillariidae	15748	65.3	MT363252	(Yan et al. 2020b)
<i>Batillaria attramentaria</i>	Batillariidae	16095	65.3	NC_047187	(Group et al. 2019)
<i>Batillaria cumingii</i>	Batillariidae	16100	65.6	MT323103	(Yan et al. 2020a)
<i>Tylomelania sarasinorum</i>	Pachychilidae	16632	65.2	NC_030263	(Hilgers et al. 2016)
<i>Turritella bacillum</i>	Turritellidae	15868	64.8	NC_029717	(Zeng et al. 2016)
<i>Maoricolpus roseus</i>	Turritellidae	15865	63.6	NC_068097	Unpublished
<i>Pseudocleopatra dartavellei</i>	Paludomidae	15368	63.8	NC_045095	(Stelbrink et al. 2019)
<i>Tarebia granifera</i>	Thiaridae	15555	65.4	MZ662113	(Yin et al. 2022)
<i>Melanoides tuberculata</i>	Thiaridae	15821	66.3	MZ321058	(Ling et al. 2022)
<i>Pirenella pupiformis</i>	Potamididae	15779	63.2	LC648322	(Kato et al. 2022)
<i>Cerithidea sinensis</i>	Potamididae	15633	66.8	KY021067	(Xu et al. 2019)
<i>Cerithidea tonkiniana</i>	Potamididae	15617	63.1	MZ168697	(Yang and Deng 2022)
<i>Cerithidea obtusa</i>	Potamididae	15708	63.0	NC_039951	(Nguyen et al. 2018)
<i>Leptoxis ampla</i>	Pleuroceridae	15591	68.8	KT153076	(Whelan and Strong 2016)
<i>Hua aristarchorum</i>	Semisulcospiridae	15691	65.3	OR522724	This study
<i>Semisulcospira gottschei</i>	Semisulcospiridae	16101	66.5	MK559478	(Lee et al. 2019)
<i>Semisulcospira coreana</i>	Semisulcospiridae	15398	65.7	NC_037771	(Kim and Lee 2018)
<i>Koreoleptoxis globus ovalis</i>	Semisulcospiridae	15866	65.1	LC006055	Unpublished
<i>Koreoleptoxis nodifila</i>	Semisulcospiridae	15737	65.8	NC_046494	(Choi et al. 2021)
<i>Koreoleptoxis nodifila</i>	Semisulcospiridae	17030	64.4	KJ696780	Unpublished
<i>Semisulcospira libertina</i>	Semisulcospiridae	15432	66.2	NC_023364	(Zeng et al. 2015)
<i>Koreoleptoxis friniana</i>	Semisulcospiridae	15474	66.0	OR567887	Unpublished
<i>Koreoleptoxis friniana</i>	Semisulcospiridae	15544	66.1	OR522723	Unpublished

of the NCR. We decided to use the result from GetOrganelle, as this software can generate assembly graphs and is more convenient for other researchers to replicate our assembly results.

The size of the complete mitochondrial genome was 15,691 bp, consisting of 13 PCGs, two rRNAs, 22 tRNAs, and one NCR measuring 346 bp (Fig. 1, Table 2). Nine PCGs (*COX1*, *COX2*, *ND4L*, *ND4*, *ND5*, *ND2*, *ATP8*, *ATP6* and *ND3*), seven tRNAs (*trnS*, *trnQ*, *trnH*, *trnF*, *trnS*, *trnD* and *trnI*), and one NCR are distributed on the heavy (H-) strand, while the other genes are distributed on the light (L-) strand (Table 2, Fig. 1). Overall, the light- and heavy-strand regions within the mitogenome of *H. aristarchorum* were concentrated and characterized by both intergenic (18 intergenic intervals, totaling 384 bp) and overlapping regions (three overlaps, totaling 56 bp) (Table 2). Two typical overlaps occur between PCGs (i.e., 7 bp between *ND4L* and *ND4*, and 47 bp between *CYTb* and *ND6*), and these overlaps are common in other freshwater gastropod sequences (Lee et al. 2019). Similar to the mitochondrial genes in other Cerithioidea species (Zeng et al. 2015; Kim and Lee 2018; Choi et al. 2021), the mitochondrial genes in *H. aristarchorum* exhibit a high A + T content of 65.3% (Table 1), with A, T, G, and C constituting 30.8%, 34.5%, 17.9%, and 16.8%, respectively (Table 3). Both the AT- and GC-skew of the mitogenome are negative, -0.056 and -0.032, respectively (Table 3), indicating that Ts and Cs are more abundant than As and Gs.

Table 2. Features of the *H. aristarchorum* mitogenome.

Gene	Position		Length (bp)	Amino	Start/stop codon	Anticodon	Intergenic region	Strand
	From	To						
<i>COX1</i>	1	1533	1533	511	ATG/TAA		32	H
<i>COX2</i>	1566	2255	690	230	ATG/TAA		19	H
<i>trnS(uga)</i>	2275	2341	67			TGA	10	H
<i>trnQ(uug)</i>	2352	2419	68			TTG	24	H
<i>ND4L</i>	2444	2734	291	97	ATG/TAA		-7	H
<i>ND4</i>	2728	4095	1368	456	GTG/TAA		35	H
<i>trnH(gug)</i>	4131	4196	66			GTG	0	H
<i>ND5</i>	4197	5915	1719	573	ATG/TAA		2	H
<i>trnF(gaa)</i>	5918	5985	68			GAA	0	H
<i>NCR</i>	5986	6331	346				0	H
<i>trnC(gca)</i>	6332	6393	62			GCA	1	L
<i>trnR(ucg)</i>	6395	6461	67			TCG	19	L
<i>trnA(ugc)</i>	6481	6548	68			TGC	20	L
<i>trnN(guu)</i>	6569	6641	73			GTT	7	L
<i>trnW(uca)</i>	6649	6717	69			TCA	9	L
<i>trnE(uuc)</i>	6727	6791	65			TTC	3	L
<i>trnY(gua)</i>	6795	6861	67			GTA	0	L
<i>trnK(uuu)</i>	6862	6930	69			TTT	69	L
<i>COX3</i>	7000	7779	780	260	ATG/TAA		3	L
<i>trnM(cau)</i>	7783	7852	70			CAT	8	L
<i>CYTb</i>	7861	9000	1140	380	ATG/TAG		-47	L
<i>ND6</i>	8954	9505	552	184	ATG/TAA		2	L
<i>trnP(ugg)</i>	9508	9573	66			TGG	4	L
<i>ND1</i>	9578	10516	939	313	ATG/TAA		0	L
<i>trnL(uaa)</i>	10517	10583	67			TAA	16	L
<i>trnL(uag)</i>	10600	10669	70			TAG	0	L
<i>l-rRNA(16S)</i>	10670	12007	1338				0	L
<i>trnV(uac)</i>	12008	12076	69			TAC	5	L
<i>trnG(ucc)</i>	12082	12150	69			TCC	1	L
<i>trnT(ugu)</i>	12152	12218	67			TGT	-2	L
<i>s-rRNA(12S)</i>	12217	13107	891				61	L
<i>trnS(gcu)</i>	13169	13236	68			GCT	0	H
<i>ND2</i>	13237	14304	1068	356	ATG/TAA		0	H
<i>trnD(guc)</i>	14305	14373	69			GTC	3	H
<i>ATP8</i>	14377	14538	162	54	ATG/TAG		9	H
<i>ATP6</i>	14548	15243	696	232	ATG/TAA		2	H
<i>trnI(gau)</i>	15246	15316	71			GAT	1	H
<i>ND3</i>	15318	15671	354	118	ATG/TAG		19	H

Genes and codon usage

The mitogenome of *H. aristarchorum* displays the standard arrangement of 13 PCGs commonly observed in Cerithioidea species. These include seven NADH dehydrogenases (*ND1-ND6* and *ND4L*), three cytochrome c oxidases (*COX1-COX3*), two ATPases (*ATP6* and *ATP8*) and one cytochrome b (*CYTb*). These 13 PCGs have a total length of 11,292 bp and encode 3,764 amino acids. With the exception of *ND4*, which starts with the GTG codon, all others begin with ATG. As for the stop codons, *CYTb*, *ATP8* and *ND3* end with the TAG codon, and the others end with TAA (Table 2), whereas in the sequences of the 13 PCGs within the

Table 3. Composition and skewness of the *H. aristarchorum* mitogenome.

	A%	T%	G%	C%	(A + T)%	AT-skew	GC-skew	Length (bp)
Mitogenome	30.8	34.5	17.9	16.8	65.3	-0.056	-0.032	15691
PCGs	26.2	38.6	18.5	16.7	64.8	-0.192	-0.051	11292
<i>COX1</i>	25.7	37.4	18.8	18.1	63.1	-0.185	-0.018	1533
<i>COX2</i>	28.4	35.9	18	17.7	64.3	-0.117	-0.008	690
<i>ND4L</i>	26.1	39.5	15.8	18.6	65.6	-0.204	0.08	291
<i>ND4</i>	27.5	38.2	19.9	14.4	65.7	-0.164	-0.16	1368
<i>ND5</i>	28.1	37.8	19.8	14.4	65.9	-0.147	-0.158	1719
<i>COX3</i>	24.2	36.2	19.7	19.9	60.4	-0.197	0.003	780
<i>CYTB</i>	24.8	37.6	21	16.6	62.4	-0.205	-0.117	1140
<i>ND6</i>	27.9	39.1	17	15.9	67	-0.168	-0.033	552
<i>ND1</i>	25	39.4	17.7	17.9	64.4	-0.223	0.006	939
<i>ND2</i>	25.2	41.7	15.3	17.9	66.9	-0.246	0.079	1068
<i>ATP8</i>	31.5	40.7	13.6	14.2	72.2	-0.128	0.022	162
<i>ATP6</i>	21.8	43.1	18.4	16.7	64.9	-0.327	-0.049	696
<i>ND3</i>	26.8	40.7	15.3	17.2	67.5	-0.205	0.061	354
<i>l-rRNA(16S)</i>	35.4	31.8	15.3	17.6	67.2	0.053	0.068	1338
<i>s-rRNA(12S)</i>	32.9	31.9	15.9	19.3	64.8	0.016	0.096	891
tRNAs	32.6	31.6	16.3	19.5	64.2	0.015	0.088	1495
NCR	39.0	24.9	18.2	17.9	63.9	0.222	-0.008	346

same family, most genes start with the codon ATG and end with the codon TAA. The AT- and GC-skews of the 13 PCGs are similarly negative, -0.192 and -0.051, respectively (Table 3). Five PCGs (*ND1*, *ND2*, *ND4L*, *COX3* and *ATP8*) exhibit positive GC-skew values, whereas the remaining eight PCGs exhibit negative values.

The 12S rRNA (891 bp) gene is located between the *trnT* and *trnS* genes, and the 16S rRNA (1,338 bp) gene is located between *trnL* and *trnV* (Table 2, Fig. 1). A total of 22 tRNA genes with lengths ranging from 62 to 73 bp were identified in the mitogenome of *H. aristarchorum*. Most of these tRNA genes exhibit a characteristic cloverleaf-like structure, except for *trnS*, which lacks a dihydrouridine arm (Suppl. material 1: fig. S1).

The relative synonymous codon usage (RSCU) values of the mitogenome were calculated and are summarized in Suppl. material 1: table S2, Fig. 2. Among the 13 PCGs, the most frequently found amino acids are *Leu* (15.57%), *Ser* (10.31%), *Phe* (9.57%) and *Ile* (8.11%). The least common amino acids are *Cys* (1.06%), *Arg* (1.63%), *Gln* (1.76%) and *Asp* (1.90%) (Fig. 2a, Suppl. material 1: table S2). RSCU analysis reveals that the most frequently found codons include UCU (*Ser*), UUA (*Leu*) and CGA (*Arg*), whereas CUG (*Leu*), ACG (*Thr*) and AGG (*Ser*) have the lowest frequencies (Fig. 2b, Suppl. material 1: table S2). RSCU analysis also indicated that codons are biased toward more A/U at the third codon, which is consistent with other Cerithioidea species (Lee et al. 2019; Choi et al. 2021).

Nucleotide diversity and evolutionary rate analysis

Nucleotide diversity analysis (Pi values) among the 13 aligned PCGs in the semisulcospirid mitogenomes revealed a substantial degree of variation within various genes (Fig. 3a). Pi values ranged from 0.108 (*COX1*) to 0.161 (*ND2*). Among all PCGs, *ND2* (Pi = 0.161) exhibited the highest variability, followed

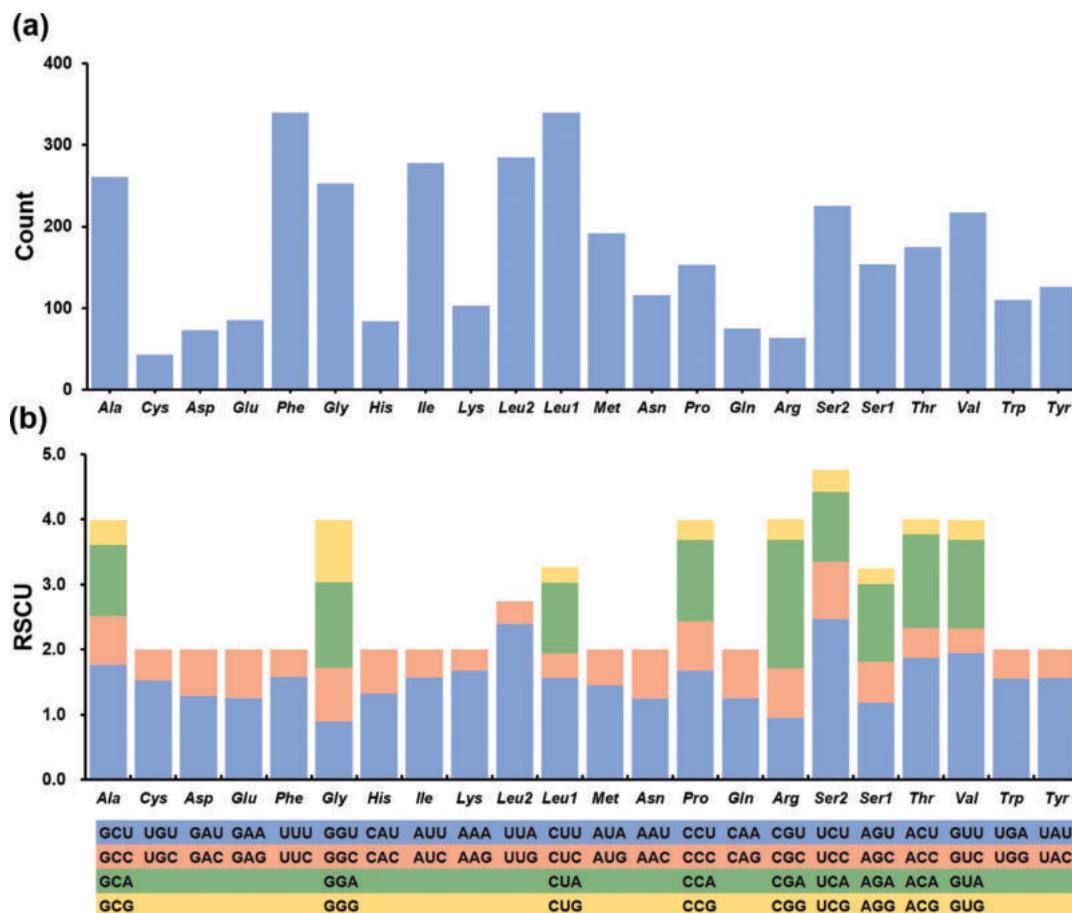


Figure 2. Amino acid composition (a) and relative synonymous codon usage (b) of the *H. aristarchorum* mitogenome. The codon families are provided under the x-axis.

closely by *ND6* ($P_i = 0.160$) and *ND4* ($P_i = 0.143$). Conversely, *COX1* ($P_i = 0.108$), *COX2* ($P_i = 0.122$) and *COX3* ($P_i = 0.122$) displayed relatively low nucleotide diversity, indicating conservation among the 13 PCGs (Fig. 3a). These observations are also reflected in the K_a/K_s ratios (Fig. 3b). These results indicate that the 13 PCGs from all Semisulcospiridae mitogenomes evolved under purifying selection (Fig. 3). Among these 13 PCGs, *COX1* ($K_a/K_s = 0.015$) underwent the strongest purifying selection and exhibited the lowest evolutionary rate. In contrast, *ND6* ($K_a/K_s = 0.160$) and *ND2* ($K_a/K_s = 0.125$) experienced comparatively weak purifying pressures, indicating a relatively rapid evolutionary rate.

Comparative analysis of mitochondrial genome components in Semisulcospiridae

We compared the mitochondrial genome of *H. aristarchorum* with those of other Semisulcospiridae species. After analyzing sequences downloaded directly from GenBank, we found that the gene positions were mostly identical. However, *S. coreana* NC_037771 did not contain *ND4L*, and there were variations in the orientation of certain genes (Fig. 4a). Notably, *K. globus ovalis* LC006055, *S. libertina* NC_023364 and *K. nodifila* NC_046494 exhibited different gene orientations, specifically *trnL* in *K. globus ovalis* LC006055 and *S. libertina* NC_023364, and *rrnL* in *K. nodifila* NC_046494, which were located on the positive strand

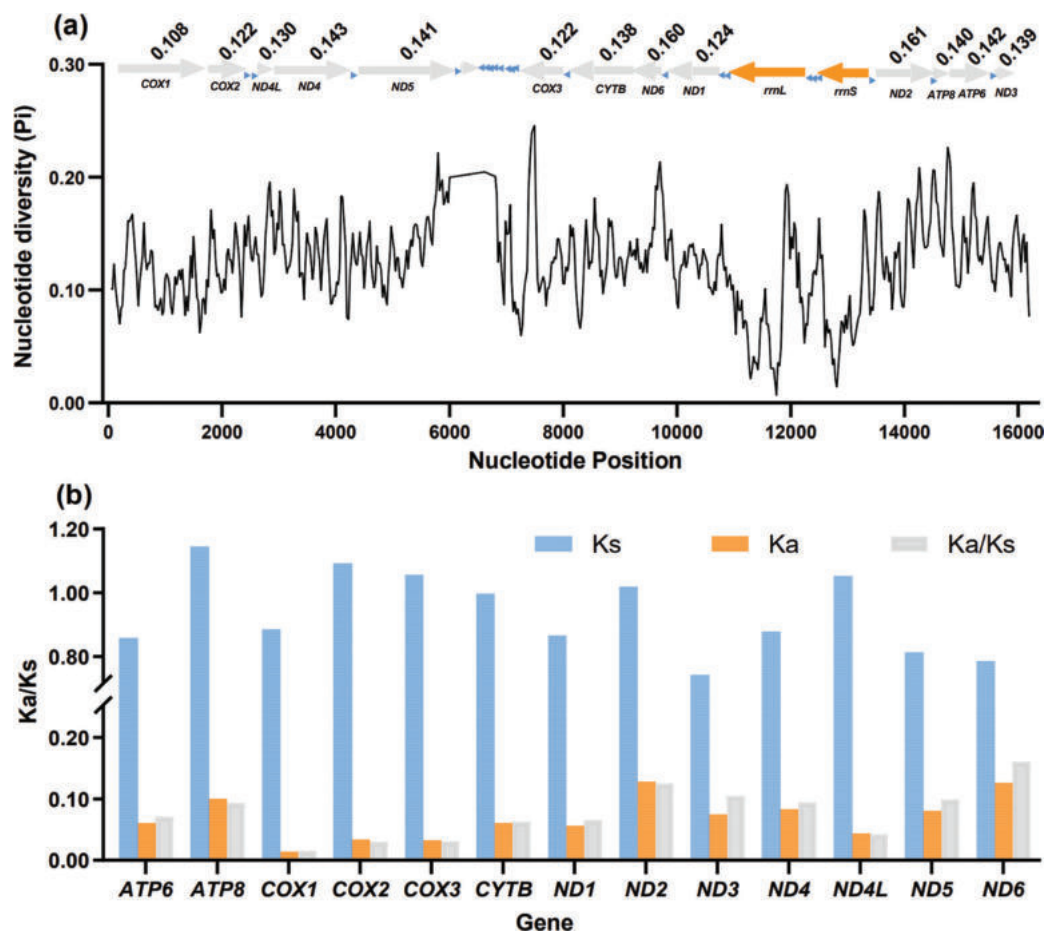


Figure 3. Nucleotide diversity analysis (a) and Ka/Ks rates (b) of 13 PCGs based on nine Semisulcospiridae species. The Pi values for the 13 PCGs is shown in the graph, with the PCGs in gray, rRNAs in orange, and tRNAs in blue. The black line represents the value of nucleotide diversity (Pi) (window size = 100 bp, step size = 20 bp). The blue, orange and gray columns represent the Ks, Ka and Ka/Ks values, respectively.

(Fig. 4a). After the re-annotation of all sequences within this family, both gene positions and orientations were found to be consistent, indicating a highly conserved gene arrangement (Fig. 4b).

In Semisulcospiridae species, duplicated *trnL* was positioned immediately after *rml*, and *trnS* preceded *rns* and *ND2*. Additionally, *trnI*, *trnP* and *trnH* were located immediately before *ND3*, *ND6* and *ND5*. Furthermore, *trnM* was located immediately after the *COX3* gene (Fig. 4b). The mitochondrial genome exhibited a highly conserved gene arrangement. These orders were *COX1-COX2*, *ND4L-ND4-ND5*, *ND1-ND6-CYTB-COX3* and *ND2-ATP8-ATP6-ND3*. The type of tRNA between certain PCGs was a common feature in all species of Semisulcospiridae (Fig. 4b).

Phylogenetic analysis

In this study, both the ML and BI methods produced identical topological structures for each dataset. The BI tree is presented here due to its higher overall support values. Datasets I (AA), II (PCG123) and III (PCG12) formed a consistent tree (Fig. 5). Among the six trees, the Bayesian posterior probability of the phylogenetic tree based on the AA dataset was the highest (Fig. 5a).

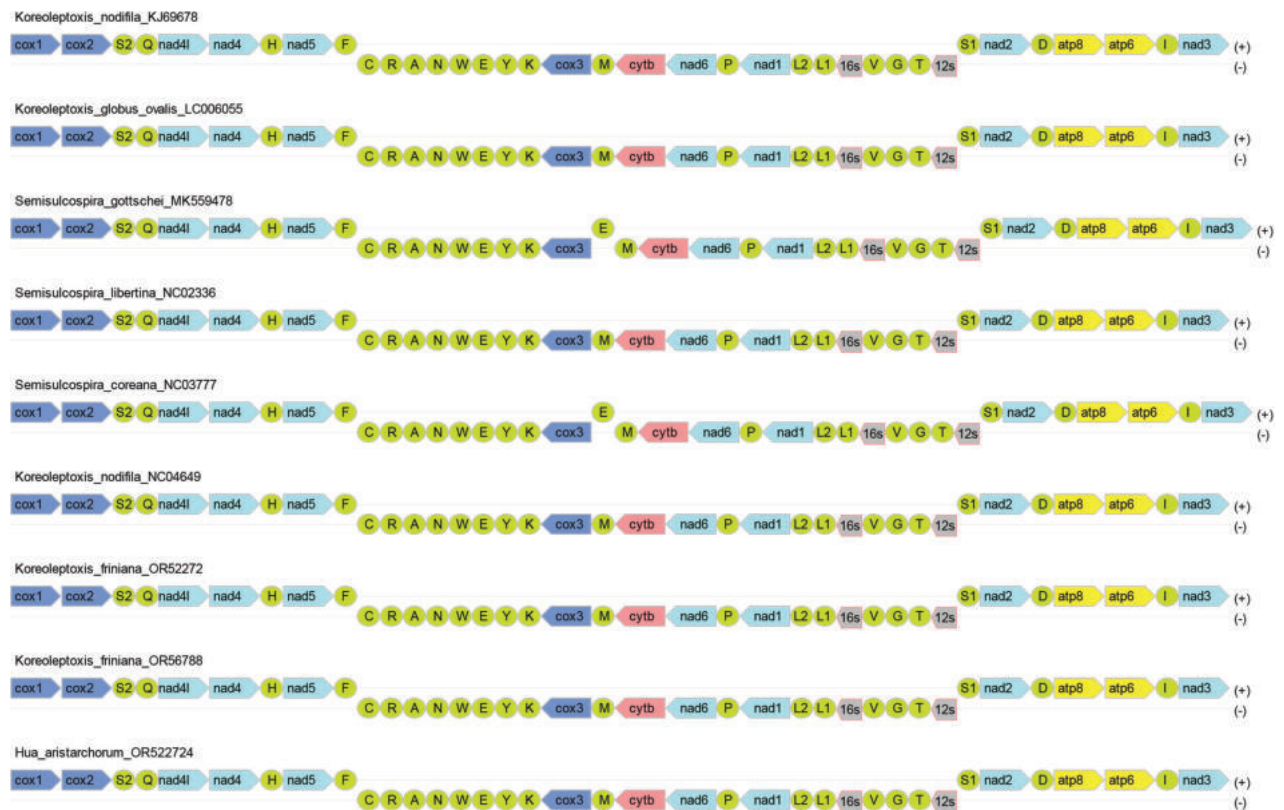


Figure 4. The mitochondrial genome composition and arrangement of Semisulcospiridae. The PCGs are colored based on their functional group (dark blue represents *COX1-3*, light blue corresponds to *ND1-6*, pink indicates *CYTB* and yellow signifies *ATP6* and *ATP8*), rRNAs (*12S* and *16S*) are represented by gray modules, and the positions of the tRNAs are portrayed using their single-letter amino acid code (green modules). The non-coding region is not displayed. Note: *H. aristarchorum* is highlighted in red.

Eight of the 22 extant families belonging to Cerithioidea were included in this study. All Semisulcospiridae species clustered into a clade. These results confirm that Semisulcospiridae is a sister group of Pleuroceridae (Fig. 5a). Within Semisulcospiridae, three of the four genera were included. The nine sequences cluster into three clades, each exhibiting high support. *Hua aristarchorum* is sister to two clades containing *Koreoileptoxis* species; however, a *Semisulcospira* species (*S. libertina* NC023 364) appears among the *Koreoileptoxis* species (Fig. 5a).

We assumed that *S. libertina* NC_023364 may have been misidentified. The distribution of freshwater snails is usually restricted (Von Rintelen and Glaubrecht 2005; Köhler 2017). The type localities of *S. libertina* are Simoda and Ousima in Japan, but specimen KF736848 originated from Poyang Lake, China (Gould 1859; Zeng et al. 2015). The mt *COX1* and *16S* rRNA sequences of NC_023364 were compared with those in the public database GenBank using a BLAST search to verify its exact affiliation. Three sequences of *16S* rRNA and two sequences of *COX1* were matched, exhibiting an identity of over 99%. The identity of the three matching *16S* rRNA sequences was 99.09% (GenBank accession No's. MK944155, MK944156, and MK944157, from *K. praenotata*), and the two matching *COX1* sequences were 99.21% and 99.08% (GenBank accession No. MK968983, from *K. praenotata*, and MK969039, from *K. davidi*). The specimens were obtained from Wuyuan County, Jiangxi Province

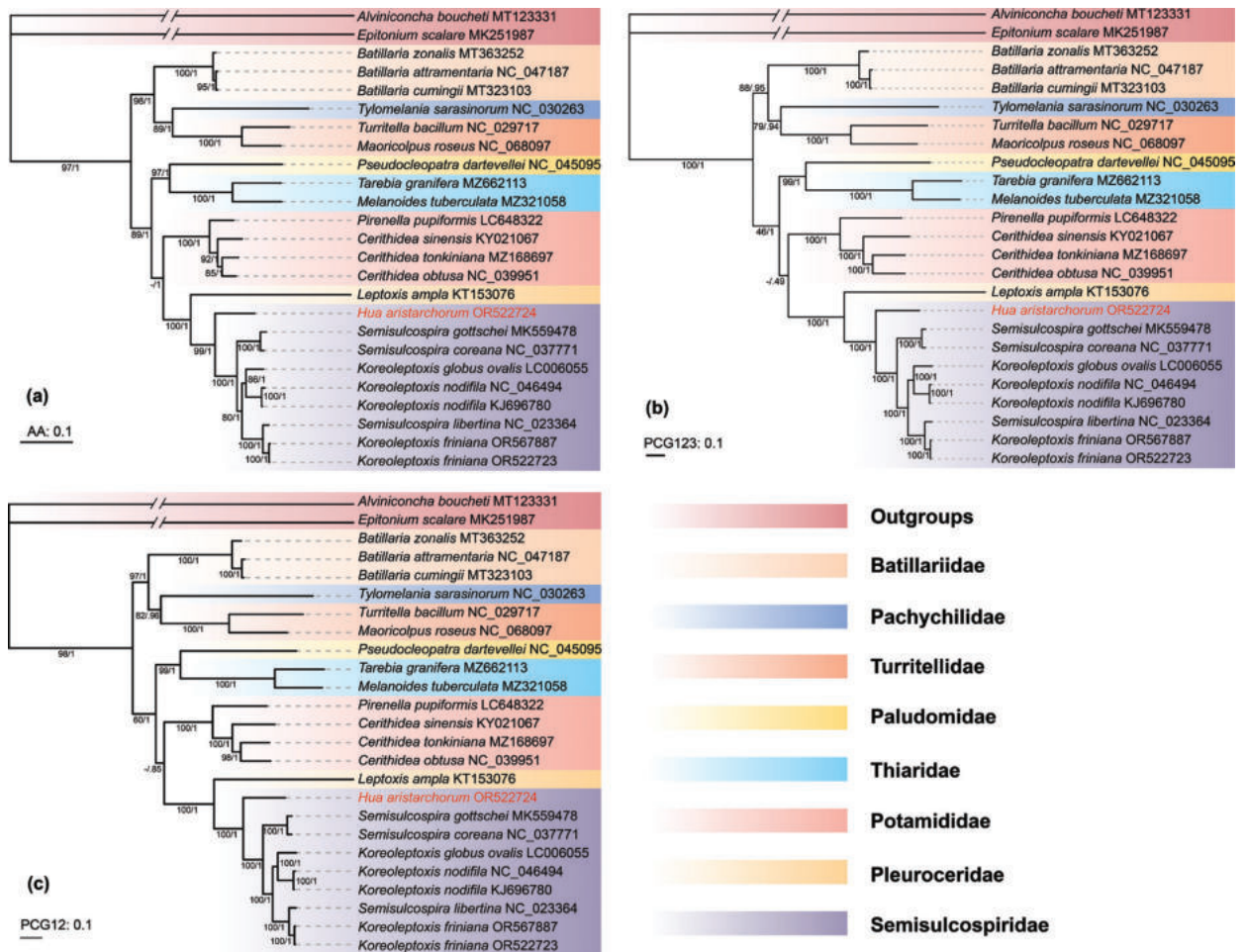


Figure 5. Phylogenetic tree (BI) of Cerithioidea species inferred from dataset I AA (a), II PCG123 (b) and III PCG12 (c). The numbers at the internodes represent maximum likelihood (ML) bootstrap (BS) and Bayesian inference (BI) posterior probabilities (PP). The GenBank accession numbers used are listed after the species names. The scale bar indicates the number of substitutions per site. Note: *H. aristarchorum* is highlighted in red.

(MK944155, MK944156, MK944157, MK969039) and Ningguo City, Anhui Province (MK969893), China (Du et al. 2019b). Based on these findings, we suspect that NC_023364 as *S. libertina* is a misidentification; it should be *K. praenotata* or *K. davidi*.

Many previous studies (Köhler 2017; Du et al. 2019a, 2019b; Du and Yang 2023) indicated that three valid genera are distributed in Asia, as indicated by the three clades shown in the phylogenetic tree (Fig. 5). However, Köhler (2017) considered that *Semisulcospira* is not a monophyletic group; of the three primary clades, two of them are viviparous, and one is oviparous. The oviparous clade is treated as a distinct genus, *Koreoleptoxis*. The other two clades are both classified as *Semisulcospira*, although they do not form a monophyletic group. However, the species involved in this study only cover two of the clades in Köhler (2017). According to these sequences, species relationships are not contrary to Köhler (2017); therefore, due to taxon sampling limitations the conclusion in Köhler (2017) has not been refuted. More sequences and further analysis are still needed to resolve relationships within *Semisulcospira*.

Conclusions

In this study, we determined and described the complete mitogenome of *Hua aristarchorum* to supplement the limited mitogenome information available for the genus. Three distinct assembly methods were employed to ensure reliability of the assembly: GetOrganelle, NovoPlasty and SPAdes. The 15,691 bp mitogenome contains 37 genes and an AT-rich region. *ND4* starts with GTG, and the other PCGs start with ATG. All of the PCGs are terminated using the TAN codon. RSCU analysis indicated that codons are biased toward the use of A/U at the third codon.

Nucleotide diversity analysis can help identify regions with significant nucleotide differences, which is useful for species-specific marker development, especially in challenging-to-identify taxa. Our results reveal that the *COX1* gene is the slowest evolving and least variable region, indicating that *COX1* as a barcode may need to be carefully tested. To identify the intricate shell sculpture of species of Semisulcospiridae or other families of Cerithioidea, we suggest the inclusion of genes with rapidly evolving rates and high Pi values, such as *ND6* or *ND2*, may be markers in diagnostic, detection, and population genetic studies of Cerithioidea.

Lee et al. (2019) mentioned concerns regarding the reliability of sequence annotation information in their study of the gene structure of Cerithioidea. This underscores the significance of mitochondrial gene annotation and the need for a uniform annotation approach. In this study, we uniformly annotated all sequences from Semisulcospiridae. In contrast to the partial gene variations that information downloaded directly from GenBank may show, our results revealed a very high level of conservation in gene structure within this family.

ML and BI methods were employed to evaluate phylogenetic relationships within Cerithioidea based on three datasets (AA, PCG123, and PCG12), yielding identical trees. The results confirm that Semisulcospiridae is closely related to Pleuroceridae, and high supports indicate that nine sequences of seven species from three genera used in this study within Semisulcospiridae form three clades, corresponding to three valid genera distributed in Asia. One clade is *H. aristarchorum*, and it is sister to the other two clades. But we find one species (*S. libertina* NC_023364) misplaced. Through analysis of its geographical distribution and comparisons with GenBank database sequences, we suspect that NC_023364 has been misidentified.

Köhler (2017) mentioned that *Semisulcospira* might not be a monophyletic group, but considering the present study only includes nine sequences from seven species, we can only reach a tentative conclusion on genus monophyly. Sequences from more species are still needed to understand the phylogeny of Semisulcospiridae in depth.

In this study, we identified annotation errors and misidentifications in public databases and highlighted their potential influence on our research results. For future research, it is crucial to adopt an appropriate approach that utilizes data from public databases. Moreover, inaccurate phylogenetic inferences are more likely to occur without sufficient specimen acquisition for intraspecific variability and geographic coverage. Therefore, comprehensive taxon sampling is necessary to resolve the phylogeny and origin of Cerithioidea with high accuracy.

Acknowledgments

Special gratitude is due to two reviewers, Xiaoping Wu and Zhongguang Chen, as well as the editor Frank Köhler for carefully and critically reading the manuscript. We are also grateful to Christopher Glasby and Zdravka Zorkova for polishing the formats of the manuscript. Their comments and suggestions helped greatly to improve the quality of the manuscript. We would like to thank Mr Bao-Gang Liu's help in collecting the specimens.

Additional information

Conflict of interest

The authors have declared that no competing interests exist.

Ethical statement

No ethical statement was reported.

Funding

This work was supported by the Monitoring of the ecological restoration status of mangroves in the first phase of Xiatanwei Mangrove Park, Xiamen City (No. 20233160A0406).

Author contributions

Conceptualization: YX, SY. Data curation: SZ. Formal analysis: SZ. Funding acquisition: SY. Investigation: YM. Methodology: DY. Project administration: YX. Resources: YM, DY. Supervision: SY, DY. Validation: DY. Visualization: SZ. Writing - original draft: YX, YM, SZ. Writing - review and editing: YX, SY.

Author ORCIDs

Yibin Xu  <https://orcid.org/0009-0004-7386-806X>

Sheng Zeng  <https://orcid.org/0009-0001-0943-3772>

Yuanzheng Meng  <https://orcid.org/0009-0006-3294-8973>

Deyuan Yang  <https://orcid.org/0000-0003-3735-9909>

Shengchang Yang  <https://orcid.org/0000-0003-3731-7872>

Data availability

All of the data that support the findings of this study are available in the main text or Supplementary Information.

References

- Aksenova OV, Bolotov IN, Gofarov MY, Kondakov AV, Vinarski MV, Beshpalaya YV, Kolosova YS, Palatov DM, Sokolova SE, Spitsyn VM, Tomilova AA, Travina OV, Vikhrev IV (2018) Species richness, molecular taxonomy and biogeography of the radicine pond snails (Gastropoda: Lymnaeidae) in the Old World. *Scientific Reports* 8(1): 11199. <https://doi.org/10.1038/s41598-018-29451-1>
- Andrews S (2010) FastQC: a quality control tool for high throughput sequence data. <https://www.bioinformatics.babraham.ac.uk/projects/fastqc/>
- Bankevich A, Nurk S, Antipov D, Gurevich AA, Dvorkin M, Kulikov AS, Lesin VM, Nikolenko SI, Pham S, Prjibelski AD, Pyshkin AV, Sirotkin AV, Vyahhi N, Tesler G, Alekseyev MA,

- Pevzner PA (2012) SPAdes: A new genome assembly algorithm and its applications to single-cell sequencing. *Journal of Computational Biology* 19(5): 455–477. <https://doi.org/10.1089/cmb.2012.0021>
- Boore JL (1999) Animal mitochondrial genomes. *Nucleic Acids Research* 27(8): 1767–1780. <https://doi.org/10.1093/nar/27.8.1767>
- Bernt M, Donath A, Jühling F, Externbrink F, Florentz C, Fritzsche G, Pütz J, Middendorf M, Stadler PF (2013) MITOS: Improved de novo metazoan mitochondrial genome annotation. *Molecular Phylogenetics and Evolution* 69(2): 313–319. <https://doi.org/10.1016/j.ympev.2012.08.023>
- Castresana J (2000) Selection of conserved blocks from multiple alignments for their use in phylogenetic analysis. *Molecular Biology and Evolution* 17(4): 540–552. <https://doi.org/10.1093/oxfordjournals.molbev.a026334>
- Chen S (1943) Two new genera, two new species, and two new names of Chinese Melaniidae. *The Nautilus* 57(1): 19–21.
- Chen S, Zhou Y, Chen Y, Gu J (2018) fastp: An ultra-fast all-in-one FASTQ preprocessor. *Bioinformatics* 34(17): i884–i890. <https://doi.org/10.1093/bioinformatics/bty560>
- Chen H, Shi B-Y, Du L-N, Sun H-Y (2023) Description of a New Species of Hua (Gastropoda: Semisulcospiridae) from Guizhou, China, Based on Morphology and Molecular Evidence. *Zoological Science* 40(5): 414–421. <https://doi.org/10.2108/zs230025>
- Choi EH, Choi NR, Hwang UW (2021) The mitochondrial genome of an Endangered freshwater snail *Koreoleptoxis nodifila* (Caenogastropoda: Semisulcospiridae) from South Korea. *Mitochondrial DNA, Part B, Resources* 6(3): 1120–1123. <https://doi.org/10.1080/23802359.2021.1901626>
- Davis GM (1972) Geographic variation in *Semisulcospira libertina* (Mesogastropoda: Pleuroceridae). *The Journal of Molluscan Studies* 40(1): 5–32.
- Davis GM, Chen C-E, Kang ZB, Liu Y-Y (1994) Snail hosts of *Paragonimus* in Asia and the Americas. *Biomedical and Environmental Sciences* 7(4): 369–382.
- Dierckxsens N, Mardulyn P, Smits G (2017) NOVOPlasty: De novo assembly of organelle genomes from whole genome data. *Nucleic Acids Research* 45(4): e18. <https://doi.org/10.1093/nar/gkw955>
- Du LN, Yang JX (2019) A review of *Sulcospira* (Gastropoda: Pachychilidae) from China, with description of two new species. *Molluscan Research* 39(3): 241–252. <https://doi.org/10.1080/13235818.2019.1572848>
- Du L-N, Yang J-X (2023) Colored Atlas of Chinese Melania. Henan Science and Technology Press, Zhengzhou, 225 pp.
- Du L-N, Köhler F, Yu G-H, Chen X-Y, Yang J-X (2019a) Comparative morpho-anatomy and mitochondrial phylogeny of Semisulcospiridae in Yunnan, south-western China, with description of four new species (Gastropoda: Cerithioidea). *Invertebrate Systematics* 33(6): 825–848. <https://doi.org/10.1071/IS18084>
- Du LN, Chen J, Yu GH, Yang JX (2019b) Systematic relationships of Chinese freshwater semisulcospirids (Gastropods, Cerithioidea) revealed by mitochondria sequences. *Zoological Research* 40(6): 541–551. <https://doi.org/10.24272/j.issn.2095-8137.2019.033>
- Gould AA 1859. Descriptions of shells collected by the North Pacific Exploring Expedition, *Proceedings of the Boston Society of Natural History*, 161–166. <https://doi.org/10.5962/bhl.part.4821>
- Group HCG, Andrade P, Arreola L, Belnas M, Bland E, Castillo A, Cisneros O, Contreras V, Diaz C, Do KT (2019) The complete mitogenome of the invasive Japanese mud snail *Batillaria attramentaria* (Gastropoda: Batillariidae) from Elkhorn Slough, California,

- USA. Mitochondrial DNA, Part B, Resources 4(2): 4031–4032. <https://doi.org/10.1080/23802359.2019.1688719>
- Guo Y, Fu Z, Feng J, Ye Y, Li J, Guo B, Lv Z (2019) The complete mitochondrial genome and phylogenetic analysis of *Epitonium scalare* (Gastropoda, Epitoniidae). Mitochondrial DNA, Part B, Resources 4(1): 1070–1071. <https://doi.org/10.1080/23802359.2019.1586462>
- Heude P (1889) Diagnoses molluscorum novorum in Sinis collectorum. Journal de Conchyliologie 37: 40–50.
- Hilgers L, Grau JH, Pfaender J, von Rintelen T (2016) The complete mitochondrial genome of the viviparous freshwater snail *Tylomelania sarasinorum* (Caenogastropoda: Cerithioidea). Mitochondrial DNA, Part B, Resources 1(1): 330–331. <https://doi.org/10.1080/23802359.2016.1172046>
- Jin J-J, Yu W-B, Yang J-B, Song Y, DePamphilis CW, Yi T-S, Li D-Z (2020) GetOrganelle: A fast and versatile toolkit for accurate de novo assembly of organelle genomes. Genome Biology 21(1): 1–31. <https://doi.org/10.1186/s13059-020-02154-5>
- Kalyaanamoorthy S, Minh BQ, Wong TK, Von Haeseler A, Jermiin LS (2017) ModelFinder: Fast model selection for accurate phylogenetic estimates. Nature Methods 14(6): 587–589. <https://doi.org/10.1038/nmeth.4285>
- Kato S, Itoh H, Fukumori H, Nakajima N, Kanaya G, Kojima S (2022) The mitochondrial genome of the threatened tideland snail *Pirenella pupiformis* (Mollusca: Caenogastropoda: Potamididae) determined by shotgun sequencing. Mitochondrial DNA, Part B, Resources 7(4): 632–634. <https://doi.org/10.1080/23802359.2022.2060143>
- Katoh K, Standley DM (2013) MAFFT multiple sequence alignment software version 7: Improvements in performance and usability. Molecular Biology and Evolution 30(4): 772–780. <https://doi.org/10.1093/molbev/mst010>
- Kearse M, Moir R, Wilson A, Stones-Havas S, Cheung M, Sturrock S, Buxton S, Cooper A, Markowitz S, Duran C, Thierer T, Ashton B, Meintjes P, Drummond A (2012) Geneious Basic: An integrated and extendable desktop software platform for the organization and analysis of sequence data. Bioinformatics 28(12): 1647–1649. <https://doi.org/10.1093/bioinformatics/bts199>
- Kim YK, Lee SM (2018) The complete mitochondrial genome of freshwater snail, *Semisulcospira coreana* (Pleuroceridae: Semisulcospiridae). Mitochondrial DNA, Part B, Resources 3(1): 259–260. <https://doi.org/10.1080/23802359.2018.1443030>
- Köhler F (2017) Against the odds of unusual mtDNA inheritance, introgressive hybridisation and phenotypic plasticity: Systematic revision of Korean freshwater gastropods (Semisulcospiridae, Cerithioidea). Invertebrate Systematics 31(3): 249–268. <https://doi.org/10.1071/IS16077>
- Köhler F, Glaubrecht M (2001) Toward a systematic revision of the Southeast Asian freshwater gastropod *Brotia* H. Adams, 1866 (Cerithioidea: Pachychilidae): an account of species from around the South China Sea. The Journal of Molluscan Studies 67(3): 281–318. <https://doi.org/10.1093/mollus/67.3.281>
- Köhler F, Li-Na D, Jun-Xing Y (2010a) A new species of *Brotia* from Yunnan, China (Caenogastropoda, Pachychilidae). Zoosystematics and Evolution 86(2): 295–300. <https://doi.org/10.1002/zoos.201000012>
- Köhler F, Panha S, Glaubrecht M (2010b) Speciation and radiation in a river: assessing the morphological and genetic differentiation in a species flock of viviparous gastropods (Cerithioidea: Pachychilidae). In: Glaubrecht M (Ed.) Evolution in Action. Springer, Berlin, Heidelberg, 513–550. https://doi.org/10.1007/978-3-642-12425-9_24

- Kumar S, Stecher G, Li M, Knyaz C, Tamura K (2018) MEGA X: Molecular evolutionary genetics analysis across computing platforms. *Molecular Biology and Evolution* 35(6): 1547–1549. <https://doi.org/10.1093/molbev/msy096>
- Lee SY, Lee HJ, Kim YK (2019) Comparative analysis of complete mitochondrial genomes with Cerithioidea and molecular phylogeny of the freshwater snail, *Semisulcospira gottschei* (Caenogastropoda, Cerithioidea). *International Journal of Biological Macromolecules* 135: 1193–1201. <https://doi.org/10.1016/j.ijbiomac.2019.06.036>
- Lee W-K, Hou BK, Ju S-J, Kim S-J (2020) Complete mitochondrial genome of the hydrothermal vent provannid snail *Alviniconcha boucheti* (Gastropoda: Abyssochrysoidea) from the North Fiji Basin. *Mitochondrial DNA, Part B, Resources* 5(2): 1848–1849. <https://doi.org/10.1080/23802359.2020.1750983>
- Letunic I, Bork P (2016) Interactive tree of life (iTOL) v3: An online tool for the display and annotation of phylogenetic and other trees. *Nucleic Acids Research* 44(W1): W242–W245. <https://doi.org/10.1093/nar/gkw290>
- Liang M, Du L-N, Luo F-G (2022) Description of a new species of *Sulcospira* (Gastropoda: Pachychilidae) from Guangxi, China based on morphology and molecular evidence. *Zoological Science* 39(2): 219–224. <https://doi.org/10.2108/zs210090>
- Ling Y, Zhang Y, Ngatia JN, Zhou H (2022) The complete mitochondrial genome of *Melanoides tuberculata* (Müller, 1774) in Guangdong, China. *Mitochondrial DNA, Part B, Resources* 7(7): 1319–1320. <https://doi.org/10.1080/23802359.2022.2054735>
- Liu Y, Zhang W, Wang Y, Wang E (1979) *Economic Fauna of China: Freshwater Mollusca*. Science Press, Beijing, 134 pp.
- Liu Y, Zhang W, Wang Y (1993) *Medical Malacology*. China Ocean Press, Beijing, 157 pp.
- Lydeard C, Cummings KS (2019) *Freshwater Mollusks of the World: a Distribution Atlas*. JHU Press, Baltimore, 242 pp. <https://doi.org/10.1353/book.66164>
- Mabuchi K, Fraser TH, Song H, Azuma Y, Nishida M (2014) Revision of the systematics of the cardinalfishes (Percomorpha: Apogonidae) based on molecular analyses and comparative reevaluation of morphological characters. *Zootaxa* 3846(2): 151–203. <https://doi.org/10.11646/zootaxa.3846.2.1>
- Meng G, Li Y, Yang C, Liu S (2019) MitoZ: A toolkit for animal mitochondrial genome assembly, annotation and visualization. *Nucleic Acids Research* 47(11): e63. <https://doi.org/10.1093/nar/gkz173>
- Minton RL, Norwood AP, Hayes DM (2008) Quantifying phenotypic gradients in freshwater snails: a case study in *Lithasia* (Gastropoda: Pleuroceridae). *Hydrobiologia* 605(1): 173–182. <https://doi.org/10.1007/s10750-008-9332-1>
- Nguyen L-T, Schmidt HA, Von Haeseler A, Minh BQ (2015) IQ-TREE: A fast and effective stochastic algorithm for estimating maximum-likelihood phylogenies. *Molecular Biology and Evolution* 32(1): 268–274. <https://doi.org/10.1093/molbev/msu300>
- Nguyen DH, Lemieux C, Turmel M, Nguyen VD, Mouget J-L, Witkowski A, Tremblay R, Gastineau R (2018) Complete mitogenome of *Cerithidea obtusa*, the red chut-chut snail from the Càn Giở Mangrove in Vietnam. *Mitochondrial DNA, Part B, Resources* 3(2): 1267–1269. <https://doi.org/10.1080/23802359.2018.1532832>
- Perna NT, Kocher TD (1995) Patterns of nucleotide composition at fourfold degenerate sites of animal mitochondrial genomes. *Journal of Molecular Evolution* 41(3): 353–358. <https://doi.org/10.1007/BF01215182>
- Ronquist F, Teslenko M, Van Der Mark P, Ayres DL, Darling A, Höhna S, Larget B, Liu L, Suchard MA, Huelsenbeck JP (2012) MrBayes 3.2: Efficient Bayesian phylogenetic

- inference and model choice across a large model space. *Systematic Biology* 61(3): 539–542. <https://doi.org/10.1093/sysbio/sys029>
- Rozas J, Ferrer-Mata A, Sánchez-DelBarrio JC, Guirao-Rico S, Librado P, Ramos-Onsins SE, Sánchez-Gracia A (2017) DnaSP 6: DNA sequence polymorphism analysis of large data sets. *Molecular Biology and Evolution* 34(12): 3299–3302. <https://doi.org/10.1093/molbev/msx248>
- Stelbrink B, Kehlmaier C, Wilke T, Albrecht C (2019) The near-complete mitogenome of the critically endangered *Pseudocleopatra dartevellei* (Caenogastropoda: Paludomidae) from the Congo River assembled from historical museum material. *Mitochondrial DNA, Part B, Resources* 4(2): 3229–3231. <https://doi.org/10.1080/23802359.2019.1669081>
- Strong EE, Köhler F (2009) Morphological and molecular analysis of '*Melania*' *jacqueti* Dautzenberg and Fischer, 1906: from anonymous orphan to critical basal offshoot of the Semisulcospiridae (Gastropoda: Cerithioidea). *Zoologica Scripta* 38(5): 483–502. <https://doi.org/10.1111/j.1463-6409.2008.00385.x>
- Strong EE, Garner JT, Johnson PD, Whelan NV (2022) A systematic revision of the genus *Juga* from fresh waters of the Pacific Northwest, USA (Cerithioidea, Semisulcospiridae). *European Journal of Taxonomy* 848: 1–97. <https://doi.org/10.5852/ejt.2022.848.1993>
- Von Rintelen T, Glaubrecht M (2005) Anatomy of an adaptive radiation: a unique reproductive strategy in the endemic freshwater gastropod *Tylomelania* (Cerithioidea: Pachychilidae) on Sulawesi, Indonesia and its biogeographical implications. *Biological Journal of the Linnean Society, Linnean Society of London* 85(4): 513–542. <https://doi.org/10.1111/j.1095-8312.2005.00515.x>
- Whelan NV, Strong EE (2016) Morphology, molecules and taxonomy: Extreme incongruence in pleurocerids (Gastropoda, Cerithioidea, Pleuroceridae). *Zoologica Scripta* 45(1): 62–87. <https://doi.org/10.1111/zsc.12139>
- Wiggering B, Neiber MT, Krailas D, Glaubrecht M (2019) Biological diversity or nomenclatural multiplicity: the Thai freshwater snail *Neoradina prasongi* Brandt, 1974 (Gastropoda: Thiariidae). *Systematics and Biodiversity* 17(3): 260–276. <https://doi.org/10.1080/14772000.2019.1606862>
- Wilke T, Kehlmaier C, Stelbrink B, Albrecht C, Bouchet P (2023) Historical DNA solves century-old mystery on sessility in freshwater gastropods. *Molecular Phylogenetics and Evolution* 185: 107813. <https://doi.org/10.1016/j.ympev.2023.107813>
- Xu Y, Luo P, Wang P, Zhu P, Zhang H, Wu H, Liao Y, Yu M, Fu J (2019) The complete mitochondrial genome of *Cerithidea sinensis* (Philippi, 1848). *Mitochondrial DNA, Part B, Resources* 4(2): 2742–2743. <https://doi.org/10.1080/23802359.2019.1644549>
- Yan C, Feng J, Ye Y, Li J, Guo B (2020a) The complete mitochondrial genome and phylogenetic analysis of *Batillaria cumingi* (Gastropoda: Batillariidae). *Mitochondrial DNA, Part B, Resources* 5(3): 2355–2356. <https://doi.org/10.1080/23802359.2020.1772685>
- Yan C, Feng J, Ye Y, Li J, Guo B (2020b) The complete mitochondrial genome and phylogenetic analysis of *Batillaria zonalis* (Gastropoda: Batillariidae). *Mitochondrial DNA, Part B, Resources* 5(3): 2256–2257. <https://doi.org/10.1080/23802359.2020.1772139>
- Yang S, Deng Z (2022) The complete mitochondrial genome of *Cerithidea tonkiniana* (Mabille, 1887) in Guangxi, China. *Mitochondrial DNA, Part B, Resources* 7(4): 669–670. <https://doi.org/10.1080/23802359.2021.2006813>
- Yang Q-Q, Yu X-P (2019) A new species of apple snail in the genus *Pomacea* (Gastropoda: Caenogastropoda: Ampullariidae). *Zoological Studies (Taipei, Taiwan)* 58: 13–19. <https://doi.org/10.6620/ZS.2019.58-13>

- Yin N, Zhao S, Huang X-C, Ouyang S, Wu X-P (2022) Complete mitochondrial genome of the freshwater snail *Tarebia granifera* (Lamarck, 1816)(Gastropoda: Cerithioidea: Thiariidae). *Mitochondrial DNA, Part B, Resources* 7(1): 259–261. <https://doi.org/10.1080/23802359.2022.2026832>
- Zeng T, Yin W, Xia R, Fu C, Jin B (2015) Complete mitochondrial genome of a freshwater snail, *Semisulcospira libertina* (Cerithioidea: Semisulcospiridae). *Mitochondrial DNA* 26(6): 897–898. <https://doi.org/10.3109/19401736.2013.861449>
- Zeng L, Wang Y, Zhang J, Wu C (2016) Complete mitochondrial genome of *Turritella terebra bacillum*. *Mitochondrial DNA, Part B, Resources* 1(1): 350–351. <https://doi.org/10.1080/23802359.2016.1144088>
- Zhang L-J, Chen S-C, Yang L-T, Jin L, Köhler F (2015) Systematic revision of the freshwater snail *Margarya* Nevill, 1877 (Mollusca: Viviparidae) endemic to the ancient lakes of Yunnan, China, with description of new taxa. *Zoological Journal of the Linnean Society* 174(4): 760–800. <https://doi.org/10.1111/zoj.12260>
- Zhang D, Li WX, Zou H, Wu SG, Li M, Jakovlić I, Zhang J, Chen R, Wang GT (2018) Mitochondrial genomes of two diplectanids (Platyhelminthes: Monogenea) expose paraphyly of the order Dactylogyridea and extensive tRNA gene rearrangements. *Parasites & Vectors* 11(1): 1–13. <https://doi.org/10.1186/s13071-018-3144-6>
- Zhang D, Gao F, Jakovlić I, Zou H, Zhang J, Li WX, Wang GT (2020) PhyloSuite: An integrated and scalable desktop platform for streamlined molecular sequence data management and evolutionary phylogenetics studies. *Molecular Ecology Resources* 20(1): 348–355. <https://doi.org/10.1111/1755-0998.13096>
- Zhang L-J, Du L-N, von Rintelen T (2023) A new genus of river snails, *Dalipaludina* (Gastropoda, Viviparidae), endemic to the Yunnan Plateau of SW China. *Zoosystematics and Evolution* 99(2): 285–297. <https://doi.org/10.3897/zse.99.102586>

Supplementary material 1

Supplementary information

Authors: Yibin Xu, Sheng Zeng, Yuanzheng Meng, Deyuan Yang, Shengchang Yang

Data type: docx

Explanation note: **table S1**. Original and Gblock lengths of the PCG and AA sequences. **table S2**. Codon numbers and relative synonymous codon usage (RSCU) of 13 PCGs in the *H. aristarchorum* mitogenome. **figure S1**. Potential secondary structures of 22 inferred tRNAs in the *H. aristarchorum* mitogenome.

Copyright notice: This dataset is made available under the Open Database License (<http://opendatacommons.org/licenses/odbl/1.0/>). The Open Database License (ODbL) is a license agreement intended to allow users to freely share, modify, and use this Dataset while maintaining this same freedom for others, provided that the original source and author(s) are credited.

Link: <https://doi.org/10.3897/zookeys.1192.116269.suppl1>

The fourth species of *Leptobrachella* (Anura, Megophryidae) found at Shiwandashan National Nature Reserve, Guangxi, China

Wei-Cai Chen^{1,2}, Peng Li¹, Wan-Xiao Peng¹, You-Jun Liu³, Yong Huang⁴

1 Key Laboratory of Environment Change and Resources Use in Beibu Gulf Ministry of Education, Nanning Normal University, Nanning 530001, China

2 Guangxi Key Laboratory of Earth Surface Processes and Intelligent Simulation, Nanning Normal University, Nanning 530001, China

3 Shiwandashan National Nature Reserve, Fangcheng 538000, China

4 Guangxi University of Chinese Medicine, Nanning 530200, China

Corresponding author: Wei-Cai Chen (chenweicai2003@126.com)

Abstract

A new species of the genus *Leptobrachella*, *L. guinanensis* **sp. nov.**, is described in this study based on morphological, molecular, and bioacoustic data. The species was discovered in the Shiwandashan National Nature Reserve in Shangsi County, Guangxi, China. Phylogenetically, *L. guinanensis* **sp. nov.** is closely related to *L. ventripunctata*. However, there are distinct morphological differences between *L. guinanensis* **sp. nov.** and *L. ventripunctata*, as well as three other sympatric species (*L. shangsiensis*, *L. shiwandashanensis*, and *L. sungi*). These differences include body size (SVL 30.5–32.5 mm in males; 38.7–41.8 mm in females in the new species vs 25.5–28.0 mm in males, 31.5–35.0 mm in females in *L. ventripunctata*), the absence of brown spots on the ventral surface (vs chest and belly creamy white with many scattered brown spots in *L. ventripunctata*), 1/3 toe webbing and wide toe lateral fringes (vs no toe webbing and no lateral fringes in *L. ventripunctata*), and distinct dermal ridges under toes (vs absent in *L. ventripunctata*). Furthermore, the dominant vocal frequencies of the new species range from 7.3 to 8.3 kHz, which is unique compared to other *Leptobrachella* species and represents the highest dominant frequencies ever recorded. The Shiwandashan National Nature Reserve is now home to four known sympatric species of *Leptobrachella*.

Key words: Bioacoustics, morphology, phylogeny, sympatric species



Academic editor: Johannes Penner

Received: 6 December 2022

Accepted: 2 February 2024

Published: 22 February 2024

ZooBank: <https://zoobank.org/96474EC4-42B1-4BEE-A68D-4F736A8A4EB9>

Citation: Chen W-C, Li P, Peng W-X, Liu Y-J, Huang Y (2024) The fourth species of *Leptobrachella* (Anura, Megophryidae) found at Shiwandashan National Nature Reserve, Guangxi, China. ZooKeys 1192: 257–279. <https://doi.org/10.3897/zookeys.1192.98352>

Copyright: © Wei-Cai Chen et al. This is an open access article distributed under terms of the Creative Commons Attribution License ([Attribution 4.0 International – CC BY 4.0](https://creativecommons.org/licenses/by/4.0/)).

Introduction

The Shiwandashan National Nature Reserve is situated in southern Guangxi, China, near the Sino-Vietnamese border, at coordinates 21°30'–22°08'N, 107°30'–108°30'E. Covering an area of 1,745 km², the reserve exhibits an elevation range from slightly below 200 m to 1,462 m at the summit of Mt. Shuliangling. With a tropical monsoon climate, the reserve lies within the tropical mountain climate zone. The average annual temperature varies between 21.3 °C and 22.4 °C, while the total amount of annual precipitation ranges from 1,203.6 to 2,820.2 mm (Tan 2014). Recent literature reports the presence of 47 amphibian species within the reserve (Ren et al. 2018). Over the past decade, six new amphibian species have been discovered in this reserve. These

include *Leptobranchella shangsiensis* Chen, Liao, Zhou & Mo, 2019 (Chen et al. 2019); *Leptobranchella shiwandashanensis* Chen, Peng, Pan, Liao, Liu & Huang, 2021 (Chen et al. 2021); *Nidirana shiwandashanensis* Chen, Peng, Li & Liu, 2022 (Chen et al. 2022a); *Occidozyga shiwandashanensis* Chen, Peng, Liu, Huang, Liao & Mo, 2022 (Chen et al. 2022b); *Odorrana fengkaiensis* Wang, Lau, Yang, Chen, Liu, Pang & Liu, 2015 (Wang et al. 2015); and *Zhangixalus pinglongensis* (Mo, Chen, Liao & Zhou, 2016) (Mo et al. 2016). Additionally, the previously recorded *L. sungi* (Lathrop, Murphy, Orlov & Ho, 1998) (Mo et al. 2008) brings the total number of *Leptobranchella* species in this reserve to three. In our recent study, we collected 14 specimens of *Leptobranchella* within the reserve and observed distinct differences to the known three species. Therefore, this study employs an integrative approach involving morphological, molecular, and bioacoustics analyses to identify and describe this newly discovered species.

Materials and methods

Sampling and morphological examination

Between 2021 and 2022, fourteen specimens were collected at the Shiwandashan National Nature Reserve (**SWDS**), Shangsi County, Guangxi, China (permission no. SWDS20210501). For comparison, nine specimens of *Leptobranchella ventripunctata* (Fei, Ye & Li, 1990) were collected at the Jinzhongshan National Nature Reserve on 22 June 2021 (**JZS**) (permission no. JZS20210605). Additionally, *L. sungi* specimens were collected at the SWDS ($n = 16$) on 4 July 2021, and the Sishuihe Nature Reserve (**SSH**) ($n = 3$) on 20 June 2020, located in Lingyun County, Guangxi, China (permission no. SSH20200615) (Fig. 1). After euthanasia using isoflurane, all specimens were fixed in 10% formalin for 48 h and finally stored in 75% ethanol. Muscle samples were taken prior to fixation and stored in 100% ethanol for subsequent molecular analyses. All specimens and muscle samples are deposited in the collection of Nanning Normal University (**NNU**) (see Table 1 for details). Specimens were measured with a digital caliper to the nearest 0.1 mm. The following measurements were taken:

SVL	snout-vent length;
HL	head length from the tip of snout to rear of jaws;
HW	head width at commissure of jaws;
SNT	snout length from the tip of snout to the anterior eye corner;
ED	diameter of the exposed portion of eyeball;
IOD	interorbital distance, the shortest distance between the anterior corners of the orbits;
IN	internarial space distance;
EN	distance from the eye to nostril, measured from the anterior corner of the eye to the posterior margin of the nostril;
TD	horizontal diameter of tympanum;
TED	distance from anterior edge of the tympanum to posterior eye corner;
TIB	tibia length with flexed hindlimb;
FLL	forelimb length from elbow to the tip of third finger;
THL	thigh length from vent to knee;

- ML** manus length from the tip of third digit to proximal edge of the inner palmar tubercle;
- PL** pes length from the tip of fourth toe to the proximal edge of inner metatarsal tubercle;
- FEM** maximum diameter of femoral gland.

Sex was determined either directly through observation of calling males, presence of vocal sacs in males, or the presence of eggs in the abdomen of females. The webbing formula was determined following Savage (1975). Morphological data were obtained from the collected vouches specimens (Suppl. material 1: table S1) as well as other museum specimens (Suppl. material 1: table S2).

Phylogenetic analyses

DNA was isolated from muscle samples using Tiangen Biotech Co. Ltd. tissue extraction kits (Beijing, China). The mitochondrial fragments of 16S (~530 bp) were amplified and sequenced using the primer pairs 16Sar_L (5'-CGCCT-GTTTACCAA AAACAT-3') and 16Sbr_H (5'-CCGGTCTGAACTCAGATCACGT-3'). Polymerase chain reaction (PCR) amplification followed the method described by Chen et al. (2021). The 16S fragments were sequenced on an ABI Prism 3730 automated DNA sequencer, and the new sequences were deposited in GenBank (OP548561–OP548567, OP548569–OP548579). Phylogenetic trees were reconstructed using the new sequences and homologous sequences of the genus *Leptobranchella* downloaded from GenBank (Table 1). The molecular data included topotypic sequences of *L. ventripunctata* (GenBank no. MH055831, KM014811, and MG520361) from Xishuangbanna, Yunnan, China (Sung et al. 2014; Chen et al. 2018; Yang et al. 2018). Bayesian inference (BI) and maximum likelihood (ML) methods were used to construct the phylogenetic trees. BI was performed using MrBayes v. 3.1.2 (Ronquist and Huelsenbeck 2003). The best-fit evolution model (GTR+I+G) was tested in JMODELTEST v. 2.1.7 (Posada 2008). Two independent runs with four Markov Chain Monte Carlo simulations were performed for 30 million iterations, and trees were sampled every 1,000th generation. The first 25% of trees were discarded as burn-in. ML analysis was carried out on the CIPRES science gateway with 100 rapid bootstrap replicates (Miller et al. 2010) (<https://www.phylo.org/portal2>). Uncorrected *p*-distances of the 16S gene were estimated using Mega v. 7 (Kumar et al. 2016) with the default settings.

Bioacoustics analysis

Advertisement calls were recorded using a SONY PCM-A10 recorder, and ambient temperature was measured using a digital hygrothermograph. The call recordings were analysed using the software Raven Pro v.1.6 (Cornell Laboratory of Ornithology, Ithaca, NY, USA). Audio-spectrograms were generated using Hanning windows, fast-Fourier transform (FFT) of 512 points, 50% overlap, and 172 Hz grid-spacing. Acoustic parameters were defined following Köhler et al. (2017) and Emmrich et al. (2020). Thus, we refer to a call refer as a group of notes, and the call duration is the time from the beginning of the first note to the end of the last note in a call. Call interval is defined as the time from the end of the last note of a call to the beginning of the first note of the subsequent call.

Table 1. DNA sequences used in this study. ‘*’ represents type locality.

ID	Species	Locality	Voucher no.	16S
1	<i>L. ventripunctata</i>	Longlin County, Guangxi, China	NNU00527	OP548575
2	<i>L. ventripunctata</i>	Longlin County, Guangxi, China	NNU00528	OP548576
3	<i>L. ventripunctata</i>	Longlin County, Guangxi, China	NNU00529	OP548577
4	<i>L. ventripunctata</i>	Longlin County, Guangxi, China	NNU00530	OP548578
5	<i>L. ventripunctata</i>	Longlin County, Guangxi, China	NNU00531	OP548579
6	<i>L. ventripunctata</i>	Xishuangbanna, Yunnan, China*	SYS a001768	KM014811
7	<i>L. ventripunctata</i>	Xishuangbanna, Yunnan, China*	SYS a004539	MG520361
8	<i>L. ventripunctata</i>	Zhushihe, Xishuangbanna, Yunnan, China*	SYSa004536	MH055831
9	<i>L. guinanensis</i> sp. nov.	Shangsi County, Guangxi, China*	NNU00557	OP548561
10	<i>L. guinanensis</i> sp. nov.	Shangsi County, Guangxi, China*	NNU00558	OP548562
11	<i>L. guinanensis</i> sp. nov.	Shangsi County, Guangxi, China*	NNU00559	OP548563
12	<i>L. guinanensis</i> sp. nov.	Shangsi County, Guangxi, China*	NNU00560	OP548564
13	<i>L. guinanensis</i> sp. nov.	Shangsi County, Guangxi, China*	NNU00561	OP548565
14	<i>L. guinanensis</i> sp. nov.	Shangsi County, Guangxi, China*	NNU00569	OP548566
15	<i>L. guinanensis</i> sp. nov.	Shangsi County, Guangxi, China*	NNU00570	OP548567
16	<i>L. shiwandashanensis</i>	Fangcheng City, Guangxi, China*	NNU202103146	MZ326691
17	<i>L. shiwandashanensis</i>	Fangcheng City, Guangxi, China*	NNU202103213	MZ326692
18	<i>L. shiwandashanensis</i>	Fangcheng City, Guangxi, China*	NNU202103214	MZ326693
19	<i>L. shiwandashanensis</i>	Fangcheng City, Guangxi, China*	NNU202103215	MZ326694
20	<i>L. shangsiensis</i>	Shangsi County, Guangxi, China*	NHMG1401032	MK095460
21	<i>L. shangsiensis</i>	Shangsi County, Guangxi, China*	NHMG1401033	MK095461
22	<i>L. shangsiensis</i>	Shangsi County, Guangxi, China*	NHMG1704002	MK095462
23	<i>L. shangsiensis</i>	Shangsi County, Guangxi, China*	NHMG1704003	MK095463
24	<i>L. sungi</i>	Shangsi County, Guangxi, China	NNU00572	OP548569
25	<i>L. sungi</i>	Shangsi County, Guangxi, China	NNU00573	OP548570
26	<i>L. sungi</i>	Shangsi County, Guangxi, China	NNU00574	OP548571
27	<i>L. sungi</i>	Lingyun County, Guangxi, China	NNU00685	OP548572
28	<i>L. sungi</i>	Lingyun County, Guangxi, China	NNU00686	OP548573
29	<i>L. sungi</i>	Lingyun County, Guangxi, China	NNU00687	OP548574
30	<i>L. aerea</i>	Quang Binh, Vietnam	ZFMK 86362	JN848409
31	<i>L. alpina</i>	Caiyanghe, Yunnan, China	KIZ049024	MH055867
32	<i>L. applebyi</i>	Phong Dien Nature Reserve, Thua Thien-Hue, Vietnam	KIZ010701	MH055947
33	<i>L. arayai</i>	Borneo, Malaysia*	AE100/S9	DQ642119
34	<i>L. ardens</i>	Kon Ka Kinh National Park, Gia Lai, Vietnam*	ZMMU-NAP-06099	MH055949
35	<i>L. aspera</i>	Huanglianshan Nature Reserve, Lyuchun, Yunnan, China*	SYS a007743	MW046199
36	<i>L. baluensis</i>	Sabah, Borneo, Malaysia*	SP 21604	LC056792
37	<i>L. bashaensis</i>	Basha Nature Reserve, Guizhou, China*	GIB196404	MW136295
38	<i>L. bidoupensis</i>	Bidoup-Nui Ba National Park, Lam Dong, Vietnam*	ZMMU-A-4797-01454	MH055945
39	<i>L. bijie</i>	Bijie City, Guizhou, China*	SYS a007313	MK414532
40	<i>L. botsfordi</i>	Lao Cai, Vietnam*	AMS R 176540	MH055952
41	<i>L. bourreti</i>	Mao'er Shan, Guangxi, China	KIZ019389	MH055869
42	<i>L. brevicrus</i>	Sarawak, Borneo, Malaysia*	ZMH A09365	KJ831302
43	<i>L. chishuiensis</i>	Guizhou, China*	CIBCS20190518047	MT117053
44	<i>L. crocea</i>	Thua Thien-Hue, Vietnam	ZMMU-NAP-02274	MH055955
45	<i>L. damingshanensis</i>	Wuming County, Guangxi, China*	NNU202103281	MZ145229
46	<i>L. dorsospina</i>	Yushe Forest Park, Shuicheng, Guizhou, China*	SYS a004961	MW046194
47	<i>L. dringi</i>	Borneo, Malaysia*	KUHE:55610	AB847553
48	<i>L. eos</i>	Phongsaly, Laos*	MNHN 2004.0274	JN848452
49	<i>L. feii</i>	Yunnan, China*	KIZ048894	MT302634

ID	Species	Locality	Voucher no.	16S
50	<i>L. firthi</i>	Kon Tum, Vietnam*	AMS: R 176524	JQ739206
51	<i>L. flaviglandulosa</i>	Xiaoqiaogou Nature Reserve, Yunnan, China*	KIZ016072	MH055934
52	<i>L. fritinniens</i>	Danum Valley Field Center, Sabah, Malaysia	FMNH 244800	MH055971
53	<i>L. fuliginosa</i>	Phetchaburi, Thailand	KUHE:20197	LC201988
54	<i>L. gracilis</i>	Bukit Kana, Sarawak, Malaysia	FMNH 273682	MH055972
55	<i>L. graminicola</i>	Mount Pu Ta Leng, Lao Cai, Vietnam*	VNMN 010909	MZ224649
56	<i>L. hamidi</i>	Borneo, Malaysia*	KUHE 17545	AB969286
57	<i>L. heteropus</i>	Peninsular, Malaysia	KUHE 15487	AB530453
58	<i>L. isos</i>	Gia Lai, Vietnam*	AMS R 176480	KT824769
59	<i>L. itiokai</i>	Gunung Mulu National Park, Sarawak, Malaysia*	KUHE:55897	LC137805
60	<i>L. jinshaensis</i>	Lengshuihe Nature Reserve, Jinsha County, Guizhou, China*	CIBJS20200516001	MT814014
61	<i>L. juliandringi</i>	Sarawak, Borneo, Malaysia*	KUHE 17557	LC056784
62	<i>L. kajangensis</i>	Tioman, Malaysia*	LSUHC:4439	LC202002
63	<i>L. kalonensis</i>	Binh Thuan, Vietnam*	IEBR A.2014.15	KR018114
64	<i>L. kecil</i>	Cameron, Malaysia *	KUHE:52439	LC202003
65	<i>L. khasiorum</i>	Meghalaya, India*	SDBDU 2009.329	KY022303
66	<i>L. laui</i>	Wutongshan, Shenzhen city, China*	SYS a001507	KM014544
67	<i>L. liui</i>	Wuyi Shan, Fujian, China *	ZYCA907	MH055908
68	<i>L. macrops</i>	Dak Lak, Vietnam*	AMS R177663	KR018118
69	<i>L. maculosa</i>	Ninh Thuan, Vietnam*	AMS: R 177660	KR018119
70	<i>L. mangshanensis</i>	Manghan, Hunan, China *	MSZTC201703	MG132198
71	<i>L. maoershanensis</i>	Mao'er Shan, Guangxi, China	KIZ07614	MH055927
72	<i>L. marmorata</i>	Borneo, Malaysia*	KUHE 53227	AB969289
73	<i>L. maura</i>	Borneo, Malaysia	SP 21450	AB847559
74	<i>L. melanoleuca</i>	Kapoe, Ranong, Thailand	KIZ018031	MH055967
75	<i>L. melica</i>	Ratanakiri, Cambodia*	MVZ 258198	HM133600
76	<i>L. minima</i>	Doi Phu Fa, Nan, Thailand	KIZ024317	MH055852
77	<i>L. mjobergi</i>	Sarawak, Borneo, Malaysia*	KUHE 47872	LC056787
78	<i>L. murphyi</i>	Doi Inthanon, Chiang Mai, Thailand*	KIZ031199	MZ710523
79	<i>L. nahangensis</i>	Tuyen Quang, Vietnam*	ROM 7035	MH055853
80	<i>L. namdongensis</i>	Thanh Hoa, Vietnam*	VNUF A.2017.95	MK965390
81	<i>L. neangi</i>	Veal Veng District, Pursat, Cambodia*	CBC 1609	MT644612
82	<i>L. niveimontis</i>	Yongde County, Yunnan, China *	KIZ028276	MT302620
83	<i>L. nyx</i>	Ha Giang Prov., Vietnam*	AMNH A 163810	DQ283381
84	<i>L. oshanensis</i>	Emei Shan, Sichuan, China*	Tissue ID: YPX37492	MH055896
85	<i>L. pallida</i>	Lam Dong, Vietnam*	UNS00510	KR018112
86	<i>L. parva</i>	Mulu National Park, Sarawak, Malaysia*	KUHE:55308	LC056791
87	<i>L. pelodytoides</i>	NA	TZ819	AF285192
88	<i>L. petrops</i>	Ba Vi National Park, Ha Tay, Vietnam	ROM 13483	MH055901
89	<i>L. picta</i>	Borneo, Malaysia	UNIMAS 8705	KJ831295
90	<i>L. pluvialis</i>	Lao Cai, Vietnam*	MNHN:1999.5675	JN848391
91	<i>L. puhoatensis</i>	Nghe An, Vietnam*	VNMN 2016 A.22	KY849586
92	<i>L. purpurus</i>	Yunnan, China *	SYSa006530	MG520354
93	<i>L. purpuraventra</i>	Guizhou, China *	SYSa007281	MK414517
94	<i>L. pyrrhops</i>	Loc Bac, Lam Dong, Vietnam*	ZMMU-A-4873-00158	MH055950
95	<i>L. rowleyae</i>	Da Nang City, Vietnam*	ITBCZ2783	MG682552
96	<i>L. sabahmontanus</i>	Borneo, Malaysia*	BORNEENSIS 12632	AB847551
97	<i>L. sola</i>	Gunung Stong, Kelantan, Malaysia	KU RMB20973	MH055973
98	<i>L. suiyangensis</i>	Guizhou, China *	GZNU20180606005	MK829649
99	<i>L. sungi</i>	Vinh Phuc, Vietnam *	ROM 20236	MH055858
100	<i>L. tadungensis</i>	Dak Nong, Vietnam*	UNS00515	KR018121

ID	Species	Locality	Voucher no.	16S
101	<i>L. tengchongensis</i>	Yunnan, China *	SYSa004598	KU589209
102	<i>L. tuberosa</i>	Kon Ka Kinh National Park, Gia Lai, Vietnam*	ZMMU-NAP-02275	MH055959
103	<i>L. wuhuangmontis</i>	Pubei County, Guangxi, China *	SYS a003486	MH605578
104	<i>L. wulingensis</i>	Hunan, China *	CSUFT194	MT530316
105	<i>L. yeae</i>	Mount Emei, Sichuan, China *	CIBEMS20190422HLJ1-6	MT957019
106	<i>L. yingjiangensis</i>	Yunnan, China *	SYSa006532	MG520351
107	<i>L. yunkaiensis</i>	Guangdong, China *	SYSa004663	MH605584
108	<i>L. zhangyapingi</i>	Chiang Mai, Thailand *	KIZ07258	MH055864
109	<i>Leptobranchium huashen</i>	Yunnan, China	KIZ049025	KX811931
110	<i>Xenophrys glandulosa</i>	Yunnan, China	KIZ048439	KX811762

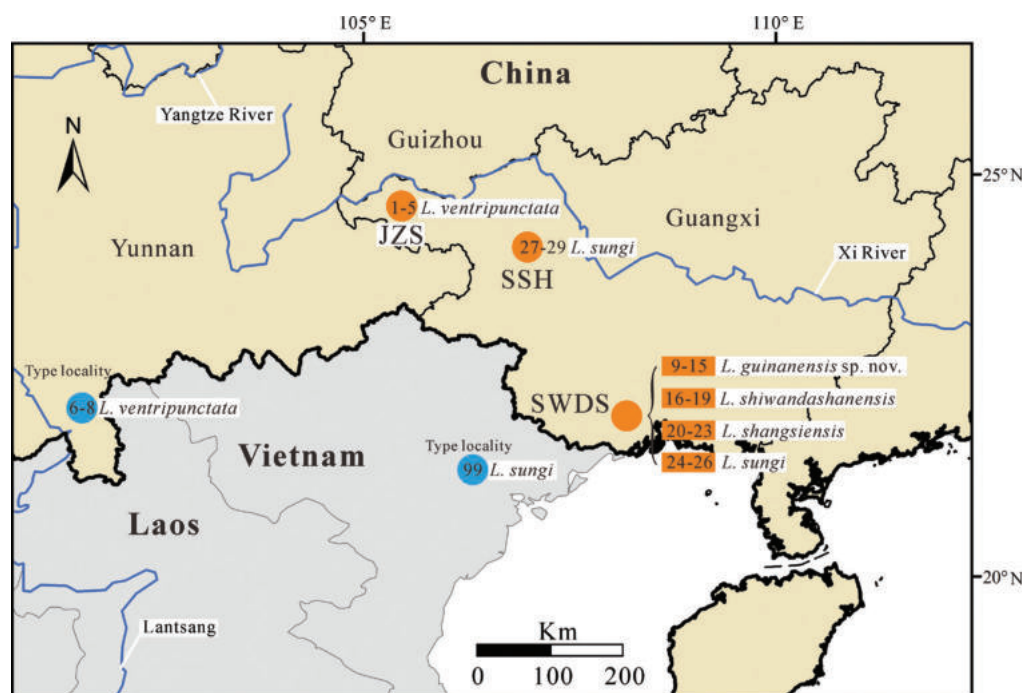


Figure 1. Localities of the new species and its sister taxa. Sample ID corresponding to those provided in Table 1.

Calls are often divided into two or more notes, which are smaller subunits that are usually separated by short intervals of silence relative to the note duration. The dominant frequency of a call is determined as the frequency with the highest energy concentration within the entire power spectrum.

Morphological analysis

According to our results of the phylogenetic analyses, the new species is closely related to *L. ventripunctata*. Consequently Mann-Whitney U tests were conducted to determine the significance of differences in morphometric characters between the new species and *L. ventripunctata* (from JZS). Differences were considered significant below a threshold of 0.05. Principal component analysis (PCA) was performed to examine the distribution of the two species based on their morphometric parameters. Prior to the analysis, morphometric parameters were adjusted by calculating the ratio of each parameter to SVL, and then log-transformed to minimise the impact of allometry. All statistical analyses were carried out using IBM SPSS v. 20.

Results

Phylogenetic analyses and genetic divergence

BI and ML analyses yielded nearly identical phylogenetic trees (Fig. 2). The preliminary phylogenetic trees revealed that all SWDS specimens were classified into four distinct lineages, corresponding to *L. shangsiensis*, *L. shiwandashanensis*, *L. sungi*, and an unidentified *Leptobrachella* lineage (Fig. 2). The newly collected specimens from SWDS formed a monophyletic group that is closely related to *L. ventripunctata*. The JZS specimens and *L. ventripunctata* from the type locality clustered together. The genetic divergences between the newly collected specimens and three sympatric species (*L. shangsiensis*, *L. shiwandashanensis*, and *L. sungi*) exceeded 8.2% (Suppl. material 1: table S3). The genetic divergences between the topotypic samples of *L. ventripunctata* and the newly collected specimens ranged from 1.6% to 2.4%, while those between the newly collected specimens and *L. ventripunctata* from JZS ranged from 1.7% to 1.9% (Suppl. material 1: table S3).

Morphology

The diagnostic characters for the new species of the genus *Leptobrachella* occurring north of the Isthmus of Kra are presented in Table 2, indicating that the newly collected specimens differ significantly from their congeners. The results of Mann-Whitney U tests revealed significant differences between the new specimens and *L. ventripunctata* from JZS in various measurements, including SVL, ED, IN, and FLL for males, and SVL, HL, HW, EN, TED, TIB, and PL for females (Table 3). There is no overlap in measurements between the new species and *L. ventripunctata* from JZS or the paratypes in terms of the measured parameters, including SVL, HL, HW, SNT, ED, TIB, FLL, ML, and PL (Table 3). Thus, PCA results showed clear differentiation between the new species and *L. ventripunctata* (Fig. 3). Furthermore, the newly described species exhibited distinct differences from *L. ventripunctata* in terms of body size (males being larger: SVL 30.5–32.5 mm vs 25.5–28.0 mm), ventral texture (ventral surface creamy white without dark brown spots vs chest and belly with dark brown spots), presence of a wide lateral fringe on toes (vs absence), presence of 1/3 toe webbing (vs absence), and presence of distinct dermal ridges under the toes (vs absence).

Bioacoustics

The calls of four individuals (NNU 00560–561, NNU 00875–876) were recorded. The main features of these calls are summarised in Table 4. The call of the newly described species consists of four notes (Fig. 4). The duration of the calls ranged from 23 milliseconds (ms) to 31 ms (mean 25.5 ± 1.4 , $n = 4$), while the intervals between the calls were 55–133 ms (mean 91.2 ± 17.5 , $n = 4$). The dominant frequencies of the calls were found to be in the range of 7.3–8.3 kHz. These characters were distinct from those of the sympatric species (*L. shangsiensis*, *L. shiwandashanensis*, and *L. sungi*) and *L. ventripunctata* (Fig. 4, Suppl. material 2: fig. S1, Table 4; Yang et al. 2018; Chen et al. 2019, 2021). Furthermore, the calls of the newly described species can also be differentiated from

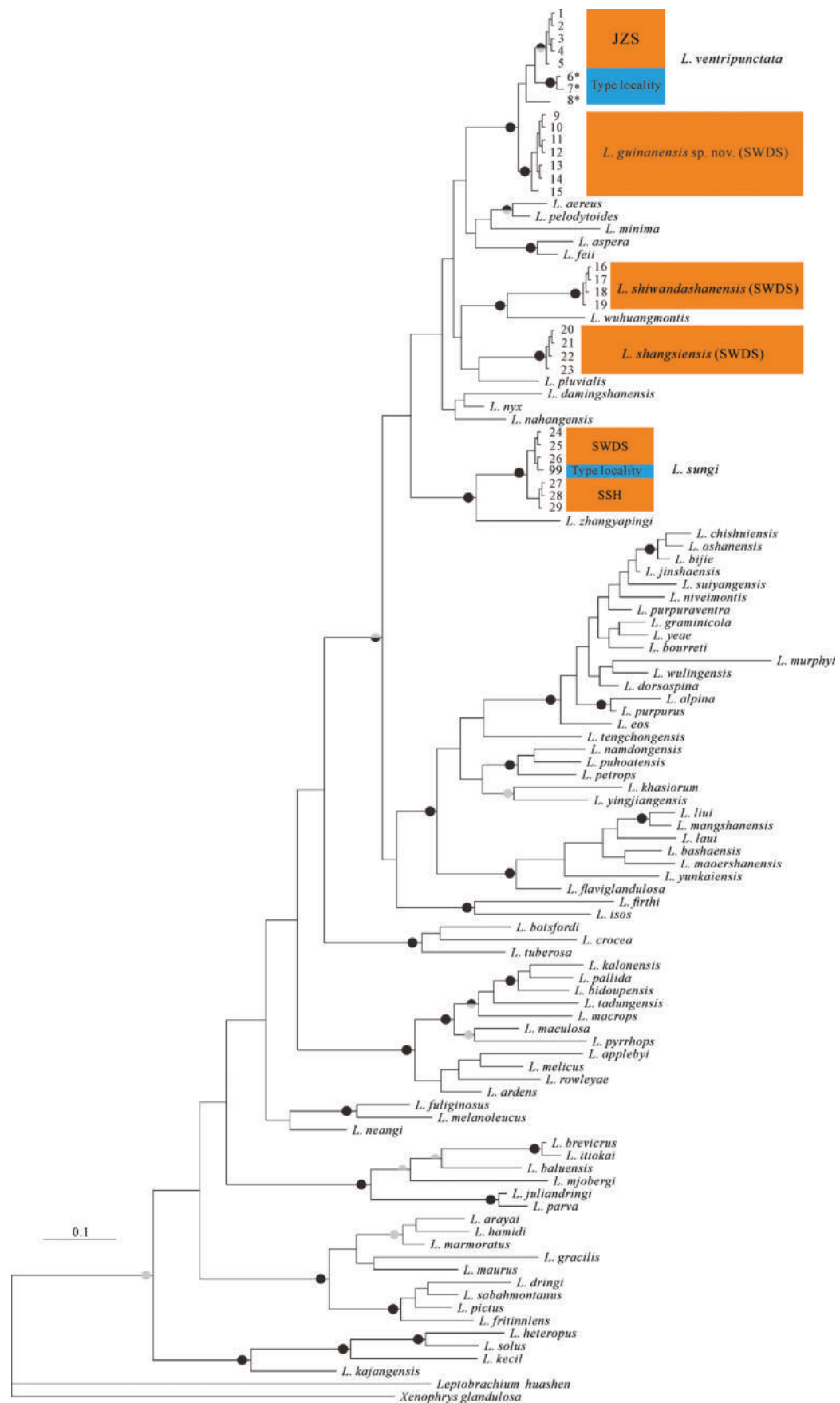


Figure 2. BI trees based on the part of the 16S gene. Node support is indicated on branches as maximum likelihood support (upper half; > 70% < 90% = grey, > 90% = black) and Bayesian posterior probabilities (lower half; > 0.95 = grey, 1 = black).

Table 2. Selected diagnostic characters for the species in the genus *Leptobranchella* occurring north of the Isthmus of Kra (modified from Rowley et al. 2017; Qian et al. 2020; and Wang et al. 2020). Toes webbing was determined following Fei et al. (2012). "Rudimentary" refers to an observable vestige of web.

ID	Species	Male SVL (mm)	Female SVL (mm)	Black spots on flanks	Toes webbing	Fringes on toes	Ventral colouration	Dorsal skin texture
1	<i>L. guinanensis</i> sp. nov.	30.5–32.5	38.7–41.8	Yes	One third	Wide	Ventral surface creamy white without dark brown spots	Dorsal surface shagreened with small, raised tubercles and longitudinal ridges
2	<i>L. aerea</i>	25.1–28.9	27.1–38.6	No	Rudimentary	Wide	Near immaculate creamy white, brown speckling on margins	Finely tuberculate
3	<i>L. alpina</i>	24.0–26.4	31.7–32.1	Yes	Rudimentary	Wide	Creamy-white with dark spots	Relatively smooth, some with small warts
4	<i>L. applebyi</i>	19.6–22.3	21.7–26.4	Yes	Rudimentary	Absent	Reddish brown with white speckling	Smooth
5	<i>L. ardens</i>	21.3–24.7	24.5	Yes	Absent	Absent	Reddish brown with white speckling	Smooth-finely shagreened
6	<i>L. aspera</i>	22.4	25.0–26.4	Yes	Rudimentary	Narrow	Creamy white with distinct dark patches on chest and abdomen	Rough with dense conical granules, tubercles, and glandular folds
7	<i>L. bashaensis</i>	22.9–25.6	27.1	Yes	Rudimentary	Narrow	Creamy-white chest and off-white belly with irregular black spots	Dorsal skin slightly shagreened with small tubercles and irregular brown stripes
8	<i>L. bidouzensis</i>	18.5–25.4	28.3–29.4	Yes	Rudimentary	Narrow	Reddish brown with white speckling	Smooth
9	<i>L. bijie</i>	29.0–30.4	Unknown	Yes	Rudimentary	Narrow	White with distinct nebulous greyish speckling on chest and ventrolateral flanks	Shagreened and granular
10	<i>L. botsfordi</i>	29.1–32.6	30.0–31.8	No	Rudimentary	Narrow	Reddish brown with white speckling	Shagreened
11	<i>L. bourreti</i>	28.0–36.2	42.0–45.0	Yes	Rudimentary	Narrow	Creamy white	Relatively smooth, some with small warts
12	<i>L. chishuiensis</i>	30.8–33.4	34.2	Yes	Rudimentary	Narrow	White with distinct nebulous greyish speckling on chest and ventrolateral flanks	Shagreened and granular
13	<i>L. crocea</i>	22.2–27.3	Unknown	No	Rudimentary	Absent	Bright orange	Highly tuberculate
14	<i>L. damingshanensis</i>	33.6–34.4	Unknown	Yes	Rudimentary	Narrow	Creamy white ventral surface with small, creamy white glands on throat, chest and belly, becoming more concentrated near lateral margin	Rough dorsal skin with sparse jacinth tubercles and some short longitudinal ridges
15	<i>L. dong</i>	29.2–34.2	34.4–43.1	Yes	Rudimentary	Wide	White with distinct nebulous brown speckling on ventrolateral flanks	Shagreened with fine tubercles
16	<i>L. dorsospina</i>	28.7–30.5	32.1–39.8	Yes	Rudimentary	Narrow	Greyish white with black spots and orange pigmentations	Rough with dense conical granules, tubercles, glandular folds, and conical spines
17	<i>L. eos</i>	33.1–34.7	40.7	No	Rudimentary	Wide	Creamy white	Shagreened
18	<i>L. feii</i>	21.5–22.8	25.7	Yes	Rudimentary	Narrow	Creamy white with black blotches	Shagreened with small tubercles and ridge
19	<i>L. firthi</i>	26.4–29.2	25.7–36.9	No	Rudimentary	Wide	Creamy white	Shagreened with fine tubercles
20	<i>L. flaviglandulosa</i>	23.0–27.0	29.3	Yes	Rudimentary	Narrow	Whitish with black speckling on margins	Shagreened with yellowish-brown tubercles
21	<i>L. fuliginosa</i>	28.2–30.0	Unknown	Yes	Rudimentary	Narrow	White with brown dusting	Nearly smooth, few tubercles
22	<i>L. isos</i>	23.7–27.9	28.6–31.5	No	Rudimentary	Wide	Creamy white with white dusting on margins	Mostly smooth, females more tuberculate

ID	Species	Male SVL (mm)	Female SVL (mm)	Black spots on flanks	Toes webbing	Fringes on toes	Ventral colouration	Dorsal skin texture
23	<i>L. jinshaensis</i>	29.7–31.2	Unknown	Yes	Absent	Narrow	Ventral surface of throat cream white, chest, and belly cream yellow with purple speckling	Dorsal skin shagreened, some of the granules forming longitudinal short skin ridges
24	<i>L. jinyunensis</i>	29.1–34.1	34.1–34.9	Yes	Rudimentary	Narrow	Basically, floral white with deep grey pigments all over	Rough, covered with dense small granules and large tubercles
25	<i>L. kalonensis</i>	25.8–30.6	28.9–30.6	Yes	Absent	Absent	Pale, speckled brown	Smooth
26	<i>L. khasiorum</i>	24.5–27.3	21.2–33.4	Yes	Rudimentary	Wide	Creamy white	Isolated, scattered tubercles
27	<i>L. lateralis</i>	26.9–28.3	36.6	Yes	Rudimentary	Absent	Creamy white	Roughly granular
28	<i>L. laui</i>	24.8–26.7	28.1	Yes	Rudimentary	Wide	Creamy white with dark brown dusting on margins	Round granular tubercles
29	<i>L. liui</i>	23.0–28.7	24.5–27.8	Yes	Rudimentary	Wide	Creamy white with dark brown spots on chest and margins	Round granular tubercles with glandular folds
30	<i>L. macrops</i>	28.0–29.3	30.3	Yes	Rudimentary	Absent	Greyish violet with white speckling	Roughly granular with larger tubercles
31	<i>L. maculosa</i>	24.2–26.6	27.0	Yes	Absent	Absent	Brown with a few white speckling	Mostly smooth
32	<i>L. mangshanensis</i>	22.2–27.8	30.2	Yes	Rudimentary	Narrow	Throat grey-white and belly creamy white, scattered with white speckles	Smooth with orange tubercles and dark brown stripes
33	<i>L. maoershanensis</i>	25.2–30.4	29.1	Yes	Rudimentary	Narrow	Creamy white chest and belly with irregular black spots	Longitudinal folds
34	<i>L. melica</i>	19.5–22.7	Unknown	Yes	Rudimentary	Absent	Reddish brown with white speckling	Smooth
35	<i>L. minima</i>	25.7–31.4	31.6–37.3	Yes	Rudimentary	Absent	Creamy white	Smooth
36	<i>L. nahangensis</i>	40.8	Unknown	Yes	Rudimentary	Absent	Creamy white with light specking on throat and chest	Smooth
37	<i>L. namdongensis</i>	30.9	32.1–35.3	Yes	Rudimentary	Absent	Creamy white with brown dusting on margins	Finely tuberculate
38	<i>L. neangi</i>	Unknown (35.4–36.3 in females)	35.4–36.3	Yes	Rudimentary (in females)	Absent (in females)	Light purplish grey with dark brown mottling on throat	Small, irregular bumps and ridges
39	<i>L. niveimontis</i>	22.5–23.6	28.5–28.7	Yes	Rudimentary	Narrow	Marbling with black speckling	Relatively smooth with small tubercles
40	<i>L. nokrekensis</i>	26.0–33.0	34.0–35.0	Yes	Rudimentary	Unknown	Creamy white	Tubercles and longitudinal folds
41	<i>L. nyx</i>	26.7–32.6	37.0–41.0	Yes, but indistinct	Rudimentary	Absent	Creamy white with white with brown margins	Rounded tubercles
42	<i>L. oshanensis</i>	26.6–30.7	28.8–32.6	Yes	Absent	Absent	Whitish with no markings or only small, light grey spots	Smooth with few glandular ridges
43	<i>L. pallida</i>	24.5–27.7	Unknown	No	Absent	Absent	Reddish brown with white speckling	Tuberculate
44	<i>L. pelodytoides</i>	27.5–32.3	35.5–37.8	Yes	One third	Narrow	Whitish	Mostly smooth with smooth warts
45	<i>L. petrops</i>	23.6–27.6	30.3–47.0	No	Absent	Narrow	Immaculate creamy white	Highly tuberculate
46	<i>L. pingbianensis</i>	28.0	30.0	Yes	Rudimentary	unknown	Chest and belly with dark brown spots	Smooth
47	<i>L. pluvialis</i>	21.3–22.3	Unknown	Yes	Rudimentary	Absent	Dirty white with dark brown marbling	Smooth, flattened tubercles on flanks
48	<i>L. puhoatensis</i>	24.2–28.1	27.3–31.5	Yes	Rudimentary	Narrow	Reddish brown with white dusting	Longitudinal skin ridges
49	<i>L. purpuraventra</i>	27.3–29.8	33.0–35.3	Yes	Rudimentary	Narrow	Grey-purple with distinct nebulous greyish speckling on chest and ventrolateral flanks	Shagreened and granular
50	<i>L. purpurus</i>	25.0–27.5	Unknown	Yes	Rudimentary	Wide	Dull white with indistinct grey dusting	Shagreen with small tubercles

ID	Species	Male SVL (mm)	Female SVL (mm)	Black spots on flanks	Toes webbing	Fringes on toes	Ventral colouration	Dorsal skin texture
51	<i>L. pyrrhops</i>	30.8–34.3	30.3–33.9	Yes	Rudimentary	Absent	Reddish brown with white speckling	Slightly shagreened
52	<i>L. rowleyae</i>	23.4–25.4	27–27.8	Yes	Absent	Absent	Pinkish milk-white to light brown with white speckles	Smooth with numerous tiny tubercles
53	<i>L. shangsiensis</i>	24.9–29.4	30.8–35.9	Yes	Rudimentary	Narrow	Yellowish creamy white with marble texture	Smooth with numerous tiny tubercles
54	<i>L. shimentaina</i>	26.4–28.9	30.1–30.7	Yes	Rudimentary	Wide	Greyish pink with distinct hazy brown speckling on chest and ventrolateral flanks	Round granular tubercles with glandular folds
55	<i>L. shiwandashanensis</i>	26.8–29.7	33.7–35.9	Yes	Absent	Absent	Creamy white ventral surface with brown spots on lateral margin and near immaculate creamy white on throat and chest	Shagreened dorsal surface with small, raised tubercles and ridges, more evident on shoulder and dorsal surfaces of limbs
56	<i>L. suiyangensis</i>	28.7–29.7	30.5–33.5	Yes	Rudimentary	Narrow	Yellowish or creamy-white with marble texture or light brown speckling	Shagreened with small granules
57	<i>L. sungi</i>	48.3–52.7	56.7–58.9	No or small	Wide	Narrow	Yellowish or creamy-white	Granular
58	<i>L. tadungensis</i>	23.3–28.2	32.1	Yes	Absent	Absent	Reddish brown with white speckling	Smooth
59	<i>L. tamdil</i>	32.3	31.8	Yes	Wide	Wide	White	Weakly tuberculate
60	<i>L. tengchongensis</i>	23.9–26.0	28.8–28.9	Yes	Rudimentary	Narrow	White with dark brown blotches	Shagreened with small tubercles
61	<i>L. tuberosa</i>	24.4–29.5	30.2	No	Rudimentary	Absent	White with small grey spots/streaks	Highly tuberculate
62	<i>L. ventripunctata</i>	25.5–28.0	31.5–35.0	Yes	Absent	Absent	Chest and belly with dark brown spots	Longitudinal skin ridges
63	<i>L. verrucosa</i>	23.2–25.9	Unknown	Yes	Absent	Narrow	Creamy white with greyish white and dark brown spots	Shagreened with numerous conical tubercles
64	<i>L. wuhuangmontis</i>	25.6–30.0	33.0–36.0	Yes	Rudimentary	Narrow	Greyish white mixed with tiny white and black dots	Rough with dense conical tubercles
65	<i>L. wulingensis</i>	24.5–32.8	29.9–38.5	yes	Rudimentary	Narrow	Creamy white, with distinct or indistinct brown speckling at margins	Shagreened with sparse large warts, sometimes with longitudinal ridges
66	<i>L. yeae</i>	25.8–32.6	33.7–34.1	Yes	Rudimentary	Narrow	Ventral belly cream white with variable brown speckling	Dorsum relatively smooth with fine tiny granules or short ridges
67	<i>L. yingjiangensis</i>	25.7–27.6	Unknown	Yes	Rudimentary	Wide	Creamy white with dark brown flecks on chest and margins	Shagreened with small tubercles
68	<i>L. yunkaiensis</i>	25.9–29.3	34.0–35.3	Yes	Rudimentary	Wide	Belly pink with distinct or indistinct speckling	Shagreened with short skin ridges and warts
69	<i>L. yunyangensis</i>	28.3–30.6	Unknown	Yes	Rudimentary	Narrow	Ventral surfaces of the throat, chest, and belly greyish white with purple-brown speckling	Rough dorsal skin, with sparse large granules and tubercles and short longitudinal ridges on the shoulder
70	<i>L. zhangyapingi</i>	45.8–52.5	Unknown	Yes	Rudimentary	Wide	Near immaculate white	Mostly smooth with distinct tubercles

the known 40 species in the genus *Leptobranchella* (Suppl. material 1: table S4), as they possess the highest dominant frequencies ever recorded.

Based on the evidence from morphology, phylogeny, and bioacoustics, it is evident that the collected specimens represent a distinct, previously undescribed species within the genus *Leptobranchella*. Therefore, we describe these specimens as a new species of the genus *Leptobranchella*.

Table 3. Morphometric measurements and comparisons between *L. guinanensis* sp. nov. and *L. ventripunctata*. “*” indicates *p*-value < 0.05; JZS = Jinzhongshan National Nature Reserve; SD = Standard deviation.

Characters	<i>p</i> -value from Mann-Whitney <i>U</i> test		<i>L. guinanensis</i> sp. nov.		<i>L. ventripunctata</i> (JZS)		<i>L. ventripunctata</i> (paratypes; Fei et al. 1992)
	Male	Female	Males (<i>n</i> = 4)	Female (<i>n</i> = 10)	Males (<i>n</i> = 5)	Females (<i>n</i> = 4)	Males (<i>n</i> = 10)
	New species vs <i>L. ventripunctata</i>	New species vs <i>L. ventripunctata</i>	Range (mean ± SD) (mm)	Range (mean ± SD) (mm)	Range (mean ± SD) (mm)	Range (mean ± SD) (mm)	Range (mean) (mm)
SVL	0.014*	0.005*	30.5–32.5 (31.8 ± 0.9)	38.7–41.8 (39.8 ± 1.5)	24.0–26.9 (26.0 ± 1.2)	32.0–34.5 (33.4 ± 1.1)	25.5–28.0 (26.5)
HL	0.806	0.011*	11.0–11.8 (11.3 ± 0.4)	14.0–15.3 (14.6 ± 0.4)	8.7–9.7 (9.3 ± 0.4)	11.1–12.0 (11.4 ± 0.4)	9.2–10.0 (9.6)
HW	0.142	0.048*	11.0–11.6 (11.4 ± 0.3)	14.0–15.5 (14.7 ± 0.6)	8.5–9.3 (9.0 ± 0.4)	11.1–12.5 (11.6 ± 0.6)	9.0–9.5 (9.5)
SNT	0.462	0.396	4.6–5.4 (4.9 ± 0.3)	5.1–6.5 (5.9 ± 0.4)	3.4–4.2 (3.8 ± 0.4)	4.6–4.9 (4.8 ± 0.1)	4.0–4.2 (4.1)
ED	0.014*	0.396	4.6–5.1 (4.9 ± 0.2)	5.2–5.9 (5.6 ± 0.2)	3.2–3.6 (3.5 ± 0.2)	4.3–5.1 (4.7 ± 0.4)	3.6–4.0 (3.8)
IOD	0.806	0.480	3.1–3.9 (3.5 ± 0.4)	3.7–4.3 (4.0 ± 0.3)	2.5–3.1 (2.9 ± 0.2)	2.9–3.2 (3.0 ± 0.1)	2.9–3.3 (3.0)
IN	0.014*	0.258	3.4–4.1 (3.7 ± 0.3)	3.7–5.0 (4.2 ± 0.4)	2.3–2.8 (2.6 ± 0.2)	3.2–3.8 (3.6 ± 0.3)	Unknown
EN	0.086	0.016*	2.1–2.8 (2.5 ± 0.3)	2.9–3.3 (3.0 ± 0.1)	1.4–2.0 (1.8 ± 0.3)	2.2–2.4 (2.3 ± 0.1)	Unknown
TD	0.142	0.120	1.9–2.2 (2.0 ± 0.1)	1.7–2.9 (2.4 ± 0.4)	1.5–2.2 (2.0 ± 0.3)	2.0–2.7 (2.3 ± 0.4)	1.7–2.0 (1.8)
TED	0.624	0.048*	1.2–1.5 (1.3 ± 0.1)	2.0–2.8 (2.3 ± 0.3)	0.8–1.3 (1.1 ± 0.2)	1.3–1.8 (1.6 ± 0.2)	Unknown
TIB	0.327	0.005*	15.2–15.9 (15.5 ± 0.4)	18.5–19.4 (19.0 ± 0.3)	12.0–12.8 (12.3 ± 0.3)	13.9–15.2 (14.6 ± 0.5)	11.4–13.3 (12.1)
FLL	0.014*	0.480	14.4–15.4 (14.9 ± 0.5)	17.9–19.4 (18.8 ± 0.6)	12.3–13.3 (12.9 ± 0.4)	14.9–16.9 (15.5 ± 0.9)	12.1–14.2 (12.9)
THL	0.462	0.157	13.0–15.8 (14.5 ± 1.5)	18.2–19.6 (18.7 ± 0.5)	11.4–13.1 (12.2 ± 0.8)	14.6–16.6 (15.2 ± 0.9)	Unknown
ML	0.221	0.322	7.8–8.4 (8.1 ± 0.2)	9.3–10.2 (9.8 ± 0.4)	6.3–6.6 (6.4 ± 0.1)	7.1–8.7 (7.8 ± 0.7)	6.4–7.3 (7.0)
PL	1.000	0.032*	13.4–15.8 (14.4 ± 1.2)	15.4–19.0 (17.4 ± 1.5)	11.4–12.1 (11.7 ± 0.3)	12.8–14.7 (13.7 ± 0.9)	10.7–12.5 (11.4)
FEM	0.327	0.671	1.2–1.5 (1.3 ± 0.1)	1.4–2.2 (1.8 ± 0.3)	0.8–1.5 (1.2 ± 0.3)	1.2–1.6 (1.4 ± 0.2)	Unknown

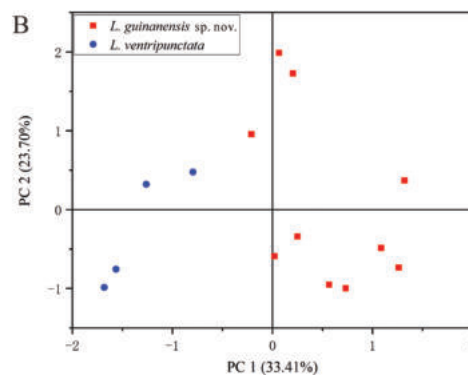
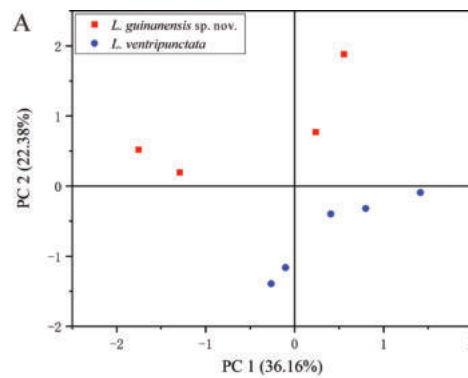


Figure 3. Scatter plot of PC1 and PC2 of PCA based on the morphometric measurements, distinguishing *L. guinanensis* sp. nov. and *L. ventripunctata* **A** male comparison **B** female comparison.

Table 4. Comparisons of characters of advertisement calls of the new species, sympatric species, and *L. ventripunctata*.

Species	Dominant frequency (kHz)	Call durations (ms)	Call intervals (ms)	Notes/call	Temperature (°C)	Reference
<i>L. guinanensis</i> sp. nov.	7.3–8.3	25.5 (23–31)	91.2 (55–133)	4–5	24.1	This study
<i>L. shiwandashanensis</i>	5.3–5.7	226.6 (194–277)	153.1 (134–186)	14–16	23.0	Chen et al. 2021b
<i>L. shangsiensis</i>	5.5–6.5	66.0 (64–69)	250.5 (184–289)	5–6	21.5	Chen et al. 2019
<i>L. sungi</i>	2.0–2.7	59.4 (56–65)	478.4 (225–996)	3	24.5	This study
<i>L. ventripunctata</i> (YJ)	6.1–6.4	145.0 (65–430)	134.0 (31–416)	3–17	15.0	Yang et al. 2018
<i>L. ventripunctata</i> (JZS)	6.2–7.1	182.8 (142–318)	215.7 (131–507)	8–9	25.1	This study

YJ, Yingjiang County, Yunnan, China; JZS, Jinzhongshan National Nature Reserve, Longlin County, Guangxi, Chin.

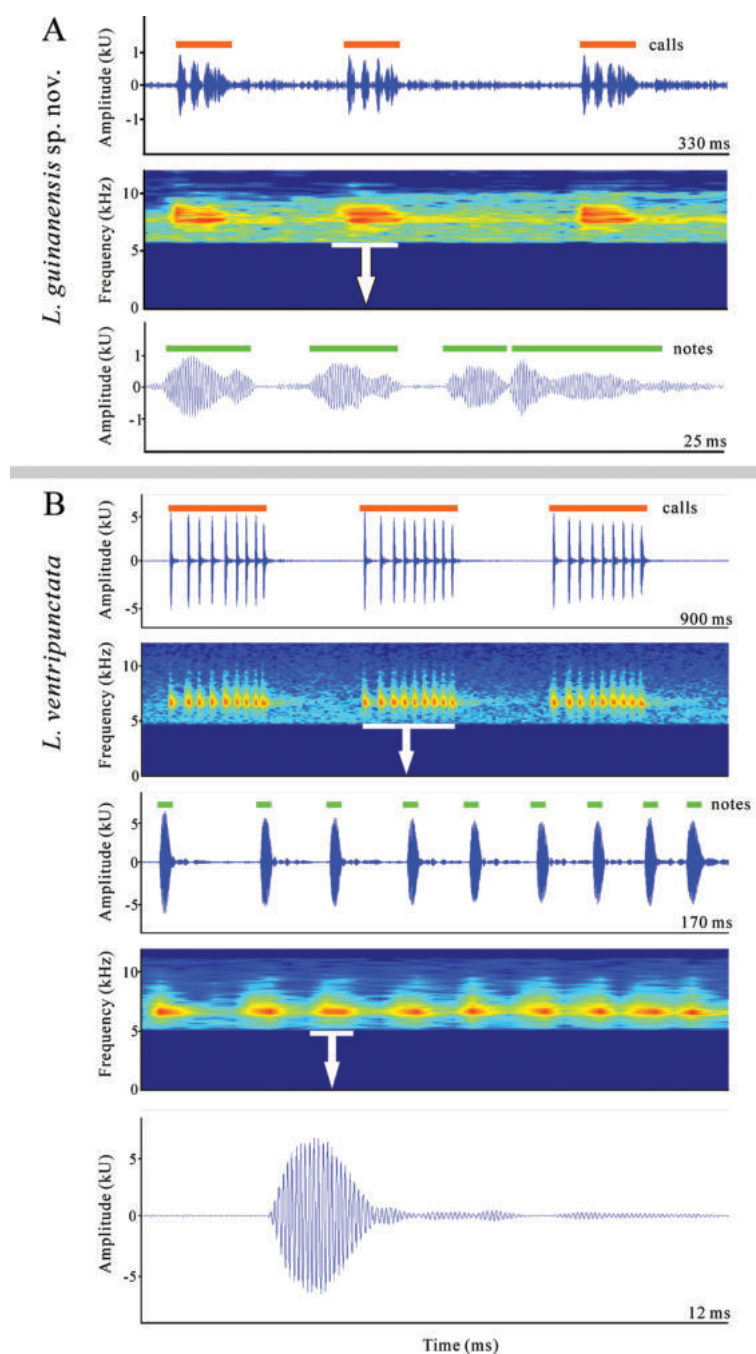


Figure 4. Advertisement calls of *L. guinanensis* sp. nov. **A** and *L. ventripunctata* **B** including waveforms and spectrograms.

Taxonomic account

Leptobranchella guinanensis Chen, Li, Peng & Liu, sp. nov.

<https://zoobank.org/412DCAC8-50F4-49D0-9F67-94D160AF1915>

Figs 5, 6

Material examined. Holotype. NNU 00876, adult male, collected at the Shiwandashan National Nature Reserve, Shangsi County, Guangxi, China (21°55'1.2"N, 107°54'10.8"E; elevation 512 m), collected by Wei-Cai Chen on 18 June 2022.

Paratypes. NNU 00560–561, two adult males, NNU 00557–559, three adult females, collected at the same locality as the holotype on 10 June 2021; NNU 00569–571, three adult females, collected at the same locality as the holotype on 1 July 2021; NNU 00875, one adult male, NNU 00877–880, four adult females, collected at the same locality and time as the holotype. All specimens were collected by Wei-Cai Chen.

Etymology. The species name *guinanensis* is derived from the geographic distribution of this species, specifically the southern Guangxi region. The suggested English name for this species is Gui Nan Leaf Litter Toad, while the Chinese name is Gui Nan Zhang Tu Chan (桂南掌突蟾).

Diagnosis. *Leptobranchella guinanensis* sp. nov. can be distinguished from its congeners by a combination of the following characters: (1) SVL 30.5–32.5 mm in males; 38.7–41.8 mm in females; (2) 1/3 toe webbing, wide lateral fringes; (3) dorsal surface shagreened with small, raised tubercles and longitudinal ridges; (4) ventral surface creamy white without dark brown spots; (5) throat immaculate creamy white and its margin concentrated brown spots; (6) iris bicoloured, upper half light copper, transitioning to silver in lower half; (7) crossbars of hindlimbs with tubercles; (8) distinct dermal ridges under the toes; (9) a pair of glands under the vent; (10) tibia-tarsal articulation reaching to centre of eye; (11) relatively higher dominant frequency of advertisement calls (7.3–8.3 kHz).

Description of holotype. Adult male, SVL = 30.5 mm, head width less than length (HW/HL = 0.93); snout protruding, projecting over the lower jaw; nostril oval, closer to the tip of snout than eye; canthus rostralis distinct; loreal region sloping and slightly concave; interorbital region flat; pupil vertical; eye diameter near equal to snout length (ED/SNT = 0.99); tympanum distinct and rounded, and its diameter conspicuously less than eye diameter (TD/ED = 0.41); supratympanic fold distinct, raised from corner of eye to supra-axillary gland; vomerine teeth absent; vocal sac openings located laterally on the floor of mouth; tongue with a shallow notch at the posterior tip.

Tips of fingers rounded and slightly swollen; relative finger lengths I < II < IV < III; nuptial pad absent; subarticular tubercles absent; prominent inner palmar tubercle, separated from the small outer palmar tubercle; finger webbing and dermal fringes absent. Tips of toes rounded, slightly swollen; relative toe lengths I < II < V < III < IV; subarticular tubercles absent, replaced by distinct dermal ridges; pronounced large, oval inner metatarsal tubercle; outer metatarsal tubercle absent; 1/3 toe webbing; lateral fringes wide. TIB/SVL = 0.51; tibia-tarsal articulation reaching to the centre of eye; heels not meeting when thighs are appressed at right angles to body (Fig. 5).

Dorsal surface shagreened with small, raised tubercles and longitudinal ridges; belly and chest smooth without tubercles; anterior throat with several

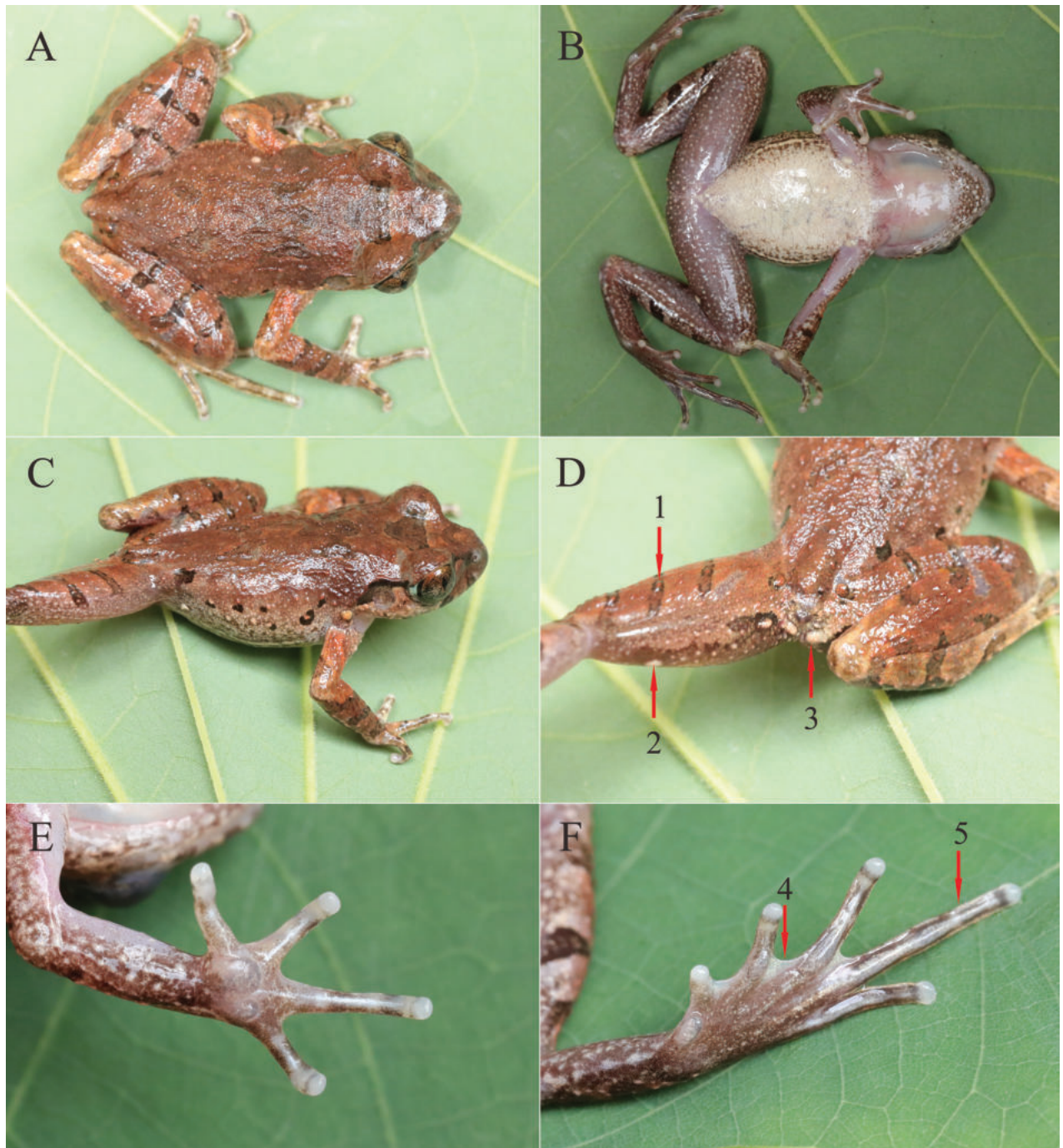


Figure 5. The holotype of *L. guinanensis* sp. nov. **A** dorsal view **B** ventral view **C** dorsolateral view **D** rear of the back and dorsal view of thighs **E** ventral view of hand **F** ventral view of foot. 1, tubercles on the crossbars; 2, femoral gland; 3, a pair of glands under the vent; 4, toe webbing; 5, wide lateral fringes on toe.

tubercles; ventral surface of limbs with creamy white tubercles; crossbars of hindlimbs with tubercles; flanks with several tubercles; pectoral glands oval, ~ 1.2 mm in diameter; femoral glands oval, ~ 1.3 mm in diameter, located on the posteroventral surface of thighs, closer to the knee than to the vent; supra-axillary glands distinct and rounded, ~ 0.9 mm in diameter; a pair of glands under the vent; and continued ventrolateral glandular line distinct (Fig. 5).

Colour of holotype in life. Dorsal surface brown, an inverted triangle marking between eyes, irregular markings on shoulder and the rear of back; flanks with



Figure 6. **A** more tubercles and longitudinal ridges on dorsum and hindlimbs surfaces (NNU00875) **B** light brown on dorsum (NNU00569) **C** ventral view of the gravid female (NNU00880) **D** eggs creamy white without black poles.

light orange tubercles; tympanum pale brown; supratympanic line black from posterior corner of eye to supra-axillary glands; posterior corner of eye silver; wide brown bars on upper lip; flanks with irregular black spots; brown transverse bars distinct on dorsal surface of forelimbs and hindlimbs; upper arm surfaces light orange; ventral surface creamy white without dark brown spots; throat immaculate creamy white and its margin concentrated brown spots; ventral surfaces of limbs purplish grey; pectoral and femoral glands, and a pair of creamy white glands under the vent, supra-axillary glands light orange; pupil black; iris bicoloured, upper half light copper, transitioning to silver in lower half (Fig. 5).

Colour of holotype in preservative. Dorsum and limbs surfaces faded to a uniform grey; brown, inverted triangle marking distinctly visible between eyes; irregular black spots distinct on flanks; throat, chest, and belly creamy white; pectoral, femoral, supra-axillary, and ventrolateral glands creamy white; dark crossbars on limbs, fingers and toes remained distinct; upper arm and tibiotarsus faded to grey.

Variation. Measurements of the type series are provided in Table 3 and Suppl. material 1: table S5. The black spots and tubercles on the flanks exhibit variation between individuals. Certain individuals possess more tubercles and longitudinal ridges on their dorsum and hindlimb surfaces (Fig. 6A), while others display a light brown colouration on their dorsum (Fig. 6B).

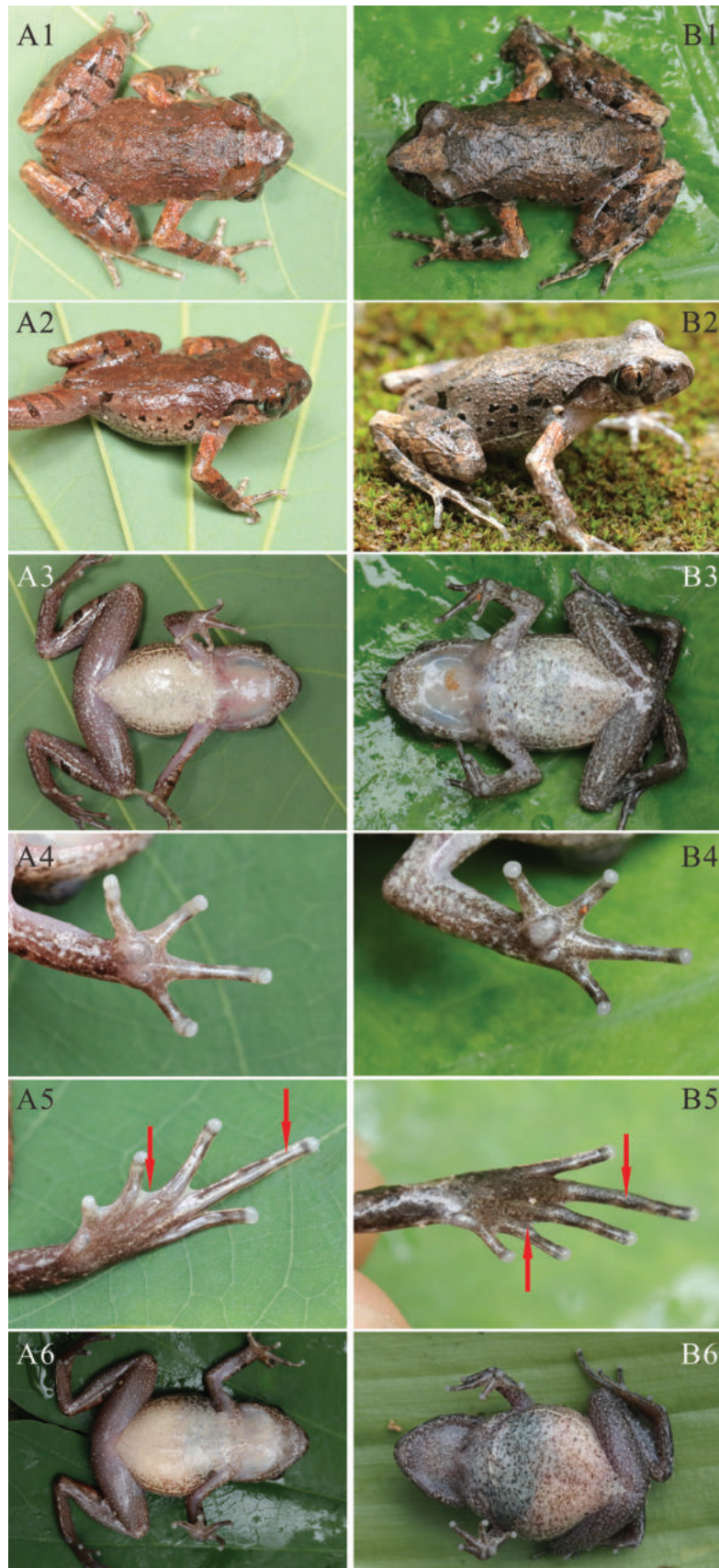


Figure 7. Morphological characters compared between *L. guinanensis* sp. nov. and *L. ventripunctata* **A1–6** *L. guinanensis* sp. nov. **B1–6** *L. ventripunctata* **A1, B1** dorsal view **A2, B2** dorsolateral view **A3, B3** ventral view **A4, B4** ventral view of hand **A5, B5** ventral view of foot **A6, B6** ventral view of the gravid female.

Ecology and distribution. *Leptobranchella guinanensis* sp. nov. was discovered in the evergreen forest at SWDS, at an elevation of 400–600 m. The individuals were observed near rocky streams between 20:00–24:00 h. Males were found calling while sitting on rocks near the stream ~ 0.5–1.0 m. Females were found to be gravid with creamy white eggs (Fig. 6C) and laid their eggs in a bag while being raised indoors (Fig. 6D). Currently, *L. guinanensis* sp. nov. is only known from SWDS. So far within this reserve, we have identified four species of *Leptobranchella*, namely *L. guinanensis* sp. nov., *L. shangsiensis*, *L. shiwandashanensis*, and *L. sungi*.

Comparison. Table 2 presents a concise overview of the diagnostic morphological characters of species found north of the Isthmus of Kra. *Leptobranchella guinanensis* sp. nov. can clearly be distinguished from its phylogenetically close congeners, *L. ventripunctata*. *Leptobranchella guinanensis* sp. nov. differs from *L. ventripunctata* by a larger body size (SVL 30.5–32.5 mm in males; 38.7–41.8 mm in females vs 25.5–28.0 mm in males, 31.5–35.0 mm in females), ventral surface creamy white without brown spots (vs chest and belly creamy white with many scattered brown spots), ventral surfaces of limbs purplish grey (vs ventral surface of limbs grey-brown with dark brown and white speckling or dots), 1/3 toe webbing and toe lateral fringes wide (vs no toe webbing and lateral fringes), dermal ridges distinct under toes (vs absent) (Fig. 7), tibia-tarsal articulation reaching the centre of eye (vs the level between tympanum and posterior of eye), heels not meeting when thighs are appressed at right angles to body (vs heels overlapping). In addition, *L. guinanensis* sp. nov. differs from *L. ventripunctata* by relatively high dominant frequencies (7.3–8.3 kHz vs 6.1–6.4 kHz), call durations (mean 25.5 ms, ranging 23–31 ms vs mean 145 ms, ranging 65–430 ms) and call intervals (mean 91.2 ms, ranging 55–133 ms vs mean 134 ms, ranging 31–416 ms) (Table 4). Secondly, *L. guinanensis* sp. nov. can be easily distinguished from its sympatric species, *L. shangsiensis*, *L. shiwandashanensis*, and *L. sungi*. *Leptobranchella guinanensis* sp. nov. differs from *L. shangsiensis* by a larger body size (SVL 30.5–32.5 mm in males, 38.7–41.8 mm in females vs 24.9–29.4 mm in males, 30.8–35.9 mm in females), crossbars of hindlimbs with tubercles (vs lack of tubercles on crossbars of hindlimbs), 1/3 toe webbing (vs toe webbing rudimentary), head width less than length (HW/HL = 0.93 vs HW/HL = 1.15), eye diameter near equal to snout length (ED/SNT = 0.99 vs ED/SNT = 0.78), a pair of glands under the vent (vs absent glands under the vent), dominant frequencies (7.3–8.3 kHz vs 5.5–6.5 kHz), call duration (mean 25.5 ms, ranging 23–31 ms vs mean 66.0 ms, ranging 64–69 ms; Table 4). *Leptobranchella guinanensis* sp. nov. differs from *L. shiwandashanensis* by relatively larger body size (SVL 30.5–32.5 mm in males; 38.7–41.8 mm in females vs 26.8–29.7 mm in males, 33.7–35.9 mm in females), 1/3 toe webbing and wide lateral fringes on toe (vs no webbing and no lateral fringes on toe), tibia-tarsal articulation reaching to the centre of eye (vs posterior of eye), a pair of glands under the vent (vs absent glands under the vent), dominant frequencies (7.3–8.3 kHz vs 5.3–5.7 kHz), call duration (mean 25.5 ms vs mean 226.6 ms; Table 4). *Leptobranchella guinanensis* sp. nov. differs from *L. sungi* by conspicuously smaller body size (SVL 30.5–32.5 mm in males; 38.7–41.8 mm in females vs SVL 48.3–52.7 mm in males, 56.7–58.9 mm in females); iris bicoloured, upper half light copper, transitioning to silver in lower half (vs uniform gold green iris), finger II longer than finger I (vs finger I and II equal in length), tympanum distinct and rounded (vs indistinct), dorsal surface brown, an inverted triangle marking between eyes, irregular markings on shoulder

and the rear of back (vs dorsum uniformly light brown or with light spots), dominant frequencies (7.3–8.3 kHz vs 2.0–2.7 kHz), call duration (mean 25.5 ms vs mean 59.4 ms), call intervals (mean 91.2 ms vs mean 478.4 ms) (Table 4).

Finally, *L. guinanensis* sp. nov. can be differentiated from other species in the genus *Leptobranchella* based on distinctive bioacoustics and morphological diagnostic characters (for details see Table 2, Suppl. material 1: table S4), as well as genetic divergences (Suppl. material 1: table S3).

Discussion

In recent years, five new *Leptobranchella* species have been discovered in the region of Guangxi: *L. damingshanensis* Chen, Yu, Cheng, Meng, Wei, Zhou & Lu, 2021, *L. maershanensis* (Yuan, Sun, Chen, Rowley & Che, 2017), *L. shangsiensis*, *L. shiwandashanensis*, and *L. wuhuangmontis* Wang, Yang & Wang, 2018 (AmphibiaChina 2023). In addition to these five species, previous studies had identified four additional *Leptobranchella* species: *L. alpina* (Fei, Ye & Li, 1990), *L. bourreti* (Dubois, 1983), *L. liui* (Fei & Ye, 1990), and *L. sungi* (Fei et al. 2012; Mo et al. 2014). Including the newly herein described *L. guinanensis* sp. nov. this elevates the known number of *Leptobranchella* species in the region of Guangxi to at least 10. Additionally, *L. ventripunctata*, originally found in Zhushihe, Mengla County, Xishuangbanna Dai Autonomous Prefecture, Yunnan, China, is widely distributed in southern Yunnan, Guizhou, China, Laos, northern Vietnam, and northern Thailand (Fei et al. 1990, 1992, 2012; Li et al. 2016; Chen et al. 2018; Luong et al. 2019; Wu et al. 2021; Frost 2023) and also Guangxi. However, this is the first recorded sighting of *L. ventripunctata* in Guangxi. The JZS specimens were identified as *L. ventripunctata* based on molecular data and morphological characters. The original diagnostic characters of *L. ventripunctata* include a relatively small body size (SVL 25.5–28.0 mm in males), absence of webbing and lateral fringes on the toes, creamy white chest and belly with scattered brown spots, relatively short hindlimbs, and tibiotarsal articulation reaching between the tympanum and the corner of the eye (Fei et al. 1990, 1992). These diagnostic characters were found to match those of the JZS specimens. However, *L. guinanensis* sp. nov. has 1/3 webbing on the toes, wide lateral fringes on the toes, no spots on the chest and belly, and tibiotarsal articulation reaching the centre of the eye, which are inconsistent with the diagnostic characters of *L. ventripunctata*. The genetic divergences between the new species and *L. ventripunctata* from the type locality are 1.6–2.4%, which is similar to the genetic divergences observed in other comparisons such as *L. brevicrus* Dring, 1983 vs *L. itiokai* Eto, Matsui & Nishikawa, 2016 (1.2%), *L. bijie* Wang, Li, Li, Chen & Wang, 2019 vs *L. oshanensis* (Liu, 1950) (1.7%), *L. jinshaensis* Cheng, Shi, Li, Liu, Li & Wang, 2021 vs *L. purpuraventra* Wang, Li, Li, Chen & Wang, 2019 (1.8%), *L. bijie* vs *L. chishuiensis* Li, Liu, Wei & Wang, 2020 (2.0%), and *L. bijie* vs *L. jinshaensis* (2.0%) (Suppl. material 1: table S3). Additionally, *L. guinanensis* sp. nov. exhibits high dominant frequencies of 7.3–8.3 kHz, which are the highest dominant frequencies ever known in the genus *Leptobranchella* (Suppl. material 1: table S4). Currently, there are no available advertisement calls of *L. ventripunctata* from the type locality. However, the advertisement calls from Yingjiang County, Yunnan, China, which is near the type locality, resemble those of the JZS specimens in terms of call durations, call intervals, and dominant frequency. It is important to note that the

advertisement calls of the new species do not overlap with those of the JZS specimens, indicating reproductive isolation between them (Köhler et al. 2017).

Leptobranchella sungi is primarily found in northern Vietnam, specifically in the provinces of Vinh Phuc, Yen Bai, Lao Cai, Dien Bien, Phu Tho, Son La, and Tuyen Quang, as well as in Guangxi, China (Frost 2023). Previous studies have indicated that *L. sungi* was only observed in the SWDS area of Guangxi (Fei et al. 2012; Mo et al. 2014). In our current study, we have identified a new range of *L. sungi* in Guangxi, specifically in the Sishuihe Nature Reserve, located in Lingyun County, Guangxi, China (SSH, Fig. 1).

The reserve harbors four different species of *Leptobranchella*, indicating a remarkably high species diversity within the genus. The four species were found in the evergreen forest at SWDS between 400–600 m. However, *L. guinanensis* sp. nov. was found near a stream that was ~ 0.5–1.0 m wide and had running currents. *Leptobranchella shangsiensis* and *L. shiwandashanensis* occur syntopically, but the former tended to call on rocks or near (~ 1.0 m) rocky streams with fast currents, while the latter called near rocky streams ~ 2.0–3.0 m away. *Leptobranchella sungi* was found to call near rocky streams that were ~ 2.0–3.0 m wide with slower currents. The breeding seasons for these species are as follows: *L. guinanensis* sp. nov. breeds in June, *L. shangsiensis* and *L. shiwandashanensis* in April, and *L. sungi* in July. Further research is required to understand how these four sympatric species interact and adapt to their respective niches within the reserve.

Acknowledgements

We would like to express our gratitude to the staff of Shiwandashan and Jinzhongshan National Nature Reserves for their valuable support during our fieldwork and for granting us permission to conduct field surveys. Additionally, we would like to acknowledge Johannes Penner, Tao Thien Nguyen, and the anonymous reviewers for enhancing the manuscript.

Additional information

Conflict of interest

The authors have declared that no competing interests exist.

Ethical statement

No ethical statement was reported.


Funding

This work was supported by the National Natural Science Foundation of China (grant numbers 32360128 and 32060116) and Guangxi Natural Science Foundation, China (grant number 2020GXNSFDA238022).

Author contributions

CWC conceived and designed the study and prepared the manuscript. CWC measured the specimens, performed the molecular experiments, and analysed the data. CWC, LP, LYJ and HY conducted field surveys. PWX drew the figures. All authors read and approved the final version of the manuscript.

Author ORCIDs

Wei-Cai Chen  <https://orcid.org/0000-0002-2398-4079>

Peng Li  <https://orcid.org/0000-0001-8311-0544>

Wan-Xiao Peng  <https://orcid.org/0000-0001-5635-9061>

You-Jun Liu  <https://orcid.org/0000-0001-7285-4943>

Yong Huang  <https://orcid.org/0000-0002-3493-9468>

Data availability

All of the data that support the findings of this study are available in the main text or Supplementary Information.

References

- Amphibia China (2023) The database of Chinese amphibians. Kunming Institute of Zoology (CAS), Kunming. <http://www.amphibiachina.org/> [Accessed 23 April 2023]
- Chen JM, Poyarkov Jr NJ, Suwannapoom C, Lathrop A, Wu YH, Zhou WW, Yuan ZY, Jin JQ, Chen HM, Liu HQ, Nguyen TQ, Nguyen SN, Duong TV, Eto K, Nishikawa K, Matsui M, Orlov NL, Stuart BL, Brown RM, Rowley JJJ, Murphy RW, Wang YY, Che J (2018) Largescale phylogenetic analyses provide insights into unrecognized diversity and historical biogeography of Asian leaf-litter frogs, genus *Leptolalax* (Anura: Megophryidae). *Molecular Phylogenetics and Evolution* 124: 162–171. <https://doi.org/10.1016/j.ympev.2018.02.020>
- Chen WC, Liao X, Zhou SC, Mo YM (2019) A new species of *Leptobrachella* (Anura: Megophryidae) from southern Guangxi, China. *Zootaxa* 4563(1): 67–82. <https://doi.org/10.11646/zootaxa.4563.1.3>
- Chen WC, Yu GD, Cheng ZY, Meng T, Wei H, Zhou GY, Lu YW (2021) A new species of *Leptobrachella* (Anura: Megophryidae) from central Guangxi, China. *Zoological Research* 42(6): 783–788. <https://doi.org/10.24272/j.issn.2095-8137.2021.179>
- Chen WC, Peng WX, Li P, Liu YJ (2022a) A new species of *Nidirana* (Anura, Ranidae) from Southern Guangxi, China. *Asian Herpetological Research* 13(2): 109–116. <https://doi.org/10.16373/j.cnki.ahr.210065>
- Chen WC, Peng WX, Liu YJ, Huang Z, Liao XW, Mo YM (2022b) A new species of *Occidozyga* Kuhl and van Hasselt, 1822 (Anura: Dicroglossidae) from Southern Guangxi, China. *Zoological Research* 43(1): 85–89. <https://doi.org/10.24272/j.issn.2095-8137.2021.252>
- Dubois A (1983) Note préliminaire sur le genre *Leptolalax* Dubois, 1980 (Amphibiens, Anoures), avec diagnose d'une espèce nouvelle du Vietnam. *Alytes* 2: 147–153. <https://doi.org/10.5962/p.297429>
- Emmrich M, Vences M, Ernst R, Köhler J, Barej M, Glaw F, Jansen M, Rödel MO (2020) A guild classification system proposed for anuran advertisement calls. *Zoosystematics and Evolution* 96(2): 515–525. <https://doi.org/10.3897/zse.96.38770>
- Fei L, Ye CY, Huang YZ (1990) Key to Chinese Amphibians. Publishing House for Scientific and Technological Literature, Chongqing, 364 pp.
- Fei L, Ye CY, Li SS (1992) Two new species of pelobatid toads of genus *Leptolalax* from Yunnan Province of China (Amphibia: Anura). *Acta Biologica Plateau Sinica* 11: 45–54.
- Fei L, Ye CY, Jiang JP (2012) Colored atlas of Chinese Amphibians and their distributions. Sichuan Publishing House of Science and Technology, Chengdu, 619 pp.
- Frost DR (2023) Amphibian Species of the World: An Online Reference. Version 6.1. American Museum of Natural History, New York. <https://doi.org/10.5531/db.vz.0001> [Accessed 21 April 2023]

- Köhler J, Jansen M, Rodríguez A, Kok PJR, Toledo LF, Emmrich M, Glaw F, Haddad CFB, Rödel MO, Vences M (2017) The use of bioacoustics in anuran taxonomy: Theory, terminology, methods and recommendations for best practice. *Zootaxa* 4251(1): 1–124. <https://doi.org/10.11646/zootaxa.4251.1.1>
- Kumar S, Stecher G, Tamura K (2016) MEGA 7: Molecular Evolutionary Genetics Analysis Version 7.0 for Bigger Datasets. *Molecular Biology and Evolution* 33(7): 1870–1874. <https://doi.org/10.1093/molbev/msw054>
- Lathrop A, Murphy RW, Orlov N, Ho CT (1998) Two new species of *Leptolalax* (Anura: Megophryidae) from northern Vietnam. *Amphibia-Reptilia* 19(3): 253–267. <https://doi.org/10.1163/156853898X00160>
- Li GG, Wei G, Zhang HB, Su HJ (2016) A new amphibian record in Guizhou Province – *Leptolalax ventripunctatus*. *Yesheng Dongwu* 37(2): 178–180.
- Liu CC (1950) Amphibians of western China. *Fieldiana. Zoology Memoirs* 2: 1–397. <https://doi.org/10.5962/bhl.part.4737>
- Luong AM, Nguyen HQ, Le DT, Nguyen SHL, Nguyen TQ (2019) New records of amphibians (Anura: Megophryidae, Ranidae) from Dien Bien Province, Vietnam. *Herpetology Notes* 12: 375–387.
- Miller MA, Pfeiffer W, Schwartz T (2010) Creating the CIPRES Science Gateway for inference of large phylogenetic trees. *Proceedings of the Gateway Computing Environments Workshop (GCE), New Orleans*, 8 pp. <https://doi.org/10.1109/GCE.2010.5676129>
- Mo YM, Jian JP, Ye CY (2008) A new record of frogs from China: *Paramegophrys (Paramegophrys) sungi* (Megophryidae, Amphibia). *Anhui Shi-da Xuebao. Zhexue Shehui Kexue Ban* 31(4): 368–370.
- Mo YM, Wei ZY, Chen WC (2014) *Colored Atlas of Guangxi Amphibians*. Guangxi Science and Technology Publishing House, Nanning, 313 pp.
- Mo YM, Chen WC, Liao XW, Zhou SC (2016) A new species of the genus *Rhacophorus* (Anura: Rhacophoridae) from southern China. *Asian Herpetological Research* 7: 139–150. <https://doi.org/10.16373/j.cnki.ahr.150070>
- Posada D (2008) jModelTest: Phylogenetic model averaging. *Molecular Biology and Evolution* 25(7): 1253–1256. <https://doi.org/10.1093/molbev/msn083>
- Qian TY, Xiao X, Cao Y, Xiao NW, Yang DD (2020) A new species of *Leptobranchella* (Anura: Megophryidae) Smith, 1925 from Wuling Mountains in Hunan Province, China. *Zootaxa* 4816(4): 491–526. <https://doi.org/10.11646/zootaxa.4816.4.4>
- Ren JL, An H, Yang T, Wang K, Xu SC, Wu PC, Wei SB, Huang XX, Li JT (2018) Preliminary herpetological resource survey and analysis in Shiwandashan National Nature Reserve, Guangxi. *Sichuan Journal of Zoology* 37(1): 95–107. <https://doi.org/10.11984/j.issn.1000-7083.20160198>
- Ronquist FR, Huelsenbeck JP (2003) MrBayes 3: Bayesian phylogenetic inference under mixed models. *Bioinformatics* 19(12): 1572–1574. <https://doi.org/10.1093/bioinformatics/btg180>
- Rowley JJ, Dau VQ, Cao TT (2017) A new species of *Leptolalax* (Anura: Megophryidae) from Vietnam. *Zootaxa* 4273(1): 61–79. <https://doi.org/10.11646/zootaxa.4273.1.5>
- Savage JM (1975) Systematics and distribution of the Mexican and Central American stream frogs related to *Eleutherodactylus rugulosus*. *Copeia* 2(2): 254–306. <https://doi.org/10.2307/1442883>
- Sung YH, Yang JH, Wang YY (2014) A new species of *Leptolalax* (Anura: Megophryidae) from southern China. *Asian Herpetological Research* 5(2): 80–90. <https://doi.org/10.3724/SP.J.1245.2014.00080>
- Tan WF (2014) *Reverses of Guangxi*. China Environment Publishing House, Beijing, 243 pp.

- Wang YY, Lau MWN, Yang J, Chen G, Liu ZY, Pang H, Liu Y (2015) A new species of the genus *Odorrana* (Amphibia: Ranidae) and the first record of *Odorrana bacboensis* from China. *Zootaxa* 3999(2): 235–254. <https://doi.org/10.11646/zootaxa.3999.2.4>
- Wang J, Lyu ZT, Qi S, Zeng ZC, Zhang WX, Lu LS, Wang YY (2020) Two new *Leptobranchella* species (Anura, Megophryidae) from the Yunnan-Guizhou Plateau, Southwestern China. *ZooKeys* 995: 97–125. <https://doi.org/10.3897/zookeys.995.55939>
- Wu YH, Pawangkhanant P, Chen JM, Gao W, Suwannapoom C, Che J (2021) Confirmation of *Leptobranchella ventripunctata* (Fei, Ye, and Li, 1990), based on molecular and morphological evidence in Thailand. *Biodiversity Data Journal* 9: e74097. <https://doi.org/10.3897/BDJ.9.e74097>
- Yang JH, Zeng ZC, Wang YY (2018) Description of two new sympatric species of the genus *Leptolalax* (Anura: Megophryidae) from western Yunnan of China. *PeerJ* 6: e4586. <https://doi.org/10.7717/peerj.4586>

Supplementary material 1

Morphological data

Authors: Wei-Cai Chen, Peng Li, Wan-Xiao Peng, You-Jun Liu, Yong Huang

Data type: xlsx

Explanation note: **table S1:** References for morphological characters for congeners of the genus *Leptobranchella*. **table S2:** Comparative material examined. **table S3:** Uncorrected p-distance in *Leptobranchella* species based on 16S gene fragments. **table S4:** Dominant frequency of advertisement calls of species available in the genus *Leptobranchella*. **table S5:** Measurements of adult specimen of *L. guinanensis* sp. nov. and *L. ventripunctata*.

Copyright notice: This dataset is made available under the Open Database License (<http://opendatacommons.org/licenses/odbl/1.0/>). The Open Database License (ODbL) is a license agreement intended to allow users to freely share, modify, and use this Dataset while maintaining this same freedom for others, provided that the original source and author(s) are credited.

Link: <https://doi.org/10.3897/zookeys.1192.98352.suppl1>

Supplementary material 2

Advertisement calls of *L. sungi*

Authors: Wei-Cai Chen, Peng Li, Wan-Xiao Peng, You-Jun Liu, Yong Huang

Data type: tif

Copyright notice: This dataset is made available under the Open Database License (<http://opendatacommons.org/licenses/odbl/1.0/>). The Open Database License (ODbL) is a license agreement intended to allow users to freely share, modify, and use this Dataset while maintaining this same freedom for others, provided that the original source and author(s) are credited.

Link: <https://doi.org/10.3897/zookeys.1192.98352.suppl2>

